12 May 2006 | $10

Science

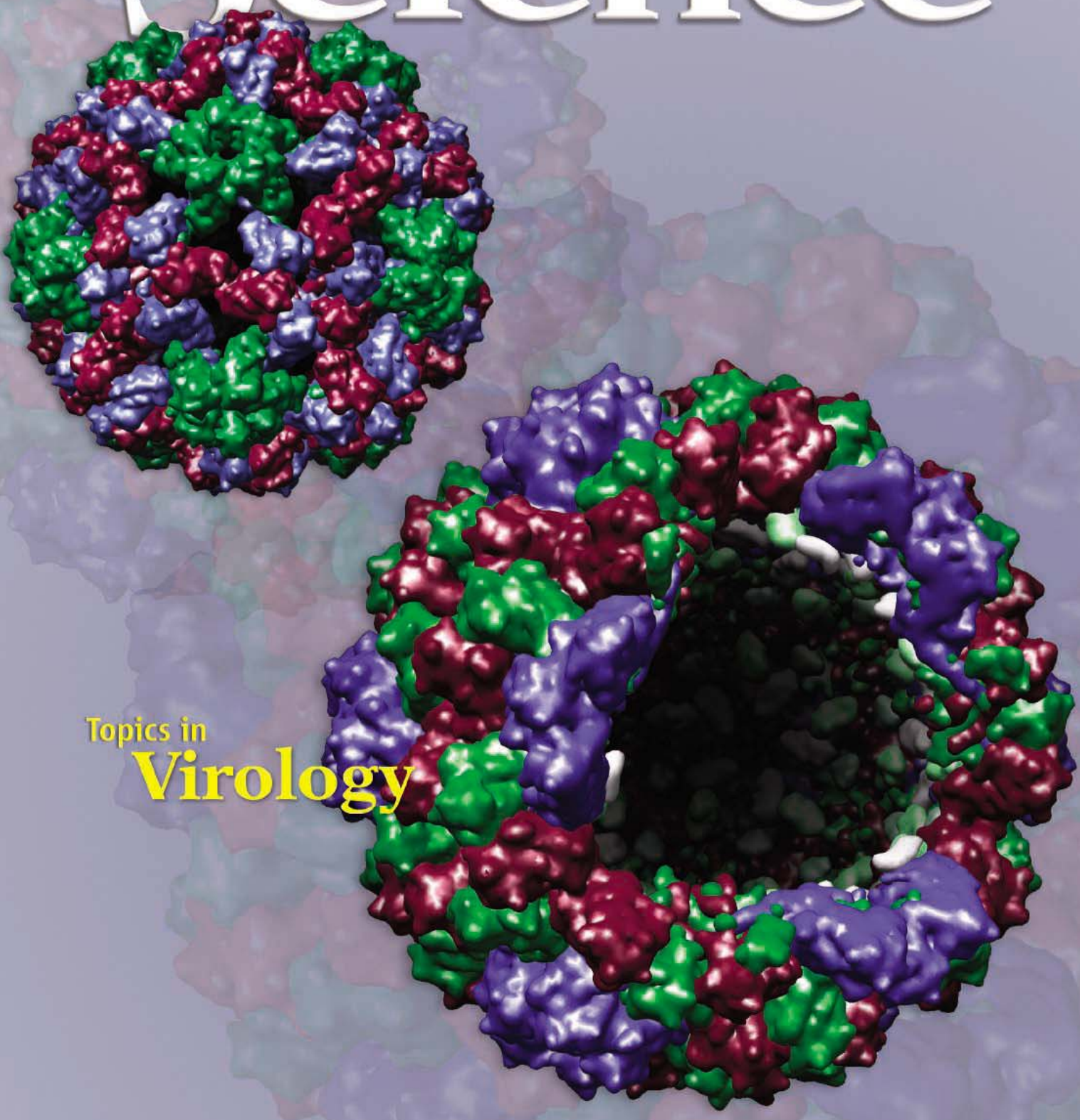

Topics in Virology

AAAS

MX3005P™ System
Most Flexible

MX3000P® System
Most Affordable

Performance runs in the family.

Choose the personal QPCR system that's right for you.

Stratagene now offers two affordable, fully-featured quantitative PCR (QPCR) systems. The new five-color Mx3005P™ QPCR System includes expanded features to support a wider range of real-time QPCR applications, such as simultaneous five-target detection and alternative QPCR probe chemistries. The Mx3000P® QPCR System is still the most affordably priced four-color 96-well system available.

- **A four- or five-color instrument, with user-selected filters**
- **Advanced optical system design for true multiplexing capability, and wider application support**
- **MxPro™ QPCR Software with enhanced data analysis and export functionality**

Need More Information? Give Us A Call:

Stratagene US and Canada
Order: 800-424-5444 x3
Technical Service: 800-894-1304 x2

Stratagene Europe
Order: 00800-7000-7000
Technical Service: 00800-7400-7400

Stratagene Japan K.K.
Order: 3-5821-8077
Technical Service: 3-5821-8076

www.stratagene.com

STRATAGENE®

TIME MACHINE

The Mini-Prep 96

A fully automatic, bench-top instrument that purifies plasmid and genomic DNA at the push of a button.

Call now or visit our website:
Your Time is Valuable.

MacConnell RESEARCH

800.466.7949 www.macconnell.com

GE Healthcare

Bringing science to life

When it comes to life sciences, GE Healthcare is setting the standard. Tens of thousands of scientists in over 100 countries around the world rely on our products every day. We have delivered more than 60 000 research protein purification systems, 1500 BioProcess™ systems and 12 000 BioProcess columns worldwide. Our Amersham family of consumables, with its 60-year heritage, is trusted to provide accurate results time and time again.

But we're never content to stand still. We constantly strive for new innovations for tomorrow's research and drug development. And the result is groundbreaking products like the ÄKTAdesign™ platform, IN Cell Analyzer, Ad-A-Gene Vectors, and MabSelect™ media. Thanks to our technological achievements and global presence, we're able to help you turn your scientific ideas into reality – bringing science to life and helping transform healthcare.

We call it Life Science Re-imagined.

Discover more at www.gehealthcare.com/life

imagination at work

Volume 312, Issue 5775

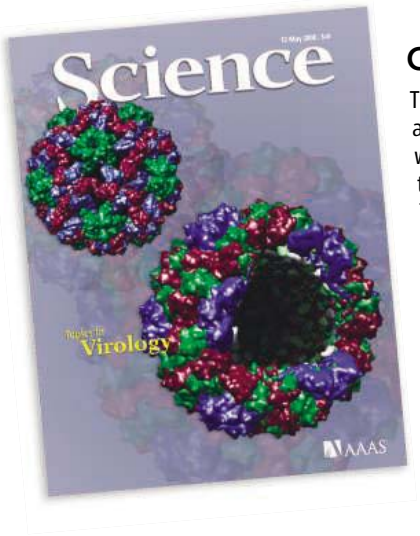

COVER

The structure of cowpea chlorotic mottle virus, a plant virus, in its open and closed forms, with a section of the capsid removed from the closed form to illustrate the interior cavity. This virus serves as a biotemplate for viral-based nanomaterials applications. See the Perspective on page 873, which is part of a special section beginning on page 869.

Image: J. Hilmer, created with UCSF Chimera

DEPARTMENTS

EDITORIAL

SPECIAL SECTION

Topics in Virology

INTRODUCTION

NEWS

PERSPECTIVE

REVIEWS

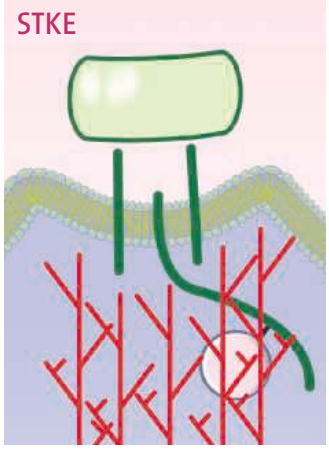

For related online content, see page 807 or go to www.sciencemag.org/sciext/virology

NEWS OF THE WEEK

NEWS FOCUS

CONTENTS continued **>>**

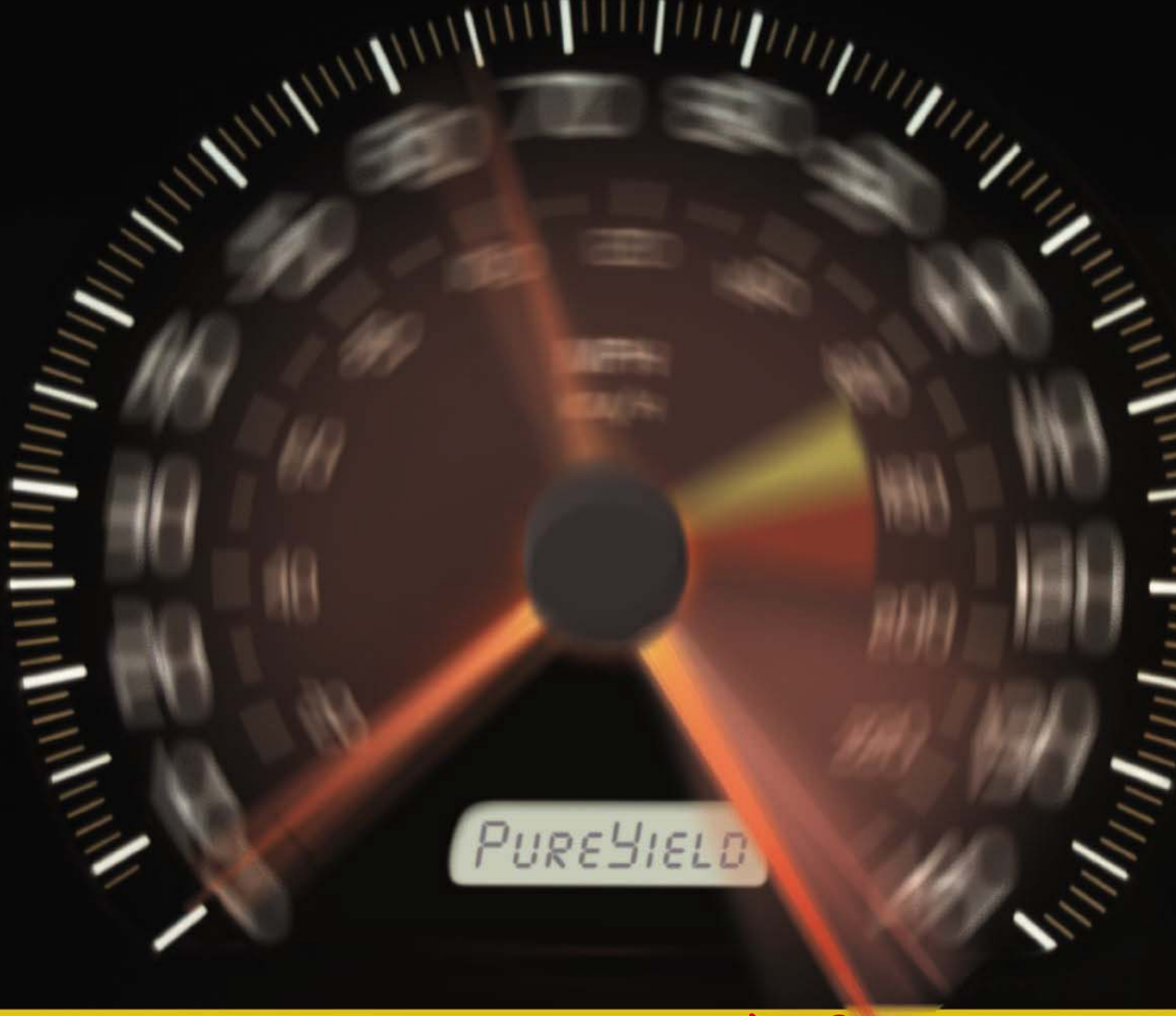

Break the midiprep and maxiprep speed limit.

New **PureYield**™ plasmid preps deliver transfection-quality DNA in record time. Recover up to 1mg of plasmid DNA in less than 60 minutes (maxiprep) or up to 200µg in only 30 minutes (midiprep). No post-elution alcohol precipitation required. Race through your next plasmid prep.

Request a FREE SAMPLE* at: www.promega.com/pureyield

*Samples to qualified customers where available, while supplies last.

PROMEGA CORPORATION • www.promega.com

Promega

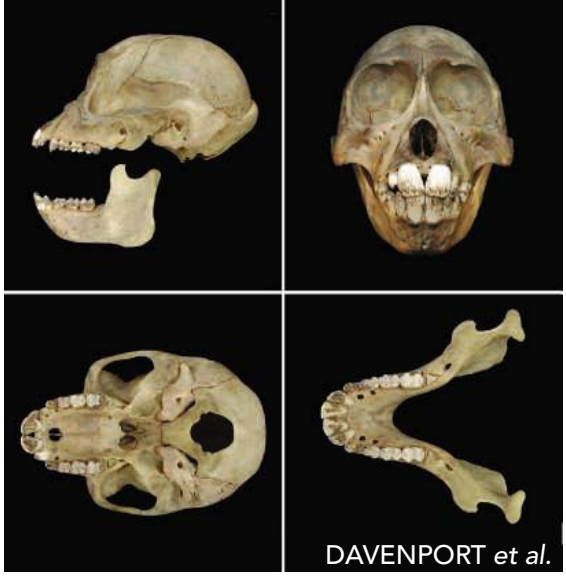

SCIENCE EXPRESS

www.sciencexpress.org

LETTERS

BOOKS *ET AL.*

POLICY FORUMS

PERSPECTIVES

TECHNICAL COMMENT ABSTRACTS

BREVIA

CONTENTS continued >>

LESS

ROUTINE.

MORE

REVOLUTIONARY.

Innovative DNA and RNA prep technologies designed to save time and produce better data downstream. Innovative ChargeSwitch® technology delivers fast, simple, effective nucleic acid purification from all types of samples. Save time and eliminate steps with fast, inhibitor-free purification. All without ethanol or chaotropic salts. And it's just one example of how Invitrogen is transforming sample prep. For good. **Get ready at www.invitrogen.com/napq.**

invitrogen™

Science

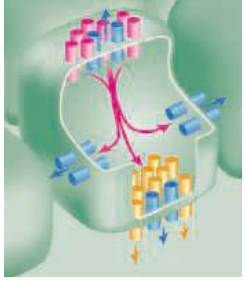

858, 883, & 914

REPORTS

AAAS
ADVANCING SCIENCE, SERVING SOCIETY

SCIENCE (ISSN 0036-8075) is published weekly on Friday, except the last week in December, by the American Association for the Advancement of Science, 1200 New York Avenue, NW, Washington, DC 20005. Periodicals Mail postage (publication No. 484460) paid at Washington, DC, and additional mailing offices. Domestic individual membership and subscription (51 issues): $139 ($74 allocated to subscription). Domestic institutional subscription (51 issues): $650; Foreign postage extra: Mexico, Caribbean (surface mail) $55; other countries (air assist delivery) $85. First class, airmail, student, and emeritus rates on request. Canadian rates with GST available upon request, GST #1254 88122. Publications Mail Agreement Number 1069624. **Printed in the U.S.A.**

Change of address: Allow 4 weeks, giving old and new addresses and 8-digit account number. **Postmaster:** Send change of address to AAAS, P.O. Box 96178, Washington, DC 20090–6178. **Single-copy sales:** $10.00 current issue, $15.00 back issue prepaid includes surface postage; bulk rates on request. The identification code for *Science* is 0036-8075. *Science* is indexed in the *Reader's Guide to Periodical Literature* and in several specialized indexes.

CONTENTS continued **>>**

One just right for you.

Whether you have 10 samples or 10,000 — discover your perfect match in the full range of Bio-Rad PCR consumables.

- Precise manufacturing ensures optimal fit in our thermal cyclers
- Optical plates and seals give dependable real-time results
- Hard-Shell® warp-free plates allow reliable laboratory automation
- Tight-sealing vessels prevent sample loss
- Products tested to be negative for DNase, RNase, and DNA contamination
- Dedicated technical support provided by experienced scientists

For more information, visit our gateway to genomics applications at **www.bio-rad.com/genomics/**

Bio-Rad offers validated consumables for the MJ Mini™ cycler, the 4-bay DNA Engine Tetrad® 2 cycler, and everything in between.

Visit us on the Web at **discover.bio-rad.com**
Call toll free at 1-800-4BIORAD (1-800-424-6723);
outside the US, contact your local sales office.

BIO-RAD

SCIENCE**NOW**

www.sciencenow.org DAILY NEWS COVERAGE

Flipper's Call Sign
Dolphins identify each other by signature whistles, not voice.

Timing Is Everything in Brain Development
Neural progenitor cells make sure the cart comes after the horse.

Up and Down, but Not Strange
A look inside the proton is helping physicists define exactly what matter is.

SCIENCE **CAREERS**

www.sciencecareers.org CAREER RESOURCES FOR SCIENTISTS

US: Postdoctoral Teaching—Savvy Career Move or Research Distraction?
M. Guinnee
Universities are offering teacher training to graduate students, postdocs, and faculty, but is it a good idea?

UK: Analyzing Corporations ... and Cosmic Structures
A. Forde
Graham Smith left a lucrative position as a business management consultant to become an astrophysicist.

US: First, Fix the Attitude
GrantDoctor
The U.S. educational system is churning out a large number of embittered young scientists who won't impress hiring and grant review committees.

GRANTSNET: International Grants and Fellowship Index
A. Kotok
Get the latest listing of funding opportunities from Europe, Asia, and the Americas.

SCIENCE'S **SAGE KE**

www.sageke.org SCIENCE OF AGING KNOWLEDGE ENVIRONMENT

PERSPECTIVE: Neuropathology in Alzheimer's Disease—Awaking from a Hundred-Year-Old Dream
A. Nunomura et al.
Are senile plaques and neurofibrillary tangles protective rather than pathogenic?

MEETINGS AND EVENTS
The 10th International Conference on Alzheimer's Disease and Related Disorders will be held in Madrid in July.

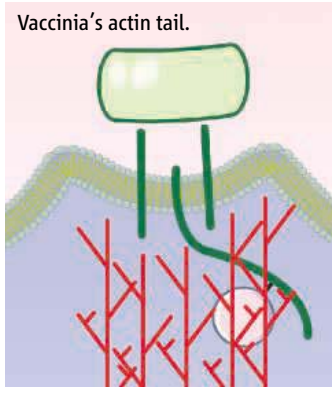
Vaccinia's actin tail.

SPECIAL CONTENT

Topics in Virology

SCIENCE'S **STKE**

www.stke.org SIGNAL TRANSDUCTION KNOWLEDGE ENVIRONMENT

EDITORIAL GUIDE: Viruses—Miniature Machiavellis of the Signaling World?
E. M. Adler
Viruses manipulate signaling pathways in the host cell to ensure their own replication and survival.

REVIEW: Signaling During Pathogen Infection
S. Münter, M. Way, F. Frischknecht
Pathogens manipulate host cell-signaling pathways to achieve efficient entry, replication, and exit during their infection cycles.

REVIEW: Notch and Wnt Signaling—Mimicry and Manipulation by Gamma Herpesviruses
S. D. Hayward, J. Liu, M. Fujimuro
EBV and KSHV exploit the Notch and Wnt pathways in B cells to advance their own life cycles.

PERSPECTIVE: Viral Modulators of Cullin RING Ubiquitin Ligases—Culling the Host Defense
M. Barry and K. Früh
Viruses hijack the host ubiquitination machinery to control a range of cellular processes.

SCIENCE**PODCAST**

Listen to the 12 May edition of the *Science* Podcast to hear about Earth's changing magnetic field, questions about the effort to wipe out polio, how viruses are emerging as a platform for nanotech, and other stories.
www.sciencemag.org/about/podcast.dtl

Separate individual or institutional subscriptions to these products may be required for full-text access.

SPECIAL INTRODUCTORY OFFER
See our website for details.

NEW ENGLAND BIOLABS

Competent Cells from New England Biolabs

SUPERIOR COMPETENT *E.COLI* STRAINS FOR CLONING AND PROTEIN EXPRESSION

For many years staff scientists at New England Biolabs have been using their own line of optimized chemically competent *E.coli* cells for cloning and protein expression. These strains have made all the difference to a highly demanding research and production program. Now when you are looking for a versatile cloning strain, rapid colony growth, or tight control of protein expression, you can benefit from the superior performance and high quality of these strains.

- **NEB Turbo Competent *E.coli*** **C2984H**
  Ligate, transform, plate and pick colonies in one day
- **NEB 5-alpha Competent *E.coli*** **C2991H**
  Versatile cloning strain
- **T7 Express Competent *E.coli*** **C2566H**
  High efficiency transformation and protein expression
- **T7 Express *I*^{q} Competent *E.coli*** **C2833H**
  Tight control of protein expression
- **dam^{-}/dcm^{-} Competent *E.coli*** **C2925H**
  Grow plasmids free of dam and dcm methylation

Advantages:

- Ready to transform – packaged in single-use transformation tubes (20 x 0.05 ml)
- Free of animal products
- 5 minute transformation protocols
- Supplied with outgrowth media and control DNA

	NEB Turbo	NEB 5-alpha	T7 Express	T7 Express *I*^{q}	dam^{-}/dcm^{-}
Transformation Efficiency (cfu/µg)	>10^{9}	1-3 x 10^{9}	2-6 x 10^{8}	2-6 x 10^{8}	>2 x 10^{6}
Strain	K12	K12	B	B	K12
T1 Phage Resistant	✓	✓	✓	✓	✓
Blue/White Screening	✓	✓	–	–	–
lac *I*^{q}	✓	✓	–	✓	–
Colonies Visible after 8 hours	✓	–	–	–	–
Endonuclease I Deficient	✓	✓	✓	✓	✓
Protease Deficient	–	–	✓	✓	–
Restriction Deficient	✓	✓	✓	✓	✓
M13 Phage Capable (F^{+})	✓	✓	–	✓	–
RecA Deficient	–	✓	–	–	–

Chemically Competent *E.coli* Strain Characteristics

For more information and international distribution network, please visit www.neb.com

- **New England Biolabs Inc.** 240 County Road, Ipswich, MA 01938 USA 1-800-NEB-LABS Tel. (978) 927-5054 Fax (978) 921-1350 info@neb.com
- **Canada** Tel. (800) 387-1095 info@ca.neb.com
- **Germany** Tel. 0800/246 5227 info@de.neb.com
- **UK** Tel. (0800) 318486 info@uk.neb.com
- **China** Tel. 010-82378266 beijing@neb-china.com

NEW ENGLAND BioLabs® Inc.
the leader in enzyme technology

EDITED BY STELLA HURTLEY AND PHIL SZUROMI

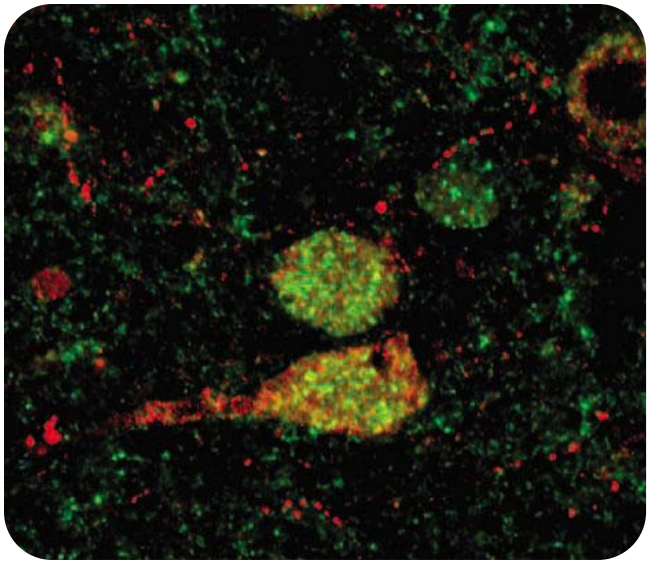

A Cellular Fuel Sensor

The brain plays a key role in body weight control. Within the hypothalamus, select populations of neurons sense changes in fuel availability and regulate food intake and metabolism, but the underlying signaling mechanisms have not been well understood. **Cota *et al.*** (p. 927; see the Perspective by **Flier**) implicate the atypical kinase mTOR (mammalian Target of Rapamycin) signaling pathway, which has been widely studied in other cell types where it regulates the rate of protein synthesis. In rodents, central administration of leucine, which increases mTOR signaling in nonneuronal cells, activated hypothalamic mTOR signaling and decreased food intake and body weight.

Getting a Charge Out of Nanowires

The protein coat of viruses has previously been used as templates for nanowires, and because some viruses can align in a liquid-crystalline phase, this approach can be used to form larger arrays of ordered nanoparticles. **Nam *et al.*** (p. 885, published online 6 April) exploit these properties to fabricate cobalt oxide nanowires for use as battery electrodes. Further modification of the virus allows for the formation of cobalt oxide–gold nanoparticle hybrid wires that enhance the charging capacity of the battery.

Light on the Fast Track

Photons travel at constant speed c, but in certain nonlinear optical media that exhibit anomalous dispersion, the speed of light pulses can appear to be faster than c, an effect called superluminal propagation. Theoretical results have suggested that the exiting pulse leaves before the entering pulse has entered the medium, and that the pulse peak propagates backward in the medium. **Gehring *et al.*** (p. 895) investigated both of these effects with a pumped erbium-doped fiber that exhibits a negative group velocity and they show that the underlying cause is the reshaping of the pulse in the gain medium. The peak of the exiting pulse is formed from the rising edge of the entering pulse, and the peak of the entering pulse becomes part of the trailing edge of the exiting pulse. **Dolling *et al.*** (p. 892) looked at the propagation of infrared femtosecond laser pulses through a negative-refractive-index metamaterial and directly measured the group and phase velocities (v_{group} and v_{phase}) by time-resolving the transmitted pulse using interferometry. This situation is the negative-index counterpart of experiments of Gehring *et al.* for positive index, where $v_{phase} > 0$ and the induced $v_{group} < 0$. They find conditions where $v_{phase} < 0$ and $v_{group} < 0$, and others where $v_{phase} < 0$ and $v_{group} > 0$. Together with the "usual" situation of $v_{phase} > 0$ and $v_{group} > 0$, all four sign combinations have now been observed in direct experiments, and in all cases, the Poynting vector is positive—energy flows in the forward direction.

CREDITS (TOP TO BOTTOM): COTA *ET AL.*; GUBBINS *ET AL.*

Not So Fast

The strength of the Earth's magnetic field has decayed since accurate measurements began in 1840, and these changes have led to speculation that the field will disappear or reverse within this millennium. Extrapolating to earlier times has been difficult, in that direct measurements, which extend back another 250 years, recorded only direction, and there paleomagnetic data that has been extracted from rocks and archaeological artifacts is limited. **Gubbins *et al.*** (p. 900; see the Perspective by **Kono**) have devised a method to use paleointensity measurements in conjunction with directional information to extend the record of the Earth's magnetic field back to 1590. Contrary to the recent steep decline, they find that the dipole moment fell hardly at all until around 1800.

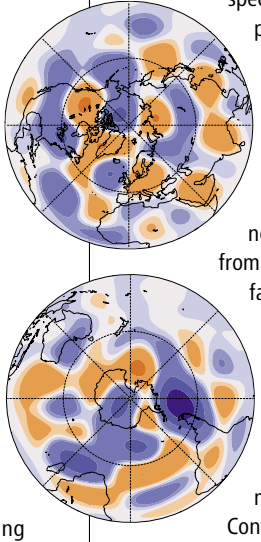

Giving Metals the Push

Crystalline metals can be thought to consist of nearly perfectly ordered grains separated by highly distorted walls. During plastic deformation, the grains will shrink and misalign, and new dislocations will form and take on ordered patterns, but it has been difficult to isolate the changes that occur to individual grains. **Jakobsen *et al.*** (p. 889; see the Perspective by **Kubin**) present an x-ray method that tracks the dynamics of individual grains deeply embedded within a crystal. They find some surprising behavior, including intermittent dynamics where the grains grow and shrink, and transient splitting of grains into subgrains.

Lost in Translation

Dyskeratosis congenita (DC) is a rare inherited disorder associated with bone marrow failure, skin defects, and an increased susceptibility to cancer. The X-linked form, X-DC, is caused by mutations in the *DKC1* gene, which encodes a pseudouridine synthase that modifies ribosomal RNA. **Yoon *et al.*** (p. 902) show that disruption of *DKC1* impairs translation of a select group of messenger RNAs (mRNAs) that initiate protein synthesis in an unusual way, through internal ribosome entry site (IRES) elements. Among the mRNAs affected were those encoding the tumor suppressor p27(Kip1) and two proteins that prevent cell death, Bcl-xL and XIAP (for X-linked Inhibitor of Apoptosis Protein). Loss of these protein functions may contribute to the pathogenesis of X-DC.

Manipulating Microtubule Motion

For small fluidic and reactor systems, one solution for controlling the transport of reagents and products would be to incorporate biological motors. Previous studies have shown that microtubules can be chemically modified to carry cargo, but controlling their motion is still a chal-

Continued on page 811

www.roche-applied-science.com

LightCycler® 480 Real-Time PCR System

Rapid by nature, *accurate by design*

LightCycler® 480 Block Cycler Unit for 96 or 384 wells, easily exchanged by users within minutes.

For years, Roche has provided real-time automated PCR solutions you can count on. Now, you can obtain the proven performance and benefits of the original LightCycler® System in a 96- or 384-well instrument platform for high-throughput applications – the new **LightCycler® 480 Real-Time PCR System**.

Speed – Save time without sacrificing the quality of your results – precise, high-speed temperature changes maximize specificity and yield.

Accuracy – Benefit from our novel thermal block cycler and data-capture technologies to minimize edge-effects for outstanding accuracy and precision.

Versatility – Combine 5 excitation and 6 detection channels, multiple probe formats, proven analysis software, and true master mix reagents to meet your specific application needs.

Compatibility – Take advantage of the instrument's automation and LIMS capabilities to interface with your current systems and future workflows.

Visit ***www.roche-applied-science.com/lightcycler480*** for more information.

Roche Diagnostics

Roche Diagnostics GmbH
Roche Applied Science
68298 Mannheim
Germany

For general laboratory use. Not for use in diagnostic procedures.

Continued from page 809

lenge. **Van den Heuvel *et al.*** (p. 910; see the Perspective by **Hess**) studied the behavior of microtubules in constant electric fields. With detailed experiments and theory, they show that individual microtubules driven by the motor protein kinesin across the surface of micrometer-sized fluidic channels can be driven in a desired direction and that the sorting occurs with high efficiency.

PINning Down Auxin Flow

The plant hormone auxin regulates a variety of growth and developmental responses and must be transported within the plant in an organized fashion. **Petrášek *et al.*** (p. 914, published online 6 April; see the Brevia by **Wiśniewska *et al.*** and the Perspective by **Sieberer and Leyser**) now show, by using inducible overexpression in plant cells and expression in human and yeast cells, that the protein PIN is responsible for the direction in which auxin flows out of the cell.

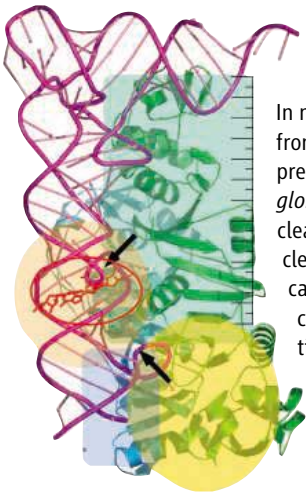

Hold and Cut

In nuclear transfer RNA and archeal RNA, introns must be removed from folded precursors to produce functional RNA. **Xue *et al.*** (p. 906) present the structure of a dimeric splicing endonuclease from *Archaeglobus fulgidus* bound to a bulge-helix-bulge RNA containing a precleaved and a cleaved splice site at 2.85 angstrom resolution. The cleavage sites are within the bulges, and an arginine pair from each catalytic domain sandwiches a flipped-out base from the bulge cleaved by the other catalytic domain. This motif leads to cooperativity in binding and cleavage of the two splice sites. Interactions between the RNA and the endonuclease at the active sites are consistent with the idea that three conserved residues form a catalytic triad.

Charting Oceanic Microbial Abundance

Prochlorococcus may represent the most abundant photosynthetic organism on Earth. **Bouman *et al.*** (p. 918) present a circumglobal sampling effort in the Southern Hemisphere of *Prochlorococcus*, its pigments, and the distribution of its specific genetic variants (such as ecotypes), across the Southern Pacific, Atlantic, and Indian oceans. The distribution of phylotypes and ecological types among the three ocean basins reflects the gradients of light and nutrients and oceanographic characteristics of the three basins.

Endocytosis and Developmental Patterning

During animal patterning in development, morphogens such as Wnt form gradients that control local developmental responses. While searching for factors involved in *Caenorhabditis elegans* larval cell migration, **Coudreuse *et al.*** (p. 921, published online 27 April) found a role for components of the conserved endocytic retromer complex. The retromer complex is required in cells that produce the Wnt ortholog EGL-20 and is needed to establish the EGL-20 concentration gradient as well as for long-range signaling. Experiments with mammalian cell lines and *Xenopus* suggest a conserved function for the retromer complex in Wnt signaling, possibly by recycling the Wnt cargo-receptor from the endosome to the Golgi.

Stroke, Ischemia, and Ion Flux

The rapid decrease of oxygen and glucose in brain tissue after an acute stroke can trigger necrotic neuronal cell death within minutes. The main underlying cause is the dysregulation of major intracellular ion concentrations, but it has been unclear which particular ion channels are activated by ischemic conditions in pyramidal neurons. Pannexin 1 (Px1) is a member of a family of gap junction proteins that are highly expressed in pyramidal neurons. In acutely isolated neurons and brain slices, **Thompson *et al.*** (p. 924) found that Px1 hemichannel opening was activated by ischemic stress. Thus, hemichannel activation by ischemia during stroke could be responsible for the profound ionic dysregulation contributing to excitotoxicity.

CREDIT: XUE *ET AL.*

www.roche-applied-science.com

Genome Sequencer 20 System

First to the Finish

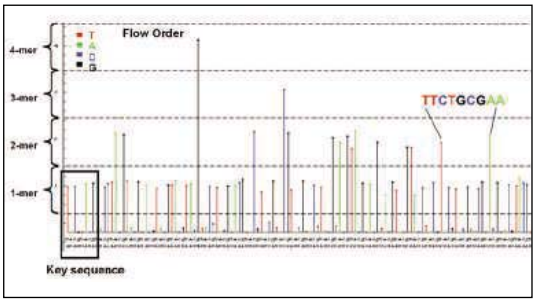

Flowgram of a GS 20 read

Sequence genomes like never before

- **Compare microbial genomes in weeks, not years**
- ***De novo* sequence a bacterial genome in fewer than 5 days**
- **Sequence more than 100 BACs per month**
- **Sequence >200,000 miRNAs, SAGE tags, or ditags (*e.g.*, CAGE) in 5.5 hours**

Coming soon:

Ultra-deep sequencing of amplicons – identify rare SNP patterns or cancer-associated mutations from complex samples

Harness the horsepower of the newest revolution in sequencing today — visit www.roche-applied-science.com/sis/sequencing/genome or contact your local sales representative.

454 LIFE SCIENCES

Roche Diagnostics

Roche Diagnostics GmbH
Roche Applied Science
68298 Mannheim
Germany

Donald Kennedy is Editor-in-Chief of *Science*

More Silliness on the Hill

THERE IS SOMETHING ABOUT GASOLINE THAT TEMPTS CERTAIN PEOPLE TO POUR IT ON A FIRE. The paroxysms of the U.S. Congress, in response to a price tag approaching $50 to fill the average automobile fuel tank, remind us that its desperate members will lunge at almost anything that might relieve constituent pain. In this respect, of course, they have no monopoly on foolishness; the White House is right in there with some questionable ideas of its own.

Consider the following list of seriously proposed solutions to this contretemps. First, give every consumer $100 as a makeup. That may pay for two fill-ups, but it will only add another tax-cut equivalent to the deficit and do nothing whatsoever to relieve the regressive character of high fuel prices. Second, mobilize the Strategic Petroleum Reserve. Well, that's another transient fix, and even the president has pointed out that it probably shouldn't be used until things get really desperate—whenever that is. Finally, because environmentalists got together to block drilling in the Arctic National Wildlife Refuge, they are really responsible for the problem, so we should go ahead and drill there just to show them.

Naturally, there has also been an effort to identify evildoers so that Americans may take comfort in pointing to an external human source of the problem. Conservatives cast the blame on environmentalists, OPEC, the bad guys who are blowing up pipelines in Iraq, and the Venezuela of Hugo Chavez. Liberals focus on the "oil guys": the corporate chieftains who met in secret with Vice President Cheney in 2001 to determine the administration's energy "policy" and reaped windfall profits; many then exited with mind-boggling separation payments.

This political theater is missing a few essentials. First, gasoline prices are getting a little closer to what they really ought to be. Europeans still pay more than Americans do with few complaints, saving those for the war in Iraq or other serious matters. The oil company executives have surely gained from the recent price rise, but it's not clear that they caused it. Some of those well-rewarded CEOs did, after all, forecast the price increases and rewarded their stockholders by negotiating future contracts at prices that seemed high at first, but later looked good against $70 per barrel. As for OPEC, they couldn't have caused this event by themselves no matter how much they might have wanted to.

Finally, no one is blaming you and me. The only sensible words the president has uttered during this episode are that Americans are "addicted to oil." No one, as far as I know, has been locked inside a dealership and forced to buy a Hummer. We reject the 55 mph speed limit whenever given the chance, and we continue to elect politicians who believe that global warming is just a myth. Americans showed in the 1973 oil crisis that they could conserve energy to a degree that astounded economists. But in the years leading up to the present price crescendo, everyone seems to have forgotten how it's done.

Now the challenge is to produce national policies that will provide incentives for Americans to cure the addiction. Stringent fuel-efficiency standards on a national basis will be essential, and reduced speed limits would add to the savings. California has shown that it can hold per-capita energy consumption flat while it has risen elsewhere, and some lessons learned there can be applied nationally. A cap-and-trade system for greenhouse gas emissions, of the general kind contained in last year's McCain-Lieberman bill, should be supported by an administration that has so far shown no appetite for emissions mitigation. Carbon-free nuclear energy is stalled because it is thought to be politically dead, but there is now every reason to weigh its risks thoughtfully against the potentially even larger ones associated with global climate change. To support more imaginative research on biofuels and other alternatives to carbon, why rule out a gas tax? After all, even at $4 per gallon, Americans would still be getting a bargain compared to the Europeans.

There's one good thing about these gas prices. They may jolt us and our political leadership out of this coma, yielding some realistic solutions once this brain-dead conversation in Washington ends.

– Donald Kennedy

10.1126/science.1129466

Advanced Quality. Reliable Performance. Better Oligos.

QSR-773

For U.S. Certification Only

100% Quality Control, 100% of the Time

Our quality standards are so high, we guarantee every oligo will work, every time. Just choose your oligo, and we'll select the best quality control procedures to ensure both accuracy and consistency. When we synthesize complex oligos, we will use a combination of state-of-the-art analytical techniques to guarantee performance. Here are just a few of the ways we lead the world in quality control:

- ***MALDI-TOF Mass Spectrometry:*** *Verified composition.*
- ***Electrospray Ionization Mass Spectrometry (ESI-MS):*** *Validated composition for oligos longer than 50 bases*
- ***Capillary Electrophoresis (CE):*** *Guaranteed consistent measurement of purity.*
- ***Polyacrylamide Gel Electrophoresis (PAGE):*** *Quality tested purity and oligo length.*

What Does ISO Mean To You?

- **Consistent Product and Service through Well-Documented Processes**
- **Reduced Cost through Continual Process Improvement**
- **Reduced Cycle Time for Quick Delivery**

ISO 9001:2000 registered: Canada, Germany, Japan and the USA.

ISO 14001:1996 registered: UK

For our latest insights on oligo quality and our performance guarantee, please visit:
sigma-aldrich.com/oligos_iso

sigma-aldrich.com

YOUR GLOBAL PARTNER FOR INNOVATIVE CUSTOM GENOMIC AND PROTEOMIC SOLUTIONS

SIGMA-GENOSYS • 1442 LAKE FRONT CIRCLE • THE WOODLANDS • TEXAS 77380 • USA

SIGMA® GENOSYS

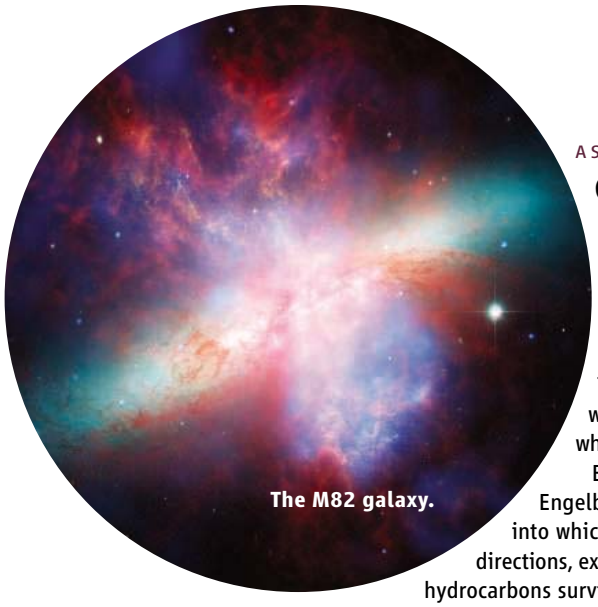

The M82 galaxy.

ASTROPHYSICS

Glowing in the Wind

Galactic winds, driven by violent bursts of star formation, are thought to spread elements heavier than hydrogen between galaxies and throughout the cosmos. The ashes of former stars thereby live on in later generations of stars and may affect galactic evolution. The loss of gas due to winds may starve galaxies of fuel and could affect the growth of different galaxy types. The nearby edge-on spiral galaxy M82 has the most thoroughly studied strong wind; this galaxy is undergoing a violent burst of star formation in its heart, which expels a bi-conical superwind of hot ionized gas.

By examining infrared images acquired with the Spitzer Space Telescope, Engelbracht *et al.* find that M82 is surrounded by a spherical halo of warm dust into which the hot wind penetrates. Spidery dust filaments emanate outward in all directions, extending well beyond the galaxy and its wind. The spectra reveal that aromatic hydrocarbons survive in the dust despite close proximity to the hot superwind. The unusually wide extent and spherical shape of the M82 dust cocoon suggest that the dust was driven out of the galaxy before the superwind commenced, and is thus more pervasive than previously thought; possible explanations include interactions with neighboring galaxies or alternative wind-related mechanisms. — JB

Astrophys. J. **642**, L127 (2006).

BIOCHEMISTRY

Flipped Out

As a consequence of their competitive upbringing, microbes have refined the art of warfare, both in the synthesis of and resistance to small molecules, many of which are used by humans as antibiotic drugs. The modes whereby the microbes resist the action of drugs fall generally into three classes: (i) chemical modification of the small molecule into a harmless derivative (for instance, by hydrolysis); (ii) protection of the protein targeted by the drug (by mutation of the gene); (iii) sequestration or transport of the drug beyond the vicinity of the target (by pumping the drug out of the cell).

Siarheyeva *et al.* have taken a closer look at the last of these pathways and address a current controversy regarding the environment and mechanism used to load substrates into the multidrug-resistance transporters for removal. By applying nuclear magnetic resonance spectroscopy to detect the interactions between (the protons of) nine representative and structurally dissimilar drugs and (the protons of) dimyristoyl phosphatidylcholine, the authors find that all of these hydrophobic compounds reside predominantly in the portion of the lipid bilayer between the choline headgroup and the aliphatic tails. This location is consistent with the view that multidrug-resistance transporters may function primarily to flip drugs from the inner to the outer leaflet of the plasma membrane, from whence the drugs diffuse into the extracellular medium, thus reducing intracellular antibiotic concentrations. — GJC

Biochemistry **45**, 10.1021/bi0524870 (2006).

PHYSICS

Brane-Induced Inflation

Inflationary cosmology seeks to explain such puzzling features of the universe as the extreme flatness of spacetime and the mutual similarity of distant regions of space that are not causally connected. A universe experiencing breakneck inflationary expansion would exhibit these and other observed characteristics, but the standard model of particle physics lacks any identifiable quantum particle, or inflaton, that could underlie this phenomenon.

A brane is a spacetime structure that inhabits the higher dimensional spaces (the "bulk") required by "theories of everything," such as string theory and M theory, and some specific assemblage of branes might act as inflatons. Shuhmaher and Brandenberger offer a model of cosmological inflation in which a hot gas of branes drives expansion of the high-dimensional bulk spacetime. At first, all spatial dimensions are extremely compact, and extra dimensions above the usual three are tucked away into a topological space called an orbifold. As the brane gas expands, its energy density decreases until the three familiar spatial dimensions can undergo conventional inflationary expansion. — DV

Phys. Rev. Lett. **96**, 161301 (2006).

CELL BIOLOGY

Stress Made Manifest

When cells attach to a surface, stress fibers (contractile actomyosin bundles) play a key role in adhesion itself and in the subsequent movements and morphology of these cells. Hotulainen and Lappalainen examined how stress fibers assemble in cultured human cells and document two pathways of formation. At the base of the cell, dorsal stress fiber assembly was driven by formin-stimulated actin assembly at focal adhesions, which are established adherent patches. In contrast, near the leading edge of the cell, unanchored ventral arcs of actin formed by means of the end-to-end assembly of bundles of the molecular motor myosin and with concomitant actin bundle assembly promoted by the Arp2/3 complex. Both dorsal stress fibers and ventral arcs were able to convert into ventral stress fibers, which are anchored to focal adhesions at the front and back of the cell.

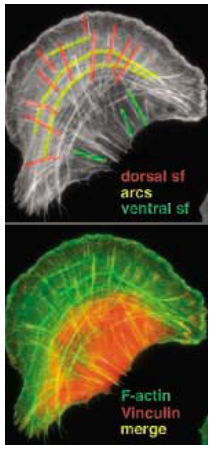

Different types of stress fibers contain actin filaments in an osteosarcoma cell line.

Continued on page 817

CREDITS (TOP TO BOTTOM): NASA/JPL-CALTECH/STSCI/CXC/UOFA/ESA/AURA/JHU; HOTULAINEN AND LAPPALAINEN, *J. CELL BIOL.* **173**, 10.1083/JCB.200511093 (2006)

Genetic Engineering that is Right on Target!

The TargeTron™ Gene Knockout System is a revolutionary method for rapid and specific disruption of genes in prokaryotic organisms. Utility of the technology has been demonstrated for prokaryotic genetic engineering, systems biology and functional genomics approaches.

The method exploits the retrohoming ability of group II introns and utilizes a simple PCR step to "re-target" the TargeTron group II intron for specific insertion into the host genome. Gene knockout using the TargeTron system has been validated in a broad range of bacterial strains such as *Escherichia coli, Staphylococcus aureus, Lactococcus lactis, Clostridium perfringens, Shigella flexneri* and *Salmonella typhimurium.*

- Targeted and permanent gene disruption
- Simple, streamlined protocol; Knockouts in 3 days or less
- Minimal screening to isolate mutants.
- No cell conjugation or specific host factor requirements
- >90% successful targeted insertion

Product	Description	Unit
TA0100A	TargeTron™AGeneAA	3EA
	KnockoutASystemA	10EA

For additional details and product availability, please visit www.sigma-aldrich.com/s1target

Continued from page 815

Both dorsal stress fibers and transverse arcs continually undergo assembly and disassembly; and within stress fibers, actin cross-linking remained dynamic, allowing for extensive remodeling during cell movement. — SMH

J. Cell Biol. **173**, 10.1083/jcb.200511093 (2006).

DEVELOPMENT

A Bug's Life History

Direct-developing insects progress through nymphal and adult stages, where nymphs are similar to but smaller than adults, whereas other insects experience a dramatic transition—metamorphosis—with distinct larval and pupal stages giving rise to the adult form. The transcription factor *broad* is known to play a critical role in metamorphosis: Its expression is limited to the larval-pupal transition, where it activates pupal-specific genes and specifies pupal development. But what does *broad* do in direct-developing insects?

Erezyilmaz *et al.* have cloned the *broad* gene from the direct-developing milkweed bug *Oncopeltus fasciatus*, which passes through five nymphal instars before molting into the adult. The *broad* gene is expressed during embryogenesis and the nymphal stages; expression peaks during the nymphal molts, but *broad* RNA is not present in the latter part of the fifth and final nymphal instar or in the subsequently formed adult. RNAi knockdown of *broad* blocks the morphological transition from one nymphal instar to the next, although it does not alter the number of nymphal instars or the transition to the adult.

***Oncopeltus fasciatus*.**

CREDIT: EREZYILMAZ *ET AL.*, *PROC. NATL. ACAD. SCI. U.S.A.* **103**, 6925 (2006)

Metamorphosis in insects is thought to have arisen in a direct-developing ancestor some 300 million years ago and may have been caused in part by changes in the expression of *broad*, from its temporally complex pattern in the milkweed bug, which directs differential growth between nymphal instars, to the highly restricted pattern during the last larval instar of insects that undergo metamorphosis. — GR

Proc. Natl. Acad. Sci. U.S.A. **103**, 6925 (2006).

CHEMISTRY

Stabilizing Ca-H

The *s*-block metals, whose valence electrons lie exclusively in *s* orbitals, are widely known for their ionic chemistry. Through careful ligand choice, metals such as sodium, magnesium, and calcium can also be coaxed into discrete coordination complexes. However, *s*-block molecular hydride complexes, which are of particular interest in light of the strong role of *p*- and *d*-block metal hydrides in organic reduction chemistry, have proven challenging to access, because they tend to decompose into insoluble aggregates.

Harder and Brettar have prepared a dimeric calcium hydride complex that is freely soluble in benzene and stable at 80°C. The solid-state structure, in which two hydride ligands bridge the two Ca centers, was characterized by x-ray crystallography. Key to the synthesis was the choice of a tightly coordinating β-diketiminate ancillary ligand on each Ca center. Surprisingly, the bulky tris(*tert*-butylpyrazolyl)borate (Tp^{tBu}) ligand failed to prevent disproportionation into $(Tp^{tBu})_2Ca$ and the insoluble CaH_2 oligomer, despite stabilizing a hydride complex of calcium's lighter congener beryllium. — JSY

Angew. Chem. Int. Ed. **45**, 10.1002/anie.200601013 (2006).

Science STKE AAAS

www.stke.org

<< Going for the Correct Orientation

Development of the *Drosophila* sensory organ depends on the polarization and subsequent asymmetric division of sensory organ precursor cells (SOPs), which give rise to the cell types that make up the mature structure. Although SOPs can become polarized and divide asymmetrically in the absence of external signals, achieving the correct orientation depends on extracellular signals transduced through the Frizzled (Fz) receptor. Fz is known to signal through heterotrimeric GTP–binding proteins containing G_o-type α subunits, and Katanaev and Tomlinson demonstrate that cells containing mutant G_o or overexpressing wild-type G_o show defects in both orientation and asymmetric division as well as in the localization of Numb, a protein whose polarized distribution in SOPs is key to cell fate determination. The phenotypic effects of overexpressing wild-type G_o depended on the expression of Fz and were enhanced by Fz overexpression. G_o thus appears to be involved both in the establishment of asymmetry and in specifying orientation, and the authors propose that it may act to integrate the two. — EMA

Proc. Natl. Acad. Sci. U.S.A. **103**, 6524 (2006).

www.sciencemag.org

Science

1200 New York Avenue, NW
Washington, DC 20005
Editorial: 202-326-6550, FAX 202-289-7562
News: 202-326-6500, FAX 202-371-9227

Bateman House, 82-88 Hills Road
Cambridge, UK CB2 1LQ
+44 (0) 1223 326500, FAX +44 (0) 1223 326501

Subscription Services For change of address, missing issues, new orders and renewals, and payment questions: 866-294-0062 or 202-326-6417, FAX 202-842-1065. Mailing addresses: AAAS, P.O. Box 96178, Washington, DC 20090-6178 or AAAS Member Services, 1200 New York Avenue, NW, Washington, DC 20005

Institutional Site Licenses please call 202-326-6755 for any questions or information

Reprints: Author Inquiries 800-635-7181
Commercial Inquiries 803-359-4578
Corrections 202-326-6501

Permissions 202-326-7074, FAX 202-682-0816

Member Benefits Bookstore: AAAS/BarnesandNoble.com bookstore www.aaas.org/bn; Car purchase discount: Subaru VIP Program 202-326-6417; Credit Card: MBNA 800-847-7378; Car Rentals: Hertz 800-654-2200 CDP#343457, Dollar 800-800-4000 #AA1115; AAAS Travels: Betchart Expeditions 800-252-4910; Life Insurance: Seabury & Smith 800-424-9883; Other Benefits: AAAS Member Services 202-326-6417 or www.aaasmember.org.

science_editors@aaas.org	(for general editorial queries)
science_letters@aaas.org	(for queries about letters)
science_reviews@aaas.org	(for returning manuscript reviews)
science_bookrevs@aaas.org	(for book review queries)

Published by the American Association for the Advancement of Science (AAAS), *Science* serves its readers as a forum for the presentation and discussion of important issues related to the advancement of science, including the presentation of minority or conflicting points of view, rather than by publishing only material on which a consensus has been reached. Accordingly, all articles published in *Science*—including editorials, news and comment, and book reviews—are signed and reflect the individual views of the authors and not official points of view adopted by the AAAS or the institutions with which the authors are affiliated.

AAAS was founded in 1848 and incorporated in 1874. Its mission is to advance science and innovation throughout the world for the benefit of all people. The goals of the association are to: foster communication among scientists, engineers and the public; enhance international cooperation in science and its applications; promote the responsible conduct and use of science and technology; foster education in science and technology for everyone; enhance the science and technology workforce and infrastructure; increase public understanding and appreciation of science and technology; and strengthen support for the science and technology enterprise.

Information for Contributors

See pages 102 and 103 of the 6 January 2006 issue or access www.sciencemag.org/feature/contribinfo/home.shtml

Now Available!
SNPlex™ Genotyping System on the 3130*xl* Genetic Analyzer.

Accept No Limitations.

The improved SNPlex Genotyping System now performs cost effective and customizable genotyping projects on the 3130*xl* Genetic Analyzer.

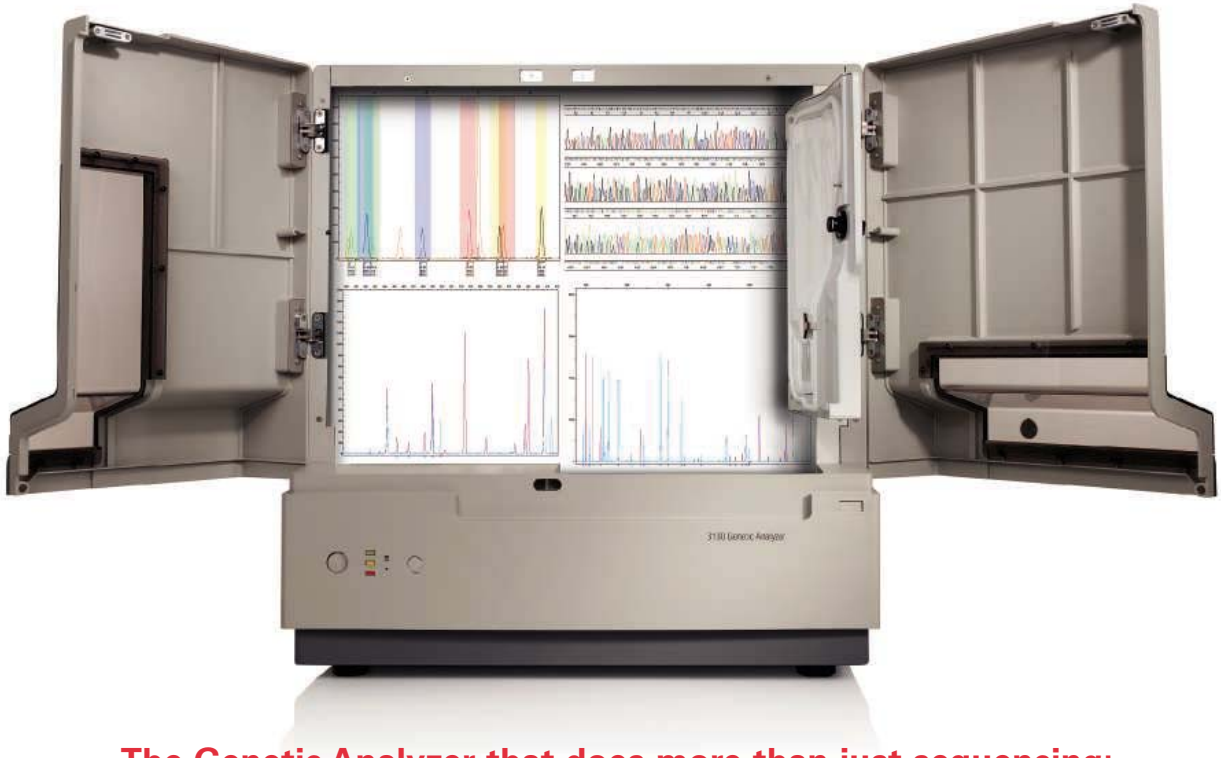

The Genetic Analyzer that does more than just sequencing:

SNPlex Genotyping System* • *De novo* sequencing • Resequencing • Comparative sequencing
Mutation/heterozygote detection • SAGE • SNP validation and screening • Genotyping • Microsatellite analysis
AFLP • Conformation analysis • T-RFLP • MLST • Relative fluorescent quantitation

Applied Biosystems 3130 and 3130*xl* Genetic Analyzers

The 4-capillary 3130 and 16-capillary 3130***xl*** Genetic Analyzers provide reference-standard data quality and sophisticated, hands-free automation capabilities across a wider range of sequencing, resequencing and fragment analysis applications. The 3130 Series systems leverage the same technology, reagents, and software interface that make our larger production-scale systems so successful, bringing superior performance within the reach of almost any lab. Learn more at: http://info.appliedbiosystems.com/3130series.

Applied Biosystems

25 YEARS ADVANCING SCIENCE

*Not supported on the 3130 Genetic Analyzer.

Imagination will often carry us to worlds that never were. But without it we go nowhere.

Carl Sagan

American astronomer, novelist (1934-1996)

Shimadzu is a participant in
the 54th ASMS Conference on Mass Spectrometry
in Seattle, Washington from May 28 to June 1, 2006.

Please visit us at
Booth # 115 or in Hospitality Suite Grand III-FGH
in the Westin Hotel

Our core strengths include not only technologies that support superior products and services, but also the spark of ideas that lights the way to a brighter future. Shimadzu believes in the value of science to transform society for the better. For more than a century, we have led the way in the development of cutting-edge technology to help measure, analyze, diagnose and solve problems. The solutions we develop find applications in areas ranging from life sciences and medicine to flat-panel displays. We have learned much in the past hundred years. Expect a lot more.

www.shimadzu.com

SHIMADZU

EDUCATION

Thinking Like a Tumor

Inside Cancer, a new primer from the Cold Spring Harbor Laboratory in New York, explains the basics of tumor biology with a snazzy mix of text and multimedia. Start with the Hallmarks of Cancer section to hear experts such as Robert Weinberg of the Massachusetts Institute of Technology talk about the abilities a cell needs to spawn a tumor, which include dodging the immune system and thwarting suicide pathways. In the action-packed Pathways to Cancer animations, visitors wend through a cell's cluttered interior and plunge into nuclear pores to see how the signaling systems that normally manage division go awry. (Above, a tumor cell tangles with an antibody-spiked B cell.) Other sections explore cancer epidemiology and new treatments. >>
www.insidecancer.org

EDUCATION

Teach Yourself Physics

At the Net Advance of Physics, you can find out how to derive the Nambu-Jona-Lasinio model of light nuclei, bone up on the motions of objects in the Kuiper belt at the edge of the solar system, and learn about hundreds of other topics. The virtual encyclopedia from Norman Redington of the Massachusetts Institute of Technology links to resources such as Wikipedia, online physics dictionaries, and articles and tutorials in the preprint server arXiv. Recent additions include biographical sketches and other information for audiences of Michael Frayn's play *Copenhagen*, about the World War II meeting between Werner Heisenberg and Niels Bohr. >>
web.mit.edu/redingtn/www/netadv/welcome.html

RESOURCES

Life With Tentacles

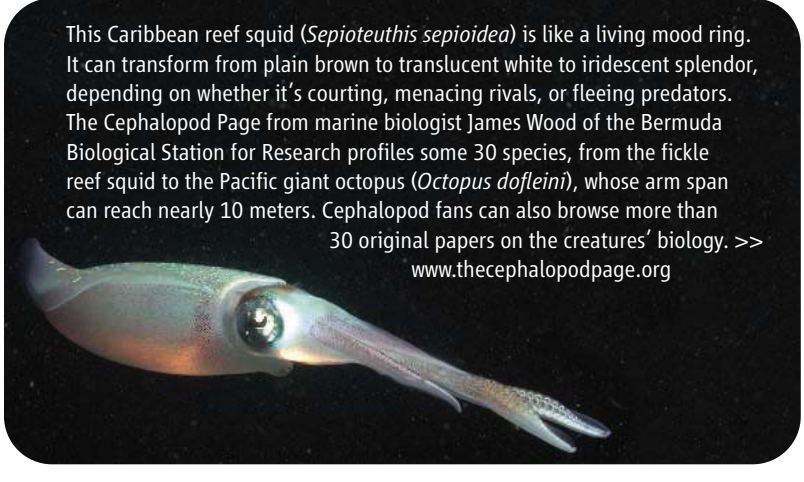

This Caribbean reef squid (*Sepioteuthis sepioidea*) is like a living mood ring. It can transform from plain brown to translucent white to iridescent splendor, depending on whether it's courting, menacing rivals, or fleeing predators. The Cephalopod Page from marine biologist James Wood of the Bermuda Biological Station for Research profiles some 30 species, from the fickle reef squid to the Pacific giant octopus (*Octopus dofleini*), whose arm span can reach nearly 10 meters. Cephalopod fans can also browse more than 30 original papers on the creatures' biology. >>
www.thecephalopodpage.org

EDUCATION

Scientists on the Record

By instilling a "great faith in mathematical models," John Maynard Smith's first career as an airplane designer during World War II prepared him to become one of the 20th century's premier evolutionary biologists. Although models incorporate unrealistic assumptions, he learned that they can still be "safe enough to trust your life to." The venerable British scientist is one of 18 researchers, mathematicians, and doctors who recounted their life stories for Peoples Archive. A London-based company has been filming the reminiscences of artists and other luminaries for the site, most of which is now free. The collection preserves the words of several scientists who have died recently, including Maynard Smith, biologists Francis Crick and Ernst Mayr, and physicists Hans Bethe and Edward Teller. >>
www.peoplesarchive.com

EXHIBITS

Home, Sweet Cave >>

Available: Roomy hillside hideaway with commanding views of France's Tautavel Valley; earth floors; stone ceilings; spacious common area great for butchering and tool-making; convenient to game trails, flint deposits.

These amenities first drew early humans to the Arago cave in southern France nearly 700,000 years ago. At this online exhibit, part of a series on archaeological sites from the French Ministry of Culture and Communication, you can visit the cave and get to know its former tenants. The beetle-browed *Homo erectus* who moved into the cave—including the famous 450,000-year-old Tautavel man (above)—may have been the ancestors of the Neandertals. The exhibit follows how human use of the cave changed over time, from a temporary hunting camp to a permanent home. Pop-up windows offer a close look at the troglodytes' tool kit of stone scrapers, choppers, and serrated denticulates for slicing flesh. >>
www.culture.gouv.fr/culture/arcnat/tautavel/en/index.html

Send site suggestions to >>
netwatch@aaas.org
Archive: www.sciencemag.org/netwatch

CREDITS (TOP TO BOTTOM): COLD SPRING HARBOR LABORATORY; JAMES WOOD

Be the 1

to dig deeper and discover answers at the exon level

1,000,000 Exons ▪ New GeneChip® Human Exon 1.0 ST Array The first system for genome-wide, exon-level expression analysis on a single microarray. Add this new tool to capture alternative splicing data and robust gene-level expression results to complement your DNA sequence and protein expression data. View the complete picture to accelerate your discovery. Use the proven GeneChip® platform to get better answers today and keep you in the lead tomorrow.

www.affymetrix.com • 1-888-DNA-CHIP (362-2447)
Europe: +44 (0) 1628 552550 • Japan: +81-(0)3-5730-8200

The Way Ahead™

AFFYMETRIX®

EDITED BY KATHERINE UNGER

SEQUENCER ON BOARD

An $85,000 on-board sequencer has enabled an international team of scientists to gather detailed genetic and morphological information on an unusually large number of species scooped up on a 20-day cruise of the Sargasso Sea in the Atlantic Ocean.

The scientists, funded by the U.S. National Oceanic and Atmospheric Administration and the Census of Marine Life, a global network of ocean scientists, found greater diversity than they expected from what is considered one of the world's least productive oceanic regions. "Sometimes the most interesting questions come from looking at places where people think it's uninteresting or unimportant," says marine biologist Russell Hopcroft of the University of Alaska, Fairbanks, a member of the expedition. The 28 scientists on board were able to identify some 444 species before their colors faded and to sequence 220 of them before returning to port. For example, *Diacria major*, a sea butterfly (above), had a mitochondrial gene sequenced and compared to that of a similar species for the first time. The goal is to form a database of DNA "barcodes" for the world's marine fish and zooplankton. Data from the cruise will be presented next week at the Barcoding Marine Life Workshop in Amsterdam, the Netherlands.

WHAT'S IN YOUR WATER?

The vast majority of Americans who rely on groundwater to drink are swigging more than just H_2O. A new survey of groundwater stores by the U.S. Geological Survey (USGS) found that volatile organic compounds (VOCs) are found in 90% of aquifers, although generally at levels considered safe for human consumption.

VOCs come from commonly used products such as gasoline, cleaning products, plastics, and paint. The 17-year USGS study, released last month, tested water samples from 98 groundwater aquifers and 3500 public and private wells for 55 compounds. Scientists identified 42 such compounds, the most common of which was chloroform. It was found in 7% of aquifers, 5% of domestic wells, and 11% of public wells. But fewer than 2% of the samples had VOC levels above those determined by the Environmental Protection Agency to be harmful to human health.

Senior author John Zogorski says the findings underscore the necessity of "continuing monitoring efforts to go back and understand the sources" of contamination. And Erik Olson, director of the drinking-water program at the Natural Resources Defense Council in Washington, D.C., cautions that many of the chemicals identified could be harbingers of worse contamination. For instance, 3% of aquifer samples contained MTBE—a highly mobile gasoline additive that affects water's taste and odor. Its presence could mean that slower moving and more toxic gasoline compounds may not be far behind.

Old in New

A three-dimensional mural based on early 20th century sketches of mouse neurons by Spanish physiologist Santiago Ramón y Cajal will grace a three-level stairway in the new Washington, D.C., headquarters of the Society for Neuroscience. Cajal shared the 1906 Nobel Prize in physiology or medicine with Camillo Golgi of Italy for work on nervous system structure.

Cajal's grandson and great-granddaughter—both Spanish physicians based in Zaragoza and Barcelona, respectively—were on hand to dedicate the 11-story building last week.

A LIBRARY'S NEW HOME

A remarkable collection of science texts will move this fall to The Huntington Library, Art Collections, and Botanical Gardens in San Marino, California. The Burndy Library, named for its founder, inventor and author Bern Dibner, has been located at the Massachusetts Institute of Technology (MIT) since 1992. But historians of science and technology expect the new site to be a shot in the arm for their field.

The Huntington already houses a strong history of science collection, with an emphasis on astronomy. And while the Dibner family provided fellowships to attract researchers to MIT, the Huntington already hosts 1700 scholars each year from a range of disciplines. "The library will be one of the richest in the country in terms of [history of science] holdings," says science historian Mordechai Feingold of the California Institute of Technology in Pasadena.

The Burndy contains some 67,000 books—a third of them rare—and various scientific instruments and paintings. Highlights of the collection include a volume belonging to Louis Pasteur, complete with margin notes, and a first edition of 17th century philosopher Robert Boyle's text on electricity (right).

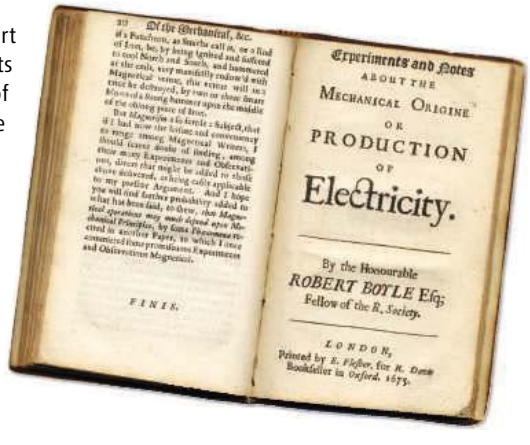

Experiments and Notes
ABOUT THE
MECHANICAL ORIGINE
OR
PRODUCTION
OF
Electricity.

By the Honourable
ROBERT BOYLE Esq;
Fellow of the R. Society.

LONDON,
Printed by E. Flesher, for R. Davis
Bookseller in Oxford, 1675.

CREDITS (TOP TO BOTTOM): RUSS HOPCROFT/UNIVERSITY OF ALASKA, FAIRBANKS/NOAA; SOCIETY FOR NEUROSCIENCE; BURNDY LIBRARY

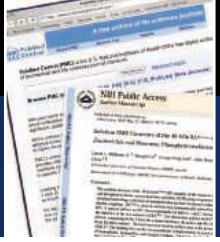

Mandating public access
828

Taking aim at social sciences
829

NASA BUDGET

Crisis Deepens as Scientists Fail To Rejigger Space Research

COLLEGE PARK, MARYLAND—With too many missions and not enough money, NASA's $5.5 billion science program is in a terrible fix. A 5-year plan that would cancel projects nearing completion, decimate disciplines, and slash funds to analyze data so upset space science researchers when NASA released it in February that officials gave the community an unprecedented shot at coming up with something better. But the scientists who met here last week as members of a newly expanded NASA advisory committee couldn't agree on an alternative approach that wouldn't bust NASA's proposed budget for 2007. That failure could leave the fate of the program to the whims of Congress.

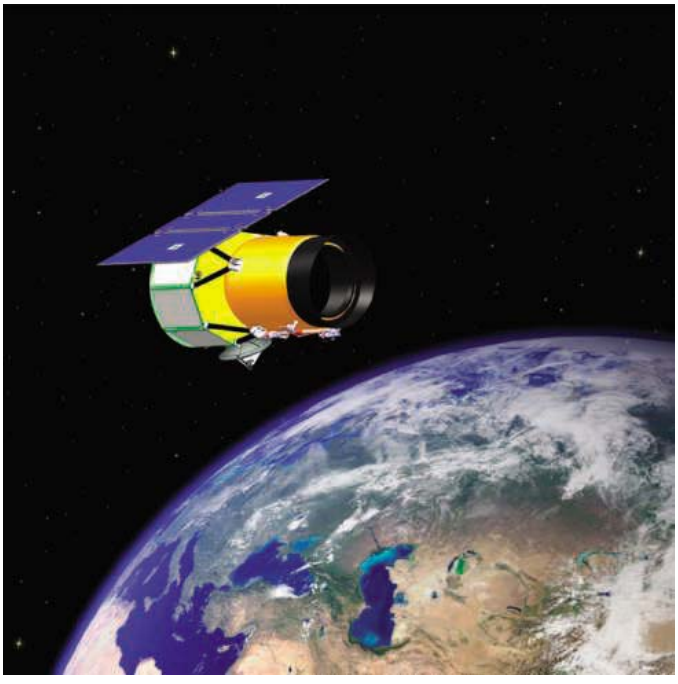

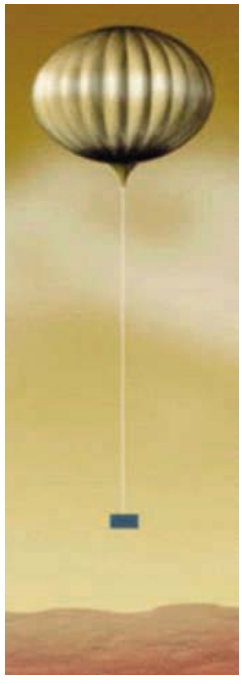

Unwise choices? NASA's budget woes could mean the end of several space science projects, including the Wide-Field Infrared Space Explorer (*left*) and a planned Mars Scout mission (*right*).

The precarious state of U.S. space and earth sciences has become clear in the past several months, as several costly birds have come home to roost. The problems—the need for more money to get the space shuttle flying again, the White House push for a new launcher to send humans to the moon, and rising costs in science projects such as the James Webb Space Telescope—are not chicken feed. And NASA Administrator Michael Griffin accepts a portion of the blame. "I made a mistake," Griffin told NASA's new science advisory panel. "I made commitments in advance that I wasn't able to keep," referring to his 2005 promise not to shift money from science to human space flight. NASA's current budget request would trim more than $3 billion from space science through 2011.

A separate effort to confront the crisis came in a 4 May report from a National Academies' National Research Council (NRC) panel. The group, chaired by Lennard Fisk, an atmospheric scientist at the University of Michigan, Ann Arbor, concludes that the program is "fundamentally unstable [and] seriously unbalanced" and that it will fall far short of the research goals laid out in earlier academy surveys. Both the committee and the NRC report say the space agency should reverse proposed cuts to research grants, restore small missions, and move quickly to control spiraling costs. But neither tells NASA which programs or missions to cut. Both groups also criticized the agency for failing to consult regularly with researchers.

The gathering of the advisory panel at the University of Maryland last week was intended to remedy that situation and come up with concrete solutions to NASA's fiscal crisis. Dividing themselves into four groups—earth sciences, astrophysics, heliospherics, and planetary science—the 70 members set out to devise an alternative budget. But they were stymied by financial and legal hurdles. When it came time to discuss the fate of the 2011 Scout balloon mission to Mars, for example, a half-dozen members recused themselves because they had proposals pending. "We can't very well make a decision to cancel the Scout mission after all the qualified people have left the room," said a frustrated Sean Solomon, a planetary geologist at the Carnegie Institution of Washington and the subcommittee chair. "We're going to punt; our hands are tied by legal restrictions."

Despite much grumbling about NASA's planned cuts, the panels could not reach agreement on a different set of priorities. William Smith, president of the Washington, D.C.–based Association of Universities for Research in Astronomy, warned that canceling or deferring flagship missions would hurt the health of the research community, noting that three of NASA's large observatories in turn award $70 million a year in small grants. Physicist Glenn Mason of the University of Maryland, College Park, argued on behalf of small missions, saying they can provide focused data in a relatively short period. And NASA's acting earth science chief Bryant Cramer cast a vote for midsize spacecraft, which he says provide a great deal of affordable science.

The panel adjourned without reaching a consensus but agreed to meet again in July for additional discussions. Simultaneously, it will help NASA come up with a long-term science strategy, which Congress wants delivered by December.

The NRC report—an independent study also requested by Congress—hammered at NASA's management of science missions, which "are being executed at costs well in excess of the costs estimated at the time when the missions were recommended." Whereas the report urged NASA to undertake detailed cost evaluations of all its missions, the ▶

CREDITS: JPL/NASA

Polio: So near, yet so far
832

Emotion control
838

Sweeping the heavens
840

advisory panel complained that some of those overruns are due to new safety requirements imposed by NASA. In fact, the only suggestion from either the advisory committee or the NRC panel about how to save money involved reducing overhead by removing some of the hurdles proposed missions must clear before launch. "Right now, we are simply too risk-averse," says Cramer, a longtime project manager. Griffin agrees that the agency must reduce red tape, and late last month, in a speech to industry, he urged companies and his staff to come up with less costly ways of doing business.

NASA officials, however, remain up against an immediate budget wall. They say they are considering canceling the Wide-Field Infrared Space Explorer, a $300 million mission well along in the planning. Also hanging by a thread is the Stratospheric Observatory for Infrared Astronomy, a joint project with Germany set for a first flight sometime next year.

Scientists are hoping that Congress will step in to save the day by providing more money than the agency requested for the fiscal year that begins on 1 October. But given competing interests, lawmakers' concerns about the growing federal deficit, and the departure next month of NASA's key ally Representative Tom DeLay (R–TX), that hope may prove illusory. And without clear direction from the science community, the missions that survive may be the ones with the strongest political allies.

In the meantime, Griffin pledges to listen more closely to scientists. He spent several hours at the advisory committee meeting answering questions and chatting informally with committee members. "I'm not the world's best communicator," he told them. But "we don't get out of bed, drive to headquarters, and try to screw the program up. … We're not out to do a Lone Ranger act." **–ANDREW LAWLER**

GLOBAL CHANGE

No Doubt About It, the World Is Warming

Global warming contrarians can cross out one of their last talking points. A report released last week* settles the debate over how the atmosphere has been warming the past 35 years. The report, the first of 21 the Bush Administration has commissioned to study lingering problems of global climate change, finds that satellite-borne instruments and thermometers at the surface now agree: The world is warming throughout the lower atmosphere, not just at the surface, about the way greenhouse climate models predict.

"The evidence continues to support a substantial human impact on global temperature increases," added the report's chief editor Thomas Karl, director of the National Climatic Data Center in Asheville, North Carolina. The additional support for global warming will not change White House policy, however. Michele St. Martin, spokesperson for the White House Council on Environmental Quality, says President George W. Bush believes that greenhouse gas emissions can be brought down through better use of energy while the understanding of climate science continues to improve.

Critics who blasted research under the White House's Climate Change Science Program (CCSP) (*Science*, 27 February 2004, p. 1269) as mere obfuscation might not have expected such a forthright conclusion from the report. Karl attributes the clarity to the CCSP approach. "For the first time, we had people [who initially disagreed] sitting down across the table. That's a tremendous advantage," he says. "The process is great for improving understanding. It led to not just synthesis but to advancing the science." The CCSP synthesis and assessment process prompted new, independent analyses that helped eliminate some long-standing differences, Karl says.

The 21 authors of the report included researchers who for years had been battling in the literature over the proper way to analyze the satellite data. Meteorologists John Christy and Roy Spencer of the University of Alabama, Huntsville, were the first to construct a long record of lower-atmosphere temperature from temperature-dependent emissions observed by Microwave Sounding Units (MSUs) flown on satellites. By the early 1990s, Christy and Spencer could see little or no significant warming of the middle of the troposphere—the lowermost layer of the atmosphere—since the beginning of the satellite record in 1979, although surface temperature had risen.

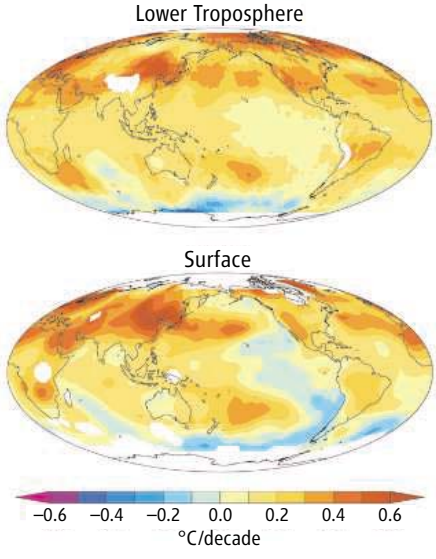

A decent match. Warming of the lower atmosphere as measured from satellites (yellows and oranges, *top*) now resembles surface warming (*bottom*) measured by thermometers.

SOURCE: NOAA

In recent years, report authors Frank Wentz of Remote Sensing Systems in Santa Rosa, California, and Konstantin Vinnikov of the University of Maryland, College Park, led separate groups analyzing the MSU data. They and others found atmospheric warming more on a par with the observed surface warming (*Science*, 7 May 2004, p. 805). Hashing out those differences over the same table "was a pretty draining experience," says Christy.

In the end, the time and effort paid off, says Karl. The report authors eventually identified several errors in earlier analyses, such as not properly allowing for a satellite's orbital drift. They had additional years of data that lengthened a relatively short record. And they could compare observations with simulations from 20 different climate models, which researchers had prepared for an upcoming international climate change assessment. The report authors found that over the 25-year satellite record, the surface and the midtroposphere each warmed roughly 0.15°C per decade averaged over the globe, give or take 0.05°C or so per decade. The tropics proved to be an exception: The models called for more warming aloft than at the surface lately, whereas most observations showed the reverse. Reconciling that discrepancy will have to wait for the next round of synthesis and assessment.

–RICHARD A. KERR

* www.climatescience.gov/Library/sap/sap1-1/finalreport/default.htm

HOT*plates*™

Patience not your virtue?
No problem!

Two-Day Plate Oligos from IDT!

Integrated DNA Technologies, inventors of *SameDay*® Oligo service, have brought the same focus on speed and service without compromise to 96-well plates. For the needs of high-throughput labs doing the most cutting-edge research, IDT now offers the HOT*plate*™. Order on our special web page today and your 96-well HOT*plate*™ ships complete tomorrow!

Only $0.18 per Base!
(expedite fee applies)

HOT*plate*™ Specifications:

- Order via the web by 2:00 P.M. ET
- Next day priority shipping!
- Normalized to 2 - 10nmoles/well or full synthesis yield
- Shipped in 300 µl V-bottom plates
- Available within the U.S. and Canada

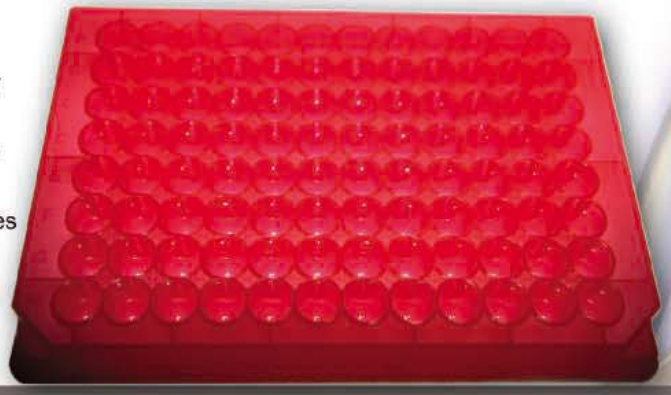

Innovation and Precision in Nucleic Acid Synthesis

www.idtdna.com **800.328.2661**

IDT
INTEGRATED DNA TECHNOLOGIES, INC.

Corporate Headquarters
Integrated DNA Technologies, Inc.
1710 Commercial Park
Coralville, IA 52241 USA

West Coast Operations
Integrated DNA Technologies, Inc.
6868 Nancy Ridge Drive
San Diego, CA 92121 USA

BSI REGISTERED
ISO 9001:2000
FM88954

INTELLECTUAL PROPERTY

Decision on NF-κB Patent Could Have Broad Implications for Biotech

In what one patent expert called a potentially "huge, huge case," a federal jury last week unanimously upheld a biotechnology patent that critics describe as exceptionally broad. If the verdict survives appeal, it could set a new precedent for the enforcement of patents on biological discoveries upstream of actual drugs.

Contrary to some predictions (*Science*, 31 March, p. 1855), on 4 May, a Boston jury ruled that Eli Lilly's osteoporosis drug Evista and sepsis drug Xigris infringed a patent held by the Massachusetts Institute of Technology (MIT), Harvard University, and the Whitehead Institute and licensed exclusively to Ariad Pharmaceuticals, a Cambridge, Massachusetts, biotech company. The jury awarded at least $65.2 million in back royalties to Ariad, which could continue collecting 2.3% of sales of the two drugs until the patent expires in 2019.

The patent covers methods for inhibiting NF-κB, a protein discovered 20 years ago at MIT by David Baltimore, now president of the California Institute of Technology in Pasadena, with help from fellow Nobel Prize winner Phillip Sharp and Harvard biologist Thomas Maniatis. (Sharp and Maniatis both testified for Ariad at the trial.) Because NF-κB, a prolific "transcription factor" that turns more than 175 other genes on and off, is so important in biology and disease—it has also been implicated in arthritis, cancer, diabetes, and stroke—the Lilly case could be the first of many involving the protein. Hundreds of compounds, including many drugs already on the market, are known to inhibit NF-κB.

It is that broad reach that has prompted debate. Ariad CEO Harvey Berger calls the patent claims "very specific" and typical for both industry and academia. "We had a very strong, crystal-clear case," he says. Law professor Arti Rai of Duke University in Durham, North Carolina, on the other hand, calls Ariad's NF-κB patent "a very broad patent." She says that an ultimate Ariad victory would herald a major change in the patent landscape, because previous decisions by the federal appeals court have led to the assumption that biotech patents must be narrow. If the Ariad patent survives appeal, "conventional wisdom gets thrown out the window," Rai says. Lilly spokesperson Philip Belt is more outspoken, calling the verdict "shockingly inconsistent with current patent law."

The patent still faces several legal hurdles. The case in Boston does not end with the jury verdict; a separate trial will be held by federal Judge Rya Zobel to decide certain legal challenges to the patent's validity and enforceability. Lilly vows to appeal last week's verdict if the judge rejects these arguments. And in late April, Amgen, a biotechnology company in Thousand Oaks, California, filed suit against Ariad to invalidate the patent and certify that its blockbuster arthritis drug Enbrel, and a second arthritis treatment, Kineret, don't infringe. Amgen spokesperson David Polk called the lawsuit "a preemptive move," because the company expected Ariad to eventually sue over Enbrel and Kineret. Berger won't comment on the Amgen claims except to say they're without merit and that licenses are available to commercial entities. (Academic scientists do not need a license, he stressed.)

CREDIT: DONNA COVENEY/MIT

High-profile witness. Nobel Prize winner Phillip Sharp, who helped discover NF-κB 2 decades ago, testified for MIT and Ariad Pharmaceuticals in the patent-infringement trial.

Berger considers the jury verdict "good for academic research, good for universities, and in the end, good for … discovering new drugs, because it speaks to important technology." But Rai sees it differently. Asked whether the verdict could hinder innovation in the drug industry, she replied: "If, as a precedent, it then led to lots of upstream players deciding that they would try to follow the lead of Ariad and try to cash in on their upstream patents, [then] yes, I think it could." **–KEN GARBER**

Ken Garber is a science writer in Ann Arbor, Michigan.

Venus Express Blues

Europe's Venus Express spacecraft, orbiting the veiled planet since 11 April, has jammed a mirror on its Planetary Fourier Spectrometer, a key instrument that looks for volcanic hot spots.

Project scientist Håkan Svedhem of the European Space Agency says the problem is "completely unrelated" to a short-lived hitch with a similar instrument on the agency's Mars Express spacecraft in 2005. "It looks like the mirror is starting to move again," says Svedhem, promising a "careful approach" to tests.

–GOVERT SCHILLING

From Lunar Hitchhiking …

NEW DELHI—After more than a year of navigating U.S. red tape, the Indian space agency and NASA have agreed that U.S. instruments will ride India's first moon mission. Concerns about both technology-sharing and security had blocked the agreement, but officials finally inked a deal earlier this week in Bangalore.

Under the pact, the Chandrayaan-I mission will carry a miniature radar to search for elusive water and a mineralogy mapper to help find helium-3 for future fusion power. NASA chief Michael Griffin, who met Indian Space Research Organization chair G. Madhavan Nair to sign the accord, hopes the launch, slated for 2008, will open a new era of Indo-U.S. space cooperation. Officials hope this summer to iron out proprietary technology agreements for future joint missions.

–PALLAVA BAGLA AND ANDREW LAWLER

… To Moon-Mulling

NASA plans to send a bevy of missions to the moon in coming years, and it has asked the National Academies' National Research Council for advice on what to do there. Among other things, NASA Science Mission Directorate Chief Scientist Paul Hertz last week told researchers that the agency wants to know what kinds of experiments could fit into a suitcase-sized box that future astronauts could deploy on the surface, similar to what Apollo astronauts left behind during their forays in the 1970s.

The work raises fears of further science budget erosion at NASA (see p. 824), and Hertz warned that "there isn't new money to do [lunar] science, but there are new opportunities." An interim version of the fast-track report is due to NASA in September, and the final report will be completed late next spring.

–ANDREW LAWLER

SCHOLARLY PUBLISHING

Bill Would Require Free Public Access to Research Papers

A proposal to require federally funded scientists to make their accepted papers freely available online within 6 months of publication has reignited a bruising battle over scientific publishing. The bill, introduced last week by senators John Cornyn (R–TX) and Joseph Lieberman (D–CT), would make mandatory a voluntary National Institutes of Health (NIH) policy and extend it to every major federal research agency, from the National Science Foundation (NSF) to the Department of Defense.

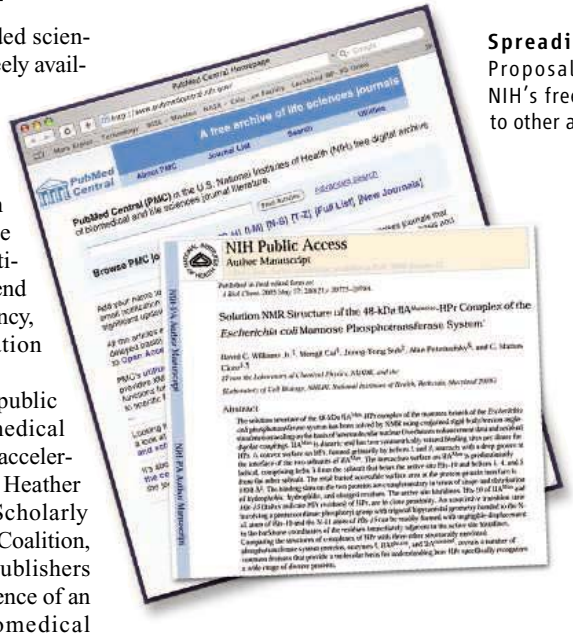

Spreading the word. Proposal would extend NIH's free archive model to other agencies.

Supporters argue that so-called public access should extend beyond biomedical research. "The ramifications for the acceleration of science are the same," says Heather Joseph, executive director of the Scholarly Publishing and Academic Resources Coalition, which represents libraries. Many publishers disagree, saying that there is no evidence of an unmet public demand for nonbiomedical papers. They warn that extending NIH's policy to other disciplines could seriously harm societies that rely on journal subscription and advertising revenues to run their organizations.

The Federal Research Public Access Act of 2006 (S.2695) follows on a 1-year-old NIH policy that asks researchers to submit accepted papers to NIH for posting in PubMed Central, NIH's full-text archive, within 12 months of publication in a journal. House and Senate appropriations committees had asked NIH to develop such a policy after patient groups argued they should have free access to biomedical studies.

The request has been ignored by most NIH grantees: A January report by NIH noted that fewer than 4% are complying. An NIH advisory committee has recommended that the policy be mandatory and that the 12-month limit be reduced to 6 months for most journals. The Cornyn-Lieberman bill would require NIH to make those changes.

But the bill also would mandate a similar plan at any U.S. agency funding at least $100 million a year in extramural research. That includes NSF, NASA, the Department of Energy, and even the Department of Transportation. The manuscripts could be posted in existing archives, such as a university server or arXiv, the physics preprint server. However, agencies would have to maintain a bibliography of all the papers they funded with links to full texts. This will give "students, researchers, and every American" access to research results, says Cornyn, which "will help accelerate science, innovation, and discovery."

Some publishers argue that there's no evidence the public is as interested in, say, high-energy physics papers as in health research. "You're just expanding this willy-nilly on the assumption that there's the same clamor," says Allan Adler, vice president for legal and governmental affairs for the Association of American Publishers. Martin Frank, executive director of the American Physiological Society, argues that if the bill became law, it could be especially damaging to "small niche area" journals in disciplines such as ecology that have not yet experimented much with open-access journals that recoup publication costs from authors rather than subscribers.

Observers don't expect the bill to be passed this year, but they anticipate a push to make the NIH policy mandatory. The 6-month deadline is also controversial: NIH Director Elias Zerhouni recently testified that he is sympathetic to publishers' desire for a 12-month delay.

In the meantime, NSF plans to add citation data to the Web-based descriptions of each award in response to a February report by its inspector general that said "other science agencies have done much more than NSF" to tell the public what it gets for its money. The report said NASA and the Defense Department already make available the full texts of some journal articles. **–JOCELYN KAISER**

CONDENSED MATTER PHYSICS

Solid Hydrogen Not So Super After All

Strike hydrogen from the list of possible "supersolids." Its conceptual cousin solid helium may flow bizarrely like a liquid with no viscosity, but solid hydrogen does *not*, say physicists who had reported that it might. "Nature has its way of having fun with us," says Moses Chan of Pennsylvania State University in State College, who alerted dozens of colleagues to the negative result this week.

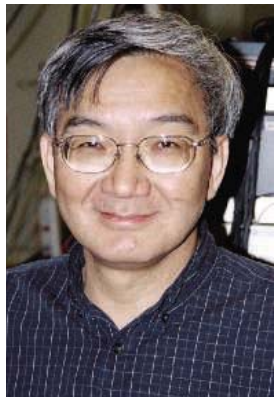

Forthright. Moses Chan e-mailed colleagues news of the negative result for hydrogen.

In 2004, Chan reported signs that a crystal of the isotope helium-4 could flow freely through itself, possibly confirming a long-hypothesized phenomenon known as supersolidity. Last year at a meeting, Chan and graduate student Anthony Clark presented data that suggested solidified molecular hydrogen flowed the same way (*Science*, 8 April 2005, p. 190). The notion was plausible because atoms of helium-4 and molecules of hydrogen are both "bosons": particles with a quantum-mechanical proclivity to bunch up.

To check the unpublished result for hydrogen, Chan and Clark ran a series of control experiments. In one, the researchers set a can full of frigid solid hydrogen twisting back and forth on the end of a thin shaft. Below a certain temperature, some of the hydrogen seemed to let go of the can and flow effortlessly through the rest of the solid, causing the frequency of twisting to increase. But when Chan and Clark blocked the path of the hypothetical flow, the frequency jump persisted. That observation suggests some other effect, such as a rearrangement of the molecules within the solid, causes the jump.

Chan deserves credit for his scientific integrity in quickly announcing the negative result, says Humphrey Maris of Brown University. "He's been completely open from the beginning," Maris says. "He certainly hasn't overstated his claims at any point."

Solid helium-4 passed both that control experiment and several others. So supersolid helium remains a tantalizing—and controversial—possibility. **–ADRIAN CHO**

CREDIT (BOTTOM): A. CHO/*SCIENCE*

U.S. SCIENCE POLICY

Senate Panel Chair Asks Why NSF Funds Social Sciences

Why is the National Science Foundation (NSF) funding a study of a women's cooperative in Bangladesh? Why are U.S. taxpayers footing the bill for efforts to understand Hungary's emerging democracy? And why are social scientists even bothering to compile an archive of state legislatures in a long-gone era when those legislators chose U.S. senators?

Senator Kay Bailey Hutchison (R–TX), chair of a panel that oversees NSF and a member of the powerful Senate Appropriations Committee, put those and other sharply worded questions to NSF Director Arden Bement last week during an unusually combative hearing on the agency's 2007 budget request. Hutchison signaled that she will be taking a hard look at NSF's $200-million-a-year social and behavioral sciences portfolio, which funds some 52% of all social science research done by U.S. academics and some 90% of the work by political scientists. Hutchison made it clear during the 2 May hearing that she doesn't think the social sciences should benefit from President George W. Bush's proposal for a 10-year doubling of NSF's budget as part of his American Competitiveness Initiative (*Science*, 17 February, p. 929). And she suggested afterward to *Science* that she's open to more drastic measures.

"I'm trying to decide whether it would be better to put political science and some other fields into another [government] department," she said. "I want NSF to be our premier agency for basic research in the sciences, mathematics, and engineering. And when we are looking at scarce resources, I think NSF should stay focused on the hard sciences."

Warning shot. Senator Kay Bailey Hutchison (R–TX) questions the value of some NSF-funded research.

CREDIT: COURTESY OF THE ALBERT & MARY LASKER FOUNDATION

Last week's hearing was not the first time Hutchison has taken a shot at NSF's support of the social sciences. In a 30 September 2005 speech honoring the winners of the annual Lasker medical research awards, she backed a doubling of NSF's budget but added that social science research "is not where we should be directing [NSF] resources at this time." Hutchison tipped her hand a few months before the hearing by asking NSF officials for abstracts of grants funded by the Directorate for Social, Behavioral, and Economic Sciences (SBE) going back several years. But the harshness of last week's attack caught the community by surprise, leaving social scientists and their supporters scratching their heads about how best to respond.

"In some ways, it's SBE that tackles the most challenging scientific questions, because its research investigates people's behavior and touches on the most sensitive issues in our society," noted Neal Lane, a physicist and former NSF director now at Rice University in Houston, Texas. "So I'm not surprised that it's been hard to articulate how it connects to innovation and improving the nation's competitiveness." Aletha Huston, a developmental psychologist at the University of Texas, Austin, who wrote a letter to Hutchison before the hearing defending NSF-funded work by herself and colleagues at UT's Population Research Center, points out that "if you want to understand how to remain competitive, you need to look at more than technology, … at the organizational and human issues that play a role."

Hutchison says she hasn't decided how to translate her concerns into legislation. One option would be to limit spending for the social sciences in the upcoming 2007 appropriations bill for NSF. Another approach would be to curtail the scope of NSF's portfolio in legislation enacting the president's competitiveness initiative or reauthorizing NSF's programs.

In the meantime, says sociologist Mark Hayward, who heads the UT population center, it would be a mistake for social scientists to ignore her concerns. "We have to be persistent and consistent in our message," says Hayward, who along with Huston hasn't heard back from Hutchison. "We can't just say, 'My goodness, she's not paying attention.' "

–JEFFREY MERVIS

Phooey on Zerhouni?

Leaders at the National Institutes of Health (NIH) are fending off new criticism of their boss, Elias Zerhouni. The kerfuffle began last month when Andrew Marks, editor-in-chief of the *Journal of Clinical Investigation*, blamed Zerhouni's "Roadmap" of trans-NIH initiatives and large clinical trials for diverting money from investigator-initiated grants. "Obviously you are not a scientist," Marks charged.

In a late April online response, all 27 directors of NIH's institutes and centers called Marks's comments a "personal attack" and a diversion from "the real issues." Marks responds that supportive e-mails show "a substantial divide" between NIH leaders and the community.

–JOCELYN KAISER

NIEHS: Doctors Wanted

The director of the National Institute of Environmental Health Sciences (NIEHS) wants his agency to get more clinical. The $641 million agency has traditionally supported research on topics as diverse as DNA repair and harmful algal blooms. But Director David Schwartz wants to boost the clinical researcher corps and focus efforts on diseases with a strong environmental component such as asthma.

Schwartz says the new focus, unveiled last week in a strategic plan, won't come at the expense of basic research: "We're not taking anything away." But observers fear Schwartz's inevitable tradeoffs. "That's what everyone will be waiting to see," says toxicologist David Eaton of the University of Washington, Seattle.

–ERIK STOKSTAD

NIH Eyes Training Support Cuts

The National Institutes of Health (NIH) wants universities to pay a greater portion of the cost of training graduate students and postdocs. NIH now pays $3000 plus 60% of the remaining tuition costs for each of the 17,000 Ph.D. students and postdocs supported through the National Research Service Award program. Under the new policy, the agency will provide 60% up to a maximum of $16,000 per year, with additional cash for health insurance and expenses.

The agency says the proposed policy, introduced this week, will save 2500 training slots that would otherwise eventually disappear if NIH's budget remains flat. Universities will "do everything we can" to bear the new cost and "avoid the loss of training slots," says Lynda Dykstra of the University of North Carolina, Chapel Hill. The comment period ends 2 June.

–YUDHIJIT BHATTACHARJEE

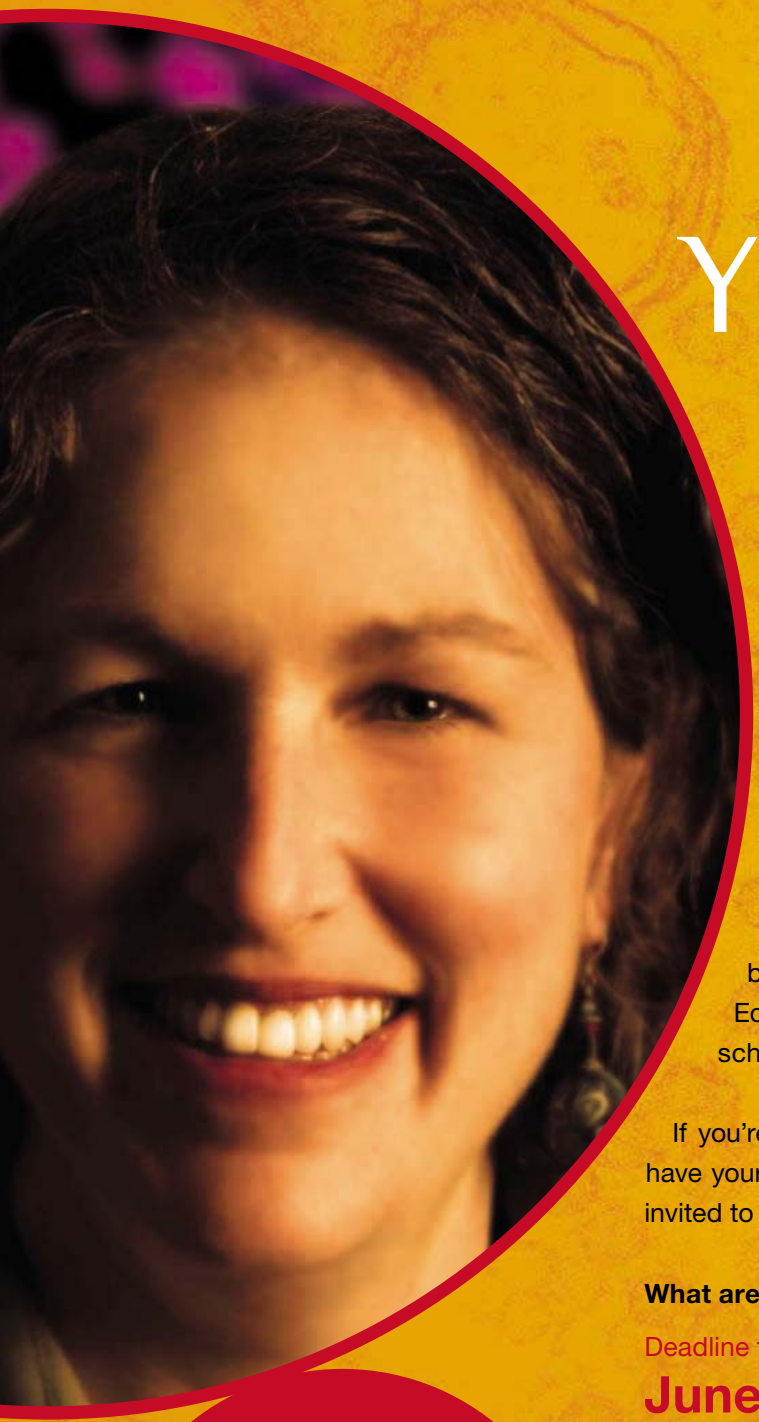

You could be next

Yes, it *can* happen to you:
If you're making inroads in neurobiology research and you've received your M.D. or Ph.D. within the last 10 years, the Eppendorf & *Science* Prize for Neurobiology has been created for YOU!

$25,000 Prize

This annual research prize recognizes accomplishments in neurobiology research based on methods of molecular and cell biology. The winner and finalists are selected by a committee of independent scientists, chaired by the Editor-in-Chief of *Science*. Past winners include post-doctoral scholars and assistant professors.

If you're selected as next year's winner, you will receive $25,000, have your work published in the prestigious journal *Science* and be invited to visit Eppendorf in Hamburg, Germany.

What are you waiting for? Enter your research for consideration!

Deadline for entries:
June 15, 2006

For more information:
www.eppendorf.com/prize
www.eppendorfscienceprize.org

"This is a unique award because it recognizes young neuroscientists for their work and their ability to communicate with a broad audience. I was surprised and honored to be a winner."

Miriam B. Goodman, Ph.D.
Assistant Professor
Stanford University
School of Medicine
2004 Winner

eppendorf & Science
PRIZE FOR NEUROBIOLOGY

CANADA

Research Budgets Are Tight Pending Science Policy Review

OTTAWA—It's an axiom of Canadian politics that new governments denounce the absence of a national science and technology (S&T) strategy, call for such a strategy to be developed, spend years creating the plan—and then get booted out of office. So why should Prime Minister Stephen Harper's new minority Conservative government be any different?

Unveiling its first budget last week since being elected in January, the Harper government put S&T relatively low on its list of fiscal priorities but said it planned to develop a new research policy based on demonstrating "value for money." In the meantime, the 2.4% increase proposed for the nation's three granting councils pales next to a 5% rise in overall government spending. The new budget, for the fiscal year that began 1 April, leaves the research councils with the unpleasant prospect of coping with a rising number of applications by chopping the number or size of awards or both, scaling back targeted programs, and at the same time, expending time and money to argue their case in the next review.

Tough times. Prime Minister Stephen Harper (*standing*) keeps a lid on Canadian research in his new budget.

The Harper government sees it differently, of course. Returned to power after a 13-year absence, Conservatives lamented the dire lack of a sound plan for investing in science and said a new national science policy should be based on determining "value for money" in the councils' grants. Officials say they have no preconceived notion of how to determine whether a research grant yields an adequate return. But Canadian Association of University Teachers Executive Director James Turk is worried that the exercise hides a "malevolent" attempt to gut basic research in favor of industrially relevant science.

The government's $210 billion budget cuts taxes while bolstering Canada's military and domestic security forces. As promised, the Conservatives have gutted climate change programs once designed to meet Canada's Kyoto Protocol commitment to reduce greenhouse gas emissions. The government says it will develop its own "made in Canada" solutions this fall.

The Canadian Institutes of Health Research (CIHR) gets a trickle-down $3.6 million a year from a 5-year, $900 million bump for "pandemic preparedness" against the avian influenza virus. The boost will supplement a tiny $15 million increase in the agency's $630 million operating budget, the same percentage increase awarded the $607 million Natural Sciences and Engineering Research Council and the $213 million Social Sciences and Humanities Research Council. CIHR President Alan Bernstein says the small rise fails to take advantage of academic investments by the previous Liberal government in more staff and the global recruitment of top scientists: "It all lands on our doorstep." Those programs will continue even if resources to fund research by those scientists are inadequate.

Still, Bernstein welcomes the S&T policy exercise. "We're not entitled to that money because of some preordained law," he says. "I think we have an obligation to demonstrate value for money." **–WAYNE KONDRO**

Wayne Kondro writes from Ottawa, Canada.

SCIENTIFIC PUBLISHING

A Call to Improve South Africa's Journals

PRETORIA, SOUTH AFRICA—In the highly competitive field of research publishing, South Africa is a giant on its continent but a dwarf in the world. A new report by the national science academy concludes that about half of the country's 255 accredited research journals have virtually no impact abroad and less than a tenth of them are even indexed on international citation lists.

The report by the Academy of Science of South Africa—a landmark as the first academy report done at the government's request—recommends that agencies tighten their accreditation of journals and take steps to make the strongest ones more influential and more accessible via the Internet. "In a developing country like South Africa which is marginalized by the 'journal power' in the United States and Europe, focusing support on journals that could be world players would make a big difference in how research is conducted and published," says the academy's executive director, biochemist Wieland Gevers, who chaired the panel that compiled the report. He expects it to trigger debate about how to make South African research more influential.

Critics say the current system, in which the education department rewards universities with subsidies based on the number of publications their researchers produce, has led to an overabundance of weak journals. To help snare these subsidies, some universities support journals that publish mainly work by their own professors that has little or no impact abroad.

Microbiologist Molapo Qhobela, chief director for higher education policy at South Africa's education department, says, "This is an important topic, and we will take the recommendations very seriously." That may include reassessing the education department's current criteria for accrediting journals, which now require that they be peer-reviewed and include contributors and editorial board members from "beyond a single institution."

Quality control. Wieland Gevers says only the best journals should get support.

Gevers says the report will be discussed at a meeting in Pretoria this week and at a series of seminars this year. "A good case can be made for robust and competitive local science publishing," Gevers says, "but we think journals should seek international indexing or develop niches that lead to recognition outside of South Africa." **–ROBERT KOENIG**

Robert Koenig is a contributing correspondent in South Africa.

CREDITS (TOP TO BOTTOM): CHRIS WATTIE/REUTERS; ACADEMY OF SCIENCE OF SOUTH AFRICA

A handful of experts have reluctantly concluded that polio may never be wiped out. They are arguing that control may be a better goal than eradication

Polio Eradication: Is It Time to Give Up?

ISAO ARITA WAS A BELIEVER. IN THE 1960s and 1970s, he was a crusader in the campaign against smallpox, the only disease ever eradicated. In 1990, he took on polio, directing the campaign that eliminated that scourge from the Western Pacific in 1997. Much of his long and distinguished career—at the World Health Organization (WHO) in Geneva, Switzerland, and the Agency for International Health in Kumanmoto, Japan—has been predicated on his faith in medicine's ability to triumph over viruses.

So it is with great seriousness that he says that he no longer believes it is feasible to wipe out polio—not in 2006, and probably not ever.

And he is not alone. Like a handful of other longtime supporters of eradication, Arita has begun to go public with his doubts. On page 852, he and his colleagues write that the 18-year, $4 billion campaign has brought enormous public good, reducing polio cases from 350,000 in 1988 to just shy of 2000 in 2005. But the old adage about the last few percent being the hardest is coming true in spades.

Since polio exploded out of Nigeria in 2003, the virus has reinfected some 18 previously polio-free countries, many of them unforgiving, conflict-torn places such as Sudan and Somalia, where it is simply too dangerous to send in health workers. And despite "heroic" efforts to achieve the highest vaccination rates ever, the virus is hanging on in the slums of India and has seeded outbreaks in four countries, most recently Bangladesh. Nor does the virus show signs of budging from the shared reservoir between Pakistan and Afghanistan.

"However diligent they are, however much the staff does its best, there are very serious obstacles that militate against eradicating polio," agrees Donald A. Henderson, the outspoken director of the earlier smallpox program and one of the few to question the feasibility of polio eradication from the start.

The skeptics, who include not only Henderson and Arita but also polio experts such as Konstantin Chumakov of the U.S. Food and Drug Administration and Vadim Agol of the Russian Academy of Medical Science's Chumakov Institute for Poliomyelitis (named after Konstantin's father), worry that the campaign is deluding itself and the world with its "ever-receding" deadline—originally 2000 and now reset at 2006. Says Henderson, who is now at the University of Pittsburgh's Center for Biosecurity in Baltimore, Maryland: "It is always 12 or 18 months away from where we are." And they contend that the program leaders are not paying sufficient attention to policies needed to control, rather than eradicate, polio over the long term—which would be a major accomplishment in its own right.

True, the case count looks bad, concedes David Heymann, another smallpox veteran who in 2002 was brought in to head the multiagency polio effort, headquartered at WHO. Global cases were higher in 2005 than in any year since 1999, and 2006 is shaping up to be even worse in Nigeria and India. But surveillance is also more sensitive, which could explain some of the increases, he says. He insists that overall, the campaign is racking up solid victories. Of the 22 countries reinfected with polio since 2003, outbreaks have been dramatically curtailed in all but nine. And the number of endemic countries—where transmission has never stopped—is down to four, an all-time low, he contends. Heymann, who runs the program with Bruce Aylward of WHO, extols the benefits of an improved, more targeted version of the oral polio vaccine. He and Aylward cite the enthusiasm and commitment of donors such as Rotary International, the G8, and the Gates Foundation—and of the polio-affected countries themselves. And they maintain that it is feasible to stop transmission of wild poliovirus in 2006 everywhere except Nigeria, which may take another year and a half, and perhaps one corner of India.

But optimism is no substitute for a contingency plan, counter the skeptics. And so the debate continues—respectful, increasingly public, and with no sign of resolution.

A reasonable target

Even now, most agree that the 1988 decision to eradicate polio made scientific sense. After all,

CREDIT: CHRIS HONDROS/GETTY IMAGES

Stepping up. The Nigerian government is recommitted to eradicating polio, but the virus is still circulating out of control in the north.

Polio warriors. David Heymann (*left*) and Bruce Aylward, who run the global campaign, are unwavering in their belief that polio can be eradicated.

the world had eradicated smallpox, and there seemed to be no overwhelming scientific obstacles to wiping out polio as well. The virus is spread from human to human, which means there's no chance of it lurking in an animal reservoir. As with smallpox, there was an effective vaccine—two, in fact: the live oral Sabin polio vaccine (OPV) and the inactivated Salk polio vaccine (IPV). The World Health Assembly endorsed the concept in 1988, setting the world on a course to wipe out polio by 2000 and then, once the threat of the virus's return was deemed negligible, to stop all control measures, as had occurred with smallpox.

It soon became clear, however, that polio would be even tougher to eradicate than smallpox, which Henderson has said was eradicated "just barely," with a lot of luck. With smallpox, there was no question who was infected, as everyone developed a telltale rash. Polio, by contrast, circulates "invisibly," causing paralysis in just one in every 100 to 200 people infected. Polio is caused by an enterovirus that replicates in the gut before sometimes invading the nervous system; it is excreted in the stool and predominantly spread by fecal-oral contamination.

And although the Sabin OPV adopted for the mass campaign proved very effective—it contains a live, attenuated virus that is also excreted in stool and thus confers immunity on people not directly vaccinated—it has decided drawbacks. The smallpox vaccine usually worked with just one shot, recalls Henderson: "The take rate was 95% to 98%, consistently, with one dose." But with OPV, "you need five, six, seven doses to be protected."

Other serious downsides have come to light. A cluster of polio cases in Hispaniola in 2000–'01 confirmed that the virus used in the Sabin vaccine can, in rare instances, regain its ability to circulate and trigger an outbreak. Scientists also discovered by chance that some immune-compromised people can shed virus for years—without showing any symptoms—and that the virus can be extremely virulent. "One man in England excreted virus for 20 years," says Henderson. Given those dangers, the global campaign advocates that OPV use be discontinued when and if transmission of the wild virus is halted.

Still, it proved relatively easy to stamp out the disease in the United States and other countries with good hygiene and good health care systems. Developing nations were tougher, as the virus thrives in crowded, unsanitary environments (*Science*, 26 March 2004, p. 1960). In Latin America in the 1980s, the Pan American Health Organization fine-tuned the mass vaccination strategy known as National Immunization Days, during which volunteer vaccinators fan out across the country to deliver polio drops to every child under age 5. By repeating campaigns several times a year and aggressively mopping up after any outbreak, the reasoning went, countries could boost immunity enough to knock out the virus. The last indigenous case in the Americas occurred 1991. Next was the Western Pacific region, where Arita led the effort, which interrupted transmission in 1997, followed by Europe in 1999.

In the process, almost inadvertently, the campaign knocked out one of the three serotypes of wild poliovirus—type 2—which has not been seen since 1999. "That is a big achievement," says Eckard Wimmer, a virologist at Stony Brook University in New York. Since then, circulation of type 3 has also been considerably curtailed. It is now confined to small areas of four countries, albeit tough ones, given their crowding and poverty: India, Pakistan, Afghanistan, and Nigeria. The polio-eradication team now thinks a sequential strategy, using new "monovalent" vaccines targeted against specific serotypes (*Science*, 28 October 2005, p. 625), might do the trick. "We want to get rid of type 1 first, then type 3," explains Heymann.

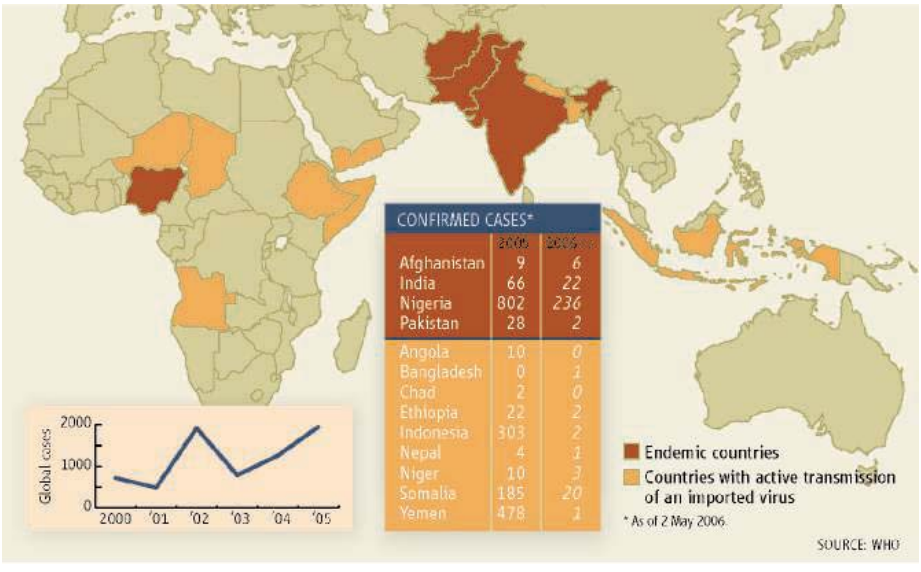

One step forward. The number of polio cases dropped from 350,000 in 1988 to a low of about 500 in 2001. But a 2002 outbreak in India, followed by a disastrous setback in Nigeria in 2003–'04, has sent cases climbing.

CREDIT (TOP): P. VIROT/WHO

Meltdown in Nigeria

Social and political problems are, however, overwhelming the campaign's scientific strategy, the skeptics point out. Take the case of Nigeria, the most populous country in Africa, and one with an abysmal health care system. (Only about 13% of Nigerian children are routinely vaccinated against childhood diseases.)

In mid-2003, amid allegations that the polio vaccine was contaminated with the AIDS virus or tainted with hormones designed to sterilize Muslim girls, several states in the northern part of the country halted polio vaccination. The virus, which was already circulating in the region, found fertile ground in the growing number of unimmunized children. By the end of 2004, the number of known cases had doubled to about 800, and the virus quickly spread across Nigeria's porous borders, taking root wherever it encountered a susceptible population (see map, left).

Although Nigeria resumed vaccination about a year later, after intense lobbying and repeated tests to confirm the vaccine's safety, the virus still rages out of control. Nigeria poses

a "grave threat" to the world, says Heymann. Recent analyses suggest that in five northern states, the immunization campaigns are missing more than 40% of children, and incidence is four times higher than at the same time last year. "With such high levels of transmission, … an additional 12 to 18 months of intensive activities may be required to interrupt polio," a 1 May update from the eradication campaign warned.

Outside Nigeria, the major problem is not so much opposition, although vaccinators still encounter it, as access. "In the Congo, between one-third and one-half [of the country] is just not accessible. You have roaming soldiers, lots of fighting in the eastern third, and it's a huge area," says Henderson. "Similarly, for Côte d'Ivoire, Angola, Afghanistan near Kandahar, … it is not possible to work there."

"Security is a big issue," concedes Heymann. Although the number of reported cases there is low, poliovirus remains entrenched in a corridor between Pakistan and Afghanistan. "The virus keeps going back and forth" between the two countries, notes Heymann, not far from where U.S. forces continue to hunt for Osama bin Laden. "Our external monitors can't get in."

Another "great risk" is Somalia, where the virus resurfaced around Mogadishu in July 2005. According to genetic sleuths at the U.S. Centers for Disease Control and Prevention in Atlanta, Georgia, one of the partner agencies in the campaign along with UNICEF and Rotary International, the virus came to Somalia from Nigeria, by way of Yemen.

Meanwhile, experience in India is suggesting that in some circumstances the virus can survive even saturation campaigns. Vaccination coverage in India has never been higher, says Heymann, who notes that the country is "pounding it," conducting nine huge campaigns last year and three already this year, to the tune of $120 million. And for the past year, vaccinators have been supplementing the standard trivalent OPV with monovalent vaccine against type 1 and, more recently, type 3.

But still, cases are being reported in Uttar Pradesh and Bihar, areas of wrenching poverty. Monitoring has confirmed that vaccinators are reaching most children; many are getting six or seven doses of vaccine a year. Epidemiologists suspect that one reason the vaccine isn't working is that the children are infected with other enteroviruses that compete with the vaccine in the gut. And because many childern have chronic diarrhea, the vaccine simply doesn't stay in the body long enough to provide sufficient immunity.

"Some pockets [of transmission] are damn near impossible," says Ellie Ehrenfeld, a polio expert at the U.S. National Institutes of Health in Bethesda, Maryland, who also advises WHO on its program. "We really don't understand why mop-ups don't knock out the virus in these areas."

House calls. Going door-to-door to deliver polio drops, as this vaccination team is doing, isn't feasible in a corridor between Afghanistan and Pakistan, where the virus is entrenched.

Meeting in Delhi in early May, India's expert advisory group decided to pound the virus even harder with monthly vaccination campaigns in the worst-afflicted parts of Uttar Pradesh and Bihar. Health workers in Uttar Pradesh will also test the feasibility of delivering a dose of OPV to all newborns in the most resilient areas of transmission within 72 hours of birth—before they become infected with competing viruses—to see whether that boosts seroconversion rates.

Redefining success

In light of these setbacks, as well as disconcerting evidence that the virus can circulate undetected even longer than people feared, prospects for stopping transmission seem grim indeed, say the skeptics. Henderson notes that last year in Sudan, surveillance turned up a strain that had been circulating silently for 5 years—while the country was labeled "polio-free." No one is ready to say emphatically that eradication is impossible, but Arita and his colleagues write that the goal is "unlikely to be achieved."

"I have no way to predict what will happen in the next 5 years, but I don't think polio will disappear," says Wimmer.

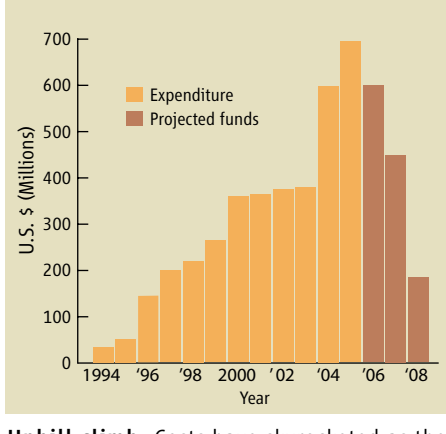

Uphill climb. Costs have skyrocketed as the polio eradication initiative has had to fight near-simultaneous outbreaks in multiple countries.

Ehrenfeld has become increasingly worried in the past few years but says she is not ready to abandon all hope. "At what point do you say we are going to give up on polio? I don't know," she asks. "Maybe these problems can be solved," she adds, noting that there was a "fair amount of progress this past year. … But it would take a very long time, much longer than anyone now expects. … And the world is tired."

And since the 2000 deadline has passed, costs have skyrocketed. It's "mind-boggling" what these massive mop-ups are costing, Ehrenfeld says. The global initiative spent almost $700 million in 2005, nearly double what it spent in 2000, and up from $600 million in 2004. One reason the world bought into the huge eradication program in the first place was the promise of money to be saved by stopping vaccination, Ehrenfeld notes—a prospect that looks increasingly unlikely. Several of the skeptics suggest that some of the vast amounts of money and energy going toward wiping out every last case of polio might be better spent increasing routine immunization against all vaccine-preventable diseases.

Unfortunately, says Chumakov, there seems to be no inclination among the program leadership to reassess whether an eradication campaign still makes sense. They "press on as if nothing had happened, as if it were 1988," says Chumakov, who calls them "captives of their own advertising. … Every year is the final one. This can't continue forever." He adds that the program should be proud of what it has achieved, and the world should "declare victory now."

In his Policy Forum in this issue, Arita urges that the reassessment begin. "The time has come for the global strategy for polio to be shifted from eradication to effective control," he writes. Henderson agrees. "Let's create a program to keep it [polio] under moderate control and say that is the best we can do."

The experts differ, however, on what, exactly, such a control strategy would consist of

CREDITS (TOP TO BOTTOM): SHAH MARAI/AFP/GETTY IMAGES; SOURCE: POLIOERADICATION.ORG

and even which vaccine—OPV, the more expensive inactivated vaccine used in wealthy countries, or a still-to-be-invented one—should be used. But any scenario, they agree, involves incorporating polio vaccine into routine immunization—which would need to be strengthened considerably and augmented with one or several special immunization weeks a year to keep up immunity. And vaccination would need to continue indefinitely, they agree. Arita and colleagues recommend continuing emergency campaigns with OPV until global cases drop below 500 and the number of nations with polio drops below 10 and then switching to a control strategy. Which vaccine to use would be reassessed in 2015.

Even if transmission of wild poliovirus could be stopped, vaccination will still be needed, adds Chumakov. One problem, as Henderson points out, is the difficulty of ever knowing for sure that the virus is gone. What's more, if immunization ceased, the world's population would soon become profoundly vulnerable to a reintroduced poliovirus, whatever its origins—whether a vaccine-derived strain, or one that escaped from a vaccine manufacturing plant, or a synthetic version released by a terrorist.

The risks are well understood and are manageable, responds Heymann. He adds that policies on whether to vaccinate posteradication are still wide open to debate, which he welcomes, noting that both Henderson and Arita were his bosses in the earlier smallpox campaign. "Nothing is cast in stone," Heymann says.

As for stopping transmission of wild poliovirus, there is no question. "We have to finish," he insists. "It would be injurious to the world's population and to its $4 billion investment to throw up our hands and say we are going back to routine immunization. … As long as the partners and countries are willing to make the effort, it is not for Isao [Arita] or me to say that eradication is not feasible."

And although it would be wonderful if polio could be controlled through routine immunization, as Arita and others propose, Heymann argues that it's simply not feasible. To keep polio in check, routine coverage would have to be maintained at consistently high levels—90% if IPV were used—and many parts of the world are not even close to achieving that. "If we had 90% or greater coverage, polio would probably have disappeared on its own," says Heymann.

Meanwhile, Heymann and his colleagues say they have an eradication program to run, and things are looking up. Not only are most countries committed and making progress, but "there are a whole series of things we are doing to improve" as well. For instance, the program is supporting development of a rapid diagnostic test that would enable countries to respond to outbreaks much more quickly. The state of Uttar Pradesh, India, will be testing a birth dose to see whether it boosts immunity. On the political front, Heymann just came back from Kabul, where the Afghani president reiterated his support, and the United Nations' Kofi Annan is committed to helping with security.

"As long as there are things we haven't tried, the polio team remains optimistic."

–LESLIE ROBERTS

CREDIT: CHRIS HONDROS/GETTY IMAGES

SCIENTIFIC PUBLISHING

A Cure for the Common Trial

A new journal aims to alleviate bias in clinical trials reporting, but some question whether it's the remedy the field needs

On the excitement spectrum, results from the LOTIS trial rank right alongside "New soil fungus identified." In the study, a Dutch team takes 402 85-year-olds and gives half access to an occupational therapist, who teaches them how to use walkers and apply for household help. The point is to see whether such interventions slow the onset of age-related disabilities. They do not.

Ordinarily, a study with negative results like this wouldn't see the light of day in a medical journal—at least not a top-tier one. But the Public Library of Science (*PLoS*) aims to be different. It's using the LOTIS study to launch its new journal, *PLoS Clinical Trials*, which begins publishing on 19 May.

The journal's credo is simple: Disappointing results can still be good news. Its editors have explicitly stated that all clinical trials submitted—regardless of outcome or significance—will be published, as long as they are methodologically sound. The policy takes aim at a pervasive problem in the clinical trials literature: a heavy skew toward studies with positive outcomes. Some say there's a "black hole" where studies with negative or ambiguous outcomes should be.

This bias can cost lives. In a particularly lethal example, a 1980 clinical trial that indicated that a prophylactic heart attack drug did more harm than good went unpublished because the drug was abandoned. Thirteen years later, the researchers involved in the trial published the study to illustrate the warning it might have provided: Estimates suggest that—in the intervening years—hundreds of thousands of people may have died prematurely from effects associated with this class of drugs, known as antiarrhythmics. More recently, industry-sponsored trials of Paxil and Vioxx have also highlighted the dangers of not reporting negative results (*Science*, 14 January 2005, p. 196).

"Science has been letting the public down very badly by not getting to grips with this problem," says Iain Chalmers, a clinical trials expert and editor of the James Lind Library in Oxford, U.K. "*PLoS Clinical Trials* is sending a message that it won't contribute to this bias." Still, Chalmers and others wonder how effective such "catch-all" journals can be—especially given that much of the bias seems to be coming from the authors. And some worry that flooding the literature with negative or ambiguous studies could itself do more harm than good.

Leveling the field

The *PLoS Clinical Trials* philosophy is hardly unique. Several medical journals, including *The New England Journal of Medicine* (*NEJM*)

ExoSAP-IT:

1 less step in PCR clean up.

1 step closer to discovery.

No Sample Loss with ExoSAP-IT®

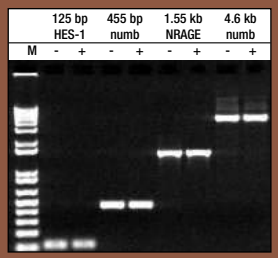

Untreated (-) and ExoSAP-IT treated (+) PCR products were analyzed by gel electrophoresis. A variety of PCR products of different lengths may be treated with ExoSAP-IT, with no sample loss.

At USB, we know the pursuit of discovery can be a time-consuming proposition. For PCR clean up, speeding up the process means ExoSAP-IT.® This unique reagent can treat PCR products in a single step, enzymatically, to remove excess primers and nucleotides. And it does it without columns. Without expensive purification plates. And most importantly, without sample loss. ExoSAP-IT is perfect for working with small sample quantities by hand or high-throughput quantities with robotics. And it can be customized to meet your precise automated specs. All to give you 100% recovery, 100% of the time. With ExoSAP-IT, you'll agree that eliminating a step is a huge step in the right direction.

usb
Fueling Innovation

For more information on ExoSAP-IT®
call 800.321.9322 or visit www.usbweb.com/exosapit

and *The Journal of the American Medical Association* (*JAMA*), claim to place a high priority on methodology.

But even the big guys admit to factoring in issues beyond study design. "Our editors are looking for research that is important" and "defines new treatments or resolves major controversies," says *NEJM* spokesperson Karen Pederson. And in meetings at which *JAMA* editors debated the merits of manuscripts, editors have frequently mentioned "journalistic goals" such as "readership needs and timeliness," according to an on-site analysis by Kay Dickersin, director of the Center for Clinical Trials at Johns Hopkins University in Baltimore, Maryland.

Such standards may give pause to authors of trials with negative or ambiguous results. Reluctance to submit such papers is a huge problem, says Kirby Lee, a clinical trials expert at the University of California, San Francisco (UCSF); it's one of the biggest drivers of publication bias. In a preliminary report presented last September at the Fifth International Congress on Peer Review and Biomedical Publication in Chicago, Illinois, Lee and UCSF colleague Lisa Bero showed that only 13% of manuscripts submitted to major biomedical journals contained ambiguous outcomes. Although these trials may not seem important on their own, they help scientists design better future trials and can be vital when combined with similar trials in so-called meta-analyses, which help determine a drug's safety or efficacy.

Getting ambiguous or negative trials into the literature can also prevent needless and potentially harmful duplicate studies. In the early 1980s, researchers at the National Cancer Institute in Bethesda, Maryland, showed that retinoic acid could turn acute myeloid leukemia (AML) cells into normal cells. Soon after, many doctors apparently began testing the acne drug Accutane—then the only clinically available form of retinoic acid—on their AML patients. The treatment didn't work, but no one reported that. Toward the end of the decade, a Chinese clinical trial showed that only a particular isomer of retinoic acid had the effect. In the interim, patients were exposed to unnecessary side effects, and alternative treatment routes were not pursued as vigorously as they might have been.

Industry suppression of unfavorable results likely plays some role in author bias, says Lee, but a lot of it comes down to human nature. "Authors don't think their studies are important, or they think editors won't be interested," he says, so they don't take the time to write them up. As a result, adds Dickersin, only about half of the studies that should be published actually are.

PLoS Clinical Trials could change that. Other journals say they are interested in methodology, but "it's a defining part of what *PLoS Clinical Trials* is," says Dickersin, who also sits on the journal's advisory board. "The editors don't care if something's hot or not." The approach "removes uncertainty on the author's end," says *PLoS Clinical Trials* publication manager Emma Veitch. And *PLoS*'s open-access policy, which makes all of the papers freely available online at the time of publication (authors pay a negotiable $2500 fee upon acceptance), assures investigators that their research will reach a much wider audience than it would at a specialty journal, she says. A number of manuscripts are coming in: "We're getting a good mix of all types of trials," says Veitch.

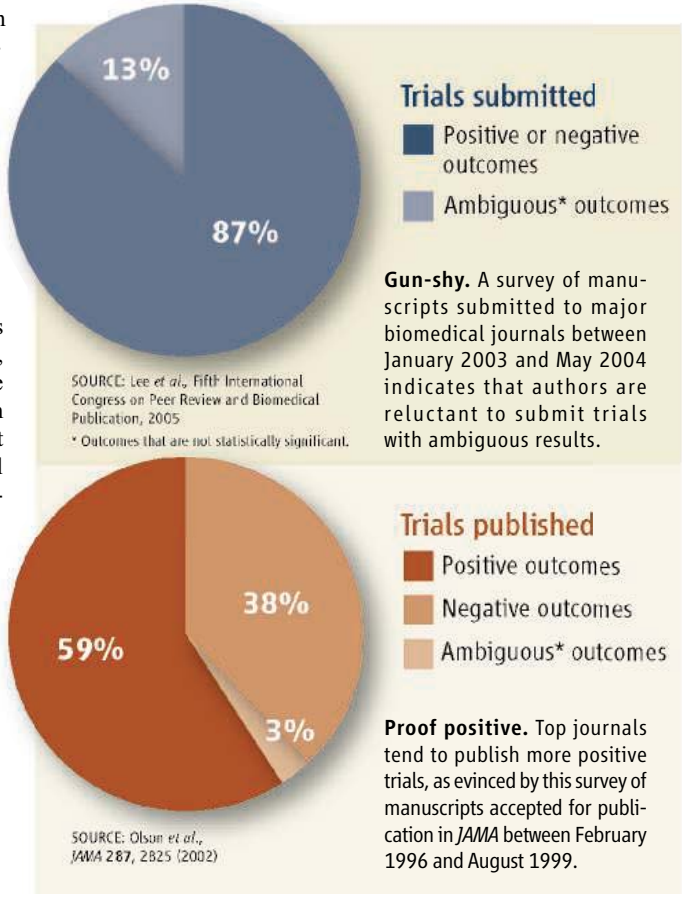

No panacea

But will getting more of these negative and ambiguous trials into the literature really address the bias problem? "Journals can help encourage the right atmosphere," says the James Lind Library's Chalmers, "but the fundamental problem is with the scientists themselves." If authors don't want to be associated with a negative trial, he says, they're still not going to submit their work. And, most say, the strategy is unlikely to stop drug companies from sitting on negative results.

The real change, says Chalmers, has to come from within the scientific community. It is "scientifically and ethically unacceptable to invite people to participate in these studies and then not publish the results," he says. The fact that medical societies have not stated this, he thinks, is "disgraceful."

Other experts worry that inundating the literature with negative and ambiguous studies could compromise patient care. "Physicians and the public rely on top-tier journals to filter out studies that are not easily interpretable or that may be misleading," says Celia Fisher, director of the Center for Ethics Education at Fordham University in New York City. "Having access to these studies could cause patients to go off medications that could be helpful" or vice versa, she says.

Publishing such trials could also hurt a journal—by marginalizing it—says Marcia Angell, a senior lecturer in social medicine at Harvard Medical School in Boston and former editor-in-chief of *NEJM*. "It sounds like a recipe for a lot of 'so-what' studies," she says, "and who wants to read a study that says the world is not flat?" UCSF's Lee agrees that readership needs to be a concern for *PLoS Clinical Trials* and any other journal that publishes such a wide range of results. "A journal that doesn't appeal to its readers won't survive," he says. That may explain the demise of a similar online journal, *Current Clinical Trials*, which began publishing in 1992 but eventually went defunct. Nevertheless, Lee is optimistic about *PLoS Clinical Trials*. "It's a great idea," he says, "and it could change the way clinical trials are published."

Robert Califf, director of the Duke Clinical Research Institute in Durham, North Carolina, believes that the new journal will encourage more authors to submit their trials, "although, personally, I'd probably try a few specialty journals before I went to *PLoS Clinical Trials*," says Califf, because the work would be more likely to reach those in his field. "Putting everything online is a good idea," he says, "but not everyone knows how to use Google." Still, he says, "if the new journal catches on, it's the right way to do things."

–DAVID GRIMM

Play it cool. Controlling emotion is crucial in many social situations—so how does the brain do it?

MEETING: COGNITIVE NEUROSCIENCE SOCIETY

Probing the Social Brain

By scanning activity within the skull, researchers are trying to understand how our brains manage interactions with other people

SAN FRANCISCO, CALIFORNIA—Whether or not we admit it, we are all armchair psychologists. Every day we analyze the behavior of friends and colleagues, trying to infer their motivations, intentions, and emotions. We even analyze ourselves. Neuroscientists are no different, except that they have access to expensive brain-scanning machines, which give them an advantage in figuring out what's going on inside someone's head.

For the first time, this year's meeting of the Cognitive Neuroscience Society (held here 9 to 12 April) included two symposia devoted to social and affective neuroscience, related fields that investigate how the human brain handles everyday situations such as figuring out what's on someone else's mind or controlling one's own emotions in dealings with other people. The presentations highlighted the excitement as well as some of the growing pains of this active area of research.

Thinking of you

Christian Keysers of the University of Groningen in the Netherlands reported new work on the neural basis of empathy. In recent years, Keysers and others have described how the brain engages in "mirror" activity that reflects the actions and experiences we see in those around us. For example, if someone sees another person grab a piece of fruit lying on a table, the region of her brain that would prepare her own arm to reach for the fruit becomes active. This happens not only when we observe actions; brain imaging studies have revealed that the brain engages in analogous mirror activity when we observe sensations and emotions as well, leading to the hypothesis that mirror activity is part of the neural mechanism that creates empathy (*Science*, 13 May 2005, p. 945).

> **"It's one of the more exciting areas** ... for understanding individual differences and psychopathology."
>
> —Cameron Carter, UC Davis

In their new study, Keysers and his grad student Valeria Gazzola investigated whether hearing rather than seeing a human action elicits mirror activity. Inside a functional magnetic resonance imaging (fMRI) scanner, 16 volunteers listened to various sounds—some associated with mouth movements, such as gargling or spitting; some associated with hand movements, such as pouring a fizzy soda into a glass; and others not caused by human activity, such as a dripping faucet. Sounds made by the mouth or hand activated brain regions involved in planning movements, including the premotor cortex, whereas environmental sounds such as the dripping faucet did not, Keysers reported. Moreover, mouth sounds activated a different region of the premotor cortex than did hand sounds. The response is very specific, Keysers says: Hearing an action activates the same brain areas that would be involved in planning that action.

The auditory-evoked mirror activity was most pronounced on the left side of the brain, where language circuitry is concentrated. This fits nicely with theories linking mirror activity to the evolution of human language, Keysers says. Other researchers have proposed that mirror activity enabled early humans to communicate by imitating each other's gestures (*Science*, 27 February 2004, p. 1316). In this view, gestures preceded vocal communication. But the new work suggests to Keysers that speech could have evolved directly from vocal imitation, aided by mirror activity in the left side of the brain.

Keysers and Gazzola also found that people who scored higher on a questionnaire that assessed their empathetic tendencies had more mirror activity. "The people who reported in everyday life that they consider the perspective of other people were the ones whose mirror systems were most active when hearing sounds made by other people," Keysers says.

"The mirror data are fantastic," says Jason Mitchell, a cognitive neuroscientist at Harvard University. But Mitchell doesn't think this is the only mechanism at the brain's disposal for reading other people's minds. "It's almost certainly part of it, but there are things we can do that the mirror system can't handle." For instance, Mitchell says, "we're really good at inferring the mental state of a character in a novel, but it's a real stretch to imagine how the mirror system could do that because it doesn't have any [firsthand] information about the person."

Other studies have shown that this sort of inference—in which no human activity has been observed—involves the medial prefrontal cortex (mPFC), Mitchell notes. In a talk at the conference, he presented new findings from his lab that suggest an intriguing refinement: People seem to use one region of mPFC to consider the mental state of someone they perceive as similar to themselves and another region of mPFC to consider someone perceived as dissimilar.

Mitchell and colleagues introduced 15 volunteers—all undergraduate or graduate students from the Boston area—to two hypothetical students by showing them photographs and short descriptions supposedly representing the students' profiles on an Internet dating site. One hypothetical student described his politics as "left of center" and said he "still can't believe Bush got reelected." The other described himself as a fundamentalist Christian and "strong supporter of the Republican Party."

The researchers then used a reaction-time test to assess which of the two hypothetical students the volunteers deemed more similar

CREDIT: JOSEPH E. LEVINE/PARAMOUNT/THE KOBAL COLLECTION

to themselves. The reaction-time test, which required students to match the faces of the two students with pronouns—such as "I" or "they"—by pressing computer keys, is more reliable than simply asking people about their preferences because it's harder to fake, Mitchell says. (In liberal Cambridge, for example, a conservative might find it socially expedient to apply a leftward adjustment to his answers.)

Their true allegiances revealed, the volunteers then slid into an fMRI scanner and answered yes-or-no questions about themselves and the hypothetical students. The questions required the volunteers to consider the mental state of the person in question, asking, for example, "Would Student #1 worry about getting a summer job?" or "Would Student #2 get upset waiting in traffic?" When volunteers thought about their own mental states in these situations, a region of ventral mPFC became active. The same area revved up when volunteers put themselves in the shoes of the student they viewed as similar to themselves. However, when volunteers considered the mental state of the dissimilar student, a nearby region, dorsal mPFC, lit up in the scans. The study will appear in the 18 May issue of *Neuron*.

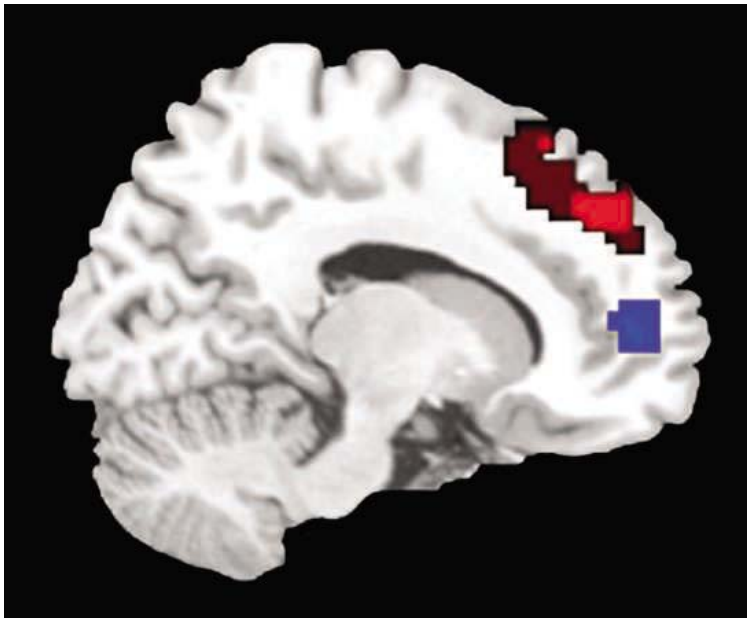

Division of labor. Different regions of prefrontal cortex fire up when people ponder the mental states of others perceived as similar (blue) or dissimilar (red) to themselves.

CREDIT: JASON MITCHELL/HARVARD UNIVERSITY

Keysers says Mitchell's findings may provide a bridge between two traditionally opposed hypotheses about how we infer the mental states of others: simulation theory and theory of mind. Simulation theory holds that we use our own experience to infer the experience of others. Mirror activity in the brain is often held up as an example of simulation theory in action. In contrast, theory of mind holds that we use abstract rules about how people behave to infer the mental states of others. The activity in dorsal mPFC seems to represent this second kind of cognition, Keysers says, but the activity in ventral mPFC seems to represent aspects of both simulation theory and theory of mind: It's abstract thought because the person under consideration isn't actually present, yet it taps into the same brain circuitry used for self-reflection. Rather than being mutually exclusive, simulation theory and theory of mind may turn out to be "two processes we can mix together," Keysers says.

Getting a grip on emotions

Reading the minds of invisible strangers isn't the only talent neuroscientists have attributed to the prefrontal cortex, a sizable swath of tissue just behind the forehead that has expanded greatly in the course of mammalian evolution. In humans, the area also appears to have much to do with personality, planning for the future, and keeping a lid on inappropriate thoughts, behaviors, and emotions—another common focus of research presented at the meeting.

Several recent studies have investigated the role of the prefrontal cortex in keeping emotions in check in social situations. In 2003, for example, Naomi Eisenberger and Matthew Lieberman of the University of California (UC), Los Angeles, and Kipling Williams of Macquarie University in Sydney, Australia, described findings suggesting that the right ventrolateral prefrontal cortex (RVLPFC) dampens the feeling of social rejection people experience when their character is shunned by other characters in a video game (*Science*, 10 October 2003, p. 290). Subjects who reported feeling less rejection showed more RVLPFC activity and less activity in the amygdala, a part of the brain whose activity reflects emotional arousal.

At the conference, Lieberman presented new work that suggests the RVLPFC region helps keep emotions in check during another type of social interaction. Lieberman and colleagues adapted a version of the "ultimatum game" used in behavioral economics. In each round, two players are told that they will split a sum of money; Player 1 decides what share to give Player 2, whose only options are to take it or leave it. The researchers scanned the brains of volunteers playing the part of Player 2 as they played one round each against what they were told were 70 different Player 1s (all of whom were actually a computer programmed to share between 5% and 50% of the total stake).

The most interesting situations, Lieberman says, are those in which the volunteer is offered a decent sum of cash that's a low percentage of the total stake. The rational thing to do is to take the money, but many people will reject an offer they deem to be insultingly low. From the brain scans, the best way to predict whether a volunteer would take an unfair offer was the amount of activation of RVLPFC. "The more they activate this area, the more likely they are to say 'Forget the insult, I'll take the money,' " Lieberman says.

Lieberman has found that the amount of RVLPFC activity in people playing the game is inversely proportional to activity in the insula, a brain region that has been linked to the perception of disgust. Although he concedes that such correlations don't prove that RVLPFC directly suppresses activity in the insula or amygdala, he says that's his working hypothesis: "What RVLPFC does well is it disengages us from our immediate responses … [and] allows higher cognitive abilities to guide thought and behavior without interference from emotional processes." Lieberman is now investigating whether RVLPFC activity is abnormal in people with anxiety disorders and whether activity in this brain region changes in people undergoing therapy.

The work is an interesting attempt to examine how people respond in a situation similar to what they might face in everyday life, says Jennifer Beer of UC Davis. Yet Beer says she's not convinced the RVLPFC activity in Lieberman's experiment represents emotional regulation per se. "In the ultimatum task, there's probably a lot of things going on when you're dealing with fair and unfair offers, not just [regulating] emotion," she says. RVLPFC activity could represent some more general cognitive process related to decision-making or response selection, Beer says.

Determining whether particular brain regions and patterns of activity are uniquely dedicated to social or emotional cognition is a major challenge for the field, says Cameron Carter of UC Davis. "This new area doesn't quite have the theoretical or methodological rigor of more traditional cognitive neuroscience" research on memory and attention, which scientists have probed with fMRI since the early 1990s, Carter says. But the field will improve as it matures, he adds: "It's one of the more exciting areas, and it's important for understanding individual differences and psychopathology."

–GREG MILLER

A Hawaiian Upstart Prepares to Monitor the Starry Heavens

Astronomers anticipate the debut of Pan-STARRS, a telescope that promises sweeping views of the nearby and distant universe

The night sky is wide and unfathomably deep, but some insatiable astronomers want to plumb everything in it. In their dream project, an all-seeing camera would film the sky with as much detail as the images from today's best telescopes. But big telescopes have tunnel vision, so they need years to assemble such a view of the heavens. And whereas smaller mirrors can take in broad chunks of the sky, faint objects elude their sight.

Now, atop a dormant Hawaiian volcano, a nimble machine that combines the best of both worlds is taking shape: the Panoramic Survey Telescope and Rapid Response System, or Pan-STARRS. The 1.8-meter telescope will use the biggest astronomical camera ever built, equipped with a novel electronic system for correcting the distortion caused by Earth's atmosphere, to take crisp images across a field of view 35 times larger than the full moon. And it will do so every 30 seconds, a pace that will capture the entire sky visible from Hawaii several times a month.

Pan-STARRS will spot thousands of things that change or move, such as supernovae, flaring stars, and asteroids. In particular, the system will find sizable asteroids that orbit dangerously close to Earth 10 times more efficiently than all current search programs combined. It also will create the most detailed all-sky atlas yet compiled, with accurate positions and brightnesses for billions of stars and galaxies. Once the telescope begins full-time science operations in early 2007, its data will flow at the rate of several terabytes (millions of megabytes) per night—a cascade that particle physicists can handle but astronomers have yet to experience.

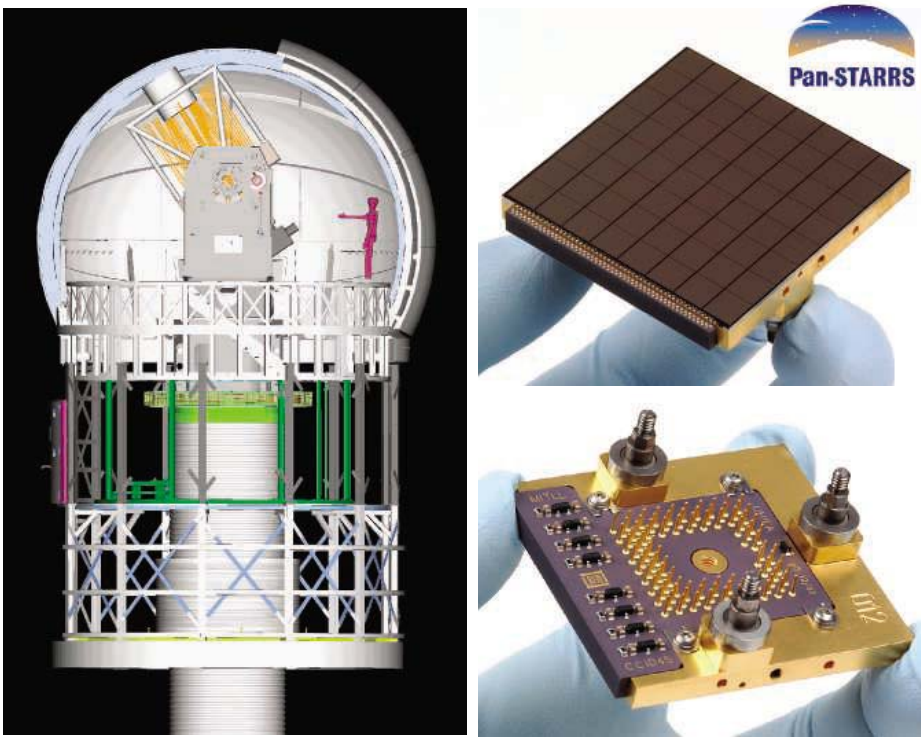

Sharp focus. Astronomers are assembling the 1.8-meter Pan-STARRS 1 telescope (engineering drawing, *left*) on Maui, Hawaii. Its camera features 1.4 billion pixels spread across 64 arrays of detectors (shown front and back, *right*) that will electronically counteract atmospheric distortions.

These ambitions have set colleagues abuzz with a blend of skepticism, envy, and praise. "The sheer volume of data processing will be a challenge, but it's a big, creative group of people," says Wendy Freedman, director of the Carnegie Observatories in Pasadena, California. Another West Coast astronomer, involved with labyrinthine plans for a giant telescope, says: "If I could start over with everything in astronomy and just join one project, it would be Pan-STARRS."

A giga-view of space

Pan-STARRS is the first in a generation of ground-based telescopes that will digitize the sky in fine detail, repeatedly. "If we had talked about terabytes of disk storage and billions of stars a decade ago, it would have been feasible but insanely expensive," says astronomer John Tonry of the University of Hawaii (UH), Manoa. "Today, buying the disk storage to do these things is trivial. Moore's Law has met the universe, and Moore's Law won."

Tonry and several UH colleagues, including Gerard Luppino and project director Nicholas Kaiser, conceived Pan-STARRS in 2000. Their inventive plans drew interest from the U.S. Air Force, which operates the Defense Department's largest telescope: a 3.67-meter satellite surveillance system on UH property near the summit of Haleakala, Maui's highest peak. The Air Force has fronted $45 million to date and is on track to provide another $45 million during the next 5 years, Kaiser says. That sum covers R&D costs and construction of a single telescope at Haleakala, called Pan-STARRS 1, and its successor of four identical telescopes (Pan-STARRS 4) planned atop Mauna Kea on Hawaii's Big Island by 2010.

Military researchers have two vested interests, says Paul Kervin, technical director of the Air Force research unit on Maui. The first is "planetary defense," the ongoing effort to find the threatening mountains of rock in space known as near-Earth objects (NEOs). The Air Force already supports R&D and provides access to its own telescopes for two programs to detect NEOs, so Pan-STARRS is the logical next step. Second, the Air Force is eager to adapt the system's groundbreaking optics to sharpen its satellite surveillance network. But the Air Force will play no role in operating Pan-STARRS; rather, UH is seeking primarily academic partners to share costs and gain access to observing time.

The star of Pan-STARRS is its camera with 1.4 billion pixels, nearly five times the pixel count of the biggest cameras now in use at other telescopes. The system is not just a passive recorder of light. Tonry and detector guru Barry Burke of the Massachusetts Institute of Technology's Lincoln Laboratory in Lexington devised special chips that can shift their electrical charges in all directions. By monitoring bright stars, the chips sense the jittering motions of starlight as it passes through Earth's atmosphere. The chips then shuffle their electrons to compensate about 10 times each second. The system thus keeps the images of objects in each frame confined within tight pinpricks, rather like a Steadicam. "This really is a major advance in imaging capability," Burke says. "The astronomy community is watching very closely."

CREDITS (LEFT): JEFFREY MORGAN/PAN-STARRS; (RIGHT) UNIVERSITY OF HAWAII

Because of these on-chip corrections, the telescope will yield a sharply focused image across 7 square degrees of the sky even without the usual deformable mirrors of adaptive optics. What's more, the chips will read out each data batch of 3 gigabytes in a few seconds, allowing rapid-fire exposures throughout the night.

A hunt for moving objects

That cadence makes Pan-STARRS ideal to watch the sky for moving blips of light. And indeed, the telescope will spend one-third of its time doing just that, with an emphasis on hunting down NEOs. UH astronomer Robert Jedicke forecasts that Pan-STARRS will chart orbits for about 90% of all NEOs larger than 300 meters across and half of those larger than 140 meters, a threshold set by NASA as worrisome. Those faint objects are beyond the reach of all five current surveys. "I think this is exactly what needs to be done," says Donald Yeomans, director of NASA's NEO office at the Jet Propulsion Laboratory in Pasadena. "This is going to completely change the NEO landscape." Along the way, Jedicke adds, Pan-STARRS will catalog millions of new main-belt asteroids and thousands of dim, cometlike bodies in the Kuiper belt beyond Neptune.

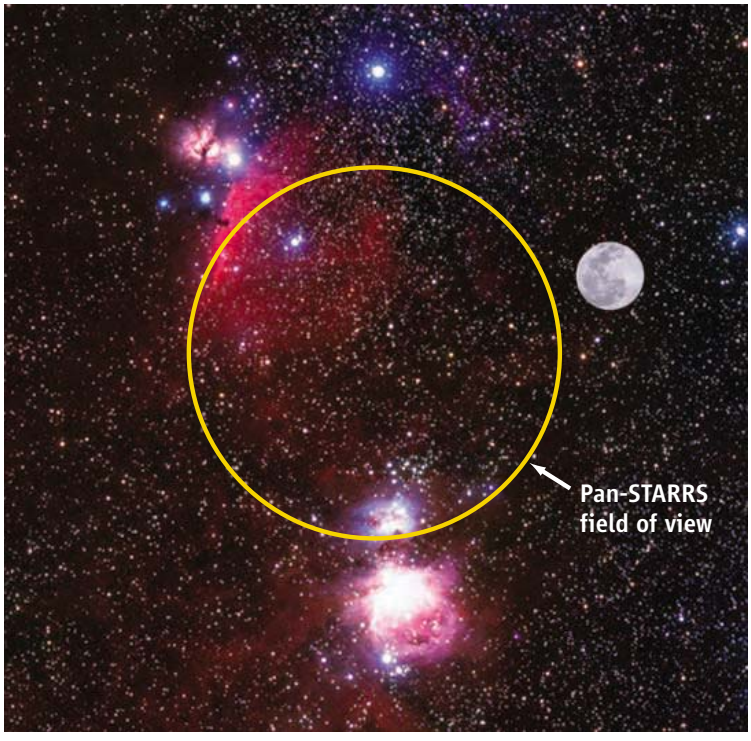

Taking the wide view. Pan-STARRS will command a sweeping vista 35 times the area of the full moon. That's seven times the scope of the largest current wide-field imager and 3500 times broader than the Hubble Space Telescope's narrow window.

Another survey calls for Pan-STARRS to stare more deeply at a dozen patches of the sky every night to look for supernovae, gamma ray bursts, and unidentified cosmic flares. The team expects to find about 5000 of the type of supernova cosmologists use to gauge the growth history of the universe, more than any other system yet funded. And astronomers elsewhere are excited by the prospect of watching the same areas with sensitive instruments at other wavelengths of light, especially radio waves and gamma rays. Simultaneous detections by several observatories and satellites would illuminate the physical causes of fleeting bursts as never before, says Joshua Bloom of the University of California (UC), Berkeley.

Finally, Pan-STARRS will scan the entire sky visible from Hawaii—about 3/4 of the full sweep of the heavens—several times every month. During 3 years of operation for Pan-STARRS 1, the team will add the images digitally to create an increasingly detailed map, both broader in scope and more precise than the results of the ongoing Sloan Digital Sky Survey. That celestial census will include the locations and motions of every star and brown dwarf within 200 light-years of the sun, an estimated half-million objects. Pan-STARRS will define stellar positions about 30 times more accurately than today's most popular astronomical catalog does, says UH astronomer Eugene Magnier, making it the de facto reference chart for professional observers.

Some of the most tantalizing science must await Pan-STARRS 4. Those telescopes, all mounted on one structure, will have the light-gathering power of a single 3.6-meter mirror. Fainter galaxies will pop into view, along with tiny distortions in their images caused by dark matter along the line of sight from Earth. This phenomenon, called weak gravitational lensing, is a promising means of probing the hidden mass of the universe (*Science*, 20 June 2003, p. 1894). "This is by far our most challenging scientific issue, because it requires very accurate control of the shapes of images," says Kaiser.

The road ahead

Pan-STARRS faces myriad near-term challenges as well. Most critical is enticing several scientific partners to share the operating costs, which Kaiser pegs at $2 million per year. Astronomy departments at Harvard University, Princeton University, the University of Pennsylvania, and UC Berkeley (in conjunction with Lawrence Berkeley National Laboratory) have piped up with interest.

Although Pan-STARRS 1 will start taking images this summer, the fate of Pan-STARRS 4 is not assured. The team covets a prime site atop Mauna Kea, with its superior atmospheric conditions. But new projects there face strict review by the state of Hawaii, and fervent opposition from native groups has torpedoed expansions at other facilities. The UH team hopes to prevent that by removing its existing 2.2-meter telescope at Mauna Kea and replacing it with Pan-STARRS 4. The new building's lower profile should please community leaders, says Rolf-Peter Kudritzki, director of the UH Institute for Astronomy.

A less tangible issue is whether Pan-STARRS might undercut a proposed national facility: the Large Synoptic Survey Telescope (LSST) (*Science*, 27 August 2004, p. 1232). This 8.4-meter telescope, planned for Chile or Baja California, Mexico, would have six times the surveying power—the product of its light-gathering capacity and its sky coverage—of Pan-STARRS 4. LSST has momentum as a high-priority project, but federal funders will need to cough up at least $200 million to build it. Some wonder whether Pan-STARRS will steal much of its scientific glory before LSST opens its wide eye on the sky.

The teams are collegial and share software, but there are undercurrents of unease. "LSST is in all senses bigger and more ambitious, yet its science case has been predicated on Pan-STARRS not existing or not getting there 5 to 10 years sooner," says UH's Tonry. "That needs to be looked at: How should LSST operate given that Pan-STARRS will have done many of these things?"

LSST director Anthony Tyson of UC Davis acknowledges that Pan-STARRS will do "marvelous work" in tracking hazardous asteroids and Kuiper belt objects. But in most other areas, he says, "Pan-STARRS 4 is not scientifically competitive." Notably, LSST will be a more sensitive probe of weak gravitational lensing—as reflected in Tyson's original name for the project, the "Dark Matter Telescope." Ideally, argues Kaiser, both should proceed. "There's great danger that if people see these as competing, it will undermine national funding [for LSST]," he says. "We will be a precursor, a stop along the way, if LSST gets funded."

Regardless of the outcome, the march of Moore's Law portends a future of digital data mining for astronomers, says Alexander Szalay of Johns Hopkins University in Baltimore, Maryland, an architect of the massive Pan-STARRS data archive. "Some people miss the lonely nights in the telescope dome," he says. "But like it or not, this is how the new astronomy will be done."

–ROBERT IRION

CREDIT: WEI-HAO WANG/UNIVERSITY OF HAWAII

“ THE FASTEST GROWING CROP IN IOWA IS NOT WHAT YOU EXPECT. ”

MORE AND MORE BIOSCIENCE COMPANIES PLANNING TO EXPAND ARE TAKING A LOOK AT IOWA. And for good reason. Iowa leads the nation in the production of raw biomass at roughly 2.75 billion bushels. The state is home to three public universities that are world-renowned for their research in plant, animal and human bioscience. And to date there are more than 1,800 Iowa establishments already involved in the bioscience industry. To learn more about expanding your business in Iowa, visit iowalifechanging.com. Because the closer you look, the more Iowa grows on you.

www.iowalifechanging.com

IOWA
life | changing™

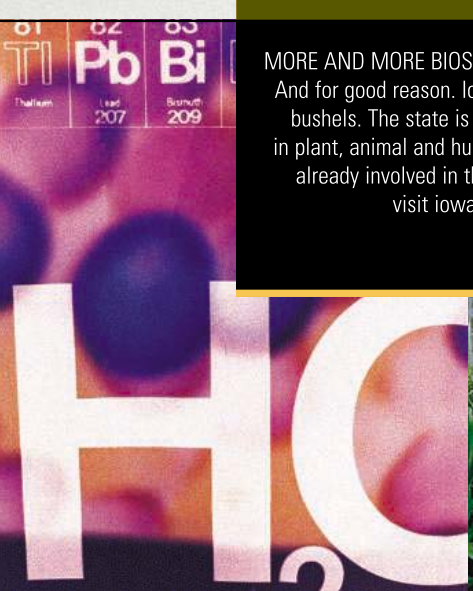

EDITED BY YUDHIJIT BHATTACHARJEE

A SALTY NAME. A new species is often named after the discoverer or a loved one. But leave it to the kids to take the scientific high road in tagging a salt- and sun-loving microbe found in the Great Salt Lake in Utah.

Salsolis was discovered by Ashlee Allred, a student at Westminster College in Utah working with biochemist Bonnie Baxter. Baxter teamed up with Maple Tree Press to hold a Name a New Species Contest. And the joint winners were Hannah Walsh, 11 (left), and Duncan Uszkay, 8 (right), of Canada, who independently chose the same Latin-based moniker.

Runners-up included "Salteenies" and "Salty the Basking Carrot," but Baxter chose salsolis because "it reflected the scientific process of naming organisms." Salsolis belongs to the *Halorubrum* genus, and Baxter is proposing *Halorubrum salsosis* as its scientific name.

AWARDS

LEMELSON PRIZE. The temperature-sensing mood rings and thermometers that James Fergason developed more than 40 years ago at Westinghouse Research Laboratories in Pittsburgh, Pennsylvania, were the first practical applications of liquid crystals. "[But] very quickly we thought about displays," says Fergason about helping to lay the cornerstone of a $24 billion annual market for liquid-crystal displays in everything from cars and cell phones to laptops and televisions. It also earned Fergason this year's Lemelson-MIT Prize and $500,000, the largest U.S. cash prize for invention.

The committee also handed out a $100,000 lifetime achievement award to Sidney Pestka, a research physician who developed a technique to purify cell-signaling proteins called interferons. They have been effective against some forms of leukemia, as well as multiple sclerosis and viral diseases.

WELCH PRIZE. Molecular biologist and former *Science* editor-in-chief Daniel Koshland has won the $300,000 Welch Award in Chemistry. Koshland, a professor emeritus at the University of California, Berkeley, receives the honor for his contributions to the understanding of enzymes and protein chemistry.

HONORING WORK FOR AFRICA. The Japanese government will create a prize for medical researchers whose work benefits Africa. Announcing the prize last week in Ghana, Japanese Prime Minister Junichiro Koizumi said it would be named after Hideyo Noguchi, a Japanese scientist who died of yellow fever in Ghana in 1928 while studying the disease. Koizumi said the first prize will be awarded in 2008 at the Tokyo International Conference on African Development.

Fact and Fiction

"Somebody told me that we graduate more majors in sports management than in engineering. I don't know if it's true, but just the idea strikes me as significant." —Representative Tom Price (R–GA) at a 3 May hearing of the House Education and Workforce Committee that examined existing federal math and science programs.

FACT: An estimated 700 sports-management degrees are awarded annually by accredited undergraduate programs, according to Mark Stevens of the United States Sports Academy in Daphne, Alabama. That's less than 1% of the 73,000 bachelor-level engineers who graduated from U.S. universities in 2004.

LAST MAN STANDING. The appointment of evolutionary biologist Mark Rausher as editor of *Evolution* caused Terry Markow, the president of the society that publishes the journal, to resign in protest of what she called gender discrimination. But society officials say Rausher, who started this month, got the job only after a dozen colleagues turned it down.

The five women and seven men declined because of the time commitment needed for the position, says Dolph Schluter of the University of British Columbia in Vancouver, Canada, past president and chair of the search committee. Even Rausher, a researcher at Duke University in Durham, North Carolina, admits to having reservations. "I agreed because I am a bit masochistic," he says.

Rausher has added two editors with an eye toward reducing publication delays and adding opinions, perspectives, or reviews. He also wants the journal to do more public outreach on evolution.

Got a tip for this page? E-mail people@aaas.org

CREDITS (TOP TO BOTTOM): MAPLE TREE PRESS; GORDON USZKAY; JIM WALLACE/DUKE UNIVERSITY PHOTOGRAPHY; CHRIS CONROY/THE LEMELSON-MIT PROGRAM

Fundación **BBVA**

II BBVA Foundation Awards for

Biodiversity Conservation

BBVA Foundation Award for Scientific Research in Ecology and Conservation Biology

Deadline for entry submission:
30 June 2006

The conditions of the call, application forms and additional information are available on the Foundation website: **www.fbbva.es**

Fundación BBVA
Gran Vía 12
48001 Bilbao
SPAIN
Fax (34) 94 487 50 97

Pº de Recoletos 10
28001 Madrid
SPAIN
Fax: (34) 91 374 34 44

convocatorias@fbbva.es

- Internationally recognising the contributions of scientists in any country that have significantly advanced the boundaries of theoretical, methodological or empirical knowledge in the fields of Ecology and Conservation Biology.

- One award will be given, consisting of a €500,000 cash prize, a diploma and a commemorative artwork.

- The award may be shared by up to three scientists and is reserved for contributions of particular significance.

The BBVA FOUNDATION Awards include two other categories, for innovative actions and knowledge dissemination in biodiversity conservation.

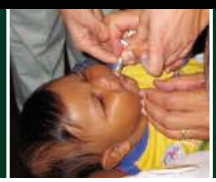

LETTERS

edited by Etta Kavanagh

Multiple Outbreaks and Flu Containment Plans

IN REPORTING ON OUR RECENT STUDY (*1*) ON THE RISK OF MULTIPLE OUTBREAKS OF PANDEMIC influenza, M. Enserink cites several scientific and political objections to our conclusions that a single introduction of pandemic flu might be followed by additional introductions in quick succession ("New study casts doubt on plans for pandemic containment," News of the Week, 24 Feb., p. 1084).

Several commentators suggest that multiple introductions are unlikely, making analogies to other emerging infections, such as SARS. In fact, SARS is thought to have entered humans several times in 2003–04 (*2*, *3*). Multiple infections have been suggested for HIV-1 (*4*), and clustered introductions have been observed for Ebola virus (*5*). The commentators suggest that the likelihood of a flu pandemic is not currently above its historical average of ~3% per year (*6*), so that containment will increase the time to a pandemic by a decade or more. Our analysis shows that containment will yield benefits on this scale only if the risk of introduction of a pandemic-capable strain is both (i) low, near its historical average, and (ii) constant over time. Neither seems likely. Although the process by which new pandemic strains emerge is poorly understood, the risk must increase with increasing encounters between livestock and humans, and populations of humans, pigs, and poultry have grown by an estimated 60%, 100-fold, and 1000-fold, respectively, in China alone since 1968 (*7*). Likewise, the past decade's geographic spread of H5N1 influenza and other influenza strains in birds must increase the opportunities for encounters between H5N1-infected birds and humans (*8*).

A Roche pharmaceuticals worker supervises the packaging of Tamiflu in Basel, Switzerland.

CREDIT: HANDOUT/EPA/CORBIS

We are disturbed by the implication from one commentator that our results should have been suppressed for fear of discouraging efforts at containment, particularly since we specifically advocate continued efforts at containment and suggest ways in which such efforts could be improved. Suppressing scientific findings or dissenting views more generally to achieve policy consensus is bad science and bad policy, for influenza (*9*) and in general (*10*).

MARC LIPSITCH,[1] JAMES M. ROBINS,[1] CHRISTINA E. MILLS,[1] CARL T. BERGSTROM[2]

[1]Department of Epidemiology, Harvard School of Public Health, 677 Huntington Avenue, Boston, MA 02115, USA. [2]Department of Biology, University of Washington, Box 351800, Seattle, WA 98195–1800, USA.

References

1. C. E. Mills, J. M. Robins, C. T. Bergstrom, M. Lipsitch, *PLoS Med* **3**, e135 (21 Feb. 2006).
2. M. Wang *et al.*, *Emerg. Infect. Dis.* **11**, 1860 (2005).
3. R. H. Xu *et al.*, *Emerg. Infect. Dis.* **10**, 1030 (2004).
4. B. H. Hahn, G. M. Shaw, K. M. De Cock, P. M. Sharp, *Science* **287**, 607 (2000).
5. X. Pourrut *et al.*, *Microbes Infect.* **7**, 1005 (2005).
6. C. Brahic, "Containing outbreak 'would only delay a flu pandemic,' " www.scidev.net/content/news/eng/containing-outbreak-would-only-delay-a-flu-pandemic.cfm (2006).
7. M. T. Osterholm, *N. Engl. J. Med.* **352**, 1839 (2005).
8. C. J. Russell, R. G. Webster, *Cell* **123**, 368 (2005).
9. R. E. Neustadt, H. Fineberg, *The Epidemic That Never Was: Policy-Making and the Swine Flu Affair* (Vintage Books, New York, 1983).
10. D. Kennedy, *Science* **311**, 917 (2006).

Migratory Birds and Avian Flu

IN HIS ARTICLE "EVIDENCE POINTS TO MIGRAtory birds in H5N1 spread" (3 Mar., p. 1225), D. Normile reports that "increasingly, scientists are attributing this remarkably fast spread [of H5N1] to migratory birds, but dissenters remain." All agreed that wild birds have a role, but attributing the spread of HPAI H5N1 entirely to migratory birds overlooks evidence that is inconsistent with this conclusion.

One cannot ignore the apparent lack of previous outbreaks along migratory pathways. Birds have been migrating along these same routes annually since this genotype of HPAI H5N1 was first identified in Asia in 1997, yet there was no spread of disease to Eurasia or Europe in the interim years. Although fewer than 0.05% of more than 13,000 healthy waterfowl tested (*1*) were positive for HPAI H5N1, billions of birds have traveled to Eurasia and Europe for 8 years. It seems suspicious that none has managed to transmit this highly pathogenic virus until now. The introduction of HPAI H5N1 onto the continent of Africa, as well as the earlier outbreaks in poultry, notably in Russia and Turkey, could have been as easily accommodated by the movement of infected poultry, poultry products, or contaminated fomites as suggested for migratory bird routes. Meanwhile, Japan, with strong controls on poultry imports, has remained H5N1-free since early 2004, when infected poultry flocks were destroyed, despite the annual arrival of large migratory bird populations from areas with known H5N1 outbreaks.

Four pathways are most likely involved in the movement of HPAI H5N1: poultry shipments; the movement of contaminated equipment, materials, and waste products; migratory birds; and the wild bird trade. At most, the evidence suggests that wild birds may be responsible for short-distance, secondary movement of HPAI H5N1. Ornithologists, virologists, veterinarians, and others must work together, sharing their specialized knowledge to understand more thoroughly the movement of this virus.

ROB FERGUS,[1] MICHAEL FRY,[2] WILLIAM B. KARESH,[3] PETER P. MARRA,[4] SCOTT NEWMAN,[3]* ELLEN PAUL[5]

[1]National Audubon Society, 545 Almshouse Road, Ivyland, PA 18974, USA. [2]Pesticides and Birds Program, American

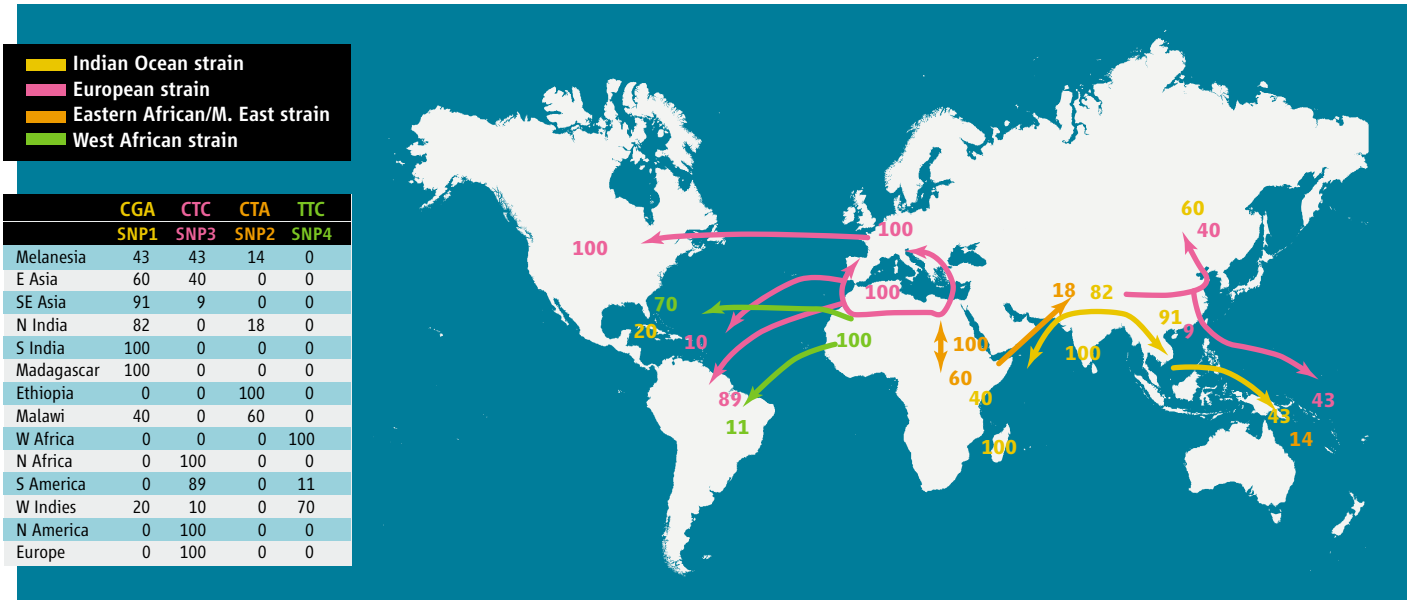

	CGA	CTC	CTA	TTC
	SNP1	SNP3	SNP2	SNP4
Melanesia	43	43	14	0
E Asia	60	40	0	0
SE Asia	91	9	0	0
N India	82	0	18	0
S India	100	0	0	0
Madagascar	100	0	0	0
Ethiopia	0	0	100	0
Malawi	40	0	60	0
W Africa	0	0	0	100
N Africa	0	100	0	0
S America	0	89	0	11
W Indies	20	10	0	70
N America	0	100	0	0
Europe	0	100	0	0

Revised regional frequency patterns for the leprosy SNPs based on Monot *et al.* Arrows indicate the primary vectors of dispersal, which can be accounted for by recent protohistoric and historic movements as well as by earlier Pleistocene dispersals.

Bird Conservancy, 1731 Connecticut Avenue, NW, Washington, DC 20009, USA. [3]Field Veterinary Program, Wildlife Conservation Society, 2300 Southern Boulevard, Bronx, NY 10460, USA. [4]Smithsonian Migratory Bird Center, National Zoological Park, 3001 Connecticut Avenue, NW, Washington, DC 20008, USA. [5]Ornithological Council, 1707 H Street, NW, Washington, DC 20006, USA.

*Previously at Wildlife Trust, 460 West 34th Street, 17th Floor, New York, NY 10001, USA.

Reference

1. H. Chen *et al.*, *Proc. Natl. Acad. Sci. U.S.A.* **103**, 2845 (2006).

Reconsidering the Antiquity of Leprosy

LEPROSY HAS CLASSICALLY BEEN CONSIDERED a disease of evolutionarily recent times, with an epidemiology related to relatively high-density living. In their Report "On the origin of leprosy" (13 May 2005, p. 1040), M. Monot *et al.* propose a scenario in which leprosy was spread around the world during the dispersal of modern humans from Africa and by recent colonial movements. We welcome this innovative model but suggest that their data are equally compatible with a more recent origin and dispersal.

The basis of their Pleistocene dispersal model is that with a low rate of mutation among mycobacteria, the preferred phylogeny of the *Mycobacterium leprae* single nucleotide polymorphisms fits the dispersal of modern humans out of Africa. However, not only is there no paleopathological evidence for leprosy before the development of urban life (*1*), its appearance around the world shows sufficient chronological differentiation to be consistent with active spread during urbanization. *M. leprae* is an obligate pathogen (*2*) dependent on high levels of human contact to be maintained in a population (*3*). This suggests it was unlikely to have thrived during the Pleistocene, when human populations lived in highly mobile, low-density groups, under conditions of relative isolation (*4*, *5*). Low host densities and the ecologically diverse geographic regions where *M. leprae* survives today indicate that mobility was the main factor determining the spread of the disease. Phylogenies should, therefore, be considered in the context of a post-Holocene pattern of dispersals associated with the appearance of higher density human populations. Finally, assessment of the coalescence of *M. leprae* strain sequences is dependent on both time and population size, and the expansion of human populations in the past 5000 years may be a critical part of the evolutionary history of the pathogen.

Relevant data on human migrations should be considered [see fig. 1; (*6*)]. Classical texts suggest that leprosy spread from the Indian subcontinent to Europe and the Middle East, possibly with the armies of Alexander the Great (*7*). The first phylogeny of Monot *et al.* suggests an East African origin. The second phylogeny suggests an Asian origin. If the origins and spread of *M. leprae* are prehistoric, an unlikely assumption, the first phylogeny is consistent with genomic analysis (*8*, *9*) and some models of modern human dispersals (*10*). However, their second phylogeny is consistent with historical texts and is compatible with the patterns of movement, trade, and contact stretching back several millennia, associated with the rise of ubanization (*11*, *12*)—in the region between the Horn of Africa and the Indus Valley.

We suggest that the distribution of *M. leprae* strains, together with paleopathological and epidemiological evidence (*13*), fits the classical model that it is a disease of evolutionarily recent times, with an epidemiology related to relatively high-density living.

RON PINHASI,[1] ROBERT FOLEY,[2] HELEN D. DONOGHUE[3]

[1]School of Human and Life Sciences, Roehampton University, Holybourne Avenue, London SW15 4JD, UK. E-mail: r.pinhasi@roehampton.ac.uk. [2]Leverhulme Centre for Human Evolutionary Studies, Henry Wellcome Building, Fitzwilliam Street, Cambridge CB2 1QH, UK. [3]Centre for Infectious Diseases and International Health, Department of Infection, Windeyer Institute of Medical Sciences, UCL, 46 Cleveland Street, London W1T 4JF, UK.

References and Notes

1. See C. A. Roberts *et al.* [C. A. Roberts, M. E. Lewis, K. Manchester, Eds., *The Past and Present of Leprosy* (BAR International Series 1054, Oxford, 2002)] for various paleopathological reports and historical reviews.
2. S. T. Cole *et al.*, *Nature* **409**, 1007 (2001).
3. R. Frothingham, *Med. Hypotheses* **52**, 95 (1999).
4. G. J. Armelagos, K. N. Harper, *Evol. Anthropol.* **14**, 109 (2005).
5. A. Cockburn, *Curr. Anthropol.* **12**, 45 (1971).
6. SNPs in our figure are color-coded according to Monot *et al.*'s fig. 1b.
7. M. F. Lechat, *Int. J. Lepr.* **63**, 460 (1999).
8. P. A. Underhill *et al.*, *Nat. Genet.* **26**, 358 (2000).
9. L. A. Zhivotovsky *et al.*, *Am. J. Hum. Genet.* **71**, 1171 (2003).
10. M. M. Lahr, R. A. Foley, *Yearb. Phys. Anthropol.* **41**, 137 (1998).
11. G. L. Cowgil, *Annu. Rev. Anthropol.* **33**, 525 (2004).
12. W. H. McNeil, *Plagues and Peoples* (Anchor, New York, 1976).
13. A. F. Aufderheide, C. Rodrigez-Martin, *The Cambridge Encyclopedia of Human Paleopathology* (Cambridge Univ. Press, Cambridge, 1998).

Species Diversity and Ecosystem Functioning

IN THEIR REPORT "NONRANDOM PROCESSES maintain diversity in tropical forests" (27 Jan., p. 527), C. Wills and colleagues provide strong

evidence that nonrandom processes play a key role in maintaining diversity in tropical forests, specifically that forest tree diversity increases as individuals age because of preferential survival by individuals of locally rare species. However, the implications are even greater than those proposed by Wills *et al.*, as all three mechanisms supported by their results imply that species diversity increases ecosystem functioning.

First, the Janzen-Connell model (*1*, *2*) predicts that species escape their specialist herbivores, predators, and pathogens when they are locally rare, whereas common species are more readily attacked. Losses of carbon and nutrients to natural enemies result in lower growth rates and thus lower primary productivity (*3*). Second, niche complementarity occurs when species exploit resources in different ways and results in more complete resource utilization and thus higher productivity (*4*) and has been shown to contribute to increased functioning with diversity (*5*, *6*). In tropical forests, tree species may differ in their ability to acquire soil resources, resulting in more complete resource capture and thus higher productivity. Third, facilitation occurs when one species directly benefits another but experiences no harm (*7*) and has been shown to contribute to increases in ecosystem functioning with diversity (*8*, *9*). In tropical forests, a tree species might fix nitrogen that becomes available to its neighbors. In this case, the tree's neighbors will experience increased growth rates if nitrogen is limiting.

When any of these three nonrandom mechanisms are operating, species extinctions will result in a decrease in productivity due to increased losses to natural enemies, failure to fully utilize essential resources, or the loss of direct benefits of facilitation. In contrast, neutral models of species coexistence (*10*–*12*) assume species are functionally equivalent, and therefore ecosystem functioning will not be dependent on species diversity. Wills and colleagues provide strong circumstantial evidence that even in highly diverse tropical forests, biodiversity enhances ecosystem functioning.

DANIEL E. BUNKER AND SHAHID NAEEM

Department of Ecology, Evolution and Environmental Biology, Columbia University, 1200 Amsterdam Avenue, New York, NY 10027–5557, USA.

References

1. D. H. Janzen, *Am. Nat.* **104**, 501 (1970).
2. J. H. Connell, in *Dynamics of Populations*, P. J. den Boer, G. R. Gradwell, Eds. (Center for Agricultural Publication and Documentation, Wageningen, The Netherlands, 1971), pp. 298–312.
3. C. E. Mitchell, *Ecol. Lett.* **6**, 147 (2003).
4. M. Loreau, *Proc. Natl. Acad. Sci. U.S.A.* **95**, 5632 (1998).
5. J. van Ruijven, F. Berendse, *Proc. Natl. Acad. Sci. U.S.A.* **102**, 695 (2005).
6. D. A. Heemsbergen *et al.*, *Science* **306**, 1019 (2004).
7. J. F. Bruno, J. J. Stachowicz, M. D. Bertness, *Trends Ecol. Evol.* **18**, 119 (2003).
8. C. P. H. Mulder, D. D. Uliassi, D. F. Doak, *Proc. Natl. Acad. Sci. U.S.A.* **98**, 6704 (2001).
9. B. J. Cardinale, M. A. Palmer, S. L. Collins, *Nature* **415**, 426 (2002).
10. S P. Hubbell, *The Unified Neutral Theory of Biodiversity and Biogeography* (Princeton Univ. Press, Princeton, NJ, 2001).
11. G. C. Hurtt, S. W. Pacala, *J. Theor. Biol.* **176**, 1 (1995).
12. J. H. Connell, *Science* **199**, 1302 (1978).

Response

BUNKER AND NAEEM CORRECTLY IDENTIFY THE key result of our analyses, i.e., that local frequency-dependent processes contribute to the maintenance of diversity in tropical forests. The commentary on our Report by E. Pennisi ("Rare tree species thrive in local neighborhoods," News of the Week, 27 Jan., p. 452) may have given readers the erroneous impression that plot-wide or forest-wide diversity increased during the census periods. Our results concerned multispecies cohorts of trees within small-scale quadrats (100 to 2500 m^2) in which species-level diversity increased through time as the result of higher mortality of locally common species. This result does not conflict with the possibility that the local (quadrat) diversity of recruits (i.e., the individuals that set the bounds within which diversity may vary for a given cohort) fluctuates through time.

Bunker and Naeem also suggest that our results support the hypothesis that tropical tree diversity may be positively correlated with

"ecosystem functioning." Even though our data and analyses do not directly address this important hypothesis, it is a testable idea. A positive relationship between biodiversity and productivity (or other ecosystem-level variables) would have important implications for tropical forest conservation.

CHRISTOPHER WILLS[1] AND KYLE HARMS[2]

[1]Division of Biological Sciences, University of California, San Diego, La Jolla, CA 92093–0116, USA. [2]Department of Biological Sciences, Louisiana State University, 202 Life Sciences Building, Baton Rouge, LA 70803, USA.

Increase in Foreign Grad Students

IN THE NEWS OF THE WEEK ARTICLE "FOREIGN grad students show renewed interest" (K. Unger, 31 Mar., p. 1845), university administrators seem to have overlooked possibly the most important reason for the recent increase in graduate school applications from foreign students. For many skilled foreigners, a change of the H-1B "work visa" quota system 2 years ago made it very difficult to obtain the necessary authorization to work in the United States. However, foreigners who hold a Master's or Ph.D. degree from a U.S. school fall under a separate quota allotment, and thus it is far easier for them to obtain the necessary H-1B visa to work in the United States. In other words, many foreigners who want science or engineering jobs in this country no longer have the option of obtaining graduate degrees in their home countries. They are applying to graduate schools here in increasing numbers because they must obtain a graduate degree from the United States to have a reasonable chance of acquiring the necessary U.S. work visa without a certain delay of one or more years. It is perhaps ironic that raising the bar on granting work visas has had the side effect of increasing the number of foreign grad student applicants.

ROBERT M. YEH

Department of Chemistry, The Scripps Research Institute, 10550 North Torrey Pines Road, La Jolla, CA 92037, USA.

Letters to the Editor

Letters (~300 words) discuss material published in *Science* in the previous 6 months or issues of general interest. They can be submitted through the Web (www.submit2science.org) or by regular mail (1200 New York Ave., NW, Washington, DC 20005, USA). Letters are not acknowledged upon receipt, nor are authors generally consulted before publication. Whether published in full or in part, letters are subject to editing for clarity and space.

TECHNICAL COMMENT ABSTRACTS

Comment on "Evidence for Positive Epistasis in HIV-1"

Kai Wang, John E. Mittler, Ram Samudrala

Bonhoeffer *et al*. (Reports, 26 November 2004, p. 1547) presented evidence for positive epistasis in a clinical data set of HIV-1 mutants and corresponding fitness values. We demonstrate that biases in the original and simulated data sets may lead to erroneous evidence for epistasis. More rigorous statistical tests must be used to account for such biases before one can infer epistasis.

Full text at www.sciencemag.org/cgi/content/full/312/5775/848b

Response to Comment on "Evidence for Positive Epistasis in HIV-1"

Sebastian Bonhoeffer, Colombe Chappey, Neil T. Parkin, Jeannette M. Whitcomb, Christos J. Petropoulos

Wang *et al*. analyzed artificially biased data to show that our results can be explained by a bias against sequences with low fitness. We explicitly acknowledged this potential caveat in our original study. Showing that an artificially introduced bias can produce a spurious signal of positive epistasis does not demonstrate that such bias exists in our original data.

Full text at www.sciencemag.org/cgi/content/full/312/5775/848c

HISTORY OF SCIENCE

Advocating Science for the People

Soraya de Charadevian

Every good biography illuminates both the life and times of its subject. In John Desmond Bernal's case, the very distinction between these two aspects seems to collapse. Not only was his knowledge encyclopedic, earning him the nickname Sage at a young age. His expansive activities—ranging from pioneering research on the minute structures of life to a visionary understanding of the role of science in society and a political engagement on a global scale—seem to embrace the times he lived in. Andrew Brown's *J. D. Bernal* rises to the challenge. Although not the first biography of Bernal, it is the first that was able to benefit from full access to his papers deposited at Cambridge University Library. Brown, a practicing radiation oncologist and biographer of the physicist James Chadwick (*1*), also conducted extensive historical research and a series of interviews with people who knew Bernal.

The main facts of Bernal's legendary life are well known; Brown recounts them with fresh detail and in a succinct and vivid style. We follow Bernal from his early childhood in rural Ireland and education in English boarding schools to his undergraduate years at Emmanuel College in Cambridge just after World War I. On trips home as a teenager, Bernal embraced the nascent Republican cause in Ireland. At Cambridge, influenced by a fellow freshman, he converted from Catholicism to Socialism, a move that would increasingly determine his intellectual and political engagement. From mathematics, he switched to the Natural Sciences Tripos. Having gained his degree, Bernal moved to William Bragg's laboratory at the Royal Institution in London. There he quickly established himself as one of the leading exponents of the burgeoning field of x-ray crystallography, while circulating at the fringes of the Bloomsbury group and leading an entangled private life. He returned to Cambridge in 1927, assuming the reinstated lectureship in structural crystallography. Here he laid the foundations for a structural approach to biologically important compounds, especially proteins, which he came to see as embodying the secret of life. Several researchers who went on to win Nobel Prizes in molecular biology—including such illustrious names as Dorothy Hodgkin, Max Perutz, John Kendrew, Francis Crick and Aaron Klug—acknowledged Bernal's pioneering work and inspiration.

The reviewer is in the Department of History and Philosophy of Science, Cambridge University, Cambridge, CB2 3RH, UK. E-mail: sd10016@hermes.cam.ac.uk

Bernal's increasing political engagements in the 1930s as a key exponent of the Scientific Left have been well documented. With the intensification of the fascist threat, the Cambridge Scientists Anti-War Group (of which Bernal was a leading figure) addressed the problem of civil protection against aerial attacks. Bernal came to see this work as the beginning of operational research, a branch of science in which he became deeply engaged as the events leading to World War II unfolded. As scientific adviser to Lord Mountbatten, Britain's chief of combined operations during the war, Bernal got entrusted with several projects. Among them was Project Habbakuk, the eventually abandoned plan (conceived by Geoffrey Pyke, another of Mountbatten's advisers) to build a landing strip of reinforced ice as a floating airbase in the Atlantic.

J. D. Bernal
The Sage of Science
by Andrew Brown
Oxford University Press, Oxford, 2005. 576 pp. $34.95, £25. ISBN 0-19-851544-8.

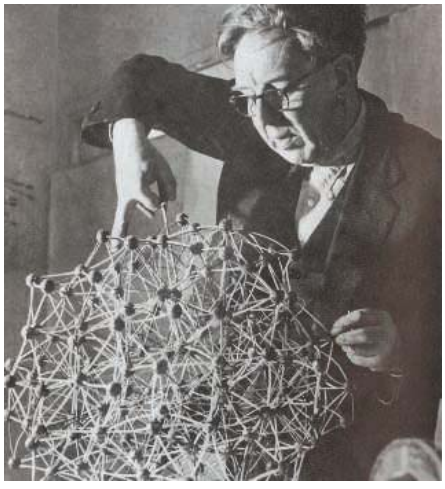

Heap of molecules. Bernal with his first ball-and-spoke model of liquid structure.

Controversy has developed around Bernal's actual role in the planning of D-Day, especially in respect to the authenticity of an account given by Bernal of his crossing of the Channel on D-Day plus 1 and 2. Here Brown comes down firmly in defense of Bernal, providing strong evidence of his decisive contributions to the preparation and the success of the invasion. As Brown documents, doubts about Bernal's role were systematically sown by Solly Zuckerman, Bernal's close wartime collaborator on operational matters. Brown cites Zuckerman's invidious character as the main reason for his deplorable action, although political divergences must have played a role as well.

Although hard to imagine, Bernal's postwar years seemed to be characterized by an even greater pace of activities. Here, Brown shifts to a thematic rather than strictly chronological account. Doing so might well have been the only way to capture Bernal's dazzling range of concerns, even if the synchronicity of events is sometimes lost. While advising on reconstruction and on how to meet Britain's urgent need for new housing, Bernal was engaged in rebuilding his own research group at Birkbeck College London, where he had been appointed to the chair in physics shortly before the war. Rosalind Franklin's virus group revitalized the x-ray crystallography tradition, while Bernal immersed himself in the question of the origins of life and then turned to the structure of liquids. At the same time, he wrote a large tome on *Science in History* (*2*) that went through several editions. Meanwhile, his socialist commitment and his vision on the transformative role of science in a planned society, first elaborated in his highly influential *The Social Function of Science* (*3*), led to a string of invitations to lecture and advise on the status of science and technology in socialist and developing countries. He undertook extended trips to the USSR, China, India, Ghana, Chile, Argentina, and Brazil, and he exchanged views with such statesmen as Nehru, Mao, Zhou Enlai, and Ho Chi Minh. His diary entries read like a tour de force through postwar history.

Bernal's belief in the progressive force of science remained unshaken by the development of the atomic bombs, but this did not prevent him from committing himself fully to the ban of nuclear weapons. Against the backdrop of the hardening Cold War, he became a driving force in the communist-led World Peace Council. He frequently had the ear of Nikita Khrushchev and may well have had a part in convincing him to step back from the brink of nuclear war in the 1962 Cuban missile crisis.

Bernal's partisan view on the future of science in socialist countries as well as his continued championing of the Soviet Union, including his defense of Lysenko, earned him criticism from many sides. Brown consistently labels Bernal's attitude as biased and shortsighted. Although agreeing that Bernal's science and communism were two sides of the same coin, the author continues to see the political side as "counterfeit" and in the end fails to make Bernal's position understandable. Aaron Klug's view, reported in the postscript, that a progressive view of history made Bernal accept rather than simply ignore the blemishes of the Soviet regime seems more helpful here. One should

not forget that Bernal was among the few who, while admitting that World War II needed to be won, denounced the inhumane character of modern warfare. His critique of the military face of modern science and his advocacy of science for the people reach beyond the divisions of the Cold War.

References

1. A. Brown, *The Neutron and the Bomb: A Biography of Sir James Chadwick* (Oxford Univ. Press, Oxford, 1998).
2. J. D. Bernal, *Science in History* (Watts, London, 1954).
3. J. D. Bernal, *The Social Function of Science* (Routledge, London, 1939).

10.1126/science.1126642

HISTORY OF SCIENCE

Overshadowed Ports of Call

Alistair Sponsel

Now that historians have demonstrated that Charles Darwin was not converted to the principle of species transmutation until a year and a half after he visited the Galapagos, does his work there deserve its disproportionate fame? It did, after all, consume only five weeks of a five-year voyage. In *Darwin's Other Islands*, Patrick Armstrong, a geographer at the University of Western Australia and longtime scholar of Darwin's fieldwork, argues that "the Galapagos Islands were important, but they were not all-important." The book draws on a variety of manuscript sources, including the captain's log kept by Robert FitzRoy, the diary of Darwin's servant Syms Covington, and the naturalist's own notes, letters, and publications. What distinguishes Armstrong from the armada of other scholars who have worked with these documents are his own voyages. Visiting half of the roughly 40 islands that the *Beagle* did between 1831 and 1836, he has retraced Darwin's footsteps in such places as the Falklands, Tierra del Fuego, Tahiti, and Cocos Atoll. In Armstrong's view, Darwin's habit of continually comparing one location to all others he had seen meant that no single destination was decisive in his work.

During the voyage, Darwin was at least as concerned to determine the origin of each island as he was intrigued by the origin of the species that inhabited them. Armstrong gives painstaking and impressively detailed accounts of Darwin using a "leaping pole" to reach the seaward-most extent of a coral reef in search of evidence for his theory of atoll formation, making geological transects in the Falklands, and chipping rocks with his hammer at virtually every port of call. Equally vivid are the reconstructions of Darwin netting fish, calculating tree heights using a pocket sextant and a piece of string, and leaving no stool unturned in his search for dung beetles. Darwin was known as a skilled shooter, but he was also deadly with his geological hammer. As well as killing innumerable birds with it, he once used the hammer to kill a fox that he had approached while it was absorbed in watching the *Beagle*'s crew at work surveying the coastline of Chiloé, Chile. (Darwin was later to write that "this fox, more curious or more scientific, but less wise, than the generality of his brethren, is now mounted in the museum of the Zoological Society.")

The book focuses intensely on Darwin, and Armstrong interjects his own experiences only occasionally and modestly. One footnote, in the chapter on Cocos Atoll, hints that the author's ambitious itinerary might deserve its own travelogue: "[Darwin] noted that it was possible to wade from island to island across the reefs.… I was advised, when planning to do this, that if small sharks approached, I should 'kick them in the head.' The advice was sound." More characteristically, Armstrong writes, "It is humbling and instructive to … see the mineralogy of the granite just as he described it, the rounded domes with their exfoliating layers, the abundance of intruded dykes." A major payoff of Armstrong's travels appears in nearly two dozen photographs of particular species, landscapes, and geological features (such as the dykes mentioned above, at King George's Sound, Australia) that Darwin described in his field notes. Several of the book's 13 maps show the routes that Darwin may have taken on his overland rambles.

Darwin's Other Islands
by Patrick Armstrong
Continuum, London, 2004. 280 pp. $150, £75. ISBN 0-8264-7531-0.

Many readers will surely be interested in learning how Darwin's impressions of the novel landscapes and species he encountered compare with the views of present-day scientists. Armstrong supplements his field observations with insights derived from recent work in geology, biology, and ethology. Unfortunately, he lets this perspective contaminate his explanations of what Darwin was thinking in the 1830s, reading more or less confidence into Darwin's notes depending on whether the ideas sound correct by modern standards. Armstrong at one point dismisses Darwin's anthropomorphic understanding of animal behavior as something "he toyed with [that] did not stand the test of time," even though Darwin would not have viewed himself as toying with an approach to which he remained committed for more than 40 years. Of Darwin's suppositions about the crystallization of molten rock, we learn that "although his views are something of a simplification, Darwin shows himself far ahead of his time." Armstrong gives ample evidence of the detail of Darwin's observations, the inventiveness of Darwin's ideas, and their intense relevance to 19th-century science. So it seems a shame to view Darwin's complex thoughts as nothing more than "simplifications" of later theories formed in other historical circumstances.

Striking scenery. From the heights of Tahiti, Darwin viewed Moorea, "standing within smooth water and encircled by a ring of snow-white breakers."

CREDIT: YANN ARTHUS-BERTRAND/CORBIS

In deftly portraying the breadth and vigor of Darwin's study during the voyage, Armstrong makes it easy to see how the observations and collections made during those years could fuel Darwin's thoughts for the rest of his career. No doubt aided by visits to so many of Darwin's field sites, but especially as a result of the author's immersion in the manuscript sources, *Darwin's Other Islands* contains a fine-grained account of Darwin's day-to-day activities that will earn it an audience among historians. Indeed many will wish that Armstrong had extended his analysis—and arguments about the value of Darwin's comparative thinking—to the spectacularly productive time Darwin spent on the continent of South America. It is a pity that the book's price is likely to keep it out of the hands of nonspecialist readers, who would otherwise surely enjoy such a concise and energetic account of the most exciting time in Darwin's life.

10.1126/science.1127303

The reviewer is in the Department of History, Princeton University, 129 Dickinson Hall, Princeton, NJ 08544, USA. E-mail: asponsel@princeton.edu

PUBLIC HEALTH

Progress Toward Rotavirus Vaccines

New childhood vaccines against rotavirus could prevent a leading cause of death among children in the developing world and do not have the dangerous side effects of the previous version.

Umesh D. Parashar* and Roger I. Glass

Many parents and even some decision-makers in public health do not know what rotavirus is, but most pediatricians are well aware of the potentially serious consequences of this common childhood infection. Rotavirus is ubiquitous, infecting children in industrialized and developing countries in the first few years of life. Rotavirus infections cause diarrhea and vomiting that is often mild, but can be severe enough in the United States to bring more than 600,000 children to their doctors, clinics, or emergency rooms; they can lead to the hospitalization of 55,000 to 70,000 and the deaths of 20 to 60 children each year (*1*). These visits and complications incur medical and societal costs estimated at $1 billion per year. In the developing world, where access to lifesaving rehydration therapy is suboptimal, rotavirus is responsible for more fatal cases of diarrhea than any other single pathogen. Each year, the disease results in about 600,000 deaths among children or about 5% of all childhood deaths (*2*).

Recent developments with rotavirus vaccines provide great promise for the prevention of severe dehydrating diarrhea in the next generation of children. On 21 February 2006, the U.S. Centers for Disease Control and Prevention's (CDC's) Advisory Committee on Immunization Practices voted to recommend universal vaccination of infants in the United States against rotavirus diarrhea (*3*). This followed by only 2 weeks the licensure by the U.S. Food and Drug Administration (FDA) of RotaTeq (Merck Vaccines, Whitehouse Station, NJ), which is now the only rotavirus vaccine available in the United States (*4*). Another rotavirus vaccine, Rotarix [GlaxoSmithKline (GSK) Biologicals, Rixensart, Belgium], has been licensed in more than 30 countries, including the countries of the European Union (*5*). It was introduced into national immunization programs in Brazil and Panama in March 2006, and launches of a national program of immunization in Venezuela and a regional program in Mexico are expected in the near future.

These events open new opportunities for prevention and control and bring to closure a 7-year saga about vaccine safety. In 1999, the first rotavirus vaccine (Rotashield; Wyeth Lederle Vaccines, Philadelphia, PA) was abruptly removed from the U.S. market because of concerns over its association with an adverse event, intestinal obstruction (*6*). This obstruction was due to intussusception, a folding of one part of the intestine into another. Consensus estimates placed the risk for intussusception at 1 case per 10,000 children immunized with Rotashield (*7*). This risk was considered unacceptable in the United States, a country in which deaths from rotavirus are uncommon. Scientists argued that in the developing world, where about 1 in 200 children die from rotavirus disease, the benefits of vaccination far exceeded its risks, and this contention was supported by ethicists (*8*). However, in the absence of data on the effectiveness of rotavirus vaccines in developing countries and in the face of political challenges to using a vaccine withdrawn from the U.S. market, further use of Rotashield in any country was untenable.

The new rotavirus vaccines from Merck and GSK are live oral preparations that recently completed safety and efficacy testing in clinical trials (*9*, *10*). These trials, each involving more than 60,000 infants, were the largest prelicensure studies ever conducted for assessment of safety alone. Each vaccine had an efficacy of 85 to 98% against severe rotavirus disease requiring hospitalization, and each reduced gastroenteritis hospitalizations of all causes by 42 to 59%. Moreover, in both trials, vaccination was not associated with an increased risk of intussusception. Both vaccines are on their way to introduction and use in real-world immunization programs. However, despite this promising start, significant challenges remain before the full potential of rotavirus vaccines can be realized.

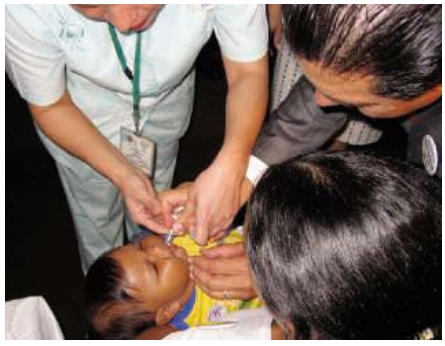

A boon for children. The president of Panama, Martin Torrijos, administers vaccine to an infant on the occasion of the national launch of the GlaxoSmithKline rotavirus vaccine in Panama, 14 March 2006.

The fundamental scientific question that remains unaddressed is whether these live oral vaccines that have worked remarkably well in affluent and middle-income countries will prove as effective in the poorest countries of Asia and Africa. Other orally administered vaccines, such as polio vaccine, cholera vaccines, and even earlier rotavirus vaccines, have each performed less favorably in these poor developing country settings (*11*–*13*). Several factors (e.g., maternal antibodies, breast-feeding, interference by other enteric pathogens, and malnutrition) might adversely affect the processing of these vaccines in the guts of infants in the developing world and could impair vaccine performance. In addition, unusual rotavirus strains that are not included in the new Merck and GSK vaccines have been detected at higher rates in some developing countries, and it is not known whether the vaccines will provide cross-protection against these strains. Thus, both RotaTeq and Rotarix will each have to demonstrate their efficacy in challenging developing country environments before the World Health Organization will recommend them for global use. Although these vaccines have not been tested simultaneously in developing and industrialized countries, as recommended after the experience with Rotashield, it is heartening to note that clinical trials of GSK's Rotarix vaccine have begun in Asia and Africa, and Merck recently committed to testing RotaTeq in the developing world.

Once these (or other) vaccines are proven efficacious against rotavirus in developing countries, the key challenges will be to provide policy-makers with data to determine the value and resources needed to finance the introduction of the vaccine and to identify mechanisms to ensure an adequate and affordable supply. The Global Alliance for Vaccines and Immunizations (GAVI) has stepped forward and has identified rotavirus as one of the two priority new vaccines (the other being pneumococcal vaccine) for accelerated development and introduction (*14*). The GAVI strategy relies on building the evidence base to evaluate vaccines through disease surveillance and key clinical trials, communicating these data to decision-makers and the public, and developing vaccine demand forecasts to ensure adequate supply. The launch price for these vaccines reflects the cost of vaccine development and expensive clinical trials and clearly puts these lifesaving vaccines out of reach for those in the developing world.

In the future, increased demand and an influx of donor funding should make it possible for manufacturers to provide their vaccines at a substantially reduced and marginal cost for children in the developing world. Although support from GAVI will help expedite early vaccine introduction, other creative financing mechanisms, such

The authors are in the Viral Gastroenteritis Section, Centers for Disease Control and Prevention, Atlanta, GA 30333, USA.

*Author for correspondence. E-mail: uap2@cdc.gov

CREDIT: PAULO FROES, UNICEF/TACRO IMMUNIZATION PLUS, PANAMA

as the recently proposed International Finance Facility (*15*) and advance purchase agreements, will be needed to ensure long-term deliverance of these vaccines to those who need them most—the world's least affluent populations. Also, 12 local manufacturers in India, Brazil, and Indonesia are already setting off to make different live oral vaccines. These efforts could increase vaccine supply and further reduce price within 3 to 7 years.

Even in industrialized countries, there are challenges, including issues of cost, awareness of rotavirus disease, and acceptance of the new vaccines in the face of safety concerns. The new vaccines initially will be expensive. The Merck vaccine (RotaTeq) has been launched in the United States at a price of $63 per dose, or $189 per child for a three-dose series, which is comparable to the current U.S. price of the vaccine against streptococcal pneumonia ($69 per dose or $276 for a complete four-dose series for young infants). The GSK vaccine (Rotarix) commands a similarly high price in private markets in Latin American and other countries. At these prices, introduction of vaccines into any national immunization program will place further stress on private and public health insurance programs for vaccine purchase. However, both companies have stated their commitment to tiered pricing, a strategy to lower the cost of vaccine substantially in the public sector markets in developing countries. In Brazil, a tiered pricing arrangement has already allowed introduction of the GSK vaccine at $7 per dose or $14 per child (*16*), making it affordable in some middle-income countries.

Few would dispute that rotavirus is one of the leading infectious causes of death among children in the developing world. However, its health burden in industrialized countries is less well appreciated. It is also not known whether and to what extent intussusception associated with the earlier Rotashield vaccine will influence the perception of providers and parents regarding the new rotavirus vaccines. Although the safety profiles in prelicensure studies of both RotaTeq and Rotarix are reassuring and should enhance vaccine acceptance, concerns might linger until additional safety data are available through postmarketing surveillance in large numbers of children.

In conclusion, the abrupt and unanticipated setback associated with Rotashield, a blow to nearly two decades of research efforts to develop rotavirus vaccines, in just 7 years has been replaced by the promise afforded by licensure and use of two new, safe, and effective rotavirus vaccines and the development of other candidates by manufacturers in developing countries. This achievement stands as a testament to the resilience and dedication of the vaccine manufacturers and the scientific community. The positive actions taken by FDA, CDC, and licensing agencies in other countries represent first steps toward making severe rotavirus diarrhea a disease of the past.

References and Notes

1. U. D. Parashar *et al.*, paper presented at the 43rd Annual Meeting of the Infectious Diseases Society of America, San Francisco, CA, 6 October 2005.
2. U. D. Parashar, C. J. Gibson, J. S. Bresee, R. I. Glass, *Emerg. Infect. Dis*. **12**, 304 (2006).
3. Centers for Disease Control and Prevention [press release] (www.cdc.gov/od/oc/media/pressrel/r060221index.htm).
4. Food and Drug Administration [press release] (www.fda.gov/bbs/topics/news/2006/NEW01307.html).
5. GlaxoSmithKline Biologicals [press release] (www.gsk.com/media/archive.htm).
6. T. V. Murphy *et al.*, *N. Engl. J. Med.* **344**, 564 (2001).
7. G. Peter, M. G. Meyers, *Pediatrics* **110**, e67 (2002).
8. C. Weijer, *BMJ* **321**, 525 (2000).
9. G. M. Ruiz-Palacios *et al.*, *N. Engl. J. Med.* **354**, 11 (2006).
10. T. Vesikari *et al.*, *N. Engl. J. Med.* **354**, 23 (2006).
11. T. J. John. *BMJ* **1**, 812 (1976).
12. M. M. Levine, *Lancet* **349**, 220 (1997).
13. R. I. Glass *et al.*, *J. Infect. Dis*. **192**, S160 (2005).
14. Global Alliance for Vaccine and Immunization (GAVI) [press release] (www.gavialliance.org/Media_Center/Press_Releases/press_110203.php).
15. Global Alliance for Vaccine and Immunization [press release] (www.gavialliance.org/Media_Center/Press_Releases/pr_IFFIm_board_21Feb2006_en.php).
16. Rotavirus Vaccine Program [newsletter] (www.rotavirus.org/Rota_Newsletter_Oct2005.html#contentBlock2).

10.1126/science.1128827

PUBLIC HEALTH

Is Polio Eradication Realistic?

Polio may be much more difficult to eradicate than smallpox. Efforts should shift from global eradication to a goal of bringing the disease under control.

Isao Arita[1]*, Miyuki Nakane[1], Frank Fenner[2]

The polio eradication campaign has been of enormous benefit to humankind, reducing the estimated 350,000 polio cases in 1988 to 1,948 in 2005. So far, it has cost $4 billion in international assistance and it has been estimated that eradication (including 3 years of follow-up) could cost another $1.2 billion (*1*, *2*). This is in sharp contrast to the experience with smallpox, for which eradication took only 10 years and international expenditure was only $100 million (1980 value) (*3*). Furthermore, we believe that global eradication is unlikely to be achieved.

The introduction of the trivalent Sabin oral vaccine (OPV) in 1962 provided a cheap and readily administered vaccine. A regional program of polio eradication was initiated in the Americas in 1985, based on the regular performance of National Immunization Days (NIDs) for all children under 5 years of age and surveillance of acute flaccid paralysis (AFP) of all children under 15 years of age. The last endemic case occurred in Peru in 1991, and regional eradication was certified by a World Health Organization (WHO) committee in 1994. Surveillance and immunization programs have been maintained, using inactivated vaccine (IPV) in North America and OPV elsewhere.

This success led the WHO to launch a global eradication program in 1988, with a target of the year 2000 for the last case. The Western Pacific region initiated its program in 1990 and, by 1997, had interrupted transmission in the region, with WHO certification in 2000.

Eradication programs in the Indian subcontinent, the Middle East, and Africa south of the Sahara were launched in the early or mid-1990s. When the target year of 2000 came, there were still 23 nations reporting cases (see table on page 853), including 9 nations where it was endemic. Intensified efforts to achieve global eradication have been made since then, but in 2005, a total of 1948 cases of poliomyelitis were reported in 16 nations. In four nations it was endemic, and six had large epidemics due to recent importations. There are four main reasons why the eradication of polio has proved so much more difficult than the eradication of smallpox: the high proportion of subclinical cases, vaccine-derived polio, population/political changes, and prolonged duration of the global program.

Subclinical cases. The most important difference between smallpox and polio that affects eradication is that in smallpox there were no subclinical cases; every infectious patient had obvious clinical disease. Smallpox vaccination could be sharply focused to small areas. In India in 1973, active village-by-village search for smallpox cases was specifically conducted and followed immediately by containment vaccination of infected villages. Within 18 months, transmission was interrupted throughout India.

There are 100 to 200 subclinical and therefore "invisible" poliovirus infections for every case of paralysis. Because every infected person excretes the virus, surveillance and containment are impossible, hence the need for NIDs. In India,

[1]Agency for Cooperation in International Health, Kumamoto-City, 862-0901, Japan. [2]The John Curtin School of Medical Research, The Australian National University, Canberra, ACT 2601, Australia.

*Author for correspondence. E-mail: arita@acih.com

although repeated rounds of NIDs were carried out between 1995 and 2005, most involving millions of children, cases have continued to be found (see table, right).

Vaccine-derived polio. The difficulties of using OPV for global eradication have recently been described (*4*). They are vaccine-associated paralytic polio (one in three million vaccines), circulating vaccine-derived polio virus (so far, five outbreak episodes with a total of 50 cases in different geographical areas), and virulent vaccine virus excreted by immune-compromised individuals (19 known cases) (*5*). A further complication is that vaccine virus may recombine with other enteroviruses; some of these recombinants have caused AFP indistinguishable from polio (*6*, *7*). Outbreaks of paralytic polio resulting from vaccine strain mutations seem to be less neuropathogenic and less transmittable. Certainly, these events require careful study, as their cause and likelihood of occurrence are unclear. In consequence, policies to be followed after termination of polio transmission are uncertain.

Changes in the world population and politics. In 1977, when the last case of smallpox occurred, the world population was 4 billion; now it is 6.2 billion, and almost all of the increase has been in the developing world, where extreme poverty has been recognized (*8*). Global eradication of infectious diseases requires "once-and-for-all" efforts by all nations; poor nations need increased investment from their limited resources, as well as assistance from outside sources.

Global coordination was easier during the Cold War period as the two superpower blocs strongly supported the smallpox program. Countrywide programs continued successfully during civil war in Nigeria, the India-Pakistan war, and the Ethiopia-Somalia war. The polio eradication program, in contrast, started approximately at the end of the Cold War and as different countries were assuming a greater degree of political independence. This had a direct influence on the polio eradication program, especially in 2003–04 in Africa, when polio vaccination was suspended in northern Nigeria because of a mistaken belief that the vaccine was unsafe (*9*). This led to extensive polio epidemics which spread to many nations in sub-Saharan Africa and Indonesia.

Duration of global eradication programs. The advantages mentioned above might give the impression that smallpox eradication was easy. It was not so. There were numerous difficulties; such as lack of transport, concealment of smallpox outbreaks by the government, guerrilla wars, chronic shortage of funds, and bureaucratic mismanagement. In 1980, D. A. Henderson, ex-WHO leader of the program, indicated, "… I realize that smallpox eradication was achieved, but just barely achieved. Had the biological and epidemiologic characteristics of the disease, or the world political situation, been even slightly more negative, the effort might have failed" (*10*).

Why, then, did smallpox eradication succeed? One reason was the short length of the program, at 10 years (*11*). In 1997, at the Dahlem Workshop on the Eradication of Infectious Diseases, Arita stated, "The duration of an eradication program should not be too long, perhaps in the range of 10–15 years…it is difficult to sustain a high level of enthusiasm throughout the period" (*11*).

It took 5 years to move from 31 nations with endemic smallpox in 1967 to 8 nations in 1973, and another 5 years to reach zero cases globally in 1977. In the polio program, 18 years have already elapsed. The eradication program succeeded in reducing the number of nations reporting polio from 150 in 1988 to the 23 in 2000 but then slowed to 16 in 2005, despite extensive synchronized campaigns in Africa (see table). By 21 March 2006, 91 total cases were reported to WHO for the year, as compared with 52 from January to March in 2005.

Poliovirus 2000–05

Country or territory	2000	2003	2005
Pakistan	199	103	28
India	265	225	66
Afghanistan	27	8	9
Nigeria	28	355	799
Somalia	46	0	185
Yemen	0	0	478
Ethiopia	3	0	22
Bangladesh	1	0	0
Niger	2	40	10
Indonesia	0	0	303
Chad	4	25	2
Angola	55	0	10
Nepal	4	0	4
Sudan	4	0	27
Mali	0	0	3
Eritrea	0	0	1
Cameroon	0	2	1
CAR	3	1	0
Côte d'Ivoire	1	1	0
Burkina Faso	0	11	0
Benin	1	2	0
Egypt	4	1	0
Ghana	1	8	0
Togo	0	1	0
Lebanon	0	1	0
DRC	28	0	0
Iran	3	0	0
Cape Verde	12	0	0
Congo	22	0	0
Myanmar	2	0	0
Iraq	4	0	0
Total	**715**	**784**	**1948**

Countries highlighted in purple are endemic in 2006 based on WHO report.

Global Eradication or Control?

The question is, should WHO proceed with its current global eradication program, in view of all the difficulties and uncertainties identified in this paper? Our answer is "No." The global eradication effort needs to be viewed in the context of the public health situation in Africa (*12*). In many sub-Saharan nations, mortality rates for children under 5 years old are ~100 to 200, as compared with 4 in Japan and 8 in the United States. A United Nations group recently concluded that the Millennium Development Goal of 70% reduction of child deaths by 2015 is too high to achieve (*13*). There are great disparities in routine immunization rates around the world; for example, 90% of children in Europe have been protected against diphtheria, pertussis, and tetanus (DPT) and measles, as compared with about 50% in sub-Saharan Africa (*14*). Vaccines are not yet available for AIDS and malaria, which represent enormous threats to the developing world.

The monetary figures for international assistance hide the reality that recipient nations, particularly poor nations in the sub-Saharan area and Indian subcontinent have to digest such assistance with extraordinary mobilization of their own health resources. Although international assistance for smallpox eradication was only $100 million for the 10-year operation, recipient nations had to spend $200 million of their own resources. We believe a similar situation has occurred and will continue in future polio eradication efforts. How can areas such as Afghanistan and the sub-Sahara cope with such enormous assistance costs? The unspoken truth is that since 2000, more than 20 poor nations could not cope. We are concerned that international assistance for polio could have negative effects on other public health efforts.

We propose an alternative for consideration by WHO and the international community. We believe the time has come for the global strategy for polio to be shifted from "eradication" to "effective control." The first priority would be to continue the current emergency measures and limit the spread of polio in Africa, the Middle East, the Indian subcontinent, and Indonesia, as well as other outbreaks which may occur in the future. The recently introduced monovalent OPV might help to achieve this goal (*1*, *15*).

As soon as the annual global number of cases is less than 500 and the number of nations with polio less than 10, all polio eradication elements should become part of the new Global Immunization, Vision, and Strategy (GIVS) program approved by WHO in 2005 (*16*). There are four major components to the GIVS strategy: "(i) protecting more people in a changing world; (ii) introducing new vaccines and technologies; (iii) integrating immunization, other health interventions, and surveillance in the health systems context; and (iv) immunizing in the context of global interdependence." Surveillance for AFP should be included in the surveillance of vaccine-preventable diseases. An international vaccine stockpile should be set up with OPV (not IPV) so that if new outbreaks occur, vaccine could rapidly be made available. OPV would continue to be used for routine vaccination in less wealthy countries until 2015, when progress toward the Millennium Development Goals will be evaluated. This strategy would sustain the benefits so far gained by the global polio program and benefit the fight against the many vaccine preventable diseases.

References and Notes

1. WHO, "Global Polio Eradication Initiative: 2004 Annual report" (WHO/VB/05.05, WHO UNICEF, IVB Document Centre, Geneva, 2005) (http://whqlibdoc.who.int/hq/2005/WHO_POLIO_05.03.pdf).
2. Funding update (www.polioeradication.org/fundingbackground.asp).
3. F. Fenner, D. A. Henderson, I. Arita, Z. Jezek, I. D. Ladnyi, *Smallpox and Its Eradication* (WHO, Geneva, 1988).
4. R. B. Aylward, R. W. Sutter, D. L. Heymann, *Science* **310**, 625 (2005).
5. O. M. Kew, R. W. Sutter, E. M. de Gourville, W. R. Dowdle, M. A. Pallansch, *Annu. Rev. Microbiol.* **59**, 587 (2005).
6. A. Nomoto, I. Arita, *Nat. Immunol.* **3**, 205 (2002).
7. M. Arita, *et al.*, *J. Virol.* **79**, 12650 (2005).
8. J. D. Sachs, in *The End of Poverty: Economic Possibilities for Our Time* (Penguin, New York, 2005), chap. 10.
9. WHO [press release] (www.who.int/mediacentre/news/releases/2005/pr49/en/index.html).
10. "Can infectious diseases be eradicated? A report on the International Conference on the Eradication of Infectious Diseases," *Rev. Infect. Dis.* **4** (5), 916 (1982).
11. I. Arita, in *The Eradication of Infectious Diseases*, W. R. Dowdle, D. R. Hopkins, Eds. (Wiley, New York, 1998), chap. 15.
12. The World Bank, *World Development Indicators 2004* (World Bank, Washington DC, 2004).
13. "Finance and economics: Recasting the case for aid." *Economist*, 22 January 2005, p. 67.
14. D. E. Bloom, D. Canning, M. Weston, *World Econ.* **6** (3), 15 (2005)
15. D. L. Heymann, R. W. Sutter, R. B. Aylward, *Nature* **434**, 699 (2005).
16. WHO, UNICEF, "GIVS global immunization vision and strategy 2006–2015" (WHO/VB/05.05, WHO UNICEF, IVB Document Centre, Geneva, 2005; (www.who.int/vaccines/GIVS/english/english.htm).
17. We are grateful for the advice from D. A. Henderson, T. Miyamura, and T. Nakano.

10.1126/science.1124959

PUBLIC HEALTH

Who Should Get Influenza Vaccine When Not All Can?

Rather than thinking only about saving the most lives when considering vaccine rationing strategies, a better approach would be to maximize individuals' life span and opportunity to reach life goals.

Ezekiel J. Emanuel* and Alan Wertheimer

The potential threat of pandemic influenza is staggering: 1.9 million deaths, 90 million people sick, and nearly 10 million people hospitalized, with almost 1.5 million requiring intensive-care units (ICUs) in the United States (*1*). The National Vaccine Advisory Committee (NVAC) and the Advisory Committee on Immunization Policy (ACIP) have jointly recommended a prioritization scheme that places vaccine workers, health-care providers, and the ill elderly at the top, and healthy people aged 2 to 64 at the very bottom, even under embalmers (*1*) (see table on page 855). The primary goal informing the recommendation was to "decrease health impacts including severe morbidity and death"; a secondary goal was minimizing societal and economic impacts (*1*). As the NVAC and ACIP acknowledge, such important policy decisions require broad national discussion. In this spirit, we believe an alternative ethical framework should be considered.

The Inescapability of Rationing

Because of current uncertainty of its value, only "a limited amount of avian influenza A (H5N1) vaccine is being stockpiled" (*1*). Furthermore, it will take at least 4 months from identification of a candidate vaccine strain until production of the very first vaccine (*1*). At present, there are few production facilities worldwide that make influenza vaccine, and only one completely in the USA. Global capacity for influenza vaccine production is just 425 million doses per annum, if all available factories would run at full capacity after a vaccine was developed. Under currently existing capabilities for manufacturing vaccine, it is likely that more than 90% of the U.S. population will not be vaccinated in the first year (*1*). Distributing the limited supply will require determining priority groups.

Who will be at highest risk? Our experience with three influenza pandemics presents a complex picture. The mortality profile of a future pandemic could be U-shaped, as it was in the mild-to-moderate pandemics of 1957 and 1968 and interpandemic influenza seasons, in which the very young and the old are at highest risk. Or, the mortality profile could be an attenuated W shape, as it was during the devastating 1918 pandemic, in which the highest risk occurred among people between 20 and 40 years of age, while the elderly were not at high excess risk (*2*, *3*). Even during pandemics, the elderly appear to be at no higher risk than during interpandemic influenza seasons (*4*).

Clear ethical justification for vaccine priorities is essential to the acceptability of the priority ranking and any modifications during the pandemic. With limited vaccine supply, uncertainty over who will be at highest risk of infection and complications, and questions about which historic pandemic experience is most applicable, society faces a fundamental ethical dilemma: Who should get the vaccine first?

The NVAC and ACIP Priority Rankings

Many potential ethical principles for rationing health care have been proposed. "Save the most lives" is commonly used in emergencies, such as burning buildings, although "women and children first" played a role on the Titanic. "First come, first served" operates in other emergencies and in ICUs when admitted patients retain beds despite the presentation of another patient who is equally or even more sick; "Save the most quality life years" is central to cost-effectiveness rationing. "Save the worst-off" plays a role in allocating organs for transplantation. "Reciprocity"—giving priority to people willing to donate their own organs—has been proposed. "Save those most likely to fully recover" guided priorities for giving penicillin to soldiers with syphilis in World War II. Save those "instrumental in making society flourish" through economic productivity or by "contributing to the well-being of others" has been proposed by Murray and others (*5*, *6*).

The save-the-most-lives principle was invoked by NVAC and ACIP. It justifies giving top priority to workers engaged in vaccine production and distribution and health-care workers. They get higher priority not because they are intrinsically more valuable people or of greater "social worth," but because giving them first priority ensures that maximal life-saving vaccine is produced and so that health care is provided to the sick (*7*). Consequently, it values all human life equally, giving every person equal consideration in who gets priority regardless of age, disability, social class, or employment (*7*). After these groups, the save-the-most-lives principle justifies priority for those predicted to be at highest risk of hospitalization and dying. We disagree with this prioritization.

Life-Cycle Principle

The save-the-most-lives principle may be justified in some emergencies when decision urgency makes it infeasible to deliberate about priority rankings and impractical to categorize individuals into priority groups. We believe that a life-cycle allocation principle (see table on page 855) based on the idea that each person should have an opportunity to live through all

Department of Clinical Bioethics, The Clinical Center, National Institutes of Health, Bethesda, MD 20892–1156, USA.

The opinions expressed are the authors' and do not reflect the policies of the National Institutes of Health, the Public Health Service, or the Department of Health and Human Services.

*Author for correspondence. E-mail: eemanuel@nih.gov

Priorities for Distribution of Influenza Vaccine

Tier*	NVAC and ACIP recommendations (subtier)†	Life-cycle principle (LCP)	Investment refinement of LCP including public order
1	Vaccine production and distribution workers Frontline health-care workers People 6 months to 64 years old with ≥2 high-risk conditions or history of hospitalization for pneumonia or influenza Pregnant women Household contacts of severely immunocompromised People Household contacts of children ≤6 months of age Public health and emergency response workers Key government leaders	Vaccine production and distribution workers Frontline health-care workers	Vaccine production and distribution workers Frontline health-care workers
2	Healthy people ≥65 years old People 6 months to 64 years old with 1 or more high-risk conditions Healthy children 6 months to 23 months old Other public health workers, emergency responders, public safety workers (police and fire), utility workers, transportation workers, telecommunications and IT workers	Healthy 6-month-olds Healthy 1-year-olds Healthy 2-year-olds Healthy 3-year-olds etc.	People 13 to 40 years old with <2 high-risk conditions, with priority to key government leaders; public health, military, police, and fire workers; utility and transportation workers; telecommunications and IT workers; funeral directors People 7 to 12 years old and 41 to 50 years old with <2 high-risk conditions with priority as above People 6 months to 6 years old and 51 to 64 years old with <2 high-risk conditions, with priority as above‡ People ≥65 years old with <2 high-risk conditions
3	Other health decision–makers in government Funeral directors	People with life-limiting morbidities or disabilities, prioritized according to expected life years	People 6 months to 64 years old with ≥2 high-risk conditions
4	Healthy people 2 to 64 years old		People ≥65 years old with ≥2 high-risk conditions

** Tiers determine priority ranking for the distribution of vaccine if limited in supply. †Subtiers in purple text establish who gets priority within the tier (starting from the top of the tier) if limited vaccine cannot cover everyone in the tier; prioritization may occur within subtiers as well. ‡ Children 6 months to <13 years would not receive vaccine if they can be effectively confined to home or otherwise isolated.*

the stages of life is more appropriate for a pandemic (*8*, *9*). There is great value in being able to pass through each life stage—to be a child, a young adult, and to then develop a career and family, and to grow old—and to enjoy a wide range of the opportunities during each stage.

Multiple considerations and intuitions support this ethical principle. Most people endorse this principle for themselves (*8*, *9*). We would prioritize our own resources to ensure we could live past the illnesses of childhood and young adulthood and would allocate fewer resources to living ever longer once we reached old age (*9*). People strongly prefer maximizing the chance of living until a ripe old age, rather than being struck down as a young person (*10*, *11*).

Death seems more tragic when a child or young adult dies than an elderly person—not because the lives of older people are less valuable, but because the younger person has not had the opportunity to live and develop through all stages of life. Although the life-cycle principle favors some ages, it is also intrinsically egalitarian (*7*). Unlike being productive or contributing to others' well-being, every person will live to be older unless their life is cut short.

The Investment Refinement

A pure version of the life-cycle principle would grant priority to 6-month-olds over 1-year-olds who have priority over 2-year-olds, and on. An alternative, the investment refinement, emphasizes gradations within a life span. It gives priority to people between early adolescence and middle age on the basis of the amount the person invested in his or her life balanced by the amount left to live (*12*). Within this framework, 20-year-olds are valued more than 1-year-olds because the older individuals have more developed interests, hopes, and plans but have not had an opportunity to realize them (*11*, *12*). Although these groupings could be modified, they indicate ethically defensible distinctions among groups that can inform rationing priorities.

One other ethical principle relevant for priority ranking of influenza vaccine during a pandemic is public order. It focuses on the value of ensuring safety and the provision of necessities, such as food and fuel. We believe the investment refinement combined with the public-order principle (IRPOP) should be the ultimate objective of all pandemic response measures, including priority ranking for vaccines and interventions to limit the course of the pandemic, such as closing schools and confining people to homes. These two principles should inform decisions at the start of an epidemic when the shape of the risk curves for morbidity and mortality are largely uncertain.

Like the NVAC and ACIP ranking, the IRPOP ranking would give high priority to vaccine production and distribution workers, as well as health-care and public health workers with direct patient contact. However, contrary to the NVAC and ACIP prioritization for the sick elderly and infants, IRPOP emphasize people between 13 and 40 years of age. The NVAC and ACIP priority ranking comports well with those groups at risk during the mild-to-moderate 1957 and 1968 pandemics. IRPOP prioritizes those age cohorts at highest risk during the devastating 1918 pandemic. Depending on patterns of flu spread, some mathematical models suggest that following IRPOP priority ranking could save the most lives overall (*13*).

Conclusions

The life-cycle ranking is meant to apply to the situation in the United States. During a global pandemic, there will be fundamental questions about sharing vaccines and other interventions with other countries. This raises fundamental issues of global rationing that are too complex to address here.

Fortunately, even though we are worried about an influenza pandemic, it is not upon us. Indeed, the current H5N1 avian flu may never develop into a human pandemic. This gives us time both to build vaccine production capacity to minimize the need for rationing and to rationally assess policy and ethical issues about the distribution of vaccines.

References and Notes

1. U.S. Department of Health and Human Services (HHS), *HHS Pandemic Influenza Plan* (HHS, Washington, DC, 2005), supplement E at (www.hhs.gov/pandemicflu/plan/) (accessed 29 March 2006).
2. S. D. Collin, *Public Health Rep.* **60**, 853 (1945).
3. D. R. Olson, L. Simonsen, P. J. Edelson, S. S. Morse, *Proc. Natl. Acad. Sci. U.S.A.* **102**, 11059 (2005).
4. L. Simonsen *et al.*, in *The Threat of Pandemic Influenza: Are We Ready?* S. L. Knobler *et al.*, Eds. (National Academies Press, Washington, DC, 2004).
5. C. J. L. Murray, A. D. Lopez, Eds., *The Global Burden of Disease* (World Health Organization, Geneva, 1996).
6. C. J. L. Murray, A. K. Acharya, *J. Health Econ.* **16**, 710 (1997).
7. R. Dworkin, in *Taking Rights Seriously* (Harvard Univ. Press, Cambridge, MA, 1978), pp. 150–205.
8. A. Williams, *Health Econ.* **6**, 117 (1997).
9. N. Daniels, in *Am I My Parents' Keeper?* (Oxford Univ. Press, New York, 1988), pp. 66–102.
10. M. L. Cropper, S. K. Aydede, P. R. Portney, *J Risk Uncertainty* **8**, 243 (1994).
11. M. Johannesson, P. O. Johansson, *J. Health Econ.* **16**, 589 (1997).
12. R. Dworkin, in *Life's Dominion* (Knopf, New York, 1993), pp.68–101.
13. M. E. Halloran, I. M. Longini Jr., *Science* **311**, 615 (2006).

14. We thank A. Fauci, A. Friedman, B. Gellin, M. Gottesman, C. Grady, B. Krohmal, S. Pearson, B. Schwartz, L. Simonsen, and the Department of Clinical Bioethics.

10.1126/science.1125347

SYMPOSIUM ANNOUNCEMENT

The Changing Landscape of Vaccine Development: Vaccines for Global Health

November 8-10, 2006 – Moody Gardens Convention Center, Galveston, Texas

The Sealy Center for Vaccine Development at The University of Texas Medical Branch in Galveston, in conjunction with the James W. McLaughlin Foundation, is proud to announce the second in a series of symposia centered around the theme of, The Changing Landscape of Vaccine Development. This second symposium is entitled, Vaccines for Global Health. Focusing on the progression of vaccine development from the bench to the bedside to the global community, this symposium will bring together experts from the fields of immunology, pathogenesis, adjuvant systems, preclinical development, clinical trials, epidemiology, risk assessment, finance, governmental regulation, and vaccine acceptance.

Session Topics

Vaccines for Zoonotic Diseases; Vaccines for Special Populations; Vaccines for Developing Countries; Therapeutic Vaccines

Confirmed Speakers

James R. Baker Jr., M.D.	**University of Michigan**
Eliav Barr, M.D.	**Merck**
David Bernstein, M.D.	**University of Cincinnati**
John Clemens, M.D.	**International Vaccine Institute**
Roy Curtiss III, Ph.D.	**Biodesign Institute**
John Donnelly, Ph.D.	**Chiron**
D. Mark Estes, Ph.D.	**University of Texas Medical Branch**
Fernando Guerra, M.D.	**San Antonio Metropolitan Health District**
Michael Houghton, Ph.D.	**Chiron**
William R. Jacobs Jr., Ph.D.	**Albert Einstein College of Medicine**
Jean Lang, M.D.	**Sanofi Pasteur**
Thomas P. Monath, M.D.	**Acambis**
Martin G. Myers, M.D.	**University of Texas Medical Branch**
Michael N. Oxman, M.D.	**University of California, San Diego**
Jean Paul Prieels, Ph.D.	**GlaxoSmithKline**
Connie Schmaljohn, Ph.D.	**USAMRIID**
Lawrence R. Stanberry, M.D., Ph.D.	**University of Texas Medical Branch**
Professor Margret Stanley	**Cambridge University**

UTMB
Sealy Center for Vaccine Development
The University of Texas Medical Branch

http://www.utmb.edu/scvd

ECOLOGY

Photosymbiosis and the Evolution of Modern Coral Reefs

The algae in coral reefs do not leave behind fossils, so deciphering their coevolution with corals is difficult. Isotope measurements can help reveal these ancient relationships.

George D. Stanley Jr.

Symbiosis is the most relevant and enduring biological theme in the history of our planet. Photosymbiosis—whereby photosynthetic microorganisms (symbionts) live inside an animal (host), deriving benefits, sometimes mutual—is found today among calcifying foraminifers and giant clams but is best exemplified in corals, the master builders of reefs. Photosymbiosis fosters diversity and novel adaptations. Recent studies on global change, coral degradation, and the future of coral reefs highlight the relevance of photosymbiosis to reef evolution (*1*–*3*).

Living corals called scleractinians, along with algae and other calcifying organisms on reefs, extract $CaCO_3$ from seawater, secreting it in massive skeletons collectively known as reefs. Reefs initiate voluminous carbonate deposition, affect ocean chemistry, and even mediate climate. Behind rapid reef growth are photosynthetic algae, especially the dinoflagellate genus *Symbiodinium* or zooxanthellae. These symbionts enhance calcification rates orders of magnitude faster than in most nonzooxanthellate species, allowing their hosts to dominate choice places on the reef. Living safely encysted within coral tissue, zooxanthellae use the host's CO_2 and nitrogenous wastes. Zooxanthellae photosynthesize carbon and transport it intracellularly to the coral, supplementing 90% of the coral's nutrition, thus resolving the paradox of why so much life flourishes on nutrient-deficient reefs (*4*). The obligate relationship restricts corals to shallow-water tropics where they modify their shapes to maximize sunlight. Protecting corals from damaging ultraviolet radiation, their symbionts even manufacture "sunscreen."

A majority of living corals are zooxanthellate and build reefs. Deciphering fossil zooxanthellate corals is problematic because symbionts aren't preserved. Symbiosis is inferred from colony size and shapes indicating light adaptation, corallite size and integration, and skeletal characteristics. Such indirect assessments relegate zooxanthellate presence to a working hypothesis. Carbon and oxygen isotopes fractionated within modern and Mesozoic coral skeletons provide quantitative methods for detecting zooxanthellae, thus serving as a proxy for photosymbiosis (*5*).

End-Permian mass extinctions decimated reefs and Paleozoic corals. Scleractinians appeared in the Middle Triassic some 8 to 10 million years later, evolving from anemone-like ancestors (*6*). Small and non–reef-building, these early corals were surprisingly diverse and integrated. Succeeding middle and early Late Triassic species remained non–reef-building. Vigorous Late Triassic (Carnian-Norian) biotic turnover and adaptive radiation culminated in the evolution of coral-framework reefs (*7*). The hypothesis that the coevolution of coral-zooxanthellate symbiosis occurred at this time is supported by skeletal stable isotopes and organic matrix analyses (*5*, *8*). Both techniques yielded positive signals for Carnian-Norian photosymbiosis. The Triassic-Jurassic dinoflagellate-cyst family Suessiacea is closely related to zooxanthellae. Triassic occurrence and increasing diversity of these dinoflagellates coincide in space and time with those of reef-building scleractinians, suggesting their coevolution (*9*). End-Triassic mass extinctions witnessed sudden reef collapse and an 8- to 10-million-year reef eclipse. Coral species suffered 98% losses followed by Jurassic coral reorganization (*7*), a trend reflected also among Suessiacea.

Reef building. Colorful life teems on a Pacific coral reef where diverse ecosystems flourish in otherwise nutrient-deficient waters. This reef and others like it owe their existence to symbiosis between algae and corals.

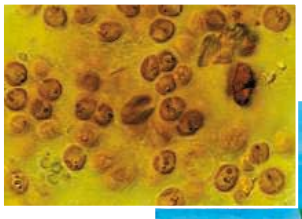

Mutual benefits. Artist's view of a living reef coral cut to reveal a polyp and massive white skeleton. Soft polyps cover the entire surface of the colony and contain a profusion of microscopic symbiotic algae (zooxanthellae). (**Upper left**) A photomicrograph of zooxanthellae cells. They live encysted in the coral's tissues, enhancing metabolism and calcification.

The author is at the University of Montana Paleontology Center, Missoula, MT 59812, USA. E-mail: george.stanley@umontana.edu

Middle and Late Jurassic reefs reveal two major radiations and coral expansions. Zooxanthellate-like seasonal growth bands and indirect criteria categorize most corals as photosymbiotic, but inexplicably, symbiosis in Triassic and Jurassic corals does not appear as efficient as in modern counterparts (*7*, *10*). Zooxanthellate and nonzooxanthellate corals existed during Cretaceous time, but reefs gradually became dominated by coral-mimicking rudistid bivalves. Zooxanthellate corals maintained diversity but rarely built reefs. Before the Cretaceous/Tertiary mass extinction, rudistids and shallow reefs died out as many ecosystems collapsed in stepwise fashion. Across the extinction boundary, greater numbers of zooxanthellates versus nonzooxanthellates perished (*11*). A 17-million-year early Tertiary reef eclipse, followed by recovery and several Paleogene biotic turnovers, led to modern reef ecosystems of the Neogene (*12*).

Reef death. Bleached Caribbean elkhorn reef coral, *Acropora palmata*, turns ghostly white when photosymbiotic algae are lost. Whether this "white death" is the beginning of the end for reefs is currently debated, underscoring the relevance of photosymbiosis for modern reef evolution.

Throughout Phanerozoic history, reefs frequently collapsed during mass extinctions, with eclipses lasting 8 to 20 million years (*13*). Collapses and recoveries were postulated to correlate with symbiont loss and symbiosis renewal, respectively (*11*, *12*, *14*). Global warming-cooling cycles, sea-level change, acid rain, eutrophication, and sunlight reduction—all of which have been proposed to accompany Mesozoic reef extinctions—appear inimical to zooxanthellae-coral symbiosis. High nutrient levels interpreted for some Paleozoic reefs don't fit this model (*15*), but post-Paleozoic nutrient-limited reef settings may do so.

Evidence of ancient reef collapse validates concerns about susceptibility of present-day reefs to climate change, bleaching, coral diseases, and nutrification—all of which involve zooxanthellae. Perceptions of coral reef fragility seem paradoxical given the resilience of Tertiary corals and rapid reef recoveries, especially after staggering Neogene upheavals, climate swings, and sea-level changes (*12*, *13*). Answers to this enigma may lie in discoveries that living zooxanthellae belong not in one species but rather combinations of diverse clades with different symbionts adapted dynamically to changing light and temperature regimes (*2*, *16*). Coral bleaching, traditionally thought detrimental, may actually be adaptive (*17*). Expulsion of less desirable symbionts in favor of more tolerant ones after environmental change would explain reef resiliency, allowing necessary adaptations to survive extinction (*18*). Brooding corals transmit zooxanthellae directly to offspring, whereas broadcasting spawners acquire symbionts from seawater, the latter promoting greater partner recombinations. Symbiont evolution among corals with geographic range expansions, driven by climatic fluctuations, could explain their adaptability and success (*19*). Coral-zooxanthellae symbiosis initially may have coevolved loosely, dissolving when advantages decreased, like the rare facultative (apozooxanthellate) corals today. If early corals lacked modern symbiont adaptations, this could account for their limited Mesozoic success (*7*, *10*). Considering symbiosis dynamics, perhaps algae and not corals are the masters of the reef. Future insights into the coevolution of photosymbiosis in both ecologic and geologic time should arise from a synthesis and integration of ideas from paleobiology, life histories, and genetics.

References

1. E. E. Sotka, R. W. Thacker, *Trends Ecol. Evol.* **20**, 59 (2005).
2. C. A. Chen *et al.*, *Mar. Ecol. Prog. Ser.* **295**, 113 (2005).
3. O. Hoegh-Guldberg, *J. Geophys. Res.* **110**, 1029 (2005).
4. P. Hallock, W. Schlager, *Palaios* **1**, 389 (1986).
5. G. D. Stanley Jr., P. K. Swart, *Paleobiology* **21**, 179 (1995).
6. G. D. Stanley Jr., D. G. Fautin, *Science* **291**, 1913 (2001).
7. E. Flügel, in *Phanerozoic Reef Patterns*, E. Flügel, W. Kiessling, J. Golonka, Eds. (SEPM, Tulsa, OK, 2002), pp. 391–463.
8. L. Muscatine *et al.*, *Proc. Natl. Acad. Sci. U.S.A.* **102**, 1525 (2005).
9. R. B. Palliani, J. B. Riding, *J. Micropaleontol*. **19**, 133 (2000).
10. R. R. Leinfelder, in *The History and Sedimentology of Ancient Reef Systems*, G. D. Stanley Jr., Ed. (Kluwer/Plenum, New York, 2001), pp. 251–309.
11. B. R. Rosen, D. Turnsek, *Mem. Assoc. Aust. Palaeontol.* **8**, 355 (1989).
12. C. Perrin, in *Phanerozoic Reef Patterns*, E. Flügel, W. Kiessling, J. Golonka, Eds. (SEPM, Tulsa, OK, 2002), pp. 587–621.
13. P. Copper, *Can. Soc. Petrol. Geol. Mem.* **13**, 271 (1989).
14. J. A. Talent, *Senckenb. Leth.* **69**, 315 (1988).
15. R. Wood, *Reef Evolution* (Oxford Univ. Press, Oxford, 1999).
16. R. Rowan, *Nature* **430**, 742 (2004).
17. D. G. Fautin, R. W. Buddemeier, *Hydrobiologia* **530–531**, 459 (2004).
18. A. C. Baker, C. J. Starger, T. R. McClanahan, P. W. Glynn, *Nature* **430**, 741 (2004).
19. T. C. LaJeunesse, *Mol. Biol. Evol.* **22**, 570 (2004).

10.1126/science.1123701

PLANT SCIENCE

Auxin Transport, but in Which Direction?

Tobias Sieberer and Ottoline Leyser

Many aspects of plant growth depend on transport of the hormone auxin across tissues, directed by specific transporter proteins .

The plant hormone auxin has remarkably diverse roles in the regulation of growth and development. Auxin, synthesized in shoot apices, is moved along specific transport routes through the plant by unique polar transport machinery (*1*). Polar auxin flow is primarily dependent on polar efflux from cells, with the resultant directed transport providing a constant stream of information. Auxin flow can be influenced by both exogenous and endogenous stimuli, triggering redistribution of auxin and specific growth and developmental responses. This intercellular communication system is conceptually similar to the animal nervous system, and its transmission rate of 1 cm/hour is fast enough for systemic signaling in a sessile organism.

Over the past decade, several classes of integral membrane proteins have been implicated in auxin flow. Mutations in these protein families perturb auxin distribution, causing diverse phenotypes, but their interrelationships and the biochemical basis for their action have remained obscure. On page 914 of this issue, Petrášek *et al.* (*2*) provide long-awaited evidence that PIN-FORMED (PIN) proteins act directly in transporting auxin out of cells, substantially independently of the PGP family of auxin pumps. Moreover, on page 883, Wiśniewska *et al.* report that polar PIN localization in cells is a primary determinant of the direction of auxin efflux (*3*). And, coming in from the opposite direction, a third report by Dharmasiri *et al.* in this week's *Science* Express (*4*) identifies a candidate regulator for the localization of AUX1, a protein that mediates cellular influx of auxin.

The PIN-FORMED family was so named because mutations in one family member,

The authors are in the Department of Biology, University of York, York YO10 4YW, UK. E-mail: ts20@york.ac.uk; hmol1@york.ac.uk

PIN1, result in failed lateral organ formation at the shoot apex of *Arabidopsis thaliana*, causing a pinlike shoot. PIN proteins are polarly localized in cells in positions correlating with auxin flow, and PIN-like phenotypes result from treatment with inhibitors of polar auxin transport, such as 1-*N*-naphthylphthalamic acid (NPA) (*1*). Although these and many other observations support a key role for PINs in auxin transport, their biochemical function has been difficult to establish definitively, earning them the delightfully noncommittal title of "auxin transport facilitator."

Meanwhile, there is evidence that the PGP family of transmembrane proteins transports auxin directly (*5*): The *Arabidopsis* proteins PGP1 and PGP19 bind NPA; PGP1 stimulates NPA-sensitive auxin efflux from plant and nonplant cells; and *pgp1/pgp19* mutants show reduction in both auxin transport and NPA binding. However, PGP proteins are often not polarly localized in cells that have directed transport of auxin, and loss of PGP function results in phenotypes that are different from those created by auxin transport inhibitor treatment.

It has been known for many years that NPA does not compete with auxin for binding to membranes. Moreover, NPA binding can be separated from auxin efflux inhibition by protein synthesis inhibitors, which suggests that the auxin efflux machinery consists of at least three separate elements: an NPA-binding component that acts through an unstable transmitter subunit to regulate an efflux catalyst (*1*). These ideas of a multisubunit efflux complex have fueled speculation about the roles of PINs and PGPs.

To resolve the biochemical function of PINs and their relationship with PGPs, Petrášek *et al.* established an inducible expression system in *Arabidopsis* and tobacco cell suspension cultures. Previous evidence that PIN2 has auxin efflux activity in yeast could not exclude the possibility of PIN action as a regulatory component of a complex with conserved elements in yeast (*6*, *7*). The cell suspension system described by Petrášek *et al.* allows more definitive analysis through quantification of substrate specificity, affinity range, inhibitor sensitivity, and transport kinetics. The authors show that increasing PIN protein expression proportionately increases auxin efflux, which is both NPA-sensitive and auxin-specific. Moreover, PIN expression in yeast and mammalian cells confers increased auxin transport, although with reduced specificity. Taken together, these experiments support a direct catalytic role for PINs in auxin transport while substantiating the need for plant-specific cofactors that define substrate specificity. These findings should satisfy all but the most doubting Thomas that PINs deserve the title "auxin efflux carrier."

But if PINs can do all this, what is the role of PGPs? The authors show that PGP-mediated auxin transport is less sensitive than PIN-mediated efflux to NPA, and that the ability of PIN1 to function in plants does not require PGP proteins, excluding direct functional interdependence. These findings suggest that PGP and PIN proteins act as distinct auxin efflux carriers (see the figure). Interestingly, computational simulations suggest that the establishment of PIN-mediated auxin transport routes across a field of cells with high auxin concentration and flux may depend on the ability of surrounding tissues to export auxin at a basal level. If this is the case, nonlocalized carriers such as PGPs may have this role (*5, 8*).

Emphasizing further the importance of PINs, Wiśniewska *et al.* bolster the evidence that PIN polarity determines the direction of auxin flow. The authors exploit a serendipitous property of a PIN1 variant that is tagged with green fluorescent protein—when expressed in root epidermal cells, it localizes at the opposite end of the cell to its hemagglutinin-tagged progenitor. Flipping the orientation of PIN1 in this way also flips the direction of auxin flow.

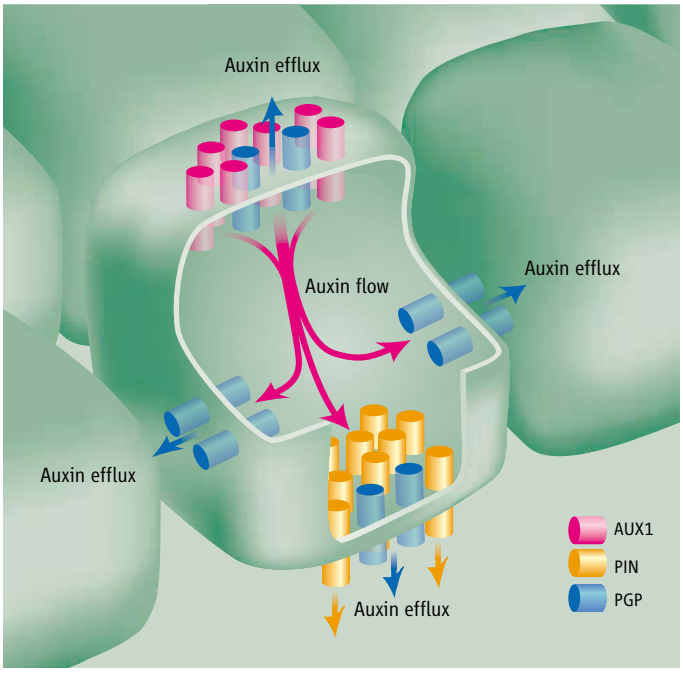

Auxin transport routes. A schematic of a hypothetical plant cell in which the directed flow of auxin is controlled by the polarized localization of PIN, an efflux carrier. Polar localization of AUX1, an auxin influx carrier, prevents dissipation of auxin gradients set up by PIN action, and PGPs are likely required for rapid movement of auxin through the tissue.

These data provide confidence that PIN orientation in the cell predicts auxin flow. However, they also spotlight our woefully inadequate understanding of the mechanism of PIN localization. Apparently, both cell type–specific and PIN protein–specific elements are involved. For example, in the root epidermis, PIN2 is oriented at the shoot end of cells (here called apical), whereas in the root cortex it is localized basally. PIN1 is also basally localized in cortical cells. When expressed from the *PIN2* promoter in the epidermis, PIN1 retains its basal orientation; however, in *pin2* mutants, the domain of PIN1 expression expands into the epidermis, and in this case it orients apically, partially replacing PIN2 function (*3*, *9*, *10*).

We have almost no mechanistic understanding of this complex phenomenology. There are numerous indications that auxin itself is involved: PINs can orient toward high auxin concentration; auxin regulates transcription of the PID protein kinase, overexpression of which can flip PIN polarity (*11*); and auxin can influence the cycling of PINs between the cell membrane and intracellular compartments (*12*). This latter phenomenon of active PIN cycling appears to be central to PIN function and is a target for NPA-mediated auxin transport inhibition (*13*). Consistent with this idea, *Arabidopsis* plants mutated in a protein similar to those required for neurotransmitter release in animals have reduced NPA binding and altered PIN trafficking (*14*). Thus, additional components are clearly needed to provide regulated directionality and auxin specificity. These elusive functions now top the most-wanted list.

Meanwhile, Dharmasiri *et al.* have identified a protein required for the localization of AUX1, a protein recently shown to have influx carrier activity (see the figure) (*15*). AUX1 has sequence similarity to amino acid permeases and exhibits polar subcellular localization in some auxin-transporting tissues (*16*). Auxin is a weak acid (indole acetic acid) and the fraction that becomes protonated at extracellular pHs can diffuse directly into cells. But much more rapid uptake is needed in some tissues to prevent diffusion of auxin in the extracellular wall space and dissipation of auxin gradients across tissues (*8*). Loss of AUX1 results in root phenotypes that include resistance to all but the most weakly acidic auxin analogs, as well as a greatly reduced root growth response to gravity. The *axr4* auxin-resistant *Arabidopsis*

mutant is phenotypically similar to the *aux1* mutant, which suggests that both genes act in the same process. Dharmasiri *et al.* now provide an explanation for this phenotypic similarity by identifying AXR4 as an endoplasmic reticulum–resident protein required for proper AUX1 sorting to the plasma membrane. AXR4 appears specific for AUX1 trafficking, because other membrane proteins such as the PINs are not mislocalized in the *axr4* mutant. Interestingly, in the root tissues examined, the only cell types affected by the *axr4* mutation were those in which AUX1 localization is polar. In the lateral root cap, where AUX1 is uniformly distributed, there are no obvious effects in the *axr4* mutant background, whereas in the epidermis and protophloem where AUX1 is polarly localized, AUX1 is retained in the endoplasmic reticulum. This suggests that AXR4 plays a specific tissue-dependent role in the polar sorting of AUX1 to a particular plasma membrane face, rather than a general chaperone-like function. The biochemical basis for AXR4 action is not yet clear. Apart from a predicted transmembrane motif and a putative α/β hydrolase fold, AXR4 does not contain any known protein domains.

These discoveries demonstrate clear tissue-specific elements in the membrane targeting of both PIN and AUX1. So far, however, there is no evidence of any coordination of these events, although there is some suggestion of common elements because both are sensitive to the protein traffic inhibitor brefeldin A (*13*, *17*). As the mechanisms for polar localization of these proteins are revealed, it will be interesting to see the extent to which they are independent.

References

1. D. A. Morris, J. Friml, E. Zazimalova, *Biosynthesis, Signal Transduction, Action*, P. J. Davies, Ed. (Kluwer Academic, Dordrecht, Netherlands, 2004), pp. 437–470.
2. J. Petrášek *et al.*, *Science* **312**, 914 (2006); published online 6 April 2006 (10.1126/science.1123542).
3. J. Wiśniewska *et al.*, *Science* **312**, 883 (2006); published online 6 April 2006 (10.1126/science.1121356).
4. S. Dharmasiri *et al.*, *Science*, 11 May 2006 (10.1126/science.1122847).
5. J. J. Blakeslee, W. A. Peer, A. S. Murphy, *Curr. Opin. Plant Biol.* **8**, 494 (2005).
6. R. Chen *et al.*, *Proc. Natl. Acad. Sci. U.S.A.* **95**, 15112 (1998).
7. C. Luschnig, R. A. Gaxiola, P. Grisafi, G. R. Fink, *Genes Dev.* **12**, 2175 (1998).
8. E. M. Kramer, *Trends Plant Sci.* **9**, 578 (2004).
9. I. Blilou *et al.*, *Nature* **433**, 39 (2005).
10. A. Vieten *et al.*, *Development* **132**, 4521 (2005).
11. J. Friml *et al.*, *Science* **306**, 862 (2004).
12. T. Paciorek *et al.*, *Nature* **435**, 1251 (2005).
13. N. Geldner *et al.*, *Nature* **413**, 425 (2001).
14. P. Gil *et al.*, *Genes Dev.* **15**, 1985 (2001).
15. S. Swarup *et al.*, *Genes Dev.* **15**, 2648 (2001).
16. Y. Yang *et al.*, *Curr. Biol.*, in press.
17. S. Swarup *et al.*, *Genes Dev.* **15**, 2648 (2001).
18. M. Grebe *et al.*, *Curr. Biol.* **12**, 329 (2002).

10.1126/science.1127659

MATERIALS SCIENCE

Toward Devices Powered by Biomolecular Motors

Biomolecular motors can be used in nanometer-scale devices to perform mechanical work. This approach will assist the development of active nanostructures.

Henry Hess

Biomolecular motors, such as the motor protein kinesin, convert chemical energy derived from the hydrolysis of individual adenosine triphosphate (ATP) molecules into directed, stepwise motion (*1*). This process enables them to actively transport designated cargo—such as vesicles, RNA, or viruses—to predetermined locations within cells. For engineers, active transport in biology inspires visions of nanofluidic systems for biosensing, of active materials that can rearrange their components, and of molecular conveyor belts and forklifts for nanometer-scale manufacturing.

Enhanced online at www.sciencemag.org/cgi/content/full/312/5775/860

Nanofluidic devices, which extend the lab-on-a-chip paradigm to systems with picoliter volumes and submicrometer channel diameters, present an immediate opportunity for the application of biomolecular motors. On page 910 of this issue, van den Heuvel *et al*. (*2*) show that kinesin motor proteins can drive the directed transport of microtubules (filamentous assemblies of thousands of tubulin proteins) in closed channels with submicrometer dimensions. Controlled application of an external electric field steers the microtubules into either one of two arms of a Y junction (see the figure).

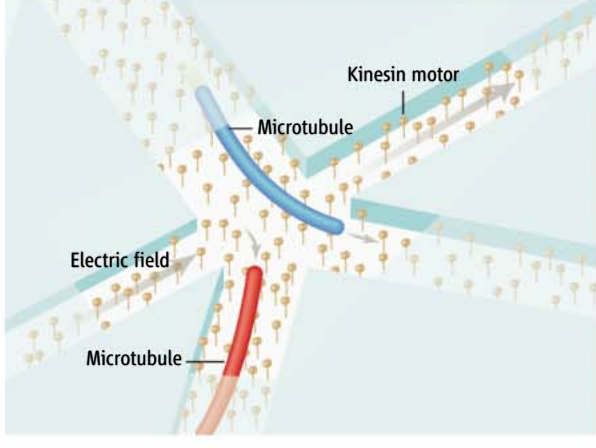

Nanofluidics with molecular motors. In van den Heuvel *et al.*'s work (*2*), an electric field is used to steer the microtubules into one of two arms of a Y junction; the microtubules move perpendicular to the field. The microtubules are transported by kinesin motor proteins.

The setup is an adaptation of the classic gliding motility assay (*3*), in which the kinesin motor proteins adhere to a surface via their rotationally flexible tails, bind to the leading ends of approaching microtubules with their two heads, and move the microtubules by stepping forward with alternating heads until they reach the trailing end and detach. In biological systems, the motors move and the microtubules are stationary. The key advantages of the inverted geometry used in the assay are that the microtubules are continuously bound to the surface over transport distances of more than a millimeter (*4*) and that the large microtubule allows the attachment of fluorescence tags for observation and of specific linkers for cargo binding (*5*).

Open or micrometer-scale closed channels have previously been fabricated to confine microtubule movements (*6*–*8*). Van den Heuvel *et al*. have now created closed channels with submicrometer dimensions. The channels not only provide better confinement, but they also mimic the dimensions of axons, in which motor–driven transport plays a central role. They may thus enable more realistic model studies at the system level of active transport in biology. Electric fields for active steering provide direct control over the paths of individual microtubules. By coupling fluorescence detec-

The author is in the Department of Materials Science and Engineering, University of Florida, Gainesville, FL 32611, USA. E-mail: hhess@mse.ufl.edu

CREDIT: P. HUEY/*SCIENCE*

tion of microtubules with this control mechanism, van den Heuvel *et al*. have integrated optics, electronics, and molecular transport, thus introducing an element of real-time programmability.

This work is related to efforts by several teams of bioengineers to envision molecular motor–based technology and build proof-of-principle devices that radically depart from current engineering concepts (*9*). For example, minute volumes of biological samples can now be rapidly analyzed in credit-card–sized microfluidic devices connected to desktop-scale peripheral instruments. Downscaling of the lateral device dimensions by a factor of 100 would result in dust-particle–sized devices reminiscent of unicellular organisms. These devices would not necessarily be useful as as microscopic extensions of macroscopic peripheral devices, but would rather lend themselves to the application of the "smart dust" concept: smart dust biosensors would be immersed in the liquid sample of interest, independently perform an analysis, and be read out collectively to generate a statistically significant signal. Biomolecular motors that coat the inner surfaces of such devices and use dissolved ATP fuel as an energy source would drive the internal transport and remove the need for peripheral pumps and batteries (*10*).

In addition to fulfilling transport functions, biomolecular motors can exert localized forces on nanostructures. They can thus cause conformational changes, such as the stretching of coiled DNA molecules into a linear configuration (*11*) or the rupture of intermolecular bonds. Molecular motors could thus push supramolecular assembly and disassembly processes away from chemical equilibrium and generate dynamic, nonequilibrium structures (*12*). The force exerted by motor proteins could also be exploited in nanorobotics, where the sequential examination or manipulation of molecules by scanning probe microscopes and optical tweezers could be complemented by a parallel approach relying on arrays of microscopic, motor-driven actuators.

A key challenge in the field of molecular motors is to replicate the direct and efficient conversion of chemical energy into mechanical work by macroscopic arrays of biomolecular motors in muscles. This would pave the way toward a "molecular engine," creating an alternative to the prevailing heat engines (whose efficiency in converting chemical energy to mechanical work is limited according to Carnot) or to the two-step process of converting chemical energy into electricity via fuel cells and then into mechanical work via electrical motors. Building on insights from muscle physiology, we can pursue the engineering of either hybrid or fully synthetic molecular motor arrays of increasing size and explore a new avenue toward the design of artificial muscles (*13*).

Biomolecular motor–based hybrid devices face limitations with respect to environmental conditions (such as temperature) and lifetime (now typically on the order of hours to a few days) (*14*). Long-term storage of these devices in an inactivated state, which is reached by freezing or lyophilization technologies already used for protein pharmaceuticals, can be used to separate device fabrication and use by at least several months. However, limited lifetime and small power density are the principal disadvantages of biomolecular motors and motivate a transition to fully synthetic molecular motors in the long term.

Molecular motors, either of biological or synthetic origin, are central in the transition from passive to active nanostructures, because they enable coupling to a reservoir of chemical energy. In previous centuries, the use of human and animal power enabled the development of a wide range of technologies—including roads, carriages, and pumps—which were augmented after the invention of the steam engine and the internal combustion engine. Similarly, biomolecular motor nanotechnology, where van den Heuvel *et al*. have devised improved roads and the first traffic control system, and the on-going development of synthetic molecular motors (*15*) contribute to the same vision of fast, efficient, and controlled nanometer-scale transport systems.

References

1. J. Howard, *Mechanics of Motor Proteins and the Cytoskeleton* (Sinauer, Sunderland, MA, 2001).
2. M. G. L. van den Heuvel, M. P. de Graaff, C. Dekker, *Science* **312**, 910 (2006).
3. S. J. Kron, J. A. Spudich, *Proc. Natl. Acad. Sci. U.S.A.* **83**, 6272 (1986).
4. P. Stracke, K. J. Bohm, J. Burgold, H. J. Schacht, E. Unger, *Nanotechnology* **11**, 52 (2000).
5. M. Bachand, A. M. Trent, B. C. Bunker, G. D. Bachand, *J. Nanosci. Nanotechnol.* **5**, 718 (2005).
6. Y. Hiratsuka, T. Tada, K. Oiwa, T. Kanayama, T. Q. Uyeda, *Biophys. J.* **81**, 1555 (2001).
7. J. Clemmens *et al.*, *Langmuir* **19**, 10967 (2003).
8. Y. M. Huang, M. Uppalapati, W. O. Hancock, T. N. Jackson, *IEEE Trans. Adv. Packag.* **28**, 564 (2005).
9. H. Hess, G. D. Bachand, V. Vogel, *Chemistry* **10**, 2110 (2004).
10. M. J. Sailor, J. R. Link, *Chem. Comm.* **2005**, 1375 (2005).
11. S. Diez *et al.*, *Nano. Lett.* **3**, 1251 (2003).
12. H. Hess *et al.*, *Nano. Lett.* **5**, 629 (2005).
13. R. H. Baughman, *Science* **308**, 63 (2005).
14. T. J. Grove *et al.*, *IEEE Trans. Adv. Packag.* **28**, 556 (2005).
15. S. P. Fletcher, F. Dumur, M. M. Pollard, B. L. Feringa, *Science* **310**, 80 (2005).

10.1126/science.1126399

NEUROSCIENCE

Regulating Energy Balance: The Substrate Strikes Back

Jeffrey S. Flier

Hormones and dietary nutrients control appetite and metabolism by acting on the brain, where the signals they elicit promote hunger or satiety. Neurons in the hypothalamus integrate these signals to regulate energy balance.

Appetite, energy expenditure, and metabolism are critically regulated by hypothalamic neural circuits, and a "wiring diagram" through which neurons and neurochemicals exert these effects is rapidly emerging. To achieve energy homeostasis, neuronal pathways in the central nervous system receive and integrate signals from the periphery that convey information about the status of energy fluxes and stores. These signals are of several types. Hormones, such as the fat-derived hormone leptin, act directly on a subset of neurons; a deficiency of leptin is interpreted by the brain as starvation. Leptin deficiency overrides other signals to produce ongoing hunger despite massive obesity, as in rare human cases and in rodent models. Other regulatory signals include gut-derived peptide hormones released with meals that promote feeding (ghrelin) or satiety (cholecystokinin and peptide YY) through actions on the same neuronal targets.

Although these endocrine effectors have received the most attention recently, metabolic fuels and substrates, the evolutionarily ancient regulators of cellular and organismic homeostasis, also affect the neurocircuitry to regulate energy balance. For example, a low glucose level sensed by this circuitry provokes hunger (*1*). More recently, free fatty acids have been shown to act on targets in the central nervous system to regulate metabolism (*2*). On page 927 in this issue, Cota *et al*. (*3*) establish a novel, and potentially important role for

The author is in the Division of Endocrinology, Beth Israel Deaconess Medical Center, and Harvard Medical School, Boston, MA 02215, USA. E-mail: jflier@bidmc.harvard.edu

Continuing Education Credits Available

AIDS 2006

Time to Deliver

Join us in Toronto to be part of the world's premier gathering of scientists and other stakeholders involved in the global response to HIV/AIDS. With a record 12,000-plus abstracts submitted, the AIDS 2006 programme will offer research findings unparalleled in scope.

XVI International AIDS Conference

Toronto Canada
13 - 18 August 2006

www.aids2006.org

CONFIRMED PLENARY SPEAKERS AND TOPICS*

Françoise Barre-Sinoussi
France
Vaccines

Christopher Beyrer, USA
Epidemiology Update
and Transmission Factors

Agnes Binagwaho, Rwanda
Universal Access –
Country Perspective

Louise Binder, Canada
Women and Girls

Kevin De Cock, UK
Treatment Access

Anand Grover, India
Human Rights and
Social Vulnerabilities

Mark Heywood, South Africa
The Price of Inaction

Musimbi Kanyoro, Kenya
Religion, Politics and Civil Society

Kerrel McKay, Jamaica
Youth and the Future

Julio Montaner, Canada
State-of-the-Art
Treatment and New Drugs

Ruth Nduati, Kenya
Children and AIDS

Julie Overbaugh, USA
Pathogenesis

Cristina Pimenta, Brazil
Prevention Response

Gita Ramjee, South Africa
New Prevention Technologies

Aleksandra Volgina, Russia
Poverty and Development

Alex Wodak, Australia
Harm Reduction

*subject to change

another class of metabolic building blocks, the branched-chain amino acids. They show that leucine, a building block for proteins, also regulates the neural circuits that control appetite and energy balance through the mTOR (mammalian Target of Rapamycin) pathway, an evolutionarily conserved mechanism for nutritional control of cellular growth and function (*4*).

mTOR is a highly conserved serine-threonine kinase present in organisms from yeast to mammals (*4*, *5*), whose activity is regulated by hormones (including insulin) and nutrients (including amino acids) (*6*, *7*). mTOR promotes protein synthesis as well as cell growth and proliferation (*8*), and it has been viewed as a sensor of cellular energy status. A possible role for an mTOR pathway in energy balance had previously been suggested, although two genetic studies suggested different roles. Mice deficient in S6 kinase, a downstream effector of mTOR, are lean, insulin sensitive, and resistant to obesity induced by high-fat diets (*9*). In contrast, suppression of S6 kinase in neurons of the fruit fly *Drosophila melanogaster* increases feeding in fasted larvae (*10*). Overexpression of mTOR is associated with aberrant cell growth, and mTOR activity has been reported to be induced in obesity in mice (*11*). However, a specific role for mTOR, its nutritional activators, and its downstream targets in hypothalamic regulation of energy balance in mammals had not previously been identified.

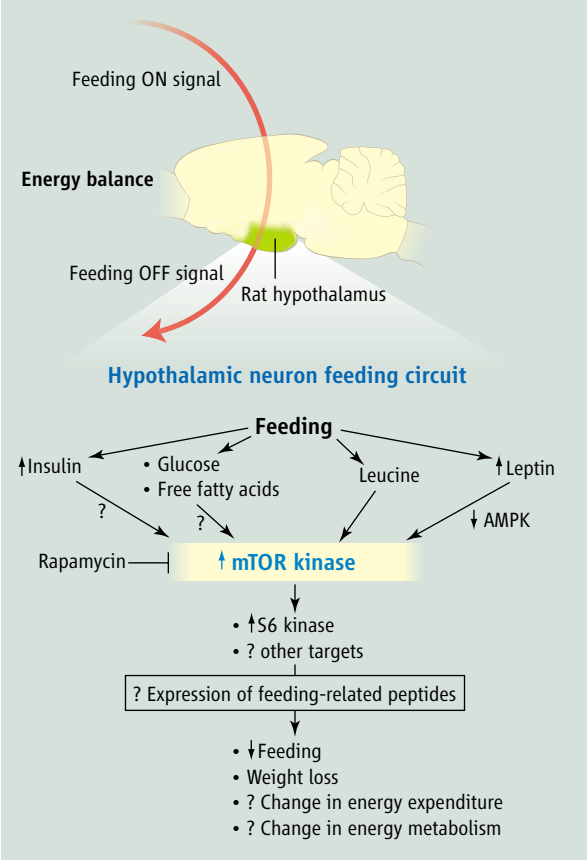

Feeding circuit in the brain. Proposed integration of signaling pathways in the hypothalamus that route through the mTOR kinase to regulate appetite, energy balance, and metabolism.

Although mTOR and S6 kinase are expressed widely in the central nervous system, Cota *et al*. show that the activated forms of these enzymes are localized to specific neurons of the hypothalamus when rats are switched from a starved to a satiated state. To further explore this, they injected leucine, which induces mTOR signaling in cultured cells (*12*), into the cerebral ventricles of the rat brain. Using antibodies that recognize activated (phosphorylated) forms of mTOR and S6 kinase, they observed that not only were mTOR and S6 kinase activated in specific hypothalamic neurons, but that feeding was suppressed (with consequential weight loss) as well. Valine, an amino acid less capable of activating mTOR, had no effect on feeding. Furthermore, inhibiting mTOR signaling with the drug rapamycin prevented both leucine-mediated mTOR and S6 kinase signaling and blocked the suppression of food intake. Finally, the authors asked whether the hypothalamic mTOR pathway mediates the anorectic effect of leptin, the canonical regulator of this circuit. Indeed, leptin also activated hypothalamic mTOR, and rapamycin substantially blocked leptin's ability to suppress food intake and body weight gain. Together, these findings suggest that specific amino acids may play a role in regulating energy balance by acting through the hypothalamic mTOR pathway, and that an ancient mTOR-sensing pathway integrates nutritional and hormonal signals in the neuronal regulation of energy balance (see the figure).

The study by Cota *et al*. raises many important questions. Because mTOR is ubiquitous in the central nervous system, how does leucine selectively regulate mTOR and S6 kinase within the neurons involved in energy balance? Although regulation of mTOR by insulin is mediated by the phosphatidylinositol 3-kinase pathway (*13*), the mechanism by which leucine activates mTOR is still uncertain, and may involve hVps34, a distinct class of phosphatidylinositol 3-kinase (*14*). How can the results indicating that hypothalamic mTOR induces leanness be reconciled with the lean phenotype of mice lacking S6 kinase, an mTOR target (*9*)? Perhaps activation of the mTOR pathway affects energy balance within hypothalamic centers differently than it does in peripheral cells. Another cellular energy sensor recently implicated in hypothalamic control of feeding circuits is the enzyme AMPK (AMP-activated protein kinase) (*15*). Whereas leptin activates AMPK in peripheral cells, it suppresses AMPK activity in the hypothalamus, and this suppression appears to be necessary for leptin's ability to reduce food intake (*16*). Because AMPK activation inhibits mTOR (*17*), reducing AMPK activity may increase mTOR activity through a pathway that mediates some or all of leptin's effects on appetite (see the figure). The finding that leptin action is inhibited both by preventing a fall in hypothalamic AMPK activity (*16*) and by preventing a rise in mTOR activity suggests the existence of such a linear pathway.

Although leucine administered to the brains of rats suppresses feeding and weight gain through actions on mTOR, it will be critical to determine whether normal physiological changes in amino acid concentration act in the hypothalamus to influence energy balance and metabolism. In this context, a rather different link between essential amino acids and appetite is well established. Unbalanced diets lacking essential amino acids (such as leucine) are sensed in the anterior pyriform cortex of the brain, where the GCN2 kinase phosphorylates eukaryotic transcription factor 2. This suppresses appetite, presumably to limit consumption of food that is nutritionally deficient (*18*). Does the brain also sense an increase in an amino acid as a signal of nutritional excess, suppressing feeding to maintain energy balance and avoid obesity? Consumption of protein is reported to decrease subsequent food intake more than a similar caloric amount of carbohydrate and fat (*19*). In addition, mechanisms for transporting amino acids across the blood-brain barrier have been identified, and concentrations of extracellular amino acids in the hypothalamus change after feeding and are influenced by dietary composition (*20*). Whether these changes affect energy regulation through actions on mTOR in hypothalamic neurons is an important question requiring further study. It will also be important to clarify the relation between metabolic substrate and hormonal signaling pathways in disease.

We should not be surprised that an ancient cellular pathway found in yeast that ensures balance between nutritional availability and synthetic pathways would be retained for parallel purposes in the hypothalamus of mammals to integrate signals regulating energy balance. Having unraveled a link between an ancient metabolic pathway and more recently evolved neural-endocrine circuits, the next

challenge will be to determine whether novel therapies for metabolic disease will emerge from pharmacological or nutritional exploitation of these insights.

References and Notes

1. B. E. Levin *et al*. *Diabetes* **53**, 2521 (2004).
2. T. K. Lam, G. J. Schwartz, L. Rossetti, *Nat. Neurosci.* **8**, 579 (2005).
3. D. Cota *et al*., *Science* **312**, 927 (2006).
4. E. Jacinto, M. N. Hall, *Nat. Rev. Mol. Cell Biol.* **4**, 117 (2003).
5. X. Long, F. Muller, J. Avruch, *Curr. Top. Microbiol. Immunol.* **279**, 115 (2004).
6. K. Inoki, K. L. Guan. *Trends Cell Biol.* **16**, 206 (2006).
7. J. Avruch *et al*., *Curr. Opin. Clin. Nutr. Metab. Care* **8**, 67 (2005).
8. P. B. Dennis *et al*., *Science* **294**, 1102 (2001).
9. S. H. Um *et al*., *Nature* **431**, 200 (2004).
10. Q. Wu *et al*., *Proc. Natl. Acad. Sci. U.S.A.* **102**, 13289 (2005).
11. L. Khamzina *et al*., *Endocrinology* **146**, 1473 (2005).
12. K. Hara *et al*., *J. Biol. Chem.* **273**, 14484 (1998).
13. A. Jaeschke, *J. Cell Biol.* **159**, 217 (2002).
14. T. Nobukuni, *Proc. Natl. Acad. Sci. U.S.A.* **102**, 14238 (2005).
15. B. B. Kahn *et al*., *Cell Metab.* **1**, 15 (2005).
16. Y. Minokoshi *et al*., *Nature* **428**, 569 (2004).
17. K. Inoki, T. Zhu, K. L. Guan, *Cell* **115**, 577 (2003).
18. S. Hao *et al*., *Science* **307**, 1776 (2005).
19. G. H. Anderson, in *Modern Nutrition in Health and Disease* (Lippincott, Williams, and Wilkins, Philadelphia, PA, ed. 7, 1994), pp. 520–538.
20. Y. H. Choi, P. J. Fletcher, G. H. Anderson, *Brain Res.* **892**, 320 (2001).

10.1126/science.1127971

MATERIALS SCIENCE

Collective Defect Behavior Under Stress

Crystals contain defects that determine how the material responds to deformation. An x-ray diffraction method reveals the dynamic behavior of these defects as the material is stressed.

Ladislas Kubin

When a piece of material is bowed or bent, it may deform in an irreversible, or plastic, manner. This property is useful to metallurgists in two ways. First, it may be used to process metallic ingots into various types of products. Second, when submitted to an overload in service conditions, materials may gently deform plastically rather than breaking abruptly. For decades, materials scientists have longed for dynamic insights into the microscopic events associated with plastic flow. On page 889 of this issue, Jakobsen *et al.* (*1*) report an important step in this direction.

Consider the uniform shearing of a crystal along a dense crystallographic plane (see the first figure, left panel). Shearing the upper part with respect to the lower part produces plastic deformation but requires the simultaneous breaking of many atomic bonds. The same task can be carried out at a much smaller expense of energy by linear defects, the dislocations (see the first figure, right panel). Dislocation motion is analogous to the movement of a caterpillar, which creates a hump at its rear and propagates it to its front. If one introduces a small shear on one side of the plane and propagates it forward, only a small number of bonds are sheared at a time. The plastic deformation of a bulk material is the sum of all the elementary shears produced by dislocation motion.

During plastic deformation, the total line length of dislocation in a material increases. At very large strains (typically when the length of a compressed specimen is halved), the total line length in a cubic meter of material can be more than 10 million times the distance from Earth to Sun. Because dislocations interact with each other at both short and long ranges, the stress needed to further deform a crystal increases continuously, up to a maximum stress beyond which the specimen breaks.

During plastic flow, the interacting dislocation populations tend to spontaneously self-organize into various types of patterns (*2, 3*). In the typical three-dimensional arrangement of dislocations (see the second figure), dislocation-dense cell walls surround almost dislocation-free regions, in a manner reminiscent of the filament-like structure of matter in the universe. This phenomenon has puzzled scientists for nearly 40 years. Dislocation theory can explain the properties of individual dislocations reasonably well, but it is still unable to deal with their collective behavior. Establishing a dislocation-based theory of plasticity therefore remains a formidable challenge.

Dislocation patterns exhibit a striking property that is not well understood: Their average diameter decreases in inverse proportion to the applied stress. This relation holds over at least five orders of magnitude in cell dimensions, depending on the applied stress. The common cell size observed in processed or deformed materials is in the micrometer range; it decreases to almost 10 nm in materials strengthened by very large deformations. At the other extreme are the giant dislocation cell structures formed in GaAs wafers under very small stresses generated by a temperature gradient. These stresses decrease from the periphery to the center, whereas the cell sizes behave in the opposite manner (see the second figure).

Dislocations induce local rotations of the lattice planes (see the first figure, right panel). In a dislocation cell wall, the sum of all these rotations does not amount to zero and induces global differences in lattice orientation between neighboring cells. These differences increase progressively during plastic flow, providing a powerful means for imaging individual dislocations and dislocation microstructures by diffraction methods.

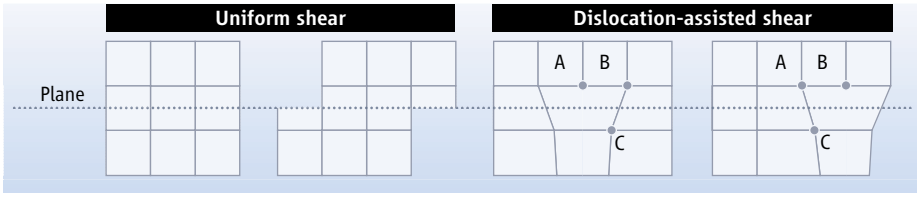

Two types of shear. (Left) Uniform shear of a crystal along a crystallographic plane. **(Right)** A dislocation, seen here end-on, induces strong local atomic disturbances in a small volume where the positions of atomic rows (e.g., A, B, and C) are severely disturbed. Dislocation glide produces a local shear that only necessitates small atomic displacements per step of motion.

By illuminating a thin film of crystalline matter with electrons or x-rays, one obtains transmitted beams that are diffracted along preferred directions. The diffraction pattern contains information about the crystal orientation, but the diffracted beams can also be used to produce images of the thin film along a certain crystallographic direction. The lattice distortions around dislocation cores disturb diffrac-

The author is at the Laboratoire d'Étude des Microstructures, CNRS-ONERA, 92322 Châtillon Cedex, France. E-mail: kubin@onera.fr

CREDIT: P. HUEY/*SCIENCE*

tion phenomena and modify the local diffracted intensities, thus revealing the dislocation lines (see the second figure, inset). The deformation of thin films can thus, in principle, be imaged in situ with electrons or x-rays. Unfortunately, in the case of imaging with electrons, the permissible film thicknesses are much smaller than the cell sizes. The use of x-rays is also limited to small dislocation densities, because the dislocation images are relatively wide and therefore overlap at moderate dislocation densities.

Jakobsen *et al.* carried out their work on polycrystals, that is, on assemblies of single crystalline grains that are misoriented with respect to each other. Using diffraction rather than direct imaging, they extended a previously developed and highly sophisticated three-dimensional x-ray diffraction method (*4*). In substance, this tomographic method allows the orientations of selected subvolumes to be mapped in situ within a single grain. This grain, with a diameter of about 30 μm, is embedded in a film that is about 10 times as thick. The method provides an insight into what happens inside a single grain during plastic flow, at a resolution that can monitor the lattice orientation changes associated with a small number of dislocations.

The examined volume clearly contains crystallites, which are convincingly identified as dislocation-free regions inside cell walls. The way in which the average dimensions of these cells are found to decrease when the applied stress increases looks a bit disconcerting. It is usually thought that these rearrangements proceed by cell splitting through the progressive construction of new individual walls. In contrast, the present observations hint at collective destructions and reconstructions of whole 3D cell structures. This is a much more catastrophic process, perhaps characteristic of small strains. Further experimentation on such collective processes will undoubtedly stimulate the imagination of theoreticians.

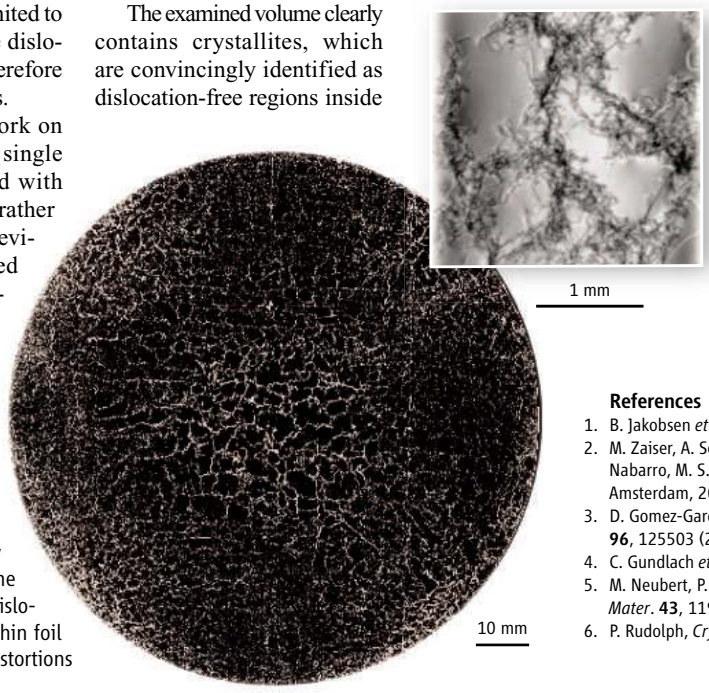

Typical dislocation cells. Optical micrograph of a giant dislocation pattern in an as-grown GaAs wafer (*5*). Chemical etching of the surface has been used to selectively dissolve the imperfect material, revealing the dense dislocation walls. **(Inset)** Magnified dislocation cell observed by x-ray imaging of a thin foil (*6*). The dark lines are images of the lattice distortions around individual dislocation cores.

References

1. B. Jakobsen *et al*., *Science* **312**, 889 (2006).
2. M. Zaiser, A. Seeger, in *Dislocations in Solids*, F. R. N. Nabarro, M. S.Duesbery, Eds. (North-Holland, Amsterdam, 2002), vol. 11, pp. 1–100.
3. D. Gomez-Garcia, B. Devincre, L. P. Kubin, *Phys. Rev. Lett.* **96**, 125503 (2006).
4. C. Gundlach *et al*., *Scripta mater.* **50**, 477 (2004).
5. M. Neubert, P. Rudolph, *Prog. Cryst. Growth Charact. Mater*. **43**, 119 (2001).
6. P. Rudolph, *Cryst. Res. Technol*. **40**, 7 (2005).

10.1126/science.1125799

GEOPHYSICS

Ships' Logs and Archeomagnetism

Ships' logs help show that the strength of Earth's magnetic field was stable until the mid-1800s. Since then, flux changes may have caused a steady decline in strength.

Masaru Kono

Since the mid-19th century, geophysical measurements have shown that the strength of Earth's magnetic field has steadily decreased by about 5% per century. At this rate, the field should disappear entirely in about 2000 years. But what about variations in the field before the start of this drop in strength? On page 900 of this issue, Gubbins and colleagues report important contributions to the study of such geomagnetic secular variations (*1*). By analyzing the record back to 1590, the authors find some surprising variations that offer clues to what is happening with Earth's field.

The regular collection of geomagnetic data at observatories and by surveys started around the time of the physicist C. F. Gauss in the mid-1800s. For earlier times, archeomagnetism in remains from human habitation (such as old bricks), and recent sediments and volcanic material can provide data back to about 20,000 years, but their accuracy is much worse (typically 10%) than that achieved by instrumental measurements (0.1% or better). Gubbins and his colleagues started a project to collect old navigational data, which consist mostly of magnetic field directions (in particular, the declination *D*, which is the angle of the field relative to geographical north, and some data on inclination *I*, which is the dip of the field relative to the level ground). Similar efforts had been made earlier by E. Sabine from 1840 to 1877, by H. Fritsche in 1893, and by others (*2*). The unique feature of the current effort is that the authors went back to the original ships' log books when they were available, and corrected wrong entries in them, such as the ship's positions, which are sources of large systematic errors. An interim summary of these findings was published in 1989 (*3*). The most recent compilation by Jonkers *et al*. (*2*) includes over 150,000 *D* and 19,000 *I* data in the interval 1510 to 1930. These data cannot attain the accuracy of the instrumental observations, but they are still very useful. Most importantly, the time of observation is exactly known. This makes them much superior to the poorly dated archeomagnetic data.

The second contribution of Gubbins is the introduction of the technique of stochastic inversion to secular variation studies (*4*). The geomagnetic field is best described by a scalar potential function, which is expressed by parameters called Gauss coefficients. The determination of the potential from observations is a typical geophysical inverse problem. For the present field analysis, it is sufficient to use the standard least-squares method (also an invention of Gauss). This method obtains the model that minimizes the misfit; that is, the sum of the squared differences between the

The author is professor emeritus at the Tokyo Institute of Technology, Tokyo, 152-8551, and Okayama University, Okayama 700-8530, Japan. E-mail: masarukono@nifty.com

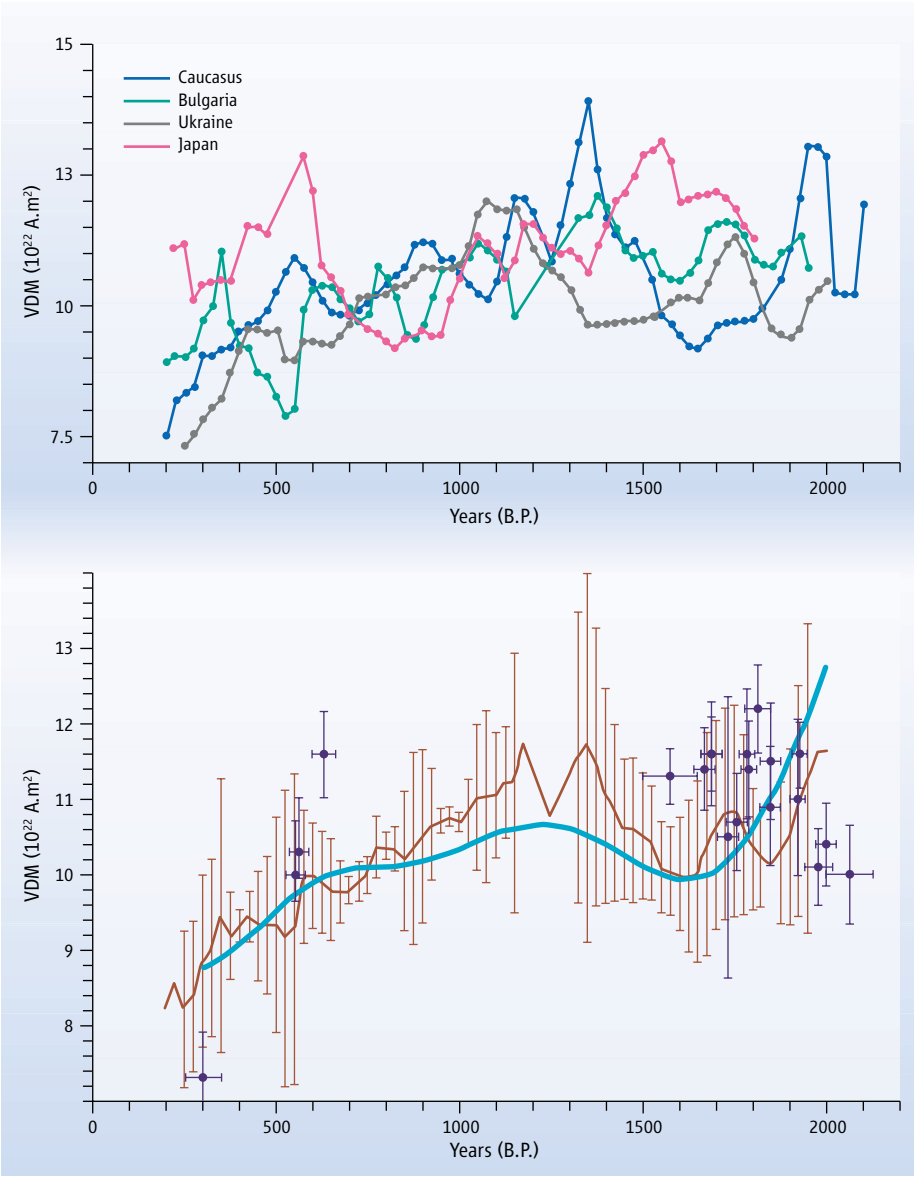

Magnetic variations. Change of Earth's magnetic field intensity in the past 2000 years (time scale is years before present, so recent times are at left). (**Top**) Averages of the virtual dipole moment (VDM) in three areas in Eastern Europe and one location in Japan. (**Bottom**) Average of the Eastern Europe curves (orange line) with the scatter indicated by thin lines, compared with a smoothed model constructed from a global database (blue line). Recent results from measurements in France are shown by dots [adapted from (*9*)].

observed and the predicted values. For older periods, the data quality is poor, their distribution is biased, and moreover, most of the data (for example, I and D) are nonlinear functions of the model parameters. These inadequacies cause a lot of problems in inversion; in many cases convergence to plausible models cannot be attained by the ordinary method. In stochastic inversion, the sum of the misfit and another quantity (usually called the penalty function) is minimized. The penalty function is chosen by physical insight (such as a minimum energy requirement, etc.), which leaves some ambiguity in the method. However, experience has shown that this method can produce quite reasonable models. Based on the collected navigational data (*2*), Jackson *et al.* (*5*) used this method to construct a very nice model called *gufm1* which covers the interval 1590 to 1990. Stochastic inversion has also been used for determination of the models of the average paleomagnetic field over a period of a few million years (*6*–*8*).

Of course, stochastic inversion is not all-powerful. It cannot say anything about a property of the field if the original data do not contain such information. Because the *gufm1* model is based on directional data, there is no information about the strength of the field. The field intensity of *gufm1* is determined with the assumption that the dipole intensity decreased in the earlier period at the same rate as observed since the time of Gauss. Gubbins *et al.* have improved the *gufm1* model by constraining the field intensity with the use of other data, such as archeomagnetic intensity data from various parts of the world. Because the geomagnetic field is dominated by the dipole term, even data from one site can give some estimate of the strength of the dipole moment. Unfortunately, the errors in these data are not small enough to give an accurate estimate. The difference in the estimates of the dipole moment from places not very far apart demonstrates that they contain errors of 10% or so (see the figure, top panel). Excluding the general decrease in the dipole intensity in the past 2000 years, it is difficult to draw a firm conclusion from a simple comparison of archeomagnetic data.

The approach taken by Gubbins *et al*. to this problem is to use standard statistical analysis. They obtained the rate of decrease of the dipole Gauss coefficient $\dot{g}_1^0 = 2.28 \pm 2.72$ nT per year for the period 1590 to 1840, which is significantly smaller than the decrease of 15 nT per year since 1840. It is interesting that the Western European average of the dipole moment shows a nearly constant value for the same period, although the scatter is quite large (see the figure, bottom panel). Gubbins *et al*. then examine the difference in field structure before and after the time of Gauss at the core-mantle boundary (which was obtained by inversion of directional data). They conclude that the fast decay in the dipole moment in recent years is due to an area of reversed flux (which decreases the magnitude of the dipole, $\dot{g}_1^0$)near Antarctica, a feature which is absent in the period 1590 to 1840. Such changes present a major puzzle to geophysicists who seek to understand these variations, as well as details of how the field is produced in the first place. Most importantly, this study provides a good example of the collaborative effort obtained by the combination of different data sets (the historical navigational data and the archeomagnetic data), as well as powerful mathematical methods (statistical analysis and inversion).

References and Notes

1. D. Gubbins, A. L. Jones, C. C. Finlay, *Science* **312**, 900 (2006).
2. A. R. T. Jonkers, A. Jackson, A. Murray, *Rev. Geophys.* **41**, 1006 (2003).
3. J. Bloxham, D. Gubbins, A. Jackson, *Philos. Trans. R. Soc. London* **A329**, 415 (1989).
4. D. Gubbins, *Geophys. J. R. Astron. Soc.* **73**, 641 (1983).
5. A. Jackson, A. R. T. Jonkers, M. R. Walker, *Philos. Trans. R. Soc. London* **358**, 957 (2000).
6. P. Kelly, D. Gubbins, *Geophys. J. Int.* **128**, 315 (1997).
7. C. Johnson, C. G. Constable, *Geophys. J. Int.* **131**, 643 (1997).
8. T. Hatakeyama, M. Kono, *Phys. Earth Planet. Int.* **133**, 181 (2002).
9. J.-P. Valet, *Rev. Geophys.* **41**, 1004 (2003).
10. I thank J.-P. Valet for providing the original figure.

10.1126/science.1126665

SCIENCE & ENGINEERING

VISUALIZATION CHALLENGE

CALL FOR ENTRIES

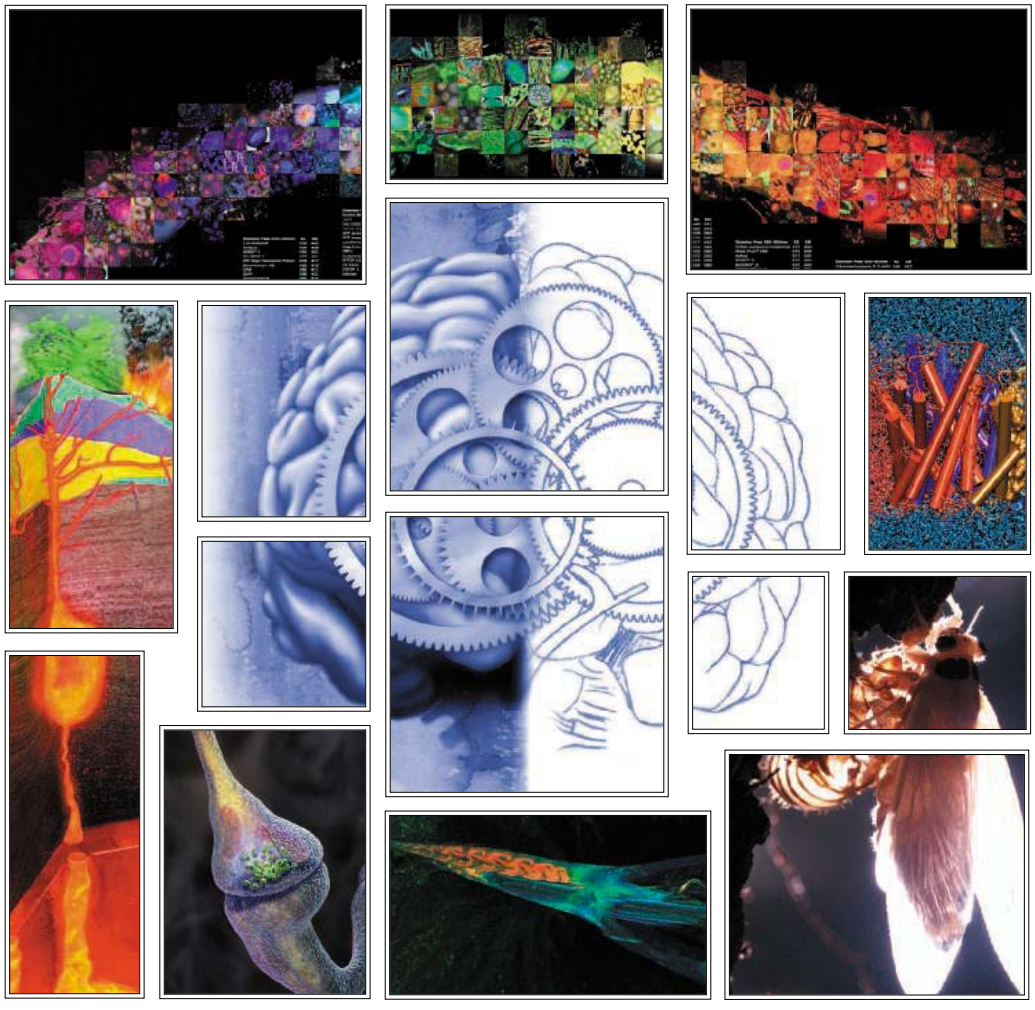

SCIENCE AND ENGINEERING'S MOST POWERFUL STATEMENTS ARE NOT MADE FROM WORDS ALONE

When the left brain collaborates with the right brain, science emerges with art to enhance communication and understanding of research results—illustrating concepts, depicting phenomena and drawing conclusions.

The National Science Foundation (NSF) and the journal *Science*, published by the American Association for the Advancement of Science, invite you to participate in the fourth annual Science and Engineering Visualization Challenge. The competition recognizes scientists, engineers, visualization specialists and artists for producing or commissioning innovative work in visual communication.

ENTRY DEADLINE: MAY 31, 2006

Award categories: Photographs, Illustrations, Interactive Media, Non-Interactive Media and Informational Graphics. Winners in each category will be published in the Sept. 22, 2006 issue of *Science* and *Science* Online, and will be displayed on the NSF Web site.

Complete Entry Information: www.nsf.gov/news/special-reports/scivis/index AND www.sciencemag.org/prizes/

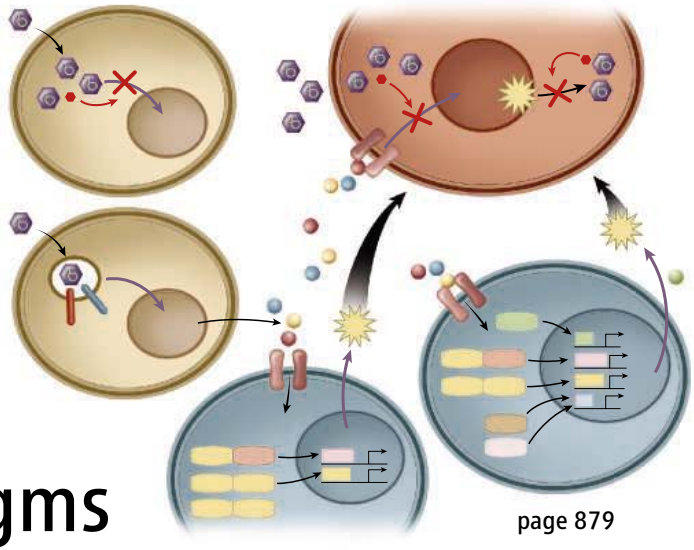

page 879

INTRODUCTION

Paradigms in the Virosphere

VIRUSES HAVE BEEN DESCRIBED AS PERFECT PARASITES: MANY ARE SO MINIMALLY assembled that they cannot strictly be classified as living organisms. Except when they damage health, we concern ourselves little about them; nevertheless, the "virosphere" (a term coined by Curtis Suttle) is ubiquitously influential in our everyday lives. Viruses continue to be the vehicles for important genetic events, from the evolution of photosynthesis to the emergence of pathogens, and play an important role in regulating the microbially dominated cycling of carbon, nitrogen, and phosphorus in the world's oceans. By means of horizontal gene transfer, viruses endow bacteria, and probably many other phyla, with clusters of distinct genes and phenotypes. Viruses infecting bacteria (bacteriophages) have been instrumental in the development of modern molecular biological techniques, and the precision and assembly of the interlocking proteins of virus capsids have inspired architects and nanotechnologists alike. In this special issue, we explore some of the attributes of viruses that are distinct from their ability to cause human disease.

Douglas and Young (p. 873) have taken virology farthest from its roots and in a Perspective explore how the flexibility of capsid structure can be exploited for diverse uses, including drug delivery and as precise templates for nanostructure assemblies. There are many challenges to the biotechnological application of artificial viruses, not least toxicity and immune responses. Initial infection with a virus can trigger a cell into an autophagic response that is similar to the cell's normal response to protein aggregates, such as those that develop during Huntington's disease. Wileman (p. 875) reviews the possibilities for subversion of the degradative activity of autophagous structures, known as aggresomes, as scaffolds for viral replication and assembly. García-Sastre and Biron (p. 879) review the subsequent lines of host defense against virus establishment: type 1 interferons. Viruses are adept at eluding host responses, but interferons can trigger a flexible network of backup responses. These backups may not result in clearance of the virus but instead give rise to its persistence, and hence a standoff develops in which yet another round of host innate or adaptive response is signaled. A News story by Zimmer (p. 870) examines a theory that viruses coexisted with the earliest organisms and perhaps helped create DNA, as Forterre argues. Three further articles at *Science*'s Signal Transduction Knowledge Environment (STKE) offer examples of how viruses and other pathogens exploit cell signaling pathways to achieve their own ends. A Review by Hayward *et al.* describes how gamma herpesviruses mimic and manipulate Notch and Wnt signaling, a Perspective by Barry and Früh focuses on viral manipulation of cullin RING ubiquitin ligases, and a Review by Münter *et al.* concerns how pathogens manipulate tyrosine kinase– and Rho GTPase–mediated pathways.

With the ongoing focus on viruses in the public eye, some may dread what the future may bring; but for most viruses, excessive virulence is a dead-end strategy. The interactions between viruses and hosts are usually subtle and unexpected; the application of nanotechnology as host defense would surely have gratified Koch, Pasteur, and Iwanowski.

–CAROLINE ASH, STELLA HURTLEY, MARC LAVINE, STEPHEN SIMPSON

Virology

CONTENTS

See also related STKE material on page 807 or at www.sciencemag.org/sciext/virology/

CREDIT: A. GARCIA-SASTRE AND C.A. BIRON

Science

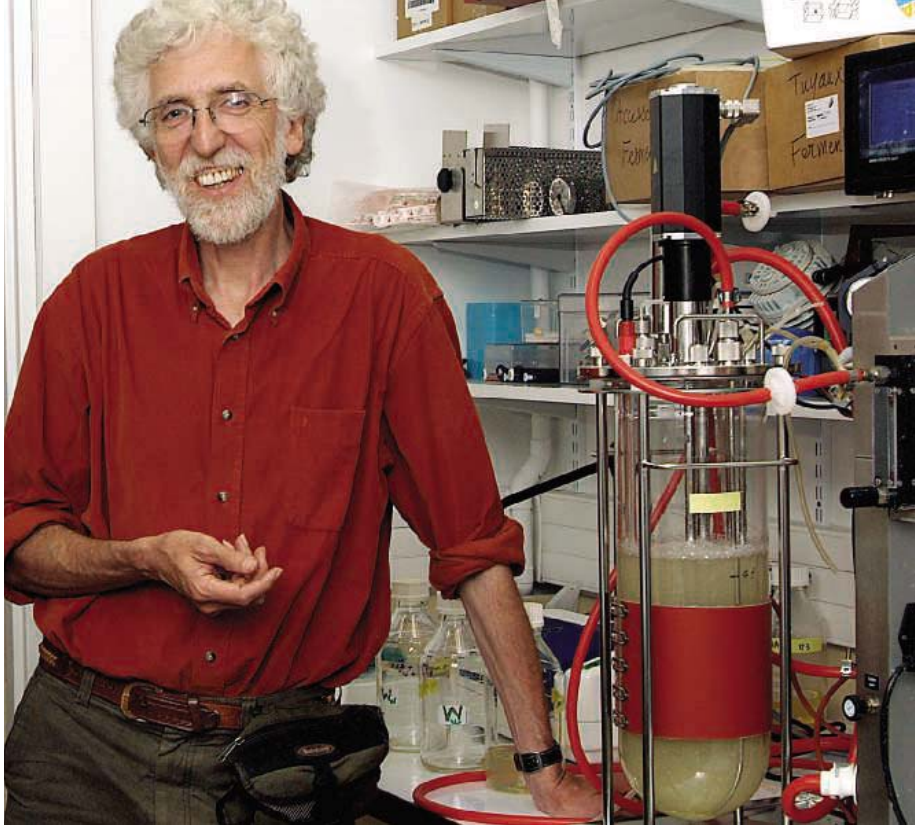

Exploring the viral world. Patrick Forterre searches for clues to the early evolution of life by investigating exotic viruses.

NEWS

Did DNA Come From Viruses?

Research that began with a study of replication enzymes used by bacteria has led to a controversial theory: Viruses may have helped shape all three major domains of life

Scientists who deal in the history of life have never been quite sure what to do with viruses. One measure of their uncertainty is the Tree of Life Web Project, a collective effort to record everything known about the relationships of living and extinct species. The first page of its Web site—entitled "Life on Earth"—shows the broadest view: From a single root come three branches representing the domains of life (www.tolweb.org). One limb, Eubacteria, includes bacteria such as *Escherichia coli*. Another, Archaea, includes microbes of a different lineage that are less familiar but no less common. The third, Eukaryotes, includes protozoans as well as multicellular organisms such as ourselves. And just below the tree there's a fourth branch floating off on its own, joined only to a question mark. It is labeled "Viruses."

A growing number of scientists hope to get rid of that question mark. They recognize that a full account of the evolution of life must include viruses. Not only are they unimaginably abundant—most of the biomass in the ocean is made up of viruses—but they are also extraordinarily diverse genetically, in part because they can acquire genes from their hosts. They can later paste these genes into new hosts, potentially steering their hosts onto new evolutionary paths.

Patrick Forterre, an evolutionary biologist at the University of Paris-Sud in Orsay, France, believes that viruses are at the very heart of evolution. Viruses, Forterre argues, bequeathed DNA to all living things. Trace the ancestry of your genes back far enough, in other words, and you bump into a virus.

Other experts on the early evolution of life see Forterre's theory as bold and significant. But although they find much to agree with—particularly the importance of viruses to evolution—many also regard Forterre's ideas as controversial.

"I really applaud the bravery and intellectual power to come up with this picture," says Eugene Koonin of the National Center for Biotechnology Information (NCBI) in Bethesda, Maryland. "But it would be strange if we agreed on all the parts of the picture."

A new domain

Forterre has been developing and elaborating his theory over many years. He began his scientific career in the early 1970s studying the replication of DNA. He investigated how *E. coli*, the common gut bacteria, use special enzymes to make new copies of their genes without letting the double helix of DNA become tangled.

As Forterre was studying bacteria, another group was developing a complex new view of simple organisms. Carl Woese of the University of Illinois, Urbana-Champaign, demonstrated that some bacteria are not bacteria at all. They belong to a separate branch on the tree of life, which came to be known as Archaea. Archaeans turned out to have a distinct biology. Forterre and his colleagues discovered that they use peculiar enzymes for DNA replication that work differently from those in bacteria and eukaryotes. Meanwhile, other scientists had begun looking at the DNA-replication enzymes used by a virus called T4 bacteriophage, which copy DNA in yet another way.

This discovery made a deep impression on Forterre. At the time, many scientists thought that viruses were merely escaped genetic fragments. After all, viruses are not truly alive: They cannot replicate on their own and have no metabolism. They simply hijack host cells to make new copies of themselves. The best explanation seemed to be that viruses evolved from genes in "true" organisms. Mutations allowed these renegade genes to leave their genomes and become encased in protective protein shells. If that were true, however, the enzymes of viruses should resemble those of their hosts. Yet the DNA-replicating enzymes of T4 bear no relation to the enzymes in the bacteria they infect.

"I thought, maybe T4 is from a fourth domain," Forterre recalls. But T4 is not unique. Scientists continued to find more DNA-copying enzymes in viruses that have no counterparts in the world of cells, and Forterre's suspicions deepened. "Maybe each of these viruses is a remnant of a domain that has disappeared," he wondered.

In 1985, Forterre offered his speculations at a scientific conference. "I suggested that viruses originated from an early cell, perhaps before the origin of the three domains," he says.

Forterre based his theories on the enzymes in viruses rather than the genes that encode them; genome information was scarce then. And for a long time, the question of viruses' origin lay dormant. But advances in DNA sequencing have brought a wealth of new information about virus genomes. In Forterre's view, it reinforces his argument that many viruses are ancient. The genes for the most common proteins in virus shells, for example, turn out to be present in viruses that infect hosts in all three domains, suggesting that these genes originated in a virus that infected an ancestor of all three domains of cellular life. "We find more and more evolutionary connec-

CREDITS: COURTESY OF PATRICK FORTERRE

tions between viruses in different domains," says Forterre. "All these findings have completely destroyed this old idea that viruses are escaped fragments of cells."

A puzzle that arose from work on microbial genes in the 1990s also gave a new dimension to Forterre's thinking. As scientists dissected the DNA that codes for enzymes used in replication, they found that the precise sequences in bacteria were radically different from those in archaea and eukaryotes. The discrepancy between the domains of life meant that DNA essential to survival had come from different sources or had been separated by a long period of evolutionary time. Koonin even proposed that DNA replication had evolved twice, once in bacteria and once in the common ancestor of archaea and eukaryotes.

Forterre had a different reaction. "I came back to this idea [of a very early origin for viruses] when genomics showed a clear difference between the DNA replication of bacteria on one side, and the system in archaea on the other," says Forterre. "Maybe in fact one of these two systems came from a virus."

Forterre proposed that the genes for DNA replication in bacteria had been donated by their viruses. Soon afterward, Luis Villarreal of the University of California, Irvine, pointed out a possible evolutionary connection between DNA-replication genes in certain viruses and those in eukaryotes. He suggested that viruses had replaced the original genes in eukaryotes. "The next step," Forterre says, "was to say, 'Why not both systems?' "

For the past several years, Forterre has been expanding his original ideas into a sort of grand unified theory of viruses and cellular life. Forterre proposes that viruses donated more than just their DNA-replication genes to cellular life. He argues that they donated DNA itself. In recent months, he has presented the scenario in a series of papers, the most recent of which appeared last month in the journal *Virus Research*.

Like many scientists, Forterre favors the theory that DNA-based organisms are descended from simpler RNA-based organisms. Experiments on RNA suggest that it could have been versatile enough to support primitive life. Not only can it carry genetic information, but it also has the capacity to act like an enzyme, carrying out chemical reactions. RNA-based life may have been able to absorb nutrients, replicate, and evolve. According to this "RNA world" theory, these organisms later evolved proteins and DNA, which then took over many of RNA's former tasks.

"I really applaud the bravery and intellectual power to come up with this picture."
—Eugene Koonin, NCBI

Forterre proposes that RNA organisms evolved into self-replicating cells that could produce their own proteins. At that point, the first viruses evolved. These RNA viruses parasitized RNA-based organisms, manipulating them to make new copies of themselves. These primordial RNA viruses may have produced lineages that are still with us today, in the form of modern RNA viruses such as influenza, HIV, and the common cold.

Although a great deal of evidence supports the idea of an RNA world, the scenario raises a number of difficult questions. Not the least of these is how RNA-based life might have evolved into DNA-based life. Many scientists have pointed out that DNA is more stable than RNA and less prone to mutations. Once DNA was established, it allowed genes to become longer and more complex. But how the transition came about is difficult to explain, Forterre points out. The stability of DNA provides long-term advantages, not the short-term ones that natural selection can favor. "This is not a Darwinian way of thinking," says Forterre. "You should explain why the first organisms in which RNA was modified had a selective advantage, not in its descendants."

Forterre offers a solution. He suggests that viruses were the intermediate agents of change. For viruses, DNA might have offered a very powerful, immediate benefit. It would have allowed them to ward off attacks from their hosts. Cells today use a number of weapons against RNA viruses. They can silence the viral RNA with special RNA molecules of their own. Or they can cut the genome of the virus into fragments.

"RNA viruses have to find a way to avoid these defenses," says Forterre. They do so by making it difficult for their hosts to grab their RNA. Living RNA viruses chemically modify their genes to thwart their hosts. Forterre proposes that some early RNA viruses altered their genes in a particularly effective way: They combined pairs of single-stranded RNA into double-stranded DNA. The vulnerable nucleotides carrying the virus's genetic information were now

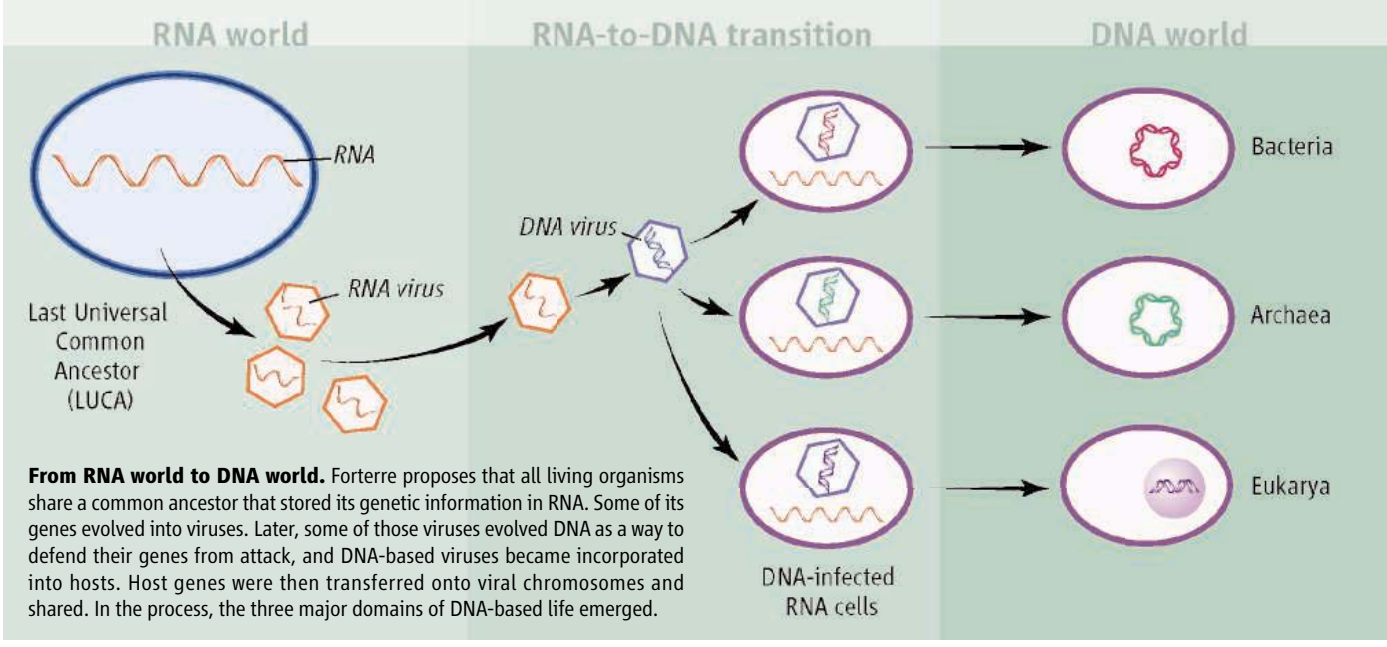

From RNA world to DNA world. Forterre proposes that all living organisms share a common ancestor that stored its genetic information in RNA. Some of its genes evolved into viruses. Later, some of those viruses evolved DNA as a way to defend their genes from attack, and DNA-based viruses became incorporated into hosts. Host genes were then transferred onto viral chromosomes and shared. In the process, the three major domains of DNA-based life emerged.

CREDIT: C. CAIN (ADAPTED FROM P. FORTERRE)

nestled on the inside of the double helix, while a strong backbone faced outward.

"The idea is that an older RNA virus could use this as a trick to modify the structure of its RNA. DNA is simply modified RNA," says Forterre.

If they were anything like viruses today, some of the viruses found a way to coexist inside the host's cells, surviving from one generation of host to the next. Forterre suggests that in the RNA world, some DNA viruses became domesticated and lost the genes they used for escaping their hosts and for making protein shells. They became nothing more than naked DNA, encoding genes for their own replication.

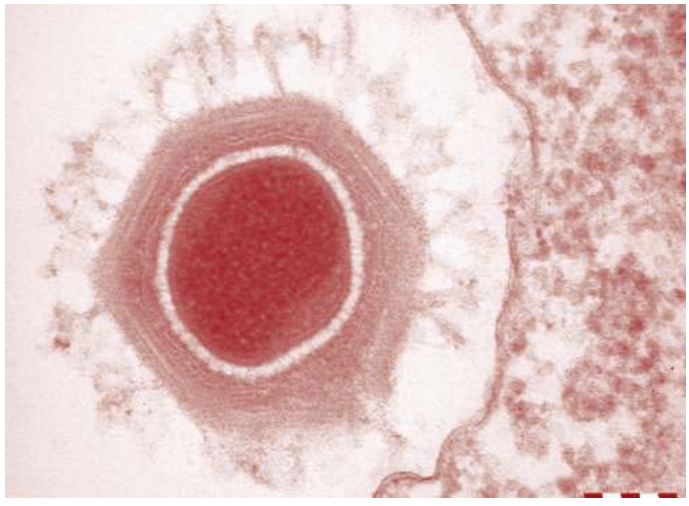

Viral diversity. Scientists are uncovering a vast diversity among viruses, such as this giant mimivirus. Their genetics and biochemistry point to an ancient origin.

Only at this point, Forterre argues, could RNA-based life make the transition to DNA. From time to time, genes from the RNA chromosome would be accidentally pasted into the virus's DNA chromosome. These genes could now enjoy all the benefits of DNA-based replication. They were more stable and less prone to devastating mutations. Natural selection favored organisms carrying important genes in DNA rather than RNA. Over time, the RNA chromosome dwindled while the DNA chromosome grew. Eventually, the organism became completely DNA-based. Forterre proposes that this viral takeover occurred three times, and each one gave rise to one of the three domains of life.

These blendings of genomes could explain the similarities and differences among the three domains, he argues. Take, for example, the fact that archaean and eukaryote DNA-replication enzymes are more similar to each other than they are to bacterial genes. Forterre suggests that it just so happened that the viruses that infected the RNA-based precursors of archaeans and eukaryotes shared a close common ancestor.

Eukaryotes in particular pose a special challenge to any account of the early evolution of life. For instance, eukaryotes keep their DNA tucked away in a nucleus, a structure whose origins scientists have debated for years. Forterre suggests that viruses may have played a part in shaping the cells of early eukaryotes. He points out that certain viruses, such as poxviruses, can form nucleuslike shells inside their hosts. Waves of viral infections could have built some of the features of the eukaryote cell. "The eukaryote cell is very strange and very complex, so I don't have a very clear idea of how they originated," Forterre admits.

After viruses ushered in these three domains of DNA-based life, the new forms proved superior to those of their predecessors. "Once this occurred, the DNA cells outcompeted all the RNA cells," says Forterre. "And once all the RNA cells were eliminated, you had a limited number of lineages."

Finding flaws

Forterre's ideas have been warmly received, even by those who dispute some of them. "Patrick's ideas need to be taken seriously," says David Penny of Massey University in Palmerston North, New Zealand. But Penny points out that in Forterre's scenario, RNA-based organisms are already relatively complex by the time viruses drive them into the DNA world.

"I doubt in the absence of DNA any organism would be very complex at all," Penny says. He points out that RNA replication suffers a high error rate. Under those conditions, genomes cannot become large without risking catastrophic damage.

Penny and his colleagues dispute the idea that natural selection could not drive RNA organisms to DNA-based replication on their own. They've argued that the organisms could have made the transition through a series of evolutionary steps, each of which reduced the error rate during replication. Once life had shifted to DNA, Penny argues, viruses might have played a part in the origin of one or more of the three domains. "I definitely do not want to exclude the possibility of viral takeover," says Penny.

Koonin, on the other hand, agrees with Forterre that viruses originated in the RNA world. "That idea makes perfect sense, in my opinion," he says. He also accepts the possibility that viruses might have invented DNA. But when Forterre argues that viruses gave rise to the three domains, Koonin parts company. "I don't believe it for a moment," he declares. Archaeans share too many genes in common with eukaryotes for this to be plausible, Koonin argues. Instead, eukaryotes must have evolved from archaeans after they had become DNA-based.

Koonin envisions a different sort of history of viruses and their hosts. He and William Martin of Heinrich Heine University in Düsseldorf, Germany, have proposed that life first evolved in honeycomb-like cavities in rocks around hydrothermal vents. These compartments played the role that cell walls and membranes would later play. Initially, RNA molecules were selected simply for fast replication. Successful molecules could spread from one compartment to another. Over time, groups of RNA molecules were favored by natural selection, working together to reproduce more successfully. It was then that viruslike things emerged—before cells yet existed.

"There would be parasites that only care for their own replication—and here Patrick's ideas might have their place," Koonin says. "DNA replication might originally have emerged in such parasitic entities."

Woese, who has influenced Forterre's work for more than 20 years, is both enthusiastic and agnostic about the virus theory. "In the most specific form, I don't know if he's right, but then it doesn't make any difference, because he's going in the right direction," he says. "I think that's a significant advance, to be able to fold the viruses into the whole process."

Woese and others believe that the best way to assess Forterre's theory would be to find and analyze more viruses. Forterre agrees. "At the moment, we know very few of the viruses in the living world," says Forterre. "We know some viruses that are human pathogens, and some that infect bacteria that are important to the food industry. But for many groups, we have no idea of their viruses."

Forterre himself is trying to fill that gap by studying viruses that live in heat-loving archaeans. Archaean viruses are proving to be particularly diverse and bizarre—such as lemon-shaped species that don't finish growing until they have left their host cell. Because viruses have such ancient roots, they preserve a remarkable range of biochemical tricks. "It's clear now that you have many more genes in the viral world, so there are many interesting new enzymes to be found," says Forterre. "If we explore the viral world more, I don't know if we will be able to be sure of one theory or the other. But I am sure we will get many more interesting molecular mechanisms."

–CARL ZIMMER

Carl Zimmer, a freelance writer, is the author of *Parasite Rex* and *Soul Made Flesh*.

PERSPECTIVE

Viruses: Making Friends with Old Foes

Trevor Douglas and Mark Young

The study of viruses has traditionally focused on their roles as infectious agents and as tools for understanding cell biology. Viruses are now finding a new expanded role as nanoplatforms with applications in materials science and medicine. Viruses form highly symmetrical monodisperse architectures and are ideal templates for engineering multifunctionality, including multivalent display of surface ligands and encapsulation of inorganic and organic materials. These developments assure that viruses will find applications as versatile nanoscale materials.

The essential nature of all viruses is to infect a host cell, replicate, package its nucleic acid, and exit the cell. In the process, viruses have evolved to move through a broad range of chemical environments. In their journey, viruses demonstrate a remarkable plasticity in their metastable structure and dynamics, including coordinated assembly and disassembly and site-specific delivery of cargo molecules. Viruses have emerged as platforms for synthetic manipulation with a range of applications from materials to medicine. Chemical or genetic manipulation makes it possible to impart new functions to protein cage architectures, combining the best of evolution and truly intelligent design. Characterized viruses represent only a fraction of the predicted viral diversity present in the biosphere. Recent revelations suggest that viruses are the most abundant biological entities on the planet and are second only to prokaryotes in terms of biomass (*1*). It is thus an exciting time for virology and the export of this field to a wide range of scientific endeavors.

If we view viruses as molecular containers, there are three important interfaces that can be exploited (Fig. 1): the exterior, the interior, and the interface between protein subunits making up the container (or capsid). Typically, viruses are assembled from repeating subunits to form highly symmetrical and homogeneous architectures (Fig. 2) (*2*, *3*). Viruses occur in a range of shapes and sizes, from 18 to 500 nm for icosahedral structures and >2 μm in length for filamentous or rod-shaped viruses. This variety provides a library of platforms for tailored applications where size, shape, and stability are required. All viruses encode, package, and transport viral nucleic acid. However, many will assemble (either naturally or through genetic manipulation) into noninfectious containers devoid of genetic material. Conceptually, this allows one to replace the natural viral cargo with a wide range of synthetic cargos. The plasticity of the structural building blocks (subunits) to both chemical and genetic modifications, without affecting the overall architecture, gives rise to a rich resource for materials and pharmaceutical applications.

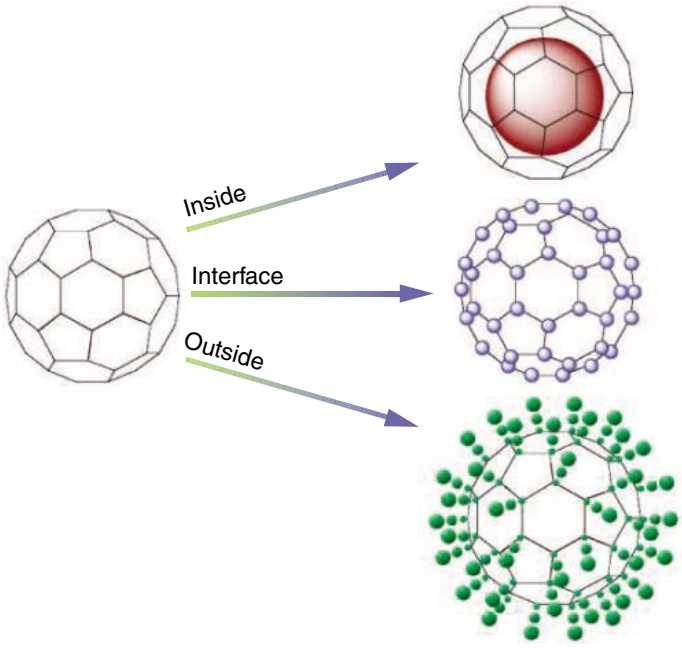

Fig. 1. A schematic of the three important interfaces available for chemical and genetic manipulation in an assembled viral protein cage architecture. The outer surface, the interior surface, and the interface between subunits have all been used for the construction of multivalent, multifunctional viral cage–based materials.

The interior interface of the viral capsid architecture has been used for directing encapsulation and synthesis of both organic and inorganic materials. All viruses package their viral nucleic acid within their capsid architecture, and the principles governing the packaging of this cargo have been exploited to package nonviral cargoes (*4*). For example, the native positive-charge density on the interior interface of empty (nucleic acid–free) cowpea chlorotic mottle virus (CCMV) capsid was used for nucleating inorganic mineralization reactions to form spatially constrained nanoparticles of polyoxometalate salts (tungstates $H_2W_{12}O_{42}^{10-}$, molybdates, and vanadates $V_{10}O_{28}^{6-}$) (*4*). In addition, through protein design and genetic engineering, the charge on the interior surface of the CCMV capsid has been altered, from positive to negative, without disrupting the ability to assemble. This negative-charge density was effective at directing the surface nucleation of transition metal oxides (Fe_2O_3, Fe_3O_4, and Co_2O_3), which proceed though cationic precursors stabilized at the highly anionic capsid interior interface (*5*). Spatially resolved elemental imaging of these materials provides a view of the hard-soft interface, an important aspect of biomaterials (Fig. 3) and one that is experimentally difficult to probe. The anisotropic rod-shaped tobacco mosaic virus (TMV) has also been used as a template for formation of metal nanowires using the interior cavity of the virus as a constraining environment (*6*). The interior interface of the capsid architectures also provides a rich, highly symmetric, and repetitive surface for encapsulation of cargo molecules through covalent attachment to site-specifically engineered residues on the interior surface. Thus, a cysteine residue genetically introduced into a subunit presents a reactive thiol group in the assembled protein cage architecture at all symmetry-related sites. Medically relevant small molecules such as therapeutics and imaging agents can be chemically attached to these reactive functional groups (*7*–*9*). The utility of this approach has been demonstrated with the use of a viruslike protein cage architecture to attach and selectively release the anticancer drug doxorubicin (*10*). This approach is medically advantageous because the protein cage acts to sequester its cargo (either natural or synthetic) until directed to be released. During administration and clearance, the encapsulated drug or imaging agent potentially remains invisible to the exterior environment and is therefore inert and biologically unavailable en route to its targeted cell.

Interactions at the subunit interface in the viral architecture provide an assembly-dependent

Center for Bio-Inspired Nanomaterials, Montana State University, Bozeman, MT 59717, USA. E-mail: tdouglas@chemistry.montana.edu (T.D.); myoung@montana.edu (M.Y.)

surface for manipulation of cage architecture and stability. Many viral capsids exhibit pleomorphism, the ability to assemble into a range of different architectures, either naturally or through genetic and chemical manipulation (*11*). This can result in alteration of the structure from icosahedral cages through tubes to planar sheetlike architectures (*12*). This structural flexibility is an example of how subtle changes to the noncovalent intersubunit interactions can direct capsid assembly and architectures. These noncovalent interactions also direct a range of programmable structural transitions and control the underlying structural dynamics of viral capsids. In general, it is likely that most virus capsids are dynamic metastable structures whose transitions are only now being revealed (*13*). In the case of CCMV, 180 metal-binding sites are created at the interface between subunits in the assembled capsid. The metal ions play a key role in controlling a structural transition in which 60 separate 2-nm pores in the capsid structure are reversibly opened and closed (*14*). This allows molecular communication between the interior of the cage and the exterior environment through a controlled gating mechanism. In a synthetic approach, using the endogenous metal-binding sites of the CCMV architecture, Gd(III) ions have been incorporated into the capsid, and the activity of the construct as a magnetic resonance imaging contrast agent is being evaluated in vitro and in vivo. In vitro, these viral-based magnetic materials exhibit some of the highest relaxivities measured to date (*15*) and demonstrate the value of precise spatial control achieved with the intersubunit interface.

The viral container interacts with its environment through the external surface and allows the cage architecture to be modified with small molecules or directed toward specific interactions to both biological and nonbiological surfaces. By design, the exterior surface of all viruses serves as a platform for multivalent presentation. Multivalent presentation allows for markedly enhanced interaction as compared with monovalent interactions. Viruses often display surface-exposed molecular apparatus for host cell–specific recognition and avoidance of host defense mechanisms. With a biomimetic approach to redirect virus cell targeting toward therapeutic applications, substantial progress has been made in genetically and synthetically incorporating ligands onto exterior viral surfaces. Incorporation of antibodies and targeting peptides to the exterior surfaces of viral capsids and other protein cage architectures has been shown to impart cell- and tissue-specific targeting, with clear implications for delivery of therapeutics and imaging agents (*16*, *17*). In a similar approach, through selective incorporation of surface-exposed thiol groups (cysteine), viral capsid monolayers have been selectively patterned onto Au surfaces (*18*). Molecular biology allows modification of amino acid residues at defined points within the cage structures. These reactive groups have been used for site-specific attachment of small molecules, including Au nanoparticles (*19*), fluorophores (*7*, *9*), carbohydrates (*20*), nucleic acids (*21*), and peptides (*16*, *17*). Contributions from synthetic chemistry will provide a broader palette of reaction chemistries for attachment of small molecules (*22*, *23*).

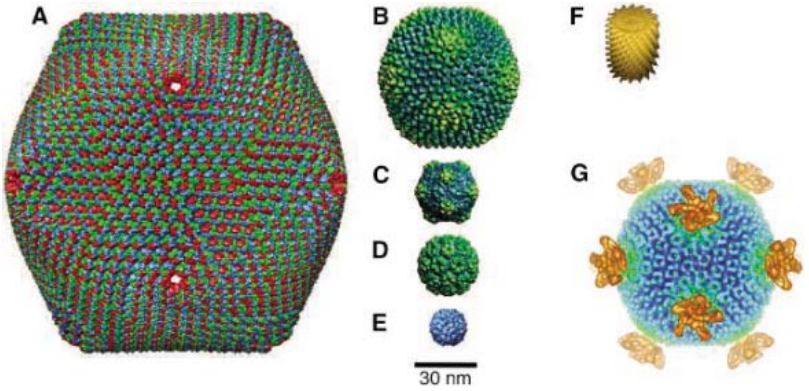

Fig. 2. Cryo–electron micrograph and image reconstructions of a library of viral capsids, including both icosahedral (*2*) and helical viruses (*3*). (**A**) *Paramecium bursaria* Chlorella virus type 1 (PCB-1), 170-nm diameter. (**B**) Murine polyoma virus, 51-nm diameter. (**C**) Cowpea mosaic virus, 31-nm diameter. (**D**) CCMV, 28-nm diameter. (**E**) Satellite tobacco mosaic virus, 18-nm diameter. (**F**) A small section of the rod-shaped TMV, which measures 18 by 300 nm. (**G**) Sulfolobus turreted icosahedral virus isolated from a boiling, acid environment in Yellowstone National Park (*30*).

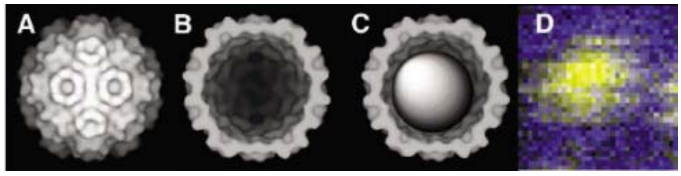

Fig. 3. (**A**) Cryo–electron micrograph reconstruction of CCMV. (**B**) Cut-away view of the CCMV cage showing the hollow interior cavity. (**C**) Schematic of a "guest" material encapsulated within the cage. (**D**) Spatially resolved spectral imaging by high-angle annular dark field scanning transmission electron microscopy of genetically modified CCMV with Fe_2O_3 synthesized within the cage [blue, N (from the protein); yellow, Fe (from the Fe_2O_3)], indicating the spatial relationship between the hard inorganic guest material (Fe_2O_3) and the soft viral protein cage (*5*).

Viruses provide a platform for the surface display of an incredible range of biological ligands. This advantage has been used in phage display technology, which provides a powerful use of biological combinatorial engineering to generate sequence diversity for practical applications. Small, randomized peptides expressed on the surface of a virus population are a powerful tool for identifying specific protein interactions with both organic and inorganic materials. Phage display has been used to identify peptide-based ligands for targeting specific cell and tissue types (*24*). Phage display libraries have also been exploited for materials applications, including specific binding to material surfaces and the ability to use those peptides to direct nucleation with control over composition, polymorph, and morphology (*25*, *26*). Identification of these active peptides has led to the synthesis of materials under mild biomimetic conditions, a notable advantage to materials processing. The phages displaying these peptides have themselves been used as templates for materials synthesis, thus exploiting two very important aspects: the organic-inorganic molecular recognition from the peptides and the unique viral architecture upon which these peptides are displayed (*26*). The nucleation peptides identified by phage display can be engineered into other virus and viruslike protein cage architectures to direct nucleation and spatial control over mineral particle growth (*27*).

As with all new approaches, there are challenges to overcome. For biomedical applications, the interactions of the protein capsids with the immune system and evaluation of toxicity need to be fully addressed. The capsid is protein based and immune responses are anticipated. While these are important issues, it is likely that they are not insurmountable, given that viruses and their hosts have coexisted and coevolved. In addition, the systems currently under investigation are all nonreplicating viral capsids, thus avoiding issues of viral mutation, recombination, replication in nontargeted tissue, and infection. Similar to other approaches using biological molecules, the effects of the immune system can be mitigated, resulting in effective therapies. This is often achieved

through preventing host recognition, either by using humanized proteins or by masking the recognition surface through attachment of poly(ethylene glycol) [pegylation (*28*)]. One can even imagine taking advantage of the immune system to enhance the utility of viral capsids through the rapid clearance of cages not localized at the cell or tissue target. This potentially would reduce the deleterious effects of exposure to nontargeted therapeutic agents.

There are other attributes of viruses that have not yet been exploited but are well within the realm of possibility. Besides delivering nucleic acids, many viruses deliver other cargo, including catalysts and regulatory molecules. One can envision the targeted delivery of synthetic catalytic capacity or designer regulatory molecules. Engineered viral capsids can be envisioned as Trojan horses, remaining quiescent until a cellular signal causes release of their cargo. The ability to sequester a cargo within a protein architecture is not exclusive to viruses; similar architectures are common in the biological world, including ferritins (*29*) and heat shock proteins, and these have also been used for pharmaceutical and materials applications. Synthetic approaches in materials science often use extreme conditions, and the biological world has been traditionally viewed as a limited source of raw materials due to the relatively narrow temperature and chemical environments in which they exist. This perception is being challenged by the amazing array of environments that support life and their associated viruses. For example, the recent discovery of viruses from extreme thermal environments (Fig. 2G) potentially expands the synthetic window in which virus architectures may be used for materials applications (*30*). An extension of the principles exemplified by viruses to biomimetic approaches with the full range of protein templates will open the range of synthetic possibilities. We have turned a corner from viewing viruses only as hostile enemies to seeing and using them as a potentially vast and beneficial resource. Ultimately, the utility of viral capsids will be limited only by our own creativity.

References and Notes

1. C. A. Suttle, *Nature* **437**, 356 (2005).
2. C. M. Shepherd *et al.*, *Nucleic Acids Res.* **34**, D386 (2006).
3. Y. Zhu, B. Carragher, D. J. Kriegman, R. A. Milligan, C. S. Potter, *J. Struct. Biol.* **135**, 302 (2001).
4. T. Douglas, M. J. Young, *Nature* **393**, 152 (1998).
5. T. Douglas *et al.*, *Adv. Mater.* **14**, 415 (2002).
6. M. Knez *et al.*, *Nano Lett.* **3**, 1079 (2003).
7. E. Gillitzer, D. Willits, M. Young, T. Douglas, *Chem. Commun.* 2390 (2002).
8. J. D. Lewis *et al.*, *Nat. Med.* **12**, 354 (2006).
9. Q. Wang, T. W. Lin, J. E. Johnson, M. G. Finn, *Chem. Biol.* **9**, 813 (2002).
10. M. L. Flenniken *et al.*, *Chem. Commun.* **2005**, 447 (2005).
11. J. Tang *et al.*, *J. Struct. Biol.* **15**, 59 (2006).
12. J. Bancroft, G. Hills, R. Markham, *Virology* **31**, 354 (1967).
13. B. Bothner *et al.*, *Virology* **334**, 17 (2005).
14. J. A. Speir, S. Munshi, G. Wang, T. S. Baker, J. E. Johnson, *Structure* **3**, 63 (1995).
15. M. A. Allen *et al.*, *Magn. Reson. Med.* **54**, 807 (2005).
16. M. L. Flenniken *et al.*, *Chem. Biol.* **13**, 161 (2006).
17. A. Chatterji *et al.*, *Bioconjugate Chem.* **15**, 807 (2004).
18. M. T. Klem, D. Willits, M. Young, T. Douglas, *J. Am. Chem. Soc.* **125**, 10806 (2003).
19. Q. Wang, T. W. Lin, L. Tang, J. E. Johnson, M. G. Finn, *Ang. Chem. Int. Ed.* **41**, 459 (2002).
20. K. S. Raja, Q. Wang, M. G. Finn, *ChemBioChem* **4**, 1348 (2003).
21. E. Strable, J. E. Johnson, M. G. Finn, *Nano Lett.* **4**, 1385 (2004).
22. Q. Wang *et al.*, *J. Am. Chem. Soc.* **125**, 3192 (2003).
23. T. L. Schlick, Z. Ding, E. W. Kovacs, M. B. Francis, *J. Am. Chem. Soc.* **127**, 3718 (2005).
24. R. Pasqualini, E. Ruoslahti, *Nature* **380**, 364 (1996).
25. S. R. Whaley, D. S. English, E. L. Hu, P. F. Barbara, A. M. Belcher, *Nature* **405**, 665 (2000).
26. C. B. Mao *et al.*, *Science* **303**, 213 (2004).
27. M. T. Klem *et al.*, *Adv. Funct. Mater.* **15**, 1489 (2005).
28. K. S. Raja *et al.*, *Biomacromolecules* **4**, 472 (2003).
29. F. C. Meldrum, V. J. Wade, D. L. Nimmo, B. R. Heywood, S. Mann, *Nature* **349**, 684 (1991).
30. G. Rice *et al.*, *Proc. Natl. Acad. Sci. U.S.A.* **101**, 7716 (2004).

31. We thank J. E. Johnson for a long-standing collaboration in developing this field and for use of cryo–electron micrograph images. Much of this work has been made possible by funding from NIH (RO1GM61340, R21EB005364, and RO1EB000432), Office of Naval Research (N00014-04-1-0672), and NSF (DMR011636 and MCB0132156).

10.1126/science.1123223

REVIEW

Aggresomes and Autophagy Generate Sites for Virus Replication

Thomas Wileman

The replication of many viruses is associated with specific intracellular compartments called virus factories or virioplasm. These are thought to provide a physical scaffold to concentrate viral components and thereby increase the efficiency of replication. The formation of virus replication sites often results in rearrangement of cellular membranes and reorganization of the cytoskeleton. Similar rearrangements are seen in cells in response to protein aggregation, where aggresomes and autophagosomes are produced to facilitate protein degradation. Here I review the evidence that some viruses induce aggresomes and autophagosomes to generate sites of replication.

Autophagy is a cellular response to starvation as well as a quality control system that can remove damaged organelles and long-lived proteins from the cytoplasm. Autophagy is involved in several developmental pathways and disease processes (*1*, *2*) and may provide defense against pathogens (*3*–*5*). In resting cells, autophagy is inhibited by the TOR (target of rapamycin) kinase and is triggered by events such as starvation or by the presence of rapamycin, either of which leads to dephosphorylation and inactivation of TOR. Autophagy begins with the sequestration of an area of the cytoplasm within a crescent-shaped isolation membrane (Fig. 1). Isolation membranes mature into large double-membraned vesicles (diameter 500 to 1000 nm) called autophagosomes, which eventually fuse with endosomes and lysosomes (*6*). Isolation membranes contain Atg5, Atg8 (also called LC3 in mammals), and Atg12 proteins. The Atg8 protein remains associated with the autophagosome and can be used to track the fusion of autophagosomes with endosomes and lysosomes.

Recent studies show that autophagy plays an important role in the removal of protein aggregates from cells. Protein aggregates—for example, those associated with neurodegenerative conditions such as Huntington's disease—are first delivered to the microtubule organizing center (MTOC) by dynein-dependent retrograde transport along microtubules (Fig. 2, step 1). When the degradative capacity of proteasomes is exceeded, protein aggregates accumulate in perinuclear inclusions called aggresomes (*7*). Aggresomes are surrounded by vimentin filaments and recruit chaperones, proteasomes, and mitochondria, suggesting a site specialized for protein folding and degradation. Many protein aggregates that cannot be refolded or degraded by proteasomes are eventually removed from aggresomes by autophagy, allowing delivery to lysosomes for degradation (*8*, *9*) (Fig. 2, step 3).

Large Cytoplasmic DNA Viruses Replicate in Factories that Resemble Aggresomes

The factories generated by large cytoplasmic DNA viruses such as vaccinia virus, irido-

School of Medicine, Health Policy and Practice, University of East Anglia, Norwich NR4 7TJ, UK. E-mail: t.wileman@uea.ac.uk

viruses, and African swine fever virus (ASFV) contain viral DNA and structural proteins concentrated within inclusions that closely resemble aggresomes (Fig. 3). In common with aggresomes, factories are located close to the MTOC and recruit vimentin, cellular chaperones, ubiquitin, and mitochondria (*10*–*14*). For ASFV, factories are absent in cells expressing the dominant negative dynein motor protein p50 dynamitin, indicating a role for the dynein motor in factory formation; also in common with aggresomes, these factories are dispersed by drugs that depolymerize microtubules (*14*).

The close structural similarity between aggresomes and virus factories raises the possibility that aggresomes offer an innate defense against infection that confines viruses within inclusions at the MTOC in preparation for degradation by proteasomes and/or autophagy (Fig. 2, step 2). The dual role played by dynein (in the formation of virus factories and in the delivery of protein aggregates to aggresomes) suggests that cells may see viruses as protein aggregates and transport them to the MTOC (*14*, *15*). Many viral core particles are of similar size (60 to 100 nm) to the aggregates that are transported to aggresomes, and the number of viruses that are recognized by dynein motors soon after entry into the cell is impressive (*16*); examples include vaccinia virus, ASFV, herpesvirus, adenovirus, and canine parvovirus. Recognition by dynein may be an innate response to viral particles. For many viruses, transport to the MTOC for storage and eventual degradation may protect cells from infection. For the large cytoplasmic DNA viruses, however, recognition by elements of the aggresome pathway may provide a site for replication.

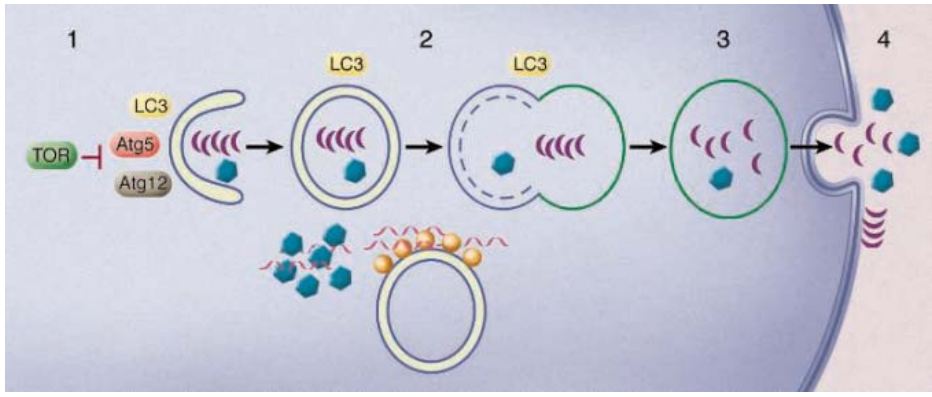

Fig. 1. Production of autophagosomes as replication sites for poliovirus and coronaviruses. Step 1: Autophagy is activated by dephosphorylation of TOR, which results in recruitment of Atg8, Atg5, and Atg12 onto crescent-shaped isolation membranes. Step 2: Isolation membranes release Atg5 and Atg12 and mature into double-membraned autophagosomes that engulf the cytosol, which may contain aggregated proteins (stacked crescents) or viruses (hexagons). The autophagosome provides a platform for the assembly of replication complexes by picornaviruses and nidoviruses (orange spheres). Step 3: Autophagosomes fuse with lysosomes, leading to degradation of content. Viruses and proteins that survive in lysosomes may be delivered to the cell surface (step 4).

Do Aggresomes Offer Advantages as Sites of Replication?

To demonstrate that aggresomes facilitate replication, it is necessary to show that replication is slowed in the absence of aggresomes. ASFV replication is blocked by p50 dynamitin, which suggests that delivery of incoming viruses to the MTOC is important to initiate virus replication (*14*). Replication of ASFV and iridoviruses also appears to require rearrangement of vimentin. During the early stages of ASFV infection, vimentin is transported by microtubules to the MTOC. Once viral DNA replication is initiated, vimentin is phosphorylated on serine by calcium/calmodulin-dependent protein kinase II (CaMKII) and is redistributed to the edge of the factory, where it forms a cage (*17*). Inhibition of CaMKII prevents vimentin cage formation and prevents virus DNA replication. Similarly, early studies showed that temperature-sensitive mutants of the iridovirus frog virus–3 that are unable to phosphorylate vimentin cannot rearrange vimentin and cannot proceed to late gene expression (*10*, *18*). Vimentin rearrangement may facilitate replication by providing a scaffold during the assembly of the virus factory (*12*), and the vimentin cage made later during infection may prevent diffusion of viral components into the cytoplasm (*14*, *17*). This would allow structural proteins to be concentrated within one site in the cell, with a steady supply of viral components and host proteins delivered from the cytoplasm along microtubules. Such a mechanism may be particularly important for complex large DNA viruses, such as vaccinia and ASFV, that are assembled from as many as 50 different structural proteins.

It is not always necessary for aggresomes to facilitate replication. It is possible that some viruses may be restricted to aggresomes because of innate cellular defenses against infection, but would replicate just as well if they remained in the cytoplasm. Rotaviruses replicate in cytoplasmic virus factories, which are globular, as in strain T3D, or filamentous, as in strain T1L. The globular factories coalesce and migrate to the MTOC, which suggests involvement of the aggresome pathway, whereas the filamentous factories align along microtubules in the cytoplasm, which are stabilized by a minor viral structural protein, μ2 (*19*, *20*). It is possible that immobilization of the factory on microtubules resists recruitment of rotavirus proteins into aggresomes (*19*). Because the filamentous strains of rotaviruses make greater quantities of viral proteins during infection and show increased virulence and broader tropism, escape from aggresomes may offer a selective advantage to rotaviruses.

How Do Viruses Avoid Degradation in Aggresomes?

One possibility is that the degradative arm of the pathway is blocked in infected cells. This could involve inhibition of transport of isolation membranes and autophagosomes into virus factories and/or inhibition of subsequent fusion with lysosomes. A second possibility is that isolation membranes are recruited into the factory and are then used as a source of membranes for virus envelopment. The membranes used for the envelopment of vaccinia virus and ASFV are poorly characterized but appear similar to the membranes used to form isolation membranes and autophagosomes (*6*). Both membranes are derived from specialized extensions of the endoplasmic reticulum (ER) and/or de novo membrane synthesis, producing perinuclear "virioplasm" or preautophagous structures, respectively. The crescent-shaped structures that form the inner envelope of vaccinia virus and ASFV are not dissimilar from the crescents formed by isolation membranes. When cells lacking Atg5 are infected with vaccinia virus, morphogenesis is normal (*21*), making it unlikely that the internal envelope of vaccinia originates from the isolation membrane.

Vaccinia virus and ASFV use microtubules to leave virus factories. Movement of vaccinia virus from factories requires intact microtubules and the viral proteins A27L and F12L, but the motor driving transport has not been identified (*22*–*24*). ASFV particles recruit the cargo-binding domain (TPR domain) of conventional kinesin light chain to factories

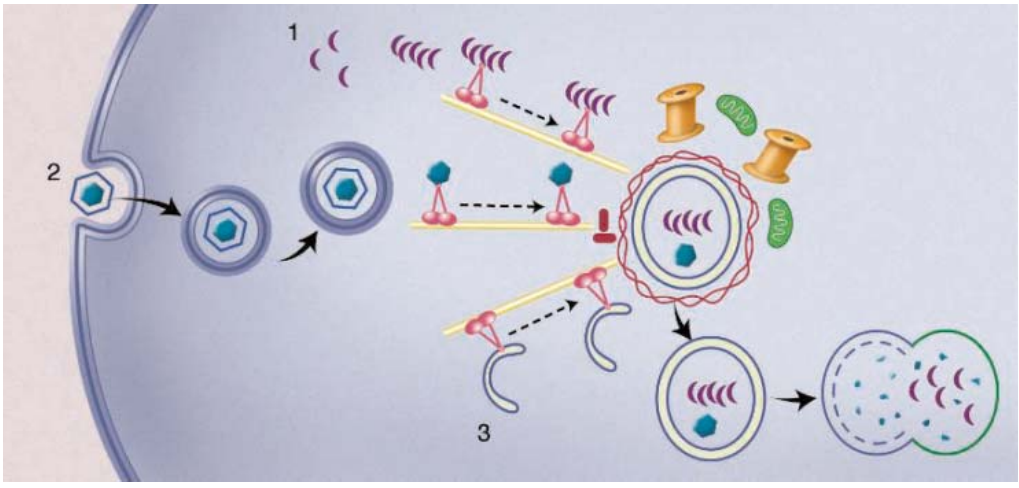

Fig. 2. Autophagy, aggresome, and virus assembly pathways converge at the MTOC. Step 1: Protein aggregates bind dynein motors and are transported to the MTOC on microtubules (yellow lines) and accumulate within aggresomes surrounded by vimentin. Step 2: Viruses (hexagons) entering cells are recognized by dynein motors and transported to aggresomes. Step 3: Isolation membranes are transported by dynein to aggresomes, where they engulf aggregated proteins. It is not known whether they also engulf viruses. The autophagosomes fuse with lysosomes, leading to degradation of protein aggregates and possibly of viruses.

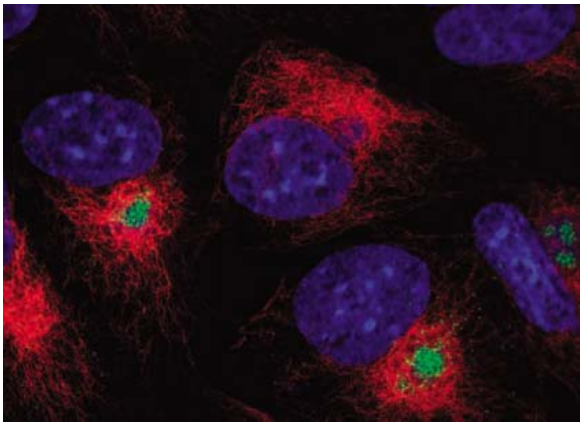

Fig. 3. African swine fever virus replicates in aggresomes. Cells infected with ASFV were labeled with antibody to the capsid protein (green). Viruses are assembled within a cage of vimentin (red) located next to the nucleus (blue). [Photo reproduced from (*47*) by permission of Blackwell Publishing; see also (*12*, *14*, *17*)]

and use kinesin to enter the cytoplasm (*25*). Recognition by kinesin needs to be linked to the final stages of virus assembly to ensure that assembly intermediates do not move away from the supply of structural proteins present in the factory before assembly is completed. ASFV lacking the pE120R protein from the outer capsid does not move from factories, which suggests a role for pE120R in recruitment of kinesin (*26*); however, direct binding of pE120R to kinesin has not been demonstrated. For vaccinia virus, recruitment of kinesin motors is regulated during envelopment by the trans-Golgi network and requires the viral membrane protein A36R, which binds to the TPR domain of kinesin light chain (*27*, *28*). This binding may be regulated by a second envelope protein, A33R, and/or by phosphorylation of A36R (*29*).

Replication of Viruses in Nuclear Aggresomes

Protein aggregation in the nucleus has been linked to neurodegenerative misfolded protein diseases such as Huntington's disease and spinocerebellar ataxias. Protein aggregates accumulate in nuclear aggresomes; because nuclear aggresomes recruit chaperones, ubiquitin, and proteasomes and expand in the presence of proteasome inhibitors, they may be sites specialized for protein degradation. Nuclear aggresomes are associated with nuclear domain 10 (ND10) bodies (*30*), which are also called promyelocytic leukemia (PML) bodies or promyelocytic leukemia oncogenic domains (PODs) and are involved in chromatin metabolism and DNA repair. ND10 structures are also associated with the genomes and/or replication complexes of herpesviruses, adenoviruses, parvoviruses, papovaviruses, and papillomaviruses (*31*). Thus, virus replication in the nucleus also takes place in structures that accumulate protein aggregates.

Aggregated proteins are continuously delivered to nuclear aggresomes and are relatively mobile. It is not yet understood how protein aggregates are recruited to, or recruit, ND10. ND10 structures are relatively static in the nucleus but can exchange their content with the rest of the nucleoplasm. When herpesvirus capsids are delivered to one side of the nucleus, ND10 is recruited to the site of incoming viruses, which suggests that viruses recruit ND10 components as they enter the nucleus (*32*). Recruitment requires association of viral DNA with viral proteins required for translation and/or replication with the genome, which suggests that ND10 is recruited to viral replication complexes. It will be interesting to follow up these studies, using infected cells containing nuclear inclusions, to determine whether viral genomes and protein aggregates colocalize in ND10. Recent studies show that autophagy markers are not recruited to nuclear aggresomes and that the turnover of aggregated protein is unaffected by conditions that modulate autophagy (*33*). Autophagy is unable to clear misfolded proteins from nuclear aggresomes, and this may be why ND10 bodies are favored as sites of virus replication in the nucleus.

Autophagosomes as Sites of Viral Replication

The Nidovirales and Picornaviridae are positive-stranded RNA viruses that assemble a replication complex containing the RNA polymerase, as well as proteins with helicase and nucleotide triphosphate activity, on the cytoplasmic face of cellular membranes. The Nidovirales constitute the arteriviruses and coronaviruses, and they replicate in association with double-membraned vesicles. The vesicles are smaller than cellular autophagosomes (diameter 500 to 1000 nm); their diameters range from 80 nm for the arteriviruses up to 100 to 300 nm for the coronaviruses (*34*–*36*). Arterivirus vesicles are connected to the ER, and those produced by the mouse hepatitis and SARS coronaviruses colocalize with Atg8 (*35*). Because coronavirus yields fall by a factor of 1000 in the absence of Atg5, the data suggest that the vesicles are related to autophagosomes. The vesicles can be produced by expression of the arterivirus Orf 1a encoding nonstructural proteins 2 to 7, which suggests that the transmembrane proteins and replicase enzymes encoded on Orf 1a stimulate production of autophagosomes (*34*).

The poliovirus replication complex also forms on double-membraned vesicles that originate either from coat protein complex II–

coated vesicles, which move proteins from the ER to the Golgi (*37*), or from autophagosomes (*38*). They are again smaller than cellular autophagosomes and range from 200 to 400 nm in diameter (*39*). A role for autophagy during replication of poliovirus is nonetheless supported by colocalization of Atg8 with virus-induced vesicles and by lowered virus yield in the absence of Atg12 and Atg8 (*40*). In common with coronaviruses, double-membraned vesicles are produced by coexpression of the membrane-targeted components of the replication complex, in this case 3A and 2BC (*38*, *40*).

Viruses may induce autophagy to generate a scaffold for the replication complex; alternatively, replication complexes may be restricted to autophagosomes as a result of innate defenses against infection. Although relatively few viruses have been studied to date, virus yields fall after loss of Atg proteins, which suggests that autophagosomes facilitate replication (*35*, *40*). The factor of 1000 fall for coronavirus is more striking than the factor of 20 fall seen for poliovirus; hence, viruses may vary in dependence on autophagosomes and/or Atg proteins. Surprisingly, suppression of Atg12 and Atg8 by RNA interference reduced extracellular poliovirus yield more than it reduced intracellular levels of virus, indicating a selective effect on virus release (*40*). Enteroviruses such as poliovirus are relatively resistant to low pH and proteases and may survive in autophagosomes and lysosomes. Viruses engulfed by autophagosomes (Fig. 1, step 2) may be released from cells after fusion of lysosomes with the plasma membrane (Fig. 1, step 4). A similar pathway leading to the extracellular delivery of protein aggregates may be responsible for the deposition of amyloid plaques associated with misfolded protein diseases. Again, the pathways followed by viruses and protein aggregates converge.

Two other families of positive-stranded RNA viruses, the alphaviruses and flaviviruses, replicate inside invaginations (diameter 50 nm) in cellular membrane compartments called spherules (*41*, *42*). The replication complexes are assembled inside spherules that are connected by a neck to the cytosol, allowing positive-sense genomes to be delivered into the cell. For poliovirus, most of the double-membraned vesicles appear to be sealed, which suggests that replication occurs on the outside of membrane vesicles, allowing direct delivery of new genomes into the cytosol. The RNA polymerase of poliovirus self-assembles into large flat ordered arrays (*43*) that are believed to coat the surface of membranes, forming a catalytic shell that may be critical for high-affinity binding of RNA and RNA elongation. The replicase complexes of alphaviruses, on the other hand, contain a low relative concentration of RNA polymerase. Replication efficiency may be enhanced by the neck of the spherule, which slows the diffusion of negative-sense RNA into the cytosol, increasing its availability as a template for genome replication.

The most striking difference between spherules and autophagosomes is their mechanism of production. Spherules are produced from existing cellular membranes by active assembly of viral proteins. This process has been likened to the coordinated assembly of viral proteins on membranes that leads to capsid assembly, genome packaging, and budding (*44*, *45*). Because autophagy is suppressed in resting cells by the TOR kinase, production of autophagosomes requires activation of signaling pathways. The structure of the vesicle is then determined by host Atg proteins rather than by the assembly of viral proteins.

Conclusions

It is clear that some viruses replicate on (or within) structures used by cells to remove protein aggregates. This may be important for virus replication, because virus yields fall if the structures are not made or if viruses are denied access to them. Aggresomes and autophagosomes are present at low levels in resting cells and are stimulated in response to specific signals. Understanding how virus infection stimulates these pathways to produce new structures for virus replication is a challenge for the future. Protein aggregation causes global inhibition of the ubiquitin-proteasome system and signals the formation of aggresomes (*46*). It will be interesting to see whether large cytoplasmic DNA viruses also modulate the ubiquitin-proteasome system to generate inclusions for replication. Virus factories share many structural features with aggresomes, but direct evidence that they are the same structure has been lacking. It will be important to demonstrate a functional link between aggresomes and factories—for example, by showing that virus factories can recruit misfolded proteins, or that viruses assemble in preformed aggresomes. Autophagosomes are formed in cells expressing the membrane-targeted components of replication complexes. These proteins provide an excellent opportunity to unravel how these viruses generate autophagosomes. Finally, it is likely that many viruses stimulate these pathways during infection and are eliminated (*4*, *5*). An understanding of how some viruses survive will provide a better understanding of the role played by autophagy and aggresome pathways during infection, leading to valuable tools for further dissection of these processes.

References and Notes

1. T. Shintani, D. J. Klionsky, *Science* **306**, 990 (2004).
2. B. Levine, D. J. Klionsky, *Dev. Cell* **6**, 463 (2004).
3. V. Deretic, *Trends Immunol.* **26**, 523 (2005).
4. Z. Talloczy *et al.*, *Proc. Natl. Acad. Sci. U.S.A.* **99**, 190 (2002).
5. K. Kirkegaard, M. P. Taylor, W. T. Jackson, *Nat. Rev. Microbiol.* **2**, 301 (2004).
6. F. Reggiori, D. J. Klionsky, *Curr. Opin. Cell Biol.* **17**, 415 (2005).
7. J. A. Johnston, C. L. Ward, R. R. Kopito, *J. Cell Biol.* **143**, 1883 (1998).
8. A. Iwata, B. E. Riley, J. A. Johnston, R. R. Kopito, *J. Biol. Chem.* **280**, 40282 (2005).
9. B. Ravikumar *et al.*, *Nat. Genet.* **37**, 771 (2005).
10. M. Chen, R. Goorha, K. G. Murti, *J. Gen. Virol.* **67**, 915 (1986).
11. A. Ploubidou *et al.*, *EMBO J.* **19**, 3932 (2000).
12. C. Risco *et al.*, *J. Virol.* **76**, 1839 (2002).
13. A. Schepis, B. Schramm, C. A. M. de Haan, J. K. Locker, *Traffic* **7**, 308 (2006).
14. C. M. Heath, M. Windsor, T. Wileman, *J. Cell Biol.* **153**, 449 (2001).
15. B. Sodeik, *J. Cell Biol.* **159**, 393 (2002).
16. K. Dohner, C.-H. Nagel, B. Sodeik, *Trends Microbiol.* **13**, 320 (2005).
17. S. Stefanovic, M. Windsor, K. Nagata, M. Inagaki, T. Wileman, *J. Virol.* **79**, 11766 (2005).
18. D. B. Willis, R. Goorha, A. Granoff, *Virology* **98**, 328 (1979).
19. J. S. Parker, T. J. Broering, J. Kim, D. E. Higgins, M. L. Nibert, *J. Virol.* **76**, 4483 (2002).
20. T. J. Broering *et al.*, *J. Virol.* **78**, 1882 (2004).
21. H. Zhang *et al.*, *Autophagy* **2**, 91 (2006).
22. C. M. Sanderson, M. Hollinshead, G. L. Smith, *J. Gen. Virol.* **81**, 47 (2000).
23. J. Rietdorf *et al.*, *Nat. Cell Biol.* **3**, 992 (2001).
24. M. Hollinshead *et al.*, *J. Cell Biol.* **154**, 389 (2001).
25. N. Jouvenet, P. Monaghan, M. Way, T. Wileman, *J. Virol.* **78**, 7990 (2004).
26. G. Andres *et al.*, *J. Virol.* **75**, 6758 (2001).
27. B. M. Ward, B. Moss, *J. Virol.* **78**, 2486 (2004).
28. U. F. Greber, M. Way, *Cell* **124**, 741 (2006).
29. T. P. Newsome, N. Scaplehorn, M. Way, *Science* **306**, 124 (2004); published online 5 August 2004 (10.1126/science.1101509).
30. L. Fu *et al.*, *Mol. Biol. Cell* **16**, 4905 (2005).
31. R. D. Everett, *Cell Microbiol.* **8**, 365 (2006).
32. R. D. Everett, J. Murray, *J. Virol.* **79**, 5078 (2005).
33. A. Iwata *et al.*, *Proc. Natl. Acad. Sci. U.S.A.* **102**, 13135 (2005).
34. K. W. Pedersen, Y. van der Meer, N. Roos, E. J. Snijder, *J. Virol.* **73**, 2016 (1999).
35. E. Prentice, W. G. Jerome, T. Yoshimori, N. Mizushima, M. R. Denison, *J. Biol. Chem.* **279**, 10136 (2004).
36. R. Gosert, A. Kanjanahaluethai, D. Egger, K. Beinz, S. C. Baker, *J. Virol.* **76**, 3697 (2002).
37. R. C. Rust *et al.*, *J. Virol.* **75**, 9808 (2001).
38. D. A. Suhy, T. H. Giddings Jr., K. Kirkegaard, *J. Virol.* **74**, 8953 (2000).
39. S. Dales, H. J. Eggers, I. Tamm, G. E. Palade, *Virology* **26**, 379 (1965).
40. W. T. Jackson *et al.*, *PLoS Biol.* **3**, e156 (2005).
41. J. Mackenzie, *Traffic* **6**, 967 (2005).
42. R. R. Novoa *et al.*, *Biol. Cell* **97**, 147 (2005).
43. J. M. Lyle, E. Bullitt, K. Bienz, K. Kirkegaard, *Science* **296**, 2218 (2002).
44. M. Schwartz *et al.*, *Mol. Cell* **9**, 505 (2002).
45. M. Schwartz, J. Chen, W.-M. Lee, M. Janda, P. Ahlquist, *Proc. Natl. Acad. Sci. U.S.A.* **101**, 11263 (2004).
46. E. J. Bennett, N. F. Bence, R. Jayakumar, R. R. Kopito, *Mol. Cell* **17**, 351 (2005).
47. P. Monaghan, H. Cook, P. Hawes, J. Simpson, F. Tomley, *J. Microsc.* **212**, 62 (2003).

48. Work in the author's laboratory was funded by the Biotechnology and Biological Sciences Research Council.

10.1126/science.1126766

REVIEW

Type 1 Interferons and the Virus-Host Relationship: A Lesson in Détente

Adolfo García-Sastre[1] and Christine A. Biron[2]*

The interface between an infectious agent and its host represents the ultimate battleground for survival: The microbe must secure a niche for replication, whereas the host must limit the pathogen's advance. Among the host's arsenal of antimicrobial factors, the type 1 interferons (IFNs) induce potent defense mechanisms against viruses and are key in the host-virus standoff. Viruses have evolved multiple tricks to avoid the immediate antiviral effects of IFNs and, in turn, hosts have adapted use of this innate cytokine system to galvanize multiple additional layers of immune defense. The plasticity that exists in these interactions provides us with a lesson in détente.

Viruses have adapted strategies to evade or even inhibit key elements of host immune responses. Because particular arms of the responses are susceptible to neutralization, the host has evolved means of activating a broad range of defense mechanisms to ensure effective protection. In the midst of this power struggle, a remarkable picture is emerging of the importance of type 1 IFNs for antiviral defense and immune regulation. This family of innate cytokines has many members, with the best characterized being a single β and multiple α gene products. The host has a variety of pathways to elicit the expression of the IFN-α/β cytokines, including pathways protected from virus-mediated inhibition in infected cells. Viruses have countered by incorporating machinery that can dampen specific defense mechanisms that type 1 IFNs induce. Host organisms have taken advantage of the cytokines to shape and enhance its panoply of independent immune effector mechanisms so that any agent overcoming the direct antiviral effects activated by type 1 IFNs will have to contend with other responses. At their best, the tools used by the virus and host achieve conditions for coexistence.

Induction of Type 1 IFNs by Viruses

Mammalian hosts have evolved a variety of cellular sensors for viral infection, and it is the engagement of these protein receptors that ultimately leads, through complex and redundant pathways, to the production of type 1 IFN. Sensors fall into two functional classes that differ fundamentally with respect to localization, associated with either the cell membrane or the cytoplasm (Fig. 1). An important biological consequence of this differential localization is the flexibility it affords the host in triggering type 1 IFN production, either in infected cells and/or before cells are exposed to viral products capable of blocking induction.

Extracytoplasmic pathways for pathogen sensing. The Toll-like receptor (TLR) family is composed of membrane proteins with domains designed to sample the environment for pathogen-associated molecular patterns (PAMPs) (*1*). Subsequently, TLRs become activated and transmit signals through their cytoplasmic Toll/interleukin-1 receptor (TIR) domains, resulting in the transcriptional induction of multiple genes involved in innate and adaptive immunity, including type 1 IFN. Different TLR molecules recognize specific PAMPs and, among these, TLR3, TLR7, TLR8, and TLR9 appear to play important roles in identifying viral products. TLR7 and TLR8 become activated by recognition of single-stranded RNA (*2*–*4*), whereas DNA activates TLR9 (*5*). Accordingly, TLR9 becomes activated in response to infection with DNA viruses such as herpesviruses, and TLR7 and TLR8 respond to RNA viruses such as influenza viruses and HIV. In contrast, TLR3 appears to represent a more general sensor of viral infection through detection of double-stranded RNA (dsRNA) (*6*), a by-product of viral replication and transcription for both RNA and DNA viruses. These four TLR molecules localize mainly in endosomal compartments of the cell, and it is upon endosome-mediated internalization of viruses (in the case of TLR7/8/9) or products of viral replication from lysed and/or apoptotic virus-infected cells (in the case of TLR3) that they are believed to come into contact with their respective activating ligands. To expose the viral genome to the corresponding TLR, this process most likely involves degradation of a subset of virus particles in the endosome. In addition, some cell surface–expressed TLRs, such as TLR4, have been shown to bind to specific viral glycoproteins and induce IFN production in a different range of cells.

TLR3 induction of type 1 IFN is mediated through the TIR domain–containing adaptor-inducing IFN-β (TRIF). TRIF mediates the activation of IκB kinase ε (IKKε) and tank-binding kinase 1 (TBK1), which phosphorylate IFN regulatory factor 3 (IRF3), resulting in its dimerization and nuclear translocation where it promotes gene transcription. TRIF also mediates the activation of neural factor κB (NF-κB) and activating protein 1 (AP1) through the kinase complex IKKα/β/γ and the mitogen-activated protein kinase (MAPK) cascade, respectively (*7*). These three transcription factors (IRF3, NF-κB, and AP1) coordinate the transcriptional regulation of the IFN-β gene (*8*).

Induction of type 1 IFN by TLR7/8/9 is mediated by the adaptor molecule myeloid differentiation primary response protein 88 (MyD88), which associates with the TIR domain of the TLRs, the interleukin-1 receptor–associated kinases IRAK1 and IRAK4, and the tumor necrosis factor receptor–associated factor 6 (TRAF6). This results in downstream activation of IRF7, and of the IKKα/β/γ and the MAPK cascades, leading to NF-κB and AP-1 activation (*7*). IRF7 is functionally similar to IRF3 and mediates the induction of IFN-β but, unlike IRF3, it also initiates the general induction of the IFN-α genes (*9*). TLR7/8/9 and IRF7 appear to be constitutively expressed in only a subset of cells, the plasmacytoid dendritic cells (PDCs), which are characterized by high IFN production and can spearhead the early IFN response (*10*).

Cytoplasmic pathways for sensing. TLR-independent pathways of sensing viral infections and triggering IFN production appear to exist as well. At least one such pathway is mediated by members of a family of DExD/H box RNA helicase proteins that contain caspase-recruiting domains (CARDs) (*11*). In contrast to TLRs, these sensors are all cytoplasmic and, thus, exclusively mediate intracellular recognition of viruses. Two such sensors have so far been described: the retinoic acid–inducible gene I (RIG-I) and the melanoma differentiation–associated gene 5 (mda5). These RNA helicases, upon binding to dsRNA, interact with a downstream molecule named independently by four different groups as mitochondrial antiviral signaling protein (MAVS) (*12*), IFN-β promoter stimulator 1 (IPS-1) (*13*), virus-induced signaling adaptor (VISA) (*14*), and CARD adaptor–inducing IFN-β (CARDIF) (*15*). This mitochondrial-resident protein interacts with the CARD of RIG-I and recruits and activates, by not yet well-defined mechanisms, IKKε/TBK1, the IKKα/β/γ complex, and MAPK, resulting in activation of IRF3, NF-κB, and AP-1 and in IFN-β induction. Evidence for a TLR and RIG-I independent pathway in recognition of cytoplasmic DNA has recently been obtained (*16*, *17*),

[1]Department of Microbiology, Mount Sinai School of Medicine, New York, NY 10029, USA. [2]Department of Molecular Microbiology and Immunology, Division of Biology and Medicine, Brown University, Providence, RI 02912, USA.

*To whom correspondence should be addressed. E-mail: Christine_Biron@brown.edu

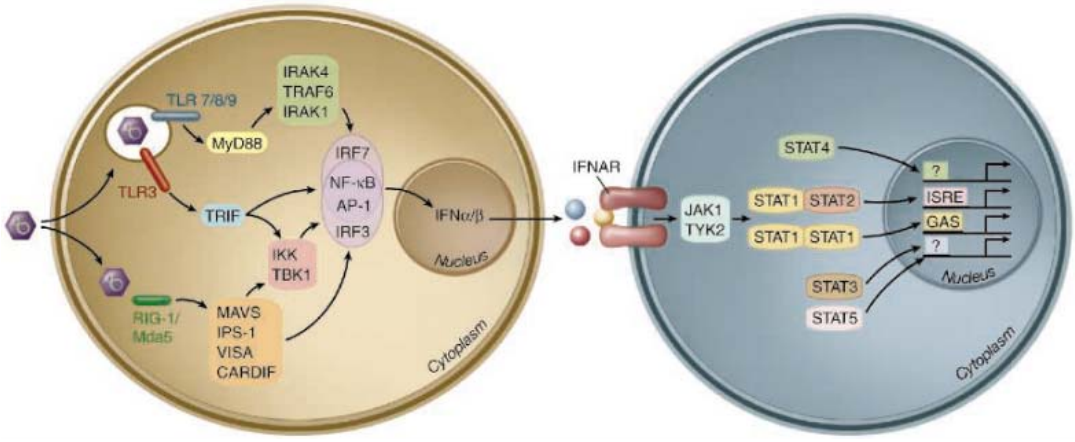

Fig. 1. The pathways to and from type 1 IFN are flexible. Families of sensors are available to detect viral products and induce expression of the cytokines. One set senses components in the cytoplasm. Another set is localized in cell membranes. There is also flexibility in the signaling pathways used by type 1 IFNs, with the potential to induce the activation of multiple STAT molecules and their downstream targets of transcription.

and additional sensors of other viral products are likely to exist.

IFN-Mediated Effects On Defense

As secreted factors, the type 1 IFNs regulate a range of immune responses through the type 1 IFN receptor, a cell surface transmembrane receptor composed of two subunits, IFN-α receptor 1 (IFNAR1) and IFNAR2 (*18*–*20*). Binding of the IFNAR results in receptor subunit dimerization and activation of kinases that associate with their cytoplasmic tails: the Janus-activated kinase 1 (JAK1) and tyrosine kinase 2 (TYK2). In turn, tyrosine phosphorylation activates the signal transducers and activators of transcription 1 and 2 (STAT1 and STAT2), to form a trimeric STAT1-STAT2-IRF9 complex, also known as IFN-stimulated gene factor 3 (ISGF3), as well as a STAT1 homodimer complex, known as the IFN-γ–activated factor (GAF). Both complexes translocate to the nucleus and bind to DNA regulatory sequences containing IFN-stimulated response elements (ISREs) and IFN-γ–activated sites (GAS), respectively. The ensuing stimulation leads to the transcription of more than 100 IFN-stimulated genes (ISGs), whose concerted action leads to the generation of an "antiviral state." Although signaling through STAT1/STAT2 and STAT1/STAT1 dimers are the best characterized of the type 1 IFN-induced intracellular pathways to gene expression, cells can differ greatly in their signaling response to type 1 IFN, and a variety of other signaling pathways can also be activated (*18*, *19*). Some of these are revealed in the absence of STAT1 (*21*), depend on STAT4 (*22*, *23*), may be STAT2 dependent but STAT1 independent (*24*), and/or are a result of STAT 3 or 5 activation (*18*). The flexibility that receptors for type 1 IFNs have for accessing downstream signaling molecules may be regulated by the relative abundance of STATs themselves (*22*).

Antiviral activities of ISGs. The myxovirus resistance gene Mx, the protein kinase stimulated by dsRNA PKR, and the 2′-5′ oligoadenylate synthetases (OAS) are among the best characterized ISGs with antiviral activity (*20*). Mx is a guanosine triphosphatase (GTPase) belonging to the dynamin family that sequesters viral ribonucleoproteins to specific subcellular compartments. PKR is a serine-threonine kinase that phosphorylates downstream substrates upon recognition of dsRNA, including the elongation initiation factor eIF2α, resulting in the inhibition of protein translation. The OAS proteins are also activated by dsRNA, leading to the generation of 2′-5′ oligoadenylates, which activate ribonuclease L (Rnase L) that degrades cellular and viral RNA. Both PKR and the OAS/RNaseL systems have profound inhibitory effects on basal cellular processes that eliminate virus-infected cells by suicide (*25*). Even in the absence of these IFN-regulated antiviral pathways, however, IFN can still induce an effective antiviral response (*26*). The existence of other multiple ISGs with antiviral activity, multiple IFN genes, and multiple pathways leading to the production of IFN raises the intriguing question of whether hosts have evolved redundant pathways to make it generally difficult for viruses to use any single mechanisms to inhibit the IFN antiviral response or whether different factors of the IFN system mediate inhibition of specific virus families.

Regulation of immune responses. Type 1 IFNs extend their antiviral defense functions to a number of other immune response components. They amplify their own expression through two independent mechanisms: the induction of IRF7 to extend IFN gene expression to a broader range of IFN-αs (*9*) and the accumulation of PDCs, major contributors to IFN-α/β responses (*27*). The cytokines also activate natural killer (NK) cells to mediate elevated cytotoxicity (*28*, *29*) and induce interleukin-15 (IL-15) to promote NK cell proliferation (*29*). At high concentrations, type 1 IFNs inhibit IL-12 (*30*) and NK cell responsiveness for IFN-γ expression (*21*). All of these effects on innate immune responses depend on STAT1. Type 1 IFNs also regulate adaptive immunity. The early STAT1-dependent induction of IL-15 contributes to short-term proliferation of memory CD8 T cells (*31*). However, only certain subsets of cells are equipped to respond to IL-15 and, consistent with the antiproliferative effects of type 1 IFNs (*32*), STAT1 acts to limit nonspecific CD8 T cell expansion, at times overlapping with the induction of innate responses (*33*). Hence, early during infections, the type 1 IFNs work to enhance proliferation of certain cell subsets and inhibit others through STAT1-dependent mechanisms.

There are many other paradoxical effects assigned to type 1 IFNs, and some of these may be explained by regulation of accessibility to different signaling pathways (*22*, *33*–*35*). STAT1 is induced by the cytokines, and the protein concentrations of this molecule are elevated at times of type 1 IFN induction during viral infection (*22*). These conditions may steer responses to STAT1/STAT2 and STAT1/STAT1 with induction of the antiviral defenses and general inhibition of proliferation as described above, but they also limit the ability of type 1 IFNs to activate STAT4 (*22*). To be effective in defense, antigen-specific CD8 T cells must expand in the presence of type 1 IFNs, and their IFN-γ production is aided by type 1 IFN- and STAT4-dependent events (*22*). Thus, the elevated STAT1 levels induced early during infection and the consequences this has for proliferation and STAT4 accessibility present inherent obstacles for generating protective T cell–mediated immunity. To overcome this, antigen-specific CD8 T cells with lower relative levels of STAT1 are induced and preferentially undergo proliferation at times when STAT1 levels are elevated in most other cells (*33*). Thus, the critical role for STAT1 in controlling the effects of type 1 IFNs may be a result of its own differential expression in different cell subsets. Linking cytokine signaling to different pathways, depending on transcription factor levels, is a sophisticated means of providing cells with a variety of downstream options using only a limited number of genes.

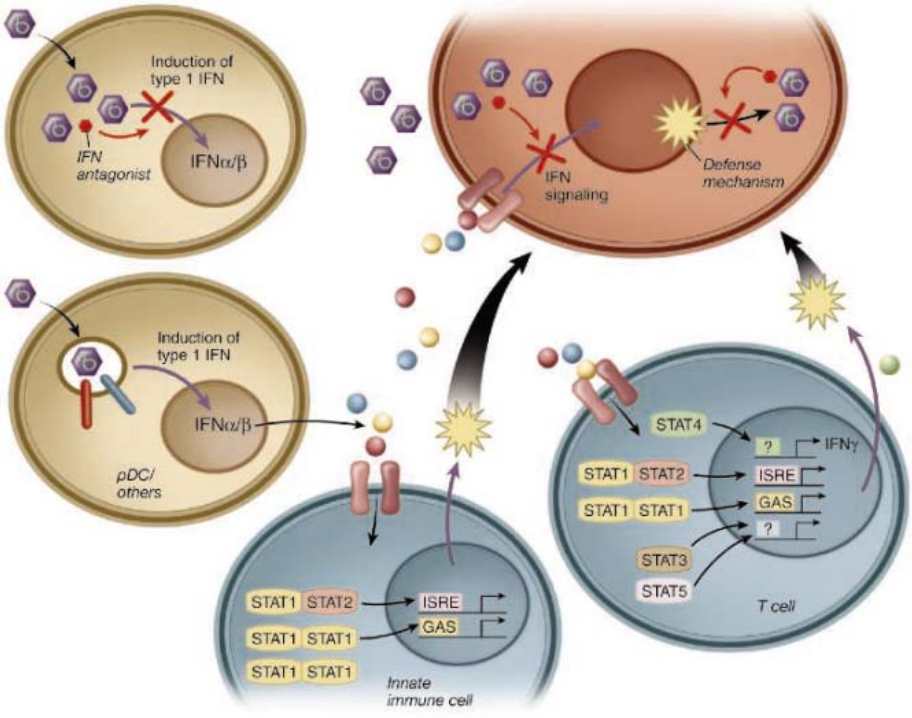

Fig. 2. The host uses type 1 IFNs to its advantage despite viral evasion mechanisms. The sensors for detecting viral products include components in the cytoplasm that are particularly sensitive to viral blocks. The set localized in cell membranes is available for sensing viral products before cells are infected. Once induced, the cytokines enhance innate and adaptive antiviral defense mechanisms as well as direct antiviral pathways. The intracellular signaling pathways used by type 1 IFNs appear to be modified to access a variety of downstream target effects in different immune cell subsets. The concentration of the various STAT molecules may act to shape accessibility to different signaling pathways. As a result of these events, an infectious agent overcoming the direct antiviral effects of type 1 IFNs has to deal with additional immune mechanisms of defense.

In addition to these effects during acute responses, the type 1 IFN receptor helps with long-term maintenance of the CD8 T cell pool (*36*). Although the role for STAT1 in this effect has yet to be defined, its ability to inhibit proliferation may serve to protect CD8 T cells from chronic stimulation and eventual depletion through clonal "exhaustion" (*37*). In the absence of STAT1, type 1 IFNs can induce growth as well as have antiapoptotic effects on T cells through possible STAT3- and/or STAT5-dependent events (*38*–*40*).

Viral Evasion of IFN Responses

Many viruses dedicate a substantial part of their genomes to down-modulating the IFN pathways. A general mechanism used by several viruses is inhibition of cellular gene expression by inhibiting transcription, RNA processing, and/or translation (*20*). Virus-induced shutoff of cellular protein expression not only favors the diversion of cellular resources for viral protein expression but also prevents the synthesis of IFN and of ISG products. Most viruses also encode viral products that specifically target pathways involved in the response to IFN, and such products are generically known as viral IFN antagonists. Typically, different virus families are characterized by the presence of specific viral IFN antagonists lacking homology with those from other families. Nevertheless, viral IFN antagonists focus inhibition on at least one of three key pathways: the IRF3, the JAK-STAT, and the PKR pathways.

Antagonism of type 1 IFN induction. Viral inhibition of IRF3, resulting in decreased type 1 IFN production, has been documented to occur at multiple levels. For example, influenza and poxviruses encode dsRNA binding proteins NS1 and E3L that prevent IRF3 activation (*41*, *42*), at least in part by sequestering viral dsRNA and preventing stimulation of cellular sensors of dsRNA, such as RIG-I and mda5. Direct binding to mda5 of a viral IFN antagonist resulting in mda5 inhibition has been shown in the case of the V protein of several paramyxoviruses (*43*). MAVS/IPS-1/VISA/CARDIF is the target for cleavage by the NS3/4A protease of hepatitis C virus (*15*). This protease also cleaves TRIF (*44*) and therefore blocks both TLR3- and RIG-I–mediated activation of IFN. In addition, the P proteins of some negative RNA viruses appear not only to be essential components of the viral RNA polymerase but also to inhibit the action of TBK1, preventing IRF3 phosphorylation (*45*). The human herpesvirus 8 encodes several analogs of IRF, known as viral IRFs (*20*), some of which act as dominant negative mutants of IRF3 action.

Antagonism of type I IFN signaling. The JAK/STAT pathway is also targeted at multiple levels by viral IFN antagonists. Poxviruses secrete a soluble form of the IFNAR that sequesters type 1 IFN before it can bind to the natural IFNAR (*46*). Inhibition of the JAK kinases has been documented for several viruses (*20*). STATs appear to be a preferred target for many paramyxoviruses, whose accessory V and W proteins bind to these factors and prevent their activation in response to IFN. Different paramyxoviruses have different specificities for STATs, with some of them inhibiting STAT1, STAT2, STAT3, or a combination of these factors. In addition, targeted degradation of the STATs is seen with a subset of paramyxoviruses (*47*). Intriguingly, paramyxovirus IFN antagonists, including the V proteins of several paramyxoviruses, and the NS1 and NS2 proteins of respiratory syncytial virus, have the remarkable property of inhibiting both IRF3 and STAT activation (*48*).

Antagonism of type 1 IFN-inducible genes and their products. It is intriguing that among more than 100 ISGs, the PKR product appears to be a common target for many viral IFN antagonists. The ways viruses inhibit the PKR pathway are again very diverse and rank from sequestration of the PKR-activating dsRNA, expression of dsRNA mimics, binding to PKR preventing its dimerization and activation, and substrate competitive inhibition (*49*). Finally, activation of cellular proteins involved in negative regulation of many aspects of the IFN response is also a strategy used by several viruses. Induction of cellular inhibitors of STATs, such as suppressors of cytokine signaling (SOCS), has been reported to occur during herpesvirus infections. Influenza virus infection activates a cellular inhibitor of PKR, the p58IPK, and herpesviruses encode a protein, γ34.5, that recruits a cellular phosphatase for the dephosphorylation of eIF2α, reverting the PKR-mediated translational block (*49*).

Smart Virus, Smart Host

As we've described, multiple offensive/defensive mechanisms have evolved to result in a balance for coexistence of hosts and viruses, and type 1 IFNs have emerged as pivotal in this conflict (Fig. 2). Antagonism of these cytokines appears to be a common feature shared by all viruses, and the variety of mechanisms for "hiding" from the direct antiviral effects of type 1 IFNs provides the virus with opportunities to replicate and infect a new host before being eliminated

by secondary innate and adaptive immune responses in the case of acute viral infections. In chronic infections, this can emerge as a means to establish viral persistence in the host. The diverse and multiple viral approaches to avoiding IFN induction and function provide persuasive evidence for the potency of these mediators in early defense. A direct consequence of disrupting the function of viral IFN antagonists is a decrease in viral replication and pathogenicity in the host, apparent, for example, in poxviruses, herpesviruses, and influenza viruses. On the far side of the spectrum, however, viruses equipped with highly refined means of disrupting innate mechanisms activated by type 1 IFN are likely to be in the highest order of pathogenicity, a notorious example being the virus strain responsible for the pandemic influenza A virus of 1918 (*50*, *51*). High pathogenicity, however, is not necessarily advantageous for the virus: Conditions that result in too rapid a destruction of the host may have deleterious effects on long-term survival of an infectious agent that requires the host for further propagation.

Although viruses evade the direct antiviral defense mechanisms activated by type 1 IFNs, hosts take advantage of these cytokines to elicit a wide range of responses. The classical signaling pathways used to induce direct antiviral defenses also activate some of these, particularly the ones elicited during innate periods of responses. The importance for protection is clearly shown by the fact that deficiencies in STAT1, and therefore in innate responses activated by type 1 IFNs, result in extreme sensitivities to viral infections (*52*–*55*). The host, however, has adapted to also use other signaling pathways to activate additional defense mechanisms, most clearly demonstrated for STAT4-dependent induction of T cell IFN-γ production. Thus, new complex and important defense responses have been attached to the critical early antiviral cytokines. One consequence of using these factors to promote downstream innate and adaptive responses is that, even if viruses have escaped their direct antiviral effects, the host can limit the window of opportunity for pathogen advancement.

Much progress has been made, but there is still much to be learned about the pathways regulating IFN induction and function during viral infections. Nevertheless, there is evidence to conclude that, as in many difficult relationships, viruses and their hosts are learning to live together and that type 1 IFNs are important players in this détente.

References and Notes

1. R. Medzhitov, C. A. Janeway Jr., *Semin. Immunol.* **10**, 351 (1998).
2. S. S. Diebold, T. Kaisho, H. Hemmi, S. Akira, C. Reis e Sousa, *Science* **303**, 1529 (2004).
3. F. Heil *et al.*, *Science* **303**, 1526 (2004).
4. J. M. Lund *et al.*, *Proc. Natl. Acad. Sci. U.S.A.* **101**, 5598 (2004).
5. H. Hemmi *et al.*, *Nature* **408**, 740 (2000).
6. L. Alexopoulou, A. C. Holt, R. Medzhitov, R. A. Flavell, *Nature* **413**, 732 (2001).
7. T. Kawai, S. Akira, *Cell Death Differ.* **13**, 816 (2006).
8. M. G. Wathelet *et al.*, *Mol. Cell* **1**, 507 (1998).
9. I. Marie, J. E. Durbin, D. E. Levy, *EMBO J.* **17**, 6660 (1998).
10. H. Kato *et al.*, *Immunity* **23**, 19 (2005).
11. M. Yoneyama *et al.*, *Nat. Immunol.* **5**, 730 (2004).
12. R. B. Seth, L. Sun, C. K. Ea, Z. J. Chen, *Cell* **122**, 669 (2005).
13. T. Kawai *et al.*, *Nat. Immunol.* **6**, 981 (2005).
14. L. G. Xu *et al.*, *Mol. Cell* **19**, 727 (2005).
15. E. Meylan *et al.*, *Nature* **437**, 1167 (2005).
16. K. J. Ishii *et al.*, *Nat. Immunol.* **7**, 40 (2006).
17. D. B. Stetson, R. Medzhitov, *Immunity* **24**, 93 (2006).
18. M. M. Brierley, E. N. Fish, *J. Interferon Cytokine Res.* **22**, 835 (2002).
19. L. C. Platanias, *Nat. Rev. Immunol.* **5**, 375 (2005).
20. C. A. Biron, G. C. Sen, in *Fields Virology, Fourth Edition*, D. M. Knipe *et al.*, Eds. (Lippincott, Williams, and Wilkins, Philadelphia, 2001), pp. 321–351.
21. K. B. Nguyen *et al.*, *Nat. Immunol.* **1**, 70 (2000).
22. K. B. Nguyen *et al.*, *Science* **297**, 2063 (2002).
23. S. S. Cho *et al.*, *J. Immunol.* **157**, 4781 (1996).
24. B. Hahm, M. J. Trifilo, E. I. Zuniga, M. B. Oldstone, *Immunity* **22**, 247 (2005).
25. C. E. Samuel, *Clin. Microbiol. Rev.* **14**, 778 (2001).
26. A. Zhou, J. M. Paranjape, S. D. Der, B. R. Williams, R. H. Silverman, *Virology* **258**, 435 (1999).
27. M. Dalod *et al.*, *J. Exp. Med.* **197**, 885 (2003).
28. C. K. Lee *et al.*, *J. Immunol.* **165**, 3571 (2000).
29. K. B. Nguyen *et al.*, *J. Immunol.* **169**, 4279 (2002).
30. C. L. Karp, C. A. Biron, D. N. Irani, *Immunol. Today* **21**, 24 (2000).
31. X. Zhang, S. Sun, I. Hwang, D. F. Tough, J. Sprent, *Immunity* **8**, 591 (1998).
32. J. F. Bromberg, C. M. Horvath, Z. Wen, R. D. Schreiber, J. E. Darnell Jr., *Proc. Natl. Acad. Sci. U.S.A.* **93**, 7673 (1996).
33. M. P. Gil, R. Salomon, J. Louten, C. A. Biron, *Blood* **107**, 987 (2006).
34. M. P. Gil *et al.*, *Proc. Natl. Acad. Sci. U.S.A.* **98**, 6680 (2001).
35. C. V. Ramana *et al.*, *EMBO J.* **19**, 263 (2000).
36. G. A. Kolumam, S. Thomas, L. J. Thompson, J. Sprent, K. Murali-Krishna, *J. Exp. Med.* **202**, 637 (2005).
37. A. Gallimore *et al.*, *J. Exp. Med.* **187**, 1383 (1998).
38. R. Gimeno, C. K. Lee, C. Schindler, D. E. Levy, *Mol. Cell. Biol.* **25**, 5456 (2005).
39. C. K. Lee, E. Smith, R. Gimeno, R. Gertner, D. E. Levy, *J. Immunol.* **164**, 1286 (2000).
40. Y. Tanabe *et al.*, *J. Immunol.* **174**, 609 (2005).
41. J. Talon *et al.*, *Proc. Natl. Acad. Sci. U.S.A.* **97**, 4309 (2000).
42. Y. Xiang *et al.*, *J. Virol.* **76**, 5251 (2002).
43. J. Andrejeva *et al.*, *Proc. Natl. Acad. Sci. U.S.A.* **101**, 17264 (2004).
44. K. Li *et al.*, *Proc. Natl. Acad. Sci. U.S.A.* **102**, 2992 (2005).
45. G. Unterstab *et al.*, *Proc. Natl. Acad. Sci. U.S.A.* **102**, 13640 (2005).
46. J. A. Symons, A. Alcami, G. L. Smith, *Cell* **81**, 551 (1995).
47. C. M. Horvath, *Eur. J. Biochem.* **271**, 4621 (2004).
48. O. Haller, G. Kochs, F. Weber, *Virology* **344**, 119 (2006).
49. M. G. Katze, Y. He, M. Gale Jr., *Nat. Rev. Immunol.* **2**, 675 (2002).
50. G. K. Geiss *et al.*, *Proc. Natl. Acad. Sci. U.S.A.* **99**, 10736 (2002).
51. T. M. Tumpey *et al.*, *Science* **310**, 77 (2005).
52. S. Dupuis *et al.*, *Nat. Genet.* **33**, 388 (2003).
53. J. E. Durbin, R. Hackenmiller, M. C. Simon, D. E. Levy, *Cell* **84**, 443 (1996).
54. S. M. Karst, C. E. Wobus, M. Lay, J. Davidson, H. W. Virgin, *Science* **299**, 1575 (2003).
55. M. A. Meraz *et al.*, *Cell* **84**, 431 (1996).

56. Work in A.G.-S.'s lab is supported by NIH grants R01AI46954, P01AI52106, P01AI58113, U54AI57158, and U19AI62623, and DOD grant W81XWH-04-1-0876. Work in C.A.B.'s lab is supported by NIH grants RO1CA41268 and RO1AI55677. In memory of Theresa P. Biron.

10.1126/science.1125676

Polar PIN Localization Directs Auxin Flow in Plants

Justyna Wiśniewska,[1,3] Jian Xu,[2] Daniela Seifertová,[1] Philip B. Brewer,[1] Kamil Růžička,[1] Ikram Blilou,[2] David Rouquié,[1]* Eva Benková,[1] Ben Scheres,[2] Jiří Friml[1]†

The phytohormone auxin plays a major role in the coordination of plant development (*1*). Classical models propose that the strict directionality of intercellular auxin transport depends on the polar subcellular localization of transport components (*2*). PIN auxin transport facilitators show such polar localization (*3*–*5*), but whether this is sufficient to determine the direction of auxin flow remains unclear. To investigate this question, we modified PIN polarity and examined directional auxin translocation during root gravitropism in *Arabidopsis thaliana*. This translocation occurs by upward PIN2-dependent auxin flow in epidermal cells along the lower side of the root from the place of gravity perception (root tip) to the place of growth response (elongation zone) (*6*, *7*).

We designed hemagglutinin (HA) epitope–tagged *PIN1* and *PIN2* genes under the transcriptional control of the *PIN2* promoter and introduced these into *pin2* mutants. PIN1 and PIN2 have distinct polar localization in their normal expression domains (*4*–*6*), and expressing them in the same cells could determine whether PIN polarity depends on cell type or PIN sequence–based signals. Consistent with normal PIN2 expression, we detected protein fusions in cortex and epidermal cells (fig. S1, A and B). In cortex cells, both proteins were localized at the lower (basal) side. However, in epidermal cells, endogenous PIN2 (in wild type) and PIN2:HA were always localized at the upper (apical) side, whereas PIN1:HA was observed at the lower side, creating a situation where PIN1 and PIN2 were localized to opposite sides of the same cell (Fig. 1A). These data demonstrate that the polarity of PIN localization is determined not only by cell type–specific signals, but also by sequence-specific signals within PIN proteins.

We also examined PIN1 constructs that may interfere with any sequence-based polarity signals, for example, the insertion of the green fluorescent protein (*GFP*) coding sequence at different positions within the *PIN1* coding sequence. These constructs were functional and showed normal localization patterns in the endogenous PIN1 domain (fig. S1H). When placed under the *PIN2* promoter, they typically (e.g., PIN1:GFP-2) showed localization, similar to PIN1:HA, at the lower side of epidermis cells, with the exception of PIN1:GFP-3, which showed localization at the upper side (Fig. 1A).

The availability of two versions of PIN1 with contrasting polarities allowed us to test the relationship between polarity and the direction of auxin flow by examining auxin translocation during gravity response. Auxin translocation to the lower side of the root (as visualized by the *DR5rev::GFP* auxin response reporter) after gravistimulation was not observed in *pin2* mutants but was completely restored in PIN2:HA lines (Fig. 1B). Whereas PIN1:HA protein at the lower side of epidermal cells failed, PIN1:GFP-3 at the upper side was able to mediate the gravitropic auxin translocation (Fig. 1B). Consequently, PIN2:HA and PIN1:GFP-3, but not PIN1:HA or PIN1:GFP-2, rescued the root gravitropic response of *pin2* mutants (Fig. 1, C and D). Thus, the localization of PIN proteins at the upper side of epidermal cells correlated with their ability to facilitate upward auxin movement for root gravitropic response.

The only variation between plants that express PIN1:HA or PIN1:GFP-3 is the engineered *PIN1* coding sequence. This difference alone is sufficient to change the polarity of PIN1 and, as a direct consequence, change its ability to mediate auxin flow in a given direction for the regulation of root gravitropism. This result shows that PIN polarity is a primary direction-determining factor in auxin transport in meristematic tissues and provides a crucial piece in the puzzle of how auxin flows can be redirected via rapid changes in PIN polarity in response to developmental and environmental signals.

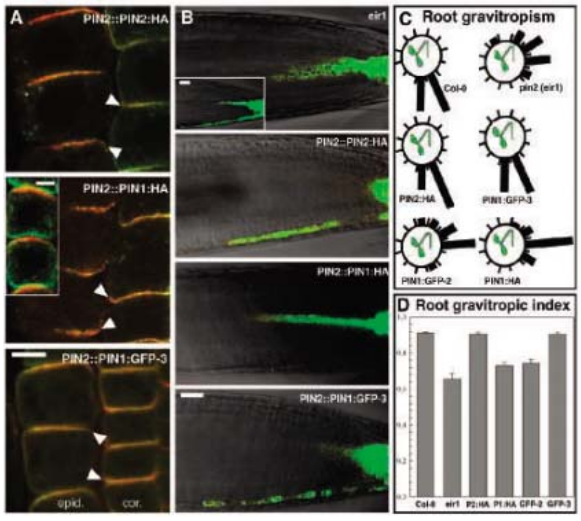

Fig. 1. (**A**) Polar localizations of PIN2:HA and PIN1:GFP-3 at the upper and PIN1:HA and PIN1:GFP-2 at the lower side of root epidermal cells as determined by coimmunolocalization with anti-PIN and anti-HA or anti-GFP antibodies. The inset shows localization of PIN1:GFP-2 (red) and PIN2 (green) on the opposite sides of the same wild-type cells. Arrowheads indicate the apical or basal polarity of PIN localization. (**B**) PIN2:HA and PIN1:GFP-3, but not PIN1:HA, when introduced in *pin2* mutants, mediate the unidirectional translocation of auxin to the lower side of the root after gravistimulation as monitored by DR5rev::GFP. The inset shows DR5rev::GFP pattern in the wild type. (**C**) In *pin2* mutants, PIN2:HA and PIN1:GFP-3, but not PIN1:HA and PIN1:GFP-2, mediate gravitropic root growth. (**D**) Quantitative evaluation of root gravitropism confirms that PIN2:HA and PIN1:GFP-3, but not PIN1:HA or PIN1:GFP-2, can functionally replace PIN2. Scale bars in (A), 5 μm; in (B), 25 μm.

References and Notes

1. S. Kepinski, O. Leyser, *Curr. Biol.* **15**, R208 (2005).
2. R. Swarup, M. Bennett, *Dev. Cell* **5**, 824 (2003).
3. J. Friml *et al.*, *Nature* **415**, 806 (2002).
4. E. Benková *et al.*, *Cell* **115**, 591 (2003).
5. J. Friml *et al.*, *Nature* **426**, 147 (2003).
6. A. Müller *et al.*, *EMBO J.* **17**, 6903 (1998).
7. C. Luschnig, R. A. Gaxiola, P. Grisafi, G. R. Fink, *Genes Dev.* **12**, 2175 (1998).
8. Supported by the VolkswagenStiftung, the EMBO Young Investigator Programme, the Foundation for Polish Science, the Margarete von Wrangell-Habilitationsprogramm, the Deutsche Forschungsgemeinschaft (grant SFB 446), and a PIONIER award from the Dutch Organization for Science.

Supporting Online Material

www.sciencemag.org/cgi/content/full/1121356/DC1
Materials and Methods
Fig. S1
References and Notes

14 October 2005; accepted 23 January 2006
Published online 6 April 2006;
10.1126/science.1121356
Include this information when citing this paper.

[1]Center for Plant Molecular Biology (ZMBP), Tübingen University, D-72076 Tübingen, Germany. [2]Department of Molecular Genetics, Utrecht University, 3584CH Utrecht, Netherlands. [3]Department of Biotechnology, Institute of General and Molecular Biology, 87-100 Toruń, Poland.

*Present address: Bayer CropScience, F-06560 Sophia Antipolis Cedex, France.

†To whom correspondence should be addressed. E-mail: jiri.friml@zmbp.uni-tuebingen.de

Isn't it time science discovered you?

GE & Science Prize for Young Life Scientists was established in 1995, and is presented by *Science*/AAAS and GE Healthcare. The prize was established to help bring science to life by recognizing outstanding PhDs from around the world and reward their research in the field of molecular biology.

This is your chance to gain international acclaim and recognition for yourself and your faculty, as well as to turn your scientific ideas into reality. If you were awarded your PhD in molecular biology* during 2005, describe your work in a 1,000-word essay. Then submit it for the 2006 GE & Science Prize for Young Life Scientists. Your essay will be reviewed by a panel of distinguished scientists who will select one grand prizewinner and four regional winners.

The grand prizewinner will get his or her essay published in *Science*, receive US$25,000, and be flown to the awards ceremony in Stockholm, Sweden. Entries should be received by **July 15, 2006**.

GE & Science Prize for Young Life Scientists: Life Science Re-imagined.

For more information on how to enter, go to www.gehealthcare.com/science

GE & Science Prize for Young Life Scientists

Dr. Ahmet Yildiz
Grand prizewinner 2005 for his essay, "Elucidating the Mechanism of Molecular Motor Movement."

Established and presented by:

Science AAAS

* For the purpose of this prize, molecular biology is defined as "that part of biology which attempts to interpret biological events in terms of the physico-chemical properties of molecules in a cell" (McGraw-Hill Dictionary of Scientific and Technical Terms, 4th Edition).

Virus-Enabled Synthesis and Assembly of Nanowires for Lithium Ion Battery Electrodes

Ki Tae Nam,[1,4] Dong-Wan Kim,[1*] Pil J. Yoo,[2,4] Chung-Yi Chiang,[1,5] Nonglak Meethong,[1] Paula T. Hammond,[2,4] Yet-Ming Chiang,[1] Angela M. Belcher[1,3,4,5]†

The selection and assembly of materials are central issues in the development of smaller, more flexible batteries. Cobalt oxide has shown excellent electrochemical cycling properties and is thus under consideration as an electrode for advanced lithium batteries. We used viruses to synthesize and assemble nanowires of cobalt oxide at room temperature. By incorporating gold-binding peptides into the filament coat, we formed hybrid gold–cobalt oxide wires that improved battery capacity. Combining virus-templated synthesis at the peptide level and methods for controlling two-dimensional assembly of viruses on polyelectrolyte multilayers provides a systematic platform for integrating these nanomaterials to form thin, flexible lithium ion batteries.

There is an increasing need for smaller and more flexible Li ion batteries and for methods to assemble battery materials. Nanoparticles, nanotubes (*1*, *2*), and nanowires (*3*), as well as several assembly methods based on lithography, block copolymer (*4*), or layer-by-layer deposition (*5*), have been introduced for constructing dimensionally small batteries. In addition to their utility in nanoelectronics, there is also growing evidence that nanostructured materials can improve the electrochemical properties of Li ion batteries compared to their bulk counterparts (*6*). However, to maximize this potential, monodisperse, homogeneous nanomaterials and hierarchical organization control are needed. Biosystems have the inherent capabilities of molecular recognition and self-assembly and thus are an attractive template for constructing and organizing the nanostructure (*7*–*13*). We have previously used viruses to assemble semiconductor and magnetic nanowires (*14*, *15*) and consider whether they can be used for device fabrication. Using batteries as our example device, we also explore whether the viruses can be modified to improve the electrode materials. Because the viruses can assemble on multiple length scales, there may be scope for designing hierarchical self-assembling batteries. For this biological approach, once the genes are programmed for a functional device, very little postsynthesis processing is necessary. Additionally, this biological route uses room-temperature, aqueous synthesis conditions.

The M13 virus consists of ~2700 major coat proteins (p8) helically wrapped around its single-stranded DNA, with minor coat proteins (p3, p6, p7, and p9) at each end of the virus. The functionality of these subunit proteins can be modified specifically through additions in the M13 genome. Modification of the major coat proteins, as well as minor coat proteins at the virus ends, has been used successfully to form functional heterostructured templates for precisely positioned nanomaterials (*16*, *17*). Furthermore, the intrinsically anisotropic virus structures are well suited for the growth of monodisperse, highly crystalline nanowires (*14*, *15*). In addition, the anisotropic virus structures are promising as elements of well-ordered nanostructure, as demonstrated in three-dimensional (3D) liquid crystal film (*18*, *19*).

Predictive-based design was used for engineering the virus to satisfy the multifunctional purpose of electrode formation and assembly with a polymer electrolyte for the Li ion battery (Fig. 1). Tetraglutamate (EEEE-) was fused to the N terminus of each copy of the major coat p8 protein with 100% expression. This clone, named E4, was designed with three objectives. (i) It can serve as a general template for growing nanowires through the interaction of the glutamate with various metal ions (Virus Biotemplating in Fig. 1). Carboxylic acid, the side chain of glutamate, binds positive metal ions via ion exchange, as demonstrated in polymeric templates (*20*). Glutamate is also believed to be important in biomineralization, as evident in its role in specific proteins that regulate the nucleation of biominerals in nature. (ii) Tetraglutamate acts as a blocking motif for gold nanoparticles (*21*), due to the electrostatic repulsion. Therefore, tetraglutamate reduces nonspecific gold nanoparticle binding to phage, thereby increasing the specificity of a gold-specific peptide to bind gold in low concentration. (iii) The E4 clone is ideally suited for electrostatically driven assembly with a charged polymer (Assembly Engineering in Fig. 1). E4 is more negatively charged than wild-type virus, which enables it to interact favorably with the positively charged electrolyte polymer. Zeta potential measurements of the E4 clone reveal a dramatic change in the potential between pH 4.5 and 5.5, thus enabling a certain degree of charge control.

To design the cobalt oxide (Co_3O_4) nanowires electrodes, we incubated the E4 virus templates in aqueous cobalt chloride solution (1 mM) for 30 min at room temperature to promote cobalt ion binding (*22*). Co_3O_4 was chosen as one of a family of new lithium-active compounds with an extremely large reversible storage capacity arising from displacement reactions (*23*), approximately three times as large as the capacity of carbon-based anodes currently used in commercial batteries. After reduction with $NaBH_4$ and spontaneous oxidation in water, monodisperse, crystalline Co_3O_4 nanowires were produced (*24*). Figure 2, A and B,

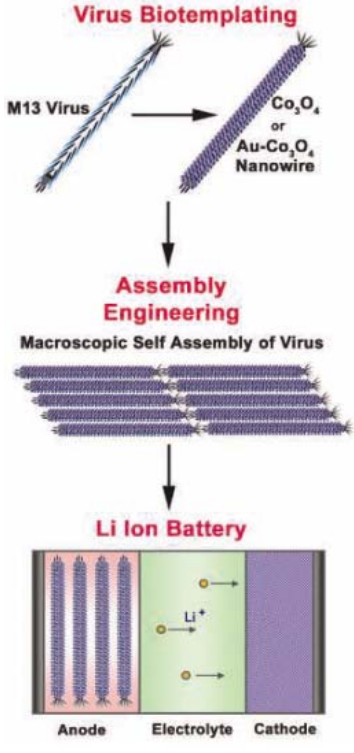

Fig. 1. Schematic diagram of the virus-enabled synthesis and assembly of nanowires as negative electrode materials for Li ion batteries. Rationally designed peptide and/or materials-specific peptides identified by biopanning were expressed on the major coat p8 proteins of M13 viruses to grow Co_3O_4 and Au-Co_3O_4 nanowires. Macroscopic ordering of the engineered viruses was used to fabricate an assembled monolayer of Co_3O_4 nanowires for flexible, lightweight Li ion batteries.

[1]Department of Materials Science and Engineering, [2]Department of Chemical Engineering, [3]Biological Engineering Division, [4]Institute for Soldier Nanotechnologies, [5]Institute of Collaborative Biotechnology, Massachusetts Institute of Technology, Cambridge, MA 02139, USA.

*Present address: Materials Science and Technology Division, Korea Institute of Science and Technology, Seoul 136-791, Korea.

†To whom correspondence should be addressed. E-mail: belcher@mit.edu

shows transmission electron microscope (TEM) images of the virus-templated Co_3O_4 nanowires, where Co_3O_4 nanocrystals of ~2 to 3 nm in diameter were uniformly mineralized along the length of the virus. For TEM observation, a dilute suspension was dropped on a carbon-coated TEM grid, washed with distilled water, and dried. The high-resolution TEM electron diffraction pattern and lattice spacing (Fig. 2), together with x-ray diffraction, confirm that the crystal structure is Co_3O_4. The inset in Fig. 2B shows that the measured lattice spacing corresponds to the planes of Co_3O_4. Because p8 proteins were genetically engineered with 100% expression and cobalt ions have a strong binding affinity to the carboxyl groups of glutamate, homogeneous and high-crystalline nanowires were synthesized. Furthermore, viral Co_3O_4 nanowires had a large surface area of 141.7 m^2/g, as measured by the Brunauer-Emmett-Teller method. The mass ratio of Co_3O_4 and virus is 0.837:0.163. Unlike E4 viruses, Co_3O_4 nucleating viruses, solutions of wild-type virus expressing no peptide insert, or solutions without viruses formed irregular and large precipitates of Co/Co_3O_4 mixtures.

For electrochemical evaluation of the Co_3O_4 nanowires, positive electrodes were prepared by mixing together 3.29 mg of the virus-based nanowires, Super P (MMM Carbon, Brussels, Belgium) carbon black, and poly(vinylidene fluoride)-hexafluoropropylene binder in a mass ratio of 74:15:11. Swagelok design cells using Li metal foil used as the negative electrode and a separator film of Celgard 2400 were assembled and saturated with the liquid electrolyte, 1 M $LiPF_6$, in ethylene carbonate and dimethyl carbonate (1:1 by volume). The assembled cells were galvanostatically cycled between 3.0 and 0.01 V using a Maccor automated tester. The behavior of voltage/capacity curves (Fig. 2C) for the Co_3O_4/Li half cell was similar to that of Co_3O_4 nanoparticles produced by other methods (*25*). The larger first-insertion capacity compared to that in subsequent discharge is characteristic of this material and is due to irreversible reactions occurring upon initial lithiation. Any biphasic nature (*25*) of Co_3O_4 and $Li_xCo_3O_4$ (~$Li_{1.47}Co_3O_4$) at the early stages of discharge was not clearly evident from the voltage traces (Fig. 2C). We observed reversible capacity (Fig. 2D) ranging from 600 to 750 mA·hour/g, which is about twice that of current carbon-based negative electrodes. The charge and discharge capacities stabilized at 600 mA·hour/g over 20 cycles. The reversible formation of Li_2O accompanying the redox of cobalt nanoparticles and the reversible growth of a gel-like polymeric layer (*26*), resulting from electrolyte degradation, are believed to contribute to this reversible capacity. The existence of higher than theoretical specific capacity in Co_3O_4 has been observed before (*27*), and it plausibly attributed to the reversible formation of a Li-bearing solid-electrolyte interface. At the nanometer scale, both the reversible formation of Li_2O, which is known to be electrochemically inactive in bulk, and the reversible formation of the gel-like layer catalyzed by cobalt nanoparticles can occur (*23*). A control experiment revealed that the virus is electrochemically inactive and stable over the electrochemical conditions of our experiments, as indicated by the absence of decomposition in cyclic voltammograms (fig. S1). The virus capsid–mediated growth of uniform-sized Co_3O_4 nanomaterials, in addition to the structural integrity and dense packing (Fig. 2B) imparted by the virus, provides electrochemical advantages. For instance, when all other experimental conditions were held constant, the capacity of samples fabricated without the virus templates faded rapidly (Fig. 2D). This phenomenon, which is most likely attributable to incomplete oxidation of cobalt, inhomogeneous composition, and large particle size, has also been observed for Co_3O_4 prepared at low temperatures, in which high polarization is a contributing factor (*25*). However, the properties of Co_3O_4 nanowires, templated by M13 virus and oxidized spontaneously at room temperature, were comparable to those of particles fabricated at temperatures above 500°C.

An added advantage of this system is that the nanotexture of viral Co_3O_4 nanowires can be manipulated by controlling the interactions between the peptides and cobalt ions. Higher cobalt chloride concentration (5 mM) with 10 mM $NaBH_4$ produced branchlike nanowire structures (Fig. 2E); in contrast, nucleation and growth of Co_3O_4 nanowires at 4°C with 1 mM

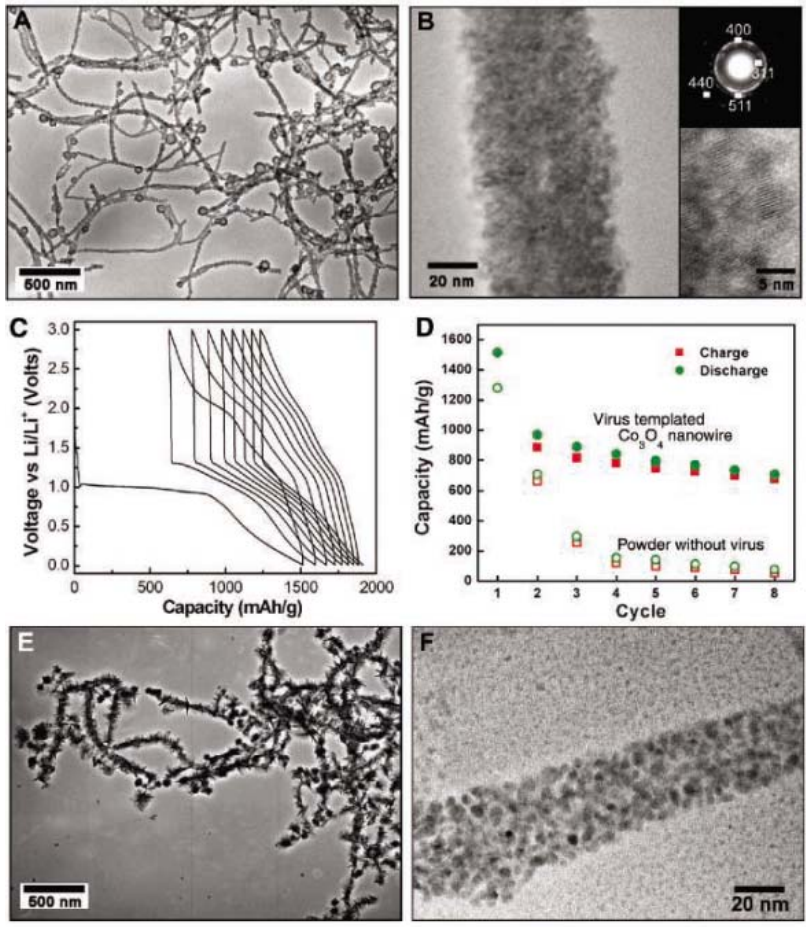

Fig. 2. Characterization of the Co_3O_4 nanowires templated by M13 virus. (**A**) TEM image of virus-templated Co_3O_4 nanowires. For visualizing the individual wires, the nanowires solution was diluted 1:100. (**B**) High-resolution TEM image of a Co_3O_4 viral nanowire. Electron diffraction pattern (Inset, upper right) confirmed that the crystal structure was Co_3O_4. Magnified image (inset, lower right) shows the lattice fringe of Co_3O_4 nanocrystals along the major coat p8 proteins of a virus. The measured lattice spacing corresponds to the (311) and (400) planes of Co_3O_4. (**C**) Charging-discharging curves for a virus-mediated Co_3O_4/Li half cell cycled between 3 and 0.01 V at a rate of *C*/26.5. *C* was defined as eight Li ions per hour. (**D**) Specific capacity versus cycle number for the same cell. The mass of Co_3O_4 only was considered. For comparison, data for the powder that was fabricated without viruses under the same condition are shown. (**E**) TEM images of differently nanostructured Co_3O_4 viral nanowires that were fabricated at a higher cobalt ion concentration. (**F**) TEM images of the assembly of discrete Co_3O_4 nanocrystals (on the p8 proteins), which were synthesized at 4°C.

cobalt ion and 5 mM $NaBH_4$ resulted in the assembly of discrete nanoparticles (Fig. 2F).

To design new hybrid material electrodes with higher capacity, we engineered additional material-specific peptide motifs into the major coat p8 protein. This provides a general method for the systematic and controlled arrangement of two distinct nanomaterials, which can enhance the electrochemical properties through the cooperative contribution of each material. Increasingly, efforts to improve battery properties have focused on composite material design (*28*, *29*). However, notable challenges, such as the achievement of uniform distributions of multiple phases, are encountered when components are combined at the nanoscale. Gold nanoparticles were chosen on the basis of their ability to provide high electronic conductivity where needed, the ability to maintain a thermodynamically stable interface with Co_3O_4, and the potential to catalyze electrochemical reactions at the nanoscale. We designed a bifunctional virus template that simultaneously expressed two different peptide motifs. To accomplish this, we isolated a gold-binding peptide motif (LKAHLPPSRLPS) by screening against a gold substrate with a phage display library (*30*), which contains random 12–amino acid peptide sequences. Then, we assembled bifunctional viruses constructed to express both Au- and Co_3O_4-specific peptides with the virus coat. Phagemid constructs (*15*) were inserted into host bacterial cells encoding the gold-binding peptide motif (*31*). Thus, upon infection of the plasmid-incorporating host cells with the E4 virus, a small percentage of the resulting E4 p8 proteins also displayed the gold-specific peptide. Therefore, two types of p8 proteins were produced: intact p8 proteins of E4 viruses and engineered p8 proteins containing the gold-binding peptide motif, randomly packaged onto the virus progeny (Fig. 3A). This hybrid clone was named AuE4 virus. Incubation of the amplified AuE4 clones with a 5-nm gold colloid suspension (5×10^{13} particles/ml; Ted Pella) resulted in 1D arrays of Au nanoparticles bound to the gold-binding peptides distributed among p8 proteins (Fig. 3B). In contrast, wild-type viruses and the E4 virus, which do not have gold-binding motifs, did not bind gold nanoparticles along the length of the virus. After removal of excess unbound gold nanoparticles by centrifugation, Co_3O_4 was nucleated and grown via the tetraglutamate functionality, resulting in hybrid nanostructures of 5-nm Au nanoparticles spatially interspersed within the Co_3O_4 wires (Fig. 3C). The crystal structure of the Co_3O_4 was confirmed by electron diffraction. Inductively coupled plasma mass spectrometry (ICPMS) analysis indicated that Au nanoparticles were associated with Co_3O_4 in a mass ratio of 0.024:0.976.

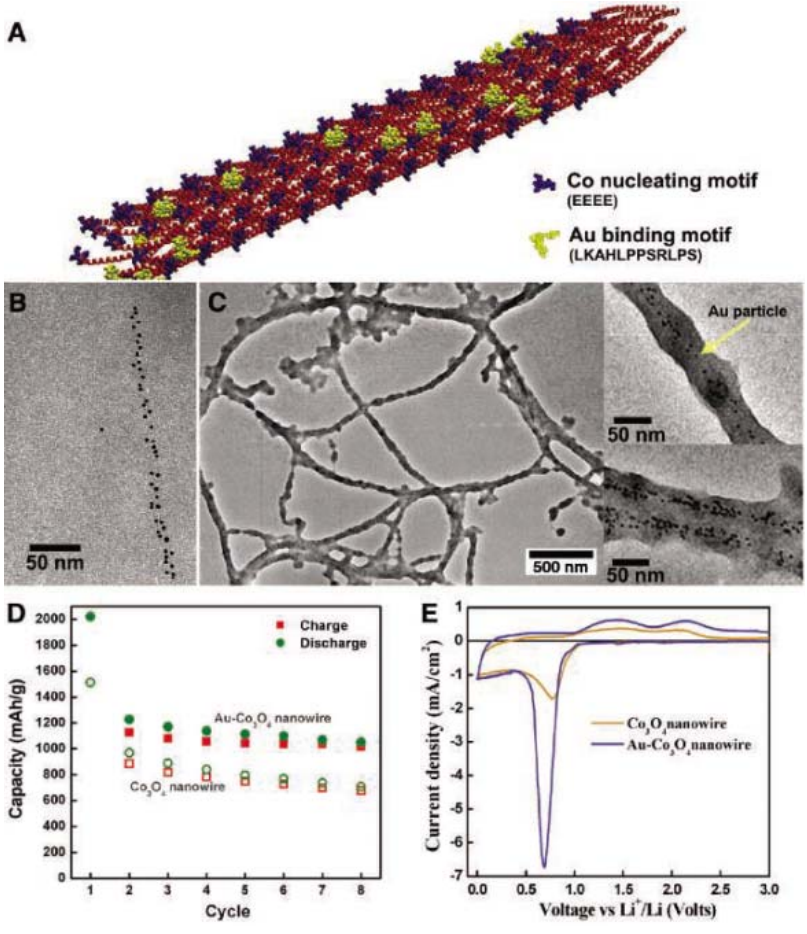

Fig. 3. Characterization of the hybrid nanostructure of Au nanoparticles incorporated into Co_3O_4 nanowires. (**A**) Visualization of the genetically engineered M13 bacteriophage viruses. P8 proteins containing a gold-binding motif (yellow) were doped by the phagemid method in E4 clones, which can grow Co_3O_4. (**B**) TEM images of the assembled gold nanoparticles on the virus. Control experiments showed that gold nanoparticles were bound by the gold-specific peptides. (**C**) TEM image of hybrid nanowires of Au nanoparticles/Co_3O_4. (**D**) Specific capacity of hybrid Au-Co_3O_4 nanowires. Half cell with Li electrode was cycled at a rate of *C*/26.5. Virus mass was subtracted and the mass of active materials such as Co_3O_4 and Au was counted. The capacity of virus-directing Co_3O_4 nanowires without Au nanoparticles was also compared. (**E**) Cyclic voltammograms of hybrid Au-Co_3O_4 and Co_3O_4 nanowires at a scanning rate of 0.3 mV/s.

We evaluated the electrochemical properties of the hybrid Au-Co_3O_4 nanowires by using galvanostatic cycling and cyclic voltammetry. The mass of Au-Co_3O_4 nanowires deposited on the Cu substrate for one electrochemical cell was 3.41 mg. The virus-mediated hybrid composite generated higher initial and reversible lithium storage capacity than the pure Co_3O_4 nanowires when tested at the same current rate (Fig. 3D). The higher lithium storage capacity may result from the formation of Au-Li intermetallic compound or the conductive or catalytic effects of Au nanoparticles on the reaction of Li with Co_3O_4. Au is known to be electrochemically active, which leads to the formation of Li_xAu alloys (*32*). However, based on the Au:Co_3O_4 ratio, the contribution of Li_xAu alloys to the lithium storage capacity is likely negligible. Cyclic voltammetry (Fig. 3E) shows no notable new redox peaks that could be associated with the lithiation of Au (*4*). Given the unique charging/discharging mechanism of Co_3O_4, wherein cobalt nanoparticles promote the reversible reaction of an organic layer that then contributes to the Li capacity, it is more likely that Au nanoparticles play a role in this displacement reaction. This role may be one of improving electronic conductivity to the Co_3O_4 nanoparticles, or it may be catalytic in nature. Indeed, decreased cell polarization was observed in the galvanostatic voltage-capacity curves, which could result from either of these mechanisms. Furthermore, incorporation of Au clearly increases the reaction rate upon reduction of Co_3O_4, as indicated by the enhanced reduction peak seen by cyclic voltammetry in Fig. 3E (measured on samples of similar mass at the same voltage sweep rate). Although the exact electrochemical mechanism is under investigation, our results show that a small amount of Au nanoparticles dispersed within Co_3O_4 to produce a hybrid material markedly improves electrochemical performance. The specific capacity of the hybrid is estimated to be at least 30% greater than that of our Co_3O_4 nanowires.

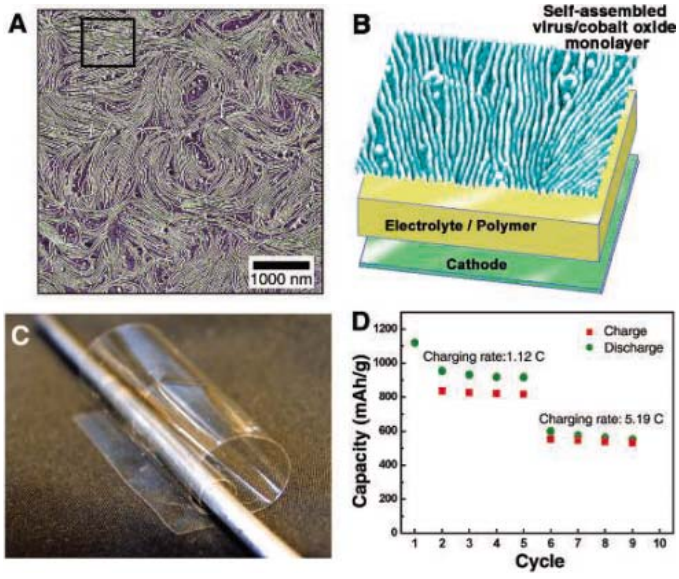

Fig. 4. Two-dimensional assembly of Co_3O_4 nanowires driven by liquid crystalline ordering of the engineered M13 bacteriophage viruses. (**A** and **B**) Phase-mode atomic force microscope image of macroscopically ordered monolayer of Co_3O_4-coated viruses. The Z range is 30° (**C**) Digital camera image of a flexible and transparent free-standing film of $(LPEI/PAA)_{100.5}$ on which Co_3O_4 viral nanowires are assembled into nanostructured monolayer with dimensions of 10 cm by 4 cm. (**D**) Capacity for the assembled monolayer of Co_3O_4 nanowires/Li cell at two different charging rates.

The principles of self-assembly and biotemplating can be further extended to control virus-virus interactions for organizing nanostructured electrodes over large length scales. Recently, we observed that negatively charged M13 viruses can form very ordered, 2D liquid crystalline layers on top of electrostatically cohesive films of linear poly(ethylene imine) (LPEI)/poly(acrylic acid) (PAA) (*33*). The ordering of engineered viruses is driven by competitive electrostatic interactions, the interdiffusion of the polyelectrolyte, and the anisotropic shape of M13 viruses. By using this technique to spontaneously order E4 viruses and subsequently grow Co_3O_4 on the virus coat proteins, we produced 2D organized ensembles of nanowires on a 10-cm length scale (Fig. 4, A and B). The spatial distance and ordering behavior between viral nanowires can be manipulated by controlling both surface charge and fluidic forces. Furthermore, the thickness of the multilayered polymer can be varied from 10 nm to several micrometers, independent of the substrate. This assembly process produces lightweight, flexible, and transparent active material/substrate multilayers, constructed as free-standing films by a simple dipping method (Fig. 4C). This process should be scalable using roll-to-roll processing. Moreover, the polymer electrolyte is believed to act as a solid electrolyte because of the relatively fast ionic conductivity of LPEI and PAA pairs (*34*, *35*). Thus, the assembled layers compose a negative-electrode material grown upon a solid electrolyte or separator membrane. For electrochemical evaluation, 100 nm of Cu, which functions as a current collector, was deposited by E-beam evaporation on the assembled Co_3O_4 nanowires/polymer layer. This assembly was then tested in Swagelok cells with a Li foil negative electrode separated from the multilayer by a separator dipped in liquid electrolyte (*36*). Figure 4D shows the capacity for the assembled monolayer of Co_3O_4 nanowires/Li cell at two different charging rates. The cell was found to sustain and deliver 94% of its theoretical capacity at a rate of 1.12 C and 65% at a rate of 5.19 C, demonstrating the capability for a high cycling rate. We believe that the power of the cell can be further increased by alternating stacks of nanowire monolayers and polymer layers of LPEI and PAA or other polyions. In addition, the Au-Co_3O_4 hybrid nanowires should also increase the total capacity.

Our results demonstrate that basic biological principles can be applied to the rational design and assembly of nanoscale battery components, exhibiting improved performance in properties such as specific capacity and rate capability. The genetic control in the viral synthesis of monodisperse oxide nanowires and the nanoarchitecture of hybrid nanowires can be advanced through further modification of other proteins. Heterostructured nanowires, composed of anode and solid electrolyte, and bioenergy-transducing nanowires, coupled with biomolecules, are currently being investigated. Moreover, we anticipate that self-organized virus monolayers for the generation of anodic as well as cathodic materials on ionically conducting polyelectrolyte films may present potential architectures for interdigitated batteries (*37*). The ease of genetic modification allows for the growth and assembly of other functional nanomaterials for applications such as photovoltaic devices, high–surface area catalysts, and supercapacitors.

References and Notes

1. A. S. Claye, J. E. Fischer, C. B. Huffman, A. G. Rinzler, R. E. Smalley, *J. Electrochem. Soc.* **147**, 2845 (2000).
2. J. S. Sakamoto, B. Dunn, *J. Electrochem. Soc.* **149**, A26 (2002).
3. A. R. Armstrong, G. Armstrong, J. Canales, R. Garcia, P. G. Bruce, *Adv. Mater.* **17**, 862 (2005).
4. S. C. Mui *et al.*, *J. Electrochem. Soc.* **149**, A1610 (2002).
5. T. Cassagneau, J. H. Fendler, *Adv. Mater.* **10**, 877 (1998).
6. A. S. Aricò, P. Bruce, B. Scrosati, J.-M. Tarascon, W. V. Schalkwijk, *Nat. Mater.* **4**, 366 (2005).
7. S. Mann, *Biomineralization: Principles and Concepts in Bioinorganic Materials Chemistry* (Oxford Univ. Press, New York, 2001).
8. A. M. Belcher *et al.*, *Nature* **381**, 56 (1996).
9. M. M. Murr, D. E. Morse, *Proc. Natl. Acad. Sci. U.S.A.* **102**, 11657 (2005).
10. N. C. Seeman, *Nature* **421**, 427 (2003).
11. S. Brown, *Nat. Biotechnol.* **15**, 269 (1997).
12. T. Douglas, M. Young, *Nature* **393**, 152 (1998).
13. S. Zhang, *Nat. Biotechnol.* **21**, 1171 (2003).
14. C. Mao *et al.*, *Science* **303**, 213 (2004).
15. C. Mao *et al.*, *Proc. Natl. Acad. Sci. U.S.A.* **100**, 6946 (2003).
16. Y. Huang *et al.*, *Nano Lett.* **5**, 1429 (2005).
17. K. T. Nam, B. R. Peelle, S.-W. Lee, A. M. Belcher, *Nano Lett.* **4**, 23 (2004).
18. S. W. Lee, C. Mao, C. Flynn, A. M. Belcher, *Science* **296**, 892 (2002).
19. Z. Dogic, S. Fraden, *Phys. Rev. Lett.* **78**, 2417 (1997).
20. S. Joly *et al.*, *Langmuir* **16**, 1354 (2000).
21. B. R. Peelle, E. M. Krauland, K. D. Wittrup, A. M. Belcher, *Langmuir* **21**, 6929 (2005).
22. The mass spectrum acquired by matrix-assisted laser desorption/ionization confirmed that cobalt was bound with p8 proteins of E4 clones.
23. P. Poizot, S. Laruelle, G. Grugeon, L. Dupont, J.-M. Tarascon, *Nature* **407**, 496 (2000).
24. A 100-μl sample of E4 viruses (10^{12} phage/ml) was incubated with 1 ml of 1 mM $CoCl_2 \cdot 6H_2O$ for 1 hour. Then, 1 ml of 5 mM $NaBH_4$ was added, and the solution was kept at room temperature for the further oxidation of nanowires.
25. D. Larcher, G. Sudant, J.-B. Leriche, Y. Chabre, J.-M. Tarascon, *J. Electrochem. Soc.* **149**, A234 (2002).
26. J.-M. Tarascon *et al.*, *C. R. Chimie* **8**, 9 (2004).
27. Z. Yuan, F. Huang, C. Feng, J. Sun, Y. Zhou, *Mater. Chem. Phys.* **79**, 1 (2003).
28. D. Gyu, B. Lestriez, D. Guyomard, *Adv. Mater.* **16**, 533 (2004).
29. Z. P. Guo, E. Milin, J. Z. Wang, J. Chen, H. K. Liu, *J. Electrochem. Soc.* **152**, A2211 (2005).
30. S. R. Whaley, D. S. English, E. L. Hu, P. F. Barbara, A. M. Belcher, *Nature* **405**, 665 (2000).
31. Bacteria containing the engineered phagemids were inoculated into 20 ml of Terrific Broth (TB) with ampicilin (100 μg/ml). The culture was maintained at 37°C until mid-log phase (optical density at 600 nm ~ 0.5). E4 bacteriophage (10 μl) and 20 μl of isopropyl-β-D-thiogalactopyranoside (100 mg/ml) were added to the bacteria culture. After 4.5 to ~5 hours of incubation at 37°C, phages were purified using standard purification procedures.
32. T. B. Massalski, H. Okamoto, P. R. Subramanian, L. Kacprzak, Eds., *Binary Alloy Phase Diagrams* (ASM International, Materials Park, OH, 1990).
33. P. J. Yoo *et al.*, *Nat. Mater.* **5**, 234 (2006).
34. D. M. DeLongchamp, P. T. Hammond, *Chem. Mater.* **15**, 1165 (2003).
35. P. T. Hammond, *Adv. Mater.* **16**, 1271 (2004).
36. To prevent the oxidation of Cu after the deposition of Cu in vacuum, we rapidly transferred the sample to a glove box for the assembly of the battery. Indeed, we observed no contribution of CuO in the charging/discharging curve. As measured by ICPMS, the mass of Co_3O_4 on the polymer was 22 μg/cm^2.
37. J. W. Long, B. Dunn, D. R. Rolison, H. S. White, *Chem. Rev.* **104**, 4463 (2004).

38. We thank S. K. Lee for engineering the E4 phage and S. T. Kottmann for the computer graphic work in Fig. 3A. We also appreciate J. Lutkenhaus for the helpful discussion. This work was supported by the Army Research Office Institute of Collaborative Biotechnologies, the Army Research Office Institute of Soldier Nanotechnologies, and the David and Lucile Packard Foundation.

Supporting Online Material

www.sciencemag.org/cgi/content/full/1122716/DC1
Fig. S1

16 November 2005; accepted 24 March 2006
Published online 6 April 2006;
10.1126/science.1122716
Include this information when citing this paper.

Formation and Subdivision of Deformation Structures During Plastic Deformation

Bo Jakobsen,[1] Henning F. Poulsen,[1*] Ulrich Lienert,[2] Jonathan Almer,[2] Sarvjit D. Shastri,[2] Henning O. Sørensen,[1] Carsten Gundlach,[1] Wolfgang Pantleon[1]

During plastic deformation of metals and alloys, dislocations arrange in ordered patterns. How and when these self-organization processes take place have remained elusive, because in situ observations have not been feasible. We present an x-ray diffraction method that provided data on the dynamics of individual, deeply embedded dislocation structures. During tensile deformation of pure copper, dislocation-free regions were identified. They showed an unexpected intermittent dynamics, for example, appearing and disappearing with proceeding deformation and even displaying transient splitting behavior. Insight into these processes is relevant for an understanding of the strength and work-hardening of deformed materials.

Metals and alloys are typically polycrystalline aggregates where each grain is characterized by the orientation of its atomic lattice. When deformed plastically, line defects (dislocations) are introduced into the lattice of each grain (*1*). These defects organize into dislocation boundaries separating (nearly) dislocation-free regions with almost perfect lattices, which we term subgrains. As an illustration, a transmission electron microscope (TEM) image is shown (Fig. 1). With increasing deformation, the flow stress increases, and the dislocation structure shrinks in length scale; the subgrains become progressively smaller, and the orientation difference between neighboring subgrains becomes larger (*2*).

Understanding the arrangement of dislocations is essential for science and industry, because their patterns determine many physical and mechanical properties, such as electrical resistivity of semiconductors or strength anisotropy and fatigue failure of (cubic) metals. Furthermore, dislocation patterns are of generic interest, because they are observed in a broad class of materials and over many different length scales, ranging from mm-sized structures in semiconductors (*3*) to structures with a size of 10 nm in severely deformed metals (*4*). Nevertheless, very central questions have not been settled. These include the following: How and when do ordered dislocation structures form? How is the shrinkage in length scale, and hence the subdivision of the deformation structure, accomplished?

Traditionally, deformed structures are characterized in two ways: by electron microscopy (EM) (*5*–*8*) and by line profile analysis of x-ray diffraction patterns (*9*–*12*). EM provides detailed maps of sections (Fig. 1), but the dynamics observed on such sections is not representative of the bulk because of artifacts such as dislocation migration toward the free surfaces and stress relaxation. Line profile analysis can, in principle, probe the bulk dynamics in polycrystals, but the results are averages over many subgrains and many grains, all with different orientations and neighboring relations.

We present results on the dynamics of individual, deeply embedded subgrains. The material was 99.99% pure Cu with an average

[1]Center for Fundamental Research: Metal Structures in Four Dimensions, Materials Research Department, Risø National Laboratory, DK-4000 Roskilde, Denmark. [2]Advanced Photon Source, Argonne National Laboratory, 9700 South Cass Avenue, Argonne, IL 60439, USA.

*To whom correspondence should be addressed. E-mail: henning.friis.poulsen@risoe.dk

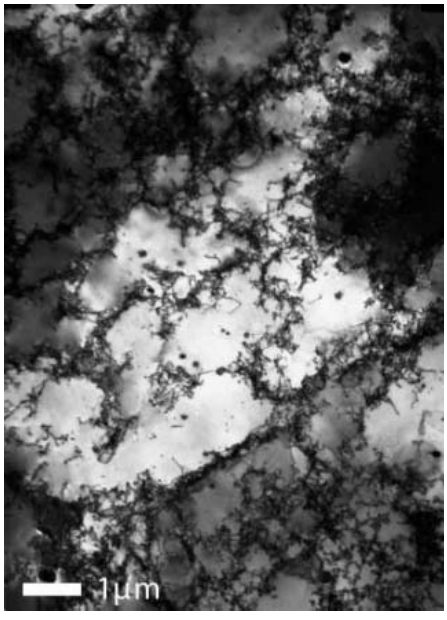

Fig. 1. TEM image of 99.99% pure Cu, deformed to a strain of 2% in tension. The dislocations (black line segments) organize into walls and dislocation-free regions.

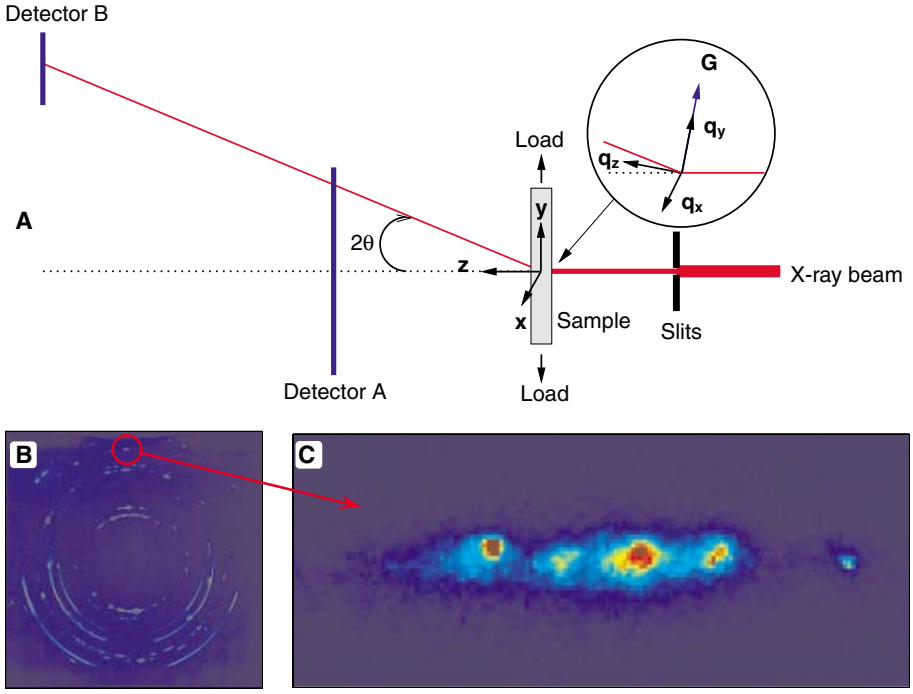

Fig. 2. (**A**) Sketch of the experimental setup. The real and reciprocal space coordinates (x, y, and z) and (q_x, q_y, and q_z), respectively, are defined, together with the scattering angle of 2θ. The directions $\mathbf{q}_y$ (the radial direction) and ($\mathbf{q}_x$ and $\mathbf{q}_z$) are parallel and perpendicular, respectively, to the ideal reciprocal lattice vector for the reflection investigated (represented by **G**). They are related to the elastic strain and orientation distributions of the grain, respectively. X-ray diffraction patterns are acquired by using the two area detectors A and B, by rotating the sample around the x axis in small intervals. (**B**) Full diffraction pattern obtained with detector A at a strain of 3%. (**C**) Corresponding high-resolution image of the 400 reflection acquired by detector B. By stacking such high-resolution images, a 3D reciprocal space map of the reflection is obtained.

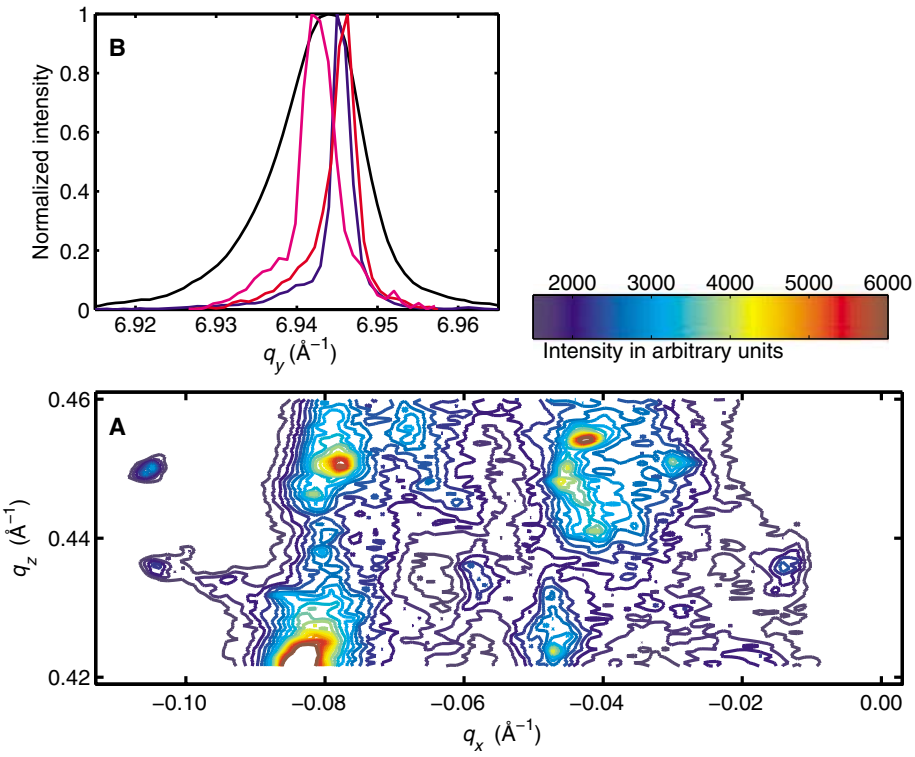

Fig. 3. (**A**) Projection onto ($\mathbf{q}_x$, $\mathbf{q}_z$) plane of an intensity map acquired at an elongation of 3.49%. The map is truncated in $\mathbf{q}_z$. The color scale is indicated above the map. (**B**) The intensity distribution of a few of the peaks appearing in the map projected onto $\mathbf{q}_y$ (red, blue, and magenta). The corresponding profile for the entire mapped intensity is indicated in black. The observed width of the individual peaks is close to the experimental resolution as measured with a standard powder.

grain size of 36 μm. Several 300 μm–thick specimens were studied during tensile deformation. To enable such measurements, we established a dedicated x-ray diffraction setup at the Advanced Photon Source synchrotron (Materials and Methods). A combination of x-ray optical elements generates a highly penetrating 52-keV x-ray beam, which at the same time exhibits high flux, narrow energy spread and divergence, and beam dimensions smaller than the average grain size. This beam impinges on the specimen and is used for in situ transmission studies. The resulting diffraction patterns are acquired concurrently by two area detectors for gathering information on the grain (detector A) and subgrain scale (detector B). Detector A is associated with an intermediate angular resolution of ~0.02 Å^{-1} (in reciprocal space units), whereas the resolution for detector B, due to a distance of 4 m to the sample, is ~0.0005 Å^{-1}. The latter corresponds to an angular resolution of ~0.004° and is an order of magnitude better than that attainable by EM. A sketch is shown in Fig. 2 along with examples of raw data.

The experiment was initiated by characterization of the undeformed state using detector A. By applying experimental procedures described in the literature (*13*–*15*), we identified the diffraction patterns from single grains, and we tested whether these selected grains are positioned near the center of the specimen. In the following, we present data

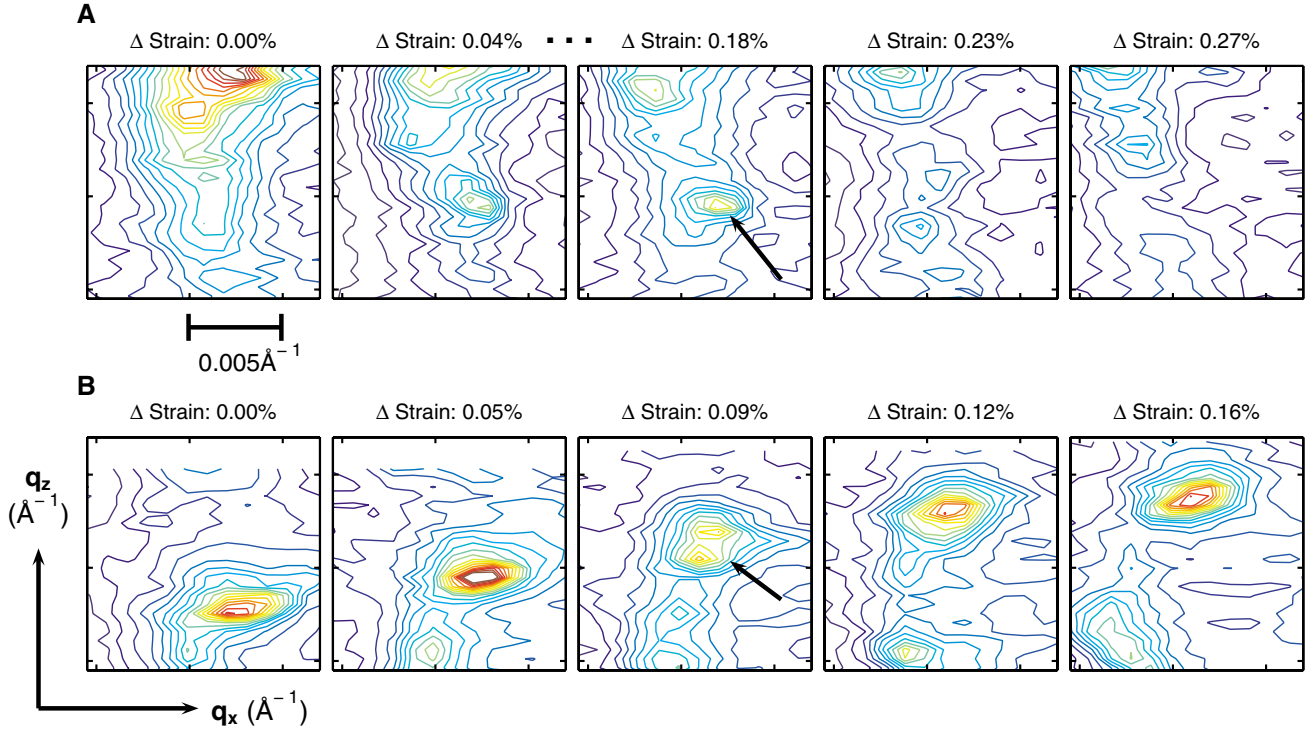

Fig. 4. Two examples of subgrain dynamics. Subfigures are excerpts from larger projections onto ($\mathbf{q}_x$, $\mathbf{q}_z$) plane of reciprocal space maps, with contour lines, axes, and color scale identical to those of Fig. 3A. These are shown left to right as a function of external strain (with strain increments relative to the first map). (**A**) An example of a peak that appeared, grew in intensity, and disappeared (the arrow indicates the peak at its maximum). (**B**) An example of a peak that split into two parts (as indicated by the arrow), which then recombined. The peak shifted simultaneously along $\mathbf{q}_z$, corresponding to a rotation of the subgrain by ~0.05°.

for a grain with a volume of ~8000 μm^3 and with its [100] direction close to the tensile axis. The beam was set to illuminate a fixed subvolume of this grain by confining it with slits (Fig. 2A) to 14 μm by 14 μm.

The sample was strained to an elongation of 3% and then from 3% to 4.2% in steps of ~0.04%. After each strain increment, a three-dimensional (3D) reciprocal space map of the 400 reflection originating from the grain subvolume of interest was generated by acquiring a set of images with detector B while rotating around the *x* axis (Fig. 2A) in intervals of 0.004°. Furthermore, at a strain of 4.07%, the sample was translated with respect to the beam in steps of 2 μm in both *x* and *y* directions (Fig. 2A), and a reciprocal space map was made at each position. By a knife-edge algorithm similar to the ones presented in literature (*13*, *16*), it is possible to determine the spatial position of features in the reciprocal space map from these scans.

All reciprocal space maps gathered show similar features, and no qualitative changes are observed in the investigated strain interval. A typical 3D map is shown in movie S1. A projection of this map, integrating along the diffraction vector, is shown in Fig. 3A. A striking feature of the high-resolution map is that the reflection comprises a set of individual peaks. Tests were performed to ensure that these peaks were not artifacts caused, for example, by the beam being partially coherent. The individual peaks were identified as diffraction spots arising from individual subgrains within the grain of choice. This claim is substantiated by three facts. First, the size of the associated diffracting entities, as deduced from the integrated intensities, were in the range of 1 to 3 μm, in good agreement with TEM results (Fig. 1). Second, the peaks were very sharp with typical full widths at half maximum of 0.001 to 0.003 Å^{-1} in all directions of reciprocal space. This implies that none or, at most, very few dislocations were present in the subgrain, which again corresponds well with TEM results. Third, most of the peaks originated from one and only one position in the grain. (Those that did not were seen as composed of overlaying contributions from several subgrains.) Consequently, individual diffraction peaks observed in reciprocal space correspond in real space to dislocation-free regions separated spatially from each other by regions of increased dislocation density. The cloud of enhanced intensity between peaks is tentatively identified as arising from these disordered dislocation boundary regions, the broad walls in Fig. 1. On the basis of intensity ratios, the volume fraction of clearly identifiable subgrains as determined by x-rays is 30%. Considering that this is a lower limit, the value corresponds well with the volume fraction of 55% found by TEM (*17*).

Examples of the intensity distribution parallel to the diffraction vector for selected peaks are provided in Fig. 3B. The centers of the peaks are clearly separated, indicating quite different elastic strains of the individual subgrains. The integrated profile in Fig. 3B (black curve) comprises contributions both from individual subgrains and from dislocation boundaries. According to the classical composite model (*11*), this curve is a superposition of two corresponding symmetric profiles, each broadened by the respective dislocation density. Forward stresses (enhancing the external load) in the dislocation walls and back stresses (opposing the load) in the dislocation-depleted regions lead to shifts in the radial positions and cause the asymmetry in the black curve. In view of our results (movie S1 and Fig. 3B), this picture holds only for the contribution of the dislocation boundaries. The contribution of the subgrains cannot be described by a shifted profile broadened by a substantial dislocation density but rather as a number of individual sharp profiles stemming from an ensemble of dislocation-free subgrains each experiencing a different stress (with a back stress in average). This finding resolves two experimentally based objections against the composite model: (i) the lack of dislocations within subgrains (*18*) and (ii) the nearly constant internal stress within individual subgrains (*19*). The existence of nearly perfect subgrains in a deformation structure has a strong impact on existing work-hardening theories in particular for larger strains, because many of them—for example, (*20*–*24*)—are built on versions of the composite model.

We created a video of the evolution of the reciprocal space map as a function of strain, and excerpts are shown in movie S2. As expected, the envelope of the reflection representing all parts of the diffracting subvolume broadens continuously with strain. Within the envelope, the evolution of nonoverlapping peaks can be traced. Because the integrated intensities and the radial and transverse positions of the peaks are linearly related to volume, elastic strain, and rotation of the corresponding subgrains, the subgrain dynamics and their reorientation can be monitored in detail.

On the basis of an analysis of about 20 peaks, the peaks display unexpected intermittent dynamics. They appear and disappear again during straining. Some peaks, such as the one in Fig. 4A, even exist only for a short strain interval. From the decrease in average boundary distance observed by TEM (*2*), following an inverse square root law, we expected a decrease of the average subgrain volume, and consequently an increase in the number of subgrains, by 67% in the strain interval from 3% to 4.2%. The decreasing boundary spacing is traditionally attributed to mutual trapping of dislocations into new boundaries. Accordingly, a dislocation-free region without orientation spread may split into two regions with distinct orientations. No such event has been observed yet. The newly appearing peaks cannot be caused by reorientation of an existing subgrain, because the maximum orientation difference caused by dislocation slip during a strain increment of ~0.04% is ~0.05° and such reorientations can be excluded from inspection of the 3D reciprocal space maps. Rather, the distinct diffraction peaks emerge from the intensity-enhanced cloud, and the corresponding dislocation-free regions materialize temporarily as islands in a sea of dislocations. Changing their volume constantly, dislocation-free regions emerge and vanish fluctuatingly, reflecting the underlying stochastic dynamics of the entire dislocation ensemble (*25*). Such an intermittent behavior of the subgrains may explain two currently unsolved questions, namely how dislocation structures remain roughly equiaxed during hot-working (*8*) and how dislocation boundaries maintain a preferred orientation during, for example, cold-rolling (*26*).

Several peaks exhibited the behavior illustrated in Fig. 4B: The peak split into two subpeaks, which then recombined with further strain. Such a splitting of ~0.002 Å^{-1} or ~0.02° can be caused by a single dislocation in the subgrain. Hence, despite the fact that the x-ray beam illuminates ~6×10^6 dislocations at one time, we stipulate that such events can provide insight into the behavior of one or a few dislocations trapped inside subgrains.

A second sample was characterized during continuous deformation with a strain rate of 2.5×10^{-6} s^{-1} from 0% up to 3% elongation. The appearance of sharp peaks on top of a structureless cloud is characteristic of all strains greater than or equal to 0.4%. This observation strongly indicates that subgrain formation is initiated shortly after onset of plastic deformation. At 3% the strain was fixed, whereas the data collection continued. These data directly address a long-standing question of whether the dislocation patterns persisting after termination of the deformation are identical to the patterns existing during deformation. [The dislocation patterns present after terminating deformation can be preserved by neutron irradiation before unloading (*27*, *28*) and hence observed by TEM after thinning.] Within observable error no changes were observed upon fixation. This is direct evidence that, at least in this case, the interruption of the test does not influence the patterning.

The method presented here can provide unique in situ information on the pattern-formation process, relevant for guiding and testing modeling efforts on the subgrain scale. In outlook, we have verified the applicability of resolving individual peaks corresponding to subgrains at much higher strains, namely 50% deformation. Furthermore, by scanning wires (*16*) or conical slits (*13*) positioned between the sample and the detector, the method can be extended to provide complete 3D spatial information. Such procedures could be added, at the expense of time, at selected strains.

References and Notes

1. F. R. N. Nabarro, *Theory of Crystal Dislocations* (Clarendon Press, Oxford, 1967).
2. D. Hughes, D. C. Chrzan, Q. Liu, N. Hansen, *Acta Mater.* **45**, 105 (1997).
3. P. Rudolph, *Cryst. Res. Technol.* **40**, 7 (2005).
4. D. Hughes, N. Hansen, *Phys. Rev. Lett.* **87**, 135503 (2001).
5. U. Essmann, *Phys. Status Solidi* **12**, 707 (1965).
6. J. W. Steeds, *Proc. R. Soc. London Ser. A* **292**, 343 (1966).
7. B. Bay, N. Hansen, D. Hughes, D. Kuhlmann-Wilsdorf, *Acta Metall. Mater.* **40**, 205 (1992).
8. P. Cizek, *Scripta Mater.* **45**, 815 (2001).
9. M. Wilkens, *Phys. Status Solidi A* **2**, 359 (1970).
10. M. A. Krivoglaz, *Theory of X-ray and Neutron Scattering by Real Crystals* (Plenum, New York, 1969).
11. H. Mughrabi, T. Ungar, W. Kienle, M. Wilkens, *Philos. Mag. A* **53**, 793 (1986).
12. R. I. Barabash, P. Klimanek, *J. Appl. Cryst.* **32**, 1050 (1999).
13. H. F. Poulsen, *Three-Dimensional X-ray Diffraction Microscopy* (Springer, Berlin, 2004).
14. E. M. Lauridsen, S. Schmidt, R. M. Suter, H. F. Poulsen, *J. Appl. Cryst.* **34**, 744 (2001).
15. L. Margulies, G. Winther, H. F. Poulsen, *Science* **291**, 2392 (2001).
16. B. C. Larson, W. Yang, G. E. Ice, J. D. Budai, T. Z. Tischler, *Nature* **415**, 887 (2002).
17. E. Göttler, *Philos. Mag.* **28**, 1057 (1973).
18. A. S. Argon, P. Haasen, *Acta Metall. Mater.* **41**, 3289 (1993).
19. M. E. Kassner, M. T. Perez-Prado, M. Long, K. S. Vecchio, *Metall. Mater. Trans. A* **33**, 311 (2002).
20. F. B. Prinz, A. S. Argon, *Acta Metall.* **32**, 1021 (1984).
21. W. D. Nix, J. C. Gibeling, D. A. Hughes, *Metall. Trans. A* **16A**, 2215 (1985).
22. M. Zehetbauer, *Acta Metall. Mater.* **41**, 589 (1993).
23. Y. Estrin, L. Tóth, Y. Brechet, A. Molinari, *Acta Mater.* **46**, 5509 (1998).
24. F. Roters, D. Raabe, G. Gottstein, *Acta Mater.* **48**, 4181 (2000).
25. P. Hähner, *Acta Mater.* **44**, 2345 (1996).
26. Q. Liu, N. Hansen, *Proc. R. Soc. Lond. A* **454**, 2555 (1998).
27. U. Essmann, *Phys. Status Solidi* **3**, 932 (1963).
28. H. Mughrabi, *Philos. Mag.* **23**, 869 (1971).

29. The sample preparation was performed by G. Christiansen, and the EM studies were performed by Q. Xing. This work was supported by the Danish National Research Foundation and the Danish Natural Science Research Council. Use of the Advanced Photon Source was supported by the U.S. Department of Energy, Basic Energy Sciences, Office of Science, under contract no. W-31-109-Eng-38.

Supporting Online Material

www.sciencemag.org/cgi/content/full/312/5775/889/DC1
Materials and Methods
Fig. S1
Movies S1 and S2

21 December 2005; accepted 16 March 2006
10.1126/science.1124141

Simultaneous Negative Phase and Group Velocity of Light in a Metamaterial

Gunnar Dolling,[1]* Christian Enkrich,[1] Martin Wegener,[1,2] Costas M. Soukoulis,[3,4] Stefan Linden[2]

We investigated the propagation of femtosecond laser pulses through a metamaterial that has a negative index of refraction for wavelengths around 1.5 micrometers. From the interference fringes of a Michelson interferometer with and without the sample, we directly inferred the phase time delay. From the pulse-envelope shift, we determined the group time delay. In a spectral region, phase and group velocity are negative simultaneously. This means that both the carrier wave and the pulse envelope peak of the output pulse appear at the rear side of the sample before their input pulse counterparts have entered the front side of the sample.

The propagation of waves through dispersive media often leads to surprising or counterintuitive behavior (*1*). For the case of positive–refractive-index media in electrodynamics, where the phase velocity v_{phase} is positive (in the forward direction), the group velocity v_{group} can become negative in the regime of anomalous dispersion. As a result, the peak of a temporally long Gaussian pulse can appear at the rear side of a sample before the peak of the Gaussian input pulse has entered the front side of the sample (*2*). This phenomenon has been directly observed (*3*) on an excitonic absorption resonance in a GaP:N semiconductor sample by time resolving the transmission of a picosecond optical pulse. Further experiments along these lines, e.g., on positive-index systems with gain (*4*–*6*), have confirmed this behavior. It has been thoroughly discussed (*2*) that superluminal or even negative group velocities are not at all in conflict with relativity or causality, essentially because the peak of the output pulse is not a cause of the peak of the input pulse. In other words, even though input and output pulses can have the same Gaussian shape, reshaping of the pulse envelope is of crucial importance.

Here we report results of corresponding experiments on negative–refractive-index materials. These highly unusual materials have only recently become available (*7*–*9*), with the optical regime becoming accessible only within the past year (*10*–*14*). The phase velocity in these materials is negative. We directly measured both group and phase velocity by propagating a femtosecond laser pulse through a negative-index metamaterial and then time resolving the transmitted pulse using interferometry. These experiments are the negative-index counterpart of the above experiments for positive-index materials (*3*–*6*), where $v_{phase} > 0$ and $v_{group} < 0$. We found conditions where $v_{phase} < 0$ and $v_{group} < 0$, and others where $v_{phase} < 0$ and $v_{group} > 0$. Together with the usual situation of $v_{phase} > 0$ and $v_{group} > 0$, all four sign combinations have now been observed in direct experiments. For all four sign combinations, the

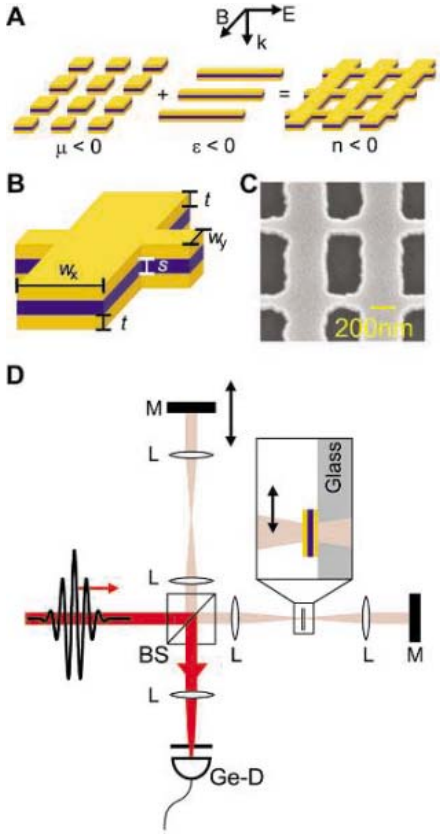

Fig. 1. (**A**) Scheme of the negative-index metamaterial design and polarization configuration used here. **E** is the incident electric-field vector, **B** the incident magnetic-field vector, and **k** the incident wave vector of light. (**B**) Definition of parameters: t = 25 nm, s = 35 nm, w_x = 307 nm, w_y = 100 nm, and a square lattice with lattice constant a = 600 nm. The metamaterial thickness is $d = 2t + s$ = 85 nm. (**C**) Top-view electron micrograph of the corresponding structure. (**D**) Scheme of the experimental setup. M, mirror; L, lens; BS, beam splitter; Ge-D, germanium photodetector.

[1]Institut für Angewandte Physik and Deutsche Forschungsgemeinschaft–Center for Functional Nanostructures, Universität Karlsruhe (TH), Wolfgang-Gaede-Straße 1, D-76131 Karlsruhe, Germany. [2]Institut für Nanotechnologie, Forschungszentrum Karlsruhe in der Helmholtz-Gemeinschaft, D-76021 Karlsruhe, Germany. [3]Ames Laboratory and Department of Physics and Astronomy, Iowa State University, Ames, IA 50011, USA. [4]Institute of Electronic Structure and Laser–Foundation for Research and Technology Hellas, and Department of Materials Science and Technology, University of Crete, 71110 Heraklion, Crete, Greece.

*To whom correspondence should be addressed. E-mail: gunnar.dolling@physik.uni-karlsruhe.de

Poynting vector is positive, i.e., along the forward direction.

The negative-index metamaterial samples used in our experiments closely follow a design proposed theoretically in (*10*) and first realized experimentally in (*11*). For the polarization configuration sketched in Fig. 1, the material can be thought of as consisting of double-plate (or double-wire) pairs (*13*, *14*), which provide the negative magnetic permeability μ, and long metal wires, which act as a diluted Drude metal. Below the plasma frequency, the latter correspond to an electric permittivity $\varepsilon < 0$. The combination of $\mu < 0$ and $\varepsilon < 0$ leads to a negative real part of the refractive index n (*15*). Our samples were fabricated using standard electron-beam lithography and electron-beam evaporation of the constituent materials. In total, we fabricated 60 different negative-index samples on glass substrate covered with a 5-nm thin film of indium-tin-oxide (ITO). Each sample has a footprint of 100 μm $\times$ 100 μm. The sample parameters of the sample discussed below are given in Fig. 1, A to C. An overview of the measured and calculated (*16*) optical transmittance and reflectance spectra is given in Fig. 2. Here, the gold dielectric function is described by the Drude model with plasma frequency $\omega_p = 1.32 \times 10^{16}$ s^{-1} and collision frequency $\omega_c = 1.2 \times 10^{14}$ s^{-1}. These values are obtained from a fit of the Drude model to the measured complex permittivity of thin gold films (*17*) in the near-infrared. The refractive index of the glass substrate is $n = 1.5$, and that of the MgF_2 spacer layer is $n = 1.38$. Experiment and theory in Fig. 2 are found to agree very well.

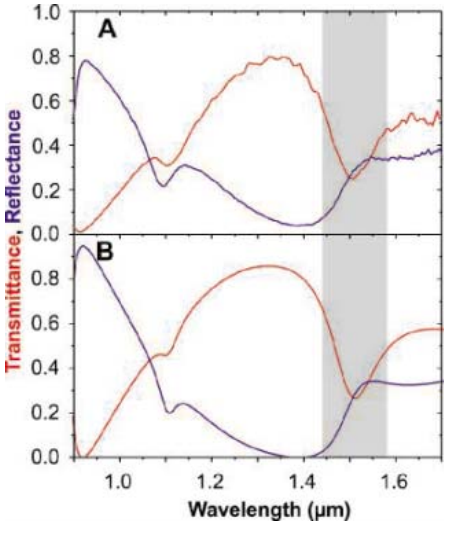

Fig. 2. Transmittance (red) and reflectance (blue) spectra for the polarization configuration and sample shown in Fig. 1. (**A**) Measurements with a white-light source. (**B**) Theory. To guide the eye, the total spectral region shown in Fig. 4 is highlighted by the gray area.

From the calculated spectra, we have retrieved (*18*) the effective metamaterial parameters and we found a negative real part of the refractive index, $\mathrm{Re}(n) < 0$ (see below). As expected from theory (*10*), we do not obtain $\mathrm{Re}(n) < 0$ for the orthogonal linear polarization.

To perform phase-sensitive experiments on these samples, different interferometer types can be used; for example, a Michelson interferometer or a Mach-Zehnder interferometer. Our setup (Fig. 1D) is essentially a compact Michelson interferometer (not actively stabilized), into one arm of which we can insert the sample. 170-fs, transform-limited Gaussian pulses from an optical parametric oscillator (OPO) that are tunable around 1500-nm wavelength are sent into this interferometer. The output of the interferometer is recorded as a function of the length of one of the interferometer arms, which can immediately be translated into an interferometer time delay. When inserting the sample, the interferogram shifts on the time-delay axis. The shift of its envelope is determined by the sample group velocity. The shift of the rapidly oscillating fringes contains information on the sample phase velocity, provided that two conditions are satisfied: (i) To infer unambiguously the phase velocity from a phase delay, one must ensure that the phase delay is smaller than one period of light. This condition translates into "thin" samples. For our conditions, the anticipated maximum phase delay Δt_{phase} is below one femtosecond and the period of light is about 5 femtoseconds at 1500-nm wavelength. (ii) Generally, an additional phase delay can arise due to the interfaces between air/metamaterial and metamaterial/substrate. Thus, the experiments must be accompanied by transmittance/reflectance spectroscopy and by theory to ensure that these phase factors do not dominate over those due to propagation (see below). This interface aspect can generally also influence the group delay, but turns out to be unimportant here.

Figure 3 shows results obtained on a negative-index metamaterial. By laterally translating the sample (Fig. 1D), we first measure the air interferogram, then that of the sample. The glass substrate is in the optical path in either case, hence it drops out when considering the difference. The zero of the interferometer time-delay axis is set to be at the maximum of the air interferogram. We measure one air interferogram within about 2 s acquisition time, then we move the sample in by computer control, take a second interferogram, move the sample out again, and

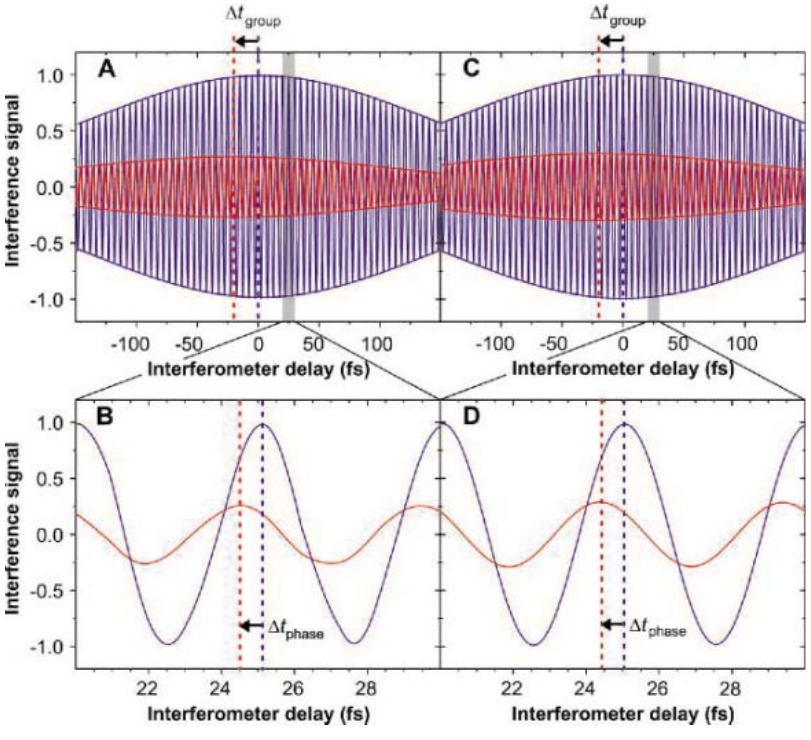

Fig. 3. (**A**) Examples of typical measured interferograms (constant background subtracted for clarity), air interferogram (blue), and interferogram with sample (red). The sample corresponds to Fig. 1, the OPO wavelength is 1500 nm. The Gaussian envelopes obtained from a least-squares fit to the interferogram extrema are depicted for both cases. The resulting negative group delay Δt_{group} is indicated. (**B**) Enlarged view of two individual interference fringes, the resulting negative phase delay Δt_{phase} is indicated. The corresponding calculated data are shown in (**C**) and (**D**).

repeat the entire procedure 20 times. In this fashion, we can identify possible drifts of our setup. Typically, we find drifts smaller than 100 attoseconds throughout the procedure. Each of the two interferograms shown in Fig. 3A results from averaging 20 individual scans with a total acquisition time of 40 s. When inserting a sample with thickness d and refractive index n, $v_{phase} = c_0/\mathrm{Re}(n)$, and the phase time delay $\Delta t_{phase} = 2d/v_{phase} - 2d/c_0$ results, where $c_0 = 2.99\times10^8$ m/s is the vacuum velocity of light. The factor of 2 stems from the double-pass geometry in the Michelson interferometer (Fig. 1D). Similarly, we get the group time delay $\Delta t_{group} = 2d/v_{group} - 2d/c_0$. For the example depicted in Fig. 4, we have $\Delta t_{phase} = -0.62$ fs < 0 and $\Delta t_{group} = -19.1$ fs < 0. The error in determining Δt_{phase} is 0.07 fs, the error in Δt_{group} is 0.3 fs. To test our apparatus, we also performed experiments on a $d = 120$ nm thin dielectric film of HfO_2 with real refractive index $n = +1.95$ on glass substrate, leading to positive phase delay $\Delta t_{phase} = +0.79$ fs > 0 and positive group delay $\Delta t_{group} = +0.78$ fs > 0. Here, phase and group delay are identical within the measurement error and consistent with the HfO_2 refractive index.

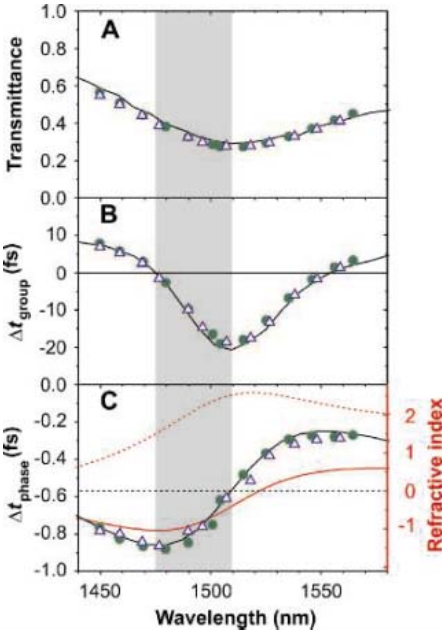

Fig. 4. Summary of two different sets of experiments (blue triangles and green circles) on the sample corresponding to Figs. 1 and 2. The black curves are calculated data. (**A**) Transmittance spectra measured with the OPO. (**B**) Group delay Δt_{group} (compare to Fig. 3). (**C**) Phase delay Δt_{phase}. A refractive index of $\mathrm{Re}(n) = 0$ together with the sample thickness of $d = 85$ nm corresponds to a propagation phase delay of -2×85 nm$/c_0 = -0.57$ fs. This condition is given by the dashed horizontal line. (C) also reveals the real (solid) and imaginary (dashed) part of the refractive index (red scale at right), as retrieved from the data of Fig. 2. The gray area highlights the regime where simultaneously $v_{phase} < 0$ and $v_{group} < 0$.

Figure 4 summarizes measured phase and group delays for various OPO center wavelengths, individually obtained along the lines of Fig. 3. The phase delay Δt_{phase} is negative for the entire spectral range depicted. The group delay is either negative or positive. All measurements agree very well with our calculations, which use the identical sample parameters as in Fig. 2. These calculations directly simulate the experiment (Fig. 3, C and D). We let a 170-fs Gaussian pulse propagate through the structure shown in Fig. 1, but we do not use the retrieved effective material parameters. However, using the retrieved material parameters would give strictly the identical result, because the complex transmittance and reflectance coefficients are strictly identical, owing to the principle of the retrieval procedure (*18*).

We start our discussion of the data in Fig. 4C by assuming that the phase delay is exclusively due to propagation. In this case, a negative refractive index requires phase delays more negative than $\Delta t_{phase} = 0 - 2d/c_0$. With the metamaterial thickness of $d = 85$ nm, we get the $\mathrm{Re}(n) = 0$ line at $\Delta t_{phase} = -0.57$ fs, which is illustrated by the dashed horizontal line in Fig. 4C. However, if the phase delay was exclusively due to propagation, the crossing of the phase-delay curve with the $\mathrm{Re}(n) = 0$ line and the zero crossing of the real part of the retrieved refractive index in Fig. 4C should strictly coincide. We find a small spectral shift between the two crossings. This shift originates from an additional phase delay due to the interfaces between air/metamaterial and metamaterial/substrate. At these interfaces, one obtains phase factors from the Fresnel equations for complex metamaterial impedances. Multiple reflections between these interfaces further modify the phase.

It is simple to understand the measured sign of the group delay in terms of an effective material (Fig. 4B). The group velocity v_{group} can be expressed as

$$v_{group} = \frac{d\omega}{dk} = \frac{c_0}{\mathrm{Re}(n) + \omega \frac{d\,\mathrm{Re}(n)}{d\omega}}$$

For the fictitious case of negligible dispersion, the group velocity is identical to the phase velocity, i.e., the group velocity is negative if the phase velocity (equivalently the real part of the refractive index) is negative. In the presence of dispersion, the second term in the denominator can be either positive or negative, depending on which part of the spectral resonance is considered. For frequencies where the derivative of the index with respect to frequency is positive (Fig. 4C, right side), the second term can overcompensate the negative refractive index. This can lead to a positive group velocity, hence to a positive group delay. Our direct experiments are consistent with indirect experiments on negative-index metamaterials in the microwave regime (*19*), where the group delay was calculated numerically on a computer from the measured dispersion of the phase delay.

We have shown in direct pulse propagation experiments on negative-index metamaterials that the phase velocity can be negative. Furthermore, contrary to common intuition, the group velocity can also be negative simultaneously. For other spectral positions, we find negative phase velocity and positive group velocity. For all sign combinations of phase and group velocity in effective metamaterials, the Poynting vector is positive—otherwise no signal would be transmitted through the sample.

References and Notes

1. L. Brillouin, *Wave Propagation and Group Velocity* (Academic, New York, 1960).
2. C. G. B. Garrett, D. E. McCumber, *Phys. Rev. A* **1**, 305 (1970).
3. S. Chu, S. Wong, *Phys. Rev. Lett.* **48**, 738 (1982).
4. L. J. Wang, A. Kuzmich, A. Dogarlu, *Nature* **406**, 277 (2000).
5. M. D. Stenner, D. J. Gauthier, M. A. Neifeld, *Nature* **425**, 695 (2003).
6. M. S. Bigelow, N. N. Lepeshkin, R. W. Boyd, *Science* **301**, 200 (2003).
7. R. A. Shelby, D. R. Smith, S. Schultz, *Science* **292**, 77 (2001).
8. D. R. Smith, J. B. Pendry, M. C. K. Wiltshire, *Science* **305**, 788 (2004).
9. S. Linden *et al.*, *Science* **306**, 1351 (2004).
10. S. Zhang *et al.*, *Opt. Express* **13**, 4922 (2005).
11. S. Zhang *et al.*, *Phys. Rev. Lett.* **95**, 137404 (2005).
12. N. Grigorenko *et al.*, *Nature* **438**, 335 (2005).
13. G. Dolling *et al.*, *Opt. Lett.* **30**, 3198 (2005).
14. V. M. Shalaev *et al.*, *Opt. Lett.* **30**, 3356 (2005).
15. V. G. Veselago, *Sov. Phys. Usp.* **10**, 509 (1968).
16. The calculations are based on a finite-difference time-domain approach and use the commercial software package CST Microwave Studio.
17. P. B. Johnson, R. W. Christy, *Phys. Rev. B* **6**, 4370 (1972).
18. Th. Koschny *et al.*, *Phys. Rev. B* **71**, 245105 (2005).
19. J. F. Woodley, M. Mojahedi, *Phys. Rev. E* **70**, 046603 (2004).

20. We thank Th. Koschny for stimulating discussions. We acknowledge support by the Deutsche Forschungsgemeinschaft (DFG) and the State of Baden-Württemberg through the DFG-Center for Functional Nanostructures within subproject A1.5. The research of M.W. is further supported by project DFG-We 1497/9-1 and that of S.L. through a Helmholtz-Hochschul-Nachwuchsgruppe (VH-NG-232). The research of C.M.S. is further supported by the Alexander von Humboldt senior-scientist award 2002, by Ames Laboratory (Contract No. W-7405-Eng-82), European Union projects DALHM, PHOREMOST, METAMORPHOSE, and by the Defense Advanced Research Projects Agency (HR0011-05-C-0068).

9 February 2006; accepted 5 April 2006
10.1126/science.1126021

Observation of Backward Pulse Propagation Through a Medium with a Negative Group Velocity

George M. Gehring,[1*] Aaron Schweinsberg,[1] Christopher Barsi,[3]
Natalie Kostinski,[1,4] Robert W. Boyd[1,2]

The nature of pulse propagation through a material with a negative value of the group velocity has been mysterious, as simple models seem to predict that pulses will propagate "backward" through such a material. Using an erbium-doped optical fiber and measuring the time evolution of the pulse intensity at many points within the fiber, we demonstrate that the peak of the pulse does propagate backward inside the fiber, even though the energy flow is always in the forward direction.

Researchers have long been intrigued by the wide range of phenomena that can occur in the propagation of optical pulses through highly dispersive media (*1*–*21*). Some of the most exotic of these effects occur for a medium with a negative value of the group velocity. In such a situation, theory predicts that the peak of the transmitted pulse will exit the material before the peak of the incident pulse enters the material, and furthermore that the pulse will appear to propagate in the backward direction within the medium (*21*–*23*). Although the first of these effects, equivalent to the occurrence of negative time delays, has been observed by previous workers (*5*, *6*, *11*, *12*, *14*, *16*, *24*), the second of these effects has apparently not been previously observed. Indeed, it has not been entirely clear whether the theoretical prediction of backward propagation is sufficiently robust that it could be observed under actual laboratory conditions.

We report on our investigations of backward propagation of an optical pulse through an erbium-doped optical fiber (EDOF) that is pumped in such a manner as to produce a negative value of the group velocity. By measuring the time evolution of the pulse intensity at many points within the fiber, our results demonstrate that the peak of the pulse does indeed propagate in the backward direction within the fiber. However, the energy flow is always in the forward direction, as the velocity of energy transport is equal to the group velocity only under special cases, notably the absence of gain or loss in the medium (*25*).

It is useful to review the theoretical understanding of slow and fast light effects (*26*, *27*) and especially of backward pulse propagation. The group velocity describing the propagation of optical pulses through a material can be expressed as $v_g = c/n_g$, where the group index is given by $n_g = n + \omega\, dn/d\omega$, n is the usual refractive index, c is the speed of light, and ω is the frequency of the radiation. In regions of anomalous dispersion (that is, for negative values of $dn/d\omega$), the second term makes a negative contribution to the group velocity, and if this term is sufficiently large the group velocity can become negative. Negative values of the group velocity thus occur under conditions of rapid spectral variation of the refractive index, which, as a consequence of the Kramers-Kronig relations, tend to appear in regions surrounding either a narrow absorption feature or a narrow dip in a gain feature. We took the latter approach, using coherent population oscillations (*13*, *14*, *28*, *29*) (CPOs) to induce a narrow dip in the gain profile of an erbium-doped fiber optical amplifier (*30*). As we showed earlier (*13*), under these conditions the spectral variation of the gain is given by

$$g(\delta) = \frac{g_0}{1 + I_0} \times \left[1 - \frac{I_0(1 + I_0)}{(T_1\delta)^2 + (1 + I_0)^2}\right] \quad (1)$$

where $\delta = \omega - \omega_0$ is the separation between the frequency ω at which the gain is measured and the frequency ω_0 of a strong wave of intensity I, g_0 is the unsaturated value of the gain coefficient, T_1 is the relaxation time of the population inversion of the erbium amplifier, and $I_0 = I/I_{sat}$ is the light intensity normalized to the saturation intensity I_{sat} of the erbium amplifier. The refractive index variation associated with this spectral feature is given by

$$n(\delta) = n_{host} - \frac{g_0 c T_1}{2\omega_1} \frac{I_0}{1 + I_0} \times \left[\frac{\delta}{(T_1\delta)^2 + (1 + I_0)^2}\right] \quad (2)$$

where n_{host} is the background refractive index of the optical fiber. The group index, evaluated for simplicity at the center ($\delta = 0$) of the spectral hole, is given by

$$n_g = n_{host} - \frac{g_0 c T_1}{2} \frac{I_0}{(1 + I_0)^3} \quad (3)$$

where for EDOF the relaxation time T_1 is equal to 10.5 ms. Under our experimental conditions,

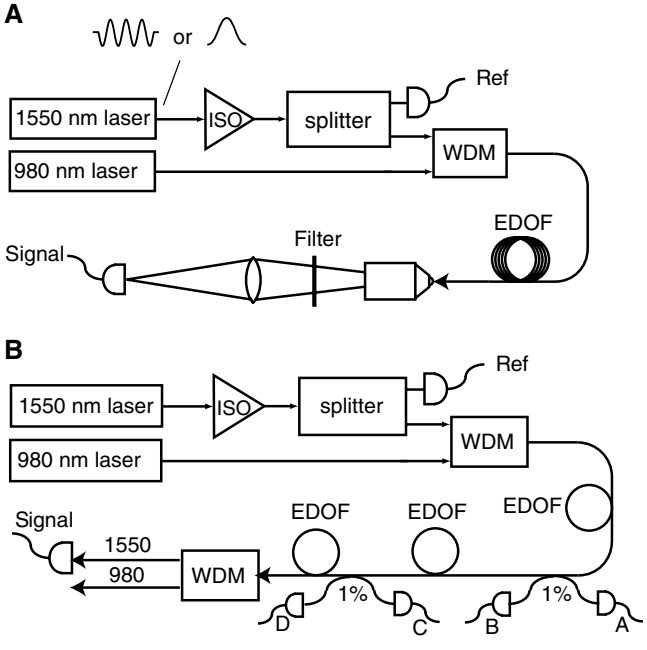

Fig. 1. (**A**) Experimental setup. The 980-nm laser acts as a pump to establish gain in the EDOF amplifier. Pulses or modulated waveforms from the 1550-nm laser probe the propagation characteristics of the fiber. A WDM combines these beams before the fiber, and an optical filter isolates the 1550-nm beam after the fiber. The time evolution of the pulse within the fiber is monitored by successively cutting back the length of the fiber and measuring the output wave form. (**B**) Alternative experimental setup used to determine the direction of energy transport in a material with a negative group index. Three 3-m sections of EDOF were placed in series, with bidirectional 1% taps placed between each pair of sections. A WDM was connected to each of the tap outputs to separate the signal wavelength from the pump wavelength. The bidirectional taps allowed measurement of energy flow in both directions.

[1]Institute of Optics, [2]Department of Physics and Astronomy, University of Rochester, Rochester, NY 14627, USA. [3]Department of Electrical and Computer Engineering, Manhattan College, New York, NY 10471, USA. [4]Department of Electrical Engineering and Computer Science, University of Michigan, Ann Arbor, MI 48109, USA.

*To whom correspondence should be addressed. E-mail: gehring@optics.rochester.edu

the measured group velocity was –75 km/s and the group index was –4000.

A group index of –4000 agrees with the predictions of Eq. 3 for a gain coefficient g_0 of 0.8 m^{-1} and a saturation parameter I_0 of 0.0032, which are reasonable estimates of the values of these parameters for our experimental setup. Even when the group index is negative, it is not necessarily easy to observe backward propagation, because this effect can be limited or obscured by competing effects such as pulse broadening and breakup as a result of dispersion of the group velocity (*31*) or by severe spectral reshaping of the pulse (*11*).

We chose an EDOF used in an optical amplifier configuration, because this enabled us to control the values of the unsaturated gain g_0 and the spectral width of the dip in the gain profile by varying the power of the 980-nm laser beam used to pump the amplifier. We were thus able to optimize the value of the time advancement associated with the group velocity (*30*). The large physical length of the material enabled us to readily measure the time evolution of the optical pulse at many locations within the fiber.

In the experimental setup (Fig. 1), the 1550-nm diode laser produces the probe pulses for our measurements. The probe laser beam is sent through an isolator, after which part of the beam is split off and sent to an InGaAs photodiode for use as a reference. The remaining light is combined with the 980-nm pump beam with the use of a wavelength-division multiplexer (WDM) and the two beams are sent through the EDOF coil. The exiting beam is collimated by a microscope objective and filtered to remove the 980-nm pump light before being focused onto a germanium photodetector. This signal and the reference are recorded by a digital storage oscilloscope.

Signal and reference traces were recorded for two different waveforms: a 1-kHz sine wave and a 0.5-ms (full width at half maximum) Gaussian pulse. In both cases, the pulse or sinusoidal waveform was superposed on a large constant background of an intensity 10 times that of peak modulation height. The presence of a large background reduces pulse distortion effects. The powers of the 980-nm pump and 1550-nm signal fields at the input to the EDOF were 128 mW and 0.5 mW, respectively. Example traces are shown in Fig. 2.

Measurements were first taken using a 9-m length of EDOF. The fiber length was then reduced by about 25 cm by cutting the fiber, and the measurement was repeated. This procedure was continued until there were only several centimeters of fiber remaining. In this way, the time evolution of the pulse could be determined at many points along the length of the fiber.

By arranging the traces according to position and playing them back in time sequence, we created movies showing the pulse evolution within the fiber (movies S1 and S2). Sequences of frames from these movies displaying the relevant behavior are shown in Fig. 3 and Fig. 4. In constructing Fig. 3, the waveforms at each spatial location have been normalized, removing the effects of the gain within the fiber; Fig. 4 presents the data without this normalization. In each case, the background has been removed.

In both figures, the peak of the transmitted pulse is seen to leave the fiber before the peak of the incident pulse enters the fiber. We also see that as the pulse exits the fiber, a small peak is created inside the fiber that moves in the backward direction, linking the input and output pulses. Movies S3 and S4 show similar results for a sinusoidally modulated input field. The apparent "backward propagation" occurs because of reshaping of the pulse profile within the gain medium as a consequence of time-dependent energy transfer between the pulse and the gain medium. There is no energy flow in the backward direction. Also, there is no violation of causality, as the peak that exits the material grows out of the rising edge of the input pulse, just as the peak of

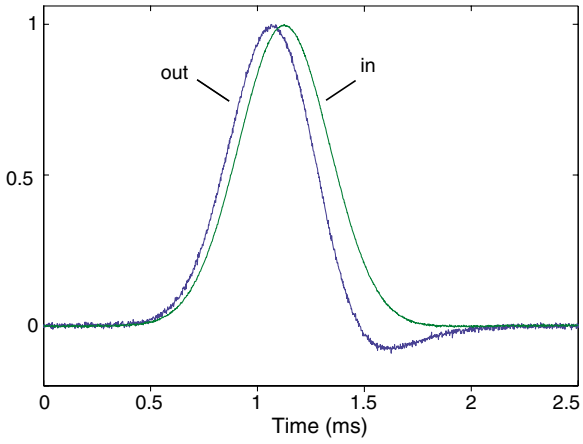

Fig. 2. Input and output waveforms after propagation through a 6-m length of erbium-doped fiber. The output waveform is seen to be advanced in time and to experience slight distortion. Pulse heights are normalized to facilitate comparison of input and output pulse shapes.

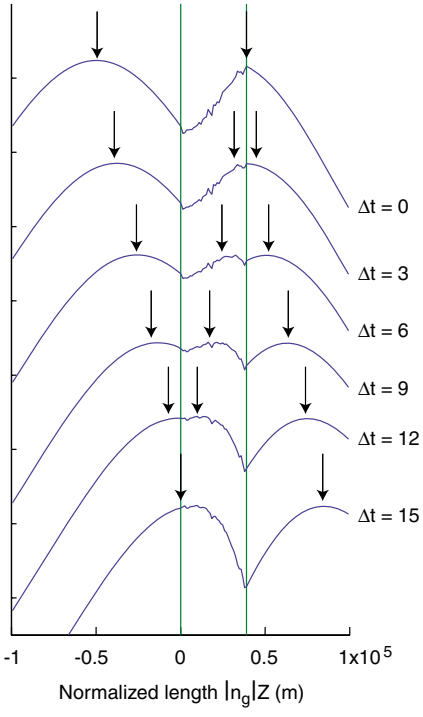

Fig. 3. Time evolution of the pulse as it propagates through the fiber. The data have been normalized at each point in the fiber to remove the effects of gain. The peak of the transmitted pulse is seen to exit the fiber before the peak of the incident pulse enters the fiber, and inside the fiber the peak moves from right to left as time increases. The arrows mark the peak of the pulse before entering the fiber (**left**), within the fiber (**center**), and after leaving the fiber (**right**). The time intervals are in milliseconds.

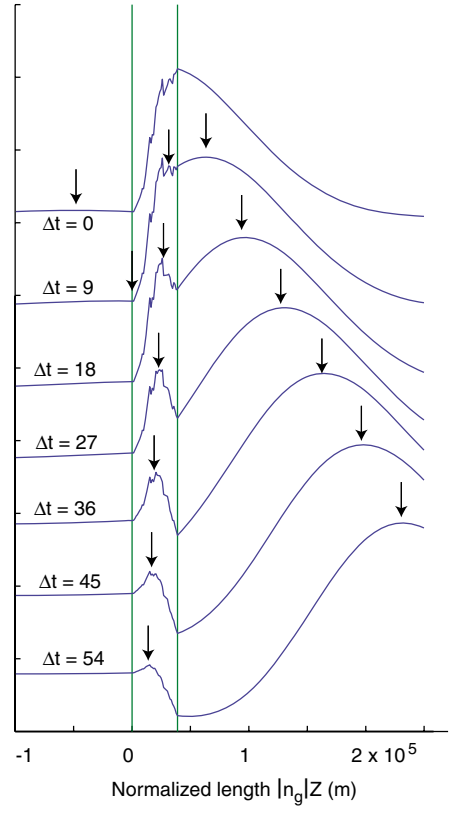

Fig. 4. Same as Fig. 3, except that the data have not been normalized to remove the effects of gain. Thus, the output pulse is much larger than the input pulse. The pulse is still seen to propagate in the backward direction, but with a different value of the pulse velocity from that of Fig. 3 as a consequence of the influence of gain. The time intervals are in milliseconds.

the input pulse becomes part of the tail of the exiting pulse.

As a further investigation into the nature of negative group velocities, we performed a second experiment to determine the direction of energy flow within the medium. The layout is shown in Fig. 1B. We observed that the signal strength measured at output ports A and C of the bidirectional 1% taps was barely above the noise floor of our detection system and was consistent with the small amount of back-reflection expected from the large number of splices present in this configuration. In contrast, strong signals were measured from ports B and D, thus demonstrating that the energy flow was only in the forward direction, even though the group velocity was negative. We also observed that the peak of the pulse arrived at port D before it did at port B, thus confirming the backward motion of the peak of the pulse within the optical fiber.

Our experiment shows that within a medium with a negative group velocity, the peak of a propagating pulse does in fact move in the backward direction, even though energy flow is always in the forward direction. These results can be understood in terms of the time dependence of the saturation of the gain of the material, whereby the leading edge of the incident pulse experiences more gain than does the trailing edge. Thus, the peak of the pulse within the medium occurs initially at the distant end of the fiber and progressively moves toward the front end of the fiber. Furthermore, all of these results are consistent with the principle of causality in that these effects are initiated by the far leading edge of the pulse.

References and Notes

1. L. Brillouin, *Wave Propagation and Group Velocity* (Academic Press, New York, 1960).
2. N. G. Basov, V. S. Letokhov, *Sov. Phys. Dokl.* **11**, 222 (1966).
3. C. G. B. Garrett, D. E. McCumber, *Phys. Rev. A* **1**, 305 (1970).
4. G. C. Sherman, K. E. Oughstun, *Phys. Rev. Lett.* **47**, 1451 (1981).
5. S. Chu, S. Wong, *Phys. Rev. Lett.* **48**, 738 (1982).
6. B. Ségard, B. Macke, *Phys. Lett. A* **109**, 213 (1985).
7. A. Kasapi, M. Jain, G. Y. Yin, S. E. Harris, *Phys. Rev. Lett.* **74**, 2447 (1995).
8. L. V. Hau, S. E. Harris, Z. Dutton, C. H. Behroozi, *Nature* **397**, 594 (1999).
9. D. Budker, D. F. Kimball, S. M. Rochester, V. V. Yashchuk, *Phys. Rev. Lett.* **83**, 1767 (1999).
10. M. M. Kash *et al.*, *Phys. Rev. Lett.* **82**, 5229 (1999).
11. Md. A. I. Talukder, Y. Amagishi, M. Tomita, *Phys. Rev. Lett.* **86**, 3546 (2000).
12. L. J. Wang, A. Kuzmich, A. Dogarlu, *Nature* **406**, 227 (2000).
13. M. S. Bigelow, N. N. Lepeshkin, R. W. Boyd, *Phys. Rev. Lett.* **90**, 113903 (2003).
14. M. S. Bigelow, N. N. Lepeshkin, R. W. Boyd, *Science* **301**, 200 (2003).
15. B. Macke, B. Ségard, *Eur. Phys. J. D* **23**, 125 (2003).
16. M. D. Stenner, D. J. Gauthier, M. A. Neifeld, *Nature* **425**, 695 (2003).
17. G. S. Agarwal, T. Nath Dey, *Phys. Rev. Lett.* **92**, 203901 (2004).
18. E. Baldit, K. Bencheikh, P. Monnier, J. A. Levenson, V. Rouget, *Phys. Rev. Lett.* **95**, 143601 (2005).
19. Y. Okawachi *et al.*, *Phys. Rev. Lett.* **94**, 153902 (2005).
20. K. Y. Song, M. González Herráez, L. Thévenaz, *Opt. Express* **13**, 83 (2005).
21. R. Y. Chiao, *Phys. Rev. A* **48**, R34 (1993).
22. M. Ware, S. A. Glasgow, J. Peatross, *Opt. Express* **9**, 506 (2001).
23. M. Ware, S. A. Glasgow, J. Peatross, *Opt. Express* **9**, 519 (2001).
24. S. Chu, S. Wong, *Phys. Rev. Lett.* **49**, 1293 (1982).
25. R. L. Smith, *Am. J. Phys.* **38**, 978 (1970).
26. R. W. Boyd, D. J. Gauthier, *Prog. Opt.* **43**, 497 (2002).
27. P. W. Milonni, *Fast Light, Slow Light, Left-Handed Light* (Institute of Physics, Bristol, UK, 2005).
28. R. W. Boyd, M. G. Raymer, P. Narum, D. J. Harter, *Phys. Rev. A* **24**, 411 (1981).
29. L. W. Hillman, R. W. Boyd, J. Krasinski, C. R. Stroud Jr., *Opt. Commun.* **45**, 416 (1983).
30. A. Schweinsberg, M. Bigelow, R. W. Boyd, S. Jarabo, *Europhys. Lett.* **73**, 218 (2006).
31. R. W. Boyd, D. J. Gauthier, A. L. Gaeta, A. E. Willner, *Phys. Rev. A* **71**, 023801 (2005).

32. Supported by the Defense Advanced Research Projects Agency/Defense Science Office Slow Light program and by NSF.

Supporting Online Material

www.sciencemag.org/cgi/content/full/312/5775/895/DC1
Movies S1 to S4

3 January 2006; accepted 5 April 2006
10.1126/science.1124524

Statistical Independence of Escalatory Ecological Trends in Phanerozoic Marine Invertebrates

Joshua S. Madin,[1]* John Alroy,[1] Martin Aberhan,[2] Franz T. Fürsich,[3] Wolfgang Kiessling,[2] Matthew A. Kosnik,[4] Peter J. Wagner[5]

Ecological interactions, such as predation and bioturbation, are thought to be fundamental determinants of macroevolutionary trends. A data set containing global occurrences of Phanerozoic fossils of benthic marine invertebrates shows escalatory trends in the relative frequency of ecological groups, such as carnivores and noncarnivorous infaunal or mobile organisms. Associations between these trends are either statistically insignificant or interpretable as preservational effects. Thus, there is no evidence that escalation drives macroecological trends at global and million-year time scales. We also find that taxonomic richness and occurrence data are cross-correlated, which justifies the traditional use of one as a proxy of the other.

Major trends in the composition of Earth's biota (*1*) are widely thought to be evolutionarily important (*2*, *3*), but statistical (*4*) and taphonomic (*5*–*7*) biases might create the appearance that such trends result from ecological interactions. The publicly available Paleobiology Database (*8*) makes it possible to test (i) the strength of long-term large-scale associations between ecology and macroevolution and (ii) the assumption that global taxonomic richness is a good proxy for ecological abundance, which previously has been demonstrated only for individual groups during certain parts of the Phanerozoic (*9*, *10*).

The two most commonly cited hypotheses explaining trends in the fossil record invoke negative interactions among ecological groups. The escalation hypothesis predicts that long-term ecological shifts are caused by the evolutionary response of prey to predation pressure (*2*), which has intensified for some groups (*11*, *12*) if not others (*13*). Two potential faunal responses are progressions to infaunality (moving into the substrate for protection from predators) and mobility (evading predators on or above the subtrate, both actively and facultatively). Alternatively, the bulldozer hypothesis (*3*), a subsidiary of the escalation hypothesis, predicts that epifaunal immobile taxa will decline when there is increased biological disturbance of the sediment by infaunal, actively mobile taxa (bioturbators). Trends involving particular taxa (*14*) or over short time scales (*15*) may conform with these predictions, but these hypotheses need to be tested by examining trends in relative diversity and counts of occurrences (fossil collections that include each taxon) among marine metazoans as a whole.

We classified marine invertebrate taxa unassociated with reefs into three ecological categories (diet, life habit, and locomotion) and one preservational category (mineralogical composition) (*16*). Trilobites were excluded from analyses because their ecological trends are quite inconsistent with escalation, with their dramatic early Paleozoic decline obscuring consistent long-term trends for other groups. Thus, excluding trilobites makes our results more conservative. To avoid problems associated with variation in sampling intensity that plague estimates of global diversity (*17*), we used proportions within each ecological category instead of raw counts (*18*).

[1]National Center for Ecological Analysis and Synthesis, University of California, Santa Barbara, CA 93101, USA. [2]Museum für Naturkunde, Humboldt-Universität, 10115 Berlin, Germany. [3]Institut für Paläontologie, Universität Würzburg, 97070 Würzburg, Germany. [4]School of Marine Biology and Aquaculture, James Cook University, Townsville 4811, Australia. [5]Department of Geology, Field Museum of Natural History, Chicago, IL 60605, USA.

*To whom correspondence should be addressed. E-mail: madin@nceas.ucsb.edu

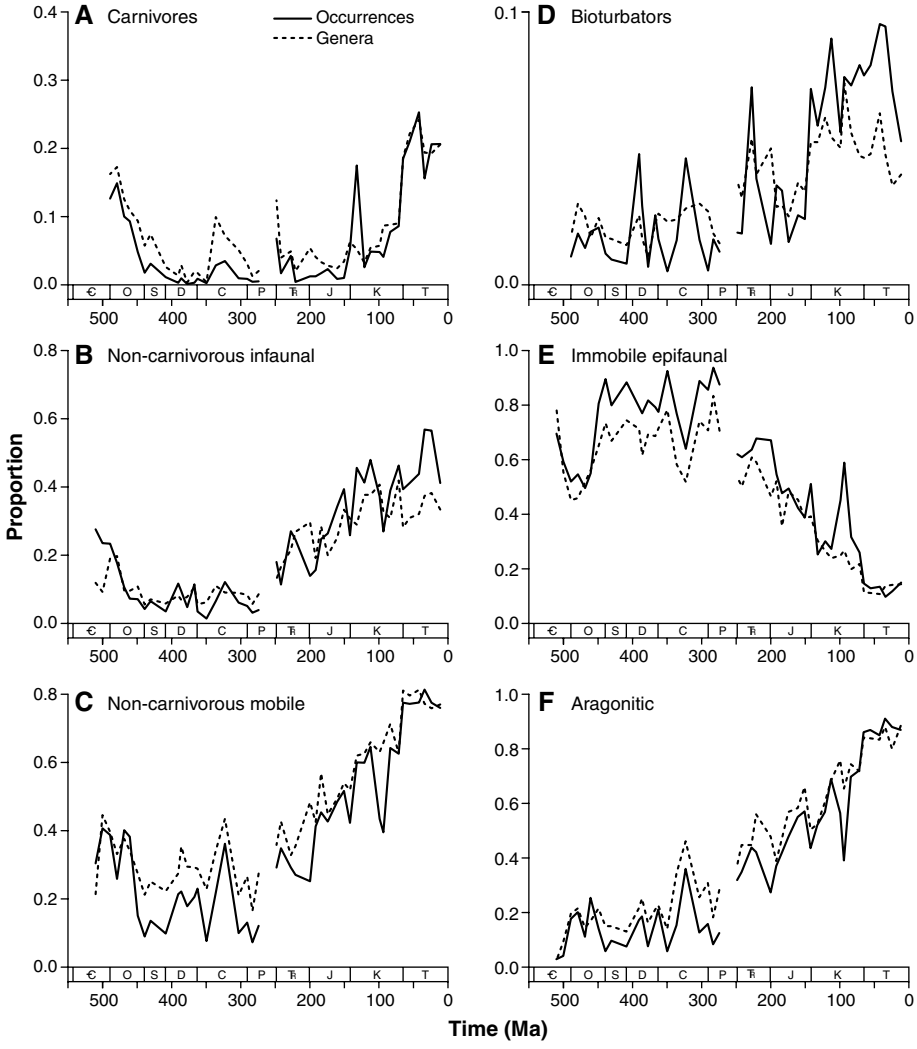

Fig. 1. Proportions of genera (dashed line) and occurrences (solid line) for taxa classified as carnivorous (**A**), noncarnivorous infaunal (**B**), noncarnivorous mobile (actively and facultatively) (**C**), bioturbating (**D**), immobile epifaunal (**E**), and aragonitic (**F**). For statistical independence of groups, proportions of carnivores are given relative to all taxa, but proportions of noncarnivorous groups [(B) and (C)] are given relative to all noncarnivorous taxa. Bioturbating and immobile epifaunal genera do not exhibit both modes of life habit or diet; therefore, proportions of bioturbators are given relative to all taxa, whereas proportions of immobile epifauna are given relative to all nonbioturbating taxa. Single letters at the bottom of each panel are abbreviations for geological periods. Ma, million years ago.

Although long-term concerted changes in the dominance of ecological strategies shown in the raw data may imply an evolutionary response (such as an increase in infaunality driven by an increase in carnivory) (Fig. 1), correspondences may be the spurious result of independent autocorrelated trends ["ships that pass in the night" (*4*)]. Process-based theories (in which changes in one variable directly cause changes in another) predict that time series will vary in concert regardless of the overall trend. Therefore, we removed autocorrelation using generalized first-order differencing of logit-transformed proportions [$\ln(p/1-p)$] (*16*) and then tested whether (i) changes in noncarnivorous infaunality or mobility were cross-correlated with carnivory and (ii) changes in immobile epifaunality were cross-correlated with bioturbation. Raw cross-correlations between the ecological categories superficially suggest that these groups were caught in an escalatory struggle (Fig. 2, A to C, and table S1). However, these cross-correlations weaken considerably after differencing (Fig. 2, D to F, and table S1), and none are significant after a Bonferroni correction (in which the alpha level of 0.05 was divided by 6, because there are six ecological comparisons). The results are unlikely to be due to a lack of power because we have adequate sample sizes (at least 40 in each case) to detect biologically interesting correlations.

Over the Phanerozoic, there has been a marked shift in the primary composition of marine invertebrate fossils from calcite to aragonite (Fig. 1F). Calcitic taxa are more taphonomically robust than aragonitic taxa (*19*). We find significant cross-correlations between the ecological proportions and shell mineralogy proportions (table S1). Such associations can exist given two causal scenarios that are not mutually exclusive. First, shifts in the ecological proportions may result from differences in the proportion of aragonitic fossils recovered from one time bin to the next (taphonomy), which in turn may be due to changes in seawater chemistry. Second, escalation may drive shifts in aragonitic taxa, and thus the proportions of aragonitic fossils shift accordingly (macroevolution).

We tested whether a preservational bias was involved by recomputing the ecological cross-correlations after excluding the occurrences from fossil collections that did not preserve aragonitic forms (14% of the total). The remaining collections should be relatively less taphonomically biased. Because other preservational indicators, such as molds or casts, were inconsistently recorded in the database, they were unusable. Two of the six cross-correlations (carnivore versus infaunal genera and bioturbating versus immobile epifaunal genera) that were not significant remained so, and the three correlations involving occurrences ceased to be significant. Although marginally significant (carnivore versus mobile genera: Spearman's $\rho = 0.398$, $P = 0.011$), this remaining correlation is not found in the corresponding occurrence data and is no longer significant after a Bonferroni correction. Thus, the relations that are weakly suggested to be important in the original analysis do not hold up, suggesting that aragonite preservation does matter in some cases [but see (*7*)].

The correlations between ecological and shell mineralogy proportions are much the same even if collections that fail to preserve aragonite, presumably for taphonomic reasons, are excluded from the analysis (table S1). Thus, the data suggest that apparent trends in the frequency of aragonitic forms are not taphonomic but are driven by the coincidental, statistically independent expansion of groups that happen to be aragonitic in composition (heterodont bivalves and neogastropods), which is a different process from escalation.

These results suggest that escalation, if it is the causal driver, does not occur within periods shorter than the 11-million-year time bins. However, a time lag might be expected if, for example, (i) dominance increased and allowed higher rates of speciation over millions of years, or (ii) dominance was depressed but taxa persisted for a long time before going extinct. To check for time lags, cross-correlations were recalculated for several lag periods in either direction (up to ±3 time bins or about 33 million years), and the resultant associations were as weak, or absent. Additional treatments of the data would be unlikely to find strong correlations. For example, analyzing the Paleozoic and post-Paleozoic data separately or increasing the length of the bins would leave so few data points that the correlations would have little power. Furthermore, restricting the data to specific environments, geographic regions, or latitudinal belts, or

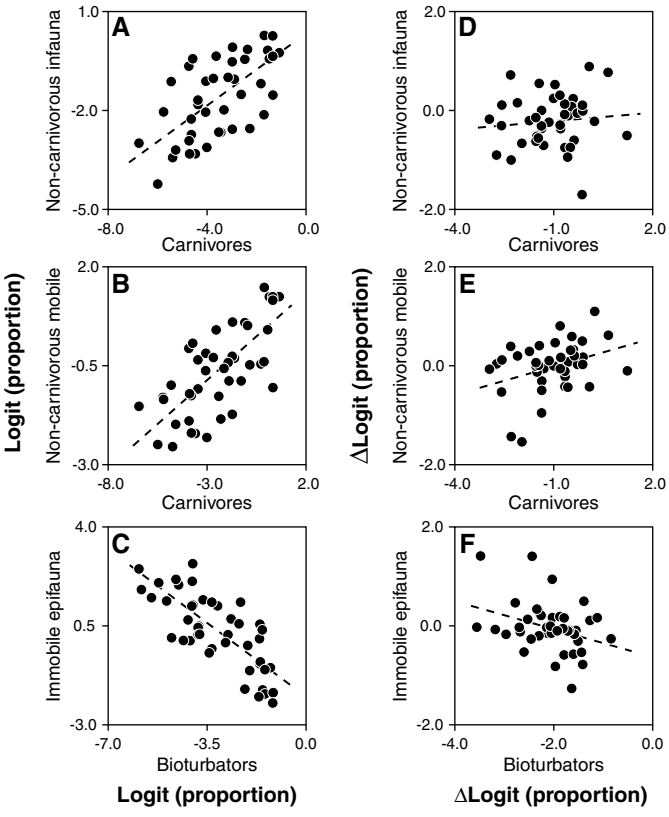

Fig. 2. Cross-correlations between logit-transformed proportions of occurrences of carnivorous and noncarnivorous infaunal (**A** and **D**), carnivorous and mobile (**B** and **E**), and bioturbating and immobile epifaunal (**C** and **F**) marine invertebrates. Correlations on the left involve raw data, whereas correlations on the right involve data after first-order differencing. Occurrences from collections including one or more aragonitic forms are tallied. Dashed lines represent least-square lines of best fit. ΔLogit, change in the logit-transformed proportion.

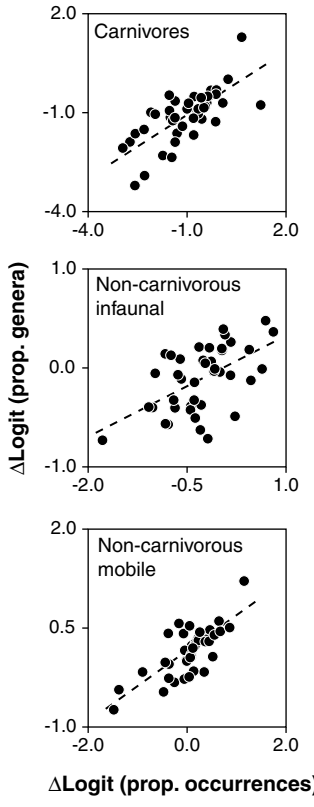

Fig. 3. Cross-correlations between changes in the proportions of genera and proportions of occurrences for carnivorous, noncarnivorous infaunal, and noncarnivorous mobile marine invertebrates. Dashed lines represent least-square lines of best fit.

using shorter bins, would create large gaps in the time series.

The raw data (Fig. 1) illustrate trends in the relative frequency of ecological groups during the Phanerozoic that seem to agree with the predictions of the two macroevolutionary hypotheses: (i) a proportional increase in carnivores corresponding with increases in noncarnivorous infaunal and mobile ecological strategies and resembling published curves showing drilling frequencies (*11*), and (ii) a proportional increase in bioturbators corresponding with a decline in immobile epifauna. However, the differencing analyses show that these correspondences are strictly coincidental, in a statistical sense.

Secular trends consistent with each hypothesis are seen even though some carnivorous groups (such as vertebrates, malacostracans, and asteroids) and bulldozing groups (such as infaunal crustaceans and polychaetes) do not fossilize well and thus are presumably undersampled. However, major predatory groups such as ammonites and neogastropods are well represented in our database, and the proportion of carnivores is quite high (~20%) by the Cenozoic. Our data also do not address alternative defensive adaptations that are not preserved, such as toxicity, but these adaptations are not the focus of the existing paleontological literature on escalation (*12*), in part because chemical defenses are less common in well-skeletonized taxa (*20*).

The dominance of ecological groups has traditionally been tracked through time using taxonomic richness (*2*, *3*, *17*), because most large-scale databases do not contain counts of occurrences (*21*). However, if one ecological group is systematically less abundant on a per-species basis, greater sampling will increase the relative taxonomic richness of that group (*9*, *10*). Counts of occurrences, on the other hand, provide an improved proxy for ecological importance because an ecological group with more occurrences is likely to have been more abundant locally and had a greater geographic range and a broader environmental distribution (*22*).

If taxonomic richness is a direct function of ecological dominance, then the proportions of genera and occurrences should have similar averages, and their changes should be cross-correlated (Fig. 1). We find significant cross-correlations between differenced proportions (*16*) of genera and occurrences for the five focal ecological groups (P values < 0.001, df = 39, Pearson's r = 0.56 to 0.77, Spearman's ρ = 0.52 to 0.70); three of these correlations are shown in Fig. 3. Moreover, two-sample t tests reveal no significant differences between average proportions. Despite the variation in total sample size per bin, the close match of the curves indicates that the frequencies of genera would not change substantially if sampling intensity were standardized. This result implies that hierarchical levels are not evolutionarily independent (*23*). Instead, taxonomic richness is a reliable surrogate for ecological importance, as is traditionally assumed (*22*).

Our results suggest either that Phanerozoic-scale patterns in the ecological proportions examined here are not driven by direct ecological interactions, or that these processes are obscured by other factors. Instead, the major ecological groups may wax and wane independently.

References and Notes

1. R. K. Bambach, in *Biotic Interactions in Recent and Fossil Benthic Communities*, M. J. S. Tevesz, P. L. McCall, Eds. (Plenum, New York, 1983), chap. 15.
2. G. J. Vermeij, *Evolution and Escalation* (Princeton Univ. Press, Princeton, NJ, 1987).
3. C. W. Thayer, in *Biotic Interactions in Recent and Fossil Benthic Communities*, M. J. S. Tevesz, P. L. McCall, Eds. (Plenum, New York, 1983), chap. 11.
4. S. J. Gould, C. B. Calloway, *Paleobiology* **6**, 383 (1980).
5. D. Sanders, *J. Afr. Earth Sci.* **36**, 99 (2003).
6. J. W. Morse, A. Mucci, F. J. Millero, *Geochim. Cosmochim. Acta* **44**, 85 (1980).
7. S. M. Kidwell, *Science* **307**, 914 (2005).
8. The Paleobiology Database (http://paleodb.org).
9. R. Lupia, S. Lidgard, P. R. Crane, *Paleobiology* **25**, 305 (1999).
10. F. K. McKinney, S. Lidgard, J. J. Sepkoski, P. D. Taylor, *Science* **281**, 807 (1998).
11. M. Kowalewski, A. Dulai, F. T. Fürsich, *Geology* **26**, 1091 (1998).
12. P. H. Kelley, M. Kowalewski, T. A. Hansen, Eds., *Predator-Prey Interactions in the Fossil Record* (Kluwer Academic/Plenum, New York, 2003).
13. M. Kowalewski, A. P. Hoffmeister, T. K. Baumiller, R. K. Bambach, *Science* **308**, 1774 (2005).
14. G. J. Vermeij, *Annu. Rev. Ecol. Syst.* **25**, 219 (1994).
15. M. Aberhan, W. Kiessling, F. T. Fürsich, *Paleobiology* **32**, 259 (2006).
16. Materials and methods are available as supporting material on *Science* Online.

17. J. Alroy *et al.*, *Proc. Natl. Acad. Sci. U.S.A.* **98**, 6261 (2001).
18. R. K. Bambach, A. H. Knoll, J. J. Sepkoski, *Proc. Natl. Acad. Sci. U.S.A.* **99**, 6854 (2002).
19. A. K. Behrensmeyer *et al.*, *Paleobiology* **31**, 607 (2005).
20. J. R. Pawlik, *Chem. Rev.* **93**, 1911 (1993).
21. J. J. Sepkoski, *Bull. Am. Paleo.* **363**, 1 (2002).
22. M. A. Buzas, C. F. Koch, S. J. Culver, N. F. Sohl, *Paleobiology* **8**, 143 (1982).
23. E. S. Vrba, S. J. Gould, *Paleobiology* **12**, 217 (1986).
24. We thank D. Bottjer, S. Holland, L. Ivany, A. Miller, and M. Patzkowsky for helpful discussions, and M. Apel, N. Bonuso, P. Borkow, B. Brenneis, M. Clapham, L. Fall, C. Ferguson, M. Foote, M. Gibson, T. Hanson, N. Heim, D. Hempfling, A. Hendy, S. Hicks, S. Holland, C. Jamet, K. Koverman, Z. Krug, K. Layou, E. Leckey, A. McGowan, P. Novack-Gottshall, S. Nürnberg, J. Sessa, C. Simpson, A. Tomasovych, and P. Wall for data collection. B. Kroeger and D. Korn helped to categorize the life habits of the Cephalopoda. This work was conducted at the National Center for Ecological Analysis and Synthesis, a center funded by NSF grant DEB-0072909, the University of California, and the University of California at Santa Barbara. This is Paleobiology Database publication number 44.

Supporting Online Material
www.sciencemag.org/cgi/content/full/312/5775/897/DC1
Materials and Methods
Table S1
References

8 December 2005; accepted 24 March 2006
10.1126/science.1123591

Fall in Earth's Magnetic Field Is Erratic

David Gubbins,* Adrian L. Jones, Christopher C. Finlay†

Earth's magnetic field has decayed by about 5% per century since measurements began in 1840. Directional measurements predate those of intensity by more than 250 years, and we combined the global model of directions with paleomagnetic intensity measurements to estimate the fall in strength for this earlier period (1590 to 1840 A.D.). We found that magnetic field strength was nearly constant throughout this time, in contrast to the later period. Extrapolating to the core surface showed that the fall in strength originated in patches of reverse magnetic flux in the Southern Hemisphere. These patches were detectable by directional data alone; the pre-1840 model showed little or no evidence of them, supporting the conclusion of a steady dipole up to 1840.

Jackson *et al.*'s historical model of the geomagnetic field (*1*) covers the period 1590 A.D. to the present (Fig. 1). Measurements of direction (declination and inclination) are available throughout this period, although inclination is scarce in the 17th century. No absolute intensity data are available until 1837, when C. F. Gauss devised the first method to measure it; intensity measurements became widespread by 1840. The EarthRef Digital Archive (ERDA) has an internally consistent paleointensity database compiled by Korte *et al.* (*2*). It contains 315 measurements on rock samples and archaeological remains from the interval 1590 to 1840 A.D., and we can, in principle, use these to determine field strength during the early period when there were no direct measurements.

The paleointensity data have error estimates on both intensity and age. Dating errors vary from 1 year, when historical records date the specimen precisely, to centuries, when only radiocarbon dates are available. Geographical coverage is poor (Fig. 2), with concentration in Europe and very little representation in the Southern Hemisphere, but temporal coverage is good (Fig. 3). Intensities have typical errors of 4000 nT, or about 10%. This error is comparable with any change expected during the entire period, so paleointensity measurements provide no usable information on intensity variation at a single site. However, given good directional information from the historical model, each intensity measurement can be converted to an estimate of the dipole moment, or g_1^0 (t), because a theorem (*3*) states that, given perfect directional information and no more than two dip-poles (places where the magnetic field is vertical, of which the Earth has only two), a single intensity measurement determines the field uniquely. The poor geographical coverage of intensity is therefore largely irrelevant, provided the global coverage of direction is good. Here we assume that g_1^0 (t) fell linearly from 1590 to 1840 and fix its value at 1840 to be that of the historical field model. This leaves just one parameter, the slope of the line, to be determined from 315 measurements. This large number of data are able to produce a meaningful estimate of a single unknown, the slope, despite the large errors on an individual datum.

We use the iterative maximum likelihood method of Williamson (*4*), closely related to that described by Press *et al.* (*5*), to fit a straight line through data having errors in both magnitude and time. g_1^0 (t = 1840) is constrained by

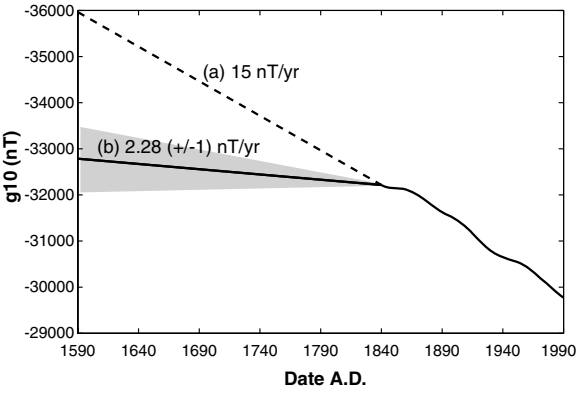

Fig. 1. Fall of the geomagnetic coefficient g_1^0 (in nT) since measurements began in 1590. g_1^0 is proportional to the Earth's dipole moment. Intensity measurements became available in 1840; the two slopes before 1840 are (a) the extrapolation back in time based on the average fall since 1840 and (b) paleointensity measurements using the method described in the present study. Shaded area gives the ±1 SD slopes.

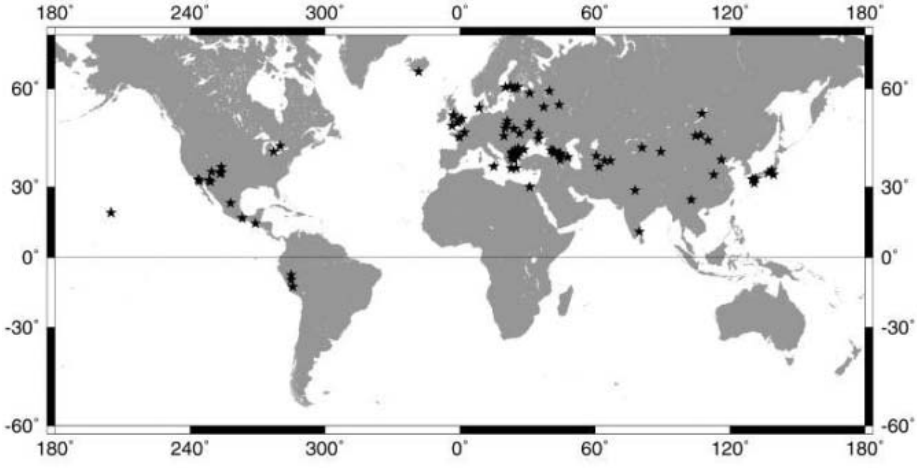

Fig. 2. Geographical distribution of the paleointensity data from 1590 to 1840 A.D. Data are mostly from the Northern Hemisphere, but the Southern Hemisphere is well covered by directional measurements.

School of Earth and Environment, University of Leeds, Leeds LS2 9JT, UK.

*To whom correspondence should be addressed. E-mail: gubbins@earth.leeds.ac.uk
†Present address: Institut für Geophysik, ETH Zürich, Switzerland.

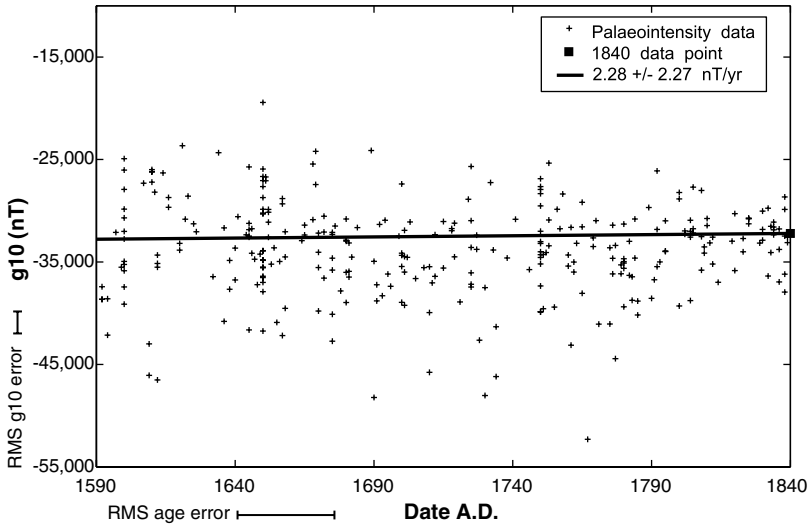

Fig. 3. Paleointensity data converted to g_1^0. The line is tied to the value at 1840 (black square), which is accurately determined by historical measurements. Root mean square (RMS) g_1^0 and age errors are shown as bars along the axes; they are 1943 nT and 35 years, respectively.

adding a single data point with very high accuracy. The method produces an estimate of the slope, its standard deviation, and a χ^2 goodness-of-fit parameter; it requires the data errors to be independent and normally distributed, which we confirmed by plotting histograms. The fit produced a slope of $\dot{g}_1^0 = 2.28 \pm 2.72$ nT/year (Fig. 1) and $\chi^2 = 258$. This value of χ^2, with 314 degrees of freedom, indicates a good fit; the probability of $\chi^2 \leq 258$ occurring by chance is 0.99. We conclude that a straight line fits the data well and a more complicated curve is not justified. A Student's t test indicates that the derived slope of 2.28 nT/year differs significantly from the post-1840 average of 15 nT/year with better than 99.999% confidence. This result is vulnerable to small systematic errors in the paleointensity data; they would need to be systematically slightly low in early times to account for the small slope. We find no reason for such a systematic error nor any systematic correlation with experimental procedure, author, or geographical site. Our result

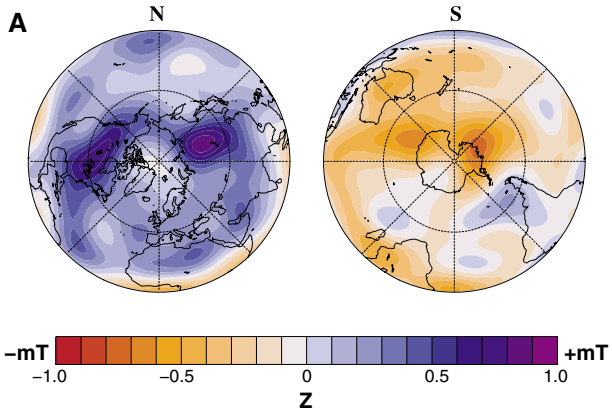

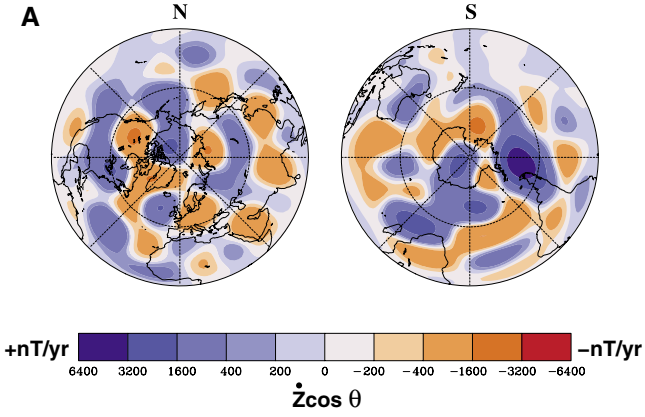

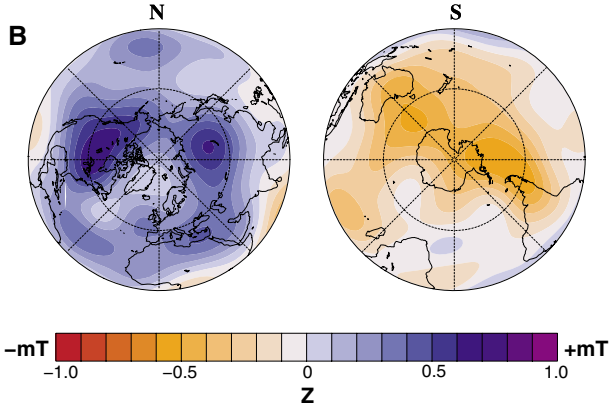

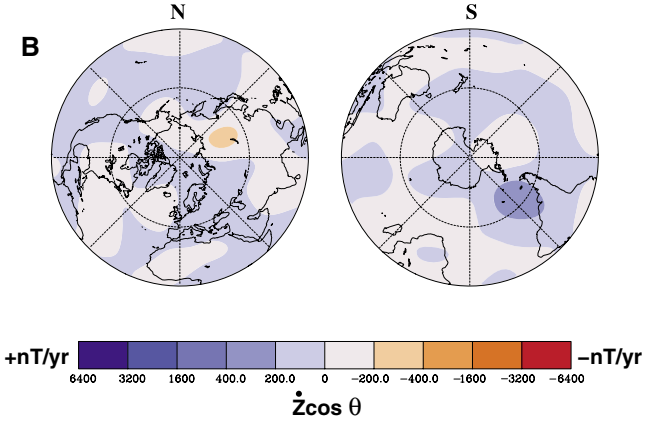

Fig. 4. (**left**). Vertical component of magnetic field Z on the core-mantle boundary in Lambert equal-area projection averaged over the interval 1840 to 1980 (**A**) and 1590 to 1840 (**B**). The general dipolar structure is reflected in the dominance of blue (inward flux) in the Northern Hemisphere (left) and orange (outward flux) in the Southern Hemisphere (right). Reverse-flux patches show up as blue in the Southern Hemisphere in 1980; these have been growing and moving south in recent decades and are the major contributor to the present fall in dipole moment. They are largely absent from the 1780 map and are not seen in earlier times. **Fig. 5.** (**right**). Contributions to the changing dipole moment over the interval 1840 to 1980 (**A**) and 1590 to 1840 (**B**). Shown is $\dot{Z}\cos\theta$, where $\dot{Z}$ is the secular variation of the vertical component of magnetic field at the core-mantle boundary and θ is the colatitude, in Lambert equal-area projection, averaged over each time interval. The fall in dipole moment over the period is given by the integral over both hemispheres (Eq. 1). The predominance of blue in the Southern Hemisphere from 1840 to 1980 [(A), right], associated with the growth and southward movement of reverse-flux patches, is responsible for almost all of the fall in dipole moment during this period.

is consistent with Korte and Constable's low-resolution geomagnetic field model CALS7K.2 (*6*, *7*), which has a slower decay of the dipole moment from 1600 to 1800 A.D. compared with that from 1800 to 1950 A.D. Their model, which spans the interval 5000 B.C. to 1950 A.D., was constructed from paleointensity and paleodirection data only (*2*, *6*) and therefore lacks information from the vastly more accurate historical measurements included in the present study.

What changed to precipitate the present fall in dipole moment? More insight comes from directional data, which are excellent from 1700 A.D. and suggest a change occurring around 1800 A.D. The geomagnetic field originates in the liquid core, and its dipole moment may be written as an average of the magnetic field at the core surface

$$g_1^0 = \frac{3c}{8\pi a^3}\int_S Z\cos\theta dS \qquad (1)$$

where Z is the downward component of magnetic field; θ is colatitude; a and c are Earth and core radii, respectively; and the integral is taken over the surface S of the liquid core. The source of any change in dipole moment can therefore be found from the change in $Z\cos\theta$ on the core surface, which comes mostly from growth and southward migration of patches of reversed flux in the Southern Hemisphere (Fig. 4). No intensity information is required to identify these reverse-flux patches; they are imaged well by the early directional data. One distinct patch first appeared in about 1780 A.D. (*8*) and continues to grow and drift south today (*8*, *9*).

An equal-area plot of $\dot{Z}\cos\theta$ reveals the regions on the core surface responsible for the fall (Fig. 5). The interval 1840 to 1980 (Fig. 5A) is dominated by the blue patch between Antarctica and the tip of South America, with additional contributions from other blue patches in the Southern Hemisphere. Orange and blue patches in the Northern Hemisphere are of similar size and cancel out. The separate contributions of the two hemispheres to the change in g_1^0 is $(\dot{g}_N, \dot{g}_S, \dot{g}_1^0) = (-0.1, 16.2, 16.1)$ nT/year, showing that almost all of the dipole decay has come from the Southern Hemisphere.

The interval 1590 to 1840 A.D. (Fig. 5B), which uses the mean fall in g_1^0 of 2.28 nT/year obtained in this study, shows much smaller amplitudes, and the patch between Antarctica and South America is almost balanced by the patches of opposite sign to the west, indicating longitudinal drift rather than southward movement or growth. The separate contributions of the integral for this interval are $(\dot{g}_N, \dot{g}_S, \dot{g}_1^0) = (-0.8, 3.1, 2.3)$; the Northern Hemisphere value is again effectively zero, but the Southern Hemisphere value is much lower than in the 19th and 20th centuries. This is consistent with a change in Southern Hemisphere behavior starting around 1800 A.D.; before that date the two hemispheres behaved in a similar manner.

Paleomagnetic data from the past 2500 years suggest a 40% fall in moment (*6*, *10*), or 1.6% per century. This is smaller than the present fall (5% per century) and is consistent with periods of rapid fall, as at present, interspersed with periods of little or no activity, as during 1590 to 1840 A.D. Patches of reverse flux almost certainly arise from expulsion of toroidal flux (*11*), and our present result suggests a quiet period up to 1800 when toroidal flux was brought up close to the core surface followed by active periods of expulsion through the core surface. The challenge now is to understand the magnetohydrodynamics of how such behavior can come about and to discover similar, earlier intervals of dipole decay interspersed with quiescence in the paleomagnetic record.

References and Notes

1. A. Jackson, A. R. T. Jonkers, M. R. Walker, *Philos. Trans. R. Soc. London A* **358**, 957 (2000).
2. M. Korte, A. Genevey, C. G. Constable, U. Frank, E. Schnepp, *Geochem. Geophys. Geosyst.* 10.1029/2004GC000800 (1 February 2005).
3. G. Hulot, A. Khokhlov, J. L. LeMouel, *Geophys. J. Int.* **129**, 347 (1997).
4. J. H. Williamson, *Can. J. Phys.* **46**, 1846 (1968).
5. W. H. Press, B. P. Flannery, S. A. Teukolsky, W. T. Vetterling, *Numerical Recipes in FORTRAN* (Cambridge Univ. Press, Cambridge, UK, 2002).
6. M. Korte, C. G. Constable, *Geochem. Geophys. Geosyst.* 10.1029/2004GC000801 (1 February 2005).
7. M. Korte, C. G. Constable, *Earth Planet. Sci. Lett.* **236**, 348 (2005).
8. J. Bloxham, D. Gubbins, A. Jackson, *Philos. Trans. R. Soc. London* **329**, 415 (1989).
9. G. Hulot, C. Eymin, B. Langlais, M. Mandea, N. Olsen, *Nature* **416**, 620 (2002).
10. M. W. McElhinny, W. E. Senanayake, *J. Geomagn. Geoelectr.* **34**, 39 (1980).
11. D. Gubbins, *Phys. Earth Planet. Int.* **98**, 193 (1996).

12. This work formed part of A.L.J.'s undergraduate project, which was supported by a Local Education Authority grant. C.C.F. was supported by a Ph.D. studentship from the Natural Environment Research Council (NER/S/A/2001/06265).

11 January 2006; accepted 14 March 2006
10.1126/science.1124855

Impaired Control of IRES-Mediated Translation in X-Linked Dyskeratosis Congenita

Andrew Yoon,[1]* Guang Peng,[1]* Yves Brandenburg,[1]* Ornella Zollo,[1] Wei Xu,[1] Eduardo Rego,[2] Davide Ruggero[1]†

The *DKC1* gene encodes a pseudouridine synthase that modifies ribosomal RNA (rRNA). *DKC1* is mutated in people with X-linked dyskeratosis congenita (X-DC), a disease characterized by bone marrow failure, skin abnormalities, and increased susceptibility to cancer. How alterations in ribosome modification might lead to cancer and other features of the disease remains unknown. Using an unbiased proteomics strategy, we discovered a specific defect in IRES (internal ribosome entry site)–dependent translation in *Dkc1^m* mice and in cells from X-DC patients. This defect results in impaired translation of messenger RNAs containing IRES elements, including those encoding the tumor suppressor p27(Kip1) and the antiapoptotic factors Bcl-xL and XIAP (X-linked Inhibitor of Apoptosis Protein). Moreover, *Dkc1^m* ribosomes were unable to direct translation from IRES elements present in viral messenger RNAs. These findings reveal a potential mechanism by which defective ribosome activity leads to disease and cancer.

X-linked dyskeratosis congenita (X-DC) is a rare and often fatal disease characterized by multiple pathological features, including bone marrow failure and increased susceptibility to cancer (*1*). X-DC is caused by mutations in the *DKC1* gene that encodes dyskerin, a protein associated with small RNAs that share the H+ACA RNA motif, including the telomerase RNA (TR), Cajal body RNAs (scaRNAs), and small nucleolar RNAs (snoRNAs) (*2*). When associated with snoRNAs, dyskerin acts as a pseudouridine synthase to mediate posttranscriptional modification of ribosomal RNA (rRNA) through the conversion of uridine (U) to pseudouridine (Ψ) (*3*, *4*). X-DC patient cell lines and mouse embryonic stem cells harboring knocked-in *DKC1* point mutations exhibit reduced rRNA pseudouridylation (*2*, *5*). Hypomorphic *Dkc1^m* mice recapitulate many of the clinical features of X-DC and display reductions in rRNA modification, suggesting that impairments in ribosome function may have a causative effect on X-DC pathogenesis (*6*). However, the role of rRNA modifications in the control of protein synthesis remains poorly understood. In addition, how alterations in the translational apparatus could lead to specific pathological features associated with human disease remains unknown. We investigated the role of rRNA modifications in the control of protein synthesis in order to understand the molecular basis of X-DC.

[1]Human Genetics Program, Fox Chase Cancer Center, Philadelphia, PA 19111, USA. [2]Center for Cell Based Therapy, Fundação Hemocentro de Ribeirão Preto, University of Sao Paulo, Brazil.

*These authors contributed equally to this work.

†To whom correspondence should be addressed. E-mail: davide.ruggero@fccc.edu

We first determined whether decreased rRNA pseudouridylation results in impaired general (cap-dependent) translation, using *Dkc1*^{m} mice. Total protein synthesis rates were no different in primary *Dkc1*^{m} cells than in wild-type cells (fig. S1), and therefore decreased rRNA pseudouridylation in *Dkc1*^{m} ribosomes does not impair general protein synthesis. We next hypothesized that the reduction of modified uridine residues in *Dkc1*^{m} ribosomes might affect the translation of specific mRNAs and hence may not be readily evident when monitoring for general cap-dependent protein synthesis. We therefore established an unbiased proteomics protocol to screen for candidate mRNAs that rely on *Dkc1*-dependent rRNA modifications for efficient protein translation. In particular, we optimized a glycerol gradient (*7*) to purify mRNAs associated with translationally active ribosomes (polysomes) from steady-state and activated primary splenic lymphocytes, one of the hematopoietic lineages affected in X-DC (Fig. 1A). Purified polysome-associated mRNAs from wild-type and *Dkc1*^{m} lymphocytes, before disease onset, were used to hybridize two commercially available mouse cDNA microarrays (*7*). These microarrays contained in total 1500 spotted cDNAs with a wide variety of biological functions, including cell signaling, cell differentiation, control of the cell cycle and apoptosis, or genes implicated in cancer initiation (*8*–*10*). Using this protocol, we identified 3 out of 1500 mRNAs that were specifically decreased in polysome association in *Dkc1*^{m} lymphocytes. In particular, the p27 tumor suppressor and the antiapoptotic proteins XIAP (X-linked Inhibitor of Apoptosis Protein) and Bcl-xL showed a significant decrease (25% or greater) in their association with polysomes in *Dkc1*^{m} cells as compared to wild-type cells. To validate the microarray results, translational control of p27, XIAP, and Bcl-xL mRNAs was monitored in *Dkc1*^{m} cells (Fig. 1, B and C). Protein levels of these target mRNAs were significantly down-regulated in *Dkc1*^{m} lymphocytes (Fig. 1, B and C), whereas no differences were apparent in mRNA transcript levels or protein stability (figs. S2 and S3). In addition, mRNAs showing less than a 25% decrease in polysome association did not reveal differences in gene expression (fig. S2). Altogether, these data reveal defects in the translation of specific mRNAs in *Dkc1*^{m} cells.

Having determined that general protein synthesis is unaffected in *Dkc1*^{m} cells, we hypothesized that a cap-independent mechanism relying on dyskerin activity may account for differences in the translation of these mRNAs. Two of the mRNAs identified in our screen, p27(Kip1) and XIAP, share a common feature in their mode of translation initiation, because they both harbor an internal ribosome entry site (IRES) element, previously shown to be important for their accurate expression (*11*–*13*). IRES elements, which are present within a subset of cellular mRNAs, are structured RNAs of variable length that bind the ribosome during translation initiation, thereby bypassing the requirement for some of the cap-binding proteins (*14*). Although IRES elements are active in normal growth conditions, IRES-dependent translation is favored during specific cellular stimuli such as the induction of programmed cell death or during distinct phases of the cell cycle, when cap-dependent translation is decreased (*15*). We therefore tested whether decreased XIAP and p27 protein expression in *Dkc1*^{m} cells was due to a defect in IRES-dependent translation. We initially analyzed endogenous levels of XIAP and p27 proteins under conditions in which IRES-mediated translation is stimulated, using mouse embryonic fibroblasts (MEFs). We examined XIAP protein levels when the MEFs were exposed to γ irradiation, a stimulus that specifically increases IRES-dependent translation of this antiapoptotic factor, thereby providing a survival advantage to the cell (*15*). A 50% increase in XIAP protein levels was evident in wild-type MEFs after this stimulus, whereas no induction was evident in *Dkc1*^{m} cells (Fig. 2A and fig. S3, C and D). We next examined the translation of the p27 mRNA during the G_0/G_1 phase of the cell cycle, which has been shown to be increased through its IRES element (*12*, *13*, *16*). Levels of p27 protein were up-regulated by 55% in wild-type cells but this induction was markedly reduced in *Dkc1*^{m} cells (Fig. 2B and fig. S3, A and B). Therefore, the translation of p27 and XIAP mRNAs in *Dkc1*^{m} MEFs is greatly impaired after specific cellular stimuli that affect endogenous IRES-dependent translation.

We next tested whether *Dkc1*^{m} ribosomes could promote the translation of a reporter mRNA directed by the XIAP and p27 IRES elements. To this end, we used the well-established bicistronic expression system to detect IRES activity (*17*, *18*), in which the first cistron is translated by a cap-dependent initiation mechanism and the second is translated by the preceding IRES element (Fig. 2, C and D). IRES-dependent translation of p27 and XIAP mRNAs has been documented with the use of this bicistronic assay (*11*, *13*, *19*). We confirmed IRES-dependent activity of these mRNAs in the primary cells used in our studies and by employing previously reported mutated IRES sequences (fig. S6). To analyze IRES function, we transfected bicistronic reporter mRNAs in wild-type and *Dkc1*^{m} MEFs and used specific stimuli that favor IRES-dependent translation (Fig. 2, C and D, and figs. S4, A to

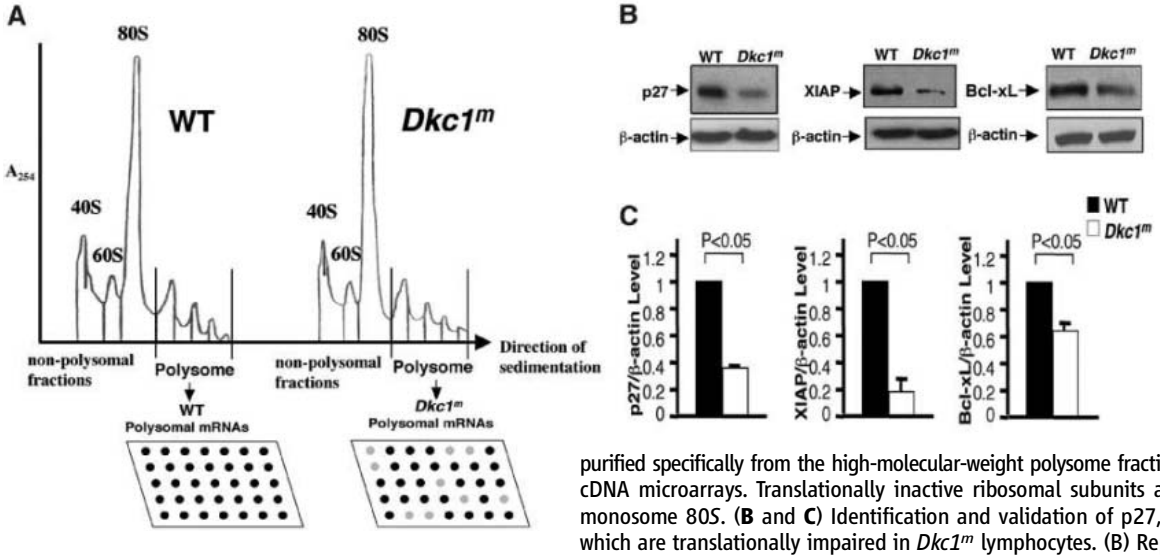

Fig. 1. An unbiased proteomics approach reveals specific translational impairments in *Dkc1*^{m} mice. (**A**) Polyribosomal profiles of wild-type (WT) and *Dkc1*^{m} cytoplasmic extracts from lipopolysaccharide-stimulated primary splenic lymphocytes fractionated on 10 to 50% glycerol gradients. The *y* axis represents the absorbance at 254 nm (A_{254}), and the *x* axis indicates fractions collected. RNA was purified specifically from the high-molecular-weight polysome fractions and used to hybridize cDNA microarrays. Translationally inactive ribosomal subunits are shown: 40*S*, 60*S*, and monosome 80*S*. (**B** and **C**) Identification and validation of p27, XIAP, and Bcl-xL mRNAs, which are translationally impaired in *Dkc1*^{m} lymphocytes. (B) Representative Western blots for p27, XIAP, and Bcl-xL in wild-type and *Dkc1*^{m} lymphocytes. (C) Densitometry analyses of p27, XIAP, and Bcl-xL values normalized against β-actin are shown as graphs. Each value represents the mean ± SD of three independent experiments, and statistical significance is indicated.

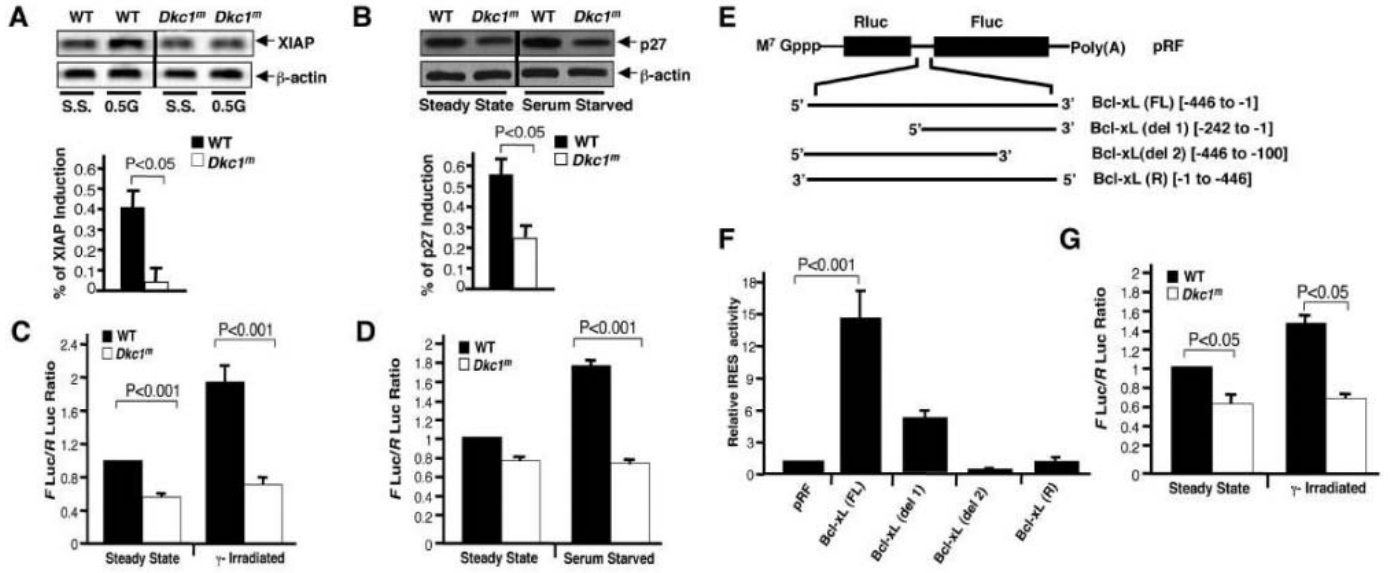

Fig. 2. Impaired IRES-dependent translation of specific cellular mRNAs identified in the proteomics screen in *Dkc1*^{m} mice. (**A**) Representative Western blot of XIAP in the steady state (S.S.) and after γ irradiation (with 0.5 Gy). Induction of XIAP expression (%) is impaired in *Dkc1*^{m} MEFs after γ irradiation. A densitometry analysis after induction (mean ± SEM) from at least three independent experiments is shown. (**B**) Representative Western blot of p27 in the steady state and after serum starvation (in 0.1% fetal bovine serum for 16 hours). Induction of p27 expression (%) is impaired in *Dkc1*^{m} MEFs after serum starvation. A densitometry analysis after induction (mean ± SEM) from at least three independent experiments is shown. (**C**) Wild-type and *Dkc1*^{m} MEFs transfected with the XIAP bicistronic reporter mRNA. The ratio of firefly luciferase to Renilla luciferase (F_{luc}/R_{luc}) (IRES/cap) activity was analyzed in the steady state or after γ irradiation (with 0.5 Gy). Each value is relative to the wild-type F_{luc}/R_{luc} ratio in the steady state, which was set to 1 and represents the mean ± SD of three independent experiments performed in triplicate. Statistical significance is indicated. (**D**) Wild-type and *Dkc1*^{m} MEFs transfected with the p27 bicistronic reporter mRNA. The ratio of F_{luc}/R_{luc} activity was analyzed in the steady state or after serum starvation. Each value is relative to the wild-type F_{luc}/R_{luc} ratio in the steady state, which was set to 1 and represents the mean ± SD of three independent experiments performed in triplicate. (**E**) Schematic diagram of the full-length (FL) Bcl-xL 5′ UTR in the reverse orientation (R) and two deletions (del 1 and del 2) used in bicistronic assays. M^{7} Gppp, 7-Methylguanasine; pRF, bicistronic reporter plasmid. (**F**) MEFs were transfected with the indicated plasmids. The F_{luc}/R_{luc} ratio was calculated, and the expression of the pRF empty vector was set as 1. Each value represents the mean ± SD of three independent experiments in triplicate. IRES-dependent translation is still retained when only 250 nucleotides of the 5′ UTR are used (Bcl-xL del1), but its activity is 35% that of the full-length UTR. The Bcl-xL (del 2) mutant indicates that an important functional domain resides with the first 100 nucleotides of the Bcl-xL IRES. (**G**) Wild-type and *Dkc1*^{m} MEFs transfected with the Bcl-xL bicistronic reporter mRNA. The ratio of F_{luc}/R_{luc} activity was analyzed in the steady state or after γ irradiation (with 0.5 Gy). Each value is relative to the wild-type F_{luc}/R_{luc} ratio in the steady state, which was set to 1 and represents the mean ± SD of three independent experiments performed in triplicate.

D and S5, A and B). At first, we confirmed that both wild-type and *Dkc1*^{m} cells responded equally to these stress stimuli (fig. S4). IRES-dependent translation of XIAP and p27 was specifically affected in *Dkc1*^{m} cells, and IRES-mediated translational induction of these mRNAs by γ irradiation and serum starvation was reduced (Fig. 2, C and D). Therefore, the translation impairment of XIAP and p27 mRNAs in *Dkc1*^{m} cells is at the level of IRES-dependent translation.

Because Bcl-xL was the third mRNA identified in our proteomics screen, we next determined the molecular mechanisms for its translational impairment in *Dkc1*^{m} cells (Fig. 1B). Although Bcl-xL had not previously been reported to contain an IRES element, we tested whether the Bcl-xL 5′ untranslated region (UTR) possesses IRES activity when cloned in a bicistronic vector. These experiments revealed that Bcl-xL contained a functional IRES that could direct the translation of a second cistron and that IRES-dependent translation was abolished when the Bcl-xL 5′ UTR was cloned in a reverse orientation or when deletion mutants were used (Fig. 2, E and F). These findings indicated that a functional IRES element is present –446 to –1 nucleotides upstream of the initiation codon and that IRES-dependent translation is still retained when only 250 nucleotides of the 5′ UTR are used (Bcl-xL del1), but its activity is 35% that of the full-length UTR. We ruled out the presence of cryptic promoters in the Bcl-xL 5′ UTR sequence because RNA transfection of the bicistronic vector retains IRES activity (Fig. 2G), and we confirmed the integrity of the transfected vectors (fig. S5, D and E). Thus, the unbiased proteomics approach identified a cellular mRNA harboring an IRES element in its 5′ UTR, affected in *Dkc1*^{m} cells. We confirmed that the defect in Bcl-xL translation was at the level of IRES-dependent translation, because Bcl-xL IRES activity in bicistronic assays was impaired in *Dkc1*^{m} cells as compared to wild-type cells (Fig. 2G). Moreover, the ratio of Bcl-xL IRES/cap activity was increased after γ irradiation in wild-type cells, whereas this was reduced in *Dkc1*^{m} cells. Taken together, these data demonstrate that *Dkc1*^{m} cells are impaired in promoting the translation of a subset of mRNAs that share a common mode of translation initiation, directed by an IRES element.

To determine the relative contribution of impaired IRES-dependent translation to X-DC pathogenesis, we undertook a direct genetic approach with one of the target mRNAs affected in *Dkc1*^{m} cells. The tumor suppressor p27 is a Cdk inhibitory protein that coordinates accurate cell-cycle progression. Haploinsufficiency in p27 expression results in susceptibility to cancer, and *p27*$^{+/-}$ mice are tumor-prone upon oncogenic challenge, without biallelic inactivation due to loss of heterozygosity (*20*, *21*). We reasoned that reduced p27 translation in *Dkc1*^{m} mice might contribute to the tumor-prone phenotype of these animals (*6*). We therefore tested for a genetic interaction between *Dkc1* and *p27* and focused our analysis on the cell-cycle status of thymocytes, the predominant cell type that shows increased proliferation in *p27*$^{-/-}$ mice (*22*–*24*). Neither *p27*$^{+/-}$ nor *Dkc1*^{m} thymocytes showed differences in cell proliferation as compared to wild-type mice. Thymocytes from *Dkc1*^{m};*p27*$^{+/-}$ mice displayed a marked increase in S phase progression, similar

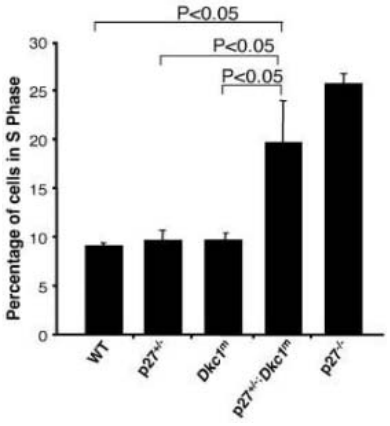

Fig. 3. *Dkc1* cooperates genetically with p27 in cell-cycle control. The cell cycle of thymocytes from indicated genotypes (8 weeks old) was analyzed by flow cytometry after propidium iodide staining. Each bar represents the mean ± SD from six mice. *P* values are indicated.

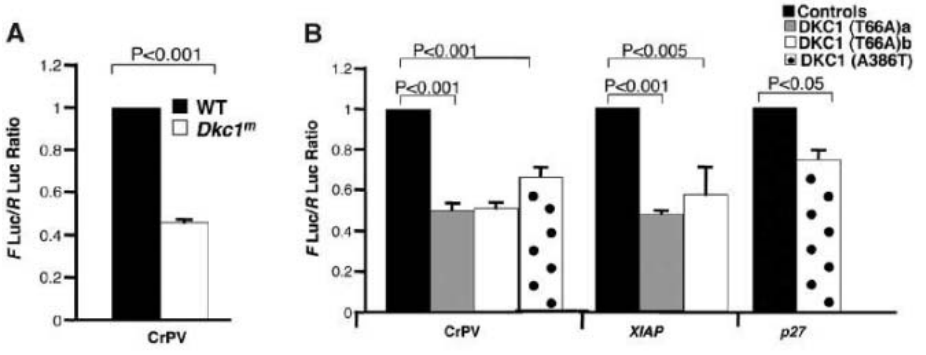

Fig. 4. Molecular role of dyskerin in IRES-dependent translation in X-DC. (**A**) Wild-type and *Dkc1m* MEFs transfected with CrPV bicistronic vector in mRNA form. Each value is relative to the wild-type F_{luc}/R_{luc} ratio, which was set to 1 and represents the mean ± SD of three independent experiments performed in triplicate. (**B**) Human X-DC B-lymphoblast and fibroblast cell lines electroporated with the bicistronic vector mRNAs as indicated. Each value is relative to the control steady state, which was set to 1 and represents the mean ± SD of three independent experiments performed in triplicate. Statistical significance is indicated. The lymphoblast cells lines were derived from two affected brothers with X-DC [DKC1 (T66A)a (DKC1a) and DKC1 (T66A)b (DKC1b)]. As controls, both a normal lymphoblast cell line derived from the unaffected carrier mother as well as two other normal lymphoblast cell lines were used (*7*). The *DKC1* mutant fibroblast cell line [DKC1 (A386T)] was, in turn, compared to three normal human fibroblast lines. All normal and/or carrier cell lines indicated as controls displayed similar values of F_{luc} IRES-mediated translation, which were averaged and set to 1. Each value represents the mean ± SD of three independent experiments performed in triplicate.

to $p27^{-/-}$ cells (Fig. 3). Thus, these findings suggest that reductions in p27 IRES-dependent translation may render *Dkc1m* mice tumor-prone, which is consistent with the cancer susceptibility phenotype manifested in X-DC pathogenesis.

To gain additional insight into the molecular mechanisms by which reductions in rRNA modifications affect IRES-dependent translation, we next investigated whether *Dkc1m* ribosomes are intrinsically impaired in their ability to translate IRES-dependent viral mRNAs via an IRES-dependent mechanism. Many viruses do not possess capped mRNAs and require IRES elements to promote translation initiation. Moreover, the translation of certain viral mRNAs occurs independently of some or all eukaryotic initiation factors (eIFs) of translation employed in cap-dependent translation (*14*). For example, the cricket paralysis virus (CrPV) IRES directly recruits the ribosome on an initiation codon without any canonical eIFs (*25*). It has previously been shown that CrPV IRES is active in mammalian cells, and we confirmed those findings in the primary cells used in our studies and by employing previously published CrPV IRES mutants (*25*–*27*) (fig. S6). To test whether the defect in IRES-dependent translation in *Dkc1m* cells resides in the ribosome, we used the CrPV IRES as a molecular tool. To this end, we transfected a bicistronic reporter mRNA in which the translation of F_{luc} is driven by the CrPV IRES element (Fig. 4A and fig. S5C). The translation of the CrPV IRES was severely impaired in *Dkc1m* cells (Fig. 4A), strongly suggesting that impairments in IRES-dependent translation in *Dkc1m* cells are attributable to an intrinsic defect in *Dkc1m* ribosomes.

We further investigated whether point mutations in the *DKC1* gene, present in X-DC patients, would result in the same translational defects as in hypomorphic *Dkc1m* mice. At first, we analyzed the efficiency of CrPV IRES translation, which relies solely on ribosomal subunits to initiate translation in human X-DC lymphoblasts and fibroblast cell lines (*7*). We observed a specific decrease in CrPV IRES activity in human X-DC patient cells as compared to normal controls (Fig. 4B). We next tested whether translational impairments of particular cellular IRES mRNAs, identified in our proteomics screen, were also evident in X-DC patient cells. A marked decrease in XIAP and p27 IRES-dependent translation was evident (Fig. 4B). Therefore, human X-DC patient cells show a specific defect in IRES-dependent translation. Moreover, mRNAs identified by an unbiased proteomics protocol in *Dkc1m* cells also show a translational impairment in X-DC human cells, thereby representing the first target genes for X-DC pathogenesis.

The full inactivation of *Dkc1* results in a lethal phenotype in yeast, fly, and mouse, supporting the notion that the complete loss of pseudouridine modifications in rRNA may not be compatible with life (*2*). How then could reductions in the activity of a housekeeping gene required for ribosome modification lead to a complex phenotype associated with X-DC disease? In this study, we addressed this question using an unbiased proteomics approach to uncover translational defects in primary cells derived from hypomorphic *Dkc1m* mice, which faithfully recapitulate X-DC pathogenesis (*6*). Our findings indicate that the activity of IRES elements, which regulate the translation of a subset of mRNAs, is affected in *Dkc1m* cells and X-DC human patient cells, thereby providing a molecular mechanism through which decreased rRNA modifications may result in specific phenotypic consequences. In this respect, our proteomics screen has identified two important cellular mRNAs previously shown to possess an IRES element: the tumor suppressor p27 and the antiapoptotic factor XIAP, which are translationally impaired in *Dkc1m* mice and X-DC human patient cells. In addition, this screen led to the unbiased identification of a previously uncharacterized IRES element present in the antiapoptotic factor Bcl-xL, and IRES-dependent translation of this mRNA was defective in *Dkc1m* cells. The deregulated IRES-dependent translation of mRNAs identified in our screen may account for two specific pathological features of X-DC: susceptibility to cancer and bone marrow failure. Because decreases in p27 protein expression are sufficient to result in tumor susceptibility (*20*), reductions in p27 IRES-dependent translation in *Dkc1m* mice and X-DC patient samples is likely to account, at least in part, for the cancer susceptibility phenotype present in X-DC. To this end, we have demonstrated a genetic interaction between *Dkc1* and p27 required for restricted cell-cycle progression. In addition, bone marrow failure, a hallmark of X-DC pathogenesis, is characterized by increased apoptosis of hematopoietic progenitors and stem cells (*28*). Many antiapoptotic factors possess an IRES element in their 5′ UTRs, which promotes translation during stress conditions, thereby providing a survival advantage to the cell (*15*). Therefore, it is tempting to speculate that a combinatorial defect in IRES translation of antiapoptotic factors such as XIAP and Bcl-xL may underlie the bone marrow phenotype in X-DC. Bcl-xL chimeric embryos display increased cell death of hematopoitic progenitors associated with anemia and lymphopenia (*29*, *30*), which are hallmarks of X-DC pathogenesis.

The fact that translation initiation directed from CrPV IRES, which relies solely on the ribosome itself, is severely impaired in *Dkc1*^{m} cells strongly implies that the molecular defect intrinsically resides in the inability of *Dkc1*^{m} ribosomes to efficiently engage the IRES element. Taken together, these findings allow us to propose a model whereby reductions in rRNA modifications due to dyskerin malfunction affect the translation of important cellular IRES mRNAs, which may require more direct interactions with the ribosome for translation initiation, thereby contributing to specific pathological features of X-DC. Although we cannot determine how defects in other cellular functions attributed to dyskerin activity may contribute to X-DC, these findings indicate a previously unknown molecular mechanism by which impairments in rRNA modifications affect translation control and lead to disease pathogenesis.

References and Notes

1. I. Dokal, *Br. J. Haematol.* **110**, 768 (2000).
2. U. T. Meier, *Chromosoma* **114**, 1 (2005).
3. J. Ni, A. L. Tien, M. J. Fournier, *Cell* **89**, 565 (1997).
4. C. Wang, C. C. Query, U. T. Meier, *Mol. Cell. Biol.* **22**, 8457 (2002).
5. Y. Mochizuki, J. He, S. Kulkarni, M. Bessler, P. J. Mason, *Proc. Natl. Acad. Sci. U.S.A.* **101**, 10756 (2004).
6. D. Ruggero *et al.*, *Science* **299**, 259 (2003).
7. Materials and methods are available as supporting material on *Science* Online.
8. N. A. Gasper, C. C. Petty, L. W. Schrum, I. Marriott, K. L. Bost, *Infect. Immun.* **70**, 4075 (2002).
9. V. Sharma, M. Delgado, D. Ganea, *J. Immunol.* **176**, 97 (2006).
10. A. J. Stauber *et al.*, *Mol. Pharmacol.* **67**, 681 (2005).
11. M. Holcik, C. Lefebvre, C. Yeh, T. Chow, R. G. Korneluk, *Nat. Cell Biol.* **1**, 190 (1999).
12. W. K. Miskimins, G. Wang, M. Hawkinson, R. Miskimins, *Mol. Cell. Biol.* **21**, 4960 (2001).
13. M. Kullmann, U. Gopfert, B. Siewe, L. Hengst, *Genes Dev.* **16**, 3087 (2002).
14. C. U. Hellen, P. Sarnow, *Genes Dev.* **15**, 1593 (2001).
15. M. Holcik, N. Sonenberg, *Nat. Rev. Mol. Cell Biol.* **6**, 318 (2005).
16. S. S. Millard *et al.*, *J. Biol. Chem.* **272**, 7093 (1997).
17. J. Pelletier, N. Sonenberg, *J. Virol.* **63**, 441 (1989).
18. M. Stoneley, F. E. Paulin, J. P. Le Quesne, S. A. Chappell, A. E. Willis, *Oncogene* **16**, 423 (1998).
19. S. Cho, J. H. Kim, S. H. Back, S. K. Jang, *Mol. Cell. Biol.* **25**, 1283 (2005).
20. M. L. Fero, E. Randel, K. E. Gurley, J. M. Roberts, C. J. Kemp, *Nature* **396**, 177 (1998).
21. J. Philipp-Staheli, S. R. Payne, C. J. Kemp, *Exp. Cell Res.* **264**, 148 (2001).
22. M. L. Fero *et al.*, *Cell* **85**, 733 (1996).
23. H. Kiyokawa *et al.*, *Cell* **85**, 721 (1996).
24. K. Nakayama *et al.*, *Cell* **85**, 707 (1996).
25. J. E. Wilson, T. V. Pestova, C. U. Hellen, P. Sarnow, *Cell* **102**, 511 (2000).
26. E. Jan, P. Sarnow, *J. Mol. Biol.* **324**, 889 (2002).
27. C. P. Petersen, M. E. Bordeleau, J. Pelletier, P. A. Sharp, *Mol. Cell* **21**, 533 (2006).
28. I. Dokal, *Curr. Opin. Hematol.* **3**, 453 (1996).
29. N. Motoyama *et al.*, *Science* **267**, 1506 (1995).
30. M. Socolovsky, A. E. Fallon, S. Wang, C. Brugnara, H. F. Lodish, *Cell* **98**, 181 (1999).

31. We are indebted to M. Barna for helpful discussions and critical reading of the manuscript. We thank A. Koff for the p27$^{-/-}$ mice; M. Holcik, L. Hengst, and P. Sarnow for reagents; K. Zaret, J. Burch, E. Golemis, and J. Testa for critical reading of the manuscript; and FCCC core facilities and J. Grant for technical assistance.

Supporting Online Material

www.sciencemag.org/cgi/content/full/312/5775/902/DC1
Materials and Methods
Figs. S1 to S6

14 December 2005; accepted 13 April 2006
10.1126/science.1123835

RNA Recognition and Cleavage by a Splicing Endonuclease

Song Xue, Kate Calvin, Hong Li*

The RNA splicing endonuclease cleaves two phosphodiester bonds within folded precursor RNAs during intron removal, producing the functional RNAs required for protein synthesis. Here we describe at a resolution of 2.85 angstroms the structure of a splicing endonuclease from *Archaeglobus fulgidus* bound with a bulge-helix-bulge RNA containing a noncleaved and a cleaved splice site. The endonuclease dimer cooperatively recognized a flipped-out bulge base and stabilizes sharply bent bulge backbones that are poised for an in-line RNA cleavage reaction. Cooperativity arises because an arginine pair from one catalytic domain sandwiches a nucleobase within the bulge cleaved by the other catalytic domain.

The removal of intervening sequences in functional RNAs is required in all domains of life. Introns found in nuclear tRNA and archaeal RNA are removed by protein enzymes—an endonuclease, a ligase, and, in some organisms, a 2′-phosphotransferase (*1*–*5*).

Critical to this splicing mechanism are the recognition of the intron-exon junctions and the subsequent breakage of the two phosphodiester bonds. This process is mediated by the endonuclease. The splicing endonucleases characterized so far belong to one of four families: homodimers (α_2) (*6*), homotetramers (α_4) (*7*), homodimers of two heterodimers ($\alpha_2\beta_2$) (*8*, *9*), or heterotetramers ($\alpha\beta\delta\gamma$) (*10*–*12*). Despite the differences in subunit composition, all splicing endonucleases comprise two conserved catalytic units and two structural units that play roles in correctly orienting the catalytic sites (*13*).

All splicing endonucleases recognize the bulge-helix-bulge (BHB) motif that is composed of two three-nucleotide bulges separated by 4 base pairs (bp) (*6*, *8*, *9*, *14*–*16*). Each bulge contains a cleavage site immediately after the second bulge nucleotide. In addition to the recognition of the canonical BHB RNA motif, splicing endonucleases of different families exhibit distinct substrate recognition properties. The localized structural fold of the BHB motif is sufficient for the removal of archaeal introns from various segments of precursor transfer RNA (tRNA), ribosomal RNA (rRNA), and some mRNA; the secondary structure of the BHB motif is solely responsible for its recognition by the archaeal splicing endonuclease (*17*–*20*). Nuclear precursor tRNAs, however, have additional recognition elements in their mature domains that are required for splicing (*16*, *21*–*23*). The eukaryal $\alpha\beta\delta\gamma$ splicing endonuclease is composed of Sen2, Sen34, Sen54, and Sen15 subunits and locates the splice sites via a "ruler mechanism." This mechanism requires the specific recognition of two features in precursor tRNAs: the cloverleaf structure of the mature domain (*21*, *24*) and an anticodon-intron base pair (A-I pair) adjacent to the 3′ bulge (*22*, *23*). It has been proposed that the eukaryal endonuclease, while maintaining the ability to recognize the minimal BHB RNA, has acquired additional RNA recognition properties.

Based on the cleavage products and conserved catalytic residues, all splicing endonucleases appear to use a similar mechanism. Cleavage by the splicing endonuclease generates 5′-hydroxyl and 2′,3′-cyclic phosphate termini (*1*, *2*, *25*). These products suggest an S_N2-type in-line attack by the nearby 2′-hydroxyl on phosphorus and a trigonal bipyramidal transition state, similar to that used by the RNase A family of ribonucleases (*26*). In previously determined archaeal-splicing endonuclease structures, three invariant residues—a histidine, a lysine, and a tyrosine—form a closely spaced triad. In the *Methanococcus jannaschii* endonuclease structure, a bound sulfate ion, which was proposed to mimic a phosphate, was found in the center of the triad (*27*), which further implicates the triad in RNA cleavage. However, there is no structural evidence to confirm the catalytic roles of each of the triad residues, and the catalytic mechanism of the splicing endonuclease remains elusive.

We have determined the cocrystal structure of a dimeric splicing endonuclease from *Archaeglobus fulgidus* (AF) bound to a BHB RNA that was formed from two annealed 21-oligomer synthetic oligonucleotide (see Fig. 1A). One strand of the RNA contains a 2′-deoxy–

Department of Chemistry and Biochemistry, Institute of Molecular Biophysics, Florida State University, Tallahassee, FL 32306, USA.

*To whom correspondence should be addressed. E-mail: hongli@sb.fsu.edu

modified uridine at position 14 (dU14) to prevent its cleavage during crystallization, whereas the other strand was cleaved at a normal 3′ splice site (*28*). The endonuclease–21-oligomer BHB RNA structure, containing two endonuclease-RNA complexes not related by crystallographic symmetry, was determined by molecular replacement methods and refined at 2.85 Å resolution to an R_{free} of 29.6% (*28*). The mean precision of the atomic coordinates is 0.45 Å (table S1).

In the complex, the AF endonuclease is the same symmetric dimer as the free AF endonuclease with the structure deviating only in local regions (*29*, *30*). In contrast, the BHB RNA differs significantly from its unbound solution structure as observed using nuclear magnetic resonance (NMR) methods (Fig. 1B). Curved when in solution (*31*), the helical portion of the BHB structure displays little bending when bound to the endonuclease (Fig. 1B). In addition, the three bulge nucleotides are completely flipped out of their stacking positions when bound, but not so when in solution. Consequently, the two bulges rise above the flat minor groove of the central helix and form two distinct protrusions to interact with the endonuclease (Fig. 1B).

The minor groove of the 4-bp central helix of the BHB RNA docks at the center of a flat surface formed by both subunits of the endonuclease (Fig. 1C). Remarkably, the entire base-paired region of the bound BHB RNA closely resembles a single A-form helix. The phosphate backbone of the uncleaved 5′ splice-site bulge bends ~180° and crosses over itself, forming an open knot (Fig. 1C). Similarly, the phosphate backbone of the cleaved 3′ splice-site bulge makes an open knot in preparation for cleavage (Fig. 1C). This tight looping brings the two base pairs flanking the bulge into stacking positions as observed in a regular A-form helix. Thus the enzyme engineers a contortion in RNA to orient it for cleavage.

The endonuclease-RNA complex buries an extensive solvent-accessible surface area (3208 Å^2). However, the "hot spots" of interactions are surprisingly confined. The primary specificity elements are the three bulge nucleotides. They interact with four positively charged residues of the endonuclease—His^{257}, Arg^{280}, Arg^{286}, and Arg^{302}—in a sequence-independent manner.

Arg^{286} is in a tight turn that connects α5 and β10 and interacts with the phosphate group of central helix nucleotides C11/u11 (fig. S1). Sequences of this tight turn are well conserved. Arg^{286} is replaced by lysine in most other organisms, with a few exceptions in eukaryal subunits, including human Sen2 which has serine at this position (fig. S2).

The hallmark of the AF endonuclease-RNA recognition is a cross-subunit arginine-nucleotide-arginine sandwich. At both splice sites, the nucleobase of the first bulge nucleotide, A13/a13, protrudes deeply into the endonuclease and is sandwiched by Arg^{280} and Arg^{302} (Fig. 2). Remarkably, the Arg^{280}-Arg^{302} pair of one subunit stabilizes the bulge that is cleaved by the other subunit (Fig. 2A). Arg^{280} is strictly conserved, whereas Arg^{302} may be replaced by an aromatic residue in other archaeal and eukaryal organisms (fig. S2). For each cation-π sandwich, the planes formed by the atoms of the two guanidinium groups are ~3.8 to 4.1 Å away from and nearly parallel to the adenine ring. This distance corresponds to the most favorable energy of interaction between the guanidinium group and the adenine base according to an ab initio quantum mechanics computation (*32*). Removal of the nucleobase from nucleotide A13 severely impairs the cleavage activity on the BHB RNA (see fig. S3A). Furthermore, the guanidinium group of Arg^{280} forms a double hydrogen bond with the phosphate group 3′ of the last bulge nucleotide (G16 or g16) and the 2′-hydroxyl oxygen atom of the first bulge nucleotide (A13/a13) (Fig. 2, B and C). This double hydrogen bond constrains the orientation of the guanidinium group and thus maximizes the cation-π interaction while stabilizing the sharply bent bulge backbone. The importance of Arg^{280} is demonstrated by the fact that it is one of four strictly conserved residues, and its mutation to lysine completely abolished RNA cleavage activity (fig. S3B).

RNA functional groups of the BHB motif also stabilized the sharply bent bulge backbone. The phosphate group of G16/g16, which closes the bulge loop, is near the center of the negatively charged bulge backbone (Fig. 2D). The nonbridging oxygens of this phosphate form short hydrogen bonds with the 2′-hydroxyl groups of C12 (2.4 Å) and A13 (2.7 Å), and a long hydrogen bond with A15 (3.5 Å) (Fig. 2D). Methylation of the 2′-hydroxyl group of C12 or A13 impairs cleavage activity on the 21-oligomer oligonucleotide BHB RNA substrate (fig. S3A).

The second bulge nucleotide (dU14/a_{23}14) is also flipped out of helical stacking, pointing in a direction perpendicular to that of the first bulge nucleotide. It is recognized primarily by its ribose ring and its connection to the well-positioned scissile phosphate group (Fig. 2B). Residue Leu^{255} in loop L7 of the endonuclease forms sequence-independent van der Waals contact with the base (Fig. 2B). This mode of

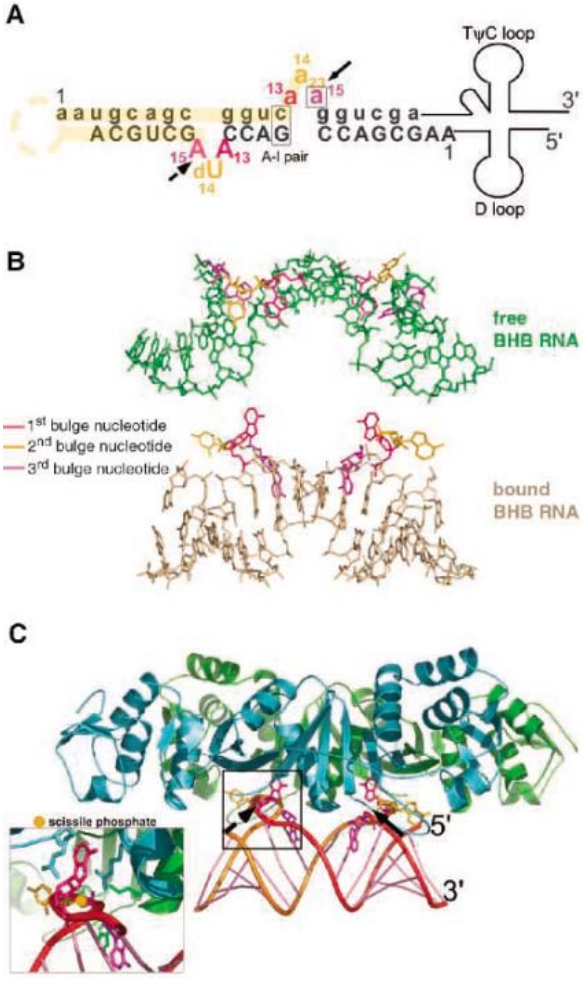

Fig. 1. AF endonuclease-BHB RNA complex structure. (**A**) A precursor tRNA structure with the primary and secondary structure of the bulge-helix-bulge (BHB) RNA used in cocrystallization represented by letters. The intron is highlighted in light orange. The two arrows depict the two splice sites where the broken arrow indicates the modified 5′ splice site. The anticodon-intron equivalent base pair (A-I pair) and the first 3′ exon nucleotide (a15) are highlighted by boxed letters. Small and capital letters of the same numbering are used for the strands containing the 3′ splice site and the 5′ splice sites, respectively. (**B**) Unstacking of three bulge nucleotides and their stabilization in the endonuclease. The bound bulge-helix-bulge (BHB) RNA structure (brown) compared with the ensemble-averaged NMR structure of a BHB RNA (green) (PDB code 2A9L). (**C**) Overview of the AF endonuclease-BHB RNA complex structure with the intron backbone colored in orange. Nucleotides in helical regions are represented by rods and those in bulges by stick models. The following color scheme for bulge nucleotides is consistently used throughout the article: first bulge nucleotide, bright red; second bulge nucleotide, orange; and the third bulge nucleotide, magenta. The two protein subunits are colored blue and green. (Insert) More detailed RNA-endonuclease interaction.

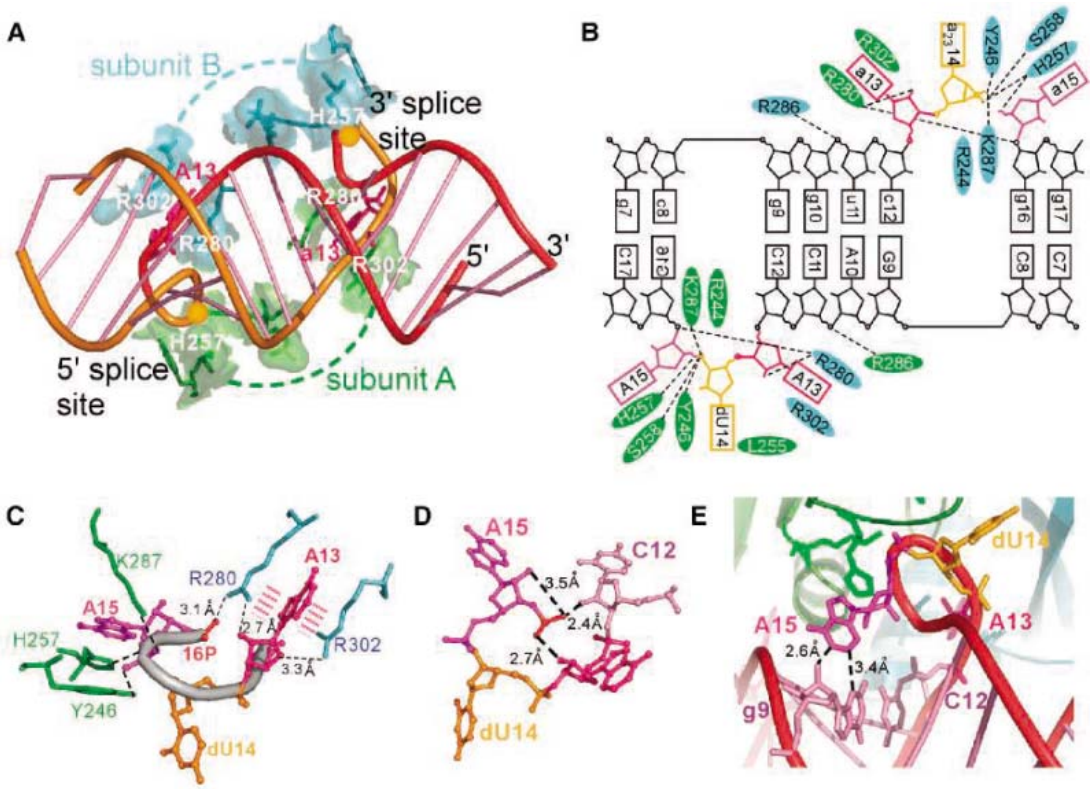

Fig. 2. Protein-RNA interactions between the bulge-helix-bulge (BHB) RNA and the endonuclease. (**A**) Cross-subunit stabilization of each splice site. The Arg$^{280/302}$ pair from one subunit recognizes the first bulge nucleotide (A13/a13) of the bulge cleaved by the other subunit. The gold spheres indicate scissile phosphates. (**B**) Protein residues contacting the BHB RNA. The color scheme is the same as that used for the structure. (**C**) Key elements of interaction between the endonuclease and bulge nucleotides. Note the stabilization of the sharply bent phosphate backbone mediated by both subunits represented by cyan and green residues. (**D**) Stabilization of the sharply bent bulge backbone by two close contacts between RNA oxygen atoms at the ends of the bulge. (**E**) A-minor interaction mediated by the last bulge nucleotide (A15/a15) and the adjacent central helix base pair g9-C12/G9-c12. Note the g9-C12 base pair corresponds to the A-I pair shown in Fig. 1A.

recognition partially explains why the second bulge nucleotide is the least conserved among the three at the 3′ splice site (fig. S4).

The third bulge nucleotide (A15/a15) is at a key location to interact with endonuclease as well as to participate in RNA folding. The flipped-out A15/a15 base protrudes toward the central helix and in the direction opposite that of the first bulge nucleotide (A13/a13). The base of A15/a15 is held in place by the conserved His^{257} residue through aromatic stacking (Fig. 2E). This interaction causes an unfavorable twist to the nucleoside moiety. Correspondingly, the torsion angles around the P–O3′ bond for both dU14 (ζ = 125°) and A15 (ζ = 134°) deviate from the typical values observed for A-form RNA (ζ = 289°) (*33*).

The adenine ring of A15/a15 forms an A-minor interaction with the g9-C12/G9-c12 base pair, although A15/a15 is slightly out of the plane of the base pair (Fig. 2E). The A-minor interaction observed in the BHB RNA is a common type of tertiary RNA interaction similar to that between the G1364-C637 base pair and A521 observed in a *Haloarcula marismortui* 50*S* ribosome structure (*34*) and that between the G212-C109 base pair and A184 in a *Tetrahymena* group I self-splicing intron structure (*35*). The stacking between the nucleobase of A15/a15 and the imidazole ring of His^{257} facilitates the A-minor interaction (Fig. 2E). Removing the nucleobase of A15/a15 abolishes enzyme activity on a modified 21-oligomer oligonucleotide BHB RNA (fig. S3A).

The unexpected interaction between A15/a15 and g9-C12/G9-c12 explains the importance of the A-I base pair in determining the 3′ splice site of eukaryal pre-tRNAs (*22*, *23*). It was previously shown that the identity of the A-I base pair required for cleavage of the 3′ splice site by *Xenopus* endonuclease is correlated with the identity of the first 3′-exon nucleotide (*22*). The A-minor interaction observed between a15 and G9-c12, which correspond to the first 3′ exon nucleotide and the A-I base pair in a eukaryal pre-tRNA, provides the structural basis for their observed interdependence (*22*, *23*).

The endonuclease-RNA complex provides structural evidence for cooperativity between the two catalytic subunits. The cross-subunit stabilization of each bulge by cation-π sandwich (Fig. 2A) suggests that cognate interactions between one bulge and both subunits may facilitate the binding of the other bulge. Consequently, disruption of the structural integrity of one bulge would cause impaired cleavage on both bulges. Indeed, in addition to impairing cleavage of the 5′ bulge, 2′-*O*-methylation of C12 or A13, or removal of the nucleobase from nucleotide A13 at the 5′ bulge, prevented the cleavage of the 3′ bulge (fig. S3A). These results lend strong support to a model of cooperative binding of the two catalytic endonuclease subunits to the BHB RNA. Remarkably, the observed cooperativity between two catalytic subunits in the AF endonuclease-RNA complex was also demonstrated in the yeast splicing endonuclease by selective mutation of its catalytic subunits (*36*).

The RNA recognition elements identified here are asymmetrically disposed between the two splice sites in eukaryal pre-tRNAs, although the sites themselves are equally utilized (*22*, *37*). This appears to conflict with cooperativity because the typically unconserved 5′ splice site in nuclear pre-tRNAs would lead to overall inefficient cleavage at both sites. We suggest that the two catalytic subunits are diverged to complement the asymmetrically conserved splice sites. Consistent with this proposal, the *Xenopus* splicing endonuclease can cleave a miniprecursor tRNA containing only the mature domain and the 3′ splice site (*16*), and mutation of the Arg^{280}-equivalent residue in yeast Sen2 only mildly impaired cleavage of the 3′ splice site (*36*).

Interactions between the RNA and the endonuclease at the active sites are consistent with the involvement of catalytic triad residues in cleavage reactions (Fig. 3). At the site of cleavage, the endonuclease facilitates a near in-line geometry of the attacking 2′-oxygen, the scissile phosphate, and the leaving 5′-oxygen that is required for RNA cleavage at this site (Fig. 3, insert). In addition, the scissile phosphates at both 5′ and 3′ splice sites are at the center of three strictly conserved residues, Tyr^{246}, His^{257}, and Lys^{287}, the same as the position occupied by the bound sulfate in the crystal structure of the *M. jannaschii* endonuclease (*27*). The pro-S_p nonbridging oxygen of the 5′ splice site is

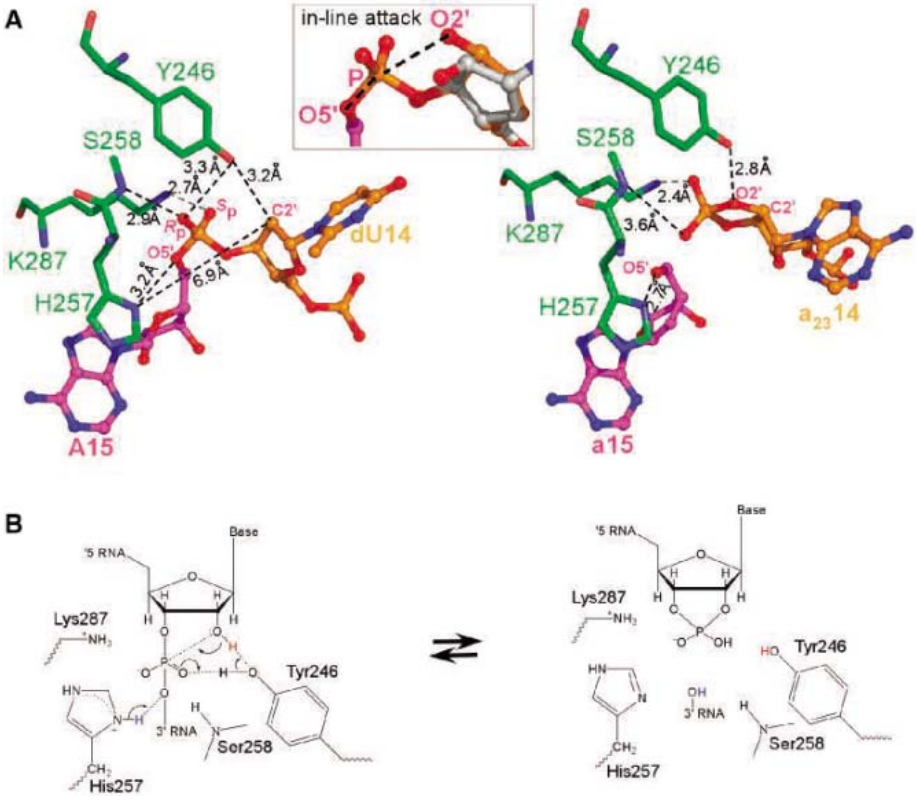

Fig. 3. Active site interaction and proposed catalytic mechanisms. (**A**) Placement of the catalytic triad residues and their distances to functional RNA groups at the 2′-deoxy modified (left) and the cleaved (right) site, respectively. The insert shows the in-line geometry formed by the attacking 2′-nucleophile oxygen, scissile phosphate, and the leaving 5′-oxygen. Gray structural model represents the same nucleotide in 3′ endo sugar-puckering conformation. (**B**) A proposed catalytic mechanism where His^{257} acts as the general acid that donates a proton to the 5′ leaving group, Tyr^{246} facilitates deprotonation of the 2′ nucleophilic oxygen, and Lys^{287} and the amide group of Ser^{258} stabilize the developing negative charge at the transition state.

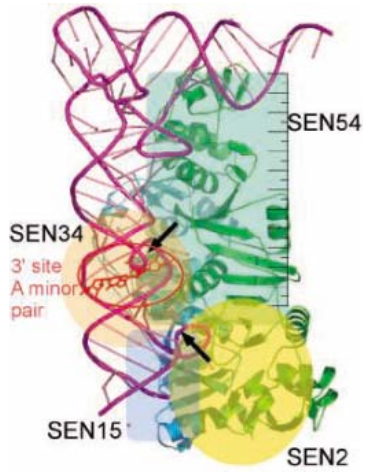

Fig. 4. A structural model of the pre-$tRNA^{Archeuka}$ bound to AF endonuclease (ribbon models) with the corresponding yeast endonuclease subunits represented in colored shapes, and the splice sites indicated by arrows. The model indicates that the structural unit of the AF endonuclease corresponding to Sen54 interacts with the mature domain of the precursor tRNA. The A-I base pair and the third bulge nucleotide involved in the A-minor interaction interact with the subunit corresponding to Sen34.

stabilized by a short hydrogen bond formed with Nε of Lys^{287} (2.7 Å, donor-hydrogen-acceptor angle 114°) and the Nδ atom of His^{257} is located 3.5 Å away from the leaving 5′ oxygen. The third catalytic triad residue, Tyr^{246}, is 2.2 Å from the modeled 2′-hydroxyl oxygen in the 2′-endo sugar-puckering conformation (3.5 Å for 3′-endo sugar-puckering). The placement of the three residues suggests a catalytic mechanism where Tyr^{246} deprotonates the nucleophilic 2′-oxygen, His^{257} protonates the leaving 5′ hydroxyl oxygen [similar to His^{119} of RNase A (*26*)], and Lys^{287} stabilizes the developing negative charge of the transition state (Fig. 3B).

The AF endonuclease-RNA cocrystal structure provides a basis for understanding the mode of RNA recognition by the eukaryal endonuclease. Based on sequence comparisons and pairwise interactions identified by yeast two-hybrid methods, it is believed that the αβγδ eukaryal endonuclease has the same overall architecture as archaeal endonucleases, with the structural subunits Sen15 and Sen54 pairing with the 5′-cleaving Sen2 and the 3′-cleaving Sen34, respectively (*7*, *10*, *11*, *27*). Thus, each AF endonuclease unit can be assigned specifically to one of the αβγδ subunits. We created a structural model of a precursor tRNA substrate by superimposing the anticodon stem of the yeast $tRNA^{phe}$ structure onto the stem 5′ of the 3′ bulge of the BHB RNA (pre-$tRNA^{Archeuka}$) and analyzed how the pre-$tRNA^{Archeuka}$ substrate interacts with the eukaryal endonuclease subunits (Fig. 4). This showed that the D arm and the acceptor stem of pre-$tRNA^{Archeuka}$ would interact with the Sen54 subunit (Fig. 4). This mode of RNA-protein interaction is consistent with the active but imprecise cleavage of a composite pre-tRNA lacking the acceptor stem by the *Xenopus* splicing endonuclease (*16*) and suggests a role of Sen54 in the ruler mechanism of splice-site selection.

The cocrystal structure of the AF endonuclease-RNA complex identifies an evolutionarily conserved RNA recognition and cleavage mechanism for the removal of introns by the splicing endonuclease. Splice-site recognition depends on the chemical features of both protein and RNA residues. The challenge will be to dissect the functional role of each of these components in RNA recognition and in catalysis.

References and Notes

1. G. Knapp, R. C. Ogden, C. L. Peebles, J. Abelson, *Cell* **18**, 37 (1979).
2. C. L. Peebles, P. Gegenheimer, J. Abelson, *Cell* **32**, 525 (1983).
3. C. L. Greer, C. L. Peebles, P. Gegenheimer, J. Abelson, *Cell* **32**, 537 (1983).
4. E. M. Phizicky, R. C. Schwartz, J. Abelson, *J. Biol. Chem.* **261**, 2978 (1986).
5. G. M. Culver *et al.*, *Science* **261**, 206 (1993).
6. L. D. Thompson, C. J. Daniels, *J. Biol. Chem.* **263**, 17951 (1988).
7. J. Lykke-Andersen, R. A. Garrett, *EMBO J.* **16**, 6290 (1997).
8. K. Calvin, M. D. Hall, F. Xu, S. Xue, H. Li, *J. Mol. Biol.* **353**, 952 (2005).
9. G. D. Tocchini-Valentini, P. Fruscoloni, G. P. Tocchini-Valentini, *Proc. Natl. Acad. Sci. U.S.A.* **102**, 8933 (2005).
10. R. Rauhut, P. R. Green, J. Abelson, *J. Biol. Chem.* **265**, 18180 (1990).
11. C. R. Trotta *et al.*, *Cell* **89**, 849 (1997).
12. S. V. Paushkin, M. Patel, B. S. Furia, S. W. Peltz, C. R. Trotta, *Cell* **117**, 311 (2004).
13. J. Abelson, C. R. Trotta, H. Li, *J. Biol. Chem.* **273**, 12685 (1998).
14. J. Kjems, J. Jensen, T. Olesen, R. A. Garrett, *Can. J. Microbiol.* **35**, 210 (1989).
15. C. Marck, H. Grosjean, *RNA* **9**, 1516 (2003).
16. E. Di Nicola Negri *et al.*, *Cell* **89**, 859 (1997).
17. L. D. Thompson, C. J. Daniels, *J. Biol. Chem.* **265**, 18104 (1990).
18. J. Lykke-Andersen, C. Aagaard, M. Semionenkov, R. A. Garrett, *Trends Biochem. Sci.* **22**, 326 (1997).
19. T. H. Tang *et al.*, *Nucleic Acids Res.* **30**, 921 (2002).
20. Y. Watanabe *et al.*, *FEBS Lett.* **510**, 27 (2002).
21. V. M. Reyes, J. Abelson, *Cell* **55**, 719 (1988).
22. M. I. Baldi, E. Mattoccia, E. Bufardeci, S. Fabbri, G. P. Tocchini-Valentini, *Science* **255**, 1404 (1992).
23. E. Bufardeci, S. Fabbri, M. I. Baldi, E. Mattoccia, G. P. Tocchini-Valentini, *EMBO J.* **12**, 4697 (1993).
24. C. L. Greer, D. Soll, I. Willis, *Mol. Cell. Biol.* **7**, 76 (1987).
25. K. Kleman-Leyer, D. A. Armbruster, C. J. Daniels, *Cell* **89**, 839 (1997).
26. R. Raines, *Chem. Rev.* **98**, 1045 (1998).
27. H. Li, C. R. Trotta, J. Abelson, *Science* **280**, 279 (1998).

28. Materials and methods are available as supporting material on *Science* Online.
29. Y. Zhang, H. Li, *Acta Crystallogr D. Biol. Crystallogr.* **60**, 447 (2004).
30. H. Li, J. Abelson, *J. Mol. Biol.* **302**, 639 (2000).
31. J. L. Diener, P. B. Moore, *Mol. Cell* **1**, 883 (1998).
32. C. Biot, E. Buisine, J. M. Kwasigroch, R. Wintjens, M. Rooman, *J. Biol. Chem.* **277**, 40816 (2002).
33. E. Hershkovitz *et al.*, *Nucleic Acids Res.* **31**, 6249 (2003).
34. P. Nissen, J. A. Ippolito, N. Ban, P. B. Moore, T. A. Steitz, *Proc. Natl. Acad. Sci. U.S.A.* **98**, 4899 (2001).
35. D. J. Battle, J. A. Doudna, *Proc. Natl. Acad. Sci. U.S.A.* **99**, 11676 (2002).
36. C. R. Trotta, S. V. Paushkin, M. Patel, H. Li, S. W. Peltz, *Nature* (in press).
37. F. Miao, J. Abelson, *J. Biol. Chem.* **268**, 672 (1993).

38. We thank J. Abelson, C. Chapman, B. Miller, C. Trotta, W. Yang (FSU), and W. Yang (NIH) for inspiring discussions and for critical reading of the manuscript and R. Dhanarajan for assistance in cloning. This work was funded, in part, by grants from Florida Biomedical Research (BM002 to H.L.), American Heart Association Florida/Puerto Rico Affiliate (030396B to H.L.), and National Science Foundation (MCB-0517300 to H.L). K.C. is an American Heart Association Florida/Puerto Rico Affiliate predoctoral fellow (0415091B). X-ray diffraction data were collected at both the Northeastern Collaborative Access Team (NE-CAT) BM-8 beamline and the Southeast Regional Collaborative Access Team (SER-CAT) 22-ID beamline at the Advanced Photon Source, Argonne National Laboratory. Supporting institutions may be found at http://necat.chem.cornell.edu/ and www.ser-cat.org/members.html. Use of the Advanced Photon Source was supported by the U.S. Department of Energy, Office of Science, Office of Basic Energy Sciences, under Contract No. W-31-109-Eng-38. Coordinates and structure factors have been deposited in the Protein Data Bank (PDB) with accession number 2GJW.

Supporting Online Material

www.sciencemag.org/cgi/content/full/312/5775/906/DC1
Materials and Methods
Figs. S1 to S5
Table S1
References

23 February 2006; accepted 5 April 2006
10.1126/science.1126629

Molecular Sorting by Electrical Steering of Microtubules in Kinesin-Coated Channels

Martin G. L. van den Heuvel, Martijn P. de Graaff, Cees Dekker*

Integration of biomolecular motors in nanoengineered structures raises the intriguing possibility of manipulating materials on nanometer scales. We have managed to integrate kinesin motor proteins in closed submicron channels and to realize active electrical control of the direction of individual kinesin-propelled microtubule filaments at Y junctions. Using this technique, we demonstrate molecular sorting of differently labeled microtubules. We attribute the steering of microtubules to electric field–induced bending of the leading tip. From measurements of the orientation-dependent electrophoretic motion of individual, freely suspended microtubules, we estimate the net applied force on the tip to be in the picoNewton range and we infer an effective charge of 12 e^- per tubulin dimer under physiological conditions.

Recent years have witnessed a strong interest in the exploration of biomolecular motors in nanotechnology (*1*–*4*). A molecular motor such as kinesin, which translocates in 8-nm steps along microtubule filaments through hydrolysis of adenosine triphosphate (ATP) (*5*), can potentially be used as the workhorse in miniaturized analytical systems or nanoelectromechanical systems (*6*, *7*). In particular, it is envisioned that microtubule shuttles translocating over kinesin-coated tracks can be used to carry a specific cargo to designated places on a chip (*8*). First steps toward such applications have been realized, such as partial confinement of microtubules to micron-sized kinesin-coated trenches (*9*–*11*), docking of shuttles to their tracks (*12*), rectification of motility (*13*, *14*), and coupling of cargo (*15*). The much-sought-after goal of dynamic control of the direction of individual microtubules, a key requirement for molecular sorting applications, has not been achieved so far. Attempts to use electric fields to manipulate the negatively charged microtubules have only resulted in large-scale alignment (*16*) or bulk transport of the filaments (*11*, *12*).

In this report, we reconstituted the kinesin-microtubule transport system in enclosed fluidic channels, which represents two major advances. First, fluidic channels achieved full confinement of the microtubules to their tracks, without the need for any surface modifications or selective patterning of kinesin molecules in open-trench structures. Second, the confined geometry of channels allowed the localized application of strong, directed electric fields, which could be exploited to steer individual microtubules, as well as to perform single-molecule biophysical experiments. By measuring the electrophoretic motion of individual microtubules, we determined the magnitude of the electric field–induced force on the microtubule tip, and we directly confirmed the predicted anisotropy in electrophoretic mobility.

We fabricated fluidic channels 800 nm deep (*17*) between entrance holes in fused-silica substrates and sealed them (Fig. 1, A and B). Microtubule motility was reconstituted in the channels by a pressure-driven flow to flush the necessary protein constituents (casein, kinesin, and fluorescently labeled paclitaxel-stabilized associated protein–free microtubules) from the entrance reservoirs into the channels (Fig. 1C). Using epifluorescence microscopy, we could discern microtubules moving on either the top or bottom surface of a channel by adjusting the focus of the objective (Fig. 1D). The enclosed geometry of the device completely confined the microtubules to their tracks (Fig. 1E). All regions could be coated with kinesin proteins, even less accessible regions in more complicated networks, such as bends (Fig. 1F). The speed of the microtubules in our channels (0.75 ± 0.02 μm/s) was the same as on a glass coverslip in a standard flow cell (0.74 ± 0.04 μm/s). By applying a voltage difference between platinum electrodes inserted in reservoirs at either end of a perpendicular cross-channel, we induced an electric field **E** perpendicular to the direction of microtubule motion (Fig. 2A). In this way, the electrical force on the negatively charged microtubules was directed opposite to the electric field.

We demonstrated that microtubules can be directed with an electric field. The trajectory of a microtubule that was subjected to an electric field of strength $|\mathbf{E}|$ = 35 kV/m (70 V over 2 mm) is shown in Fig. 2B. At the beginning of the path, the microtubule was oriented perpendicular to the electric field. As the microtubule progressed, its leading end gradually oriented itself opposite to the applied field, until the microtubule finally changed course by 90° and moved parallel to the electric field and toward the positive electrode. A trace of the leading- and trailing-end coordinates of the microtubule showed that they followed exactly the same path (Fig. 2B). This clearly indicates that there was no motion of the microtubule perpendicular to its long axis, which is expected if kinesin molecules hold onto the microtubule. Up to 110 kV/m, we did not observe a measurable increase or decrease of the microtubule velocity due to the electric field (*18*).

The electric force was used to actively steer individual microtubules into a desired channel of a Y junction, across and through which a perpendicular channel was fabricated in order to confine the electric field. As a microtubule approached the junction, it was steered into the right channel by adjustment of the perpendicular electric field, whose magnitude was between 0

Kavli Institute of Nanoscience, Section Molecular Biophysics, Delft University of Technology, Lorentzweg 1, 2628 CJ Delft, Netherlands.

*To whom correspondence should be addressed. E-mail: dekker@mb.tn.tudelft.nl

and 50 kV/m (Fig. 2C). Figure 2D shows an experiment in which many microtubules were selectively steered into the right or the left channel.

We attribute the observed steering of the microtubules to a biased search of the free leading tip of the microtubule for the next kinesin motor (Fig. 2E) (*16*). As a microtubule is propelled by kinesin molecules, its tip fluctuates freely by Brownian motion until it binds to a new kinesin motor (*19*). In the absence of applied force, the equilibrium position of the free tip is collinear with the microtubule's long axis, which gives an equal probability of finding the next motor in either direction from this axis. The presence of a perpendicular force, however, will bias the

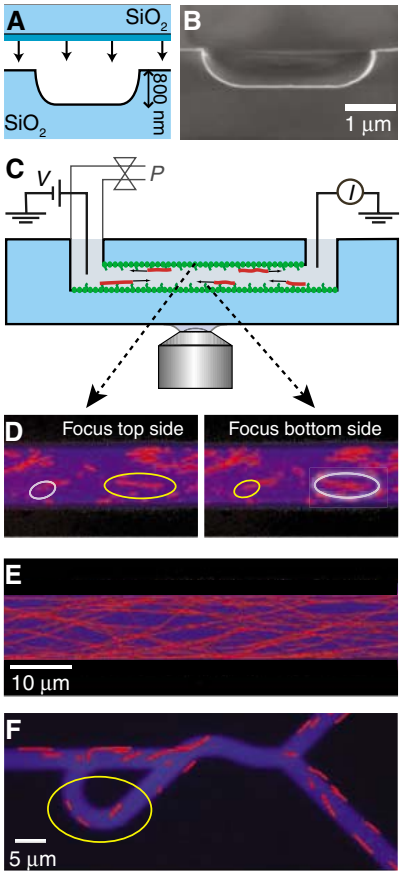

Fig. 1. Enclosed submicron channels allow for full confinement of microtubules. (**A**) E-beam lithography and wet etching create 800-nm-deep trenches in SiO_2 substrates. A coverslip coated with a sodium-silicate solution (dark blue) seals the channel after annealing. (**B**) Scanning electron microscopy image of a cross section of a nanochannel. (**C**) Schematic cross section along a channel. Kinesin motor proteins (green) and microtubule filaments (red) are added to the channels by a pressure-driven flow. Electric fields can be induced in the channels by applying a potential difference between the reservoirs. (**D**) Fluorescence microscopy shows that microtubules (red) move on both sides of the channels (blue). Yellow ovals indicate microtubules in the focal plane; white ones denote microtubules just out of focus. (**E**) Traces of several microtubules moving through a confined channel. The figure is an overlay of microtubule traces traversing the image during a period of 7 min. No microtubules are observed outside of the tracks. (**F**) More complex geometries, such as the bend in a rectifying geometry, could also be well coated with kinesin molecules and could support microtubule motility.

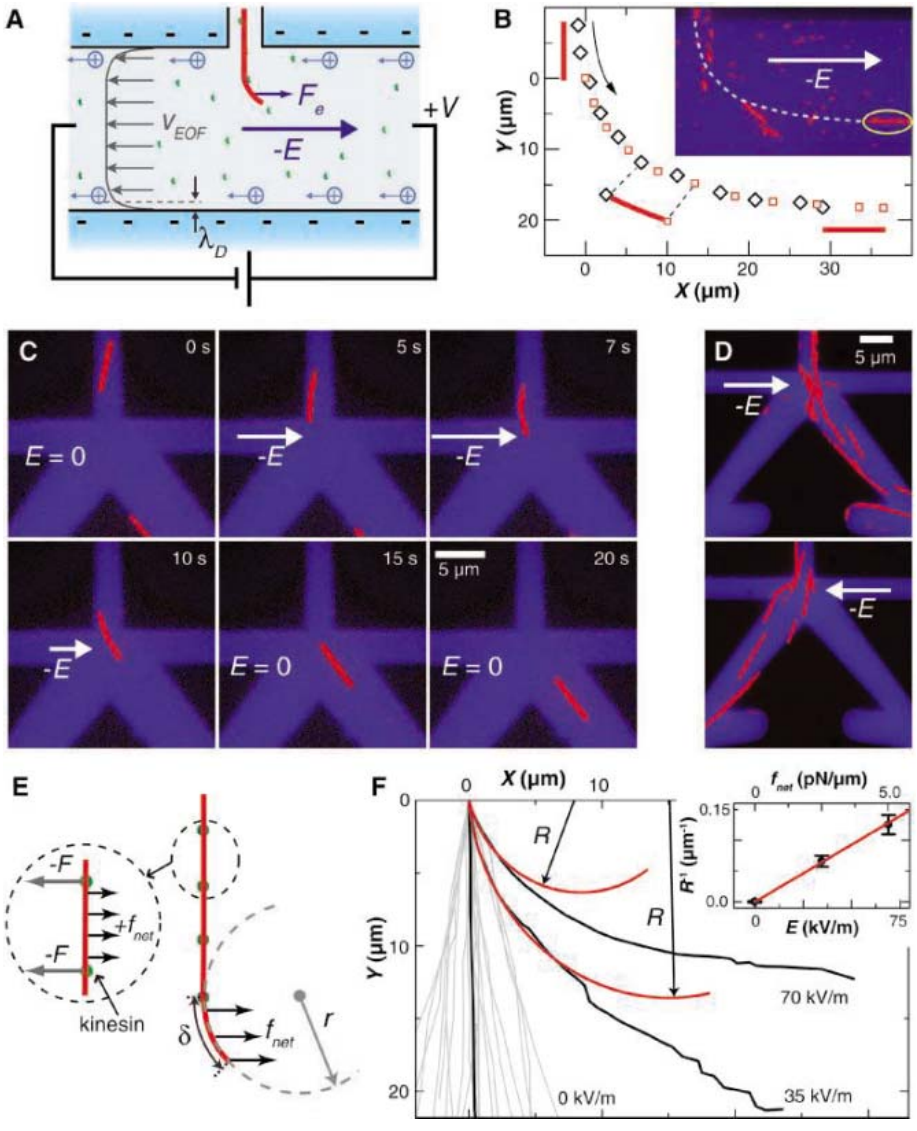

Fig. 2. Bending and steering of microtubules by an electric field. (**A**) An electric field (**E**) is induced in a horizontal channel perpendicular to the vertical direction of microtubule (red) motion. The electric force on the negatively charged microtubule is along –**E**, denoted by the blue arrow. Furthermore, the applied electric field will induce motion of the positive ions in the double layer at the channel walls (characteristic thickness λ_D), causing an electro-osmotic flow in the channel. (**B**) Overlapping coordinates of leading (red symbols) and trailing (black symbols) ends of a microtubule oriented in a field $|\mathbf{E}| = 50$ kV/m. (Inset) The positions trace (dashed) in a fluorescence image. (**C**) A microtubule entering from the central channel at the top is steered into the right lead of the Y junction by application of a perpendicular electric field that varies in magnitude between 0 and 50 kV/m (indicated by length of arrow). (**D**) By using magnitude and direction of the electric field, many microtubules are steered to the right (top panel) and left (bottom panel). (**E**) Bending of a microtubule by a net force. The main part of the microtubule is held fixed by kinesin molecules; only the free leading tip (length δ) is subject to a force density f_{net}, which bends it with curvature r^{-1}. (**F**) Measurements of the average trajectories that microtubules travel under three different applied fields $\mathbf{E}_x$. Black traces represent averages of many individual paths. Gray lines are the individual trajectories at $|\mathbf{E}| = 0$. At $|\mathbf{E}| \neq 0$, the spread in the individual trajectories is similar, but they are not shown for clarity. Initial curvatures of the trajectories are denoted by red circles. (Inset) The linear relation between electric field strength $|\mathbf{E}|$ and curvature R^{-1}. The values of f_{net} were calculated from **E** (see text).

equilibrium position toward the direction of higher potential and thereby increases the probability of finding the next binding site in this direction.

The field-dependent trajectories of microtubules were traced to quantify the microscopic bending in experiments analogous to Fig. 2B. For $|\mathbf{E}| = 0$, the average path of several ($N = 18$) microtubules was indeed a straight line in the initial direction of motion (Fig. 2F). For $|\mathbf{E}| = 35$ kV/m, the average microtubule path deviated from the straight path, ultimately orienting itself along the electric field ($N = 17$). The curvature of the trajectory upon entering the electric field was fitted by a circle of radius $R = 15 \pm 2$ μm. At a higher $|\mathbf{E}| = 70$ kV/m, the average bending of the path ($N = 10$) was more pronounced, and the curvature was described by a circle of $R = 8 \pm 1$ μm. The observed curvature of the microtubule path increased linearly with applied electric field (Fig. 2F, inset). The average bending radius did not depend on microtubule length.

The forces that act on the microtubules in the presence of an electric field have a nontrivial origin. The net force per unit length on the microtubule, f_{net}, stems from two components. First, the electric force was shown to equal the drag that moving counterions in the microtubule's double layer experience from the surrounding fluid: $f_e = c\mu_e\mathbf{E}$ (*20*–*22*). Here, c is the Stokes drag coefficient per unit length and μ_e the (negative) electrophoretic mobility of the microtubule. The second contribution to the force on the microtubule results from the fluid motion in the channel due to the field-driven motion of counterions at the glass channel walls. This electro-osmotic flow (EOF) (Fig. 2A) exerts a drag force on the microtubule opposite from the electric force, $f_{EOF} = c\mu_{EOF}\mathbf{E}$. Here, μ_{EOF} is the (positive) electro-osmotic mobility. At the beginning of the microtubule path, the electric field is perpendicular to the microtubule, resulting in a net force:

$$f_{net} = c_\perp(\mu_{e,\perp} + \mu_{EOF})\mathbf{E} \qquad (1)$$

Electrokinetic measurements were performed on single microtubules in order to measure the magnitude of this force. The electrophoretic mobility of rodlike polymers, such as microtubules, has only been treated theoretically, and is predicted to be anisotropic for perpendicular ($\mu_{e,\perp}$) and parallel ($\mu_{e,\parallel}$) orientations of the rod to the electric field (*20*, *23*):

$$\mu_{e,\parallel} = \frac{\varepsilon\zeta}{\eta} \text{ and } \mu_{e,\perp} = {}^2\!/_3 g_\perp \frac{\varepsilon\zeta}{\eta} \qquad (2)$$

Here, η and ε are the viscosity and dielectric constant of the fluid, respectively, and ζ is the electrostatic potential at the no-slip plane of the microtubule. The anisotropy factor $g_\perp$ accounts for the perturbation of the ionic atmosphere around the rod (*20*, *23*) and approaches a maximum value of $^3\!/_2$ for infinitely small Debye lengths (*24*). Measurements of these anisotropic electrophoretic mobilities of colloidal cylinders have not, as far as we know, been reported. The small height of our channels allowed us to observe individual microtubules in a single focal plane, which enabled us to test the predicted anisotropy of the mobility. The anisotropic mobilities induced an observable orientation-dependent velocity of microtubules, with components perpendicular (v_x) and parallel (v_y) to the electric field (fig. S1):

$$v_x = {}^1\!/_2(\mu_{e,\parallel} - \mu_{e,\perp})\sin 2\theta\cdot\mathbf{E}$$
$$v_y = [(\mu_{e,\parallel} - \mu_{e,\perp})\sin^2\theta + (\mu_{e,\perp} + \mu_{EOF})]\mathbf{E} \qquad (3)$$

Here, θ is the orientation of the filament with respect to the x axis (Fig. 3A). Note that the velocity is not necessarily collinear with the electric field. The EOF adds linearly as an orientation-independent velocity decrease in the y direction.

The electrophoretic motion of individual microtubules in channels without kinesin is shown in Fig. 3A. In accordance with the bending experiments, we observed that freely suspended microtubules move opposite to the applied electric field along the channel. Values of orientation-dependent v_x (Fig. 3B) and v_y (Fig. 3C) were measured for different $\mathbf{E}$. The red lines are fits of Eq. 3 through the binned data and clearly describe the θ dependence of the velocities very well. These data are direct evidence of the anisotropic electrophoretic microtubule mobility, and the amplitudes of the curves provide a straightforward measure of the anisotropy. As expected from Eq. 2, microtubules move fastest if they are oriented parallel to the

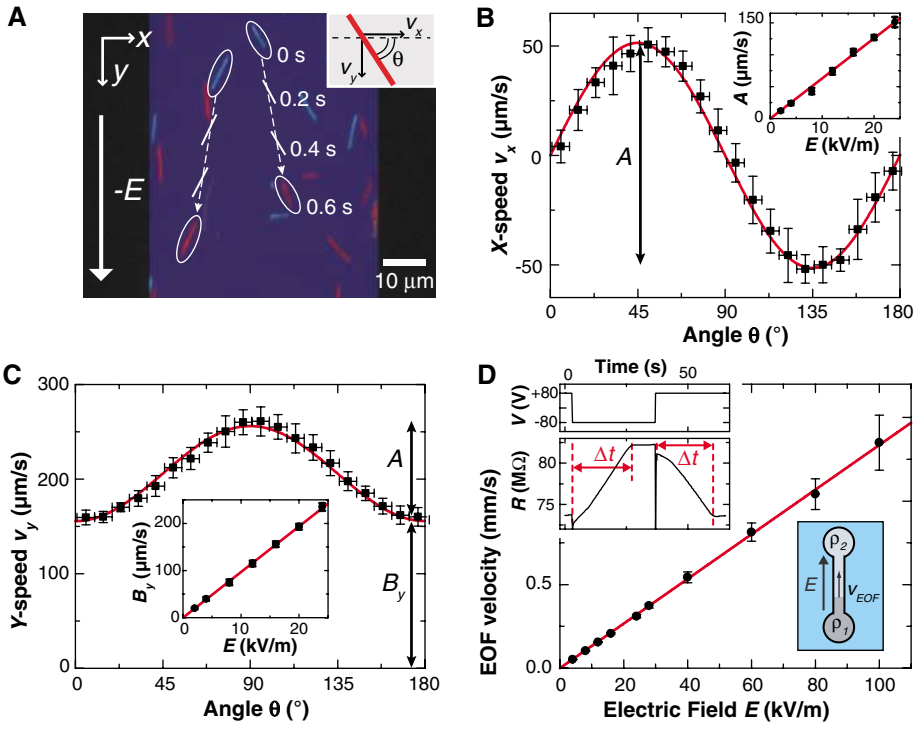

Fig. 3. Electrophoresis of single microtubules and measurement of the EOF velocity. All measurements were performed at neutral pH in the presence of 160 mM K^+. (**A**) Electrophoresis in channels of individual microtubules. Shown is an overlay of images at 0 s (blue microtubules) and at 0.6 s (red microtubules). Intermediate positions of two selected microtubules are indicated by white lines. The selected microtubules not only move in the direction of the electric field, but also perpendicular to it. (**B** and **C**) Binned data ($N = 1496$) of orientation-dependent electrophoretic velocities of microtubules in the x direction [perpendicular to the electric field (B)] and in the y direction [parallel to the electric field (C)]. Error bars denote standard deviation of binned data. The amplitudes A in both curves equal $(\mu_{e,\parallel} - \mu_{e,\perp})\mathbf{E}$. The offset of the v_y graph, $B_y = (\mu_{e,\perp} + \mu_{EOF})\mathbf{E} \propto f_{net}$, applied during steering as in Fig. 2A. (Insets) Linear relation between B_y and $\mathbf{E}$. There was no significant dependence of the velocity on microtubule length. (**D**) EOF velocity as a function of electric field, measured by monitoring the change in resistance of a channel that is replenished by a solution of a different resistivity ρ by an EOF. (Inset) Two typical measurements of the time Δt that it takes the EOF to replace a channel volume (length 5 mm) at $|V| = 80$ V. Each data point in the main graph represents an average of 4 to 6 separate measurements. The slope of the graph equals μ_{EOF}.

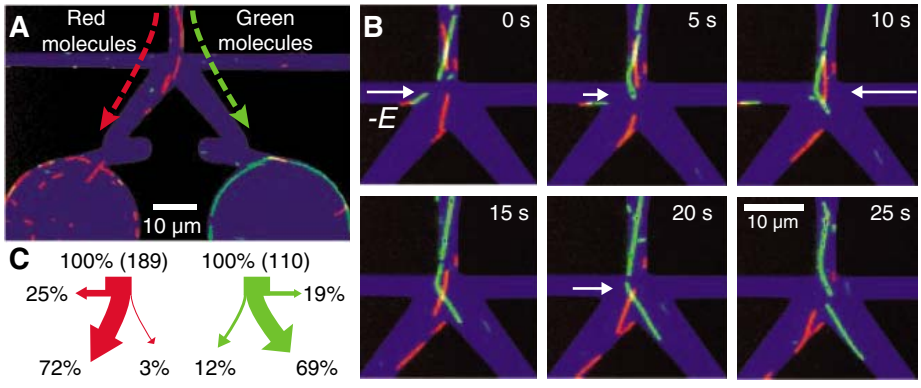

Fig. 4. Demonstration of molecular sorting. (**A**) Color image of a mixture of red- and green-labeled microtubules approaching a Y junction. Electrical force is used to steer microtubules carrying green and red fluorophores into the right and left reservoirs, respectively. (**B**) Example of successful sorting events for a green- and a red-labeled microtubule. As a function of time, first a green microtubule is steered into the right reservoir ($t \leq 10$ s), and subsequently a red microtubule is sent into the left reservoir. (**C**) Steering efficiencies for 189 red and 110 green microtubules. Steering of microtubules into the wrong reservoir (3 and 12%) was mainly due to differences in stiffness between microtubules or due to the simultaneous arrival of microtubules of opposite color. The fractions 19 and 25% of microtubules in the perpendicular channels are artificially high because microtubules were sometimes purposely directed into the perpendicular steering channel so as to avoid such errors.

electric field and slowest for perpendicular orientations (Fig. 3C). To extract the values of the anisotropic microtubule mobilities, we measured $\mu_{EOF} = (1.33 \pm 0.01) \times 10^{-8}$ m^{2}V^{-1}s^{-1} in our kinesin-coated channels (Fig. 3D), yielding $\mu_{e,\perp} = -(2.30 \pm 0.04) \times 10^{-8}$ m^{2}V^{-1}s^{-1} and $\mu_{e,\parallel} = -(2.93 \pm 0.02) \times 10^{-8}$ m^{2}V^{-1}s^{-1}. The anisotropy in electrophoretic mobility is not related to the well-known factor 2 anisotropy in Stokes drag coefficients (*25*), because, in electrophoresis, the retarding shear acts on the length scale of the Debye length λ_D, whereas, in Stokes drag, this length scale is on the order of the size of the object. The values of μ_{EOF}, $\mu_{e,\perp}$, and $\mu_{e,\parallel}$ are all constant over the probed range of electric fields (insets of Fig. 3, B to D).

These mobility measurements permit a calculation of the net force applied in the bending experiments (Eq. 1). From the values $c_\perp = (7.4 \pm 2.0) \times 10^{-3}$ kg/ms (*26*) and $(\mu_{e,\perp} + \mu_{EOF}) = -(9.7 \pm 0.2) \times 10^{-9}$ m^{2}V^{-1}s^{-1}, we calculated the net electrokinetic applied force on the microtubule as $f_{net} = [-(7.2 \pm 2.0) \times 10^{-11}$ N/V$]$ **E**. The forces applied in the bending experiments (Fig. 2F) thus ranged up to 5.0 ± 1.4 pN/μm at $|\mathbf{E}| = 70$ kV/m. Knowledge of the magnitude of this force allowed determination of both the persistence length and the surface charge of the microtubules.

The persistence length of the microtubule was determined from observations of the bending radius under a known perpendicular force. The bending of the microtubule tip can be expressed in terms of the free tip length δ [inversely proportional to motor density (*19*)] and its persistence length L_p. For perpendicular forces f_{net}, the induced curvature r^{-1} of the free tip, in the limit of small deflections, is as follows (Fig. 2E and fig. S2):

$$r^{-1} = \frac{1}{4k_BT}\frac{\delta^2}{L_p}f_{net} \qquad (4)$$

where k_B is Boltzmann's constant and T is temperature. We assert that the microscopic tip curvature r^{-1} equals the macroscopic path curvature R^{-1}. From the linear relation of R^{-1} versus f_{net} (Fig. 2F, inset, and Eq. 4), we determined $\delta^2/L_p = 0.41 \pm 0.12$ nm. We estimated $\delta = 0.26 \pm 0.06$ μm for the free tip length from our observations of the length of the shortest microtubules (0.52 ± 0.13 μm) that still moved in smooth trajectories in our channels. The persistence length of the microtubule's free tip was thus determined to be $L_p = 0.16 \pm 0.09$ mm. This value is on the low end of published values on paclitaxel-stabilized microtubules that find $L_p = 0.2$ to 5.2 mm (*27*, *28*), but the persistence length of the tip does not necessarily represent the persistence length of the entire microtubule (*29*).

The electric charge of a microtubule is determined in two independent ways from the electrophoretic mobilities. First, the value of $\mu_{e,\parallel}$ is proportional to ζ (Eq. 2), which is a direct measure of the surface charge density σ via the linear Grahame equation $\sigma = \varepsilon\zeta/\lambda_D$. From $\mu_{e,\parallel}$, we find that ζ = –37 mV, which yields a surface charge density of 0.20 e$^-$/nm^2. A second measure of the surface charge follows from the value of $g_\perp$ (*20*, *23*). The experimentally determined anisotropy factor $g_\perp = {}^3/_2\,\mu_{e,\perp}/\mu_{e,\parallel} = 1.18$ yields a value of ζ = –50 mV via the inverse transformation (*24*) $\zeta = \Im^{-1}(g_\perp, a/\lambda_D)$. This ζ corresponds to σ = 0.27 e$^-$/nm^2. The average of both measurements gives σ = 0.24 ± 0.04 e$^-$/nm^2, with the error estimated from the difference between the two values (*30*).

From the measured σ and the known 25-nm diameter of a 13-protofilament microtubule, we calculated an effective charge of 12 ± 2 e$^-$ for the solution-exposed surface of the tubulin dimer. A rough estimate of the bare charge of the free dimer of 47 e$^-$ at pH = 6.9 follows from the crystal structure of the tubulin dimer (*31*), if one assumes the isolated dissociation constants of the individual amino acids. The effective charge constituted only about 25% of the bare charge, which can be attributed mainly to screening by counterions that are tightly bound to the microtubule surface.

Having developed an understanding of the steering mechanism of individual microtubules, we demonstrated the applicability of the electrical steering of microtubules in nanostructures by sorting a population of two different molecules on a chip (Fig. 4A, movie S1). To this end, we introduced a mixture of rhodamine- (red) and fluorescein-labeled (green) microtubules into our nanostructures. Using a color-sensitive camera, red microtubules approaching a Y junction were sent into the red-collecting reservoir and green microtubules into the green reservoir (Fig. 4B) by reversing the polarity of the electric field. After a series of successful single-molecule redirections, one reservoir contained predominantly red microtubules, whereas the other reservoir contained mainly green microtubules (Fig. 4A).

We quantified the sorting efficiency in Fig. 4C. A large fraction (72%) of the red microtubules approaching the junction were directed, as intended, into the red reservoir. Only 3% of the red microtubules incorrectly ended up in the green reservoir. The remainder of the red microtubules (25%) was steered into the perpendicular channel. A similar analysis was made for the green microtubules (69, 12, and 19%, respectively, Fig. 4C). The final result is that 91% of the microtubules sent into the left reservoir are red (136 out of 149), and 94% of the microtubules in the right reservoir are green (76 out of 81). Real use of this sorting method, e.g., for purification, will benefit from automation, which can be incorporated straightforwardly. The use of biomolecular motors for sorting forms an interesting alternative to existing pressure- or EOF-driven microfluidic devices (*32*–*34*) by which whole cells are sorted.

In conclusion, our experiments demonstrate the ability to electrically steer individual microtubules in enclosed submicron channels, as demonstrated by the single-molecule sorting of fluorescein- and rhodamine-labeled microtubules. The steering of microtubules is described in terms of force-induced bending of the free tip of the microtubule, which yields a persistence length $L_p = 0.16 \pm 0.09$ mm. Our single-microtubule electrophoresis experiments revealed an orientation-dependent electrophoretic

mobility and yield a charge of $12 \pm 2\ e^-$ per tubulin dimer under physiological conditions. This value may be important to elucidate the effect of in vivo electric forces on microtubules. Endogenous physiological electric fields, with a typical value up to 10^3 V/m, are shown to be involved in cell division, wound healing (*35*), and embryonic cell development (*36*), but their microscopic effect has so far not been understood. The application of biomotors in nanofabricated environments is an exciting development, offering novel possibilities for future developments in lab-on-chip sorting or purification applications.

References and Notes

1. R. K. Soong *et al.*, *Science* **290**, 1555 (2000).
2. F. Patolsky, Y. Weizmann, I. Willner, *Nat. Mater.* **3**, 692 (2004).
3. J. Xi, J. J. Schmidt, C. D. Montemagno, *Nat. Mater.* **4**, 180 (2005).
4. H. Hess, V. Vogel, *J. Biotechnol.* **82**, 67 (2001).
5. M. J. Schnitzer, S. M. Block, *Nature* **388**, 386 (1997).
6. K. J. Bohm, J. Beeg, G. M. zu Horste, R. Stracke, E. Unger, *IEEE Trans. Adv. Packag.* **28**, 571 (2005).
7. R. Yokokawa *et al.*, *Nano Lett.* **4**, 2265 (2004).
8. H. Hess, G. D. Bachand, V. Vogel, *Chemistry* **10**, 2110 (2004).
9. J. Clemmens *et al.*, *Langmuir* **19**, 10967 (2003).
10. S. G. Moorjani, L. Jia, T. N. Jackson, W. O. Hancock, *Nano Lett.* **3**, 633 (2003).
11. L. Jia, S. G. Moorjani, T. N. Jackson, W. O. Hancock, *Biomed. Microdevices* **6**, 67 (2004).
12. M. G. L. van den Heuvel, C. T. Butcher, S. G. Lemay, S. Diez, C. Dekker, *Nano Lett.* **5**, 235 (2005).
13. Y. Hiratsuka, T. Tada, K. Oiwa, T. Kanayama, T. Q. P. Uyeda, *Biophys. J.* **81**, 1555 (2001).
14. M. G. L. van den Heuvel, C. T. Butcher, R. M. M. Smeets, S. Diez, C. Dekker, *Nano Lett.* **5**, 1117 (2005).
15. S. Ramachandran, K. Ernst, G. D. Bachand, V. Vogel, H. Hess, *Small* **2**, 330 (2006).
16. R. Stracke, K. J. Bohm, L. Wollweber, J. A. Tuszynski, E. Unger, *Biochem. Biophys. Res. Commun.* **293**, 602 (2002).
17. Materials and methods are available as supporting information on *Science* Online.
18. At large fields, higher than ~110 kV/m, we observed an effect on the microtubule velocity along the electric field. Microtubules moving parallel to the electric field displayed higher and lower speeds depending on the direction of the field. For fields oriented perpendicular to the long axis, microtubules displayed sideward motion. We are investigating these effects.
19. T. Duke, T. E. Holy, S. Leibler, *Phys. Rev. Lett.* **74**, 330 (1995).
20. D. Stigter, *J. Phys. Chem.* **82**, 1417 (1978).
21. D. Stigter, C. Bustamante, *Biophys. J.* **75**, 1197 (1998).
22. The electrophoretic force on stationary microtubules in the absence of a bulk EOF consists of a direct force on the negative microtubule charge, $-|\sigma|\mathbf{E}$, and an opposing indirect friction, τ, exerted by the microtubule's counterions moving along the electric field. The velocity of the counterions increases from 0 at the microtubule surface to $|\mu_e|\mathbf{E}$. If $\lambda_D \ll R$, the magnitude of $\tau = +|\sigma|\mathbf{E} - c|\mu_e|\mathbf{E}$ and also equals the total force density exerted on the double layer, plus the drag force exerted on the moving counterions (*21*).
23. D. Stigter, *Biopolymers* **31**, 169 (1991).
24. The value of $g_\perp$ only depends on the ζ potential of a microtubule and the relative thickness of the double layer (λ_D) with respect to the cylinder radius a, i.e., $g_\perp = \Im(\zeta, a/\lambda_D)$, and numerical values have been tabulated (*20*). In the limit of infinitely small λ_D, $g_\perp$ reaches its maximum value of 1.5 and $\mu_{e,\perp} \rightarrow \mu_{e,\parallel}$. The experimentally determined value of $g_\perp$ is thus a measure of the ζ potential by $\zeta = \Im^{-1}(g_\perp, a/\lambda_D)$, using $a = 12.5$ nm and $\lambda_D = 0.8$ nm for the Debye length in our 160 mM buffer.
25. A. J. Hunt, F. Gittes, J. Howard, *Biophys. J.* **67**, 766 (1994).
26. We calculate $c_\perp$ using the analytical result from Hunt *et al*. (*25*) with the following numerical values: Microtubule radius $a = 12.5 \pm 1$ nm, viscosity $\eta = 0.89 \pm 0.09 \times 10^{-3}$ kg/ms, and $h = 30 \pm 10$ nm for the distance of the microtubule axis to the surface.
27. F. Gittes, B. Mickey, J. Nettleton, J. Howard, *J. Cell Biol.* **120**, 923 (1993).
28. H. Felgner, R. Frank, M. Schliwa, *J. Cell Sci.* **109**, 509 (1996).
29. For long microtubules and high kinesin density, the persistence length of the microtubule trajectory L_{tr} equals the persistence length of the tip L_p (*19*). This trajectory persistence length of microtubules in the absence of electric fields has been quantified to be 0.11 mm (*37*). Our value of the tip persistence length is close to this value. The suggestion of Kis *et al*. (*38*) that protofilament sliding reduces the stiffness of short lengths of microtubules could serve as a possible explanation of the low L_p, together with possible defects in the tip structure.
30. The use of the linear Grahame equation is strictly speaking only valid for $\zeta \ll k_BT/e = 26$ mV. However, at $\zeta = 50$ mV, the use of the linearized Grahame equation introduces an error in σ of only 14%. The use of the nonlinear version of the Grahame would invoke an unknown source of error, because we would then have to assume a value for the double-layer capacitance of the microtubule.
31. E. Nogales, S. G. Wolf, K. H. Downing, *Nature* **393**, 191 (1998).
32. P. S. Dittrich, P. Schwille, *Anal. Chem.* **75**, 5767 (2003).
33. A. Y. Fu, C. Spence, A. Scherer, F. H. Arnold, S. R. Quake, *Nat. Biotechnol.* **17**, 1109 (1999).
34. H. A. Stone, A. D. Stroock, A. Ajdari, *Annu. Rev. Fluid Mech.* **36**, 381 (2004).
35. B. Song, M. Zhao, J. V. Forrester, C. D. McCaig, *Proc. Natl. Acad. Sci. U.S.A.* **99**, 13577 (2002).
36. K. R. Robinson, L. F. Jaffe, *Science* **187**, 70 (1975).
37. T. Nitta, H. Hess, *Nano Lett.* **5**, 1337 (2005).
38. A. Kis *et al.*, *Phys. Rev. Lett.* **89**, 248101 (2002).

39. We thank J. Howard and S. Diez for kindly providing us with the kinesin expression vector and for advice with protocols; S. G. Lemay, I. Dujovne, and D. Stein for useful discussions; Y. Garini and Olympus Netherlands for lending optical equipment; and Hamamatsu Germany for kindly providing us a C7780 color camera. This work was funded by the Dutch Organization for Scientific Research (NWO) and the European Community Biomach program.

Supporting Online Material

www.sciencemag.org/cgi/content/full/312/5775/910/DC1
Materials and Methods
SOM Text
Figs. S1 and S2
References and Notes
Movie S1

23 December 2005; accepted 9 March 2006
10.1126/science.1124258

PIN Proteins Perform a Rate-Limiting Function in Cellular Auxin Efflux

Jan Petrášek,[1,2] Jozef Mravec,[3] Rodolphe Bouchard,[4] Joshua J. Blakeslee,[5] Melinda Abas,[6] Daniela Seifertová,[1,2,3] Justyna Wiśniewska,[3,7] Zerihun Tadele,[8] Martin Kubeš,[1,2] Milada Čovanová,[1,2] Pankaj Dhonukshe,[3] Petr Skůpa,[1,2] Eva Benková,[3] Lucie Perry,[1] Pavel Křeček,[1,2] Ok Ran Lee,[5] Gerald R. Fink,[9] Markus Geisler,[4] Angus S. Murphy,[5] Christian Luschnig,[6] Eva Zažímalová,[1]* Jiří Friml[3,10]

Intercellular flow of the phytohormone auxin underpins multiple developmental processes in plants. Plant-specific pin-formed (PIN) proteins and several phosphoglycoprotein (PGP) transporters are crucial factors in auxin transport–related development, yet the molecular function of PINs remains unknown. Here, we show that PINs mediate auxin efflux from mammalian and yeast cells without needing additional plant-specific factors. Conditional gain-of-function alleles and quantitative measurements of auxin accumulation in *Arabidopsis* and tobacco cultured cells revealed that the action of PINs in auxin efflux is distinct from PGP, rate-limiting, specific to auxins, and sensitive to auxin transport inhibitors. This suggests a direct involvement of PINs in catalyzing cellular auxin efflux.

Auxin, a regulatory compound, plays a major role in the spatial and temporal coordination of plant development (*1*–*3*). The directional active cell-to-cell transport controls asymmetric auxin distribution, which underlies multiple patterning and differential growth processes (*4*–*7*). Genetic approaches in *Arabidopsis thaliana* identified candidate genes coding for regulators of auxin transport, among them permease-like AUX1 (*8*), plant-specific PIN proteins (*9*) (fig. S1), and homologs of human multiple drug resistance transporters PGP1 and PGP19 (*10*, *11*). PGP1 has been shown to mediate the efflux of auxin from *Arabidopsis* protoplasts and heterologous systems such as yeast and HeLa cells (*12*). Similarly, PIN2 in yeast conferred decreased retention of structural auxin analogs (*13*, *14*). Plants defective in PIN function show altered auxin distribution and diverse developmental defects, all of which can be phenocopied by chemical inhibition of auxin efflux (*1*, *4*–*7*, *9*). All results demonstrate that PINs are essential components of the auxin transport machinery, but the exact mechanism of their action remains unclear.

Studies of the molecular function of PINs have been hampered mainly by the technical inability to quantitatively assess auxin flow across the plasma membrane (PM) in a multicellular system. We therefore established *Arabidopsis* cell suspension culture from the *XVE-PIN1* line, in which we placed the *PIN1* sequence under control of the estradiol-inducible promoter (*15*). Treatment with estradiol led to the activation of *PIN1* expression as shown by the coexpressed green fluorescent protein (GFP) reporter and reverse transcription polymerase chain reaction (RT-PCR) of *PIN1* in seedlings (Fig. 1A) and cultured cells (fig. S2). In estradiol-treated *XVE-PIN1* cells, the overexpressed PIN1 was localized at the PM (Fig. 1, B and C). The syn-

thetic auxin naphthalene-1-acetic acid (NAA) enters cells easily by diffusion and is a poor substrate for active uptake but an excellent substrate for active efflux (*16*). Therefore, change in accumulation of radioactively labeled NAA inside cells provides a measure of the rate of auxin efflux from cells. Untreated *XVE-PIN1* cells as well as nontransformed cells displayed [^{3}H]NAA accumulation kinetics indicative of saturable auxin efflux and sensitive to a well-established (*1*, *9*) noncompetitive inhibitor of auxin efflux: 1-naphthylphthalamic acid (NPA) (Fig. 1D). Estradiol did not influence control cells but led to substantial decrease of [^{3}H]NAA accumulation in *XVE-PIN1* cells (Fig. 1, D and E). This demonstrates that PIN1 overexpression leads to the stimulation of efflux of auxin from *Arabidopsis* cultured cells.

Arabidopsis cultured cells are not sufficiently friable to be useful in transport assays. Instead, we used tobacco BY-2 cells, a well-established model for quantitative studies of cellular auxin transport (*17*). PIN7, the most representative member of the subfamily including *PIN1*, *PIN2*, *PIN3*, *PIN4*, *PIN6*, and *PIN7* (fig. S1), was placed under the control of a dexamethasone (DEX)–inducible system (*18*) and stably transformed into BY-2 cells. The resulting line (*GVG-PIN7*) showed up-regulation of *PIN7* expression as early as 2 hours after DEX treatment and the up-regulated PIN7 protein was detected at the PM (Fig. 2A). Nontransformed cells displayed saturable, NPA-sensitive [^{3}H]NAA efflux, which was unaffected by DEX (Fig. 2B). Induction of expression of PIN7 or its close (PIN4) and the most distant (PIN6) homologs (fig. S1) resulted in a decrease in [^{3}H]NAA accumulation, to roughly half of the original level (Fig. 2C). The kinetics of NAA efflux after the initial loading of BY-2 cells (Fig. 2D), as well as displacement curves using competitive inhibition by nonlabeled NAA (fig. S3A), clearly confirm that PIN7 overexpression stimulates saturable efflux of auxin from cells. The efflux of other auxins—such as synthetic 2,4-dichlorophenoxyacetic acid (2,4-D) or naturally occurring indole-3-acetic acid (IAA), but not its precursor tryptophan—was also stimulated (Fig. 2, E and G). The PIN7-dependent efflux of all auxins was NPA sensitive (Fig. 2G), competitively inhibited by nonlabeled NAA, and unaffected by the structurally related but biologically inactive weak organic acid, benzoic acid (BeA) (fig. S3B). Furthermore, the increasing levels of induced PIN7, as achieved with the use of different concentrations of DEX for induction, and monitored by dot blot, clearly correlated with the gradual increase in [^{3}H]NAA efflux (Fig. 2F). These data imply that different PIN proteins are rate-limiting factors in NPA-sensitive, saturable efflux of auxins from BY-2 cells. This similarity in the molecular function of PINs, together with the diversity in their regulation, provides a basis for their complex functional redundancy observed in planta (*6*, *19*, *20*).

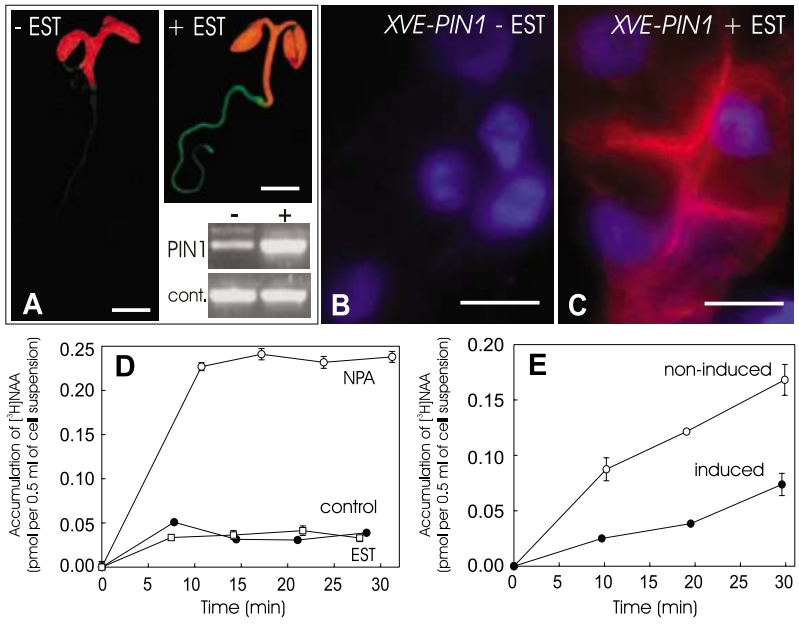

Fig. 1. PIN1-dependent auxin efflux in *Arabidopsis* cultured cells. (**A**) Up-regulation of PIN1 expression in *XVE-PIN1 Arabidopsis* seedlings after estradiol (EST) treatment (1 μM, 4 hours). The expression of coupled GFP reporter (green) and RT-PCR of *PIN1* [PGP19 expression was used as a control (cont.)] are shown. Scale bars, 3 mm. (**B** and **C**) Anti-PIN1 immunostaining (red) at the PM of *XVE-PIN1* cultured cells after EST treatment (1 μM, 24 hours) (C). There was no signal in the untreated control (B). Nuclear counterstain is shown in blue. Scale bars, 10 μm. (**D**) Auxin accumulation in *Arabidopsis* wild-type cells. NPA (10 μM) increased [^{3}H]NAA accumulation inside cells, demonstrating inhibition of auxin efflux. EST treatment (1 μM, 24 hours) had no effect on [^{3}H]NAA accumulation. (**E**) [^{3}H]NAA accumulation kinetics in *XVE-PIN1* cells, demonstrating PIN1-dependent stimulation of NAA efflux after PIN1 overexpression. Error bars show SEM (n = 4); where error bars are not shown, the error was smaller than the symbols.

The evidence from cultured cells shows that PIN proteins are key rate-limiting factors in cellular auxin efflux. This approach, however, cannot distinguish whether PINs play a catalytic role in auxin efflux or act as positive regulators of endogenous plant auxin efflux catalysts. To address this issue, we used a nonplant system: Human HeLa cells contain neither PIN-related genes nor auxin-related machinery and allow efficient heterologous expression of functional eukaryotic PM proteins (*21*). We transfected HeLa cells with *PIN7* and its more distant homolog *PIN2*. Transfected cells showed strong PIN expression (Fig. 3A), which resulted in a substantial stimulation of net efflux of natural auxin [^{3}H]IAA, compared with empty vector controls (Student's t test: $P < 0.001$) (Fig. 3B). Efflux of [^{3}H]BeA was also stimulated but to a lesser extent. These data show that PIN proteins are capable of stimulating cellular auxin efflux in the heterologous HeLa cell system, albeit with decreased substrate specificity.

To test the role of PIN proteins in another evolutionarily distant nonplant system, we used yeast (*Saccharomyces cerevisiae*). PIN2 and PIN7 were expressed in yeast and showed localization at the PM (Fig. 3A). Kinetics of relative [^{3}H]IAA retention demonstrated that expression of the PINs led to a substantial increase in IAA efflux (Fig. 3C). Efflux assays in conjunction with control experiments, including testing metabolically less active yeast in the stationary phase, or after glucose starvation (Fig. 3D), confirmed an active PIN-dependent export of IAA and, to a lesser extent, of BeA from yeast (Fig. 3C and fig. S4B). To test the requirements of the subcellular localization for PIN2 action in yeast, we performed a mutagenesis of the PIN2 sequence to isolate mistargeted mutants. One of the mutations, which changed serine-97 to glycine (pin2Gly97), led to the localization of pin2Gly97

[1]Institute of Experimental Botany, the Academy of Sciences of the Czech Republic, 165 02 Prague 6, Czech Republic. [2]Department of Plant Physiology, Faculty of Science, Charles University, 128 44 Prague 2, Czech Republic. [3]Center for Plant Molecular Biology (ZMBP), University Tübingen, D-72076 Tübingen, Germany. [4]Zurich-Basel Plant Science Center, University of Zurich, Institute of Plant Biology, CH 8007 Zurich, Switzerland. [5]Department of Horticulture, Purdue University, West Lafayette, IN 47907, USA. [6]Institute for Applied Genetics and Cell Biology, University of Natural Resources and Applied Life Sciences–Universität für Bodenkultur, A-1190 Wien, Austria. [7]Department of Biotechnology, Institute of General and Molecular Biology, 87-100 Toruń, Poland. [8]Institute of Plant Sciences, University of Bern, 3013 Bern, Switzerland. [9]Whitehead Institute for Biomedical Research, Nine Cambridge Center, Cambridge, MA 02142, USA. [10]Masaryk University, Department of Functional Genomics and Proteomics, Laboratory of Molecular Plant Physiology, Kamenice 5, 625 00 Brno, Czech Republic.

*To whom correspondence should be addressed. E-mail: eva.zazim@ueb.cas.cz

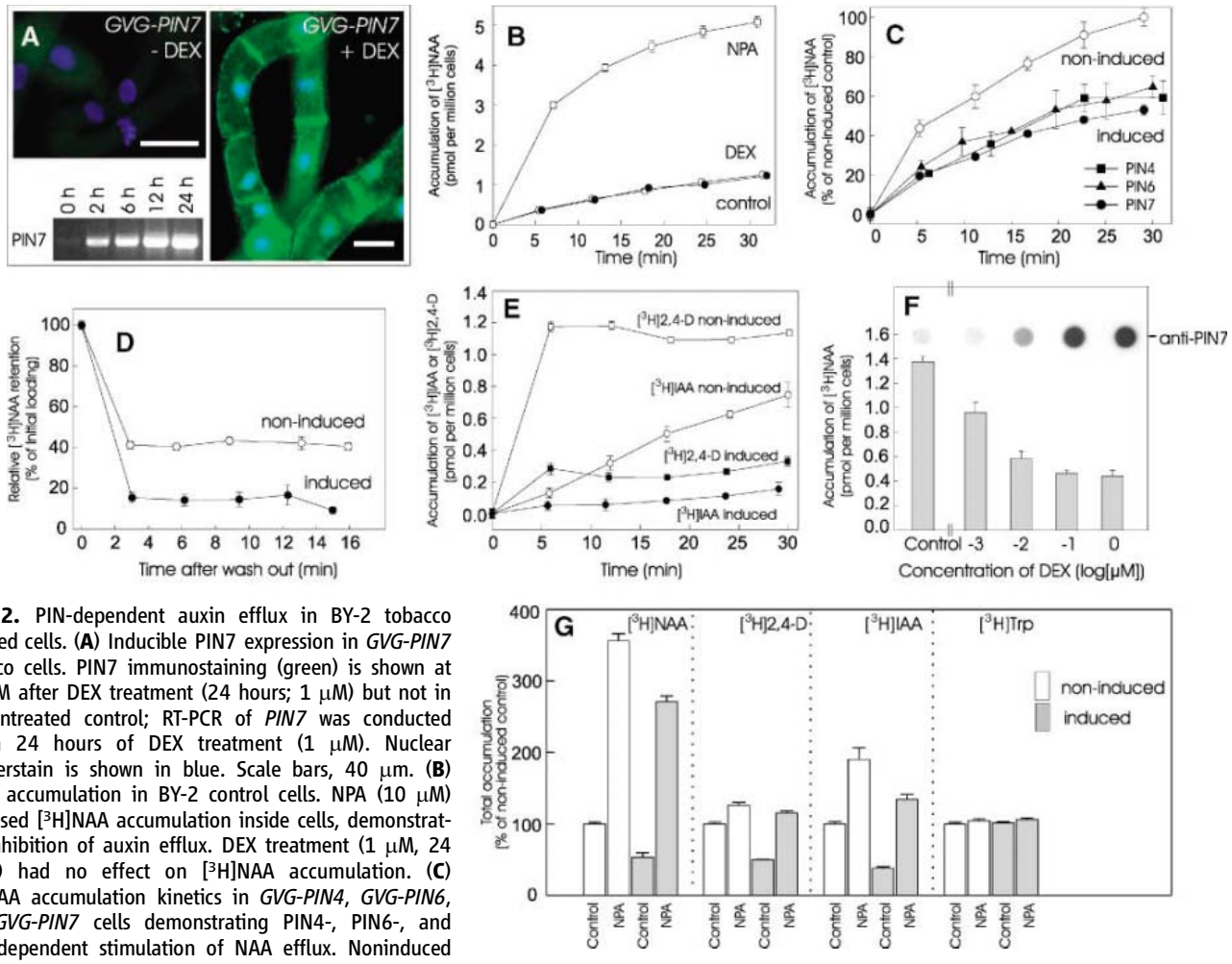

Fig. 2. PIN-dependent auxin efflux in BY-2 tobacco cultured cells. (**A**) Inducible PIN7 expression in *GVG-PIN7* tobacco cells. PIN7 immunostaining (green) is shown at the PM after DEX treatment (24 hours; 1 μM) but not in the untreated control; RT-PCR of *PIN7* was conducted within 24 hours of DEX treatment (1 μM). Nuclear counterstain is shown in blue. Scale bars, 40 μm. (**B**) Auxin accumulation in BY-2 control cells. NPA (10 μM) increased [^{3}H]NAA accumulation inside cells, demonstrating inhibition of auxin efflux. DEX treatment (1 μM, 24 hours) had no effect on [^{3}H]NAA accumulation. (**C**) [^{3}H]NAA accumulation kinetics in *GVG-PIN4*, *GVG-PIN6*, and *GVG-PIN7* cells demonstrating PIN4-, PIN6-, and PIN7-dependent stimulation of NAA efflux. Noninduced control is shown only for PIN7; those for PIN4 and PIN6 were within the range ±8% of the values for PIN7. Data are expressed as a percentage of noninduced control at 30 min after application of labeled [^{3}H]NAA. (**D**) Induced *GVG-PIN7* cells showed decreased retention of [^{3}H]NAA compared with noninduced control. (**E**) Accumulation kinetics in induced *GVG-PIN7* cells revealed PIN7-dependent stimulation of [^{3}H]IAA and [^{3}H]2,4-D efflux. (**F**) Treatments with increasing concentrations of DEX led to gradually higher levels of PIN7 in *GVG-PIN7* cells, as determined by dot blot (top) and to concomitant decrease of [^{3}H]NAA accumulation. (**G**) NPA inhibition of both endogenous and PIN7-dependent efflux of [^{3}H]NAA, [^{3}H]2,4-D, and [^{3}H]IAA. PIN7 overexpression or NPA treatment did not affect accumulation of related compound, [^{3}H]Trp. Open bars, noninduced cells; gray bars, induced cells. For all experiments, error bars show SEM (n = 4); where error bars are not shown, the error was smaller than the symbols.

in intracellular compartments (Fig. 3A). When tested in the [^{3}H]IAA efflux assay (fig. S4A), pin2Gly97 failed to mediate auxin efflux but rather increased [^{3}H]IAA accumulation inside cells (Fig. 3D). This shows that pin2Gly97 is still functional but fails to mediate auxin efflux, suggesting importance of PIN localization at PM. Overall, the results suggest that in yeast as well, PM-localized PIN proteins mediate, although with decreased specificity, a saturable efflux of auxin.

A role in auxin efflux has also been reported recently for PGP1 and, in particular, PGP19 proteins of *Arabidopsis* (*12*). PIN and PGP proteins seem to have a comparable effect on mediating auxin efflux in yeast and HeLa cells, but the genetic interference with their function in *Arabidopsis* has distinctive effects on development. All aspects of the *pin* mutant phenotypes can be mimicked by chemical interference with auxin transport (*4*–*7*, *9*). In contrast, *pgp1*/*pgp19* double mutants show strong but entirely different defects (*10*, *11*), which cannot be phenocopied by auxin transport inhibitors.

To compare the roles of PINs and PGPs in auxin efflux, we constructed the *GVG-PGP19:HA* (hemagglutinin) cell line of BY-2. DEX treatment led to the up-regulation of PGP19:HA protein, which was detected at the PM (Fig. 4A), and to a decrease in [^{3}H]NAA accumulation, similar to that observed in the *GVG-PIN4*, *GVG-PIN6*, and *GVG-PIN7* lines (Fig. 4B, compare with Fig. 2C). BeA did not interfere with [^{3}H]NAA accumulation and [^{3}H]Trp accumulation did not change after DEX treatment. However, compared with PIN-mediated auxin efflux, the PGP19-mediated NAA efflux was notably less sensitive to NPA. Whereas PIN-mediated transport was completely inhibited by NPA, about 20% of PGP19-dependent transport was NPA insensitive (Fig. 4C).

To address whether PIN action in planta requires PGP1 and PGP19 proteins, we analyzed effects of PIN1 overexpression on plant development in *pgp1*/*pgp19* double mutants. PIN1 overexpression in *XVE-PIN1* led to pronounced defects in root gravitropism, which could be detected within 4 hours after estradiol treatment. Quantitative evaluation of reorientation of root growth revealed that PIN1 overexpression in *pgp1*/*pgp19* had the same effects (Fig. 4D). These data show that PIN1 action on plant development does not strictly require function of PGP1 and PGP19 proteins, and they suggest that PINs and PGPs molecularly characterize distinct auxin transport systems. This is also supported by evidence that PIN2 mediates auxin efflux in yeast, which is known to lack homologs to *Arabidopsis* PGP proteins (*21*). It is still unclear whether these two auxin transport machineries act in planta entirely independently or in a coordinated fashion.

Rate-limiting, saturable, and specific action of PIN proteins in mediating auxin movement

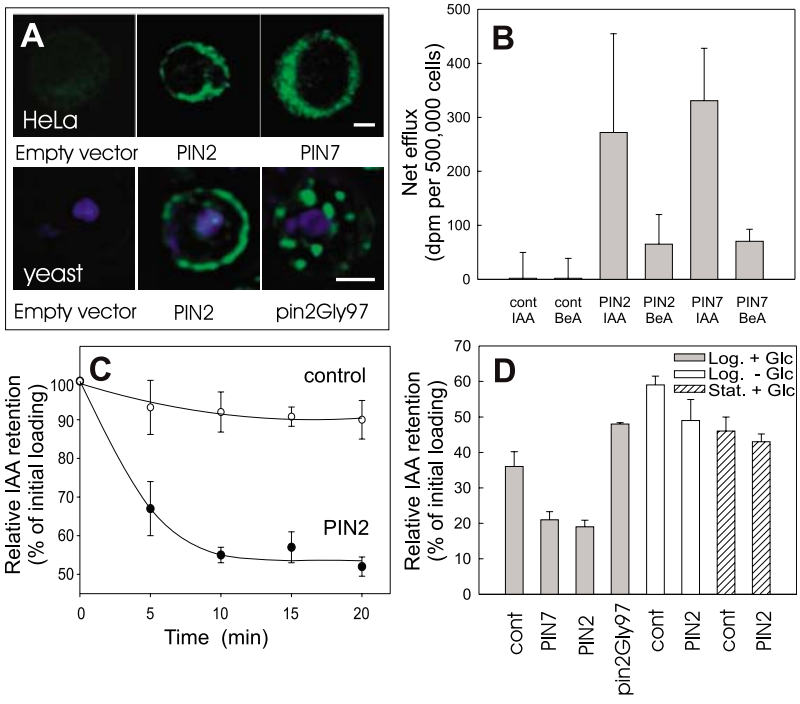

Fig. 3. PIN-dependent auxin efflux in mammalian and yeast cells. (**A**) PIN2:HA and PIN7:HA expression in HeLa and yeast. Anti-HA immunostaining detected PIN2:HA and PIN7:HA at the PM of transfected but not control (empty vector) HeLa cells (top). Anti-PIN2 immunostaining detected PIN2 at the PM and pin2Gly97 in intracellular compartments, compared with empty vector controls (bottom). Scale bars, 2 μm. (**B**) Transfected HeLa cells display PIN2- and PIN7-dependent net efflux of [^{3}H]IAA and to a smaller extent also of [^{3}H]BeA. dpm, disintegration per minute. (**C**) The kinetics of [^{3}H]IAA efflux. PIN2 stimulated saturable [^{3}H]IAA efflux in yeast JK93da strain. (**D**) [^{3}H]IAA retention measured 10 min after loading: PIN2 and PIN7 mediated [^{3}H]IAA efflux; pin2Gly97 failed to mediate efflux but increased [^{3}H]IAA retention. Yeast in stationary phase or without glucose showed much less [^{3}H]IAA efflux. Error bars show SEM (n = 4).

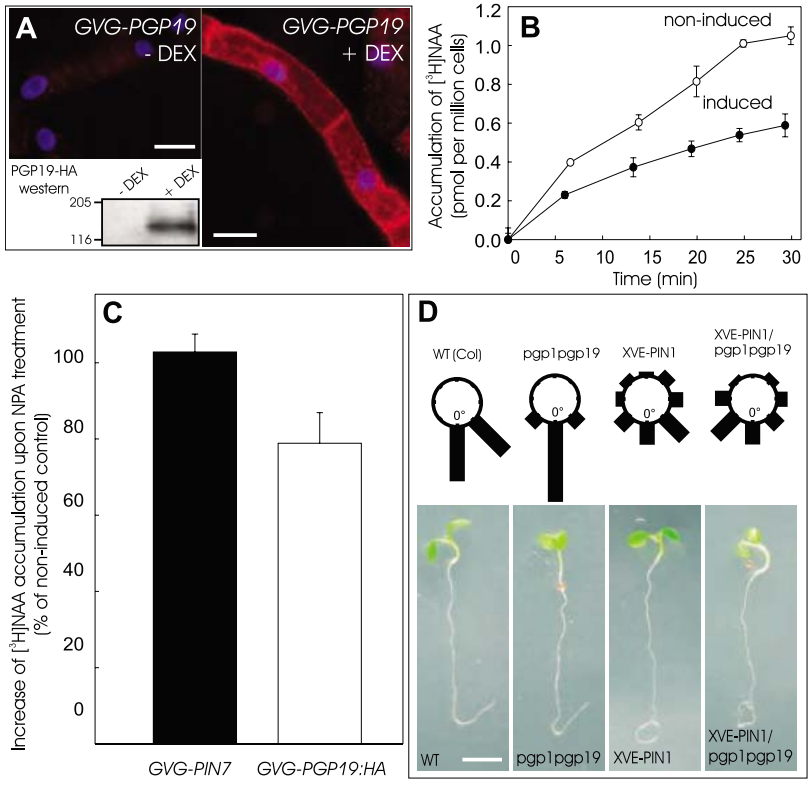

Fig. 4. Requirement of PGP function for PIN role in auxin efflux. (**A**) Inducible PGP19 expression in *GVG-PGP19:HA* tobacco cells. PGP19:HA immunostaining (red) at PM after DEX treatment (24 hours, 1 μM) is shown; no PGP19:HA immunostaining was present in the untreated control. An anti-HA immunoblot was conducted after 24 hours of DEX (1 μM) treatment. Nuclear counterstain is shown in blue. Scale bars, 40 μm. (**B**) [^{3}H]NAA accumulation decreased upon PGP19 expression, revealing function in auxin efflux in BY-2 cells. (**C**) Different sensitivities of PIN7- and PGP19-dependent [^{3}H]NAA efflux to NPA treatment (10 μM, 20 min) in *GVG-PIN7* and *GVG-PGP19:HA* cells (*23*). (**D**) Root gravitropism in *XVE-PIN1* seedlings. PIN1 overexpression (4 hours, 4 μM EST) led to gravitropic defects in *pgp1/pgp19* mutants in contrast to gravitropic growth of EST-treated nontransformed wild-type (WT) and *pgp1/pgp19* seedlings. Root gravitropism was scored 12 hours after gravity stimulation (n > 40). Scale bar, 3 mm. For (B) and (C), error bars show SEM (n = 4); where error bars are not shown, the error was smaller than the symbols.

across the PM out of plant cells largely clarifies a role of PIN proteins in intercellular auxin transport. Furthermore, the polar, subcellular PIN localization provides a vectorial component to the directional auxin flow (*22*). Therefore, transport function of PINs together with their asymmetric subcellular localization defines directional local auxin distribution underlying different developmental processes.

References and Notes

1. J. Friml, *Curr. Opin. Plant Biol.* **6**, 7 (2003).
2. A. W. Woodward, B. Bartel, *Ann. Bot. (Lond.)* **95**, 707 (2005).
3. S. Kepinski, O. Leyser, *Curr. Biol.* **15**, R208 (2005).
4. J. Friml, J. Wisniewska, E. Benková, K. Mendgen, K. Palme, *Nature* **415**, 806 (2002).
5. J. Friml *et al.*, *Cell* **108**, 661 (2002).
6. J. Friml *et al.*, *Nature* **426**, 147 (2003).
7. E. Benková *et al.*, *Cell* **115**, 591 (2003).
8. M. Bennett *et al.*, *Science* **273**, 948 (1996).
9. I. A. Paponov, W. D. Teale, M. Trebar, I. Blilou, K. Palme, *Trends Plant Sci.* **10**, 170 (2005).
10. B. Noh, A. S. Murphy, E. P. Spalding, *Plant Cell* **13**, 2441 (2001).
11. J. J. Blakeslee, W. A. Peer, A. S. Murphy, *Curr. Opin. Plant Biol.* **8**, 494 (2005).
12. M. Geisler *et al.*, *Plant J.* **44**, 179 (2005).
13. R. Chen, *Proc. Natl. Acad. Sci. U.S.A.* **95**, 15112 (1998).
14. C. Luschnig, R. A. Gaxiola, P. Grisafi, G. R. Fink, *Genes Dev.* **12**, 2175 (1998).

15. J. Zuo, Q. W. Niu, N. H. Chua, *Plant J.* **24**, 265 (2000).
16. A. Delbarre, P. Muller, V. Imhoff, J. Guern, *Planta* **198**, 532 (1996).
17. J. Petrášek *et al.*, *Plant Physiol.* **131**, 254 (2003).
18. T. Aoyama, N. H. Chua, *Plant J.* **11**, 605 (1997).
19. I. Blilou, *Nature* **433**, 39 (2005).
20. A. Vieten *et al.*, *Development* **132**, 4521 (2005).
21. M. Geisler, A. S. Murphy, *FEBS Lett.* **580**, 1094 (2006).
22. J. Wiśniewska, *Science* **312**, 883 (2006).
23. Materials and methods are available as supporting material on *Science* Online.
24. We thank N. H. Chua for providing material, V. Croy for help with HeLa studies, and P. Brewer and M. Sauer for critical reading of the manuscript. This work was supported by the European Molecular Biology Organization Young Investigator programme (J.F.), the Volkswagenstiftung (J.F., J.M., D.S., P.D.), the Grant Agency of the Academy of Sciences of the Czech Republic, project A6038303 (E.Z., M.Č., M.K., P.K., J.P., L.P., D.S., and P.S.), the Ministry of Education of the Czech Republic, projects MSM0021622415 and LC06034, the Alexander von Humboldt Foundation (Feodor Lynen fellowship to M.G.), the Foundation for Polish Science (J.W.), Margarete von Wrangell-Habilitationsprogramm (E.B.), NSF grant 0132803 (A.M., J.B., and O.L.), and Austrian Science Fund (FWF) grant 16311 (L.A. and C.L).

Supporting Online Material
www.sciencemag.org/cgi/content/full/1123542/DC1
Materials and Methods
Figs. S1 to S4
References

7 December 2005; accepted 14 March 2006
Published online 6 April 2006;
10.1126/science.1123542
Include this information when citing this paper.

Oceanographic Basis of the Global Surface Distribution of *Prochlorococcus* Ecotypes

Heather A. Bouman,[1]* Osvaldo Ulloa,[1] David J. Scanlan,[3] Katrin Zwirglmaier,[3] William K. W. Li,[4] Trevor Platt,[4] Venetia Stuart,[5] Ray Barlow,[6] Ole Leth,[2] Lesley Clementson,[7] Vivian Lutz,[8] Masao Fukasawa,[9] Shuichi Watanabe,[9] Shubha Sathyendranath[5]

By using data collected during a continuous circumnavigation of the Southern Hemisphere, we observed clear patterns in the population-genetic structure of *Prochlorococcus*, the most abundant photosynthetic organism on Earth, between and within the three Southern Subtropical Gyres. The same mechanisms that were previously invoked to account for the vertical distribution of ecotypes at local scales accounted for the global (horizontal) patterns we observed. Basin-scale and seasonal variations in the structure and strength of vertical stratification provide a basis for understanding large-scale horizontal distribution in genetic and physiological traits of *Prochlorococcus*, and perhaps of marine microbial communities in general.

Prochlorococcus is the smallest and most abundant phytoplankter in the global ocean and contributes significantly to the primary productivity of tropical and subtropical oceans (*1*). That the genus thrives throughout a wide range of photic zone conditions has been explained by the discovery of genetically and physiologically distinct populations, commonly referred to as high light (HL)– and low light (LL)–adapted ecotypes (*2*). *Prochlorococcus* ecotypes partition themselves according to depth in a stratified water column (*3*); however, the coexistence of multiple ecotypes (*2*) and phylotypes (*4*–*6*) has also been reported and attributed to vertical mixing in response to local physical forcing. But the effect of physical forcing on *Prochlorococcus* ecotypes at the global scale has not been explored. By using data collected during a circumnavigation of the Southern Hemisphere, we investigated whether the genetic structure of *Prochlorococcus* populations changes in response to vertical mixing within and between the major ocean basins of the world.

Samples were collected during the Blue Earth Global Expedition (BEAGLE) (Fig. 1A). The 7-month expedition spanned the southern Pacific (winter), Atlantic (late spring), and Indian (summer) Oceans (*7*); covered several biogeochemical provinces (*8*); and provided a rare opportunity to study physical forcing of phytoplankton at the global scale. We used the depth of the surface mixed layer (z_m) and the strength of the vertical density gradient (N) as indicators of the physical state of the water column (*9*). The three ocean basins differed markedly in these properties (Fig. 1B). The basin-scale variations in the vertical structure of the water column observed in the BEAGLE data are partly due to seasonal and latitudinal differences in the sampling of the three ocean basins. Mixed-layer–depth climatology reveals strong seasonality in z_m, with high values of z_m occurring during the Austral winter in all three ocean basins, and relatively uniform and shallow z_m values in the summer months (fig. S1). However, differences among basins are also found. Thus, spatial differences in vertical mixing as indexed by z_m observed during the BEAGLE have a seasonal as well as a geographical component.

Prochlorococcus cell abundance was determined by flow cytometry, and the concentration of divinyl chlorophyll a (DV Chla), a pigment marker for this genus, was measured by high performance liquid chromatography (HPLC). A clear difference between the geographic patterns of these two indices of abundance was found (Fig. 2A). *Prochlorococcus* abundance has a minimum in the well-mixed, mesotrophic waters of the Western Pacific Basin and a maximum in the strongly stratified oligotrophic waters of the Indian Ocean, a pattern that is consistent with our current understanding of the distribution of this genus (*1*, *10*, *11*). However, the concentration of divinyl chlorophyll a is high in the Pacific Basin (except near 140°W) and low in the Atlantic and Indian Basins. This is perhaps counterintuitive; it can be explained as follows. Because all samples were collected within the top 10 m of the water column, vertical mixing would be an important mechanism altering the growth conditions (light and nutrients) of the phytoplankton cells. Thus, the high divinyl chlorophyll a concentrations in the Pacific may arise from photoacclimatory (physiological) or photoadaptive (genetic) response of the cells to a decrease in mean light intensity. Basin-scale patterns in the intracellular concentration of divinyl chlorophyll a (C_i) for *Prochlorococcus* are evident (Fig. 2B), with low C_i values observed in the strongly stratified Indian Ocean during the summer (averaging 0.14 fg DV Chla per cell), consistent with those found in the surface waters of the subtropical North Atlantic (*12*), and high values observed in the well-mixed Archipelagic Deep Basins Province (*8*) during the winter (averaging 1.00 fg DV Chla per cell), similar to those typically found deeper in the water column in subtropical gyres (*12*).

Because light decreases exponentially with depth, phytoplankton cells mixed deeper in the water column would experience a lower mean daily irradiance than if they remained at the sea surface. Phytoplankton respond to this reduction in irradiance by increasing the concentration of pigment per cell. An inverse relation between C_i

[1]Laboratorio de Procesos Oceanográficos y Clima, Departamento de Oceanografía, and Centro de Investigación Oceanográfica en el Pacífico Sur-Oriental, [2]Departamento de Geofísica, Universidad de Concepción, Casilla 160-C, Concepción, Chile. [3]Department of Biological Sciences, University of Warwick, Coventry CV4 7AL, UK. [4]Bedford Institute of Oceanography, Dartmouth, Nova Scotia, B2Y 4A2, Canada. [5]Department of Oceanography, Dalhousie University, Halifax, Nova Scotia, B3H 4J1, Canada. [6]Marine and Coastal Management, Private Bag X2, Rogge Bay 8012, Cape Town, South Africa. [7]Commonwealth Scientific and Industrial Research Organization, Marine Research, Post Office Box 1538, Hobart, Tasmania, Australia, 7001. [8]Instituto Nacional de Investigación y Desarrollo Pesquero, Paseo Victoria Ocampo 1, 7600 Mar del Plata, Argentina. [9]Japan Agency for Marine-Earth Science and Technology, 2-15, Natsushima, Yokosuka, 237-0061, Japan.

*To whom correspondence should be addressed. E-mail: heather@profc.udec.cl

and daily mean irradiance in the mixed layer ($\bar{I}_m$) was seen (Fig. 3A), consistent with the physiological response of *Prochlorococcus* in culture experiments (*13*). The ratio of the sum of photoprotective accessory pigments to the sum of both photoprotective and photosynthetic accessory pigments (*D*) can also be used as an index of the response of the phytoplankton community to ambient light conditions and has been shown to be strongly correlated with available irradiance within the mixed layer (*14*). Again, this pigment index is significantly correlated with C_i (Fig. 3B).

The cellular properties of *Prochlorococcus*, in particular cell fluorescence, have been known to change in response to vertical mixing (*15*). Thus, in the absence of genetic information, the relationship between the C_i and vertical mixing could be interpreted as simply the response of a single genotype to changes in light history. But vertical variation in both cell fluorescence and C_i has also been associated with a change in genotype (*3*, *12*). In fact, the unique fluorescence properties of surface and deep populations of *Prochlorococcus* led to the isolation and identification of HL and LL ecotypes (*2*).

Culture experiments have shown that HL ecotypes have optimal growth rates at higher irradiance levels than their LL counterparts (*13*). Pronounced differences in the regulation of light harvesting between HL and LL ecotypes have also been observed (*16*). Genomic comparison between HL- and LL-adapted strains of *Prochlorococcus* has shown that the HL strain has a photolyase gene, which serves to repair ultraviolet damage, and which is absent in the LL-adapted strain (*17*). Both culture experiments and genomic analysis have revealed that HL ecotypes must exclusively rely on reduced forms of nitrogen, whereas several LL ecotypes can use both nitrite and ammonium (*17*, *18*). The relatively high nitrite concentration and low mean irradiance in the Pacific Basin caused by seasonal mixing, compared with those of the Atlantic and Indian Oceans (Fig. 4A), imply conditions resembling those found at depth in stratified water columns. Thus, we would anticipate major differences in the population genetic structure of *Prochlorococcus*

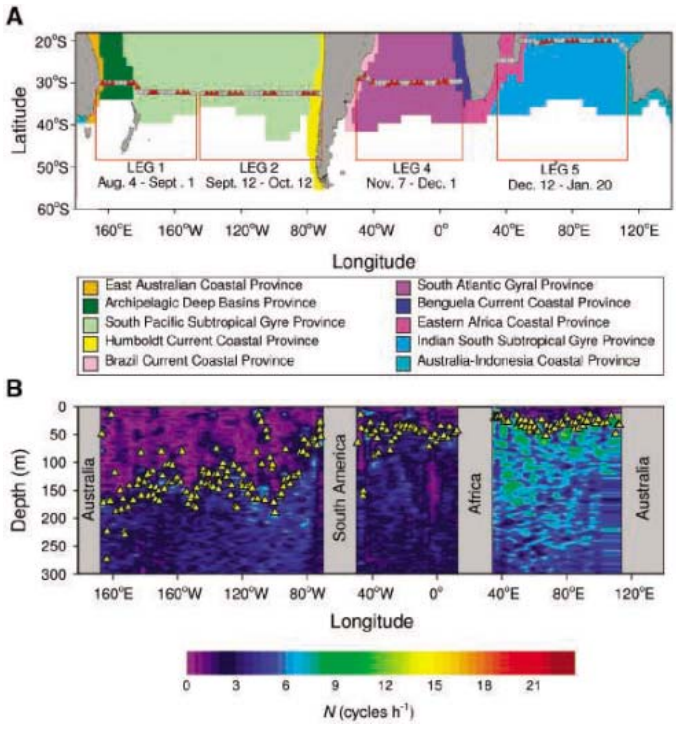

Fig. 1. (**A**) Map of the biological sampling stations for the BEAGLE and the biogeochemical provinces defined by Longhurst (*8*). The gray dots indicate routine sampling stations where all regular biological and physicochemical data were obtained. The red triangles represent stations from which DNA samples were used for dot blot hybridization analysis; each analysis was done on combined samples of three stations. (**B**) Contour plot of the strength of the vertical density gradient index, *N* (*9*), with corresponding estimates of the depth of the mixed layer (z_m) using conductivity-temperature-depth (CTD) density profiles represented by the yellow triangles. Values of the maximum observed *N* for the water column (N_m) for the Indian Ocean were high, averaging 14.2 ± 3.45 cycles per hour, whereas in the Pacific and Atlantic Basins, average values of N_m were 7.3 ± 1.70 and 8.9 ± 2.29 cycles per hour, respectively. The average (±1 SD) z_m in the Pacific, Atlantic, and Indian Ocean Basins were 126 ± 46.1 m, 52.1 ± 26.3 m, and 29.5 ± 9.3 m, respectively.

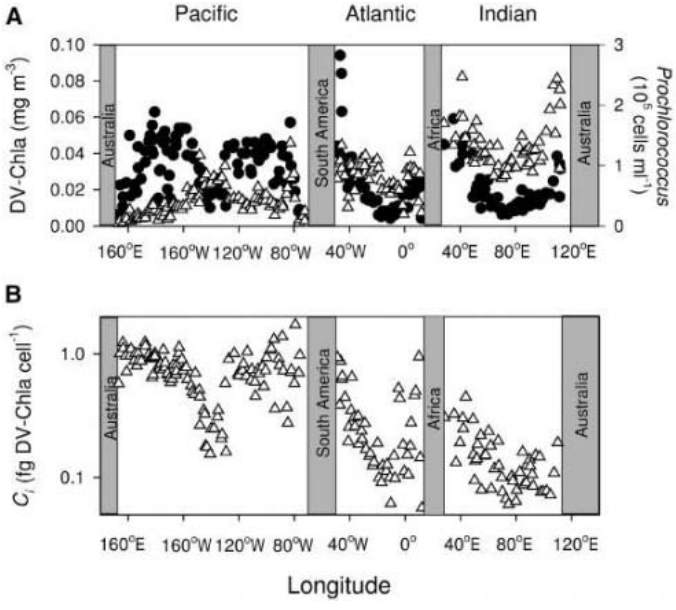

Fig. 2. (**A**) Distribution of divinyl chlorophyll a (DV Chla) concentration and cell abundance; the black dots indicate the concentration of divinyl chlorophyll a and the open triangles indicate the *Prochlorococcus* abundance. (**B**) The intracellular concentration of divinyl chlorophyll a (C_i). All samples were collected within the top 10 m of the water column.

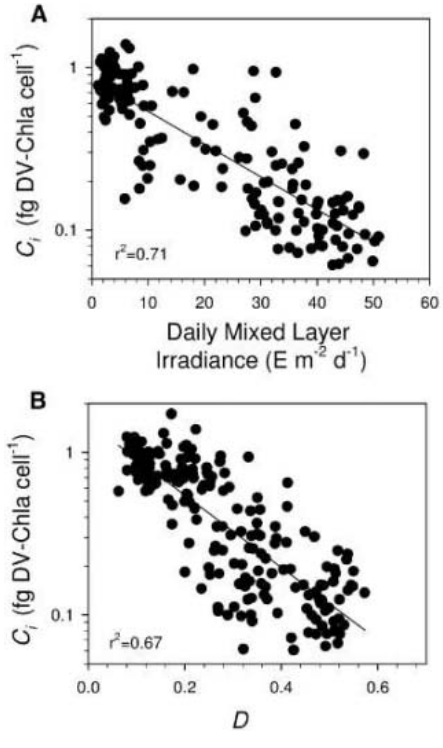

Fig. 3. Relationship between the intracellular concentration of divinyl chlorophyll a (C_i) for *Prochlorococcus*. (**A**) The average daily irradiance within the mixed layer ($\bar{I}_m$) and (**B**) the ratio of the sum of the concentration of photoprotective pigments to the total pigment concentration (*D*) for samples collected during the BEAGLE expedition.

between the three ocean basins as a result of changes in vertical mixing.

To test this expectation, polymerase chain reaction (PCR) amplified oxygenic phototroph 16S ribosomal DNA (rDNA) sequences derived from environmental DNA were hybridized with genotype-specific oligonucleotide probes (*3*, *19*) designed to detect the two HL adapted clusters (HLI and HLII), the LL adapted strains, and the specific LL adapted genotype SS120 (fig. S2). This method has been shown to yield similar results to those obtained using quantitative PCR (qPCR) (*20*). The analysis was conducted on surface samples selected to cover a broad range in the C_i and mixing conditions. To ensure ample DNA for the dot blot hybridization analysis, filters from three alternate stations were combined (Fig. 1A).

Prochlorococcus probes hybridized faintly but significantly at stations located at the edge of the Pacific Basin and more strongly in the central Pacific, Atlantic, and Indian Oceans (Fig. 4B). This pattern reflects changes in the relative contribution of *Prochlorococcus* to the total phytoplankton biomass, which can also be represented by the ratio of the concentration of divinyl chlorophyll a, a pigment found exclusively in *Prochlorococcus*, to the sum of the concentration of divinyl and monovinyl chlorophyll a (DV Chla/TChla) (Fig. 4B). At the eastern and western Pacific Basin, where nutrient concentrations were high because of winter mixing, we found a low percent hybridization and DV Chla/TChla, revealing high concentrations of *Synechococcus* and eukaryotic picoplankton (fig. S3), whereas *Prochlorococcus* cell abundance decreased.

Several factors may contribute to the observed distribution of *Prochlorococcus*. First, under strong vertical mixing, *Prochlorococcus* is believed to have limited ability for chromatic adaptation, compared with that of *Synechococcus* (*21*). Furthermore, the higher chlorophyll concentrations in nitrate-rich regions also result in a light field rich in green photons, which the accessory pigments in *Synechococcus* cells absorb preferentially (*21*). Second, no known strain of *Prochlorococcus* is able to use nitrate, a nutrient associated with mixed waters (*17*, *18*). Third, vertical mixing reduces the temperature of surface waters, which may affect the relative contribution of *Prochlorococcus* to total biomass, given that the dominant ecotypes of *Prochlorococcus* achieve their temperature optimal for growth at ~25°C (*22*).

Our observations harmonized with these expectations. For example, we found the abundance of HLII was positively correlated with *D*, $\overline{I}_m$, and temperature, but negatively associated with the concentration of nitrite and phosphate (table S1). At lower temperatures, LL was less abundant. However, the abundance of other *Prochlorococcus* genotypes (HLI and SS120) was related only weakly to the covariates of physical forcing. Our results also revealed that within the LL and HL groupings there is further niche partitioning among genotypes. For example, HLII dominates in surface waters of regions with high stratification (Indian Ocean), whereas HLI is more prevalent in surface waters with moderate stratification and mixed-layer depth (middle of the Pacific Basin and Atlantic Basin). By contrast, LL and SS120 disassociate, which may be explained in part by the inability of SS120 to use nitrite (*23*), whereas several LL-adapted strains can use this form of nitrogen (*18*).

The influence of vertical mixing on the population structure of *Prochlorococcus* becomes clear when we examine the relative proportions of HL and LL ecotypes occurring in the three ocean basins (Fig. 4C). In the well-mixed Pacific Basin, relative hybridization for HL and LL genotypes is similar. In contrast, in the Atlantic Basin hybridization showed greater abundance of HL compared with LL. This is accentuated in the highly stratified Indian Ocean, where HL ecotypes dominate over their LL counterparts, with HLII genotypes being particularly abundant. However, the highly stratified, summer conditions present in the Indian Ocean would likely result in a dominance of LL ecotypes near the base of the photic zone (*3*, *12*, *22*). One could argue that the high relative abundance of LL ecotypes in the Pacific is the result of resuspension of cells from depth toward the sea surface. However, given that *Prochlorococcus* division rates are on the order of 1 day, and given that the samples were collected in August, which was months after the initiation of deep winter mixing and after the maximum in mixed-layer depth (fig. S1), the population structure of *Prochlorococcus* is likely the result of a successional change to environmental conditions.

In the surface ocean, the occurrence of the LL ecotype appears to be significantly correlated not only with temperature, but also with $\overline{I}_m$ and *D*. The abundances of the ecotypes are correlated positively (LL) and negatively (HLII) with phos-

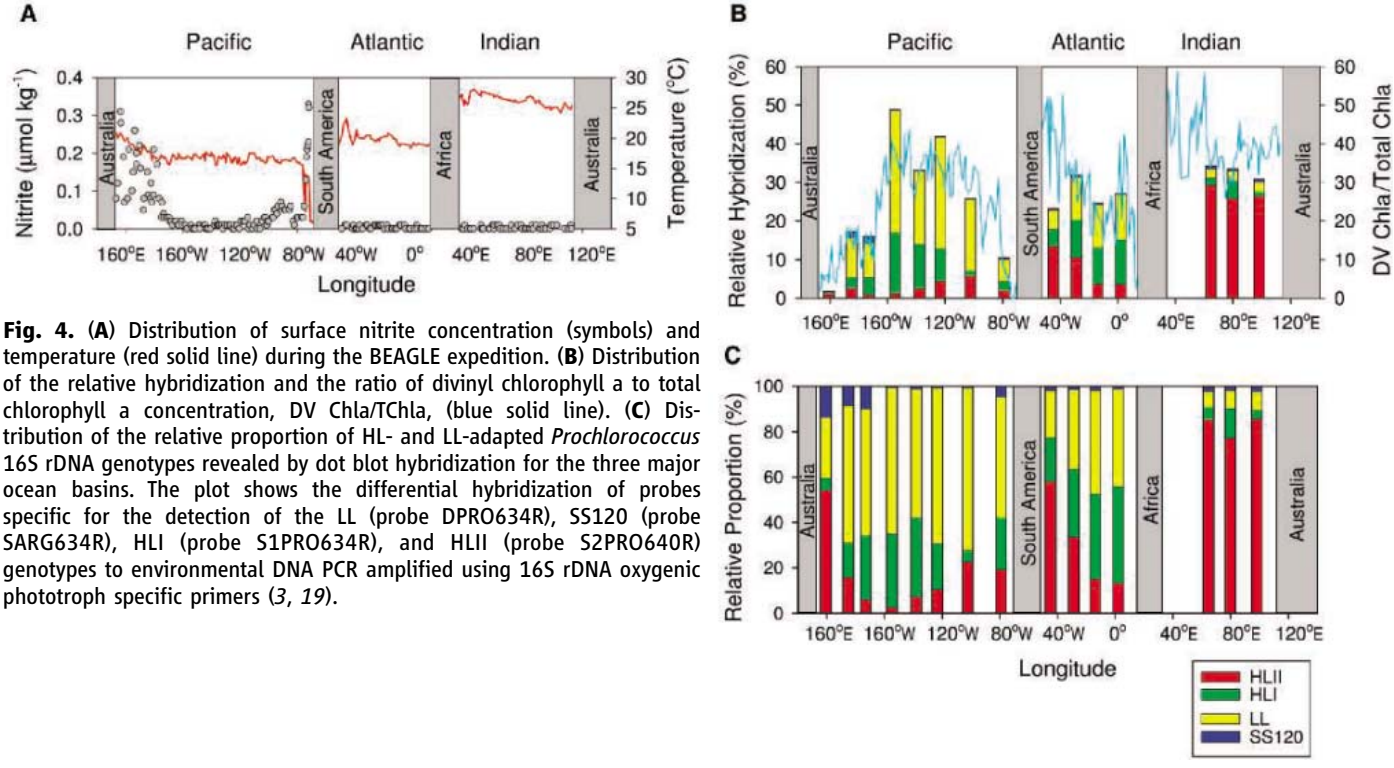

Fig. 4. (**A**) Distribution of surface nitrite concentration (symbols) and temperature (red solid line) during the BEAGLE expedition. (**B**) Distribution of the relative hybridization and the ratio of divinyl chlorophyll a to total chlorophyll a concentration, DV Chla/TChla, (blue solid line). (**C**) Distribution of the relative proportion of HL- and LL-adapted *Prochlorococcus* 16S rDNA genotypes revealed by dot blot hybridization for the three major ocean basins. The plot shows the differential hybridization of probes specific for the detection of the LL (probe DPRO634R), SS120 (probe SARG634R), HLI (probe S1PRO634R), and HLII (probe S2PRO640R) genotypes to environmental DNA PCR amplified using 16S rDNA oxygenic phototroph specific primers (*3*, *19*).

phate concentration, whereas the relationship between nitrite and these ecotypes is markedly weaker (table S1). The differences we observe in the BEAGLE data can be explained by the presence of organic forms of phosphorus in the surface oligotrophic water and high concentrations of inorganic forms occurring at depth. Physiological differences in both phosphorus (P) uptake and in the P stress response, as well as differences in genes implicated in P acquisition and regulation have been reported in various *Prochlorococcus* genotypes (*24*).

We have provided evidence that the relative abundance of surface *Prochlorococcus* ecotypes is related to changes in vertical mixing across the three major ocean basins of the Southern Hemisphere. In particular, we have found associations among the phenotypic (C_i) and genotypic (HL:LL relative abundance) attributes of *Prochlorococcus* with water column stability, the mean irradiance in the mixed layer, and photoacclimation across the entire breadth of the Southern Hemisphere. Based on seasonal climatology of the three ocean basins, one would anticipate that changes in ecotypes would also occur over an annual cycle at a given place due to seasonal changes in physical forcing. It is probable that the relation between genotype, light, and vertical mixing is characteristic not only of the smallest of ocean microbiota, but also of the phytoplankton community in general (*25*, *26*). Our findings may help explain some of the known phytoplanktonic community response (size structure and taxonomic composition) to changes in physical forcing (*27*–*30*), as well as emerging patterns in the global distribution of marine microorganisms (*31*, *32*), and even genes (*33*), in the upper ocean.

References and Notes

1. F. Partensky, W. R. Hess, D. Vaulot, *Microbiol. Mol. Biol. Rev.* **63**, 106 (1999).
2. L. R. Moore, G. Rocap, S. W. Chisholm, *Nature* **393**, 464 (1998).
3. N. J. West, D. J. Scanlan, *Appl. Environ. Microbiol.* **65**, 2585 (1999).
4. B. Palenik, *Appl. Environ. Microbiol.* **60**, 3212 (1994).
5. M. J. Ferris, B. Palenik, *Nature* **396**, 226 (1998).
6. E. Urbach, S. Chisholm, *Limnol. Oceanogr.* **43**, 1615 (1998).
7. H. Uchida, M. Fukasawa, Eds., *WHP P6, I3/I4 Revisit Data Book Blue Earth Global Expedition 2003* (JAMSTEC, Yokosuka, Kanagawa, 2005).
8. A. Longhurst, *Ecological Geography of the Sea* (Academic Press, San Diego, 1998).
9. Materials and methods are available as supporting material on *Science* Online.
10. F. Partensky, J. Blanchot, D. Vaulot, *Bull. Inst. Oceanogr. Monaco* **19**, 457 (1999).
11. W. K. W. Li, in *Marine Macroecology*, J. Witman, K. Roy, Eds. (Univ. Chicago Press, in press).
12. M. J. W. Veldhuis, G. W. Kraay, *Deep Sea Res.* **51**, 507 (2004).
13. L. R. Moore, S. W. Chisholm, *Limnol. Oceanogr.* **44**, 628 (1999).
14. M. Babin *et al.*, *Deep Sea Res.* **43**, 1241 (1996).
15. J. A. Dusenberry, R. J. Olson, S. W. Chisholm, *Limnol. Oceanogr.* **44**, 431 (1999).
16. S. Bailey, N. H. Mann, C. Robinson, D. J. Scanlan, *FEBS Lett.* **579**, 275 (2005).
17. G. Rocap *et al.*, *Nature* **424**, 1042 (2003).
18. L. R. Moore, A. F. Post, G. Rocap, S. W. Chisholm, *Limnol. Oceanogr.* **47**, 989 (2002).
19. N. J. Fuller *et al.*, *Limnol. Oceanogr.* **50**, 363 (2005).
20. E. Zinser *et al.*, *Appl. Environ. Microbiol.* **72**, 723 (2006).
21. C. S. Ting, G. Rocap, J. King, S. W. Chisholm, *Trends Microbiol.* **10**, 134 (2002).
22. Z. I. Johnson *et al.*, *Science* **311**, 1737 (2006).
23. A. Dufresne *et al.*, *Proc. Natl. Acad. Sci. U.S.A.* **100**, 10020 (2003).
24. L. R. Moore *et al.*, *Aquat. Microb. Ecol.* **39**, 257 (2005).
25. E. V. Armbrust *et al.*, *Science* **306**, 79 (2004).
26. R. F. Strzepek, P. J. Harrison, *Nature* **431**, 689 (2004).
27. R. Margalef, *Oceanol. Acta* **1**, 493 (1978).
28. J. Rodriguez *et al.*, *Nature* **410**, 360 (2001).
29. W. K. W. Li, *Nature* **419**, 154 (2002).
30. H. A. Bouman *et al.*, *Mar. Ecol. Prog. Ser.* **258**, 19 (2003).
31. N. Selje, M. Simon, T. Brinkhoff, *Nature* **427**, 445 (2004).
32. T. Pommier, J. Pinhassi, Å. Hagström, *Aquat. Microb. Ecol.* **41**, 79 (2005).
33. N.-U. Friggard, A. Martinez, T. J. Mincer, E. F. DeLong, *Nature* **439**, 847 (2006).

34. The authors would like to thank the instructors of BEAGLE Bio-optics Program (B. Irwin, Leg 1; G. Alarcón, Leg 2; and P. Bonham, Leg 5) for the collection of samples and the many students and researchers who participated in the bio-optics training program funded by the Partnership for Observation of the Global Oceans, the International Ocean-Colour Coordinating Group, and the Intergovernmental Oceanographic Commission. The assistance and support of the research scientists and crew onboard the *R.V. Mirai*, in particular the captain, M. Akamine, is also appreciated. We also thank E. Devred and the Japan Agency for Marine-Earth Science and Technology administration, in particular T. Hirano. This research was also funded by the Department of Fisheries and Oceans Strategic Science Fund, the Chilean National Commission for Scientific and Technological Research through the Funds for Advanced Research in Priority Areas Program, and by Natural Environment Research Council (D.J.S.). H.A.B. was supported by a Natural Sciences and Engineering Research Council of Canada Postdoctoral Fellowship and Canadian Space Agency Postdoctoral Supplement.

Supporting Online Material

www.sciencemag.org/cgi/content/full/312/5775/918/DC1
Materials and Methods
Figs. S1 to S4
Table S1
References

16 November 2005; accepted 11 April 2006
10.1126/science.1122692

Wnt Gradient Formation Requires Retromer Function in Wnt-Producing Cells

Damien Y. M. Coudreuse, Giulietta Roël,* Marco C. Betist,* Olivier Destrée, Hendrik C. Korswagen†

Wnt proteins function as morphogens that can form long-range concentration gradients to pattern developing tissues. Here, we show that the retromer, a multiprotein complex involved in intracellular protein trafficking, is required for long-range signaling of the *Caenorhabditis elegans* Wnt ortholog EGL-20. The retromer functions in EGL-20–producing cells to allow the formation of an EGL-20 gradient along the anteroposterior axis. This function is evolutionarily conserved, because Wnt target gene expression is also impaired in the absence of the retromer complex in vertebrates. These results demonstrate that the ability of Wnt to regulate long-range patterning events is dependent on a critical and conserved function of the retromer complex within Wnt-producing cells.

During *C. elegans* early larval development, EGL-20 is expressed by a group of cells located at the posterior end of the animal (*1*). EGL-20 controls the anterior migration of the HSN neurons (*2*) and the polarity of the division of the epidermal seam cell V5 (*3*). In addition, EGL-20 regulates the left/right asymmetric migration of the more distantly located Q neuroblasts (*2*) (fig. S1A). EGL-20 generates this asymmetry by specifically activating the expression of the Hox gene *mab-5* in the left Q cell (QL) (*1*). MAB-5 in turn directs the migration of the QL daughter cells (QL.d) toward the posterior (*4*). The Q daughter cells on the right side (QR.d) migrate in the default anterior direction. We used this asymmetric migration as an assay to identify novel components of the EGL-20 pathway. In a genome-wide RNA-mediated interference (RNAi)–based screen (*5*), we found that an ortholog of the yeast retromer complex subunit Vps35p (table S1) is required for posterior localization of the QL.d. In yeast, the retromer directs endosome-to-Golgi retrieval of proteins such as the carboxypeptidase Y receptor Vps10p (*6*). In vertebrate epithelial cells, it physically interacts with the immunoglobulin receptor (IgR) and mediates basal-to-apical transcytosis of the IgR-IgA complex (*7*).

We isolated a deletion allele that likely represents the *vps-35* null phenotype (fig. S1B).

Hubrecht Laboratory and Center for Biomedical Genetics, Uppsalalaan 8, 3584 CT, Utrecht, Netherlands.

*These authors contributed equally to this work.
†To whom correspondence should be addressed. E-mail: rkors@niob.knaw.nl

vps-35(hu68) mutants showed loss of *mab-5* expression in the QL lineage and anterior migration of the QL.d (Fig. 1, A and B). Further analysis of *vps-35(hu68)* showed that the *vps-35* and *egl-20* mutant phenotypes are strikingly similar. Thus, *vps-35* is also required for the EGL-20–dependent anterior migration of the QR.d and HSN neurons and for establishing the correct polarity of the V5 division (fig. S2A and table S5). Apart from these phenotypes, *vps-35* mutants showed no obvious additional defects, indicating that other signaling pathways are not substantially affected. Mutation of the two additional core retromer components *vps-26* and *vps-29* resulted in similar phenotypes (fig. S2A and table S2). Loss of *vps-5*, which encodes an accessory subunit of the retromer (*6*, *8*), did not affect Q cell migration. However, it did enhance the QL.d migration defect of *vps-29(tm1320)* and *vps-26(RNAi)* (fig. S2A and table S2), indicating that VPS-5 has a minor role in this process.

EGL-20 signaling is mediated by canonical as well as noncanonical Wnt pathways (*9*), and the requirement of the retromer complex for both signaling functions indicates that it acts before the divergence point of these different pathways. Epistatic analysis showed that VPS-35 functions upstream of the BAR-1/β-catenin destruction complex (fig. S2A and table S2), suggesting that it acts at the level of Frizzled or Dishevelled, or upstream of EGL-20 itself. To distinguish between these possibilities, we investigated whether the retromer complex is required in EGL-20–responding or –producing cells. Because *vps-35* is widely expressed, we used different tissue-specific promoters to express *vps-35* in a *vps-35(hu68)* mutant background (table S3 and fig. S2B). We found that expression of *vps-35* in cells that respond to EGL-20, such as the Q neuroblasts and the HSN neurons, failed to rescue the mutant phenotype. Rescue was, however, obtained when *vps-35* was expressed in all or part of the EGL-20–producing cells (see supporting online material). Taken together, these results demonstrate that the presence of the retromer complex in EGL-20–producing cells is necessary and sufficient for its function in EGL-20 signaling.

Mutation of the retromer complex strongly disrupts EGL-20 function, but other Wnts such as MOM-2 and LIN-44 are only mildly affected (table S4). The known functions of MOM-2 and LIN-44 depend on short-range signaling (*10*, *11*), whereas EGL-20 is the only Wnt that has been demonstrated to signal over a distance (*1*). We therefore investigated whether loss of retromer function differently affects long- and short-range functions of EGL-20. To test this, we compared the effect of different mutations in *egl-20*, *vps-35*, and *vps-26* on the Q neuroblasts, which are located relatively far from the group of EGL-20–producing cells, and the V5 cell, which is positioned closer. All mutations similarly disrupted QL.d migration (fig. S2), but V5 polarity was more strongly affected in *egl-20* null mutants than in *vps-35(hu68)* and *vps-26(tm1523)* (table S5). These results suggest that long-range EGL-20 signaling is more dependent on retromer function than is short-range signaling.

In the *Drosophila* wing imaginal disc, Wingless forms a concentration gradient that enables signaling over a distance (*12*). In *C. elegans*, *egl-20* is expressed in the posterior of the animal and triggers responses in more anteriorly located cells (fig. S1A). Together with the different effects on long- versus short-range EGL-20 signaling, this suggests that the retromer may be required for the formation of an EGL-20 gradient. We therefore investigated whether loss of retromer function affects EGL-20 localization. Immunostaining of animals expressing a functional EGL-20::proteinA fusion under the control of the *egl-20* promoter revealed that EGL-20 forms an anteroposterior gradient (Fig. 2, A to C, and E). The gradient is mainly visible at early stages, when EGL-20–dependent processes such as *mab-5* regulation in the Q neuroblasts take place. As observed for Wingless in *Drosophila* (*12*), EGL-20 shows a punctate staining. The EGL-20 gradient was absent in *vps-35(hu68)* mutants (Fig. 2D). Taken together, these results show that the retromer is involved in a critical step within EGL-20–expressing cells that allows EGL-20 to spread anteriorly.

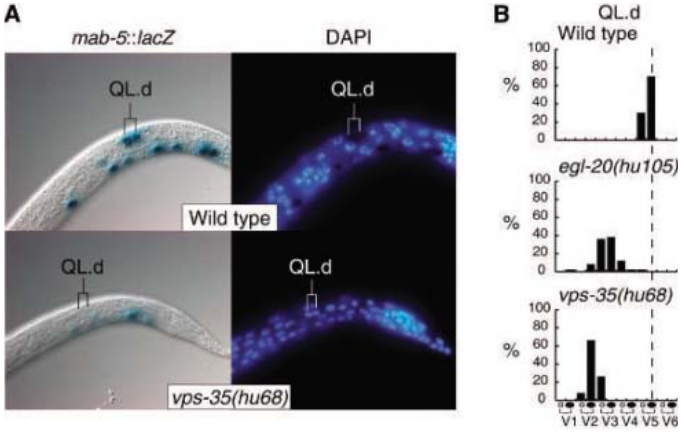

Fig. 1. The retromer complex is required for Q cell migration. (**A**) In *vps-35(hu68)*, a *mab-5::lacZ* reporter is not expressed in the QL.d. Whole-mount larvae were fixed 3 to 5 hours after hatching and stained for β-galactosidase activity. The DNA stain 4′,6′-diamidino-2-phenylindole (DAPI) was used for cell identification. (**B**) Anterior localization of the QL.d in *vps-35(hu68)*. The final positions of the QL.d ($n = 50$) were determined relative to the invariant positions of the seam cells (V1 to V6) after their first division. Bars indicate the percentage of cells at each position. Dashed lines indicate the wild-type position.

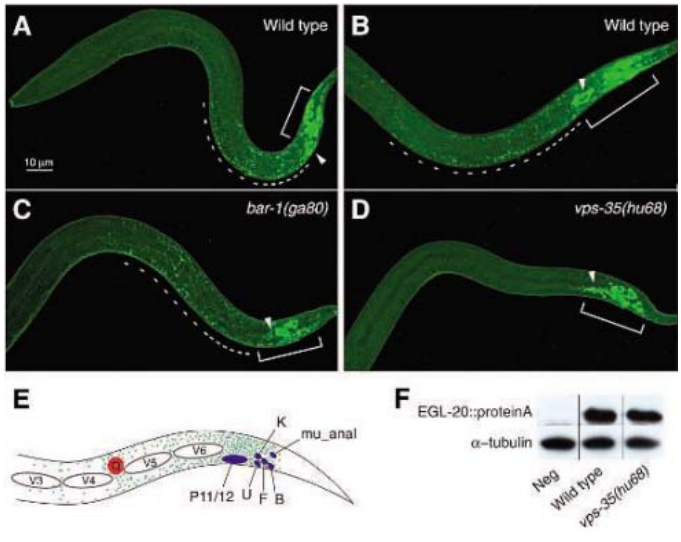

Fig. 2. The retromer complex is required for EGL-20 gradient formation. Whole-mount larvae carrying the integrated *Pegl-20::egl-20::proteinA* transgene were fixed 1 to 5 hours after hatching and stained with a fluorescein isothiocyanate–coupled antibody. (**A** and **B**) In wild-type animals, EGL-20 forms a punctate anteroposterior gradient. (**C**) This gradient is not affected in *bar-1(ga80)* mutants. (**D**) In *vps-35(hu68)* mutants, the EGL-20 gradient is absent. Arrowheads indicate P11/12 (*23*). White bars delimit the group of *egl-20*–expressing cells. Dashed lines represent the range of the gradient. A similar gradient was observed in live animals using an EGL-20::Venus fusion (fig. S4). (**E**) Schematic representation of the EGL-20 gradient. The punctate EGL-20 staining is indicated by green dots; *egl-20*–expressing cells are in blue. (**F**) Loss of *vps-35* does not affect global levels of EGL-20. Western blots of total first and second larval stage lysates were stained for EGL-20::proteinA. Neg, nontransgenic animals. Equal loading was confirmed using an antibody to α-tubulin.

The retromer complex is conserved from yeast to vertebrates (table S1). Therefore, we investigated its potential role in vertebrate Wnt signaling. RNAi-mediated knockdown of Vps35 in human embryonic kidney (HEK) cells inhibited the activation of a TCF reporter gene upon Wnt3A transfection (Fig. 3, A and B). As expected from the *C. elegans* data, Vps35(RNAi) had no effect when the reporter was activated downstream of Wnt by overexpression of a constitutively active TCF–β-catenin fusion (*13*). This shows that Vps35 has a conserved function that is also required for effective signaling in tissue culture. Furthermore, to address the in vivo effect of Vps35 knockdown in vertebrates, we used a morpholino (MO) approach in *Xenopus tropicalis* (fig. S3). Ectopic ventral activation of the Wnt pathway induces a secondary body axis (*14*, *15*). When a Vps35 MO was co-injected ventrally with Wnt1 RNA, axis duplication was strongly inhibited (Fig. 4A). Again, Vps35 knockdown had no effect on axis duplication when Wnt target gene expression was ventrally induced by a constitutively active TCF3-Armadillo fusion (*16*). The absence of a functional retromer complex also impaired endogenous Wnt signaling. Asymmetric injection of Vps35 MO specifically inhibited the expression of the Wnt target genes XmyoD (*17*) and Xslug (*18*) on the injected side (Fig. 4B) but did not affect the mesodermal marker Xbra. Co-injection of β-catenin or TCF3-Armadillo expression constructs rescued XmyoD and Xslug expression, showing that the vertebrate retromer specifically acts in the Wnt pathway, upstream of β-catenin (Fig. 4B and table S6). By analogy with our results in *C. elegans*, we propose that Wnt spreading and long-range signaling in vertebrates are dependent on a functional retromer.

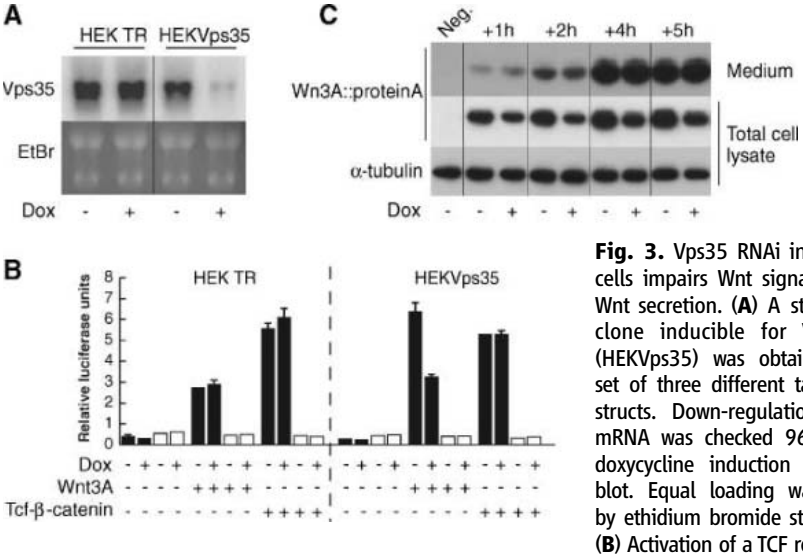

Fig. 3. Vps35 RNAi in mammalian cells impairs Wnt signaling but not Wnt secretion. (**A**) A stable HEK TR clone inducible for Vps35 RNAi (HEKVps35) was obtained using a set of three different targeting constructs. Down-regulation of Vps35 mRNA was checked 96 hours after doxycycline induction by Northern blot. Equal loading was confirmed by ethidium bromide staining (EtBr). (**B**) Activation of a TCF reporter (black bars) by Wnt3A transfection is inhibited by doxycycline-induced Vps35 RNAi. Activation by TCF–β-catenin is not affected. White bars represent negative controls. Data are presented as means ± SD. (**C**) Wnt3A levels are identical in the medium of cells induced or noninduced for Vps35 RNAi, demonstrating that Wnt secretion was not impaired despite a slightly lower amount of Wnt3A::proteinA in the corresponding total cell lysates. Neg., Nontransfected control; Dox, doxycycline.

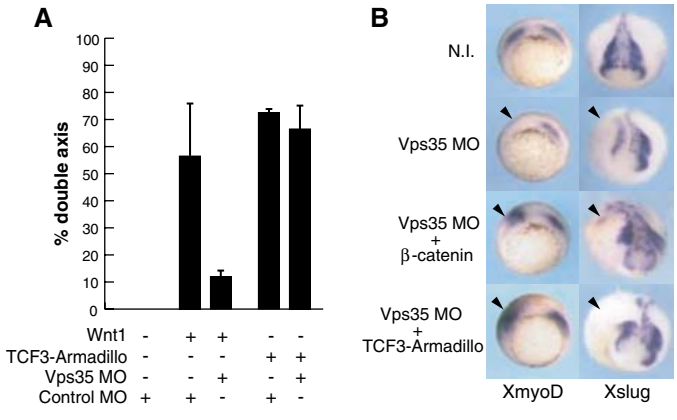

Fig. 4. The retromer complex is required in vivo for vertebrate Wnt signaling. (**A**) Vps35 MO inhibits Wnt1-induced double axis formation but has no effect on a constitutively active TCF3-Armadillo fusion ($n \geq 50$ in each assay). Data are presented as means ± SD. (**B**) Vps35 knockdown inhibits endogenous Wnt target gene expression on the MO-injected side. In situ hybridizations for the Wnt target genes XmyoD and Xslug were performed at the appropriate stages. Co-injection of β-catenin or TCF3-Armadillo expression constructs rescued Wnt target gene expression (representative embryos are shown). Arrowheads indicate the side of injection. N.I., noninjected control.

Retromer function may be required for the formation of an active Wnt protein, for secretion, or for other processes within the expressing cells that enable long-range Wnt signaling. Several lines of evidence suggest that retromer function is not required for the formation and secretion of an active form of Wnt. First, the specificity of the retromer mutant phenotype argues against a general role in active Wnt formation. Thus, whereas mutation of the Porcupine ortholog MOM-1 (which is required for active Wnt formation) (*19*, *20*) leads to embryonic lethality (*10*, *21*), mutation of the retromer complex primarily disrupts EGL-20 function. Second, our observation that loss of retromer function mainly affects long-range EGL-20 signaling indicates that short-range–acting forms of EGL-20 and other Wnts are still produced and secreted. Third, mutation of *vps-35* did not affect EGL-20 levels within the EGL-20–producing cells (as observed by immunostaining and with a functional EGL-20::GFP fusion) (Fig. 2, D and F), indicating that EGL-20 is normally produced and secreted. Finally, knockdown of Vps35 in transfected HEK cells did not affect Wnt3A secretion (Fig. 3C).

It has recently been shown that binding of Wnt to lipoprotein particles is important for long-range gradient formation (*22*). The association of Wnt with these particles may take place within Wnt-producing cells, in an endosomal compartment that contains both Wnt and internalized lipoprotein particles. This mechanism would require Wnt to be sorted out of the default secretory pathway by a specific cargo receptor and to be transported to endosomes before secretion. We speculate that, similar to its function in Vps10p trafficking, the retromer complex may recycle the Wnt cargo receptor from the endosome to the Golgi network. In the absence of retromer, a lack of Wnt cargo receptors in the Golgi would lead to Wnt secretion via the default pathway. This would impair Wnt association with lipoprotein particles and limit its range of signaling.

Wnt gradient formation is a complex and tightly regulated process. Factors expressed at the surface of cells along the gradient domain control its spatial extension and determine the range of its effects. However, our results show that the establishment of a Wnt concentration gradient is not dependent only on the capacity of neighboring cells to attract and spread Wnt proteins. An early permissive mechanism within the Wnt-producing cells, which requires retromer function, is an essential step that allows secreted Wnt molecules to respond to the different cues that will shape the gradient.

References and Notes

1. J. Whangbo, C. Kenyon, *Mol. Cell* **4**, 851 (1999).
2. J. Harris, L. Honigberg, N. Robinson, C. Kenyon, *Development* **122**, 3117 (1996).
3. J. Whangbo, J. Harris, C. Kenyon, *Development* **127**, 4587 (2000).
4. S. J. Salser, C. Kenyon, *Nature* **355**, 255 (1992).
5. A. G. Fraser *et al.*, *Nature* **408**, 325 (2000).
6. M. N. Seaman, J. M. McCaffery, S. D. Emr, *J. Cell Biol.* **142**, 665 (1998).
7. M. Verges *et al.*, *Nat. Cell Biol.* **6**, 763 (2004).
8. B. F. Horazdovsky *et al.*, *Mol. Biol. Cell* **8**, 1529 (1997).
9. H. C. Korswagen, *Bioessays* **24**, 801 (2002).
10. C. J. Thorpe, A. Schlesinger, J. C. Carter, B. Bowerman, *Cell* **90**, 695 (1997).
11. M. A. Herman, H. R. Horvitz, *Development* **120**, 1035 (1994).
12. K. M. Cadigan, M. P. Fish, E. J. Rulifson, R. Nusse, *Cell* **93**, 767 (1998).
13. F. J. Staal, B. M. Burgering, M. van de Wetering, H. C. Clevers, *Int. Immunol.* **11**, 317 (1999).
14. J. Noordermeer, F. Meijlink, P. Verrijzer, F. Rijsewijk, O. Destree, *Nucleic Acids Res.* **17**, 11 (1989).
15. A. P. McMahon, R. T. Moon, *Cell* **58**, 1075 (1989).
16. J. Roose *et al.*, *Nature* **395**, 608 (1998).
17. S. Hoppler, J. D. Brown, R. T. Moon, *Genes Dev.* **10**, 2805 (1996).
18. J. Vallin *et al.*, *J. Biol. Chem.* **276**, 30350 (2001).
19. T. Kadowaki, E. Wilder, J. Klingensmith, K. Zachary, N. Perrimon, *Genes Dev.* **10**, 3116 (1996).
20. K. Tanaka, Y. Kitagawa, T. Kadowaki, *J. Biol. Chem.* **277**, 12816 (2002).
21. C. E. Rocheleau *et al.*, *Cell* **90**, 707 (1997).
22. D. Panakova, H. Sprong, E. Marois, C. Thiele, S. Eaton, *Nature* **435**, 58 (2005).
23. J. E. Sulston, H. R. Horvitz, *Dev. Biol.* **56**, 110 (1977).
24. We thank C. McNulty, H. Clevers, and R. Plasterk for critically reading the manuscript; J. Ahringer, A. Fire, C. Haft, D. Hermand, R. Moon, J. Smith, and C. Wolkow for reagents; B. Bowerman, J. Kuipers, W. Stoorvogel, and M. van de Wetering for help and advice; Shohei Mitani (National Bioresource Project for the Nematode, Tokyo) for deletion mutants; and the *Caenorhabditis* Genetic Center (University of Minnesota, Minneapolis) for strains. This work was supported by the Dutch Cancer Foundation, the EU FP6 program Cells into Organs (H.C.K.), and EU grant QLRT-2000-01275 (O.D.).

Supporting Online Material

www.sciencemag.org/cgi/content/full/1124856/DC1
Materials and Methods
Figs. S1 to S4
Tables S1 to S6
References

11 January 2006; accepted 13 April 2006
Published online 27 April 2006;
10.1126/science.1124856
Include this information when citing this paper.

Ischemia Opens Neuronal Gap Junction Hemichannels

Roger J. Thompson, Ning Zhou, Brian A. MacVicar*

Neuronal excitotoxicity during stroke is caused by activation of unidentified large-conductance channels, leading to swelling and calcium dysregulation. We show that ischemic-like conditions [O_2/glucose deprivation (OGD)] open hemichannels, or half gap junctions, in neurons. Hemichannel opening was indicated by a large linear current and flux across the membrane of small fluorescent molecules. Single-channel openings of hemichannels (530 picosiemens) were observed in OGD. Both the current and dye flux were blocked by inhibitors of hemichannels. Therefore, hemichannel opening contributes to the profound ionic dysregulation during stroke and may be a ubiquitous component of ischemic neuronal death.

The rapid decrease of O_2 and glucose in the infarct region of ischemic tissue can trigger necrotic cellular death within a few minutes as a result of Ca^{2+}, Na^+, K^+, and Cl^- dysregulation (*1*, *2*). An unexplored contributor to unregulated ionic fluxes in neurons is hemichannel opening. Hemichannels are open unapposed half gap junctions that form large-conductance channels and allow flux of ions and molecules (<1 kD). Connexin (Cx) hemichannels function physiologically during inhibition in the outer retina (*3*), and metabolic inhibition or divalent cation free solutions open Cx43 hemichannels in astrocytes and cardiomyocytes (*4*–*6*). Pyramidal neurons in the central nervous system do not express connexins but express pannexin 1 (Px1), which forms gap junctions and hemichannels in oocytes, and can open as a hemichannel at negative resting membrane potentials or in physiological Ca^{2+} concentrations (*7*–*9*).

Our recording conditions were designed to isolate nonselective channels by including a cocktail of blockers against glutamate receptors and voltage-dependent K^+, Na^+, and Ca^{2+} channels (*10*). OGD activated a large inward current in acutely isolated hippocampal neurons within 9.7 ± 1.2 min (Fig. 1, A and E; range, 3 to 19 min; n = 19). The current had a large amplitude (–74.7 ± 16 pA/pF at –60 mV) versus the control (–4.4 ± 1.1 pA/pF), a linear current-voltage (*I-V*) relationship, and a reversal potential near 0 mV (Fig. 1, B and E). The current declined (Fig. 1B) if O_2/glucose was returned within ~5 min of activation (about 15 min after OGD). However, longer durations of OGD (>20 min) resulted in irreversible current activation, neuronal swelling, and membrane breakdown.

The amplitude and linear *I-V* of the OGD-activated current suggested activation of hemichannels. To determine hemichannel involvement, we tested the gap junction/hemichannel blocker carbenoxolone (Cbx). After OGD activated the current, Cbx (100 μM) was applied and block was observed (Fig. 1C, top trace, and Fig. 1D). In other experiments, the current was not induced when Cbx was applied concomitantly with OGD. Lanthanum chloride (La^{3+}; 100 μM), which blocks Cx hemichannels, significantly (P = 0.042) reduced the amplitude of the OGD-activated current (Fig. 1C, lower trace, and Fig. 1E).

We eliminated the possibilities that the acid-sensitive ion channel ASIC1a (*11*) and the large-pore purinergic P2X7 receptor contribute to the OGD-activated current. ASIC1a and P2X7 activation were unlikely because extracellular pH was maintained at 7.4 and the isolated neurons were constantly perfused at ~4 ml/min to prevent the accumulation of secreted molecules (*10*). Nevertheless, amiloride (100 μM, to block ASIC1a channels) or brilliant blue G (BBG; 10 μM, to block P2X7 receptors) were bath-applied after current activation or concomitantly with OGD; both failed to affect the large OGD-activated current (Fig. 1F).

After inhibition of the OGD-activated hemichannel by Cbx or La^{3+}, a small residual current remained (Fig. 1, D and E) that was consistent with the transient receptor potential (TRP) family—specifically, TRPC4 or TRPC5 homomeric channels—because this current had a doubly rectifying *I-V* relationship and was augmented by 100 μM La^{3+}. TRP channels have been reported to be activated by OGD and cyanide in cultured cortical neurons (*12*). We chose to focus the remainder of our investigation on the hemichannel because the very large amplitude of this current would make it a major contributor to ionic dysregulation during OGD.

If the large current in OGD is from hemichannel opening, then influx or efflux of gap junction/hemichannel permeable dyes should be measurable in neurons. Acutely isolated hippocampal neurons were loaded with calcein green AM (Fig. 2A), a largely nonreactive green fluorescent dye with a molecular weight of 0.66 kD that is known to cross gap junctions (*13*). In control solutions, calcein did not leak from acutely isolated neurons because fluorescence was stable (control; Fig. 2B). In OGD, calcein fluorescence decreased steadily (Fig. 2, A, B, and D), indicating that ischemia triggered dye efflux. The OGD-induced dye efflux was not affected by antagonists to glutamate receptors and ion channels (*10*) [Fig. 2D, OGD + blockers + D,L-2-amino-5-phosphonovaleric acid (APV)]. If dye efflux was mediated by hemichannel opening, Cbx should block it. Figure 2C shows examples from three different hippocampal neurons where dye efflux was blocked by Cbx; data from a number of neu-

Department of Psychiatry and Brain Research Centre, University of British Columbia, Vancouver, British Columbia V6T 2B5, Canada.

*To whom correspondence should be addressed. E-mail: bmacvica@interchange.ubc.ca

rons are summarized in Fig. 2D. In neuron 1 in Fig. 2C, the neuron was concomitantly exposed to Cbx and OGD, and dye loss was not observed (Fig. 2A, lower panels). In neuron 2, Cbx and OGD were applied simultaneously and Cbx was removed after 35 min; only then did the calcein fluorescence decrease. Finally, in neuron 3, dye efflux was inhibited by a transient exposure to Cbx. The strong Cbx sensitivity indicates that the decrease in dye signal was not due to photobleaching or to a loss of plasma membrane integrity.

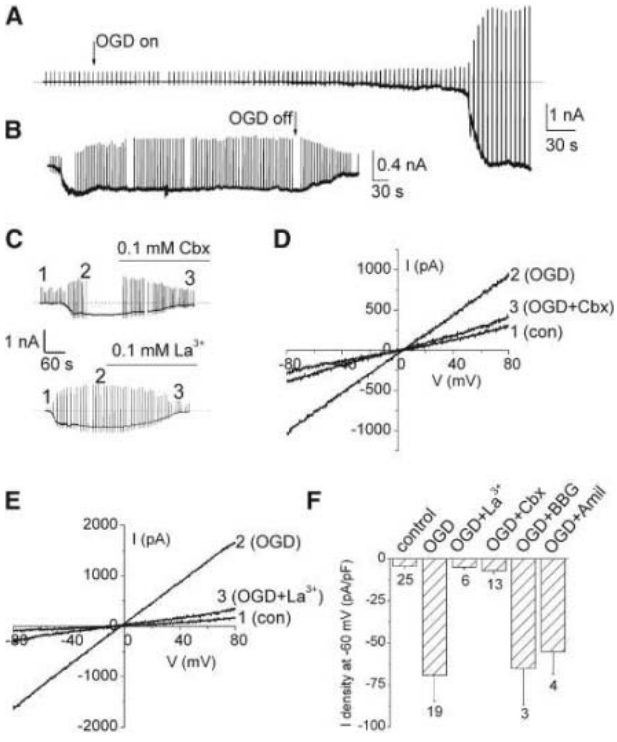

Fig. 1. Effects of OGD on hippocampal neurons. (**A**) Voltage-clamp recording of an acutely isolated rat hippocampal neuron showing activation of a large inward current during ischemia (OGD). The spike-like events are 150-ms voltage ramps from –80 to 80 mV. (**B**) Return to control solutions within 5 min of activation of the large current resulted in reversal. (**C**) The hemichannel blockers Cbx and La^{3+} blocked the OGD-activated inward current. The numbers above each trace indicate the voltage ramps shown in (D) and (E). (**D**) The OGD-activated current was blocked by Cbx. (**E**) La^{3+} also blocked the OGD-activated current. (**F**) Average inward current density at –60 mV (the number of cells is indicated under each bar).

We next used two-photon laser scanning microscopy of identified yellow fluorescent protein–positive (YFP^+) cortical neurons (*10*, *14*) to measure the influx of another gap junction permeable dye, sulforhodamine 101 (SR101). SR101 is normally completely excluded from neurons but is a selective and stable marker of astrocytes in situ (*15*). YFP^+ neurons imaged at least 100 μm from the surface of a 400-μm brain slice did not stain with SR101 under control conditions (Fig. 3A). The YFP (green neurons) and red (SR101 in the bath) signals did not overlap. However, after exposure of brain slices to OGD for 12 min, SR101 loading of YFP^+ neurons was observed (Fig. 3, A to C), as indicated by the merging of the YFP and SR101 signals (yellow). YFP-negative neurons also loaded with SR101 during OGD (Fig. 3A).

If SR101 loading in situ was due to hemichannel opening by OGD, as predicted by the in vitro calcein efflux data, then the hemichannel blocker Cbx should abolish SR101 loading. As a semiquantitative measure of dye influx, the intensity of SR101 inside the YFP^+ neuron was subtracted from that for the same sized region outside of the neuron and normalized to the peak SR101 intensity. Thus, a negative number indicates a higher extracellular SR101 fluorescence relative to that inside the neuron. The average time course (Fig. 3B) shows clearly that SR101 loading of neurons occurred only during OGD, and that this was blocked by Cbx. Neither

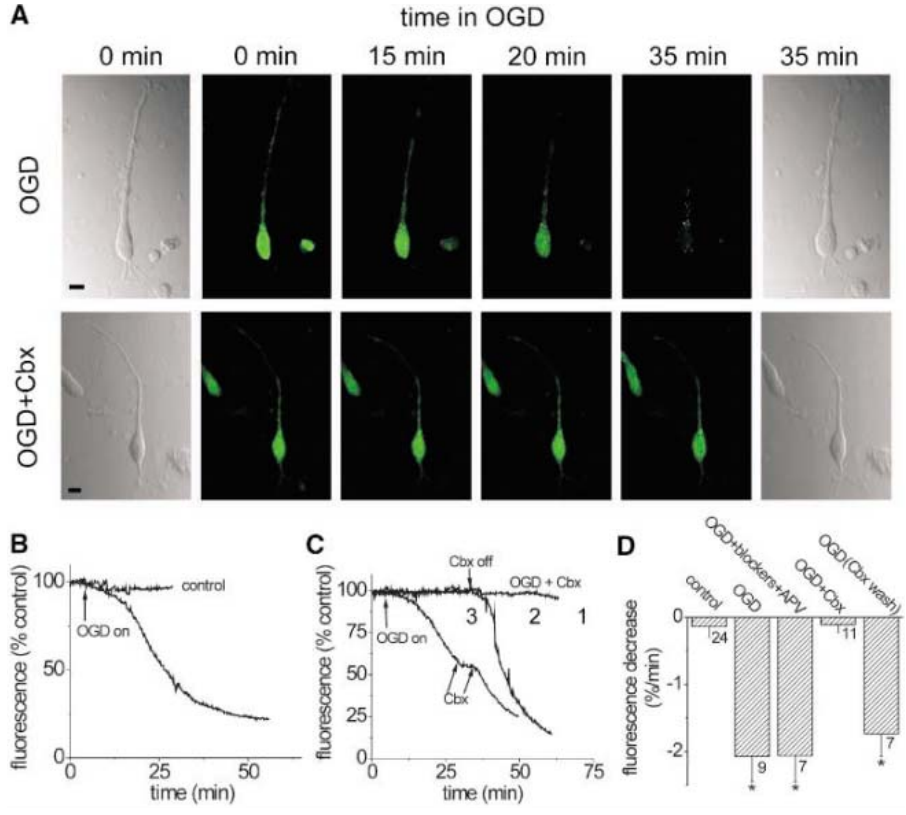

Fig. 2. Ischemia-mediated efflux of small molecules from neurons. (**A**) Confocal images of a calcein-loaded, acutely isolated hippocampal neuron. OGD resulted in rapid calcein efflux, which was inhibited by the hemichannel blocker Cbx (bottom row). Scale bars, 10 μm. (**B**) Calcein fluorescence during control and OGD. Each trace represents data from different neurons, expressed as the percentage of the average control fluorescence. (**C**) Calcein fluorescence from three separate neurons exposed to OGD (OGD on) in the presence of Cbx for variable times as indicated. Cbx prevented dye loss from the neurons. (**D**) Average calcein fluorescence decrease, calculated as the slope over 5-min periods.

BBG nor kyenurinic acid plus APV included with the cocktail of blockers (*10*) (OGD + blockers + APV) prevented the SR101 staining of identified neurons, indicating that P2X7 and ionotropic glutamate receptors were not involved (Fig. 3C).

The most likely candidate for the proteins constituting OGD-activated hemichannels in pyramidal neurons is Px1, because it may be the only gap junction protein expressed in these cells (*9*, *16*). Cx36, Cx45, and Cx52 are unlikely to contribute to the hemichannel current because they are closed by negative membrane potentials and physiological Ca^{2+} concentrations (*8*, *11*). The conductance of homomeric Px1 (550 pS) (*7*) is at least 200 pS larger than those reported for connexin hemichannels (*17*). We therefore performed cell-attached single-channel recording from acutely isolated hippocampal neurons to determine the single-channel conductance of OGD-activated channels.

Openings of large-conductance channels (Fig. 4A) were rare under control conditions, as illustrated by the single peak in the all-points amplitude histogram of Fig. 4D and the low open probability (Fig. 4G, control). In OGD, 5 of 13 patches showed activation of two or more large-conductance channels (Fig. 4, B and C). The average single-channel current amplitude and conductance were –31.6 ± 2.2 pA (n = 5) and 527 ± 36 pS at –60 mV (Fig. 4D). Open probability was increased by a factor of 4.5 over control (Fig. 4G). The channels had a linear *I-V* plot with a reversal potential near 0 mV (Fig. 4E). Full single-channel transitions were observed (Fig. 4F), which is a biophysical criterion indicating the presence of bona fide large-conductance channels and not the summated openings of many smaller ones (*18*). All of these single-channel biophysical properties are similar to those of homomeric Px1 hemichannels expressed in oocytes (*7*). Finally, Cbx was bath-applied after appearance of the large channels and resulted in a slowly reversible block in all four cell-attached patches that were tested (Fig. 4, C, D, and G).

We propose that ischemic insults open Px1 hemichannels, and that this is a central component of the increased plasma membrane permeability leading to neuronal necrosis. Px1 hemichannel opening may have several severe physiological consequences for neurons. First, these nonselective cation channels could mediate the dysregulated ionic fluxes that are known to occur during ischemia (*1*, *2*). Other pathways may be involved, such as ASIC1a channels (*11*), voltage-dependent Na^+ channels (*19*), *N*-methyl-D-aspartate (NMDA) receptors (*20*), and TRP channels (*12*). However, we argue that the extremely large amplitude of the

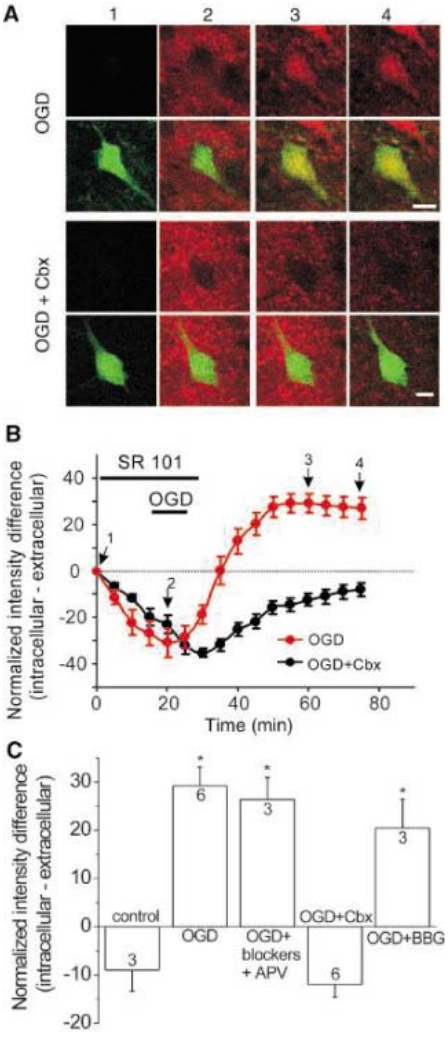

Fig. 3. Effect of OGD on dye loading in situ. (**A**) Two-photon laser scanning microscopy images of YFP^+ mouse cortical neurons in a 400-μm brain slice. SR101 (red; first and third rows) was excluded from the cells under control conditions. Dye influx occurred during OGD (top rows) and was prevented by hemichannel block (Cbx, bottom rows). Scale bar, 10 μm. (**B**) Time course of SR101 intensity inside YFP^+ neurons. (**C**) Average SR101 difference intensities (outside minus inside) 45 min after OGD.

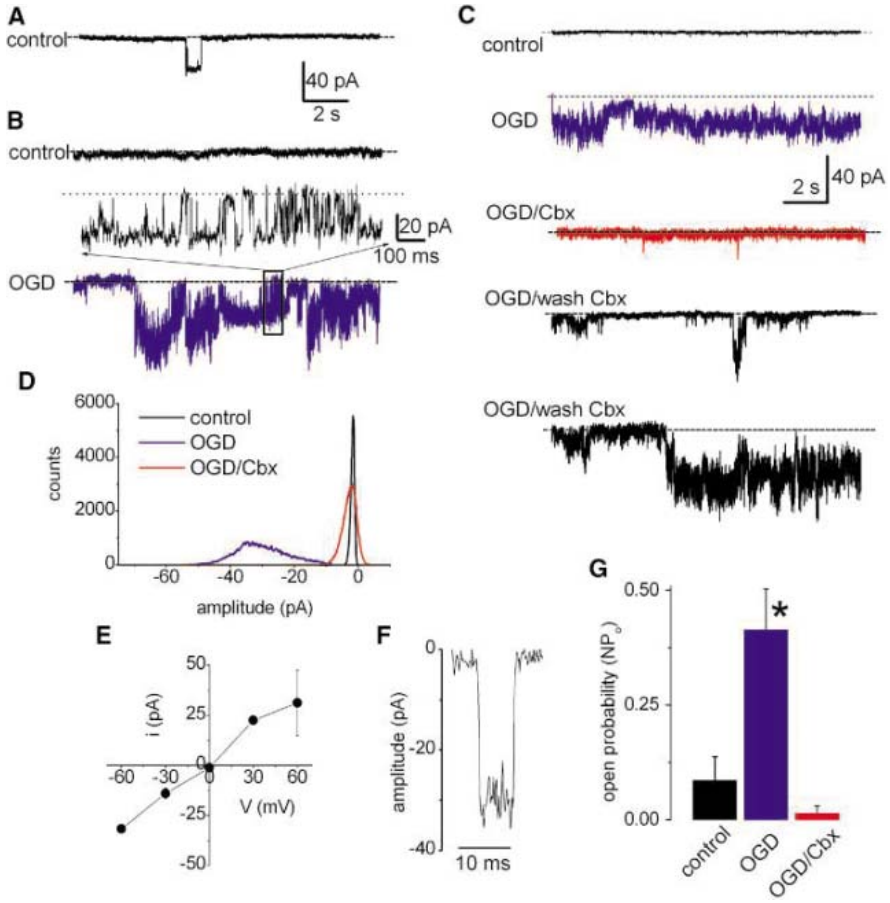

Fig. 4. OGD activates single large-conductance channels. (**A**) Cell-attached patch recording (duration 15 s) under control conditions. (**B**) Recordings from a hippocampal neuron under control (black) and during exposure to OGD (blue). The boxed region is expanded to show large single-channel transitions. (**C**) Cell-attached recordings from a neuron showing hemichannel activation by OGD (blue), inhibition by carbenoxolone (Cbx; red), and reversal after washout of Cbx. (**D**) All-points amplitude histograms from the traces in (C), showing the closed (control) and open amplitudes (OGD). (**E**) Average *I-V* plot of OGD-activated hemichannels from five different neurons. (**F**) A single opening (and closing) of the hemichannel in OGD. (**G**) Hemichannel open probability (NP_o) was significantly increased during OGD (n = 5) and blocked by Cbx.

hemichannel makes it a major contributor to ionic dysregulation in ischemia. Second, Px1 hemichannel opening may result in efflux of glucose and adenosine triphosphate (ATP), further compromising the neuron's recovery from an ischemic insult. Consistent with this was our observation that fluorescent dyes became membrane-permeable only during OGD. Hemichannels are putative conduits for ATP release from astrocytes (*21*) and in the cochlea (*22*). Third, the large amplitude of the Px1 hemichannel current at holding potentials near the neuron's resting membrane potential (~ –60 mV) indicates that these currents likely contribute substantially to "anoxic depolarization," a poorly understood but well-recognized and key component of ischemic neuronal death (*2*, *23*, *24*). Therefore, hemichannel opening may be an important new pharmacological target to prevent neuronal death in stroke.

References and Notes

1. A. J. Hansen, *Physiol. Rev.* **65**, 101 (1985).
2. P. Lipton, *Physiol. Rev.* **79**, 1431 (1999).
3. M. Kamermans *et al.*, *Science* **292**, 1178 (2001).
4. J. E. Contreras *et al.*, *Proc. Natl. Acad. Sci. U.S.A.* **99**, 495 (2002).
5. R. P. Kondo, S. Y. Wang, S. A. John, J. N. Weiss, J. I. Goldhaber, *J. Mol. Cell. Cardiol.* **32**, 1859 (2000).
6. H. Li *et al.*, *J. Cell Biol.* **134**, 1019 (1996).
7. L. Bao, S. Locovei, G. Dahl, *FEBS Lett.* **572**, 65 (2004).
8. R. Bruzzone, M. T. Barbe, N. J. Jakob, H. Monyer, *J. Neurochem.* **92**, 1033 (2005).
9. R. Bruzzone, S. G. Hormuzdi, M. T. Barbe, A. Herb, H. Monyer, *Proc. Natl. Acad. Sci. U.S.A.* **100**, 13644 (2003).
10. See supporting material on *Science* Online.
11. J. Gao *et al.*, *Neuron* **48**, 635 (2005).
12. M. Aarts *et al.*, *Cell* **115**, 863 (2003).
13. C. Tomasetto, M. J. Neveu, J. Daley, P. K. Horan, R. Sager, *J. Cell Biol.* **122**, 157 (1993).
14. G. Feng *et al.*, *Neuron* **28**, 41 (2000).
15. A. Nimmerjahn, F. Kirchhoff, J. N. Kerr, F. Helmchen, *Nat. Methods* **1**, 31 (2004).
16. G. Sohl, S. Maxeiner, K. Willecke, *Nat. Rev. Neurosci.* **6**, 191 (2005).
17. J. C. Saez, M. A. Retamal, D. Basilio, F. F. Bukauskas, M. V. Bennett, *Biochim. Biophys. Acta* **1711**, 215 (2005).
18. R. J. Thompson, M. H. Nordeen, K. E. Howell, J. H. Caldwell, *Biophys. J.* **83**, 278 (2002).
19. M. L. Fung, G. G. Haddad, *Brain Res.* **762**, 97 (1997).
20. H. Benveniste, J. Drejer, A. Schousboe, N. H. Diemer, *J. Neurochem.* **43**, 1369 (1984).
21. C. E. Stout, J. L. Costantin, C. C. Naus, A. C. Charles, *J. Biol. Chem.* **277**, 10482 (2002).
22. H. B. Zhao, N. Yu, C. R. Fleming, *Proc. Natl. Acad. Sci. U.S.A.* **102**, 18724 (2005).
23. T. R. Anderson, C. R. Jarvis, A. J. Biedermann, C. Molnar, R. D. Andrew, *J. Neurophysiol.* **93**, 963 (2005).
24. G. G. Somjen, *Physiol. Rev.* **81**, 1065 (2001).
25. Supported by the Canadian Institutes for Health Research and the Canadian Stroke Network. B.A.M. has a Tier 1 Canada Research Chair in Neuroscience and a Michael Smith Foundation for Health Research distinguished scholar award. We thank Y.-T. Wang, C. C. Naus, and T. Snutch for critical reading of the manuscript.

Supporting Online Material

www.sciencemag.org/cgi/content/full/312/5775/924/DC1
Materials and Methods

14 February 2006; accepted 31 March 2006
10.1126/science.1126241

Hypothalamic mTOR Signaling Regulates Food Intake

Daniela Cota,[1] Karine Proulx,[1] Kathi A. Blake Smith,[1] Sara C. Kozma,[2] George Thomas,[2] Stephen C. Woods,[1] Randy J. Seeley[1]*

The mammalian Target of Rapamycin (mTOR) protein is a serine-threonine kinase that regulates cell-cycle progression and growth by sensing changes in energy status. We demonstrated that mTOR signaling plays a role in the brain mechanisms that respond to nutrient availability, regulating energy balance. In the rat, mTOR signaling is controlled by energy status in specific regions of the hypothalamus and colocalizes with neuropeptide Y and proopiomelanocortin neurons in the arcuate nucleus. Central administration of leucine increases hypothalamic mTOR signaling and decreases food intake and body weight. The hormone leptin increases hypothalamic mTOR activity, and the inhibition of mTOR signaling blunts leptin's anorectic effect. Thus, mTOR is a cellular fuel sensor whose hypothalamic activity is directly tied to the regulation of energy intake.

A subset of neurons in the central nervous system (CNS) plays a role in regulating both blood plasma fuel levels and nutrient intake (*1*, *2*). An emerging concept is that specific neuronal populations integrate fuel availability signals with signals mediated by hormones such as leptin (*3*). However, the signaling pathways that are involved are poorly understood.

In peripheral cells, the mammalian mTOR signaling pathway integrates nutrient signals with hormonal signals to control growth and development (*4*, *5*). mTOR is a highly conserved serine-threonine kinase, which, in the presence of mitogens and available nutrients (including amino acids), stimulates protein synthesis and inhibits autophagy (*6*). In vitro, cellular levels of adenosine triphosphate (ATP) increase mTOR signaling, and mTOR itself is thought to serve as an ATP sensor (*7*). mTOR thus functions as a checkpoint by which cells sense and decode changes in energy status, which in turn determines the rate of cell growth and proliferation (*6*). Complete loss of TOR function is lethal in mice (*8*); in *Drosophila*, defects in TOR signaling result in the formation of smaller cells in all tissues (*9*). Conversely, increased or otherwise aberrant mTOR activity has been linked to the development of cancer, diabetes, and obesity (*10*, *11*). As is consistent with the development of these diseases, the activation of the mTOR pathway is markedly elevated in the liver and in the skeletal muscle of insulin-resistant obese rats maintained on a high-fat diet (*12*), whereas the absence of the downstream mTOR target [S6 kinase 1 (S6K1)] protects against diet-induced obesity and enhances insulin sensitivity in mice (*13*). Given these observations, we hypothesized that mTOR might integrate cellular fuel status with hormonal-related signaling in specific populations of neurons that use this information to regulate food intake.

To test this hypothesis, we used antibodies to localize mTOR and two downstream targets of mTOR action [S6K1 and S6 ribosomal protein (S6) (*5*, *6*)] in the rat brain. Consistent with previous work (*14*), antibodies recognizing total mTOR had a ubiquitous distribution in the CNS, and there was scattered expression of specific phosphorylation of mTOR at Ser^{2448} (pmTOR) in extra-hypothalamic areas, including the hippocampus, thalamus, and cortex. In the hypothalamus, pmTOR was highly localized in the paraventricular (PVN) and arcuate (ARC) nuclei (fig. S1A) (*15*). Likewise, total S6K1 stained broadly throughout the CNS, whereas the hypothalamic expression of the activated form of S6K1, phosphorylated at Thr^{389} (pS6K1), was also largely limited to the PVN and ARC. Further, dual labeling for pmTOR and pS6K1 revealed that they are localized in the same cells in both of these regions (fig. S1B). Although most of these cells appear to be neurons, some may be glia.

The ARC contains at least two populations of neurons that are linked to the regulation of energy balance and whose activity is regulated by leptin: (i) orexigenic neurons that express both neuropeptide Y (NPY) and agouti-related peptide (AgRP) and (ii) anorexigenic neurons that express proopiomelanocortin (POMC) and cocaine- and amphetamine-regulated transcript (CART). Both pmTOR and pS6K1 were found in ~90% of ARC NPY/AgRP neurons (Fig. 1A), whereas only 45% of ARC POMC/CART neurons revealed phosphorylation of these proteins (Fig. 1B).

We next investigated whether changes in the body's energy status modulate mTOR signaling

[1]Department of Psychiatry, [2]Department of Genome Science, University of Cincinnati, Genome Research Institute, 2170 East Galbraith Road, Cincinnati, OH 45237, USA.

*To whom correspondence should be addressed. E-mail: Randy.Seeley@uc.edu

in the brain. There was a notable decrease in both hypothalamic pS6K1 and S6 phosphorylated at Ser^{240} and Ser^{244} (pS6) in rats that were fasted for 48 hours as compared with rats that were re-fed for 3 hours (Fig. 2A), but no significant changes in protein phosphorylation were found in extra-hypothalamic areas, such as the cortex and hippocampus (fig. S2A). After a 48-hour fast, the number of hypothalamic cells expressing pmTOR and pS6K1 was significantly decreased in the ARC, whereas no significant changes were observed in the PVN (Fig. 2B and fig. S2B). Thus, mTOR activity in the ARC is low when available fuels are low and the organism is predisposed to consume more calories.

If mTOR signaling is linked to the regulation of energy balance in the CNS, then manipulations of mTOR activity in the hypothalamus would be predicted to alter food intake. In a variety of model systems, mTOR activity is sensitive to levels of branched-chain amino acids, especially L-leucine (*16*, *17*). If increased hypothalamic mTOR signaling suppresses food intake, then the administration of L-leucine in the vicinity of the ARC (*15*) should produce anorexia. Intracerebroventricular administration of L-leucine [1.1 μg in 2 μl of phosphate-buffered saline (PBS) into the third ventricle] to 24-hour fasted rats before the onset of the dark cycle caused a decrease in food intake that was apparent 4 hours after treatment and lasted for 24 hours (Fig. 3A). The L-leucine–induced anorexia was accompanied by significant weight loss (Fig. 3B). In separate experiments, L-leucine also decreased food intake during the light cycle (fig. S3, A and B).

Unlike L-leucine, the intracerebroventricular administration of L-valine, another branched-chain amino acid, did not potently stimulate mTOR signaling (*16*, *17*), nor did it affect food intake and body weight (fig. S3, C and D). If our hypothesis is correct, doses of L-leucine that suppress food intake should also increase mTOR activity in the hypothalamus. Consistent with this, 45 min after intracerebroventricular administration of L-leucine, levels of pS6K1 were significantly increased in the hypothalamus (fig. S3E) whereas no changes were observed in pS6 levels at that time point (pS6/S6 L-leucine, 94.8 ± 5.3% versus pS6/S6 PBS, 100 ± 3.3%, $P = 0.4$). L-leucine–induced anorexia was also accompanied by significantly reduced NPY mRNA levels in the ARC (NPY mRNA after L-leucine, 85.6 ± 4.3% versus NPY mRNA after PBS, 100 ± 5.0%, $P < 0.05$), suggesting that hypothalamic mTOR signaling is selectively linked to the NPY system. Moreover, control experiments revealed that the L-leucine–induced anorexia was not due to the development of conditioned taste aversions (fig. S3, F and G).

We next investigated the effects of the well-characterized mTOR inhibitor rapamycin (*18*). Intracerebroventricular administration of

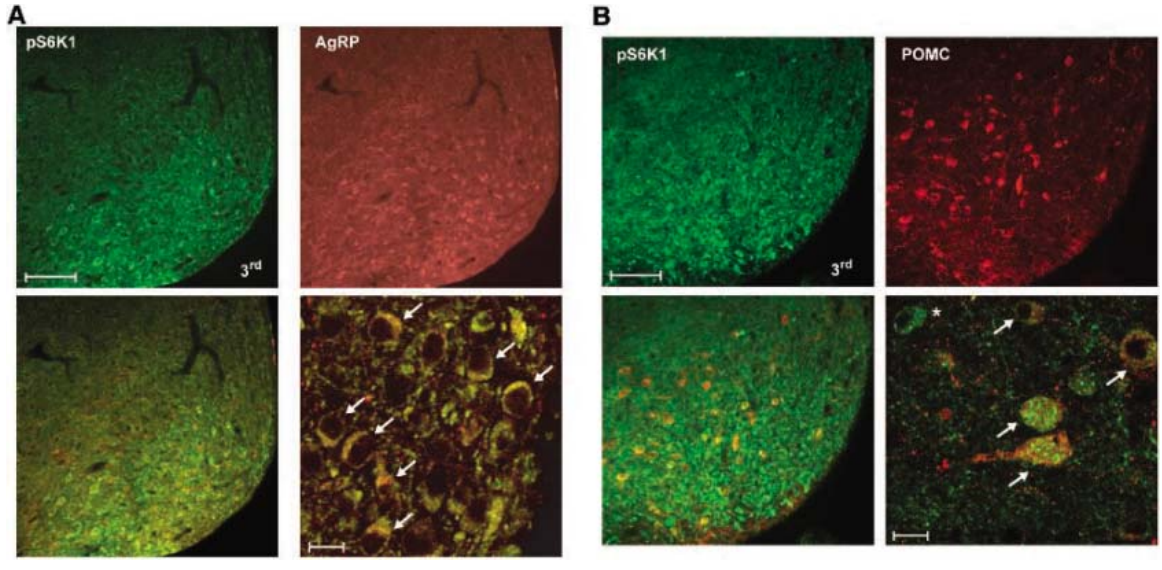

Fig. 1. Localization of mTOR signaling in the rat hypothalamus. (**A**) Immunohistochemistry showing colocalization (yellow, bottom left) of pS6K1 (green, top left) and AgRP (red, top right) in the ARC of the hypothalamus. Scale bar, 50 μm. (Bottom right) High-resolution image depicting the colocalization of pS6K1 and AgRP (arrows). 3rd indicates the third ventricle. Scale bar, 10 μm. (**B**) Immunohistochemistry showing colocalization (yellow, bottom left) of pS6K1 (green, top left) and POMC (red, top right) in the ARC of the hypothalamus. Scale bar, 50 μm. (Bottom right) High-resolution image depicting the colocalization of pS6K1 and POMC (arrows). The asterisk indicates a cell expressing only pS6K1. Scale bar, 10 μm.

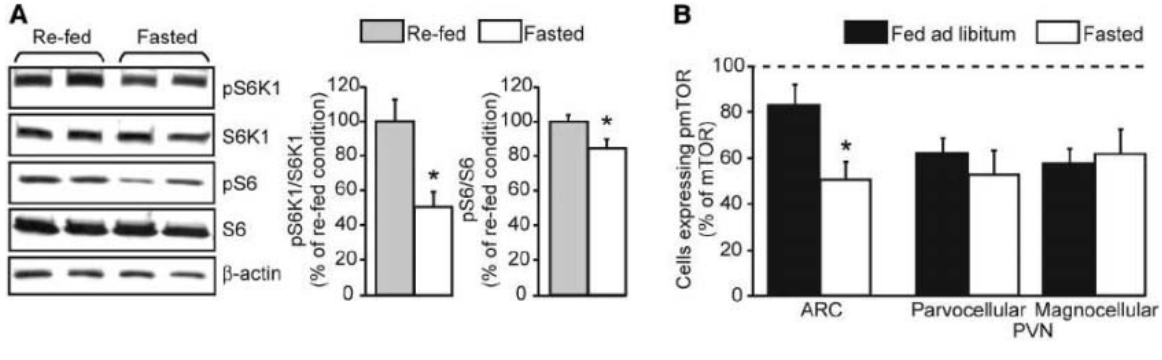

Fig. 2. Modulation of hypothalamic mTOR signaling by energy status. (**A**) (Left) Representative Western blot from re-fed rats or rats fasted for 48 hours. β-actin was the loading control. (Right) Quantification by image analysis of hypothalamic S6K1 and S6 phosphorylation. Error bars indicate SEM. *$P < 0.05$ versus rats in the re-fed condition. Five brains were examined for each condition. (**B**) Quantification of immunoreactivity for pmTOR in the ARC and PVN of rats fed ad libitum and rats fasted for 48 hours. The mean ± SEM of the number of cells positive for pmTOR is expressed as a percentage of mTOR-labeled cells. *$P < 0.05$ versus rats in the fed–ad libitum condition. Five brains were examined for each condition.

rapamycin [50 μg in 2 μl of dimethyl sulfoxide (DMSO)] rapidly inhibited hypothalamic S6K1 and S6 phosphorylation (Fig. 3C) and significantly increased the short-term intake of chow in pre-satiated rats, which were exposed to a highly palatable diet (Ensure) during the light cycle (fig. S4).

To determine whether the stimulation of hypothalamic mTOR signaling is required for the L-leucine–induced reduction of food intake, we combined intracerebroventricular administration of rapamycin, at a dose that does not affect food intake, with a subsequent intracerebroventricular injection of L-leucine. Rapamycin significantly inhibited the L-leucine–induced anorexia 4 hours after the administration of the amino acid (Fig. 3D), an effect that persisted up to 24 hours after treatment (Fig. 3D). Moreover, whereas L-leucine–treated rats lost a significant amount of weight, the rapamycin pre-treatment was associated with changes in body weight that were comparable to those observed in vehicle-treated animals (Fig. 3E).

A number of hormones and cytokines mediate their cellular effects through the mTOR signaling pathway. For example, the activation of mTOR and S6K1 by insulin is dependent on the phosphatidylinositol 3-kinase (PI3K)/Akt pathway (*10*) and in the hypothalamus, the anorectic actions of both insulin and leptin can be blocked by the inhibition of PI3K (*19*, *20*). To determine whether leptin's anorectic effects depend on mTOR activation, we examined hypothalamuses from leptin-treated rats [10 μg in 2 μl of saline, intracerebroventricular (icv)] 2 hours after the administration of the hormone (Fig. 4A). Leptin treatment increased the phosphorylation of both S6K1 and S6 relative to saline. Moreover, a significant positive correlation was found between the hypothalamic phosphorylation levels of signal transducer and activator of transcription 3 (pSTAT3) and both pS6K1 (Pearson's $r = 0.6$, $P = 0.03$) and pS6 (Pearson's $r = 0.86$, $P = 0.0006$). To determine whether increased mTOR activity is required for the leptin-induced anorexia, we combined the administration of leptin with rapamycin. Rapamycin greatly attenuated the anorexia and body weight loss that was induced by leptin over a 24-hour period (Fig. 4, B and C). This contrasts with the results obtained with the potent melanocortin receptor 3 and 4 agonist, melanotan II (MTII) (0.26 μg in 1 μl of saline, icv), whose effect on food intake and body weight was unaffected by rapamycin (fig. S5, A and B). This finding suggests that the interaction between mTOR signaling and leptin is relatively specific.

Our data highlight an important role for hypothalamic mTOR signaling in food intake and energy balance regulation in a mammalian model. Analogous changes in S6K activity affect the feeding behavior of *Drosophila* larvae

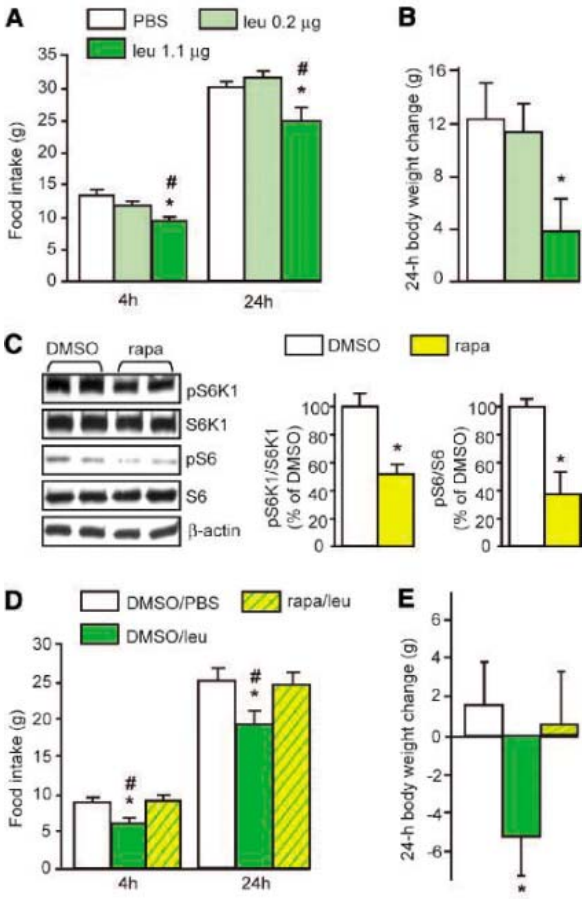

Fig. 3. L-leucine and rapamycin oppositely modulate hypothalamic mTOR signaling. (**A** and **B**) Intracerebroventricular administration of L-leucine decreases food intake (A) and body weight gain (B) in rats fasted for 24 hours. The mean ± SEM of 6 to 7 rats used for each treatment group is shown. *P < 0.05 versus PBS-treated rats; #P < 0.05 versus rats treated with 0.2 μg of L-leucine in 2 μl of PBS (leu 0.2). Leu 1.1, treatment with 1.1 μg of L-leucine in 2 μl of PBS. (**C**) Rapamycin (50 μg in 2 μl of DMSO, icv) inhibits hypothalamic mTOR signaling. (Left) Representative Western blot from DMSO- or rapamycin (rapa)–treated rats. β-actin was the loading control. (Right) Quantification by image analysis of hypothalamic S6K1 and S6 phosphorylation. Error bars indicate SEM. *P < 0.05 versus DMSO-treated rats. Three brains were examined for each condition. (**D** and **E**) Rapamycin (25 μg in 2 μl of DMSO, icv) blocks the L-leucine–induced effects on food intake (D) and body weight (E). The mean ± SEM of 6 to 7 rats used for each treatment group is shown. *P < 0.05 versus DMSO/PBS-treated rats; #P < 0.05 versus rapamycin/leucine-treated rats.

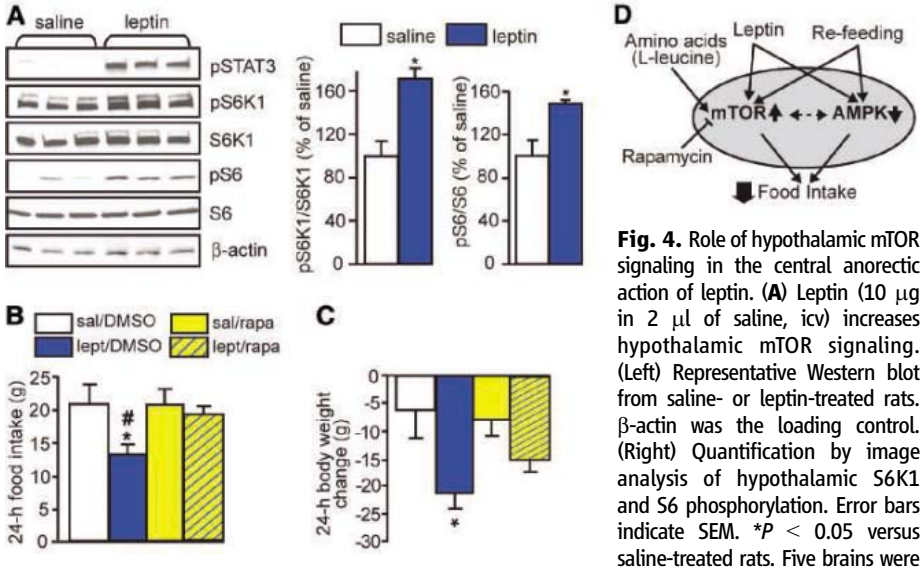

Fig. 4. Role of hypothalamic mTOR signaling in the central anorectic action of leptin. (**A**) Leptin (10 μg in 2 μl of saline, icv) increases hypothalamic mTOR signaling. (Left) Representative Western blot from saline- or leptin-treated rats. β-actin was the loading control. (Right) Quantification by image analysis of hypothalamic S6K1 and S6 phosphorylation. Error bars indicate SEM. *P < 0.05 versus saline-treated rats. Five brains were examined for each condition. (**B** and **C**) Rapamycin (25 μg in 2 μl of DMSO, icv) blocks the central action of leptin (10 μg in 2 μl of saline, icv) on food intake (B) and body weight changes (C). The data are shown as the mean ± SEM. Saline- or DMSO-treated rats ($n = 3$) were compared with treated rats ($n = 8$). *P < 0.05 versus saline/DMSO- or saline/rapamycin-treated rats; #P < 0.05 versus leptin/rapamycin-treated rats. (**D**) Proposed model for the role of mTOR signaling in the hypothalamic regulation of energy balance. Anorectic signals, such as amino acids (L-leucine), leptin, and re-feeding, increase hypothalamic mTOR signaling. Increased mTOR activity leads to a decrease in food intake. Rapamycin inhibits hypothalamic mTOR, causing an increase in food intake. Opposite to their effect on mTOR, leptin and re-feeding decrease hypothalamic AMPK (*27*). mTOR is inhibited by AMPK-dependent mechanisms in vitro (*28*). Thus, reciprocal interaction might exist between hypothalamic mTOR and AMPK.

(*21*). Cells suppress protein synthesis when there is insufficient energy or amino acid substrate, and mTOR plays a critical role in this regulatory mechanism. Similarly, the CNS must monitor fuel and substrate levels to coordinate the availability of fuel for the entire organism. Whereas a signal of low fuel in a single peripheral cell may curtail its own protein synthesis, causing a localized catabolic action, a signal of low fuel in key areas of the CNS might be expected to increase food intake, producing an overall anabolic effect.

CNS circuits can directly sense glucose and specific fatty acids, integrating this information to modulate caloric intake (*1*, *22*). Our findings expand the knowledge of these CNS sensing mechanisms to include a protein component: the amino acid L-leucine. However, the degree to which amino acids act as physiological signals to centrally modulate energy balance, in situations other than amino acid imbalance (*23*), is unclear. The ability of L-leucine to activate mTOR in the hypothalamus and to inhibit food intake may be an example of CNS circuits using an evolutionarily conserved signaling mechanism as a fuel sensor rather than as an amino acid sensor.

An important feature of the mTOR pathway is that its activity is modulated by growth factors and hormones. Our data indicate that hypothalamic mTOR signaling can be modulated by leptin and that leptin's effect on food intake is mTOR-dependent.

One implication of our experiments relates to recent findings describing leptin induced rapid reorganization of synapses in the ARC (*24*). Local regulation of mRNA translation plays an important role in axon guidance and neuronal plasticity, which are processes that involve mTOR activity (*25*). Conceivably, the inhibition of mTOR signaling may block leptin's anorectic effect by suppressing the hormone's synaptic remodeling activity.

Other fuel-sensitive kinases have been implicated in the hypothalamic control of energy balance. Like mTOR, AMP-activated protein kinase (AMPK) is regulated by intracellular AMP/ATP ratios. However, in contrast to mTOR, AMPK activity is increased during fuel deficiency (*26*) and inhibited by leptin and nutrient signals (*27*). AMPK overexpression in the hypothalamus increases food intake and body weight, and its down-regulation inhibits feeding (*27*). Moreover, the activation of AMPK-dependent mechanisms leads to the inhibition of mTOR activity (*28*). Thus, AMPK and mTOR may have overlapping and reciprocal functions (Fig. 4D).

These fuel-sensitive signaling pathways may ultimately provide important insights into the link between obesity and type 2 diabetes. In peripheral organs such as the liver, and in skeletal muscle, fuel overabundance is deleterious because it alters the activity of fuel-sensitive kinases (increased mTOR and decreased AMPK), causing insulin resistance, which in turn suppresses nutrient uptake into tissues (*10*, *26*). In the CNS, an overabundance of fuel and nutrients may produce similar changes in mTOR and AMPK signaling, leading, conversely, to a beneficial reduction in nutrient intake and in the level of stored fat. As long as the CNS responses are adequate, the organism can remain in a state of metabolic balance. However, an imbalance between peripheral and CNS fuel-sensing pathways may predispose toward the development of obesity and/or diabetes.

References and Notes

1. B. E. Levin, A. A. Dunn-Meynell, V. H. Routh, *Int. Rev. Neurobiol.* **51**, 219 (2002).
2. S. Ritter, K. Bugarith, T. T. Dinh, *J. Comp. Neurol.* **432**, 197 (2001).
3. R. J. Seeley, S. C. Woods, *Nat. Rev. Neurosci.* **4**, 901 (2003).
4. D. M. Sabatini, H. Erdjument-Bromage, M. Lui, P. Tempst, S. H. Snyder, *Cell* **78**, 35 (1994).
5. T. Schmelzle, M. N. Hall, *Cell* **103**, 253 (2000).
6. E. Jacinto, M. N. Hall, *Nat. Rev. Mol. Cell Biol.* **4**, 117 (2003).
7. P. B. Dennis *et al.*, *Science* **294**, 1102 (2001).
8. Y. G. Gangloff *et al.*, *Mol. Cell. Biol.* **24**, 9508 (2004).
9. J. Montagne *et al.*, *Science* **285**, 2126 (1999).
10. B. D. Manning, *J. Cell Biol.* **167**, 399 (2004).
11. K. Inoki, M. N. Corradetti, K. L. Guan, *Nat. Genet.* **37**, 19 (2005).
12. L. Khamzina, A. Veilleux, S. Bergeron, A. Marette, *Endocrinology* **146**, 1473 (2005).
13. S. H. Um *et al.*, *Nature* **431**, 200 (2004).
14. C. J. Sabers *et al.*, *J. Biol. Chem.* **270**, 815 (1995).
15. Materials and methods are available as supporting material on *Science* Online.
16. A. J. Meijer, P. F. Dubbelhuis, *Biochem. Biophys. Res. Commun.* **313**, 397 (2004).
17. C. G. Proud, *Eur. J. Biochem.* **269**, 5338 (2002).
18. M. A. Bjornsti, P. J. Houghton, *Nat. Rev. Cancer* **4**, 335 (2004).
19. K. D. Niswender *et al.*, *Nature* **413**, 794 (2001).
20. K. D. Niswender *et al.*, *Diabetes* **52**, 227 (2003).
21. Q. Wu, Y. Zhang, J. Xu, P. Shen, *Proc. Natl. Acad. Sci. U.S.A.* **102**, 13289 (2005).
22. T. K. Lam, G. J. Schwartz, L. Rossetti, *Nat. Neurosci.* **8**, 579 (2005).
23. D. W. Gietzen, L. J. Magrum, *J. Nutr.* **131**, 851S (2001).
24. S. Pinto *et al.*, *Science* **304**, 110 (2004).
25. G. M. Schratt, E. A. Nigh, W. G. Chen, L. Hu, M. E. Greenberg, *J. Neurosci.* **24**, 7366 (2004).
26. B. B. Kahn, T. Alquier, D. Carling, D. G. Hardie, *Cell. Metab.* **1**, 15 (2005).
27. Y. Minokoshi *et al.*, *Nature* **428**, 569 (2004).
28. K. Inoki, T. Zhu, K. L. Guan, *Cell* **115**, 577 (2003).

29. We thank L. De, E. Matter, K. Parks, J. Reed, E. Richer, D. Russell, J. Sorrell, and M. Toure for expert technical assistance; J. P. Herman and C. M. Padgett for assistance with artwork preparation; and H. Shi for assistance with the quantification of the immunohistochemistry. Supported by NIH grants DK 17844, DK 54080, and DK 54890. G.T. receives research support from Novartis.

Supporting Online Material

www.sciencemag.org/cgi/content/full/312/5775/927/DC1
Materials and Methods
Figs. S1 to S5
Table S1
References

21 December 2005; accepted 25 March 2006
10.1126/science.1124147

High-Throughput HPLC

The Prominence high-performance liquid chromatograph (HPLC) is designed to meet a wide array of research and testing needs by combining high sensitivity detection with a fast autosampler and web-based instrument control. The Prominence HPLC features high pump motor resolution, stable temperature control, 10-sec injection speed with excellent accuracy and low carryover, and a fast-response ultraviolet detector. The Shim-pack XR-ODS column increases analysis speed while decreasing back pressure. The instrument offers reliable operation at 85°C for elevated temperature LC. The Prominence MD Method Development System features full automation from injection to report generation and the ability to configure four solvent pairs and up to 10 columns. It features automatic flushing of flow lines whenever the mobile phase is changed to allow easy comparison of chromatographic results.
Shimadzu Scientific Instruments For information 800-477-1227 www.ssi.shimadzu.com

RNA from a Single Cell

The ArrayPure Nano-scale RNA Purification Kit provides all the reagents needed to purify RNA from one or more eukaryotic cells, including quantities typically obtained with laser capture procedures. The kit contains only aqueous solutions and requires no toxic organic solvents. This protocol has been tested with quantitative real-time polymerase chain reaction on 1 to 10,000 eukaryotic cells. Very low cell numbers were trapped in a microcapillary pipet and enumerated by observation with an inverted microscope. Microgram amounts of RNA have been produced from 20 HeLa cells using two rounds of RNA amplification.
Epicentre Biotechnologies For information 800-284-8474 www.EpiBio.com

PTFE Membranes

Omnipore hydrophilic membrane filters are compatible with virtually all solvents, acids, and alkaline solutions. The polytetrafluoroethylene (PTFE) membrane filters are available as 13-mm, 25-mm, and 47-mm cut disks in a range of pore sizes from 0.1 to 10 μm. The membranes are optimized for low drug- and protein-binding, with excellent throughput in typical aqueous and solvent sample preparation. Millipore also offers the LCR membrane, manufactured specifically for high-performance liquid chromatography solvent filtration applications.
Millipore For information 800-MILLIPORE www.millipore.com

Protein Crystallization

Analysis of a protein's three-dimensional structure is essential to understanding its function, but identifying the chemical conditions that lead to highly diffracting protein crystals has been a tedious, time-consuming, hit-or-miss process. Qiagen's EasyXtal and NeXtal products offer a chance of obtaining protein crystals in a short time using the minimum amount of protein. The chance of finding the right conditions is increased by systematic screening with the world's largest offering of protein crystallization screening conditions. Each Screening Suite provides 96 different, systematically formulated conditions based around chemical species that have been proven to promote crystallization. Screening Suites are available in a range of volumes, from microplates to 10-ml tubes.
Qiagen For information 800-426-8157 www.qiagen.com

NMR CryoProbe

The QNP CryoProbe is for multipurpose nuclear magnetic resonance (NMR) measurements of four different nuclei—phosphorus, carbon, nitrogen, and hydrogen. This unique, 5-mm, general purpose, cryogenically cooled probe is automated to easily switch between these nuclei, eliminating the need to change probes. Phosphorus, carbon, nitrogen, and hydrogen are present individually or together in a majority of organic, biological, and inorganic compounds. The direct observation of these nuclei can provide quantitative information in addition to small molecule structural data, and the most significant advantage of the new probe is that it enables more complete characterization of molecules that contain all four of the nuclei. While traditional CryoProbes are aimed at biological research, the new QNP CryoProbe is suitable for applications in organic and inorganic chemistry.
Bruker BioSpin For information 978-667-9580 www.bruker-biospin.com

Tangential Flow Filtration

Two tangential flow filtration (TFF) products allow researchers to easily purify large volumes of protein-containing solutions. Applications typically include concentrating and desalting proteins from cell culture supernatants and fermentation broths. The high-flux, low-binding Millipore membranes used in these devices provide high protein retention and recovery. Pellicon XL Devices are available with a choice of Durapore PVDF membrane (microporous), Ultracel regenerated cellulose membrane (ultrafiltration), or Biomax polyethersulfone membrane (ultrafiltration), and membranes for concentrating and desalting from 100 ml to 2 l of protein-containing solution. Compared with large stirred cell systems, Pellicon XL Devices offer better flow rate with less processing time. Pellicon 2 Mini-Cassettes are available with either regenerated cellulose or polyethersulfone membranes for processing up to 10 l of protein-containing solution. Larger cassette systems are available for processing 250 l or more of solution.
Millipore For information 800-MILLIPORE www.millipore.com/bioscience

Newly offered instrumentation, apparatus, and laboratory materials of interest to researchers in all disciplines in academic, industrial, and government organizations are featured in this space. Emphasis is given to purpose, chief characteristics, and availability of products and materials. Endorsement by *Science* or AAAS of any products or materials mentioned is not implied. Additional information may be obtained from the manufacturer or supplier by visiting www.science.labvelocity.com on the Web, where you can request that the information be sent to you by e-mail, fax, mail, or telephone.

POSITIONS OPEN

ASSISTANT/ASSOCIATE PROFESSOR
Bioinformatics
Clemson University/Greenwood Genetic Center

The Department of Genetics and Biochemistry **(website: http://www.clemson.edu/genbiochem/)** and the Greenwood Genetic Center **(website: http://www.ggc.org/)** jointly invite applications for an Assistant or Associate Professor position in bioinformatics. This joint position is a tenure-track, 100 percent research appointment at Clemson University. The individual will be physically located in the J.C. Self Research Institute of Human Genetics at the Greenwood Genetic Center campus in Greenwood, South Carolina. Faculty at the Greenwood Genetic Center hold faculty appointments in the Department of Genetics and Biochemistry and are involved in training students and performing research.

Successful applicants must have a Ph.D. degree, a strong publication record, and at least two years of postdoctoral experience in bioinformatics or a related discipline. Experience in sequence analysis and data mining is essential. Additionally, knowledge of statistics and human genetics is desired. Special consideration will be given to candidates with experience in gene phylogeny, microarray analysis, proteomics, and comparative genomics. Successful candidates will be expected to collaborate with other researchers at the Greenwood Genetic Center, develop extramurally funded research programs, and mentor undergraduate and graduate students from the Department of Genetics and Biochemistry. To apply, submit a cover letter, curriculum vitae, future research plan, and contact information for three references as a PDF file to **e-mail: gblss@clemson.edu** with Bioinformatics Position in the subject heading. Applications received by June 9, 2006, will receive full consideration. *Clemson University is an Equal Employment Opportunity/Affirmative Action Employer and does not discriminate against any individual on the basis of age, color, disability, gender, national origin, religion, sexual orientation, or veteran status.*

ASSISTANT PROFESSOR
Microbiology and Cell Science
University of Florida

The Microbiology and Cell Science Department at the University of Florida invites applications for an Assistant Professor tenure-track position to develop an externally funded research program in microbiology. The research interest is open but candidates with interests in evolutionary microbiology, systems biology, structure-function relationships of microbial model systems, or host-microbe interactions, are especially encouraged to apply. Applicants must have a Ph.D., postdoctoral experience, and a strong publication record. The successful candidate is expected to develop an outstanding program and participate in our undergraduate and graduate programs. A very competitive startup package and salary are available to the successful candidate. Details of the Department and the position may be found at **website: http://microcell.ufl.edu.** Submit applications as a single PDF file containing a cover letter, curriculum vitae, and summary of research interests to **Dr. Madeline Rasche (e-mail: mrasche@ufl.edu).** Three letters of reference should also be sent directly to **e-mail: mrasche@ufl.edu.** Review of applications will begin June 1, 2006. *The University of Florida is an Equal Opportunity Employer.*

MOLECULAR CARDIOLOGIST. The Division of Cardiology at the Weill – Cornell University Medical Center seeks highly qualified applicants (M.D., Ph.D., M.D./Ph.D.) for tenure-track positions in basic and/or translational cardiovascular research at the Assistant or Associate Professor level. The Molecular Cardiology Program is a multidisciplinary team currently devoted to human genetics, cardiovascular development, vascular biology, genomics, electrophysiology, and gene therapy. Please send curriculum vitae to: **Bruce B. Lerman, M.D., Chief, Division of Cardiology, Cornell University Medical Center, 525 East 68th Street, Starr 409, New York, NY 10021.**

POSITIONS OPEN

ASSISTANT PROFESSOR
Microbiology and Cell Science
Citrus Research and Education Center
University of Florida

The Department of Microbiology and Cell Science at the University of Florida invites applications and nominations for a 12-month tenure-accruing position as Assistant Professor at 90 percent research and 10 percent teaching located at the Citrus Research and Education Center at Lake Alfred. Applicants must have a Ph.D in microbiology, plant pathology, or related field. Postdoctoral experience is preferred. The successful candidate is expected to develop an outstanding research program supported with extramural funding as well as recruit, mentor, and train graduate students. The research component is to focus on fastidious bacterial diseases of citrus, with particular emphasis on Huanglongbing (citrus greening). The causal agent of this disease is believed to be an uncultured α-proteobacterium that lives within the phloem of citrus. This is a terrific opportunity for anyone interested in the culturing, physiology, and genomics of a novel α-proteobacterium. Application should include a letter of application, curriculum vitae, list of publications, copies of transcripts of all university work, and three letters of recommendation. Send all application materials to: **William O. Dawson, Chair, Search and Screen Committee, Citrus Research and Education Center, 700 Experiment Station Road, Lake Alfred, FL 33850** or by **e-mail: wodtmv@ufl.edu.** Review of applications will begin on June 1, 2006. *Women and minorities are encouraged to apply. The University of Florida is an Equal Opportunity Employer.*

FACULTY POSITIONS
Lung Pathobiology

The Ohio State University, Division of Pulmonary, Allergy, Critical Care and Sleep Medicine **(website: http://www.internalmedicine.osu.edu/pulmonary/index.cfm)** and the Dorothy Davis Heart and Lung Research Institute **(website: http://heartlung.osu.edu/)** are seeking four basic science faculty working in areas related to human genetics of lung disease, acute lung injury/sepsis, or chronic inflammation and repair of the lung. Ph.D. scientists or physician-scientist candidates with a strong record of publications and grant support are encouraged to apply. Send curriculum vitae, statement of research interests and direction, three reference contacts, and cover letter to: **Dr. Clay Marsh, Division Director, The Ohio State University, Pulmonary Critical Care, Allergy and Sleep Medicine, 201 HLRI, 473 W. 12th Avenue, Columbus, OH 43210. Telephone: 614-247-7707; e-mail: clay.marsh@osumc.edu.** *The Ohio State University is an Equal Opportunity/Affirmative Action Employer. Qualified women, minorities, Vietnam era veterans, and individuals with disabilities are encouraged to apply.*

FACULTY POSITION
University of Wisconsin, Madison
Integrative Physiology

The Department of Comparative Biosciences, School of Veterinary Medicine invites applications for a tenure-track faculty position (Assistant or Associate Professor). Qualifications include a Ph.D., postdoctoral experience, commitment to excellence in teaching, and the ability to develop an extramurally funded research program in an area of physiology integrating cellular and molecular studies in a whole organism perspective. Teaching responsibilities include participation in a physiology course in the veterinary medical curriculum and/or the undergraduate level. To apply, send curriculum vitae, brief statements of research interests and teaching philosophies, and three letters of reference to: **Gordon S. Mitchell, Chair, Department of Comparative Biosciences, University of Wisconsin, 2015 Linden Drive, Madison, WI 53706.** Apply by July 1, 2006. For additional information, see **website: http://www.vetmed.wisc.edu/jobs.html.** *Equal Opportunity/Affirmative Action Employer.*

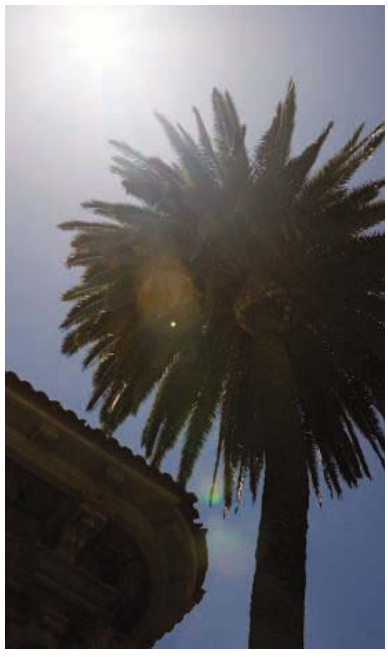

FOCUS ON CAREERS

California
A Sunny State of Opportunities

The high concentration of academics and industry in California makes this state a desirable destination for many job seekers in life sciences. In this article, experts from academic, government, and industrial settings describe the skills in highest demand and techniques for gaining the best job. BY MIKE MAY

California hosts a range of life science employers: hundreds of biotechnology and pharmaceutical companies, state and private academic institutions, private research organizations, and government laboratories. In addition, "California has some of the most attractive urban areas on the planet," says Elbert Branscomb, associate director of biosciences at the Lawrence Livermore National Laboratory.

Getting a job in that sunny environment, however, takes some doing. Branscomb says, "My impressionistic view from people applying to jobs here and gossip on the streets is that the market is fairly flat. We see quite a few people out looking for jobs because a corporation has failed or changed directions."

When it comes to biotechnology, though, optimism sometimes shines as brightly as the sun in San Diego. Madeline Butler, academic coordinator for undergraduate laboratories in the division of biological sciences at the University of California, San Diego (UCSD), says, "Our students with undergraduate degrees in biology seem to do well getting jobs in academic institutions and at biotechnology companies." Likewise, Holly Butler, principle staffing consultant in research staffing at Genentech, also sees many opportunities. She says, "The California job market for life sciences remains strong. San Diego and the San Francisco Bay Area are home to the majority of the jobs, but new biotechnology companies are sprouting up throughout the state." Rich Pennock, regional director at Kelly Scientific Resources, also sees growing job opportunities in California. He says, "We are seeing unemployment dropping in California, and a lot of the companies—especially pharmaceutical companies—are hiring." He adds, "Biotech money is also loosening up, so some of the incubator companies are also hiring."

Like all life science markets, California's can be divided into two general areas. Michael French, senior vice president of corporate development at Sirna Therapeutics, says. "The biotech job market can be divided into the business side and the research side." Biotech business opportunities are dynamic in the San Francisco Bay Area, says French. "People move around a lot in that space. So the job opportunities there are very good." For bench scientists, French says there are solid opportunities at many companies. "California is a great area for both of these types of jobs," says French.

Whether the current California job market is flat or growing, experts interviewed here expect a bustling future. Branscomb CONTINUED »

Genentech
http://www.gene.com

Kelly Scientific Resources
http://www.kellyscientific.com

Lawrence Livermore National Laboratory
http://www.llnl.gov

Sirna Therapeutics
http://www.sirna.com

University of California, San Diego
http://www.ucsd.edu/

says, "There seems to be no doubt that biology is going through a phase transition and will emerge as a dominant scientific, technological, and economic force." He adds, "This century will surely be the time in which mankind finally figures out how life works. We are suddenly broaching into the real central chambers of the mystery of life and developing the tools to take it on in meaningful ways."


ELBERT BRANSCOMB

Marketable Abilities

The breadth of employers in California generates equally broad needs for scientists. "For R&D," Madeline Butler of UCSD says, "we see a demand for people with capabilities in molecular biology and biochemical techniques. These are still very big areas for bench jobs." She also sees considerable demand for experience in bioengineering and chemical engineering. Experience in a lab also improves an undergraduate's employability. For example, Madeline Butler says, "There's a lot of interest in students with some whole animal physiology and in vivo pharmacology experience. Students do not get much hands-on experience in these areas in undergraduate classes but they can get it through research opportunities and internships, which we encourage them to do."

Chemistry also offers many opportunities. "For chemists, there is a huge need across the board—medicinal chemists, organic chemists, formulation chemists, and so on," says French. If a biologist happens to have knowledge related to a target area that interests pharmaceutical companies, says French, "That person will be in great demand, but the therapeutic target du jour varies." That variation, though, does not hurt a biologist's attractiveness as much in core therapeutic areas such as metabolism, cardiovascular, and inflammation, according to French.

When asked about the categories of skills in greatest demand, Pennock mentions two. First, he agrees with the demand for chemists. He says, "Analytical chemists have always been in demand. The demand is very robust for skills in areas like high pressure liquid chromatography and gas chromatography." He adds, "Wet lab chemists are also in high demand." The second area of skills in demand, according to Pennock, is molecular biology. Here, he points out demand for capabilities in assay development, cell culture, enzyme linked immunosorbent assay (ELISA), and the polymerase chain reaction (PCR). He also says that his company is seeing an increased need for people with backgrounds in good laboratory and manufacturing practices. A cross-disciplinary background, such as biochemistry, is also valuable, says Pennock.

According to Holly Butler of Genentech, "We are interested in candidates who have targeted research experience." She adds, "Employers are looking for well qualified, passive job seekers—meaning people who already have jobs and are good at what they do, especially those with superior academic records and proven success at learning and growing in their chosen field while adding value to their employer in the process." In terms of the most readily available positions, she says, "The disciplines that employers typically need help filling positions in are research and development, clinical, regulatory, quality assurance and quality control, manufacturing, pharmacology, and bioinformatics, genomics, toxicology, and immunology."

Branscomb sees needs for people with a variety of modern capabilities. "Most of what we see advertised for and what we are often interested in," he says, "has been dominated by a few themes, such as a combination of solid biological and computational skills." He explains: "Someone is golden who understands an area of biology, can use algorithms, and is computer comfortable or can even write serious code." Branscomb also sees lots of opportunities in "techniques that are transforming scientific methodology, such as array technology, comparative genomic approaches, proteomics, sequence analysis." He adds, "The fact that we can query entire genomes for the state of play at a specific moment is absolutely transforming the science."

The opportunities, though, extend beyond brand new science. Branscomb also sees advances in classical areas of biology. He says, "Immunology is rising on the tide of transformations in methodological power." He adds that rapid advances in developmental biology are also refreshing that area of research.


MADELINE BUTLER

Riding the Rising and Crashing Waves

Some geographical areas offer the highest density of opportunities. Branscomb says that some areas of California—such as San Diego and the San Francisco Bay area—always seem hot for jobs in the life sciences. Madeline Butler agrees. She says, "There's definitely a demand here in San Diego. Some of the diagnostics companies, for instance, are expanding, and there's been an influx of big pharma into the area recently." She adds, "There seems to be a growing need for people with expertise in antibody therapies, pharmacokinetics, and toxicology. Companies also seem to be looking for people with a knowledge of biology and manufacturing." CONTINUED »

Visit **www.sciencecareers.org** and plan to attend upcoming meetings and job fairs that will help further your career.

Others
call it research.

We call it changing the medical textbooks.




For 30 years, Genentech has been at the forefront of the biotechnology industry, using human genetic information to discover, develop, commercialize and manufacture biotherapeutics that address significant unmet medical needs. Today, Genentech manufactures and commercializes multiple biotechnology products that have helped patients suffering from serious diseases and conditions, including breast cancer, colorectal cancer, non-Hodgkin's lymphoma, lung cancer, rheumatoid arthritis, cystic fibrosis and allergic asthma. The company is the leading provider of anti-tumor therapeutics in the United States.

Genentech's research organization features world-renowned scientists who are some of the most prolific in their fields and in the industry. Our more than 650 scientists have consistently published important papers in prestigious journals and have secured more than 5,500 patents worldwide (with an equal number pending). Genentech's research organization combines the best of the academic and corporate worlds, allowing researchers not only to pursue important scientific questions but also to watch an idea move from the laboratory into development and out into the clinic. We are proud of our long history of groundbreaking science leading to first-in-class therapies, and we hope you'll consider joining us as we continue the tradition.

Our continued growth has created opportunities in Research in our South San Francisco headquarters. Please take this opportunity to learn about Genentech, where the creativity and openness of an academic environment meet the rigorous dedication of industry-leading professionals focused on improving and extending people's lives.

We have opportunities for Postdoctoral Fellows, Research Associates and Scientists in the following areas:

- Angiogenesis
- Antibody Engineering
- Assay Technology
- Bioinformatics
- Biomedical Imaging
- Cell Biology
- Immunology
- Medicinal Chemistry
- Molecular Biology
- Molecular Diagnostics
- Molecular Oncology
- Pathology
- Protein Chemistry
- Protein Engineering
- Translational Oncology
- Tumor Biology

Genentech was named #1 on FORTUNE's 2006 "100 Best Companies to Work For" list.

To learn more about these opportunities, please visit **www.gene.com/careers**. Please use "Ad - Science" when a "source" is requested. Genentech is an equal opportunity employer.

Genentech
IN BUSINESS FOR LIFE
www.gene.com

Pennock sees the geographical areas of demand as centered around three hubs: San Diego, San Francisco, and Los Angeles. "The farther you get from one of those hubs," says Pennock, "the fewer job opportunities you will see." In some cases, though, new job areas do develop now and then. For example, Pennock says, "Big pharma manufacturing is on the rise in Vacaville, California."

In general, though, Branscomb sees a life in biology as a life of change. "For many biotech firms, this has been an era of high instability," he says. "A firm can be bought by another and then change direction and get rid of much of the staff." He adds, "Even for very able people, biotech is not necessarily a very stable job. If stability matters to you, then this may not be not be the field for you."

Despite this draw back, Madeline Butler sees ways to survive. She says, "One of the advantages is that San Diego offers an abundance of opportunities. Although downsizing and layoffs are always disruptive, in this area there are so many companies and institutes that experienced people can often land new jobs quickly and can avoid having to relocate."

As with all of the experts interviewed here, Madeline Butler sees California as a great place to live. She says, "The weather and proximity to the beach are big pluses here." Then she adds, "Unfortunately, the housing prices balance the pluses. Relocating here from where housing is less expensive can be a bit of a shock." Branscomb agrees about California's high cost of living. He says, "It's so expensive to live here, and you have to live close to your work or suffer intolerably from the traffic. On average, though, we judge ourselves to be very advantaged for being in California." Perhaps best of all, Holly Butler notes: "California's the only state where you can ski and surf in the same day."

Nonetheless, the shortcomings of working in California can be significant. "One of the things we're seeing," says Pennock, "is that it is very difficult for someone outside California to make the transition into this state, because they are not familiar with the costs. When they find out about California's cost of living, it's pretty negative." He adds, "You really need a salary that overcomes those shortcomings." In some cases, in Pennock's perspective, companies in California do try to take the cost of living into account in offering a salary. "This is typically only true in mid-career to more experienced positions," he says. "At the entry level, we don't see that."

For further valuable career advice, visit **www.sciencecareers.org**, click on **Career Development**.

RICH PENNOCK

Personalizing the Possibilities

To get a life science job in California, Madeline Butler says, "getting experience—in academics or industry—is the primary thing." Then she adds, "As you move up, though, you must decide if you want academics or industry. They are very different environments."

French agrees that a job seeker should decide what environment is most appealing. He says, "California offers a variety of opportunities from the high risk 'working out of a garage' environment to the more solid mid to large pharmaceutical and biotech companies." In thinking over such options, French advises: "Be true to yourself about what you want." For example, the high risk garage job might sound great until you find yourself working till midnight when your family expected you home hours earlier. Likewise, French says, "People who are great researchers at a university might not find that they can accommodate the pressures of performing in a commercial environment."

After deciding what kind of job sounds most appealing, Branscomb recommends a personal touch. He says, "First of all, I'd do the standard thing: search, search, search." Then he adds, "Quickly bend that search to personal contacts. Personalize your search as aggressively as possible. Find people in similar areas to your interest and training who recently found jobs and go talk to them."

Moreover, different organizations may hire in different ways. Holly Butler says, "Larger companies have pretty sophisticated websites and online recruiting systems that work pretty well. Some smaller ones still will respond to the personal touch and will appreciate it."

Pennock thinks that a job seeker should first decide which of the three geographical hubs—San Diego, San Francisco, or Los Angeles—is most appealing. "These are distinct hubs, with distinct cultural scenarios," he says. "Decide which one offers the quality of life that you want." Then he says that a job hunter should put together a skill inventory—essentially a list of capabilities—and see how that matches up with jobs in the chosen hub. After that, Pennock says, "Turn to networking. Get referrals from friends." He adds, "You can also turn to professional associations and services like Kelly Scientific Resources."

The overall key to gaining employment and building a successful career in the life sciences, though, depends most on desire. "This is a line of work like being an actor," Branscomb says. "If you're not driven to it by idiosyncratic madness, you probably shouldn't do it." He adds, "The ones who really succeed have an almost irrational desire."

Mike May (mikemay@mindspring.com) is a publishing consultant for science and technology based in the state of Minnesota, U.S.A.

DIRECTOR OF RESEARCH

The California Academy of Sciences is recruiting for a Director of Research to help develop and implement a vision for the Academy's research departments, library, technical laboratories, and the training of students in systematic and evolutionary biology. The new Director will advance the Academy's research agenda and provide leadership in: collections and associated data, budgets, long-term planning, administration and integrated programming across the Academy. As part of the senior management team, the Director will serve as liaison with the Science Council, Fellows of the Academy, and members of the scientific community.

A Ph.D. in one of the Academy's scientific disciplines is required, with a focus on systematics and evolutionary biology, and the experience and qualifications of an Associate or Full Curator. The successful candidate must be able to articulate the Academy's research mission to diverse constituencies at local, national and international levels, seek funding for the research enterprise, and have demonstrated experience in the administration of research organizations or complex organizations.

Founded in 1853, and located in San Francisco, the Academy includes a natural history museum, aquarium, planetarium, research division and education programs. The Academy will begin the move from its current temporary space to a new facility in Golden Gate Park in late 2007.

Interested applicants should send a letter of interest, curriculum vitae and the names and contact information of three references to:

California Academy of Sciences
Attn: HR#DirRA
875 Howard Street
San Francisco, CA 94103-3098

Review of applications will commence on **September 1, 2006**.

The Academy, an Equal Opportunity Employer, offers a competitive salary and an excellent benefits package.

www.calacademy.org

PROFESSOR/RESEARCH SCIENTIST AND DIRECTOR
AIR POLLUTION RESEARCH CENTER
UNIVERSITY OF CALIFORNIA, RIVERSIDE

Applications and nominations are invited for the position of Professor/Research Scientist who will also serve as Director of the Air Pollution Research Center (APRC) of the University of California, Riverside. The APRC is an Organized Research Unit within the University of California system, with responsibilities for research and, through appointments with academic departments, teaching at the undergraduate and graduate levels. APRC's research mission has historically focused on atmospheric processes, including the chemical processes involved in the formation of air pollution and the atmospheric transformations of organic compounds, and the subsequent effects on the environment, including on plants.

Candidates should have a record of outstanding, internationally recognized, research productivity in atmospheric sciences. It is expected that the successful candidate will hold a Ph.D. in chemistry, physics, environmental sciences, engineering, or a related discipline, and have a research emphasis in some area of atmospheric processes. He or she will be expected to maintain an active and highly visible research program while providing leadership as Director of APRC. In keeping with the policy of integrating the APRC research programs with the academic research and instructional activities of the campus, the Director/Research Scientist will also hold a 50% tenured appointment at the Full Professor level in an appropriate academic department, where he or she will participate in the undergraduate and graduate instructional programs. A commitment to excellence in both teaching and research and a vision of interconnections between APRC and academic programs are especially important. Salary will be commensurate with education and experience. The anticipated start time for this position is July 2007.

Applicants should send a complete resume, a statement of research interests and a statement of teaching interests, in addition to the names of five individuals who may be contacted for letters of reference, to: **APRC Search Committee Chair, c/o Department of Environmental Sciences, Room 2208 Geology, University of California, Riverside, CA 92521-0424**. Evaluations of applications will begin **July 1, 2006**, but applications will be accepted until the position is filled.

The University of California is an Affirmative Action Equal Opportunity Employer.

CALIFORNIA CAREERS

The Chemistry is right.

Anadys Pharmaceuticals (NASDAQ: ANDS) is a rapidly growing biopharmaceutical company committed to advancing patient care by discovering, developing and commercializing novel small molecule medicines for the treatment of hepatitis, other serious infections, and cancer. The Company has core expertise in Toll-Like Receptor-based small molecule therapeutics and structure-based drug design coupled with medicinal chemistry. Anadys' clinical development programs include ANA975 for the treatment of HCV and HBV, and ANA380 for the treatment of HBV. Backed by strong core values and an ongoing commitment to human health, our goal is to improve the quality of life worldwide. If you share our values and our goal, consider these opportunities:

- **Head of Document & Information Management**
- **Head of Pharmaceutical Research & Development**
- **Associate Director, Analytical Chemistry**

Anadys offers excellent salaries, stock options, advancement opportunities, ongoing training, 401(k), generous vacation, and a choice of PPO or HMO options with most employee health benefits provided at no cost. For more information about the above positions or to see additional opportunities, visit: **www.anadyspharma.com**

ANADYS
PHARMACEUTICALS, INC.

We are proud to be an equal opportunity employer.

UCIrvine
University of California, Irvine

Faculty Position in Immunology

The Department of Microbiology and Molecular Genetics at the University of California, Irvine (UCI) is seeking applicants for a faculty position at the Assistant or Associate Professor level, depending upon qualifications. More senior candidates also may be considered. The applicant's previous work should have been judged by peer review to have been scientifically rigorous. We are seeking a faculty member whose research is in one of several areas of **molecular immunology**, including but not limited to: **(1) Lymphocyte signaling; (2) Mechanisms of tolerance or autoimmunity; (3) Lymphocyte differentiation; (4) Host-pathogen interactions**. Candidates must have a Ph.D. and/or M.D. degree. The successful candidate will have teaching responsibilities typical of a medical school, but will have considerable time available for research and research-related activities. The successful candidate will have the opportunity to be a member of the UCI Center for Immunology, which includes 26 faculty members in both the School of Medicine and School of Biological Sciences with research interests broadly related to immunology. Please send curriculum vitae, summary of research interests, and names of three references to: **Dr. Eric J. Stanbridge, Search Committee Chair, Department of Microbiology and Molecular Genetics, School of Medicine, University of California, Irvine, CA 92697-4025.**

The University of California, Irvine has an active career partner program and an NSF ADVANCE Program for Gender Equity and is an Equal Opportunity Employer committed to excellence through diversity.

CALIFORNIA CAREERS

EACH THERAPY SHOULD BE TOO.

GENITOPE CORPORATION is a biotechnology company focused on the research and development of novel immunotherapies for the treatment of cancer. Genitope Corporation's lead product candidate, MyVax® Personalized Immunotherapy, is a patient-specific active immunotherapy based on the unique genetic makeup of a patient's tumor and is designed to activate the patient's immune system to identify and attack cancer cells. Genitope is conducting a pivotal Phase 3 clinical trial of MyVax® Personalized Immunotherapy in previously untreated indolent non-Hodgkin's lymphoma patients.

If you're looking for an opportunity to play a key role in the development of an innovative and personalized approach for treating cancer, please forward your resume and cover letter to:

GENITOPE CORPORATION
HR Department
Attn: Job#
525 Penobscot Drive
Redwood City, CA 94063
FAX: (650) 482-2002
Email: HR@genitope.com
No phone calls please. *EOE*

We currently have positions available in the following areas:

- **Development**
- **Project Management**
- **Quality Assurance/Control**
- **Regulatory Affairs**
- **Research**

We're seeking both Ph.D. and non-Ph.D. candidates.

To view a list of our current openings and to apply online, please visit our web site at:

www.genitope.com

Please reference Job# when applying.

Genitope Corporation
Delivering on the Promise of Personalized Medicine™

CAREERS IN MICROBIOLOGY

PNNL – Pacific Northwest National Laboratory
Associate Director of Microbiology

Pacific Northwest National Laboratory is seeking a Senior Scientist with expertise in microbiology with an emphasis on one or more of the following areas: environmental microbiology; systems microbiology; microbial genomics; or synthetic biology. Topics of research focus should include, but not necessarily be limited to, primary Department of Energy (DOE) mission areas of bioenergy, contaminant fate and transport, environmental remediation, and carbon cycling. The applicant will have the opportunity to lead a well-established research group in environmental microbiology funded primarily by DOE's Office of Biological and Environmental Research. The applicant will have line management responsibilities for the group ensuring significant scientific impact and serve as an interface between microbiology staff and other groups across the Laboratory. This position features access to extensive research capabilities such as controlled microbial cultivation facilities (e.g., bioreactors), global proteomics, microarray facilities, electron and confocal microscopies, and computational modeling. This position is located in Richland, WA.

Minimum Requirements: Ph.D. in microbiology, molecular biology, or related discipline and 7+ years' relevant experience. A complete list of requirements can be viewed at our webiste noted below.

Qualifications: The ideal candidate will demonstrate an interest in multi-disciplinary research; systems and synthetic biology-based approaches to problem solving; an interest in applying new knowledge to DOE missions of bioenergy, contaminant fate and transport, environmental remediation, and carbon cycling is desired. The successful candidate will have a demonstrated record of strong leadership qualities, scientific talent, team building and motivation skills, and managing to outcomes, as well as a proven commitment to the mentoring and development of junior scientific staff. The candidate will participate in setting the national and/or international research agenda and will have obtained recognition via publications, awards, citations, or other honors.

About Systems Biology and Biology at PNNL: **www.sysbio.org** ; **www.pnl.gov/biology** • About PNNL: **www.pnl.gov** • About the William R. Wiley Environmental Molecular Sciences Laboratory (EMSL): **www.emsl.pnl.gov** • About Tri-Cities: **www.visittri-cities.com** • Apply online: **www.jobs.pnl.gov**, Reference Requisition **#111629**

For more information, contact: **Josie Villa, Human Resources Manager, Josie.villa@pnl.gov**.

POSITIONS OPEN

Xishuangbanna Tropical Botanical Garden, the Chinese Academy of Sciences is a comprehensive research institution engaged in biodiversity conservation and sustainable uses of plant resources, focusing on forest ecosystem ecology, conservation biology and resource plant development. We are inviting applications for the following four positions:

1. PI for Research and development of biomass energy;
2. PI for Biodiversity management and policy issues;
3. PI for Ecological evolutionary biology;
4.Curator for the Living collections management.

Applicants should have a Ph.D. degree and relevant post-doctoral experience in biological sciences or a related discipline, and have an excellent record of productivity. Successful candidates will be appointed at the professorship level and provided with a competitive salary, startup package, and generous laboratory space. Appointees are expected to develop extramurally funded and internationally recognized research programs.

Interested individuals should submit (1) a letter of application, (2) curriculum vitae including list of publications, (3) a summary of research interests and future plans electronically as PDF files to **yuping@xtbg.ac.cn** and copy to **cj@xtbg.org.cn**

Review of applications will begin on August 15, 2006, and continue until suitable candidates are selected.

For more information about us, please visit **http://www.xtbg.ac.cn**

CAREERS IN MICROBIOLOGY

U.S. Environmental Protection Agency
Office of Research and Development

HIGH-LEVEL CAREER OPPORTUNITIES IN MICROBIOLOGY

EPA's Office of Research and Development (ORD) is seeking internationally recognized scientists to fill two positions: one in the National Exposure Research Laboratory (NERL) **http://www.epa.gov/nerl/** and another in the National Center for Environmental Assessment (NCEA) **http://www.epa.gov/ncea/**. Both positions are located in Cincinnati, Ohio.

ORD plans to fill these positions using EPA's Title 42 Authority, which offers up to 5-year renewable term appointments at highly competitive, market-based salaries. The positions are part of a larger EPA effort to use state-of-the-science approaches and technologies in its mission of protecting human health and the environment. The ideal candidates will have a doctoral level degree in a pertinent science discipline and extensive specialized experience. For more information about the two organizations and their respective job announcements, please refer to their websites as listed above.

Positions and major duties include:

NERL-06-42-04 Research Microbiologist

- Establishing and conducting a research program to address critical needs related to the assessment of exposure to microbiological hazards in water. An area of particular relevance to NERL is the development of innovative approaches for reliable concentration, detection and characterization of pathogens of concern to EPA. Other areas of research could involve studies to support the assessment of pathogenicity and the development of quantitative models of microbial risk.

NCEA-06-42-05 Microbial Risk Assessor

- Developing and implementing ORD's research agenda for microbial risk assessment, particularly (1) characterizing environmental exposures of humans to pathogenic microorganisms, (2) characterizing infectivity, virulence, and transmissibility of environmental microbial agents, and (3) characterizing both individual and population susceptibility to diseases caused by environmental microorganisms.
- Overseeing the conduct of microbial risk assessments which are of significant strategic importance to EPA risk management and rule-making decisions.

Responsibilities for both positions include providing leadership of ORD's microbiology research program, serving as a senior spokesperson/representative, identifying collaborative opportunities with outside organizations, and playing a vital role in the leadership of a proposed virtual EPA Institute for Environmental Microbiology.

Salary and Benefits: Salary is up to $200,000 per annum, dependent upon qualifications, experience, and other factors. The selected applicant will be eligible for full benefits including health and life insurance, retirement, and vacation and sick leave.

How to Apply: Send the following information: (a) a vision statement (1-2 pages) including your research goals and how they relate to the duties of the position for which you are applying; (b) curriculum vitae; (c) the names of three references; (d) citizenship status; and (e) compensation requirements. **Candidates must reference the specific vacancy number(s) of the position(s) for which they are applying.**

Applications should be mailed to the attention of: **Ms. Dorothy Carr, U.S. EPA, MD-C639-02, RTP, NC 27711** or sent via email to **title42@epa.gov** by **May 31, 2006**. For additional information, **Ms. Carr** can also be reached at **(800) 433-9633**. Technical questions pertaining to vacancy **NERL-06-42-04** may be addressed to **Dr. Al Dufour** at **(513) 569-7330**. Technical questions regarding vacancy **NCEA-06-42-05** may be addressed to **Dr. Glenn Suter** at **(513) 569-7808**.

The U.S. EPA is an Equal Opportunity Employer.

National Cancer Institute

U.S. DEPARTMENT OF HEALTH AND HUMAN SERVICES

National Institutes of Health

POSTDOCTORAL FELLOWSHIP (Ph.D./M.D.) OPPORTUNITIES

The National Cancer Institute offers numerous postdoctoral fellowship opportunities in a large variety of science disciplines (chemistry, biochemistry, bioinformatics, biology, biostatistics, cancer biology, cell biology, epidemiology, genetics, HIV research, immunology, microbiology, molecular biology, nuclear radiochemistry, nutrition, optical probe chemistry, pathology, pharmacology, virology, etc.).

Fellowship opportunities can be viewed on our training and employment Web site "StarCatcher" **http://generalemployment.nci.nih.gov**. We recommend that you post your resume in either job category "Postdoctoral Fellowship (U.S. citizens and permanent residents)" or "Postdoctoral Fellowship (foreign visiting fellows)" for viewing by our principal investigators. Then use the links to our research divisions to apply for current positions and communicate directly with the principal investigators. The **Center for Cancer Research** (NCI's largest clinical and basic science research division) lists multiple fellowship opportunities on their link and provides the opportunity to search their index of branches/labs/programs to find areas of research of particular interest to you. The **Division of Cancer Epidemiology and Genetics** provides an online application for fellowships in molecular, nutrition, radiation and genetic epidemiology. The **Division of Cancer Prevention** offers an online application process for fellowship opportunities in cancer prevention.

NCI facilities located in Bethesda, Rockville, Gaithersburg and Frederick Maryland, present a professional environment and possess the best-funded and equipped laboratories in the United States. As the largest institute within the National Institutes of Health, NCI provides postdoctoral fellows the opportunity to interact with scientists from a wide range of life/medical sciences, and to attend lectures given by international renowned scientists. Stipend range $38,500 to $71,000 commensurate with experience. Standard self and family health insurance is provided and high-option coverage is available. Program duration is 2 to 5 years.

Open to graduating doctorate degree (Ph.D. and/or M.D.) students and current postdoctoral fellows with less than 5 years postdoctoral experience. U.S. citizenship, permanent residency (green card), or current authorization (F-1 or J-1 visa) for training in the United States is required.

Apply online at **http://generalemployment.nci.nih.gov**

DHHS, NIH and NCI are EQUAL OPPORTUNITY EMPLOYERS

CAREERS IN MICROBIOLOGY

FACULTY POSITION IN MICROBIOLOGY/BACTERIOLOGY

The **Department of Veterinary and Biomedical Sciences, University of Minnesota**, invites applications for a full-time tenure-track faculty position in microbiology/bacteriology at the level of Assistant or Associate Professor. The selected candidate will join a Departmental program with demonstrated leadership in molecular biology, microbial and animal genome analysis, and infectious diseases. The successful candidate will receive a competitive salary and start-up package. Rank (Assistant or Associate Professor) will depend on qualifications and experience consistent with Collegiate and University policy. The successful candidate will become part of an expanding University commitment to cutting-edge research in infectious diseases, biomedical and agricultural genomics, and bioinformatics, and will have access to new facilities for high throughput screening, DNA sequencing, proteomics, microscopy and imaging.

Candidates must have a Ph.D. or foreign equivalent in a relevant field of biomedical, biological or agricultural sciences, and two or more years of postdoctoral experience. Demonstrated ability to publish in peer-reviewed journals, obtain extramural research support, and teaching experience are desired. The successful applicant is expected to develop or maintain an externally funded research program in an area of infectious diseases, participate in teaching of undergraduate microbiology and participate in graduate student programs.

Applicants must provide an introductory letter, curriculum vitae, a statement of research and teaching goals, and should arrange to have three letters of reference sent to the Search Coordinator. Letters of reference should include assessment of the applicant's background and abilities in research and interpersonal skills. Send materials to: **Ms. Lea Schwartz, Search Coordinator, Department of Veterinary and Biomedical Sciences, University of Minnesota, 205 Veterinary Science, 1971 Commonwealth Avenue, St. Paul, MN 55108: Fax (612) 625-5203; Email schwa142@umn.edu**. For inquiries, please contact **Dr. Randall Singer**, Search Committee Chair, **singe024@umn.edu**. Reviews of applications will continue until the position is filled.

The University of Minnesota is an Equal Opportunity Educator and Employer.

POSITIONS OPEN

HEAD OF DEPARTMENT CHEMISTRY & BIOCHEMISTRY

Worcester Polytechnic Institute invites applications and nominations for Head of the Department of Chemistry and Biochemistry. The Department is integral to a major new life science research initiative at WPI, supported by a new, state-of-the-art research facility scheduled to open in spring 2007. This $40M facility will host life science-related departments and the Bioengineering Institute. WPI seeks a Department Head with a clear and creative vision for building and sustaining ambitious departmental research programs during a period of growth. This vision will include enhancing the department's role in the life sciences and the successful candidate will be expected to oversee a vigorous faculty recruitment program. The Department Head will have an earned doctorate in chemistry or biochemistry, an international reputation in research, and a distinguished record of publication and funding in an area at the interface of chemistry and biochemistry. She or he must demonstrate outstanding leadership and mentoring abilities.

The Department of Chemistry and Biochemistry at WPI offers undergraduate and graduate (MS, Ph.D.) degrees in chemistry and biochemistry. WPI is a private, selective technological university with an undergraduate student body of 2800 and 1000 full-time and part-time graduate students. Worcester, New England's third largest city, offers ready access to diverse economic, cultural, and recreational resources of the region. Further information about WPI and the department can be accessed at **http://www.wpi.edu.**

The application should consist of a detailed curriculum vita, a letter of intent that describes professional interests (research, teaching, and administrative), and a vision statement for the future development of the department. Applicants should also supply the addresses, e-mails and telephone numbers of at least three references. Applications should be sent to: **WPI, Chemistry and Biochemistry Department, 100 Institute Rd., Worcester, MA 01609.** Nominations only may be sent by e-mail to **chem.-biochem@wpi.edu.** Further inquiries can be directed to **Dr. José Argüello (arguello@wpi.edu)** or **Dr. John MacDonald (jcm@wpi.edu).** Review of applications will continue until an appropriate candidate is identified.

WPI offers a smoke free environment, competitive compensation and an excellent benefits package including health insurance, family tuition reimbursement and generous vacations.

To enrich education through diversity, WPI is an affirmative action, equal opportunity employer.

Positions @ NIH
THE NATIONAL INSTITUTES OF HEALTH

Postdoctoral Research Opportunity
Dr. Karen L. Adelman
adelmank@niehs.nih.gov

Our laboratory's goal is to elucidate the dynamic interplay between signals from the extracellular environment and chromatin architecture, and to probe how chromatin structure and epigenetics influence gene activity. Although it has been known for many years that the compaction of DNA into chromatin can occlude protein binding sites and gene promoters, the ways in which the cellular machinery manipulates chromatin structure to influence gene expression remain poorly understood. We are investigating the transcriptional responses to specific stimuli to better appreciate the biological events that result from gene-environment interactions, including the pathological outcomes that result from transcription dysregulation.

The primary aim of our research is to address two key questions: (i) How do histone modifications and nucleosome remodeling affect Pol II initiation and elongation through a gene? (ii) What are the structural rearrangements that take place in a nucleosome to allow Pol II to access the information within the wrapped DNA?

We are currently undertaking both in vivo and in vitro approaches to probe the relationship between transcription by Pol II and chromatin (e.g. Adelman, et al., Mol. Cell, 2005; Mol. Cell. Biol., 2006), including a comprehensive RNAi screen and ChIP-on-chip location analysis. In addition, the successful applicant will help implement novel, single-molecule biophysical techniques to monitor transcription elongation in real-time (e.g. Adelman, et al., Mol Cell, 2004). These studies will also take advantage of the availability of cutting-edge microarray, protein expression, structural biology and mass spectrometry facilities at the NIEHS.

Applicants must possess a Ph.D. degree in Biochemistry, Biophysics or a related field and have less than three years of postdoctoral experience. Candidates with experience in optical imaging techniques, fluorescence microscopy and/or Labview are especially encouraged to apply. Salary will be commensurate with experience. Applications should be received no later than **June 23rd, 2006**. For consideration, send cover letter, curriculum vitae including list of publications, and the names/phone numbers/email addresses of three people who could provide letters of reference to:

Dr. Karen Adelman, Laboratory of Molecular Carcinogenesis, National Institute of Environmental Health Sciences, Room D454A, Mail Drop D4-02, 111 Alexander Drive, Research Triangle Park, NC 27709, FAX: 919-541-0146, Email: adelmank@niehs.nih.gov, http://dir.niehs.nih.gov/dirlmc/transcript.htm

Postdoctoral, Research and Clinical Fellowships at the National Institutes of Health

www.training.nih.gov/pdopenings

www.training.nih.gov/clinopenings

Train at the bench, the bedside, or both

Office of Intramural Training and Education
Bethesda, Maryland 20892-0240
800.445.8283

Postdoctoral Fellowship Opportunity
Molecular Mechanisms of Cancer

The Molecular Pathology Group within the Laboratory of Experimental Pathology is interested in early molecular mechanisms of cancer. We are recruiting a talented Postdoctoral fellow to define epigenetic mechanisms of cancer. Cancer models used in our research are related to studies conducted in the National Toxicology Program (Robert C. Sills et al., Carcinogenesis 2004, Yongbaek Kim et al., Toxicology and Applied Pharmacology, 2005). These studies take advantage of cellular, molecular and genomic approaches which are used to examine mechanisms of carcinogenesis following environmental exposures. Along with the exceptional pathology and molecular facilities and resources at the National Institute of Environmental Health Sciences (NIEHS), the Molecular Pathology Group provides a highly interactive and unique scientific environment with several research groups within the NIEHS, so as to create an exceptional training opportunity. NIEHS is in a highly attractive area of North Carolina that is central to prominent research institutions. Applicants should have a DVM and/or PhD with experience in molecular biology. Salary and benefits are competitive.

For prompt consideration, send or e-mail cover letter, curriculum vitae, and the names/phone numbers of three people who could provide letters of reference to:

Dr. Robert C. Sills, Head, Molecular Pathology, NIEHS/NIH, P.O. Box 12233, Mail Drop B3-08, 111 Alexander Dive, Research Triangle Park, NC 27709, sills@niehs.nih.gov, TEL: 919-541-0180

WWW.NIH.GOV

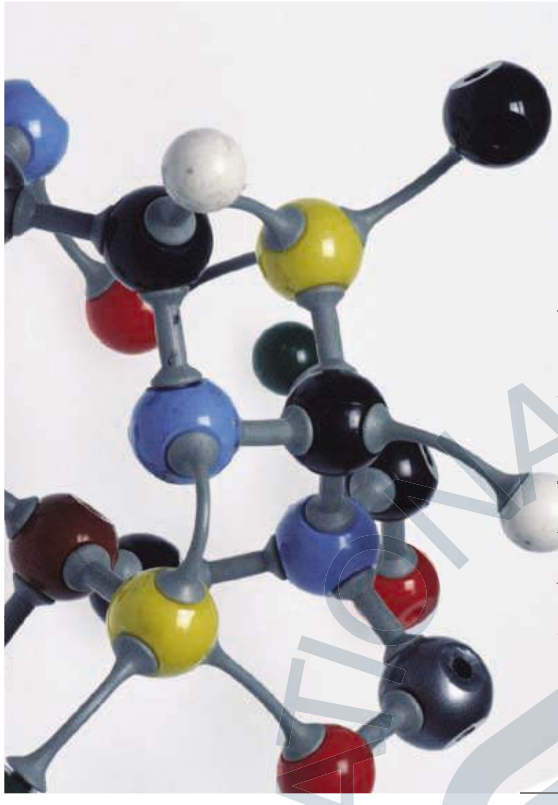

Postdoctoral Research Training at NIH

- Launch a career to improve human health
- Work in one of 1250 of the most innovative and well-equipped biomedical research laboratories in the world
- Explore new options in interdisciplinary and bench-to-bedside research
- Develop the professional skills essential for success
- Earn an excellent stipend and benefits
- Click on www.training.nih.gov

Office of Intramural Training and Education

Hire the World's Best Scientists

- Advertise your positions to the more than 3800 doctoral scientists and clinicians who are in training at the National Institutes of Health
- Reach scientists who are at the forefront of their fields
- Access a population large enough to guarantee interest in your position
- Post new positions with a click of your mouse
- Visit the NIH Virtual Job Fair @ www.training.nih.gov/careers

Office of Intramural Training and Education

Highthroughput Screening Staff Scientist
H. Lee Moffitt Cancer Center & Research Institute

The Staff Scientist is responsible for providing management/oversight and technical support for the HTS and Chemistry Core Facility. Duties include, but are not limited to: Managing the daily activities of the HTS Laboratory, providing technical assistance to our researchers to configure their assays for High-Throughput format, experimental design, performing experimental HTS assays, data analysis and chemical compound management, instrument (including robotics) trouble-shooting, and project trouble-shooting.

Education: Minimum of a Ph.D. in biochemistry, pharmacology, bioorganic chemistry, molecular biology or related field.

Training/Experience: 5-7 years hands-on research in the area of HTS, or related field. Academic or industrial experience is acceptable. Must have background in HTS assay development, screening and analysis. Also, a track record that demonstrates publications in peer-reviewed journals. Five years supervisory experience is required. Past experience in a customer-service oriented laboratory/core facility is highly preferred as is experience supervising a High-Throughput screening core facility.

Competencies: Knowledge of enzymology, protein-protein interactions, signal transduction, apoptosis and cancer biology. Ability to plan, organize and coordinate work assignments. Ability to establish and maintain effective working relationships with others as well as communicate verbally and in writing.

For detailed information, contact Dr. Wayne Guida, guidawc@moffitt.usf.edu
or visit **www.MoffittCancerCenter.org**
Phone: 813-745-6047
Fax: 813-745-6748

H.LEE MOFFITT Cancer Center & Research Institute
A National Cancer Institute Comprehensive Cancer Center
At the University of South Florida

EO/AAE & drug-free workplace.

BLOODCENTER of WISCONSIN™
Blood Research Institute

Research Faculty Openings in:
Stem Cell Biology • Vascular Biology • Immunology

The Blood Research Institute of BloodCenter of Wisconsin is undergoing major expansion of its research facilities and programs, and is seeking qualified research faculty at all levels in the areas of (1) Stem Cell Biology, (2) Vascular Biology, and (3) Immunology. Candidates will join existing vigorous programs in Immunology or Vascular Biology. The newly developed Program in Stem Cell Biology seeks applicants actively conducting research on basic and/or translational aspects of hematopoietic, embryonic, and various other types of adult stem cells.

The 85,000 square foot Blood Research Institute provides state-of-the-art facilities on the campus of the Milwaukee Regional Medical Center, adjacent to the Medical College of Wisconsin (MCW), with an outstanding academic environment for scientific interaction and interdisciplinary collaboration.

Successful junior candidates will have a Ph.D. and/or M.D. degree, relevant postdoctoral experience in the above areas, and a very strong publication record. More established candidates will have a demonstrated record of scholarly contributions to the scientific literature and a history of continuous grant funding. In all cases, ample laboratory and office space, as well as generous start-up funds will be provided.

For further information please visit our web site at **www.bcw.edu**. To submit an application, send your CV, a letter detailing your specific training and research interests and the names and addresses of three references, either via e-mail to **search@bcw.edu** or to: **Gilbert C. White II, M.D., Blood Research Institute, 8727 Watertown Plank Road, PO Box 2178, Milwaukee, WI 53201-2178.**

BloodCenter of Wisconsin is an Equal Opportunity/Affirmative Action Employer. Women and minorities are encouraged to apply.

DUKE NUS
GRADUATE MEDICAL SCHOOL SINGAPORE

Faculty Positions - All Ranks

Tenure-track faculty positions at all levels are available at the Duke-NUS Graduate Medical School Singapore (GMS). The GMS is unique in bringing post-baccalaureate, research-intensive medical education to Asia, and represents a truly global partnership between two leading U.S. and Asian universities. The GMS shares a modern campus with Singapore's largest hospital and several national research centers.

We are seeking creative individuals who are focusing on discovery biology and translational medicine in any thematic area, but with particular emphasis on Cancer and Stem Cell Biology, Degenerative and Metabolic Disorders, or Emerging Infectious Diseases. Special opportunities and infrastructure exist for research involving non-human primates, well-annotated patient populations and biorepositories, advanced imaging of animals and humans, and cell processing. The pioneering faculty will join a number of Duke and Singapore investigators already affiliated with the GMS (see www.gms.edu.sg). Faculty positions include full salary, generous start-up, and five years of annual research funding of up to S$500K/p.a., assuring a stable base of support that can be supplemented by competitive grant awards, which are expanding rapidly in Singapore.

Interested candidates should send a CV, a statement of research interests, and arrange for three letters of reference to be sent (Assistant Professor candidates), or provide contact information for three references (Associate and Full Professor candidates), to:

Patrick J. Casey, Ph.D., Senior Vice Dean of Research,
Duke-NUS Graduate Medical School Singapore,
2 Jalan Bukit Merah, Singapore 169547,
or by email to: hrgms@gms.edu.sg

The GMS is a collaboration of the Duke University School of Medicine and the National University of Singapore.

Pfizer
Expect More From Your Career.®

Imagine a career that touches the lives of people everywhere. Imagine an opportunity to reach beyond your area of expertise to make an impact on something greater than the bottom line. Imagine playing a key role in some of the most critical issues facing healthcare today. This is your career at Pfizer – a career unlike any other.

Our Ann Arbor, MI facility currently has an opportunity for:

Biologics Scientist

As part of a multi-disciplinary drug discovery group working to develop novel macromolecule based therapies, you will be responsible for design, development and screening of assays required to identify the lead molecules.

A Master's Degree in Molecular Biology, Cell Biology or Immunology, with 8 or more years experience in macromolecule drug discovery and a proven track record of developing in vitro screening assays for the identification of lead macromolecules are required. Hands on experience with FACS, immunoassays, multiplex cytokine analysis, reporter gene assays, and primary cell culture as well as with siRNA or aptamers, either as therapeutics or as tools for in vitro or in vivo target validation is highly desirable. The successful candidate will be able to design experiments independently, analyze and present data and work effectively in a diverse, team-based environment.

We offer competitive compensation, full benefits and talented professional colleagues...some of the best and brightest in the industry. To find out more about this position and submit your resume, visit our website at: **www.pfizer.com/careers** and search by **Req # 054166.**

Prizer is proud to be an Equal Opportunity Employer and welcomes applications from people with different experiences, backgrounds and ethnicities.

PGRD
Pfizer Global Research & Development

MOTOR NEURON CENTER

Program Manager

COLUMBIA UNIVERSITY

Center for Motor Neuron Biology and disease

This new center (www.ColumbiaMNC.org) brings together 40 scientists and clinicians working on motor neuron biology and disease (ALS and SMA). We seek a Program Manager with a scientific and administrative background to coordinate and catalyze scientific interactions and to organize administration, meetings, faculty recruitment, grant programs, and fund-raising. The Manager reports to co-directors of the Center.

Requirements: Graduate-level education, 2+ years' experience in program management or equivalent for a foundation, government organization, academic institution, or corporation. Demonstrated project management skills, including project design and budget management.

E-mail CV and cover letter to
dgl2102@columbia.edu.

Columbia University takes affirmative action to ensure equal employment opportunity.

UNIVERSITY OF SOUTHERN DENMARK

WWW.JOBS.SDU.DK

▸ Professorship in Molecular Oncology

SDU - Odense

Applications are invited for a position as professor in molecular oncology at the Institute of Medical Biology, Faculty of Health Sciences, University of Southern Denmark. The professorship is established at the Medical Biotechnology Center, which forms part of the Insitute of Medical Biology.

Further information can be obtained from the Head of the Institute of Medical Biology, prof. dr. med.Ole Skøtt, tel. +45 6550 3752, e-mail: oskott@health.sdu.dk or the Dean of the Faculty of Health Sciences, prof. dr. med. Mogens Hørder, phone: +45 6550 3015, e-mail mhorder@health.sdu.dk

See the full job description on	**www.jobs.sdu.dk**
Deadline for applications:	**June 15, 2006, at 12 noon sharp**
The application must be marked	**"Position no: 061017"**

SYDDANSKUNIVERSITET**.DK**

Flow Cytometry Core Manager/ Staff Scientist

The Division of Viral Pathogenesis at Beth Israel Deaconess Medical Center, Harvard Medical School seeks a full time manager and staff scientist for the flow cytometry core laboratory.

The core laboratory currently serves 90 investigators with a strong AIDS emphasis. It is equipped with a FACSVantage SE DiVa cell sorter, two FACSCaliburs, one FACSArray, a 16 color LSR II and multiple analysis work stations.

The successful candidate will be a highly self-motivated individual, willing to collaborate with multiple researchers and with proven supervisory skills. The position requires an in-depth knowledge of flow cytometry including cell sorting, data analysis, data presentation, fluorochromes and optics. Furthermore, a broad knowledge of computer hardware including server maintenance and software is required. Pursuit of independent research will be encouraged and supported.

Candidates should have an M.D. or a Ph.D. in immunology, virology or related fields with 5 years of relevant flow cytometry experience. Candidates without doctoral degrees will be considered based on experience.

Send letter of introduction, CV and three references by e-mail to: **Dr. Joern Schmitz**, e-mail: **jschmitz@bidmc.harvard.edu**.

"Come build the company of

the future"

Fred Hassan, CEO Schering-Plough

Our plans for tomorrow are as bold as yours. Schering-Plough has new drugs on the horizon, new partnerships and a renewed dedication to leadership, values and hard work — the same qualities that made us an industry leader for decades. Each day, we grow our relationships and establish the trust of doctors and patients alike, while providing them with a steady flow of the most innovative and effective science-based medicines and services.

As we strive to achieve these goals, our commitment to building a diverse, global, highly skilled workforce has become even stronger, with performance driven incentives, leading-edge training and development, and excellent opportunities for professional advancement. "We are building a new and special kind of healthcare company. The change, the excitement, the opportunity are infectious."

We have the following opportunity available in Cambridge, MA:

Associate Director/Director, High Throughput Screening Technology

Req #15043BR

In this position, you will be responsible for overall management of the ALIS operation at our Cambridge, MA facility. ALIS (Automated Ligand Identification System) is a proprietary high throughput screening technology based upon interface of affinity selection and mass spectrometric technologies. The selected candidate will be expected to manage the ALIS operation, including screening of new targets from various therapeutic areas, working closely with chemists on ALIS-based hit and lead optimization projects, and innovating new applications of ALIS in drug discovery.

Qualified candidates will have a Ph.D. in Chemistry or Biochemistry and a minimum of 8-10 years of experience in a biotechnology/ pharmaceutical company, preferably including 3-5 years managing an interdisciplinary group of scientists. The ideal candidate will have a background in high throughput screening operations with strong knowledge of mass spectrometry-based technologies.

As part of the New Schering-Plough team, you'll benefit from strong leadership, a new vision and an empowering corporate culture...while enjoying a very competitive compensation and benefits package. For more information and to apply, visit: **www.schering-lough.com/careers.** Select 'search jobs', enter corresponding req. # and click 'search'. CVs may also be sent directly to john.memmel@spcorp.com. We value the diversity of our global workforce. We are an equal opportunity employer.

Schering-Plough

U.S. DEPARTMENT OF ENERGY
Office of Science
Office of Biological and Environmental Research
Intergovernmental Personnel Act (IPA)
Appointment for two Research Program Managers

The U.S. Department of Energy's (DOE) Office of Biological and Environmental Research (OBER), Office of Science, is soliciting applications from university scientists interested in a 2-year assignment (with an option for an additional 2 years) under an Intergovernmental Personnel Act (IPA) assignment. The respective incumbents will serve as research program managers in the Climate Change Research Division of OBER located in Germantown, Maryland. One assignee would serve as the research program manager for the Terrestrial Carbon Sequestration Research Program and manage selected components of DOE's Terrestrial Carbon Cycle Research Program. Information on these two programs is available at: **http://cdiac2.esd.ornl.gov/index.html** and **http://www.science.doe.gov/ober/CCRD/tcp.html**, respectively. A second IPA assignee would manage DOE's Integrated Assessment Research Program. Information on the Integrated Assessment Research Program is available at: **http://www.science.doe.gov/ober/CCRD/ia.html**. To ensure that research sponsored by these programs is effectively coordinated within and among these and other Climate Change Research Programs in DOE, the incumbents would be expected to work in a team setting with other program managers in OBER.

An IPA assignment is a temporary transfer of skilled personnel between the Federal Government and State or local governments, institutions of higher education, Native American tribal governments, and eligible non-Federal "other organizations," including Federally Funded Research and Development Centers. Assignments are implemented through written Assignment Agreements between DOE, the non-Federal employer, and the assignee. For information on Intergovernmental Personnel Act assignments, please refer to the DOE Directive on IPAs at **http://www.directives.doe.gov/cgi-bin/explhcgi?qry1347894433;doe-110**.

Individuals interested in either IPA assignment position are requested to send their resume to: **Dr. Jerry W. Elwood, Director, Climate Change Research Division, Department of Energy, SC-23.3/Germantown Building, 1000 Independence Avenue, SW, Washington, DC 20585-1290 (Phone: 301-903-3281, email: (jerry.elwood@science.doe.gov)**. Applicants are requested to describe their expertise and experience that would enable them to effectively manage the Terrestrial Carbon Sequestration Research and Carbon Cycle Research Program or manage the Integrated Assessment Research Program. These vacancies will remain open until filled. Prior to submitting an application, prospective applicants should know whether their employer would approve the temporary assignment through the IPA Assignment Agreement.

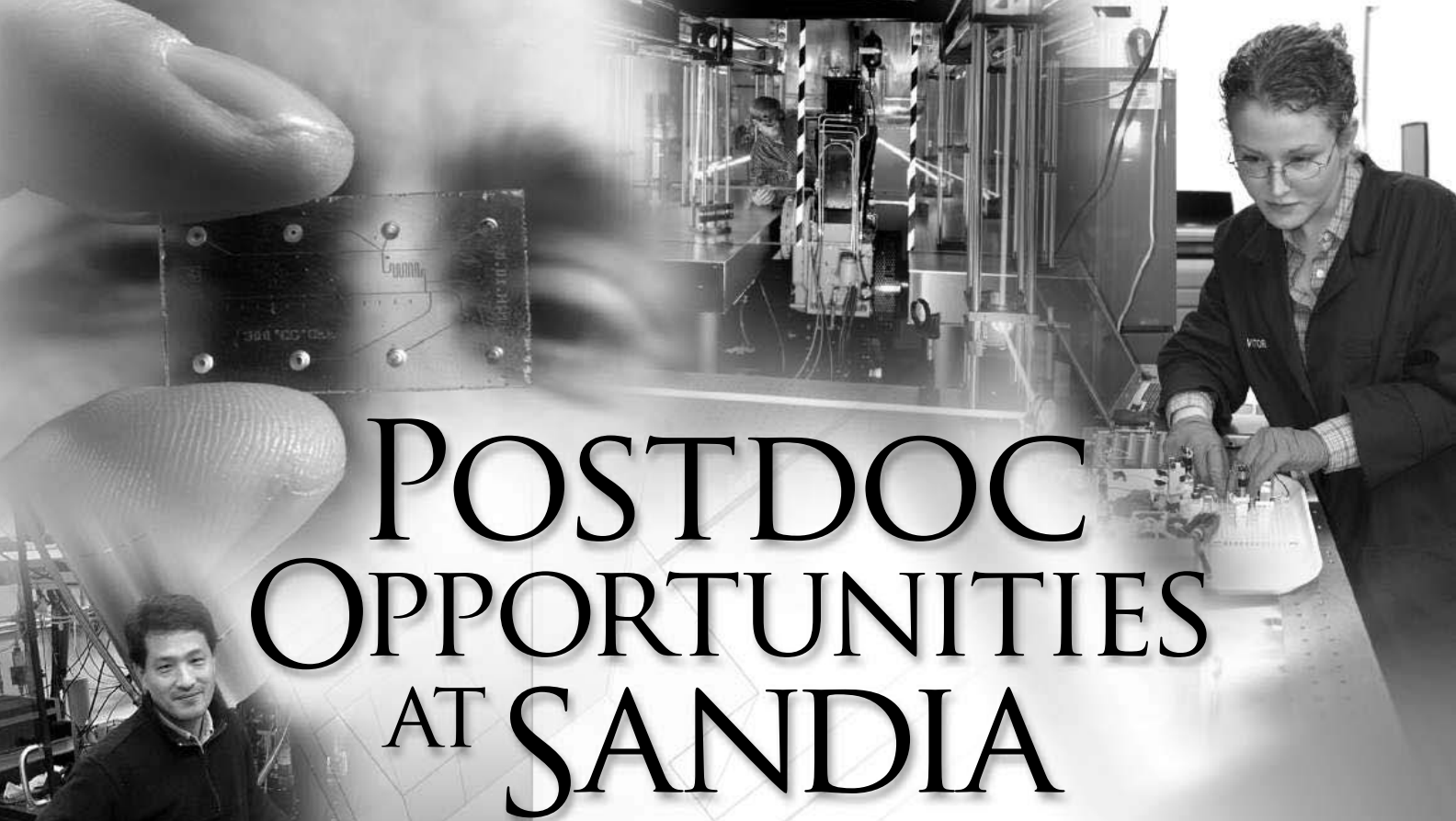

Postdoc Opportunities at Sandia

Division 8000 of Sandia National Laboratories is offering postdoctoral positions for entry level Ph.D. graduates in a variety of technical disciplines. Most positions are located in Livermore, CA, (San Francisco Bay Area) with some situated in Albuquerque, NM.

A Ph.D. in biological, chemical or physical sciences, engineering, or related fields, a strong academic record, and demonstrated research accomplishments are required.

Our success is closely tied to our interactions with collaborators. Researchers from universities, industry, and other laboratories work closely with Sandia scientists, engineers, technologists, and postdocs on problems of mutual interest.

Candidates must possess excellent quantitative, verbal and written communication skills and an ability to work effectively with others. U.S. citizenship is desirable, but not required for many of these openings.

Annual salary is $72,100 with a comprehensive benefits package.

Information on these and other opportunities can be found at:
http://www.sandia.gov/employment/career-opp/index.html
Please submit an online application using the reference number associated with each position.

- Nanostructure Electronics & Photonics (54723), CA
- Molecular Immunology (54673), CA
- Chemical Kinetics (54657), CA
- Fluid Mechanics/Multiscale Modeling (54653), CA
- Surface Science (54635), CA
- Mechanics of Materials (54621), CA
- Nanoscale Materials (54603), CA
- Computational Biology (54600), NM
- Molecular Dynamics (54459), NM
- Biomolecular Imaging (54444), NM
- Biology/Immunology (54217), NM
- Molecular Modeling (54151), NM
- Microfluidics (54090), CA
- Experimental Combustion (54015), CA
- Fluorescence Spectroscopy (54014), NM
- Microfluidics (53979), CA
- Laser-based Sensing (53879), CA
- Picosecond Diagnostics (53744), CA
- Combustion Chemistry (53567), CA
- Combustion Kinetics (53561), CA
- Experimental Biophysics (53546), CA
- Mass Spectroscopy (53490), CA
- Hydrogen Storage (52791), CA
- Radiation Detection (52765), CA

Sandia National Laboratories

Sandia National Laboratories is an Equal Opportunity Employer. M/F/D/V.

Careers in Translational Medicine

Advertising Supplement

Be sure to read this special ad supplement devoted to translational medicine opportunities in the upcoming **26 May issue of *Science*.**

You can also read it online on **www.sciencecareers.org.**

To advertise in this issue, please contact:

U.S. Daryl Anderson
phone: 202-326-6543
e-mail: danderso@aaas.org

Europe and International
Tracy Holmes
phone: +44 (0) 1223 326 500
e-mail: ads@science-int.co.uk

Japan Jason Hannaford
phone: +81 (0) 52 789-1860
e-mail: jhannaford@sciencemag.jp

ScienceCareers.org
We know science AAAS

School of Medical Sciences

Two Senior Lectureships in Neurosciences and Cell and Developmental Biology

The University require two senior lecturers/readers to enhance its strong research programmes in Neuroscience and in Cell and Developmental Biology.

Individuals studying the cell and molecular basis of normal or regenerative biology are especially welcome. With an international research reputation, clear research vision and strong research funding, you will be joining the internationally excellent physiology group (RAE2001: 5 rated). Current research strengths include neural development, regeneration, regulation of gene expression, cell signalling and adhesion, stem cells, neurological disease and brain ageing, learning, memory and synaptic plasticity and neurophysiology and neuropharmacology. You will also undertake an element of undergraduate and postgraduate teaching.

The post will be based in the University's flagship Institute of Medical Sciences with state-of-the-art facilities.

Informal enquiries to Professor Colin McCaig, Head of School of Medical Sciences (tel: 01224 273047, e-mail: c.mccaig@abdn.ac.uk).

Online application forms and further particulars are available from www.abdn.ac.uk/jobs Alternatively telephone (01224) 272727 (24 hour answering service) quoting reference number MSU990A for an application pack.

Closing date: 9 June 2006.

Promoting Diversity and Equal Opportunities throughout the University

1495 UNIVERSITY OF ABERDEEN

NANOCENTER USC

ENDOWED CHAIR POSITION

Polymer Nanocomposite Research
University of South Carolina NanoCenter

The University of South Carolina seeks to hire an endowed chair for its Research Center of Economic Excellence in polymer nanocomposites. This recently formed Center was created after the University of South Carolina competed and received a $3.5 million award from the state of South Carolina. This funding, when matched with an additional $3.5 million, creates a substantial endowment to support the center's activities. The successful applicant will be expected to lead and grow the university's polymer nanocomposites program by hiring additional faculty, staff, and students to support this institutional research priority.

The ideal candidate will be hired at the associate or full professor level in the department and college most closely aligned with their research and academic interests. Applicants should be internationally recognized for their work in this emerging field and will possess significant external funding to support his/her scholarly activities. The successful applicant will benefit from this state's significant plastics industry, and will be responsible for nurturing relationships between the University, the nanocenter (http://nano.sc.edu), and these companies in order to support the development of new commercially relevant products that will positively impact the state's industry and economy. The University has made substantial investments in this program and this is an ideal opportunity for anyone interested in being provided sufficient resources to grow a research program to international prominence.

Candidates are encouraged to submit in confidence a complete curriculum vitae, publication list, statement of research interests and accomplishments to: **Professor Tom Vogt, Chair of the Polymer Nanocomposite Search Committee, USC NanoCenter, Sumwalt College, University of South Carolina, Columbia, SC, 29208**. Letters of recommendation will be sought after an initial review of applications. E-Mail applications can be sent to **tvogt@gwm.sc.edu**.

Evaluation of applicants will begin **August 1, 2006**, and will continue until the position is filled.

The University of South Carolina is an EO/AA Employer and encourages applications from minorities and women.

POSITIONS OPEN

VIROLOGY FACULTY POSITION

The Department of Microbial and Molecular Pathogenesis is recruiting an outstanding Virologist for a tenure-track position at the **ASSISTANT PROFESSOR** level. Investigators whose research complements existing strengths in molecular virology and pathogen-host interactions will be given priority. State-of-the-art facilities for animal housing, genomics, proteomics, structural biology, and biocontainment (BL-3) are available on campus or within the Department. The candidates are expected to establish an independent, externally funded research program and to participate in medical and graduate education programs through Department, including an NIH fellowship program in Host-Pathogen Interactions. Numerous opportunities exist for collaborations in basic and clinical sciences within the Health Science Center as well as with interdisciplinary programs in conjunction with Texas A&M University (e.g. the Intercollegiate Faculty of Virology, 22 members). Appointments are for 12 months with a competitive startup package and laboratory space. Review of applications will begin immediately. Applicants should submit curriculum vitae, a statement of research interests and goals, and have letters of recommendation sent from three referees. These materials should be submitted online **(e-mail: wilson@medicine.tamhsc.edu)** and through the postal service to: **Dr. Van G. Wilson, Search Committee Chair, Department of Microbial and Molecular Pathogenesis, College of Medicine, Texas A&M University System Health Science Center, College Station, TX 77843-1114.** For more information visit our **website: http://medicine.tamhsc.edu/basic_sciences/mmp/.**

The Texas A&M University System Health Science Center is an Affirmative Action/Equal Opportunity Employer and encourages applications from women and minorities.

We are seeking a **POSTDOCTORAL FELLOW** with expertise in electrophysiology to join an active group of NIH-funded pain researchers in the Disorders of Neuroregulatory Function Center of Excellence. Our team is conducting cutting edge research on the ability of neurotrophins to modulate nociceptive processing in the brainstem and spinal cord using a variety of chronic and neuropathic pain models. Projects will include exploring the phenotype of knockout mice using these model systems.

Qualified applicants must hold a Ph.D. in neuroscience or a related field and must be proficient in the setup, organization, and performance of in vivo extracellular recording in the mouse spinal cord. The ability to perform nocifensive behavioral testing and assist with the maintenance and expansion of genetically engineered mouse strains is desired.

Interested candidates should submit a cover letter, curriculum vitae or resume, names of three references, and a summary of research interests to:

Dr. Susan G. Dorsey
University of Maryland School of Nursing
c/o Lois Reisig
655 West Lombard Street, Room 505
Baltimore, MD 21201

The University of Maryland is an Equal Opportunity/Affirmative Action/ADA Employer.

CHIEF MEDICAL OFFICER

Highly intelligent individual with exceptional communication skills sought by prominent Manhattan family to research and coordinate family medical and healthcare issues. Act as liaison with leading medical researchers and consultants in academia and industry, with full responsibility for technical, financial, and administrative functions. Considerable weight given to evidence of unusual academic or other intellectual distinction. Ph.D. or M.D. required, clinical experience a plus but not essential. Possible entrepreneurial opportunities involving delivery of ultrahigh-end medical care to other, similar families. Full- time position. Excellent compensation with significant upside potential and management possibilities. Resume to **e-mail: fmc4@spsfind.com.**

POSITIONS OPEN

TENURE-TRACK FACULTY MEMBER
Medical Oncology

Stanford University School of Medicine and the Stanford Cancer Center . We are searching for a physician scientist at the level of **ASSISTANT** or **ASSOCIATE PROFESSOR** in the University Tenure Track in the Division of Oncology, Department of Medicine. The predominant criterion for appointment in the University Tenure Track is a major commitment to research and teaching. Candidates should have an M.D. or M.D./Ph.D., be trained in the subspecialty of medical oncology, and be accomplished in research. They should be prepared to establish an independent laboratory program in cancer research. Applicants with expertise in molecular and cell biology, immunology, molecular therapeutics, or genetics and in translational research in solid tumors are especially encouraged. Salary support, laboratory space, and startup funds are available for this position. Successful candidates will have demonstrated their ability to obtain peer reviewed research funding. Participation in clinical care and in teaching will be expected. Please send curriculum vitae, a statement of career plans, and three names of references to: **Ronald Levy, M.D., Professor of Medicine, Chief, Division of Oncology, Stanford University School of Medicine, CCSR Building, Room 1126, Stanford, CA 94305-5151.** *Stanford University is an Equal Opportunity Employer and is committed to increasing the diversity of its faculty. It welcomes nominations of and applications from women and members of minority groups, as well as others who would bring additional dimensions to the University's research, teaching, and clinical missions.*

Virginia Commonwealth University (VCU) School of Medicine is seeking several scientists for tenure-eligible positions in the areas of diabetes, metabolism, and nutrition for the establishment of major broad-based interdisciplinary research programs. Candidates should qualify for an appointment at the **ASSOCIATE** or **PROFESSOR** level, possess an M.D. and/or Ph.D. degree, and be nationally recognized for achievement in basic or clinical research as demonstrated through extramural grant support and publications. Areas of research represented at VCU include insulin resistance, metabolic syndrome, insulin signaling, islet cell electrophysiology, lipidology, islet cell transplantation, nonalcoholic steatohepatitis, polycystic ovary syndrome, and obesity. Candidates with research interests that integrate several of these areas are especially encouraged, as are those with a translational component to their research. VCU has considerable resources available to invest in successful candidates. Send letter of interest and curriculum vitae to: **John E. Nestler, M.D., Chair, Division of Endocrinology and Metabolism, P.O. Box 980111, Richmond, VA 23298-0111.** These positions will remain open until they are filled. *Virginia Commonwealth University is an Equal Employment Opportunity/Affirmative Action Employer. Women, minorities, and persons with disabilities are encouraged to apply.*

POSTDOCTORAL POSITIONS IN SIGNAL TRANSDUCTION
Harvard Medical School/
Massachusetts General Hospital

Positions are available in the laboratory of **Joseph Avruch, M.D.,** Departments of Medicine and Molecular Biology, now through fall 2006, for recent graduates with strong skills in mammalian molecular biology and/or protein chemistry. Ongoing work involves Rheb and mTOR signalling (*Curr. Biol.* **15:**702,2005), Nore1A and the MST1/2 kinases (*B.J.* **381:**453, 2004), and the Nek kinases (Nek1, 6, 9, *MBC* **16:**4827, 2005). Prior experience with protein phosphorylation desirable. Outstanding scientific environment.

Please send curriculum vitae, the names and addresses of three references to **e-mail: avruch@molbio.mgh.harvard.edu.**

POSITIONS OPEN

HEAD, DIVISION OF HEMATOLOGIC ONCOLOGY
Memorial Sloan-Kettering Cancer Center

The Department of Medicine at Memorial Sloan-Kettering Cancer Center (MSKCC) is seeking a Head of the Division of Hematologic Oncology. The Division consists of more than 45 board-certified oncologists on the Leukemia, Lymphoma, Bone Marrow Transplantation and Hematology Services and has recognized programs in laboratory and clinical translational research and clinical care. The Head of the Division oversees the Division's research programs, clinical activities, and teaching. The successful candidate will have an outstanding record of accomplishments as a widely recognized and active scientific leader in the study of the hematologic neoplasms. An M.D., M.D./Ph.D., or equivalent degree and board certification in internal medicine and oncology and/or hematology are required. The successful candidate will bring her/his research activities to the vibrant research environment of MSKCC, including the Sloan-Kettering Institute, the Gerstner Sloan-Kettering Graduate School, and the Human Oncology and Pathogenesis Program, as well as the neighboring Weill Medical College of Cornell University and Rockefeller University. Interested candidates are invited to submit curriculum vitae and bibliography to: **Alan Houghton, M.D., Chair, Division of Hematologic Oncology Search Committee, c/o Ms. Kendra Eaglin, Memorial Sloan-Kettering Cancer Center, 1275 York Avenue, C1289, New York, NY 10021** or at **e-mail: eaglink@mskcc.org.** *Memorial Sloan-Kettering Cancer Center is an Equal Opportunity Employer with a strong commitment to enhancing the diversity of its faculty and staff. Women and applicants from diverse racial, ethnic, and cultural backgrounds are encouraged to apply.*

FACULTY POSITION
Microbiology

The Department of Microbiology and Immunology at Des Moines University, Osteopathic Medical Center invites applicants for a tenure-track position at the level of **ASSISTANT PROFESSOR.** The successful candidate must possess the knowledge and skills necessary to participate in the teaching of pathogenic bacteriology to medical and health professional students. In addition, it is expected that the individual develop an innovative and extramurally funded research program using contemporary approaches to study host-pathogen interaction. Applicants should have a Ph.D. and relevant postdoctoral experience. Applicants should send curriculum vitae, a concise statement of teaching and research interests, and the names of three professional references to:

Microbiology Faculty Search
Department of Microbiology and Immunology
Des Moines University
Osteopathic Medical Center
3200 Grand Avenue
Des Moines, IA 50312

Visit **website: http://www.dmu.edu.**

For full consideration applications should be received by June 30, 2006.

ASSISTANT PROFESSOR IN MOLECULAR BIOSCIENCES, University of Hawaii, tenure track, to teach biochemistry and develop a research program integrating biochemistry with other biosciences. Ph.D. in biochemistry or closely related area, two years of postdoctoral training desirable. To apply: Send cover letter, curriculum vitae, statement of research and teaching interests, reprints, and three reference letters to: **Search Committee Chair, Department of Molecular Biosciences and Bioengineering, Center of Tropical Agriculture and Human Resources, University of Hawaii at Manoa, 1955 East West Road, Honolulu, HI 96822.** Further information on the position can be viewed at **website: http://www.ctahr.hawaii.edu/mbbe/.** Inquiries, **telephone: 808-956-8384.**

IBC's 11th Annual World Congress

Drug Discovery Technology® & Development

Science Subscribers Register Early and Save

See website for details

Conference: August 7-10, 2006 • Exhibition: August 8-10, 2006 • World Trade Center Boston/Seaport Hotel • Boston, MA

Keynote Speakers

Andrew C. von Eschenbach, M.D.
Acting Commissioner, **FDA**
and Director, **National Cancer Institute**

Steven M. Paul, M.D.
Executive Vice President, Science and Technology, President, Lilly Research Laboratories, **Eli Lilly and Company**

Peter B. Corr, Ph.D.
Senior Vice President, Science & Technology
Pfizer Inc

Susan Hockfield, Ph.D.
President
Massachusetts Institute of Technology

Providing Coverage of the Most Vital Topics in Drug Discovery and Development

More *Sessions than Ever Before ... Six Dedicated Conferences*

- **Targeting Disease and Evaluating Disease-Relevant Targets**
- **Lead Discovery and Lead Optimization**
- **Discovery to Development:** *Case Studies, Safety, PK/PD and Pharmacogenomics*
- **Biomarkers:** *Utility, Validation and Applications from Discovery to Clinic*
- **R&D Strategies and Business Alliances**
- **The Interface between Drug Discovery and Informatics**

Plus! 7 In-Depth, Focused Pre-Conference Workshops

200+ Speakers

Plus! *The Top Ten Reasons You Can't Afford to Miss this Event*

1. **Discover new approaches for targeting disease** and next generation target prioritization techniques including the re-emergence of genetics approaches
2. **Gain insights** to reduce cost and attrition, improve innovation, implement new R&D models and develop productive alliances **from the perspective of 60+ thought leaders**
3. **Improve your lead discovery and optimization efforts** by attending 14 case studies, and hear about innovative chemistry techniques, compound collection strategies and the latest in fragment-based approaches from 30+ speakers
4. **Hear cutting-edge biomarker applications** from 35+ leading voices and get the latest updates on the FDA's pharmacogenomics guidance and biomarker validation
5. **Find out which approaches to safety and PK/PD are adding value** and how pharmacogenomics and personalized medicine are being applied from discovery to clinic
6. **Bridge the gap between Science and Informatics** in your company and learn how to put your scientific data to use. Attend the informatics sessions featuring 40+ speakers, 5 interactive panel discussions and new exciting debates
7. **Evaluate over 300 exhibit booths** showcasing the latest technologies, products and services in drug discovery and development....all under one roof
8. **Participate in 16 thought provoking panels** on cost reduction, the role of Asia & Eastern Europe, VC funding, strategic alliances dos and don'ts and more....
9. **Network with 4000+ attendees** by taking advantage of DDT Event Connect...the on-line networking tool that lets you set up meetings before the event
10. **Learn from 200+ speakers, 150+ poster presentations** covering all facets of drug discovery and development

VIP CODE: 3200SADM

Presidential Sponsor ELSEVIER MDL

Executive Sponsors CCS Caliper LifeSciences

Executive Support Sponsors Roche GENE LOGIC

Sponsoring Publication Science AAAS

Association Sponsor MBC Massachusetts Biotechnology Council

Organized by ibc Life Sciences

To Register: Call (800) 390-4078 • Fax: (941) 365-0104 • Email: reg@ibcusa.com

www.drugdisc.com

POSITIONS OPEN

SUPERVISORY PHYSICAL SCIENTIST, GS-1301- 15, or **SUPERVISORY SOCIAL SCIENTIST,** GS-101-15, salary range: $107,521 to 139,774. The Climate Program of the National Oceanic and Atmospheric Administration (NOAA) is seeking an energetic individual with considerable experience in outcome-oriented, applied environmental research to lead a new division known as Climate Assessments and Services. The incumbent is responsible for managing a division that leads the effort to connect climate assessments, research, and services to broader public interest goals associated with adapting to climate variability and change. The ideal candidate will have demonstrated him/herself to be an innovator and initiator, will have experience working across public and private sector organizations, will have worked in the field of applied climate and environmental research or in a setting which required ongoing interaction with the environmental research community, and will have a vision for the implementation of federal investments linking new climate-related interdisciplinary research with national needs for building adaptive capacity for climate variability and change. Excellent verbal and written communication skills are essential as is the ability to work in a team of Senior Program Managers in support of agency goals and mission requirements. Ph.D. or equivalent experience required. Detailed job information and applicant instructions will be found at **website: https://jobs1.quickhire.com/scripts/doc.exe** under vacancy numbers OAR-HQ-2006-0092, 93, 94 and 96. *Open to all U.S. citizens. The U.S. Department of Commerce is an Equal Opportunity Employer.*

PH.D. RESEARCH SCIENTISTS

Biocept, a San Diego Biotech Company, is developing technology for Non-invasive Prenatal Diagnosis of Chromosomal Disorders. We have immediate need for innovative Ph.D. scientists with a demonstrated record of accomplishments in molecular biology and human genetics. The prospective candidates must be proficient in state-of-the-art molecular biology techniques including all aspects of QF-, Q-RT-, and real time polymerase chain reaction in situ hybridization, and functional genome analysis. These individuals are expected to be vigorously involved in ongoing discovery programs to develop gene expression markers for rare cells and identify novel cell surface proteins for immunohistochemical staining and cell capture. The successful candidates will have a Ph.D. degree and two to seven years of experience in a related field, and excellent communication skills. Meticulous work habits, attention to details, and ability to analytically design, execute experiments, and interpret experimental data are a must.

Biocept is located minutes away from the University of California, San Diego, Salk and Scripps Research Institutes, as well as La Jolla beaches. It offers competitive salaries and an excellent benefit package to its employees. Interested candidates may send their resume in confidence to **e-mail: khoughtaling@biocept.com.**

The Protein Nanotechnology Group at National Aeronautics and Space Administration (NASA) Ames Research Center is seeking **TWO POSTDOCTORAL ASSOCIATES.** Both should have experience in molecular biology and protein engineering. One project is in the area of protein-based chemosensors. This work seeks to create sensing elements for small molecule analytes using proteins evolved by living organisms to sense compounds in their surroundings. Experience with fluorescence spectroscopy or optics is desirable. The other project requires experience in surface science or biomaterials, and the successful candidate will join efforts to genetically manipulate the structure and function of molecular chaperones to create useful nano-devices (**McMillan et al.,** *Nature Materials* **1**:247, 2002). E-mail curriculum vitae and cover letter to **e-mail: chad.paavola@nasa.gov.**

POSITIONS OPEN

The Division of Endocrinology, Metabolism, and Lipids at Emory University in Atlanta, Georgia, is seeking applicants with interests in either basic bone biology, bone diseases, or diabetes for **TENURED** and **TENURE-TRACK FACULTY POSITIONS.** Applicants must have an M.D., Ph.D., D.D.S.P.H. or M.D./Ph.D. degree and a strong background in molecular and/or cell biology. Openings are available at the Assistant, Associate and Full Professor level. Excellent laboratory space and competitive startup and compensation packages are available. Candidates at the Associate/Full Professor level must have an established, extramurally funded research program while candidates at the Assistant Professor level need to demonstrate the potential for establishing an independent research program within three years of their initial appointment. Interested candidates should contact:

Roberto Pacifici, M.D.
Herndon Professor of Medicine
Director, Division of Endocrinology, Metabolism and Lipids
Emory University School of Medicine
101 Woodruf Circle, WMRB 1307
Atlanta, GA 30322

E-mail: roberto.pacifici@emory.edu; telephone: 404-712-8420; fax: 404-727-1300.

POSTDOCTORAL FELLOW
University of the Pacific, Stockton, California
Deadline: Open Until Filled
Field: Molecular Biology

NIH-supported postdoctoral position in research focused on diabetes/vascular biology at the University of the Pacific, T.J. Long School of Pharmacy, Stockton, California. Requires expertise in molecular biology (microarray, et cetera). Interested individuals should e-mail a cover letter, curriculum vitae, and two references to **Dr. Roshanak Rahimian,** e-mail: rrahimian@pacific.edu.

ANNOUNCEMENTS

SECOND CALL FOR PROPOSAL-2006 INDO-U.S. SCIENCE AND TECHNOLOGY FORUM
Fulbright House, 12 Hailey Road,
New Delhi-110 001, India
Website: http://www.indousstf.org

The Indo-U.S. Science and Technology Forum (Forum), established under an agreement between the governments of India and the United States of America, is an autonomous, not-for-profit society that promotes and catalyzes the Indo-U.S. bilateral collaborations in science, technology, engineering, and biomedical research through substantive interaction among government, academia, and industry.

The Forum seeks to support innovative programs aimed to stimulate interactions that have a strong potential for generating follow-on activities and building long-term Indo-U.S. science and technology relationships. The Forum promotes a program that nurtures contacts between young and mid career scientists and technologists and fosters active public-private partnership in R&D.

The Forum solicits proposals thrice a year (January, May, October) jointly submitted by the U.S. and Indian principal investigators from academia, government funded institutions/laboratories, and private R&D entities for: (1) Knowledge R&D Networked and Public-Private Networked Indo-U.S. Centers; (2) Bilateral workshops, conferences, symposia, schools, etc.; (3) Travel grants: (a) to avail already awarded fellowship and sabbatical positions in U.S./India; (b) for selected U.S. participants to attend international conferences/events in India; (c) for specific exploratory/planning visits aimed at large-scale collaborations.

Detailed format available at **website: http://www.indousstf.org.** For further details and electronic submission, contact: **Arabinda Mitra, e-mail: amitra@indousstf.org;** and **Michael Cheetham, e-mail: mcheetham@si.edu.**

Submission deadline is 15 June 2006, and award announcement is mid September 2006.

POSITIONS OPEN

POSTDOCTORAL ASSOCIATE

A Postdoctoral Position is immediately available to study the cellular and molecular mechanisms of neuronal migration disorders in genetically modified mice. Independent, ambitious postdoctoral scientist with training in biochemistry, molecular biology, glycobiology, or developmental neurobiology is required. Experience with transgenic mice, protein analysis, and purification or protein-protein interactions are desirable but not required. Apply to position 021427 online at **website: http://www.upstate.edu.** *An Affirmative Action/Equal Employment Opportunity/ADA employer committed to excellence through diversity.*

RESEARCH FELLOW, POSTDOCTORAL sought by A.I. DuPont Hospital Laboratory of Human Genetics. Must have Ph.D. in cell biology, biochemistry, genetics or related, and knowledge of immuno assays (Western Blot and immuno fluorescence); recombinant DNA methods (sequencing, mutagenesis, cloning, PCR and RT-PCR); protein expression and purification of recombinant proteins and from mammalian cells; cell biology techniques (transfection and generation of cell lines); and microscopy (light and fluorescence). Send resume to: **A. M. Riddle, Adminstrator for Nemours Biomedical Research, A.I. DuPont Hospital for Children, P.O. Box 269, Wilmington, DE 19899.**

KARLSTAD UNIVERSITY, SWEDEN

Tenured **SENIOR LECTURER/ASSOCIATE PROFESSOR** in freshwater ecology, working on benthic macroinvertebrates or vertebrates in area that complements Departmental research. See **website: http://www.kau.se/eng/vacancies/index.lasso?to_do=detail&tjanst_id=1850.** Applications are due 22 May 2006.

MARKETPLACE

ENDOGEN®
SEARCHLIGHT®

SearchLight® Protein Arrays

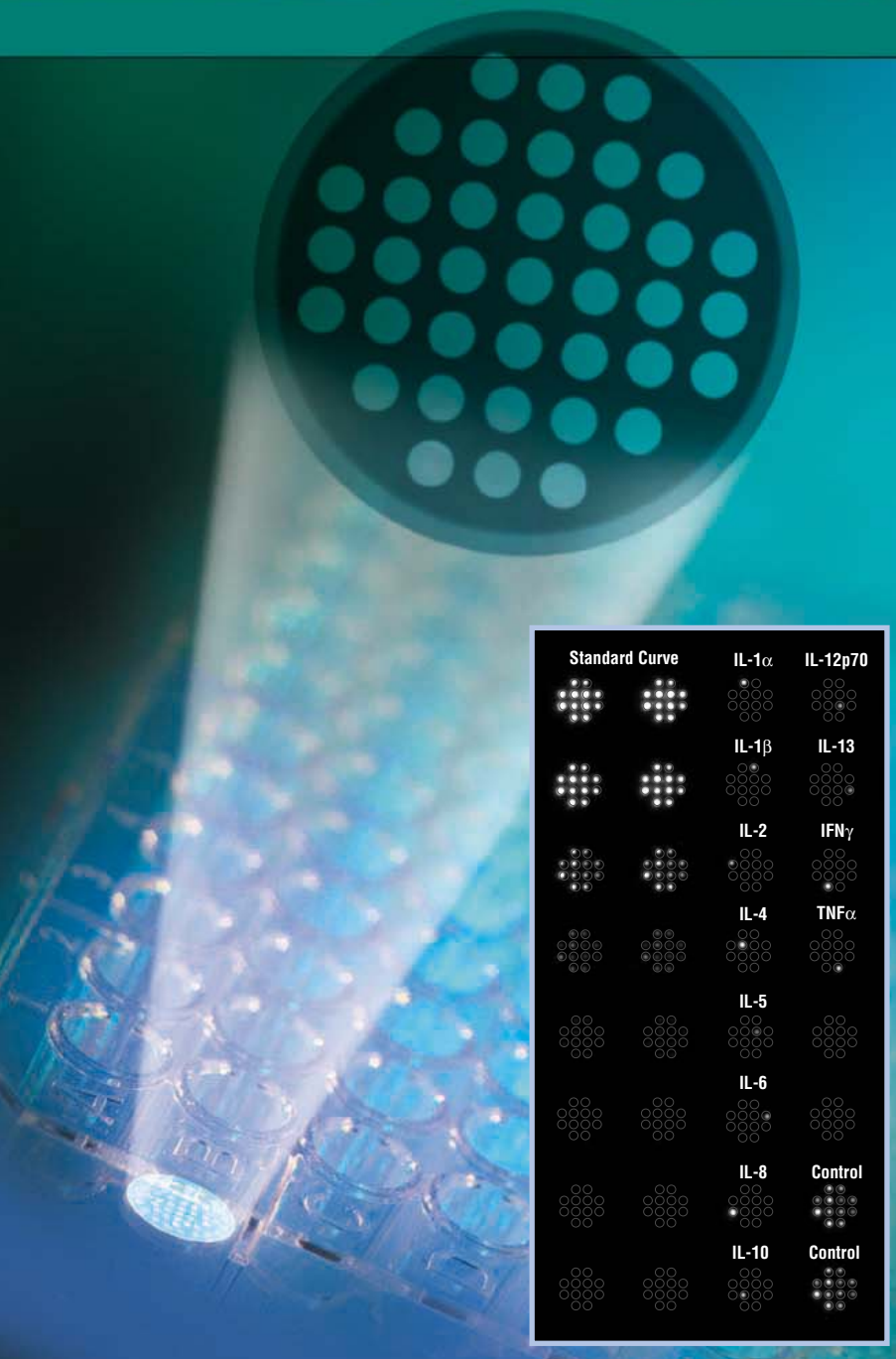

Cytokine and Biomarker Profiling

Now the choice **is yours.**

SearchLight® Infrared or Chemiluminescent Protein Arrays

Choose from the best technologies

- **New** arrays are compatible with the Odyssey® and Aerius® Infrared Imaging Systems from LI-COR® Biosciences
- Sensitive chemiluminescent arrays are compatible with the SearchLight® CCD Imaging System for up to 12 proteins per well

Choose quality results

- Sensitivity and dynamic range comparable to or better than traditional colorimetric ELISAs
- Comprehensive specificity testing for each new antibody combination
- More than 200 protein markers and growing … cytokines, MMPs, biomarkers and more

Choose our reputation

- We have pioneered innovative assay technologies and are highly trusted for our excellent customer support
- We can test your samples for you. Get your data back in 7-10 days. For Sample Testing Service from Pierce, contact us online

Choose from a growing menu of plate-based arrays, slide arrays, ELISA kits and reagents for protein quantification.
Visit our web site or call 815-968-0747 to locate your local Endogen/Pierce representative.

www.endogen.com

Tel: 815-968-0747 or 800-874-3723 • Fax: 815-968-7316
Technical Assistance E-mail: TA@piercenet.com • Customer Assistance E-mail: CS@piercenet.com

For distributors outside the U.S. and Europe, visit www.piercenet.com

For European offices and distributors, visit www.perbio.com

PERBIO